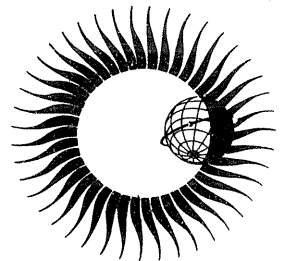


WORLD DATA CENTER A
for
Solar-Terrestrial Physics



COLLECTED DATA REPORTS
ON
AUGUST 1972 SOLAR - TERRESTRIAL EVENTS



JULY 1973

WORLD DATA CENTER A

National Academy of Sciences

2101 Constitution Avenue, N. W. Washington, D. C. U.S.A., 20418

World Data Center A consists of the Coordination Office

and eight subcenters:

World Data Center A
Coordination Office
National Academy of Sciences
2101 Constitution Avenue, N.W.
Washington, D. C., U.S.A. 20418
Telephone (202) 961-1478

Solar and Interplanetary Phenomena,
Ionospheric Phenomena, Flare-Associated
Events, Geomagnetic Variations, Magnetospheric
and Interplanetary Magnetic Phenomena,
Aurora, Cosmic Rays, Airglow:

World Data Center A
for Solar-Terrestrial Physics
National Oceanic and Atmospheric
Administration
Boulder, Colorado, U.S.A. 80302
Telephone (303) 499-1000 Ext. 6467

Geomagnetism, Seismology, Gravity (and
Upper Mantle Project Archives):

World Data Center A:
Geomagnetism, Seismology and Gravity
Environmental Data Service, NOAA
Boulder, Colorado, U.S.A. 80302
Telephone (303) 499-1000 Ext. 6311

Glaciology:

World Data Center A:
Glaciology
U. S. Geological Survey
1305 Tacoma Avenue South
Tacoma, Washington, U.S.A. 98402
Telephone (206) 383-2861 Ext. 318

Longitude and Latitude:

World Data Center A:
Longitude and Latitude
U. S. Naval Observatory
Washington, D. C., U.S.A. 20390
Telephone (202) 698-8422

Meteorology (and Nuclear Radiation):

World Data Center A:
Meteorology
National Climatic Center
Federal Building
Asheville, North Carolina, U.S.A. 28801
Telephone (704) 254-0961

Oceanography:

World Data Center A:
Oceanography
National Oceanic and
Atmospheric Administration
Rockville, Maryland, U.S.A. 20852
Telephone (202) 426-9052

Rockets and Satellites:

World Data Center A:
Rockets and Satellites
Goddard Space Flight Center
Code 601
Greenbelt, Maryland, U.S.A. 20771
Telephone (301) 982-6695

Tsunami:

World Data Center A:
Tsunami
National Oceanic and Atmospheric
Administration
P.O. Box 3887
Honolulu, Hawaii, U.S.A. 96812
Telephone (808) 546-5698

Notes:

- (1) World Data Centers conduct international exchange of geophysical observations in accordance with the principles set forth by the International Council of Scientific Unions. WDC-A is established in the United States under the auspices of the National Academy of Sciences.
- (2) Communications regarding data interchange matters in general and World Data Center A as a whole should be addressed to: World Data Center A, Coordination Office (see address above).
- (3) Inquiries and communications concerning data in specific disciplines should be addressed to the appropriate subcenter listed above.

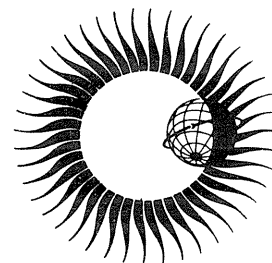
WORLD DATA CENTER A for Solar-Terrestrial Physics



REPORT UAG - 28 PART II

COLLECTED DATA REPORTS ON AUGUST 1972 SOLAR - TERRESTRIAL EVENTS

Helen E. Coffey, Editor
WDC-A for Solar - Terrestrial Physics
Boulder, Colorado U.S.A.



Prepared by World Data Center A for
Solar-Terrestrial Physics, NOAA, Boulder, Colorado
and published by

U.S. DEPARTMENT OF COMMERCE
NATIONAL OCEANIC AND ATMOSPHERIC ADMINISTRATION

ENVIRONMENTAL DATA SERVICE
Asheville, North Carolina, USA 28801

July 1973

SUBSCRIPTION PRICE: \$9.00 a year; \$2.50 additional for foreign mailing; single copy price varies.* Checks and money orders should be made payable to the Department of Commerce, NOAA. Remittance and correspondence regarding subscriptions should be sent to the National Climatic Center, Federal Building, Asheville, NC 28801, Attn: Publications.

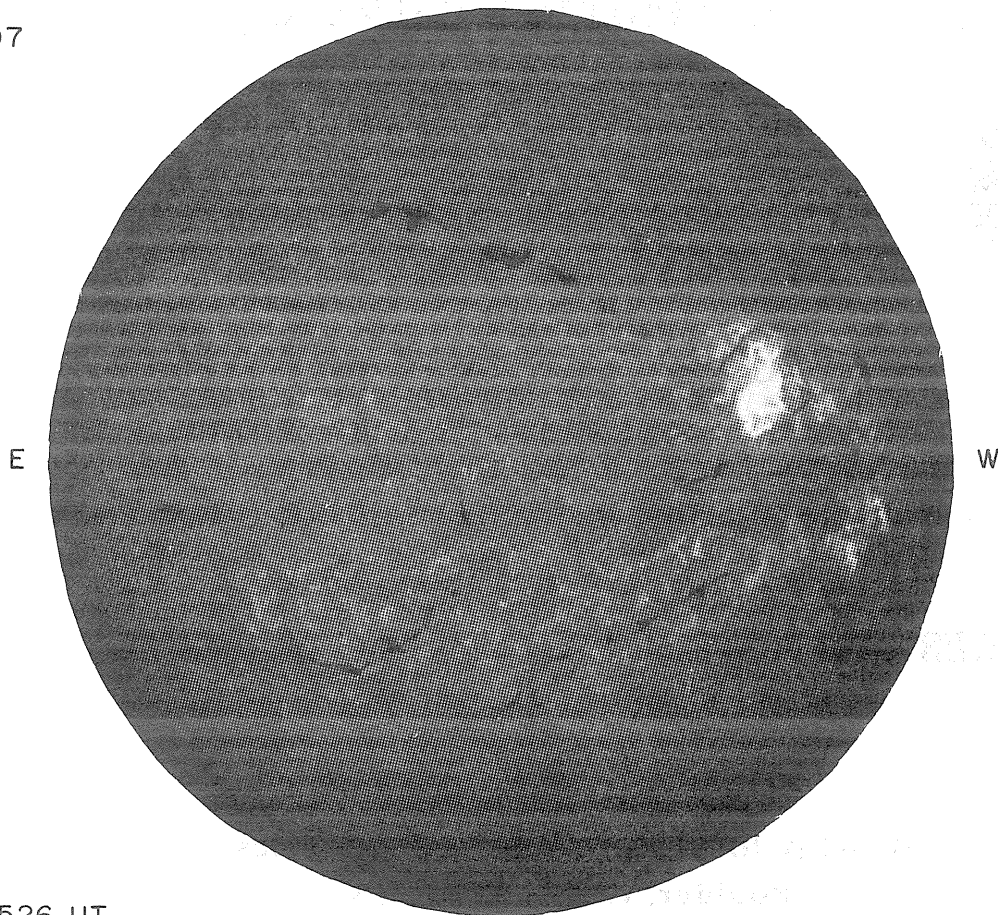
* PRICE THIS ISSUE \$1.50

BOULDER

Np

H α

07



E

W

1526 UT

Sp

FLARE OF 07 AUGUST 1972

SUMMARY TABLE OF CONTENTS

PART I

FOREWORD

1. SUMMARIES OF AUGUST 1972 EVENTS
2. SOLAR OPTICAL DATA
3. SOLAR RADIO DATA

PART II

4. SPACE OBSERVATIONS
5. COSMIC RAYS
6. IONOSPHERE

PART III

6. IONOSPHERE (continued)
7. GEOMAGNETISM
8. AERONOMY AND MISCELLANEOUS

APPENDIX I: Miscellaneous Data and Information from WDC-A

APPENDIX II: Other References

APPENDIX III: Explanation of Solar Radio Chart and Table

ALPHABETICAL INDEX

AUTHOR INDEX

TABLE OF CONTENTS FOR PART II

	<u>Page</u>
4. SPACE OBSERVATIONS	287
"Kilometric Wave Observations of the Great Type III Burst of August 7, 1972" (Paul J. Kellogg, James C. Lai and David G. Cartwright)	288
"OSO-7 Observations of Solar X-Ray Bursts from 28 July to 9 August 1972" (Dayton W. Datlowe and Laurence E. Peterson)	291
"Solar X-Ray Emission Measured by SOLRADS 9 and 10 during the Period July 26 - August 14, 1972" (K. P. Dere, D. M. Horan and R. W. Kreplin)	298
"Solar Flares Observed by the Hard X-Ray Spectrometer on Board the ESRO TD-1A Satellite" (H. F. van Beek, P. Hoyng and G. A. Stevens)	319
"Gamma Ray Observations from OSO-7 (26 July to 14 August 1972)" (E. Chupp, D. Forrest, C. Reppin, A. Suri and C. Tsai)	325
"Particle Observations of the August 1972 Solar Events by Explorers 41 and 43" (J. W. Kohl, C. O. Bostrom and D. J. Williams)	330
"Low Energy Electron and Proton Observations July 19 - August 14, 1972" (R. P. Lin and K. A. Anderson)	334
"Low Energy Interplanetary Particles during the August 1972 Events" (L. J. Lanzerotti and C. G. MacLennan)	338
"MeV Electrons, Protons and Alpha Particles, August 2-13, 1972" (V. Domingo, D. Köhn, D. E. Page, B. G. Taylor and K-P. Wenzel)	342
"Proton and Alpha Particle Fluxes Observed Aboard OV5-6 in August 1972" (G. K. Yates, L. Katz, B. Sellers and F. A. Hanser)	348
"Energy Dependent Composition of Solar Flare Particles on 4 August 1972" (P. B. Price, J. D. Sullivan and H. J. Crawford)	354
"Lunar Surface Observations of the August, 1972 Solar Flare Activity" (Patricia R. Moore, David L. Reasoner, William J. Burke, and Frederick J. Rich)	356
"Penetrating Solar Flare Particle and Solar Wind Observations in the Lunar Night, August, 1972" (René A. Medrano, John W. Freeman, Jr., H. Kent Hills and Richard R. Vondrak)	361
"Radio Scintillation Measurements of the Solar Wind following the Flares of August 1972" (J. W. Armstrong, W. A. Coles, J. K. Harmon, S. Maagoe, B. J. Rickett and D. G. Sime)	371
"The Distribution of Small-Scale Irregularities in the Solar Plasma during July 26 - August 14, 1972" (Z. Houminer)	375
"The August 1972 Events; Pioneer 9 Plasma Wave Observations" (Frederick L. Scarf)	378
"Solar Wind Density Variations Observed on a Long Path during August 1972" (Thomas A. Croft)	381
"VLF Emissions and Whistlers Observed in Japan for the August 1972 Events" (Tadanori Ondoh and Yoshihito Tanaka)	389
5. COSMIC RAYS	393
"Asymptotic Directions for Selected High Latitude Stations Appropriate for the August 1972 Ground Level Cosmic-Ray Events" (M. A. Shea and D. F. Smart)	394
"Observations Relevant to the August 1972 Storm" (P. J. Tanskanen, H. Kananen and K. A. Blomster)	415
"The Unprecedented Cosmic Ray Disturbances of Early August 1972" (J. C. Dutt, J. E. Humble and T. Thambyahpillai)	423
"Remarkable Cosmic Ray Storm and Associated Relativistic Solar Particle Events of August 1972" (M. A. Pomerantz and S. P. Duggal)	430
"The Rigidity Dependence of Cosmic-Ray Variations during the August, 1972 Solar Events" (P. H. Stoker)	441
"Three Dimensional Analysis of Cosmic Rays during Forbush Decreases of August 1972" (S. Yoshida and N. Ogita)	445

TABLE OF CONTENTS FOR PART II (continued)

	<u>Page</u>
"The August 1972 Cosmic Ray Storm at High Rigidities" (Derek B. Swinson)	448
"Energy-Dependent Phenomena of Muons and Nucleons in August 1972" (Robert L. Chasson)	450
"The Event of August 1972 Studied with Cosmic Rays at Magnetic Cut-off Rigidity of 8.72 GV" (A. Apostolakis, H. Mavromichalaki and X. Moussas)	454
"A Comparison of Recordings of the Forbush Effect of the 4th August 1972 by Several Terrestrial Cosmic Ray Monitors" (V. J. Kisselbach)	458
"Solar Cosmic Ray Flares of August 4 to 9, 1972 as Measured in the Stratosphere" (G. A. Bazilevskaya, Yu. I. Stozhkov, A. N. Charakhchyan and T. N. Charakhchyan)	460
"Cosmic Ray Variations on August 1-14, 1972 from Data of Neutron Supermonitors in Siberia and Far East" (N. P. Chirkov, A. M. Novikov, I. S. Samsonov, A. A. Upolnikov, A. A. Luzov, A. V. Sergeev, Yu. A. Kurchenko, V. N. Nikolayev, V. L. Yanchukovsky and G. G. Todikov)	465
"Data of the Events of August 1972 from the Cosmic Ray Installation Complex in Yakutsk" (V. A. Filippov, A. I. Kuzmin, A. N. Prikhodko, I. S. Samsonov, G. V. Skripin, G. V. Shafer and A. A. Upolnikov)	469
"Mexico City Cosmic Ray Observations during the Large Solar Events of August 1972" (Oscar Troncoso Lozada)	475
"Cosmic Ray Hourly Intensities during August 1 - 10, 1972" (Y. Miyazaki, S. Kawasaki, M. Kodama, K. Murakami, M. Wada, L. S. Chuang and Y. Nakano)	476
"Multi-directional Meson Intensities at Mt. Norikura and Nagoya, August 1972" (Y. Sekido, K. Nagashima, I. Kondo, H. Ueno, K. Fujimoto and Z. Fujii)	479
"Cosmic Ray Neutron Intensity during the Interval July 26 - August 14, 1972 at Morioka, Japan) (Hachiro Takahashi and Toshimi Chiba)	484
"Unusual Cosmic Ray Intensity Variations in August 1972" (U. R. Rao)	486
"Forbush Decrease of August 4, 1972" (H. Razdan and M. M. Bemaikhedkar)	487
 6. IONOSPHERE	 489
"Overview of Solar Events and Related Auroral-Zone Geophysical Observations during the August 1972 Storm" (Robert D. Hunsucker)	490
"Electron Density Variations at Chatanika, Alaska, during the Storm of August 4-9, 1972" (B. J. Watkins, H. F. Bates, A. E. Belon and R. D. Hunsucker)	492
"Millstone Hill Incoherent Scatter Observations" (J. V. Evans)	497
"Data of the Radar Echoes from Electrojet Irregularities" (C. L. Jain)	502
"Variations of Noon Electron Density at Wallops Island July 31 - August 11, 1972, and Related Parameters" (T. N. Gautier and L. R. Wescott)	505
"Ionospheric and Geomagnetic Behavior at Mid-Latitudes during the Solar Events of August 1972" (Michael Mendillo, John A. Klobuchar and Dae-Hyun Chung)	508
"Total Electron Content of the Ionosphere over Lindau/Harz by Dispersive Doppler Effect, July 26 - August 12, 1972" (G. K. Hartmann, G. Schmidt and A. Tauriainen)	511
"Faraday Rotation Measurements of the Equatorial Ionosphere for the Period July 26 - August 14, 1972" (D. Yeboah-Amankwah and J. R. Koster)	525
"Ionospheric Electron Content Data 2-8 August 1972 Observed at the NASA- Goddard Space Flight Center, Greenbelt, Maryland" (S. Rangaswamy and P. E. Schmid)	526
"Total Electron Content Measurements during July 26 - August 15, 1972" (Elizabeth A. Essex)	529

TABLE OF CONTENTS FOR PART II (continued)

	<u>Page</u>
"Satellite Scintillation Observations at Sagamore Hill, Mass. and Narsarsuaq, Greenland during the Solar Events of August 3 - 10, 1972" (Jules Aarons and Eileen Martin)	532
"Australian Ionospheric Observations during the Magnetic Storm of August 1972" (D. G. Cole, L. F. McNamara and F. E. Cook)	536
"Ionospheric and Geomagnetic Effects of the Solar-Activity Event in August 1972" (R. A. Zevakina, E. E. Goncharova and L. A. Yudovitch)	549
"Ionospheric Behavior during August 2-11, 1972 Derived from Data of the Ionosphere Vertical Sounding over Khabarovsk" (E. G. Mirmovich)	557
"Ionospheric Report for July 24 - August 14, 1972 for Slough, South Uist and Port Stanley Observatories" (R. W. Smith)	561
"Manila Ionospheric Soundings in the Interval July 26 - August 14, 1972" (J. J. Hennessey, S. J. and Florencio Rafael, Jr.)	562
"HF Doppler Observations at Boulder, Colorado, August 1-12, 1972" (G. M. Lerfald and R. B. Jurgens)	566
"HF Doppler Observations Associated with Magnetic Storm of August 4 to 6, 1972" (T. Ichinose and T. Ogawa)	571
"SID Effects during July/August Event 1972" (R. Knuth and K.-H. Ohle)	574
"Shortwave Fadeouts and Ionospheric Absorption Measured at Lindau (N52.6; E8.7) in the Period 15 July to 15 August 1972" (H. Schwentek)	579
"Sudden Phase Anomalies Observed at Uji" (Y. Naito, S. Kato and T. Araki)	584

4. SPACE OBSERVATIONS

Summary on page 4.

For basic data and indices for this section and others, see Appendix I for Table of Contents to Report UAG-21.

For data papers presented or published elsewhere which contain additional information on space observations and the other categories included in this report, see Appendix II.

KILOMETRIC WAVE OBSERVATIONS OF THE
GREAT TYPE III BURST OF AUGUST 7, 1972

By
Paul J. Kellogg, James C. Lai and David G. Cartwright
University of Minnesota
Minneapolis, Minnesota

With our experiment on the satellite IMP-6 we have observed radio emission of Type III from the large solar eruption on August 7. Our experiment is a plasma wave receiver which is connected to six antennas, three orthogonal electric dipoles and three single turn magnetic loops. The receiver tunes to 64 different frequencies, logarithmically spaced between 200 kHz and 23 Hz, i.e., with a frequency difference of about 15% between adjacent channels. The bandwidth of each channel is also of the order of 15% so that we have essentially continuous coverage. The Type III burst of August 7th was observed in all electric field channels down to about 10 kc.

Figure 1 shows an overall view of the observations. For clarity we have plotted two of our channels on each graph and we have only plotted the first part of the event. The numbers along the top part of the graph indicate the range of IMP-6 from the earth in kms, the numbers along the bottom part of the graph give the time in universal time. Each plot is marked with the frequency (i.e. 177 K means 177 kHz). The signal plotted is the sum of the squares of the signal in the X antenna and the Y antenna. It shows some spin modulation because of gain differences in the receivers attached to each of the antennas and because the X antennas are only 170 feet tip to tip while the Y antennas are 300 feet tip to tip. In the lower lefthand corner of the graph are marks indicating 20 dB intervals and the signal plotted is very roughly in units of dB above a threshold of approximately 10 v per channel at the receiver input.

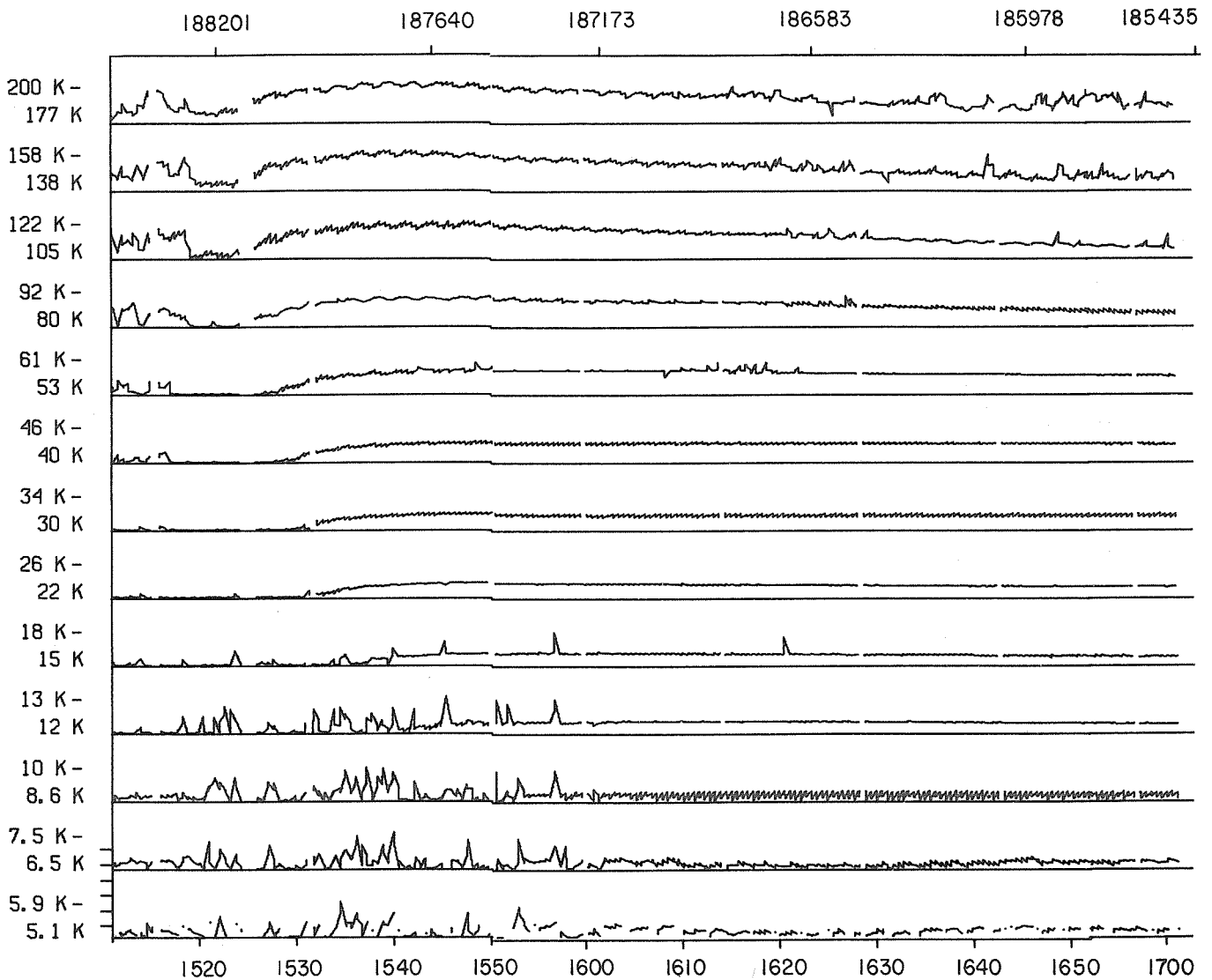
This is by far the most intense Type III burst which we have observed in the two years of observations with IMP-6. The peak intensity is plotted as a function of frequency in Figure 2. The experiment was operating in a mode which is very insensitive to the magnetic component of the electromagnetic waves and we were not able to measure B, so the intensity has been calculated from the electric vector assuming an index of refraction of 1. An arrow on one of the points shows the correction to the intensity which would result if the index of refraction is calculated from

$$n^2 = 1 - \frac{f_p^2}{f^2}$$

assuming a plasma frequency f_p of 10 kc. The correction is obviously small for most of the points.

In Figure 3 we present a plot of the onset time of the observations as a function of frequency. The onset time in the highest frequency channels is somewhat masked by emission from the earth, (the irregular noise before the beginning of the burst). Then unfortunately the experiment went into a calibrate cycle which masks the onset of time at a few more frequencies; however, there are still quite a few points on the exponentially rising part of the burst and we have made extrapolations of the observations to recover the missing onset times. For Type III bursts, the onset time as a function of inverse frequency is often approximately a straight line. If we take the simple model that (1) the electron density of the solar corona is proportional to $1/R^2$ and (2) that the radiation we are seeing is all second harmonic (or all first harmonic) of the plasma frequency, and (3) the velocity of the source is constant, then the plot of (frequency)⁻¹ vs. onset time is approximately linear (neglecting light travel time). Here the plot is not linear so that at least one of the above assumptions is not valid. At the present time we believe that we are seeing a mixture of first harmonic radiation early in the event and second harmonic later, and that the corona is not spherical, but we need more analysis before these conclusions are firm.

The signal is observed in all channels down to 10 kHz. It may possibly be present below but the data are confused by local noise in the plasma. This is lower by a factor of 2 than the lowest frequency which we have observed in any other Type III burst. Presumably, however, this is not a property of the



1972 DAY 220

Fig. 1.

Type III burst but of the adjacent plasma and indicates merely that the plasma frequency has dropped below 10 kHz or that the plasma density has dropped below about 1 particle/cm³. Our identification of the plasma frequency as being 10 kHz is strengthened by the noise burst at about 1522. Noise bursts of this nature are quite commonly observed in the solar wind and are generally centered at 20 kHz which we interpret as being the plasma frequency. The fact that this one is centered at about 10 kHz confirms our suspicion that the interplanetary plasma density is at an unusually low value.

We have not shown the end of the event in order to use an expanded scale for the more interesting onset; however, the event was still present in the 20 kHz channel at 2140. After that time, all channels are masked by plasma noise.

We have also seen the great Type III burst of August 4, but the experiment was in a mode which makes data analysis more difficult, even impossible during part of the event, and we have done little with it.

This work was supported by the National Aeronautics and Space Administration under Contract No. NAS 5-11060. One of us (P.J.Kellogg) is grateful for support from the James-Minna-Heineman Foundation and the Scientific Affairs Division of NATO.

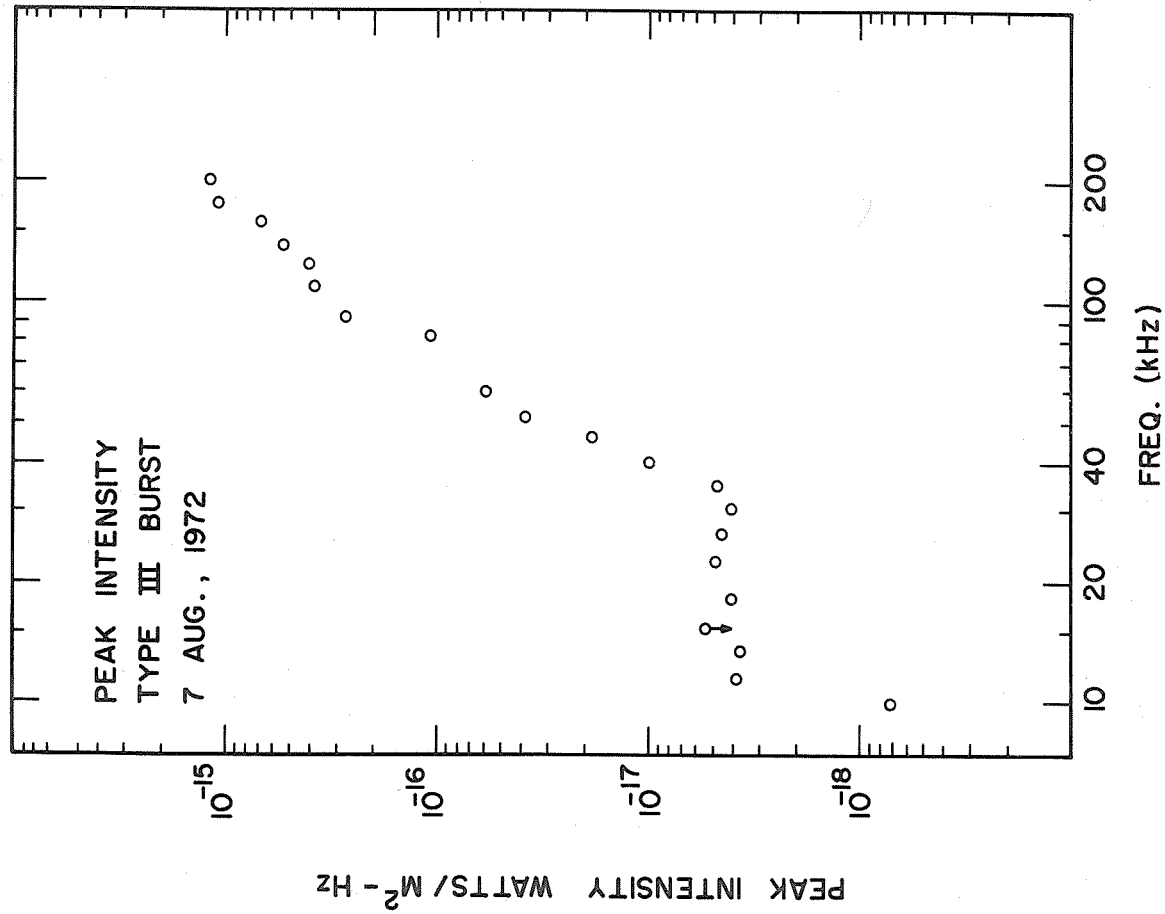


Figure 2

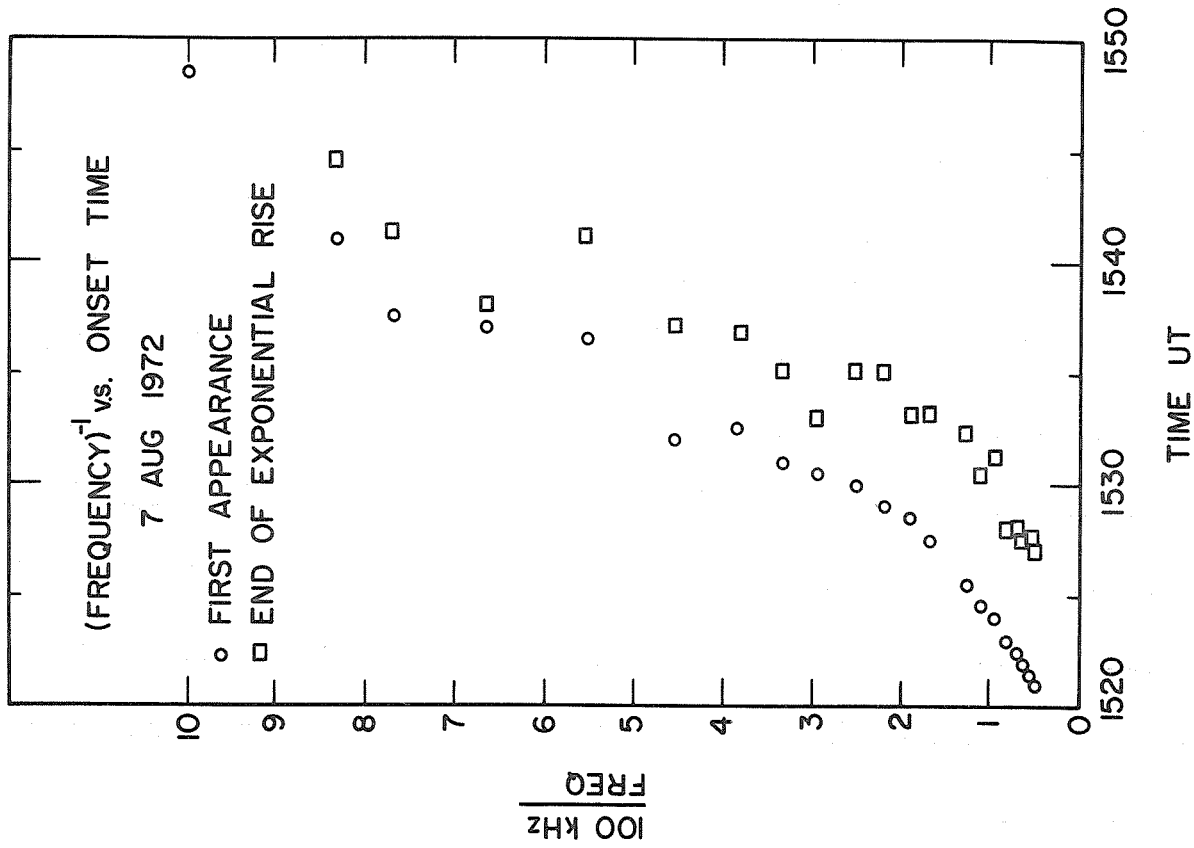


Figure 3

OSO-7 Observations of Solar X-Ray Bursts From 28 July to 9 August 1972

by

Dayton W. Datlowe and Laurence E. Peterson
University of California, San Diego
LaJolla, California 92037

Solar X-ray bursts contain emission of two general types. In the range below 10 keV the emission is believed to come from a hot plasma on the sun with a temperature of the order of 10^7 [Culhane & Phillips, 1970]; the spectrum in the range 3-10 keV is an exponential and the slope is interpreted as $1/kT$. This emission tends to evolve slowly, with significant changes taking place in time scales on the order of minutes. Emission above 10 keV is dominated by bremsstrahlung from non-thermal electrons colliding with the solar atmosphere [Brown, 1972]. The spectrum of the X-rays can be fitted to a power law, and from this information the spectrum of the non-thermal electrons at the sun can be inferred. This emission is frequently impulsive, with large changes taking place on time scales on the order of seconds [Kane & Anderson, 1970; Frost, 1969]. Non-thermal X-ray emission is not seen in all bursts; for bursts with a thermal flux of greater than 10^3 photons/cm²-sec-keV there is approximately a 50% chance of detecting non-thermal X-ray above a threshold of .1 photon/cm²-sec-keV between 20 and 30 keV [Datlowe *et al.*, 1973].

Early August 1972 was an especially interesting time to be observing solar X-ray bursts. In addition to a relatively high frequency of bursts, two of the largest bursts detected by the OSO-7 Solar X-ray Instrument since its launch in September 1971 occurred on 4 and 7 August. Also, between 28 July and 9 August, essentially 100% of the bursts detected by the OSO-7 instrument showed significant non-thermal flux. In what follows, we will present our observations of the major bursts on August 2, 4 and 7, discuss the August 2 event, and present a table of the 23 events observed during the period of observation.

The Instrument

The University of California at San Diego, Solar X-ray Instrument on OSO-7 [Harrington *et al.*, 1972] has two X-ray detectors, one to observe the thermal X-ray region from 3-14 keV and one to observe the non-thermal X-ray region from 10 to 300 keV. The detector of thermal X-rays is a proportional counter with a Xe/CO₂ fill and with a 115 mg/cm² Beryllium window. The aperture of .32 cm² is determined by a passive aluminum collimator. The detector for the 10-300 keV region is a sodium iodide (NaI(Tl)) scintillator with a 41 mg/cm² Aluminum window. The detector has an area of 9.57 cm² and is collimated by an active anti-coincidence shield. Events from the detectors are sorted by pulse height analysis, with proportional counter having 8 channels and the scintillator having 9 channels. We show plots of X-ray flux versus time. These are obtained by plotting channel 4 of the proportional counter (5.1-6.6 keV) and channel 3 of the scintillator (20-30 keV). The counting rates have been converted to flux by numerical factors determined by computing the response of the detector systems to sample spectra. The dynamic range of the detectors from background to saturation is as follows:

<u>Detector</u>	<u>Energy</u>	<u>Background</u>	<u>Saturation</u>
Prop. counter	5 keV	100 c/cm ² -sec-keV	3×10^4 c/cm ² -sec-keV
Scintillator	20	.05	300

Above saturation the counting rates continue to increase, but the flux value is uncertain.

Out of each satellite orbit, two thirds is spent during spacecraft day and the remainder is spent during spacecraft night. Since the orbital period is approximately 90 minutes, long term plots of the data will show 60 minute stretches of data separated by 30 minute gaps. Contamination of the data by charged particles trapped in the geomagnetic field is detected by three solid state detectors on board the instrument, and any such data is discarded. During the early August period losses due to charged particle contamination were small.

The Major Events

The solar X-ray flux from 1800 UT on August 2 to 0230 UT August 3 is plotted in Figure 1. The upper trace shows the thermal X-rays from 5.1-6.6 keV and the lower trace shows the non-thermal X-rays from 20-30 keV, with the same vertical axis applicable to both traces. Each data point represents an average over 61.44 seconds. The dotted line at the top shows the approximate saturation level of the proportional counter.

The first of the three events shown began at 1839 UT and lasted until 1851 UT. The maximum flux in the 20-30 keV X-rays was 108 which occurred at 1840:02 UT and the maximum of the 5.1-6.6 keV X-rays was 5×10^4 which occurred at 1842:05 UT. The accuracy of the timing is 5 seconds. The event is associated with the 1B flare in McMath region 11976 which began at 1839 UT [Lincoln *et al.*, 1972].

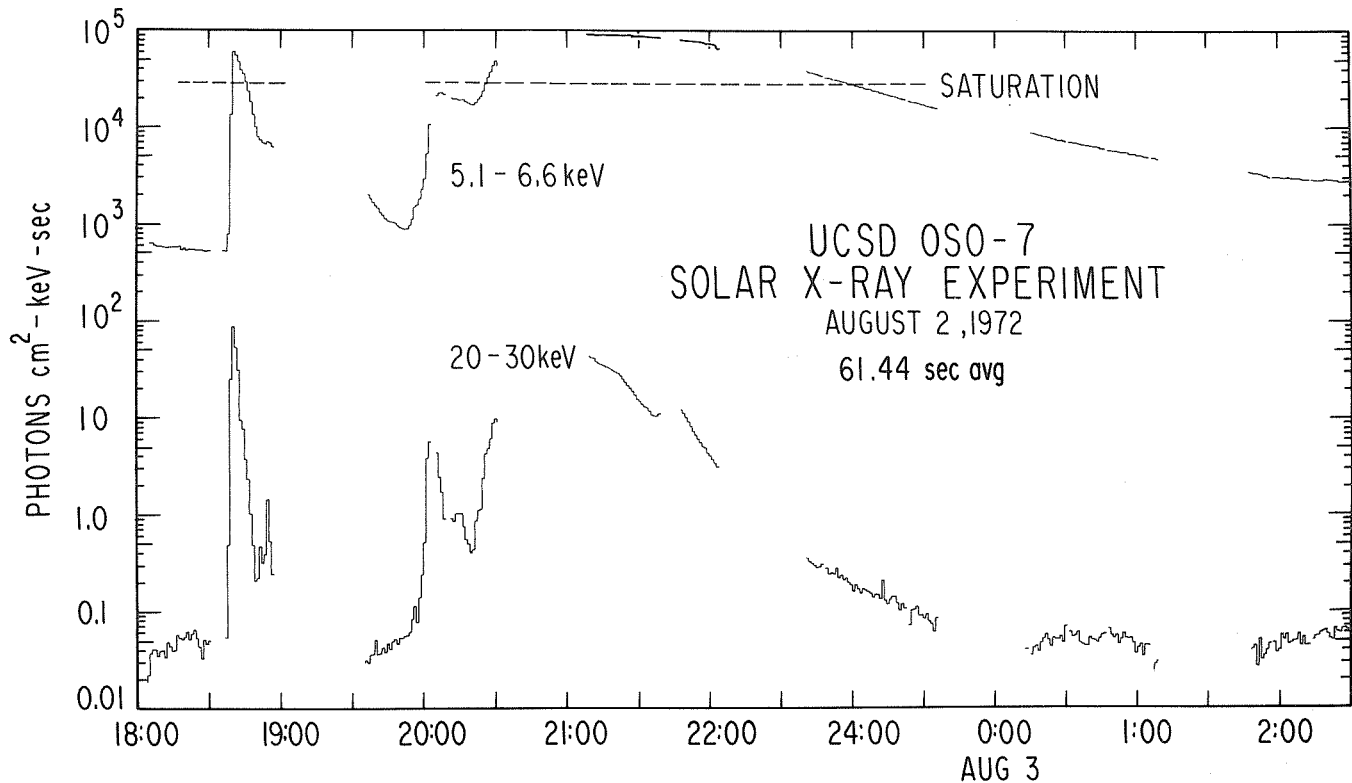


Fig. 1. Solar X-ray flux is presented covering the energy ranges 5.1-6.6 keV and 20-30 keV for the period 1800 UT August 2 to 0230 UT August 3, 1972.

Two more bursts occurred at 1956 and 2021 UT, respectively. For the first event the peak flux in the 20-30 keV channel was 6.8 photons/cm²-sec-keV and the peak flux in the 5.1-6.6 keV channel was 23,000. The peak of the second burst occurred during spacecraft night. These events were associated with flares of classification 2B and 1B, respectively, in plage region 11976.

The X-ray burst associated with the 3B flare on August 4 is shown in Figure 2. The peak flux for a ten second interval occurred at 0628 UT just prior to spacecraft night: the value of the peak flux is comparable to 10³ photons/cm²-sec-keV but the exact value is uncertain since the scintillation counter was saturated. The peak of the thermal X-ray flux occurred during spacecraft night.

Figure 3 shows the X-ray fluxes associated with the 3 B flare on August 7. This graph is different from the preceding two in that each point represents 10.24 seconds of data rather than 61.44 seconds. The flare, which began at about 1505 UT, was in progress at spacecraft dawn, which occurred at 1536 UT. The maximum of both the thermal and non-thermal fluxes occurred during spacecraft night. Excess thermal emission from this burst was still detectable at 0800 UT on the next day.

The Flare of August 2, 1972 at 1839 UT

As an example of the kind of analysis which can be carried out with the Solar X-ray data, we present more details of the event of August 2 at 1839 UT. Figure 4 is a spectrum of the X-rays above 10 keV observed in the ten second interval starting at 1839:5₂ UT just prior to the peak of the non-thermal X-ray event. The vertical axis is flux in photons/cm²-sec-keV and the horizontal axis is photon energy, in a log-log scale. The data points are rates which have been divided by a numerical factor to convert to flux. The solid line shows the power law $AE^{-\gamma}$ which, when folded through the detector response including gain, efficiency, and resolution, gives the best fit to the scintillation counter rates. The computations are carried out on a computer. It will be seen that a good fit to a power law is obtained over the range 13-140 keV with an exponent $\gamma = 3.7$.

Once the spectrum of the X-rays can be expressed in the form of a power law, the spectrum of the electrons at the sun which generated these X-rays and the energy dissipated by the electrons in collisions can be computed, using the formulae of Brown [1972]. In these computations it is assumed that the electrons lose all of their energy in collisions and stop in the solar atmosphere. The computation can also be carried through for the case in which the electrons escape from the X-ray emitting region before losing a significant amount of their energy in collisions; however, Zirin and Tanaka [1973] have presented good evidence that the former case is applicable to this particular event.

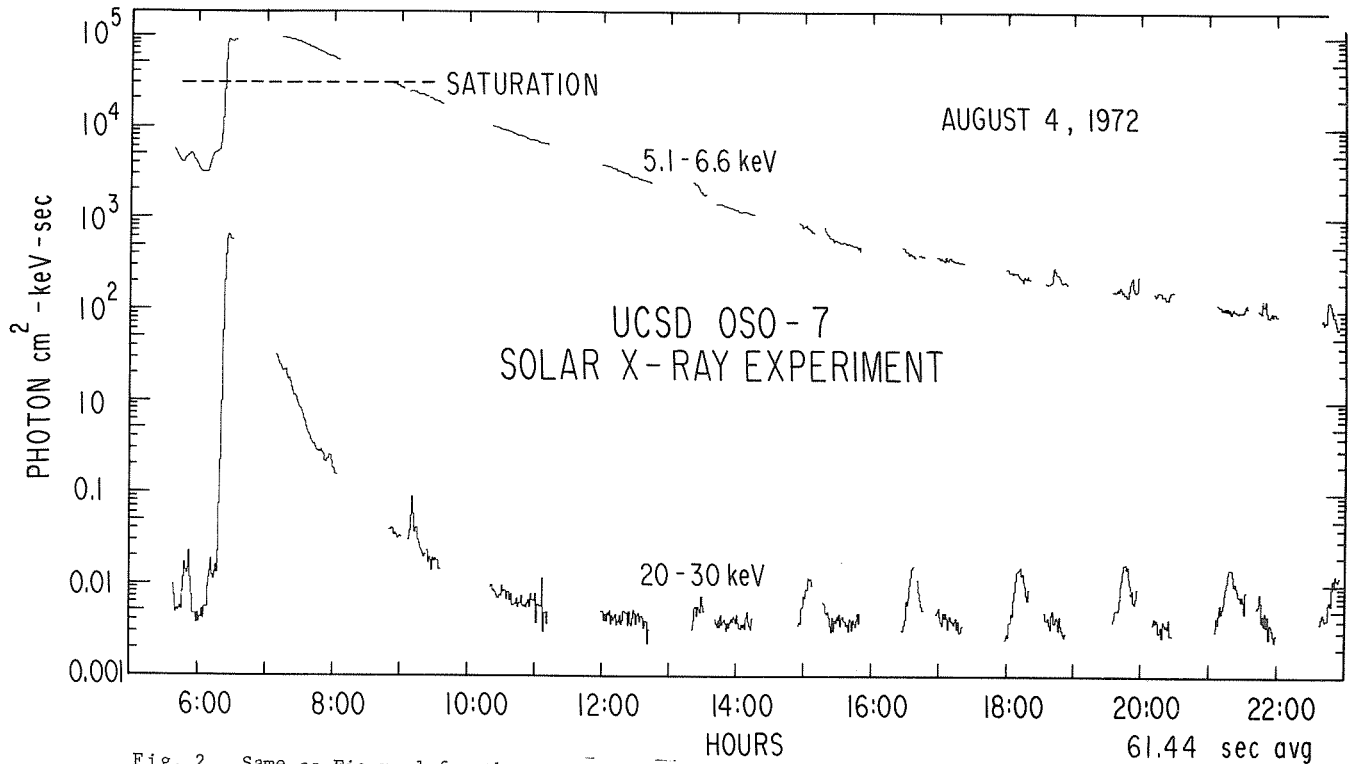


Fig. 2. Same as Figure 1 for the period 0600-2200 UT August 4, 1972

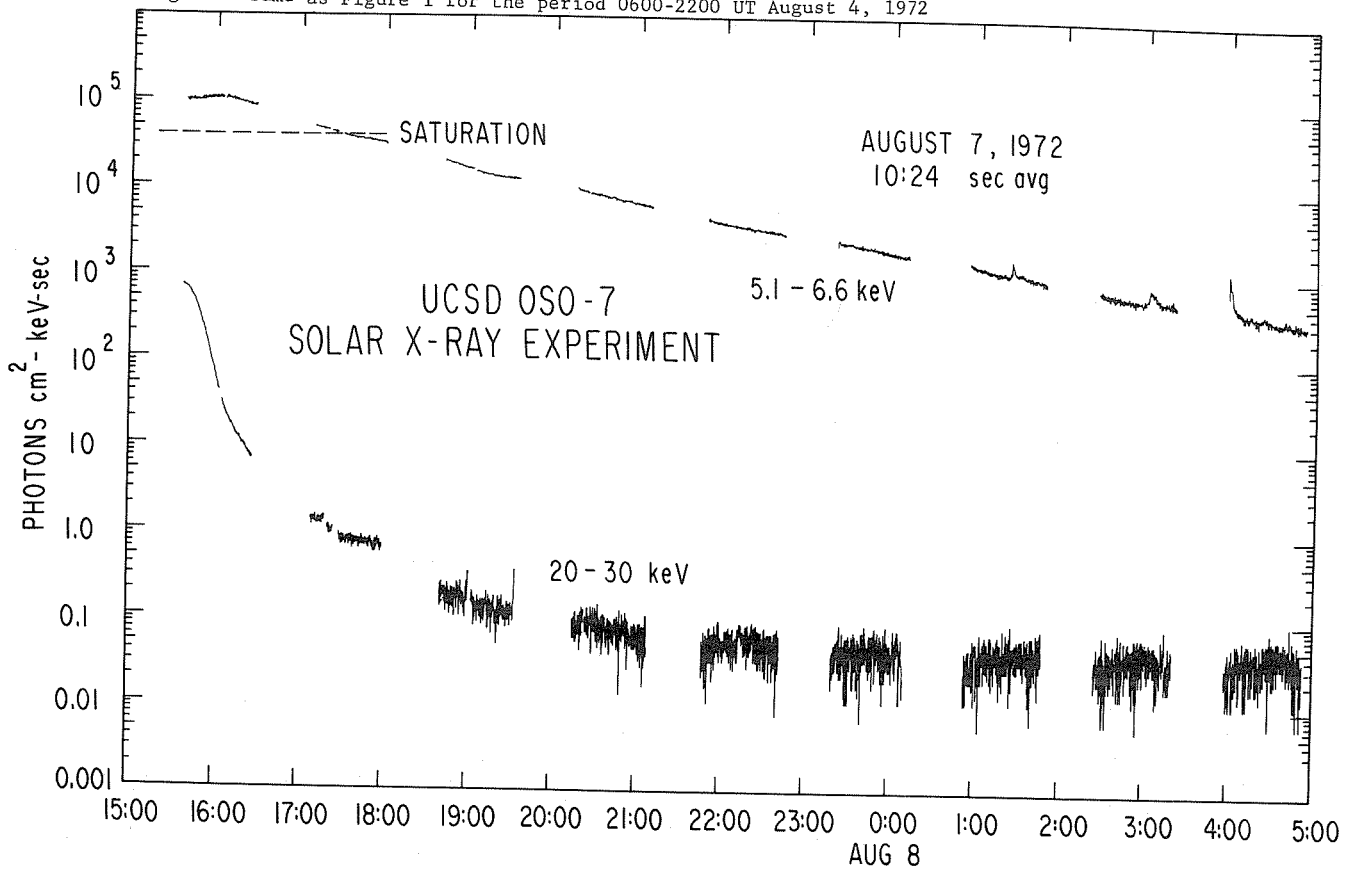


Fig. 3. Same as Figure 2, except for the shorter time span for each data point, covering the period 1500 UT August 7 to 0500 UT August 8, 1972.

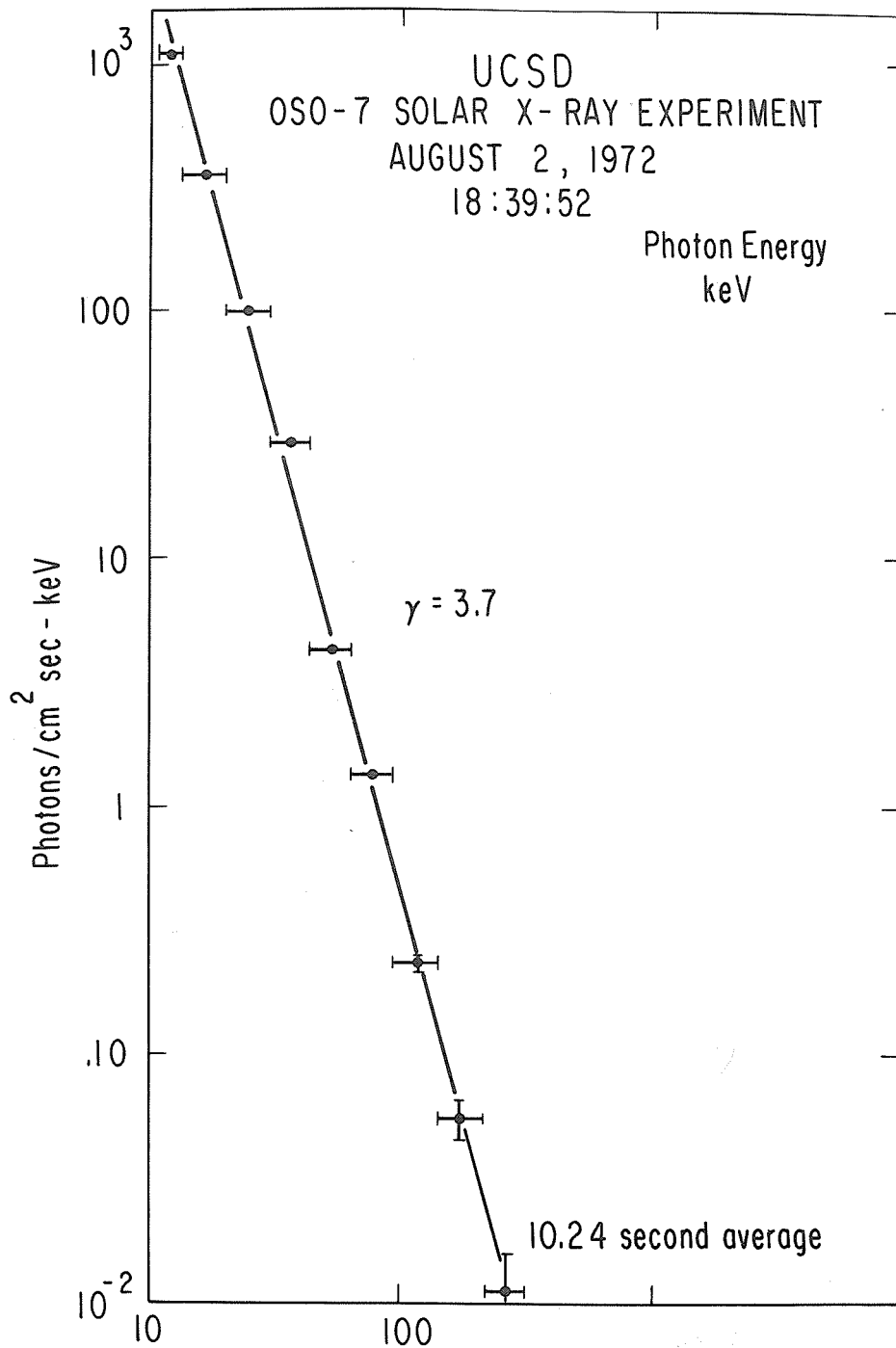


Fig. 4. Spectrum of X-rays above 10 keV observed at 1839:52 UT August 2, 1972, plotted on a log-log scale.

10.24 second spectra for this event have been computed from 1838:20 to 1840:53 UT and one minute average spectra have been computed out to 1848:23 UT. For each spectrum the power dissipated by electrons above 10 keV and 40 keV in collisions has been computed. The results are shown in Figure 5. At the bottom the spectral exponent γ is plotted. The slope of the spectrum is nearly constant at 3.6 from the start of the burst until 1840:23 UT; thereafter the slope of the spectrum increases slowly until the end of the burst, reaching $\gamma=7$. The upper two traces show the power in ergs/second dissipated by collisions. The closed circles represent electrons above 10 keV, and the open circles represent electrons above 40 keV. The latter data points have been multiplied by 100 to compress the plot. It will be seen that the power dissipated by electrons above 40 keV peaks earlier than the power dissipated by electrons above 10 keV.

Catalog of Events

Table 1 is a catalog of the solar X-ray bursts detected by the OSO-7 solar X-ray experiment from

28 July to 9 August. Only events with a peak flux in the 5.1-6.6 keV channel greater than 10^3 photons/cm²-sec-keV are included. The onset of an event is readily determined to an accuracy of one minute: however, in one case the event occurred during spacecraft night and the time of the onset of the optical flare is inserted in parentheses. For short events the end time is readily determined to an accuracy of one to two minutes if the end time occurred during spacecraft day. Four of the events (10, 14, 15, and 20) exhibited long slow decays in the 5.1-6.6 keV X-rays. The time listed is, to the nearest hour, when the X-ray flux declined to below 10^2 photons/cm²-sec-keV at 5 keV.

The right four columns give the time of the maximum flux and the value of the maximum flux for the 5.1-6.6 keV and 20-30 keV channels. The time quoted is the beginning of the 10.24 second interval during which the sample was accumulated: in some cases a plot of 1 minute averages of the flux shows a value which is noticeably lower than this peak 10.24 second sample. Fluxes greater than 3×10^4 in the 5.1-6.6 keV channel and 300 in the 20-30 keV channel indicate that the respective detectors are operating outside the normal dynamic range and the quoted fluxes should be understood as lower limits.

Additional X-ray data from these solar events and plots covering the entire time span from 28 July to 9 August are available. Inquiries should be sent to:

Prof. Laurence E. Peterson
Department of Physics
University of California, San Diego
La Jolla, Calif. 92037, U.S.A.
Telephone (714) 453-2000, Ext. 2186

REFERENCES

- | | | |
|--|------|--|
| CULHANE, J. L. and
K. J. H. PHILLIPS | 1969 | Solar X-ray Bursts at Energies less than 10 keV Observed with OSO-4, <u>Solar Phys.</u> , <u>11</u> , 117. |
| DATLOWE, D. W.,
H. S. HUDSON and
L. E. PETERSON | 1973 | OSO-7 Observations of Solar X-ray Bursts in the Energy Range 5-15 keV. (to be published). |
| FROST, K. | 1969 | Rapid Fine Structure in a Burst of Hard Solar X-rays Observed by OSO-5, <u>Ap. J.</u> , <u>158</u> , 1159. |
| HARRINGTON, T. M.,
J. O. MALOY,
D. L. MCKENZIE and
L. E. PETERSON | 1972 | Design of the Solar X-ray Instrument for OSO-H, <u>IEEE Trans on Nuc. Sci.</u> <u>NS-19</u> , 506. |
| KANE, S. R. and
K. A. ANDERSON | 1970 | Spectral Characteristics of Impulsive Solar Flare X-rays >10 keV, <u>The Astrophysical Journal</u> , <u>162</u> , 1003. |
| LINCOLN, J. V. and
H. I. LEIGHTON | 1972 | Preliminary Compilation of Data for Retrospective World Interval July 26 - August 14, 1972, <u>World Data Center A for Solar-Terrestrial Physics</u> , Report <u>UAG-21</u> , November 1972. |
| ZIRIN, H., and
K. TANAKA | 1973 | The Flares of August 1972, to be published (see abstract elsewhere in this compilation). |

TABLE 1

Solar X-ray Bursts Observed by the UCSD Solar X-ray Instrument on OSO-7

Date	Onset	End	Time	Maximum Flux*		20-30 keV
				5.1-6.6	Time	
1 28 July	13:14	--	13:26:32	25000	13:24:18	1.2
2 30 July	16:04	16:10	16:06:13	6000	16:05:42	1.9
3 31 July	1:19	1:38	1:21:40	4700	1:20:40	2.7
4	4:25	--	4:28:22	5600	4:26:29	0.7
5	6:24	6:35	6:26:28	3500	6:25:47	0.6
6	15:00	15:10	15:08:19	1700	15:07:38	1.2
7 1 Aug.	6:54	--	7:02:58	30000	6:59:23	5.2
8	14:52	--	14:58:14	3500	14:57:33	1.3
9 2 Aug.	1:40	--	1:42:27	--	1:40:14	1.5
10	3:08	16:00	> 3:30	--	3:30	> 90.0
11	10:45	11:00	10:46:19	23000	10:45:17	6.2
12	18:39	18:51	18:42:05	> 50000	18:40:02	109.0
13	19:56	16:00**	20:07:05	23000	20:01:47	6.8
14 3 Aug	22:04	--	20:16:14	4000	20:14:01	0.5
15 4 Aug	6:18	15:00	--	--	6:28	> 1000.0
16	23:21	23:28	6:26:21	1650	6:24:39	1.4
17 5 Aug.	21:10	--	21:12:21	2000	21:10:18	0.3
18 6 Aug.	4:19	4.27	4:19:51	5700	4:19:30	0.8
19 7 Aug.	3:33	~ 4:12	3:58	> 60000	4:57:58	20.0
20	(15:05)	8:00**	15:36***	> 10 ⁵	15:36	190.0
21 8 Aug.	21:22	21:50	21:32:04	> 34000	21:29:10	4.2
22 9 Aug.	16:12	16:25	16:14:58	20000	16:14:17	7.0
23	22:13	22:35	22:19:19	4500	22:18:27	3.7

*Maximum photons/cm²-sec-keV in the energy ranges 5.1-6.6 and 20-30 keV in a 10.24 second interval.

** End time occurred on the following day

*** Peak occurred during spacecraft night. This is the time of the start of the X-ray observations.

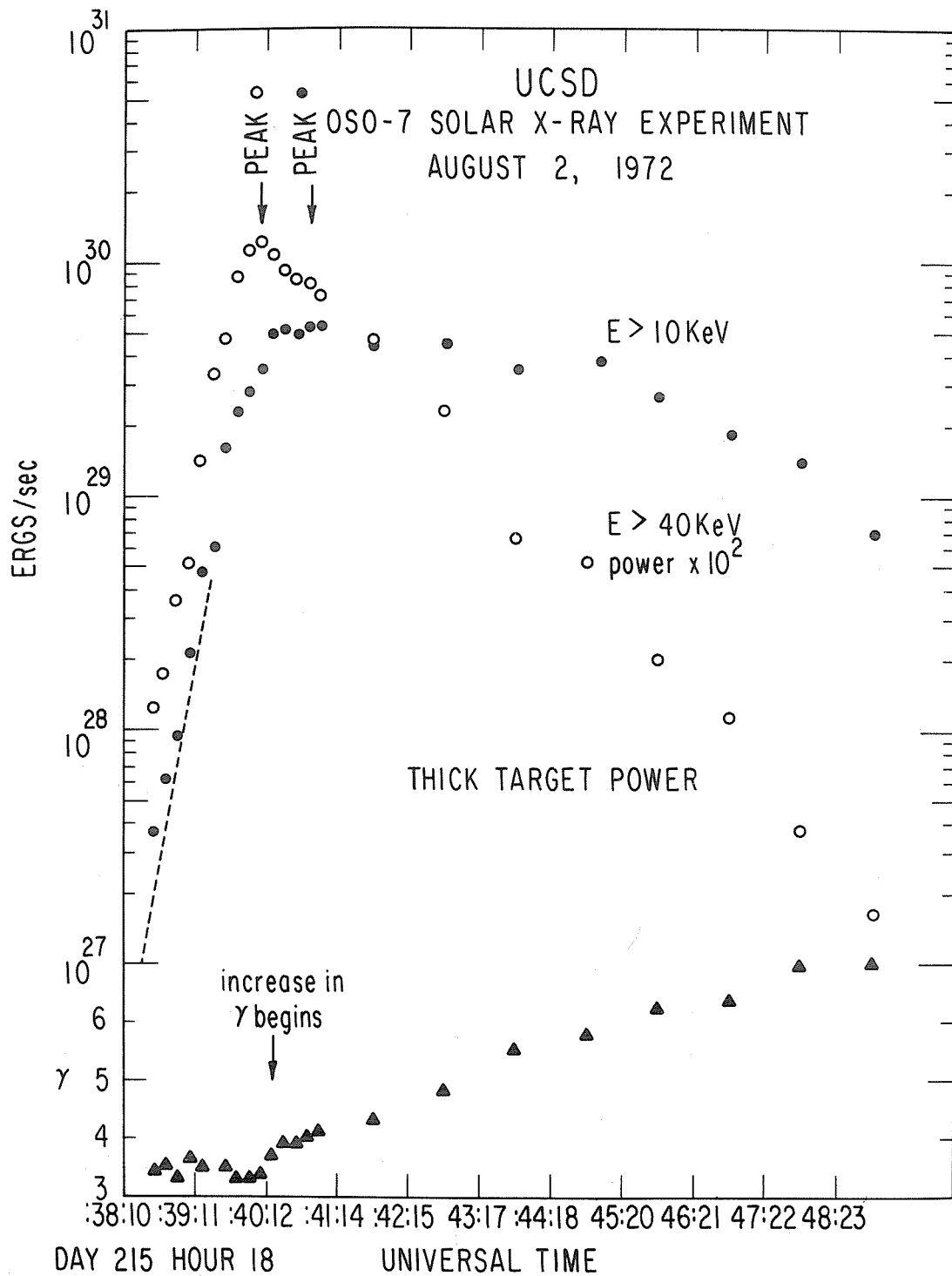


Fig. 5. One minute average electron spectra for $E > 10 \text{ keV}$ and $E > 40 \text{ keV}$ are presented along with the spectral exponent γ for the period 1838:10-1848:23 UT August 2, 1972.

Solar X-ray Emission Measured by SOLRADS 9 and 10
during the Period July 26 - August 14, 1972

by

K. P. Dere, D. M. Horan and R. W. Kreplin
E. O. Hulburt Center for Space Research
Naval Research Laboratory
Washington, D. C. 20375

During the period July 26 through August 14, 1972, the Naval Research Laboratory's SOLRAD 9 and SOLRAD 10 satellites were monitoring the soft X-ray emission from the sun. Measurements were made by ionization chambers sensitive in the following bands: 0.5 to 3Å, 1 to 5Å (SOLRAD 10 only), 1 to 8Å and 8 to 16Å. The currents induced in the detectors by the solar X-rays are converted to solar flux values ($\text{ergs cm}^{-2} \text{sec}^{-1}$) using an assumed graybody solar emission model with an appropriate temperature: 10×10^6 °K for the 0.5 to 3Å detector and 2×10^6 °K for the other detectors. At times, the actual solar flux values can be lower by up to a factor of 4 as shown by computations based on use of thermal bremsstrahlung, radiative recombination and line spectrum. Bragg spectrometer data has shown that the true flare emission spectrum is of this form. A further discussion of this matter can be found in a recent NRL Report [Dere et al., 1973].

The data are presented in two plots for each day, the first showing SOLRAD 9 data and the second showing SOLRAD 10 data. The flux values in $\text{ergs cm}^{-2} \text{sec}^{-1}$ for each experiment are plotted logarithmically on the vertical scale versus the universal time on the horizontal scale. For the SOLRAD 9 plots, starting from the top are the 8-20Å flux values, the 1-8Å flux values, the 0.5-3Å flux values and background values. Often the SOLRAD 9 0.5-3Å flux is below the detector threshold. The SOLRAD 10 plot is similar, with the 1-5Å flux values between the 1-8Å and 0.5-3Å values. The background values are an indication of the amount of interference by charged particles penetrating the detectors such as during passage of the satellite through the Earth's particle belts. The gaps in the data are usually produced by satellite night or passage through intense portions of the particle belts. Usually the 8-20Å detector is relatively unaffected by the particle belts, but when the energy spectrum of the particles is changed as a result of proton flares, the 8-20Å detector will show an increased response to the trapped radiation. Also, large X-ray flares can induce a response in the background detectors and examples of this can be seen in these data. Late on August 10, 1972, SOLRAD 9 developed a data transmission problem that cured itself later in the month. However, it was possible to reduce the data on August 11 although some of the flux values are spurious. During some periods following flares, the SOLRAD 10 1-8Å detector will fail to function resulting in a lack of 1-8Å data during these times. Due to the use of updated mass absorption coefficients, the conversion constant for the SOLRAD 10 8-16Å detector is a factor of 1.43 higher than that for SOLRAD 9. Further information on these two satellites can be obtained from the NRL Reports concerning them [Kreplin and Horan, 1969; Horan and Kreplin, 1972].

Corresponding with the arrival of McMath Region 11976 on the east limb the X-ray background levels showed a moderate rise on July 27 and 28 and continued at this level. However, these levels were not so high that major activity would be expected. There was very little flare activity until a number of moderately sized flares occurred on July 31 and August 1. By the end of August 1, the background levels had risen to values that have been indicative of increased flare activity in the past. Then on August 2 the first two major flares of this period occurred: The first flare began at 0240 UT in the 0.5-3Å band and reached a broad minimum around 0410 UT with a 1-8Å flux of $1.8 \times 10^{-1} \text{ ergs cm}^{-2} \text{sec}^{-1}$. The average flare temperature at the maximum flux was about 20×10^6 °K with an emission measure ($\int N_e^2 dV$) of $2.2 \times 10^{49} \text{ cm}^{-3}$. In general, the temperature of the flare plasma peaks when the flux levels are rising and the emission measure reaches its maximum value somewhat after the time of the peak fluxes and remains fairly constant for the duration of the flare. The X-ray emission from this first flare continued to decay for about 14 hours until 1830 UT when an impulsive flare occurred. The second large flare began with a precursor flare at 1955 UT. The main part of the flare began around 2020 UT and reached a maximum 1-8Å flux of $1.8 \times 10^{-1} \text{ ergs cm}^{-2} \text{sec}^{-1}$ at 2057 UT. The maximum flare temperature was $\geq 20 \times 10^6$ °K. By 2124 UT the average flare temperature was 17×10^6 °K with an emission measure of $2.5 \times 10^{49} \text{ cm}^{-3}$. A very prolonged decay continued until about 2000 UT on August 3.

Aside from these large flares, there was very little activity and only moderately high background levels until the large flare on August 4. As evidenced by the data obtained during passage through the particle belts on August 4, the trapped radiation had already been affected by the particle emission from the previous flares. This was recorded by the SOLRAD 9 8-20Å detector perhaps as early as 0220 UT on August 4 and definitely at 0400 to 0420 UT and 0540 to 0600 UT. SOLRAD 10 did not show this until 1130 to 1150 UT on August 4 when it began to pass through the particle belts again and the cyclic increases appeared in the 8-20Å response.

On August 4, a precursor flare began at 0507 UT in the 0.5-3Å detector. The main event began at about 0610 UT in the 0.5-3Å detector and exhibited a very fast rise. A peak flux greater than a saturated 1-8Å value of 5.1×10^{-1} ergs $\text{cm}^{-2} \text{sec}^{-1}$ was attained around 0645 UT. By 0652 UT, early in the decay phase, the average flare temperature was 17×10^6 °K with an emission measure of $1.5 \times 10^{50} \text{cm}^{-3}$. The flare continued to decay until about 2200 UT. Throughout August 5 and 6, the background levels were only moderate and there was very little flare activity.

On August 7, two class M flares occurred early in the day. At around 1100 UT, a small flare began an increased level of activity preceding the major flare that day. The high background levels were indicative of a plasma at 0.5-3Å band after a small precursor. Again the risetime was very short. The 1-8Å detector was saturated with a flux greater than 5.1×10^{-1} ergs $\text{cm}^{-2} \text{sec}^{-1}$ when peak flux levels were reached at about 1528 UT. At 1605 UT, the average flare temperature was 19×10^6 °K with an emission measure of $5.6 \times 10^{49} \text{cm}^{-3}$. The flare then continued its decay for about 18 hours until 1000 UT on August 8.

There was little flare activity on August 8 and 9 but this picked up somewhat on August 10. On August 11, another major flare began with an impulsive precursor at 1212 UT. The main event began at 1233 UT and reached a maximum 1-8Å flux of 2.5×10^{-1} ergs $\text{cm}^{-2} \text{sec}^{-1}$ at 1241 UT. Assuming a flare temperature of 20×10^6 °K, the emission measure was about $3.4 \times 10^{49} \text{cm}^{-3}$. The decay phase lasted for about 11 hours until 2400 UT. August 12 was a fairly active day but flare activity was decreasing so that by August 14 there was very little activity.

In general, the whole period of August 1-11 produced five class X flares (1-8Å flux greater than 1×10^{-1} ergs/ $\text{cm}^2 \text{sec}$). Otherwise, it did not produce a larger number of smaller flares. August 5 and 6 were very quiet days. The X-ray background levels did reach values that have been associated with increased X-ray flare activity in the past but by August 3 the background was again below these critical levels.

One interesting feature of this group of flares is in the preflare activity. Two types of preflare activity are shown in the flares on August 2. Before 0300 UT the background levels are high and are produced by an active area with an average electron temperature between 8 and 10×10^6 °K, which is a high non-flare temperature. The second type is evident as a moderately sized impulsive flare preceding the major event by from 10 to 60 minutes. The fluxes in these impulsive precursors can be characterized as arising from a region with electron temperature $\geq 15 \times 10^6$ °K or as having a power-law photon spectrum:

$$\frac{dN}{dE} = k E^{-\alpha}$$

with α between 4 and 5. These precursive spikes have been seen before in SOLRAD 9 data but not too frequently. However, NRL experiments on OSO-5 which also covered the 0.5-3Å, 1-8Å, 8-20Å, and 44-60Å bands but with a 15 second time resolution, often showed impulsive events during the rising phases of flare although not as distinctly as seen in some of these flares.

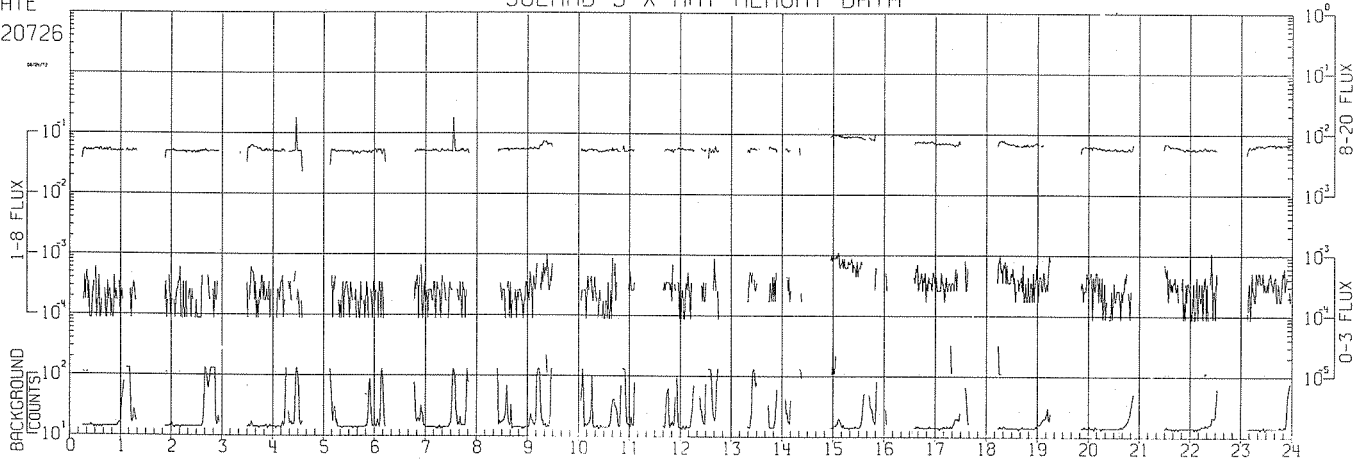
McMath region 11976 produced five very significant X-ray flares in early August 1972. Those on August 4 and 7 were of an intensity rarely reached in the 4½ years that SOLRAD 9 has been monitoring solar X-rays. There are a number of similarities between these flares and some of the X-ray flares that occurred during the October 26 through November 4, 1968 period in the intensity of the flares and in the precursor activity. However, background levels in early August were only moderate and the number of smaller flares produced was small.

REFERENCES

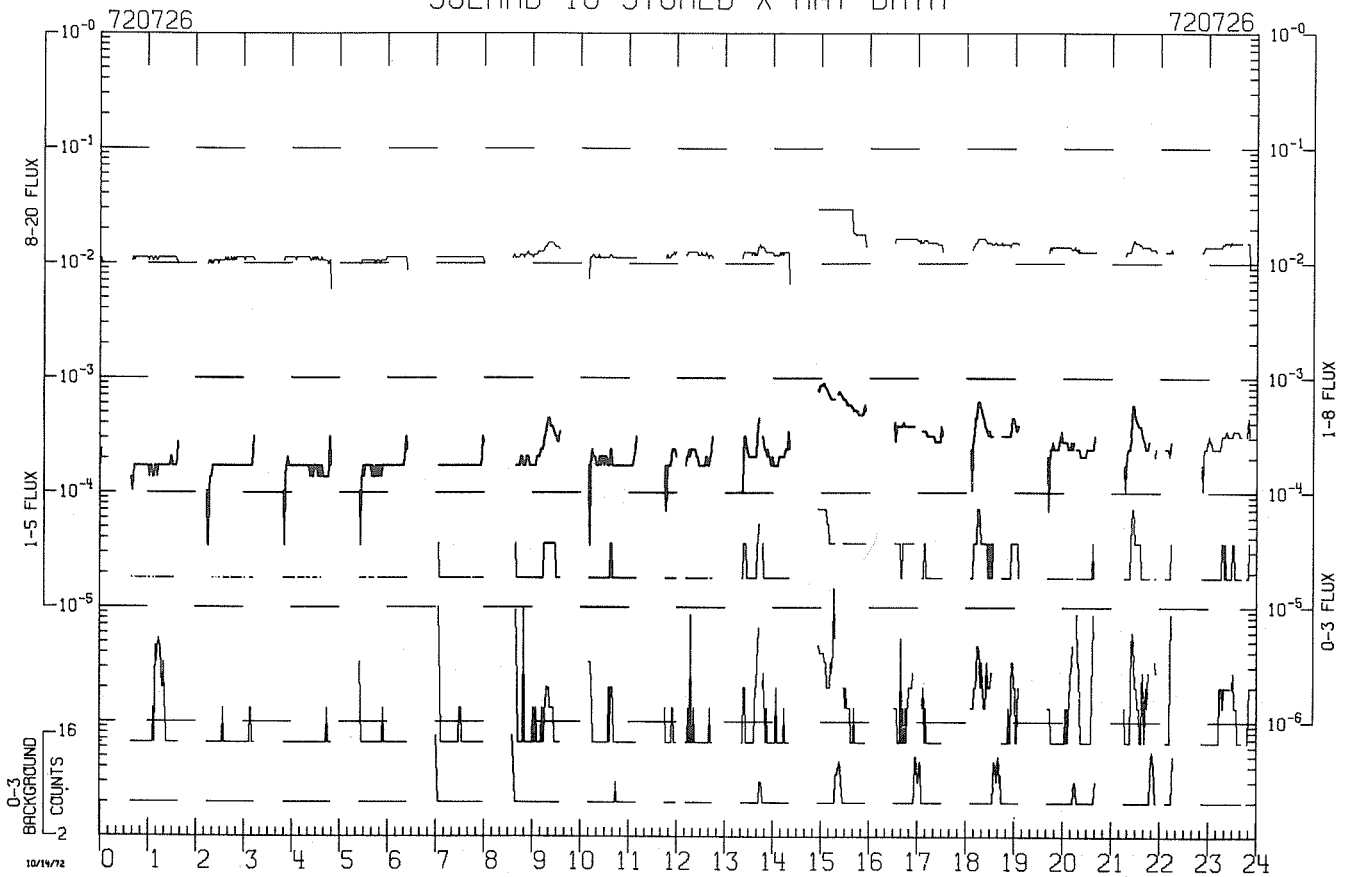
- | | | |
|--|------|---|
| DERE, K. P.,
D. M. HORAN and
R. W. KREPLIN | 1973 | Corrections to Solar Soft X-ray Flux Values Measured by NRL Ionization Chamber Experiments, <u>NRL Report</u> , in press. |
| HORAN, D. M. and
R. W. KREPLIN | 1972 | The SOLRAD 10 Satellite, <u>NRL Report 7408</u> . |
| KREPLIN, R. W. and
D. M. HORAN | 1969 | The NRL SOLRAD 9 Satellite, <u>NRL Report 6800</u> . |

DATE
720726

SOLRAD 9 X-RAY MEMORY DATA



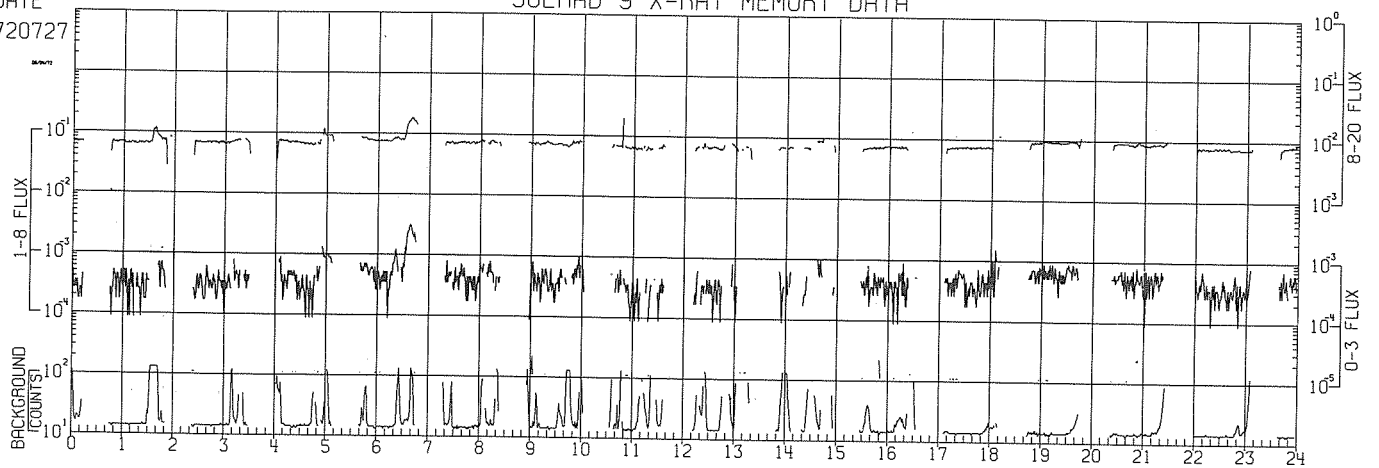
SOLRAD 10 STORED X-RAY DATA



DATE

SOLRAD 9 X-RAY MEMORY DATA

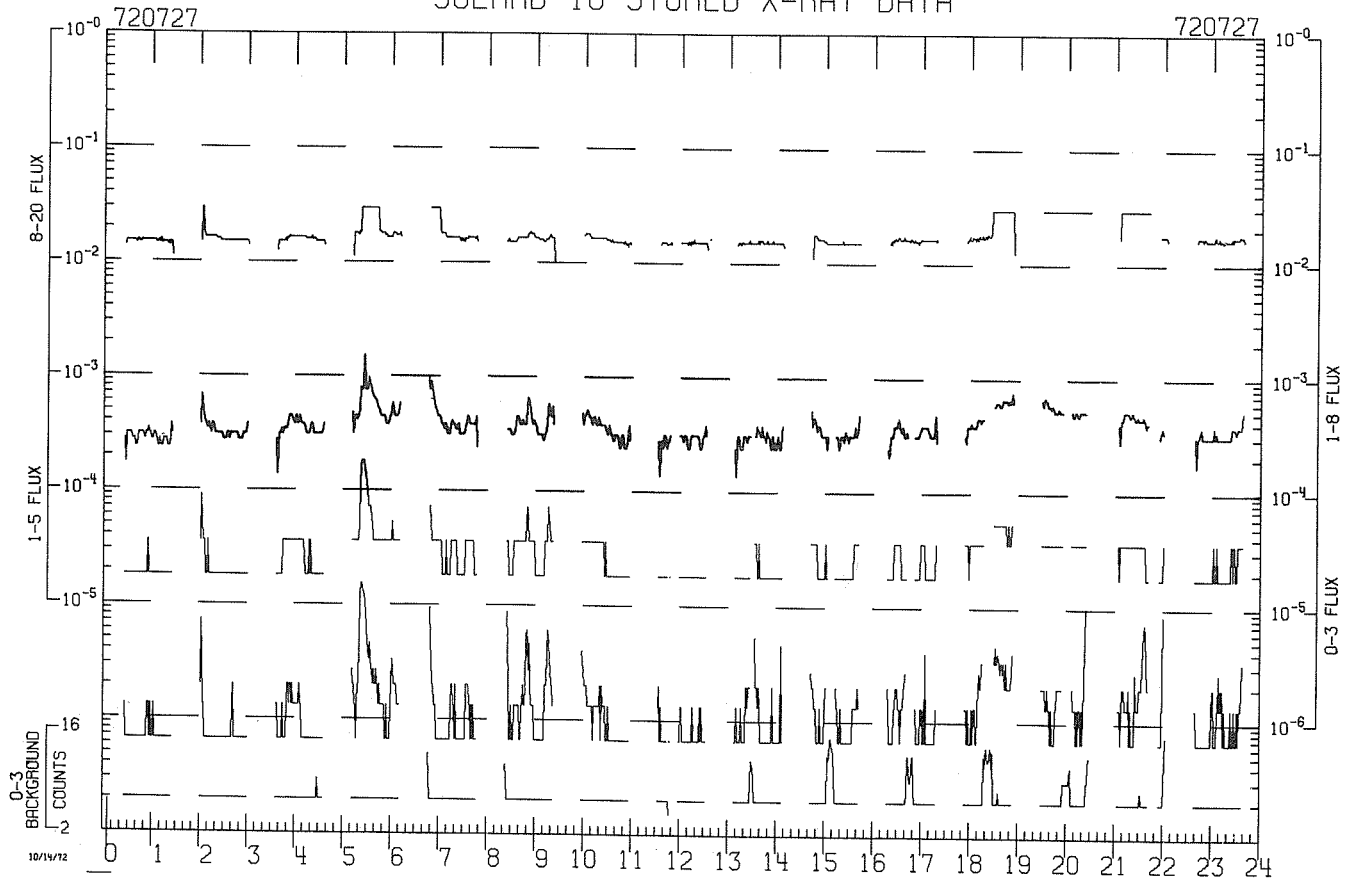
720727



SOLRAD 10 STORED X-RAY DATA

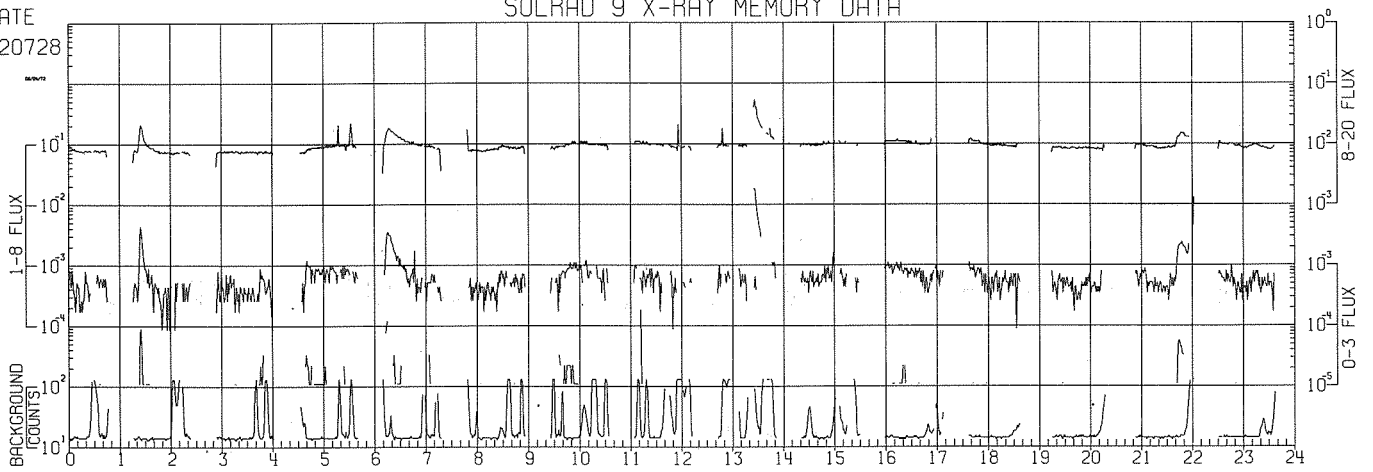
720727

720727

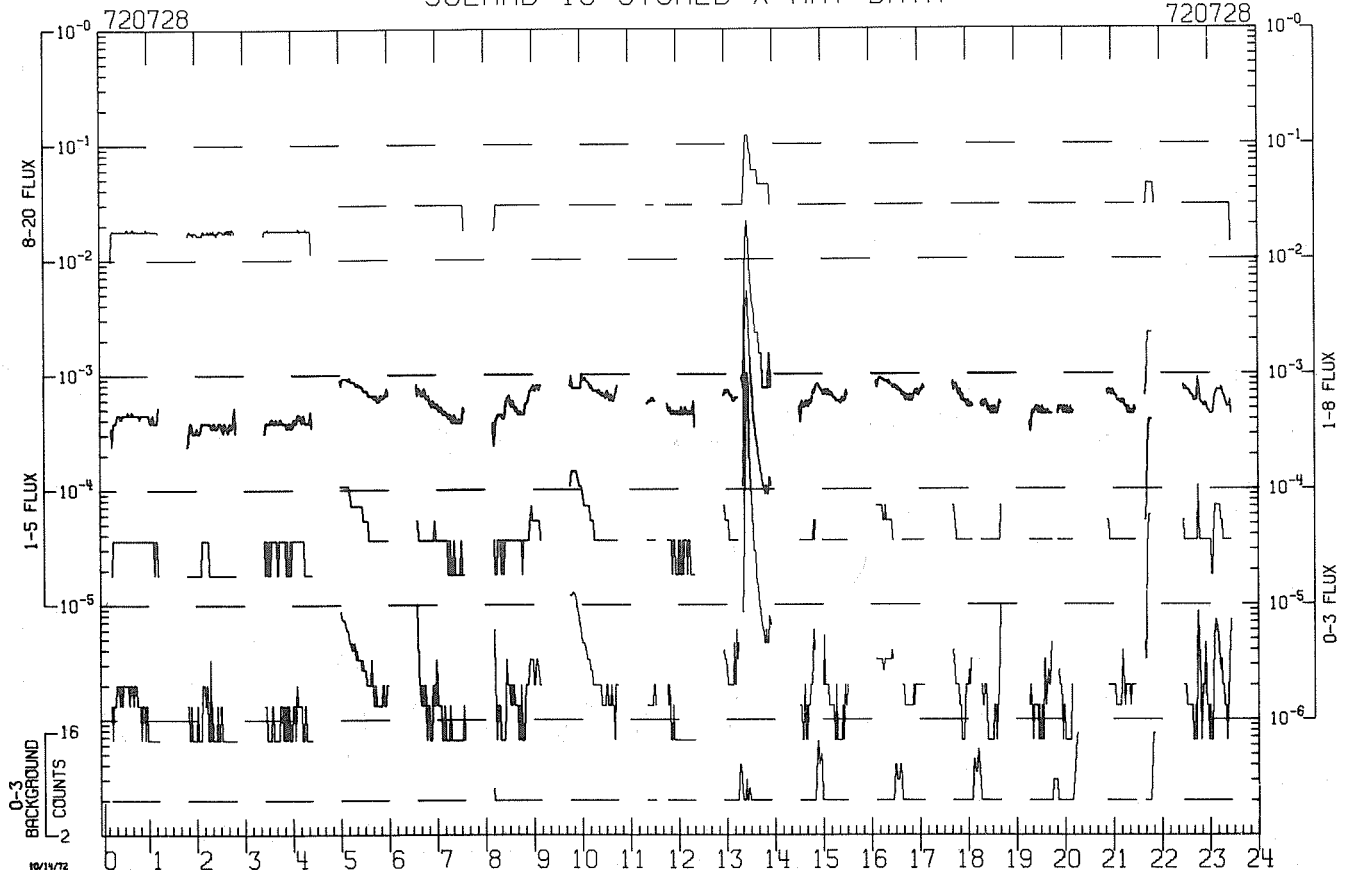


DATE
720728

SOLRAD 9 X-RAY MEMORY DATA



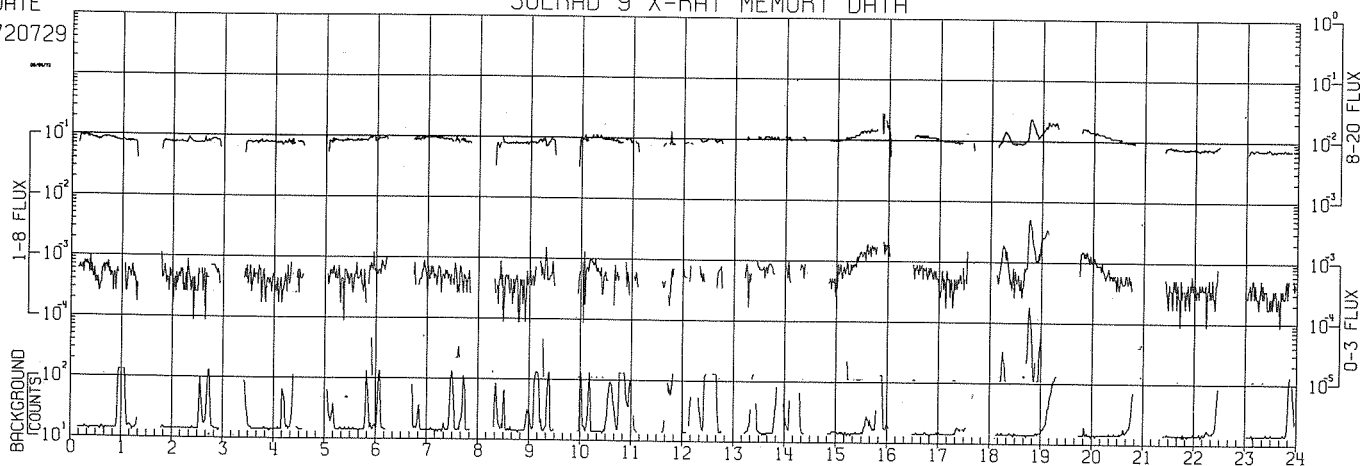
SOLRAD 10 STORED X-RAY DATA



DATE

SOLRAD 9 X-RAY MEMORY DATA

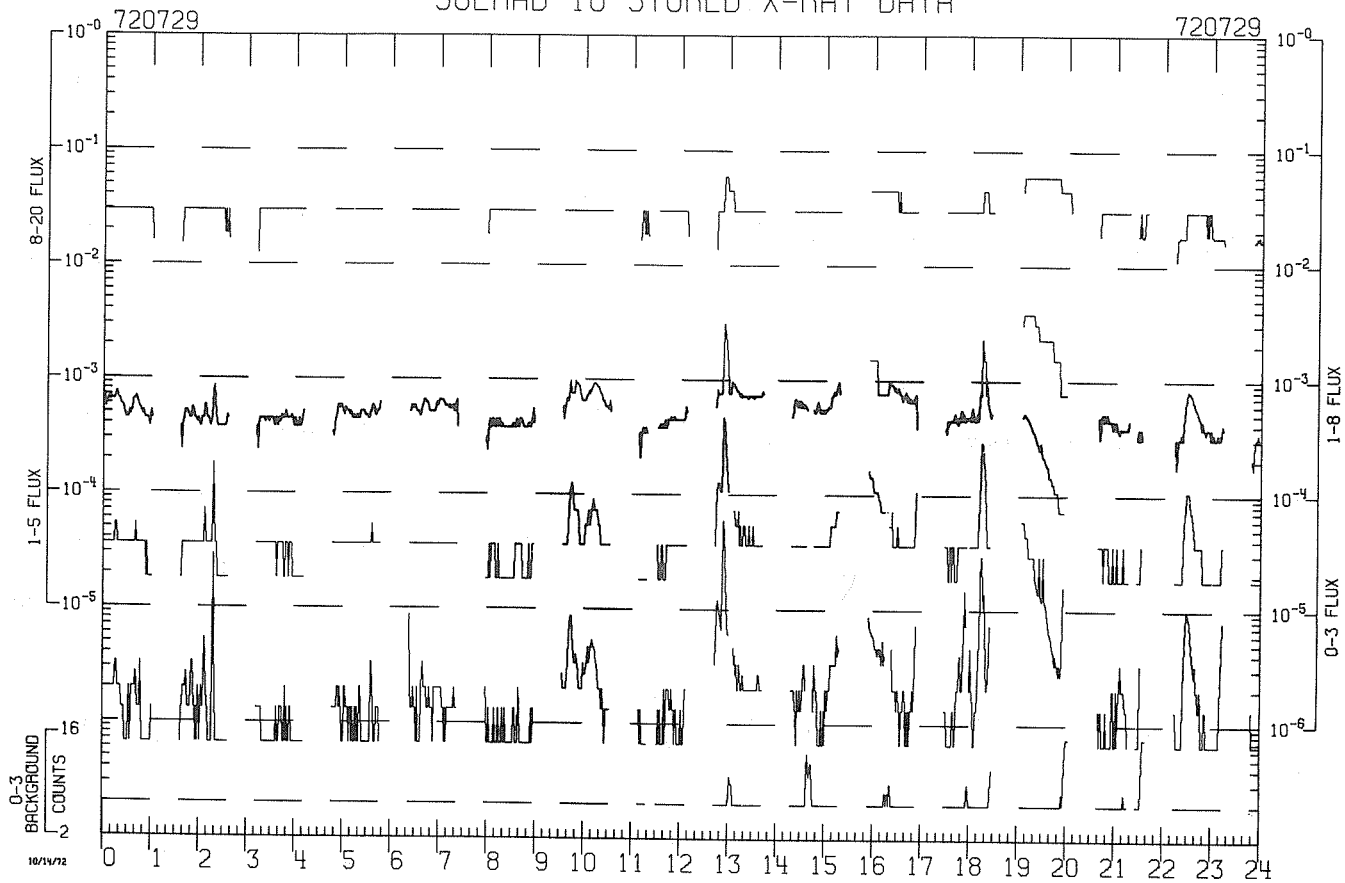
720729



SOLRAD 10 STORED X-RAY DATA

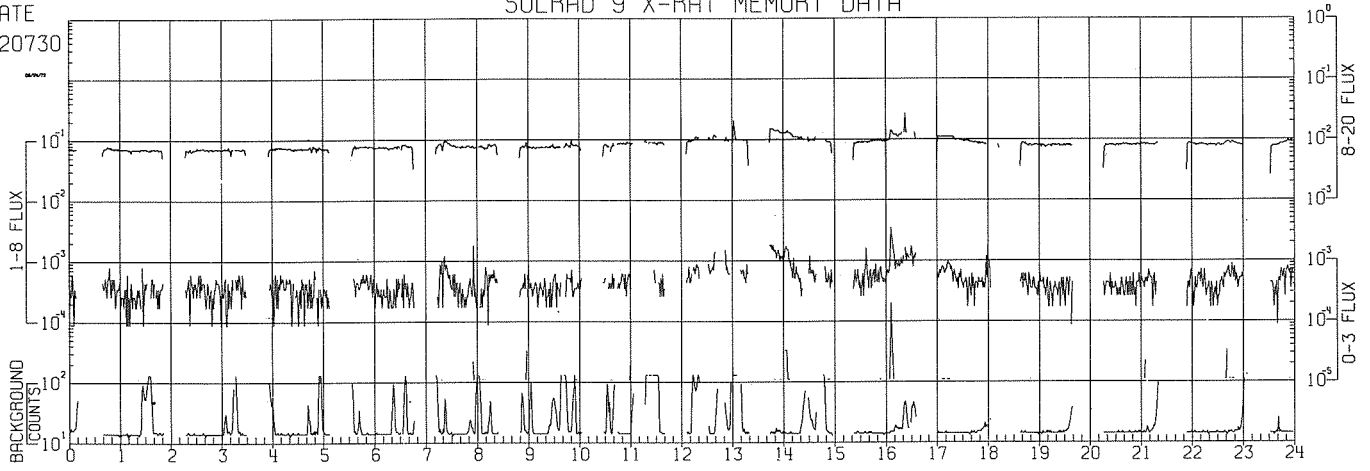
720729

720729

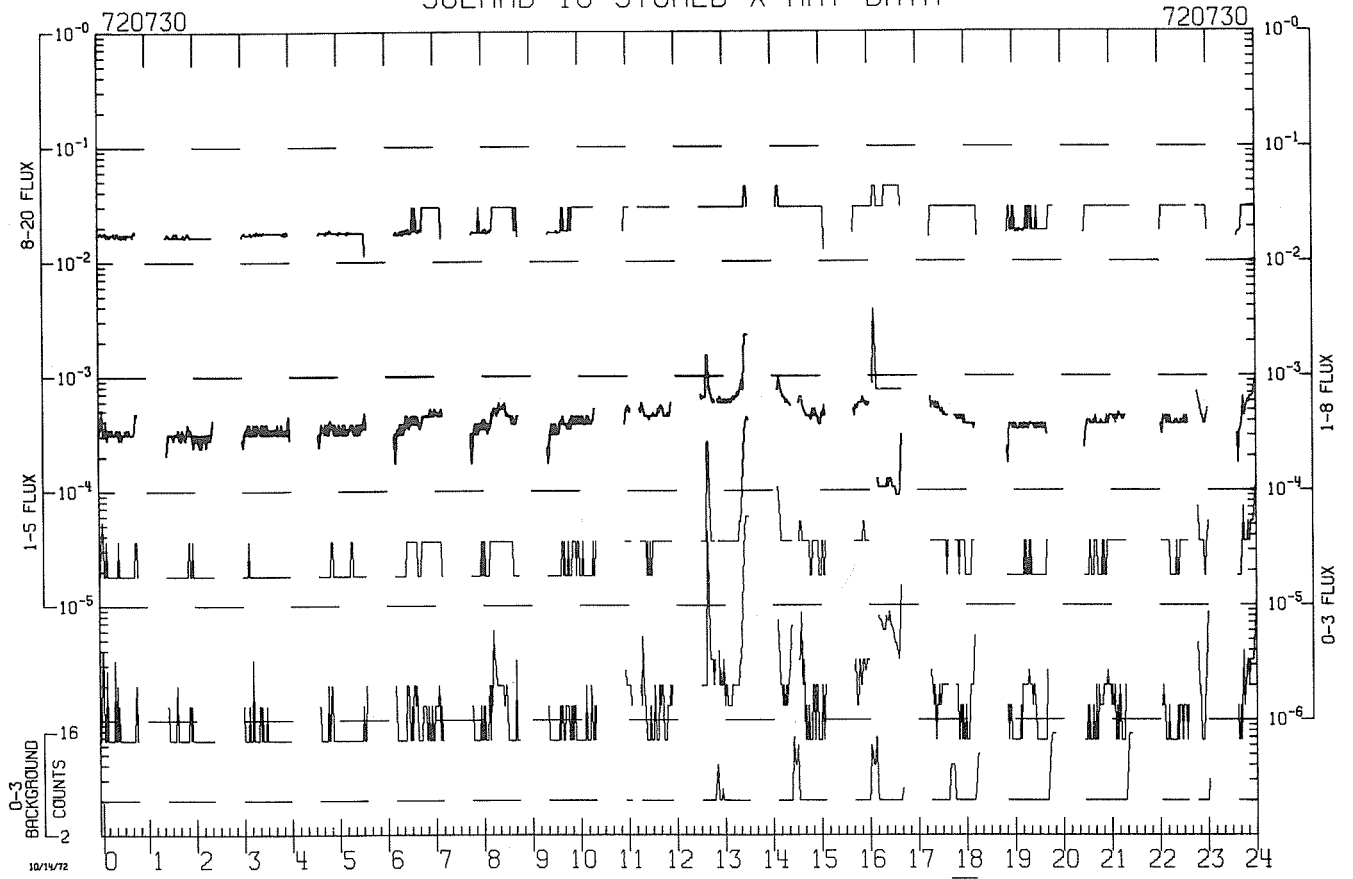


DATE
720730

SOLRAD 9 X-RAY MEMORY DATA

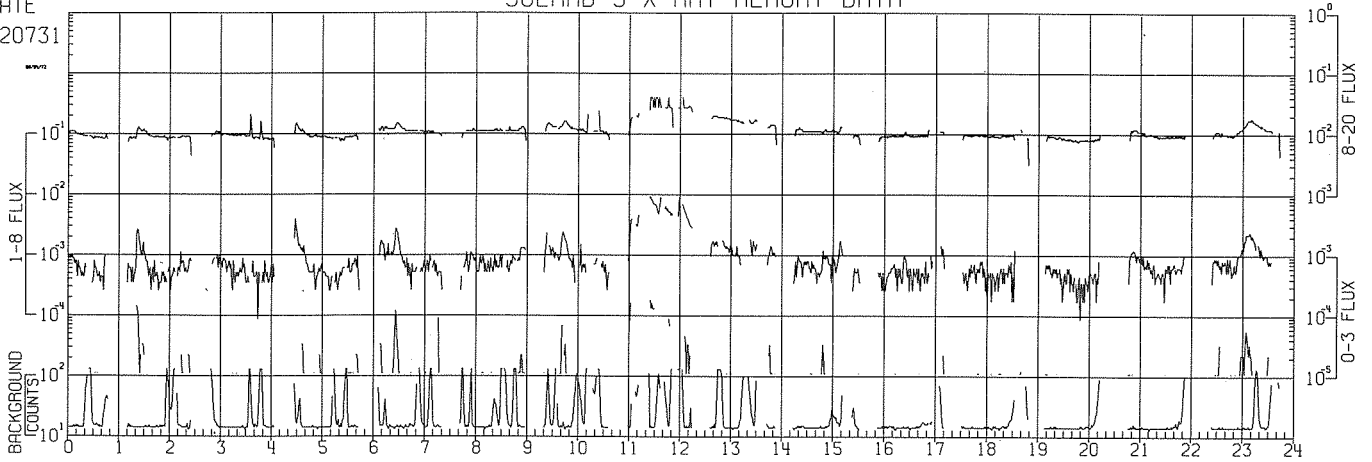


SOLRAD 10 STORED X-RAY DATA

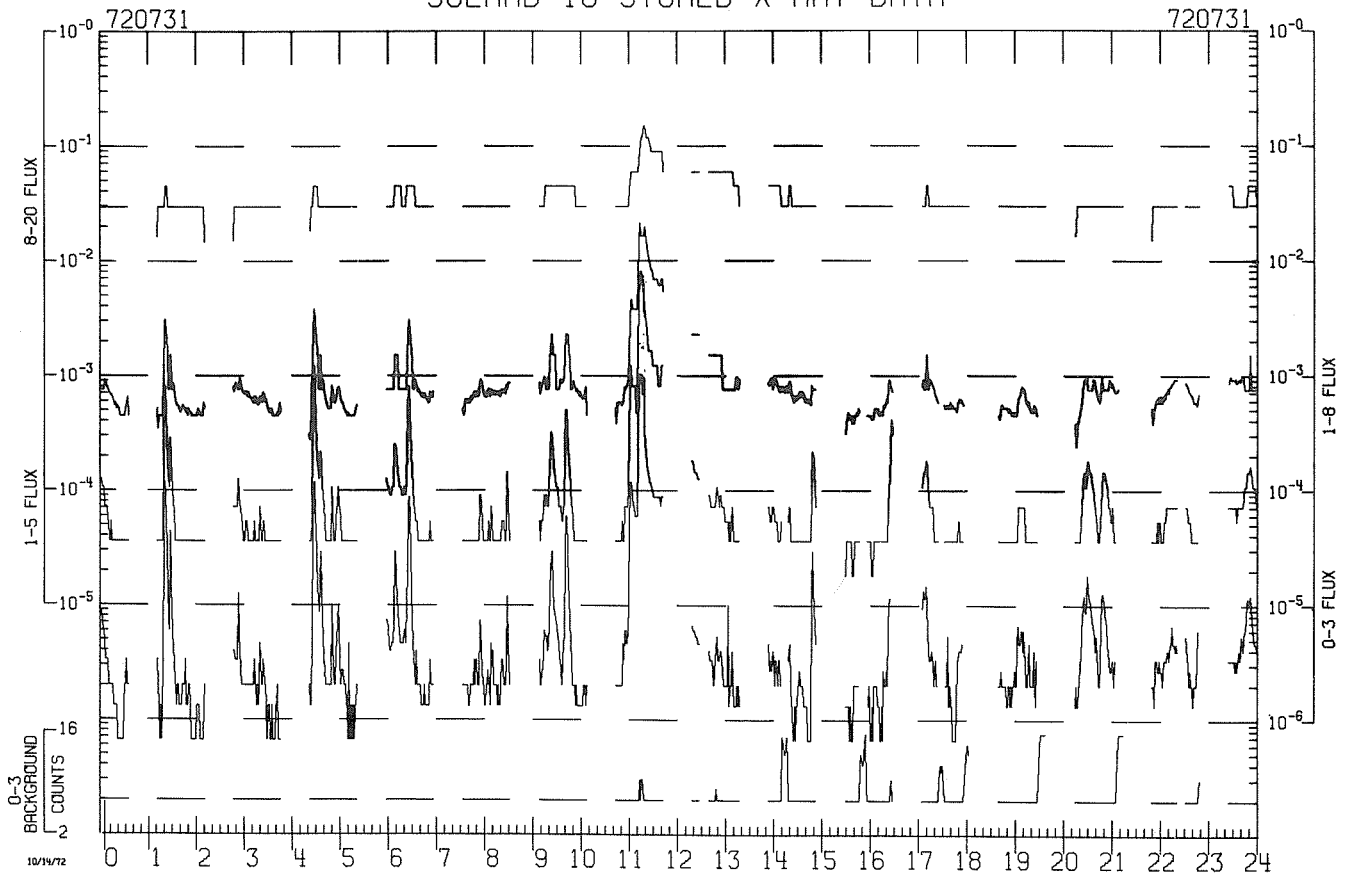


DATE
720731

SOLRAD 9 X-RAY MEMORY DATA

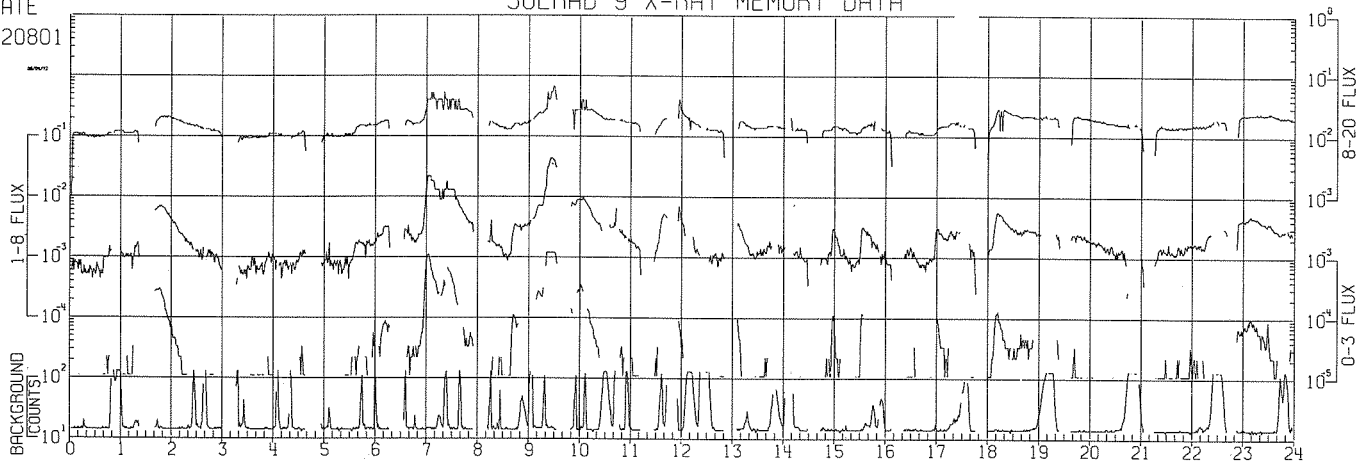


SOLRAD 10 STORED X-RAY DATA

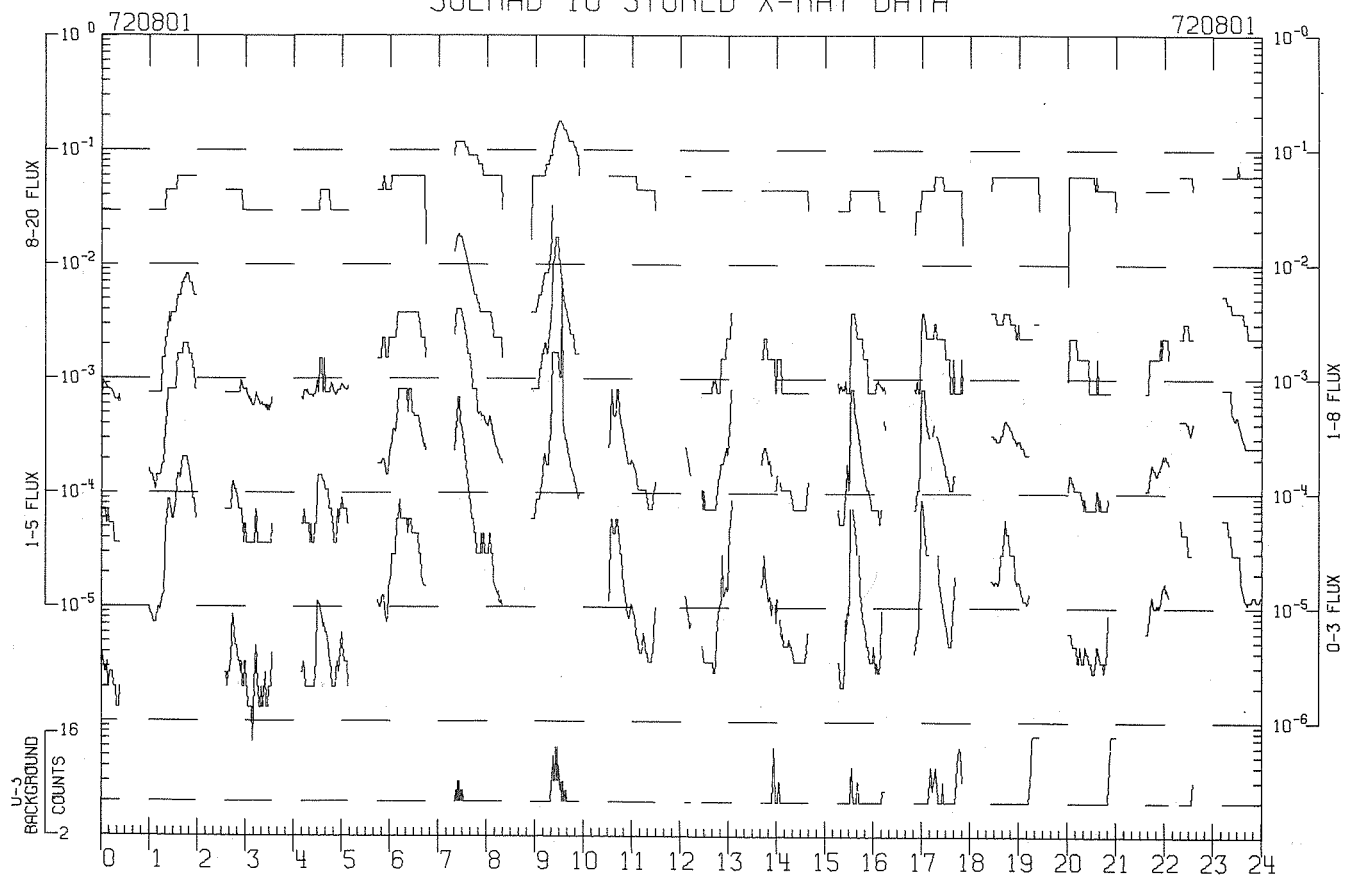


DATE
720801

SOLRAD 9 X-RAY MEMORY DATA

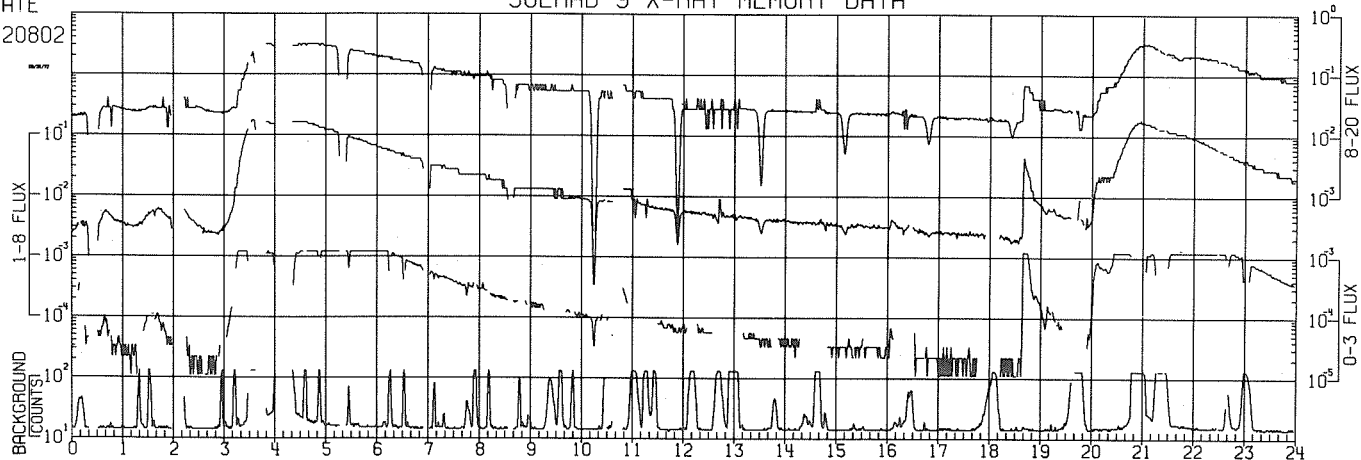


SOLRAD 10 STORED X-RAY DATA

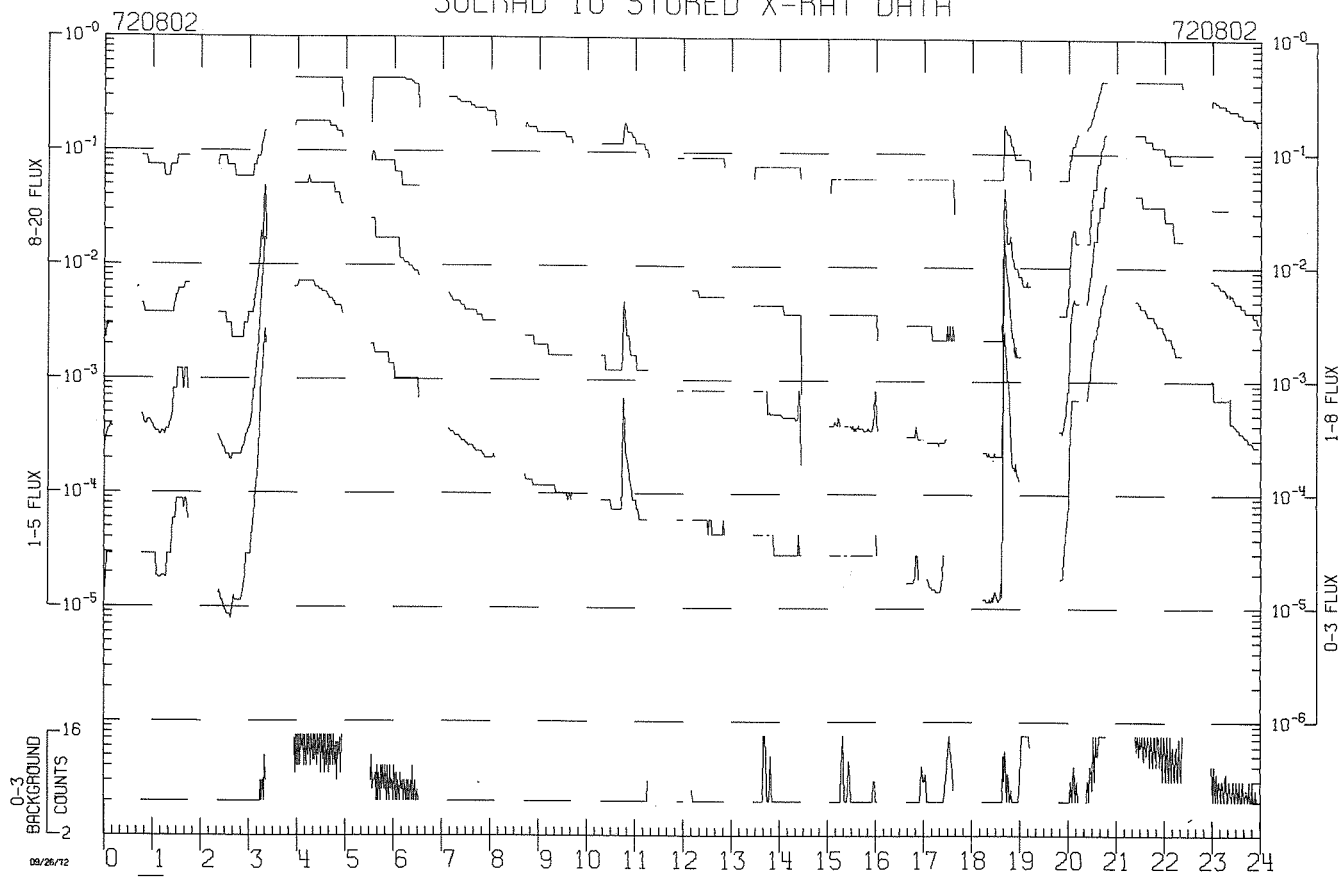


DATE
720802

SOLRAD 9 X-RAY MEMORY DATA

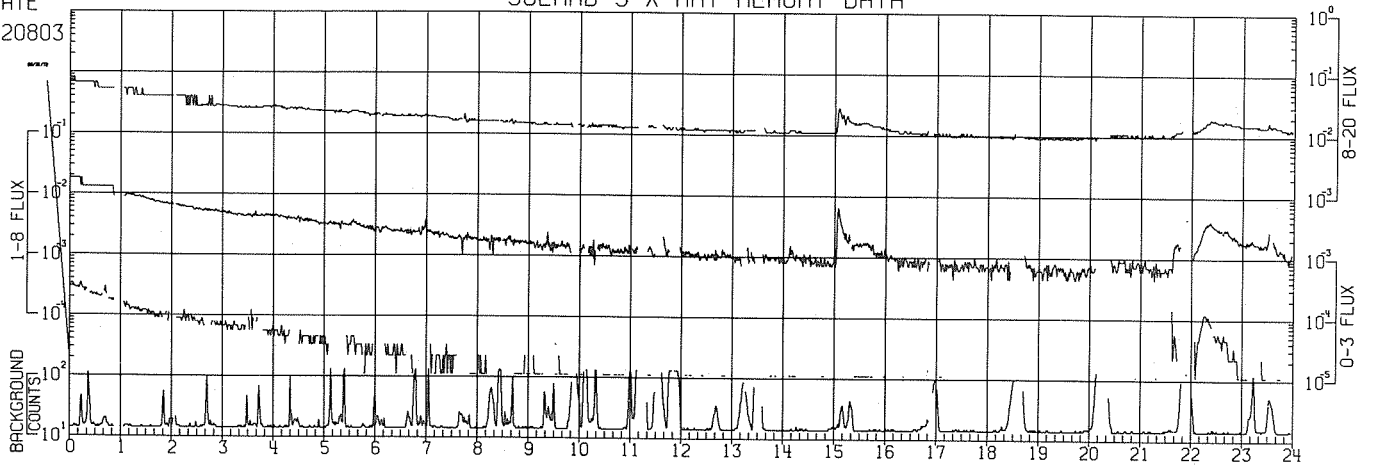


SOLRAD 10 STORED X-RAY DATA

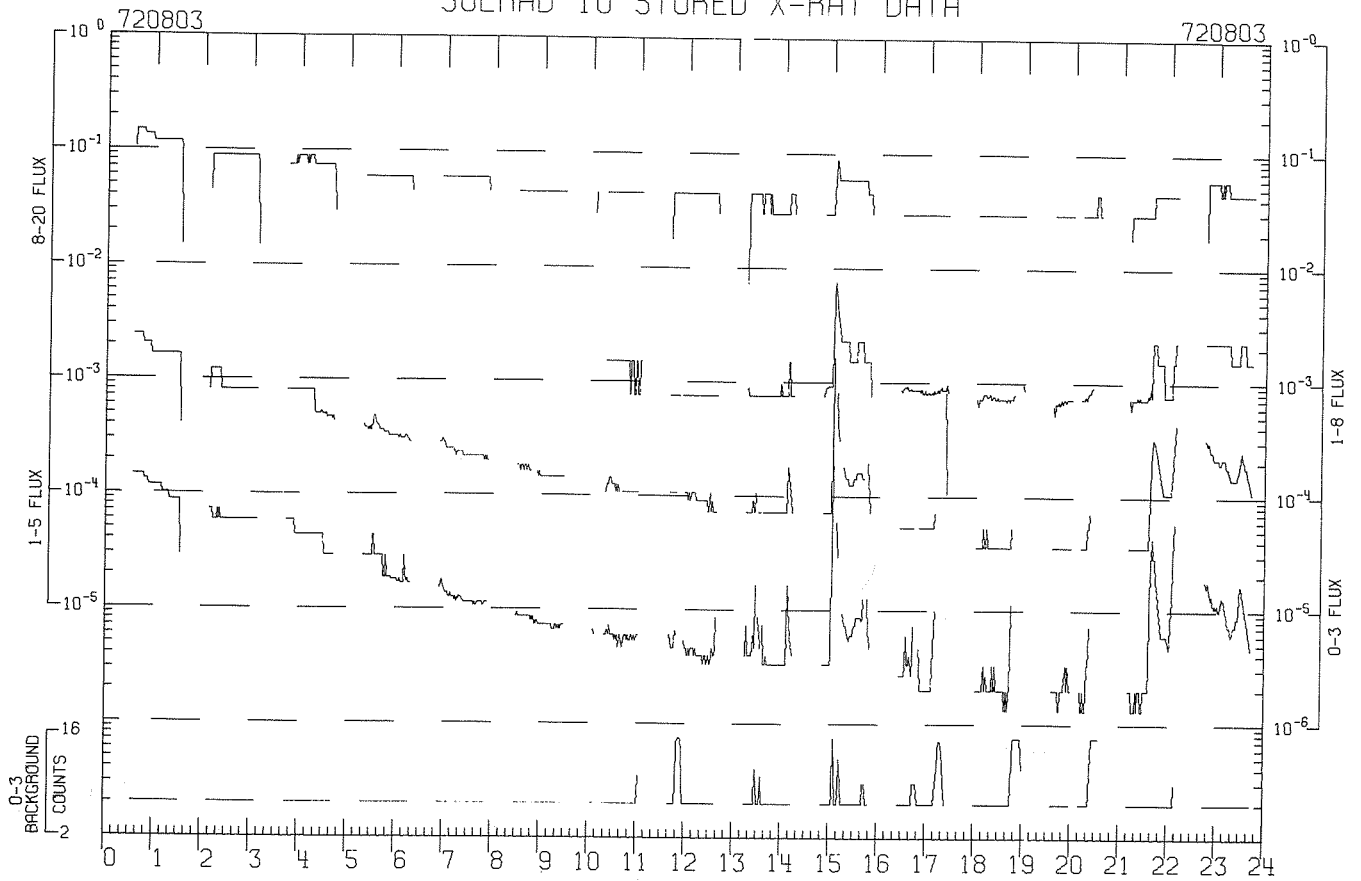


DATE
720803

SOLRAD 9 X-RAY MEMORY DATA

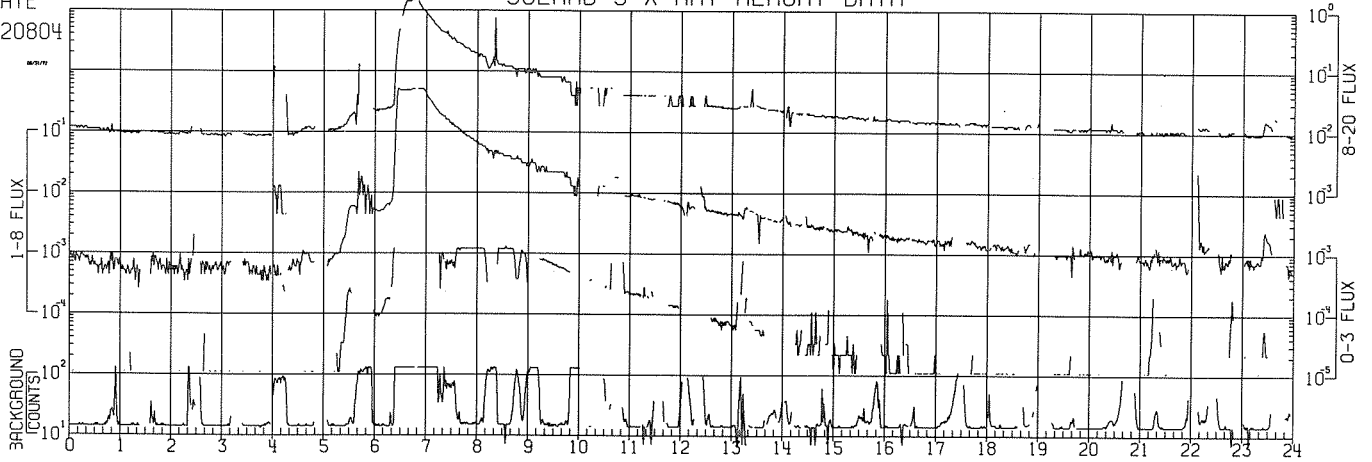


SOLRAD 10 STORED X-RAY DATA

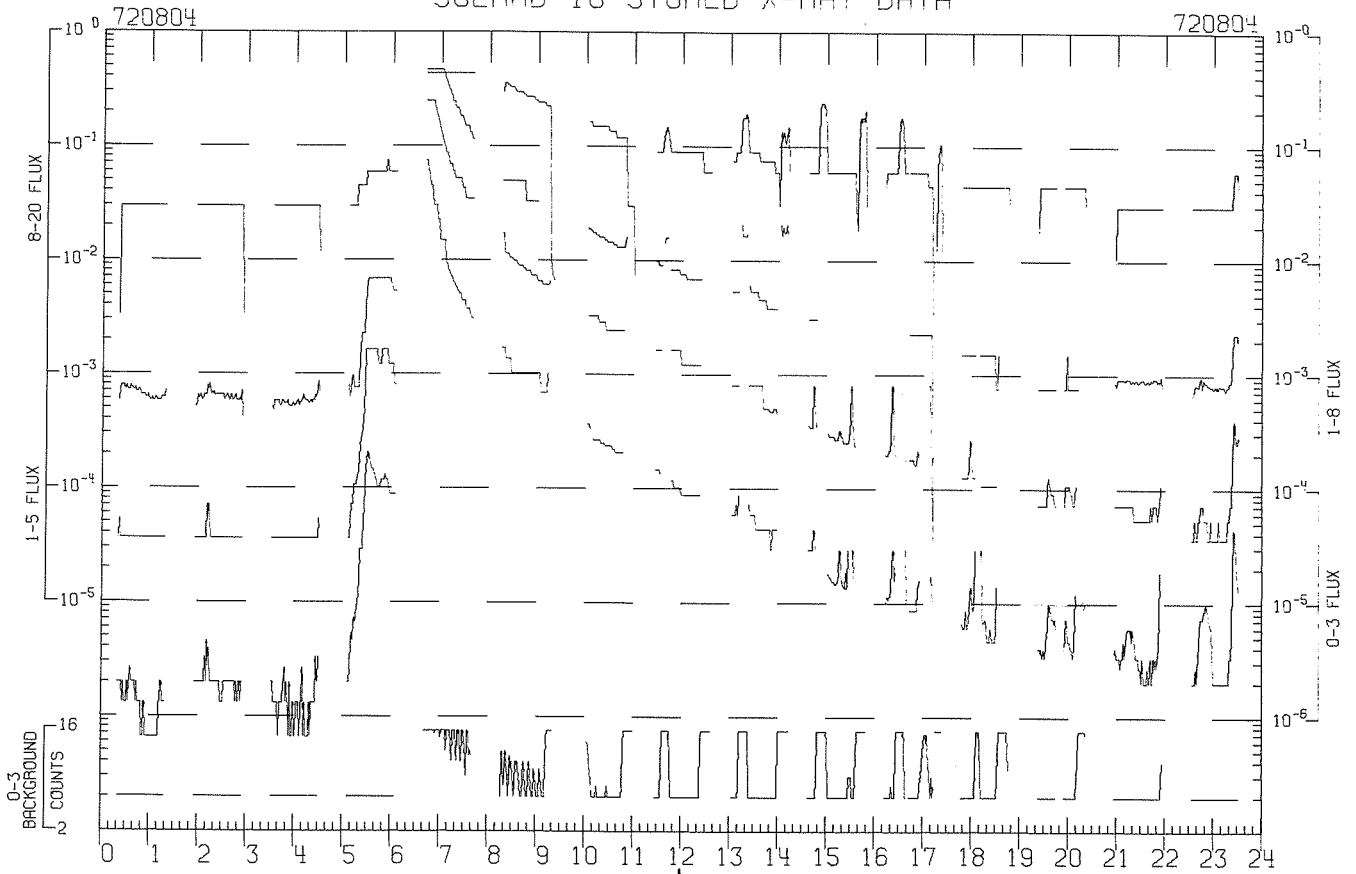


DATE
720804

SOLRAD 9 X-RAY MEMORY DATA

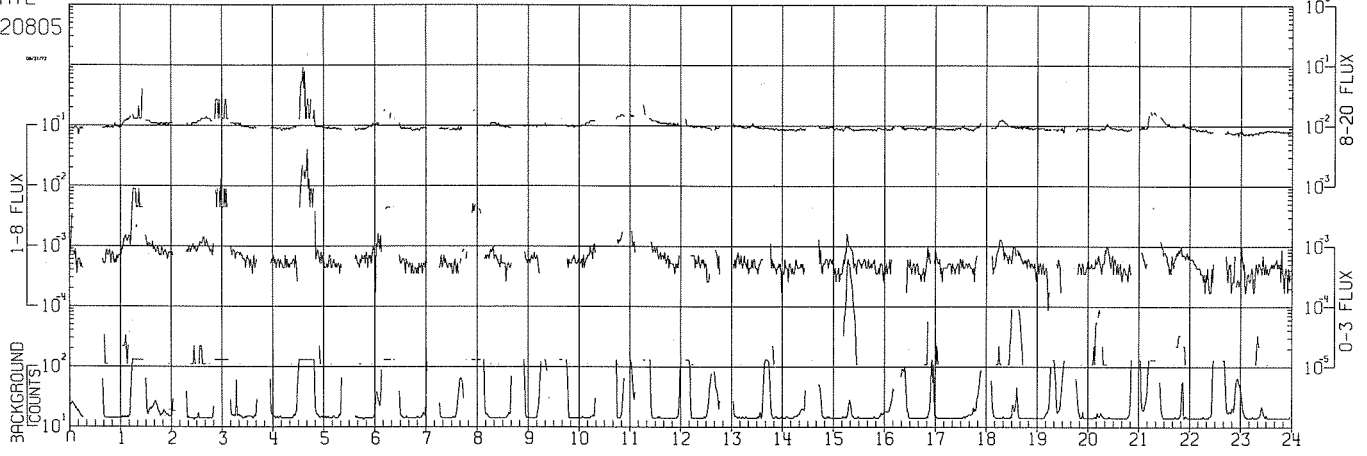


SOLRAD 10 STORED X-RAY DATA

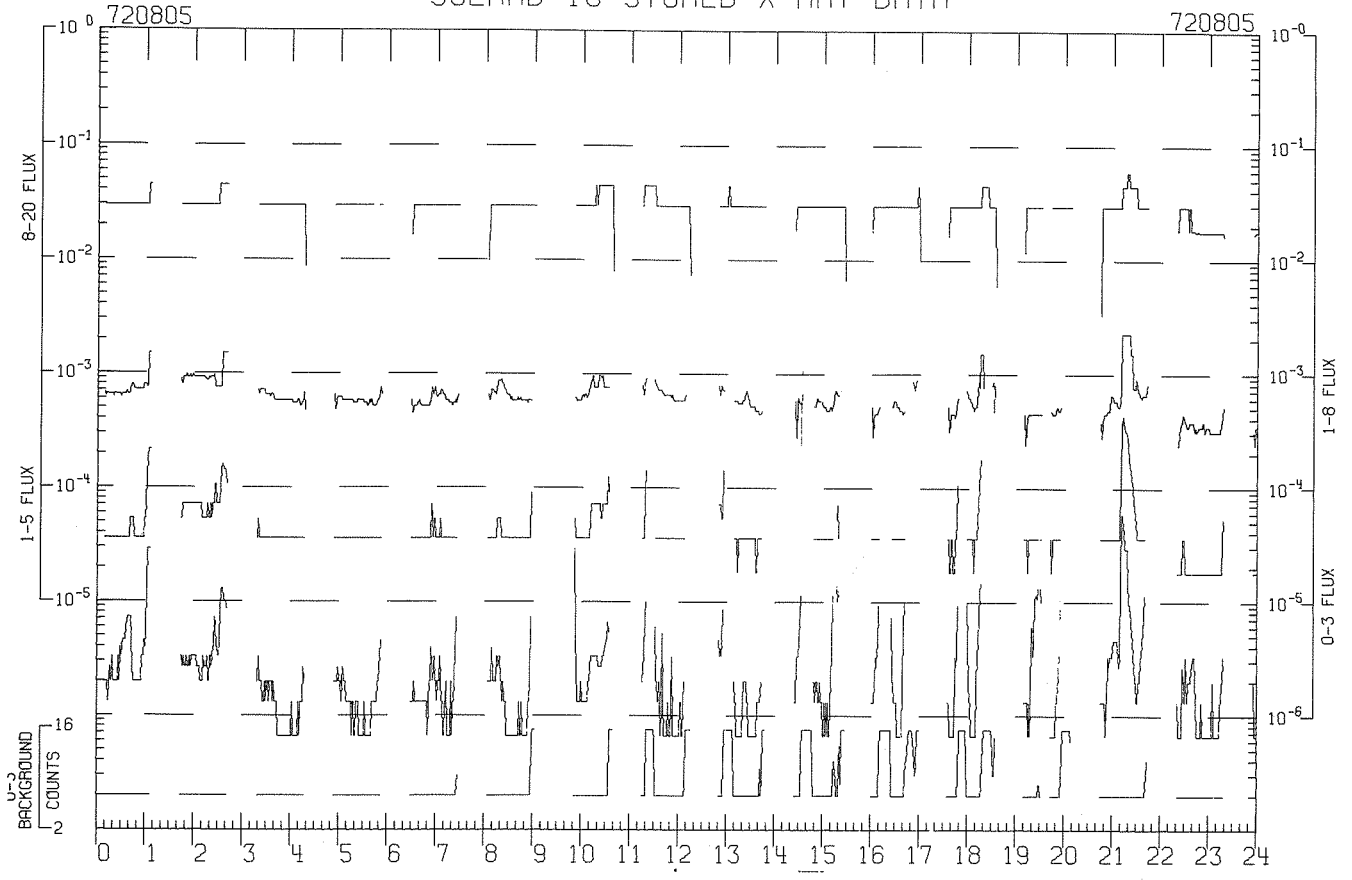


DATE
720805

SOLRAD 9 X-RAY MEMORY DATA

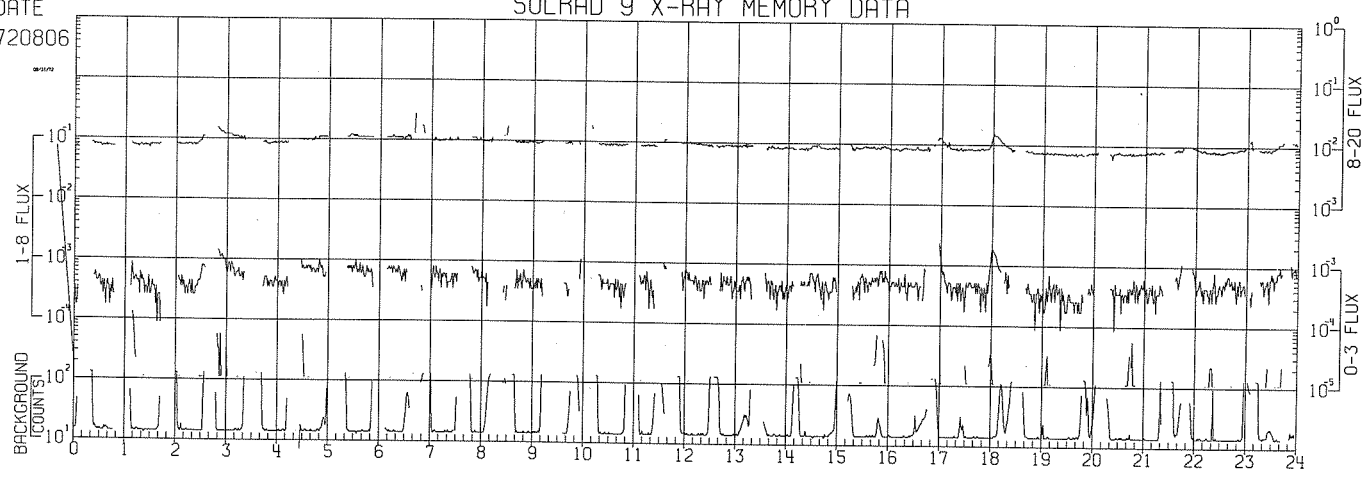


SOLRAD 10 STORED X-RAY DATA



DATE
720806

SOLRAD 9 X-RAY MEMORY DATA

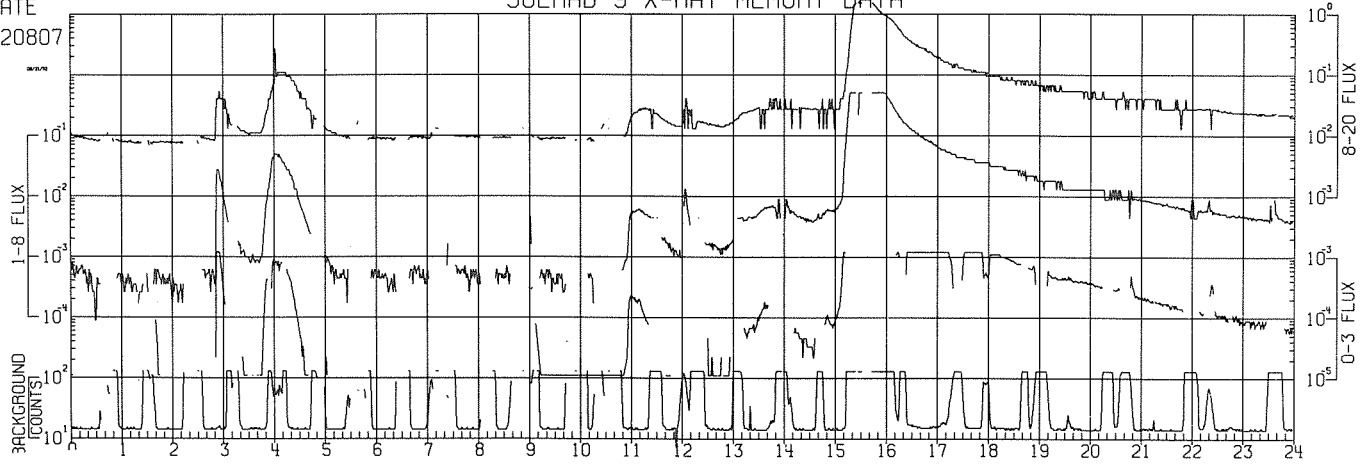


SOLRAD 10 STORED X-RAY DATA

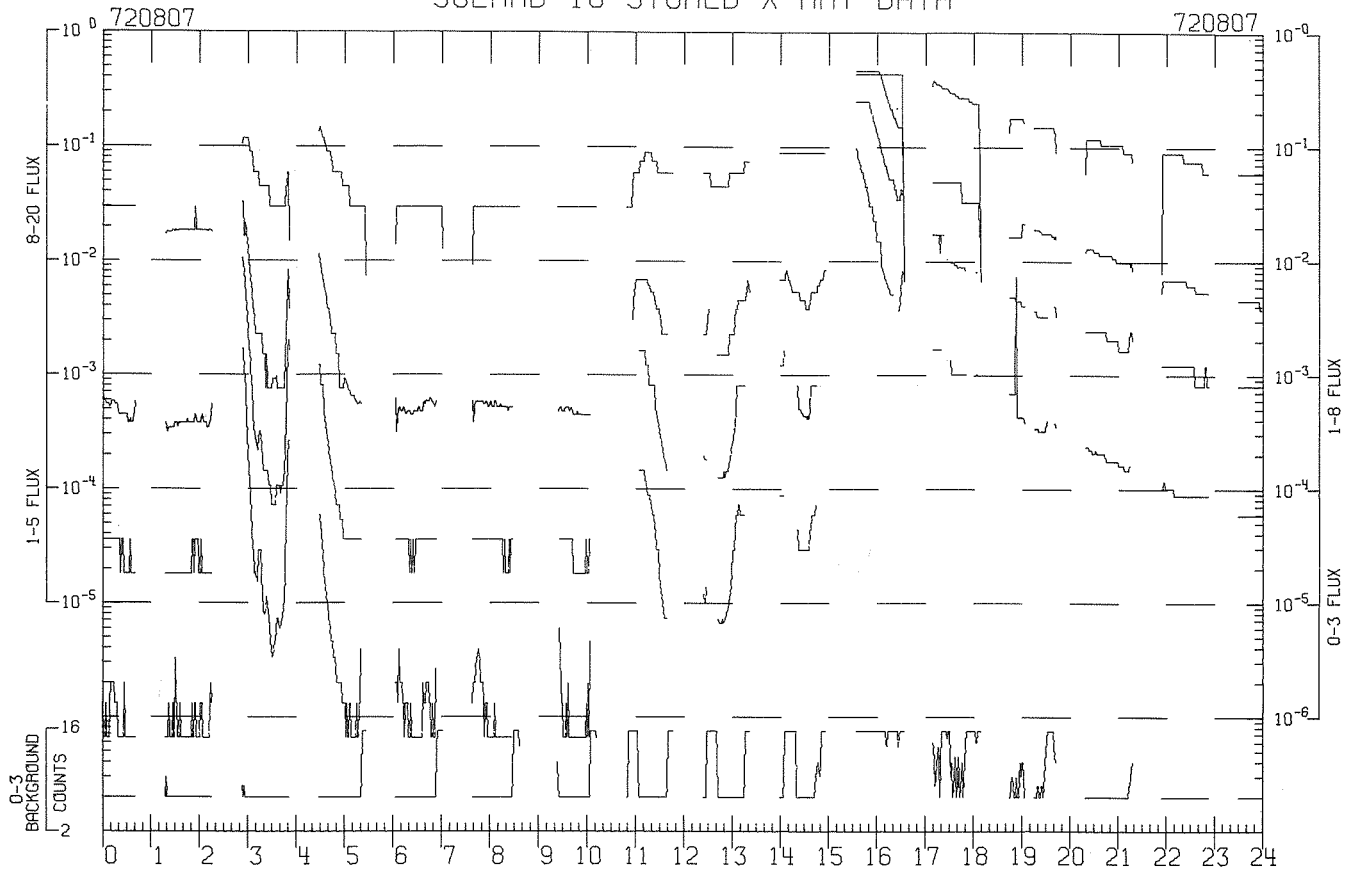


DATE
720807

SOLRAD 9 X-RAY MEMORY DATA

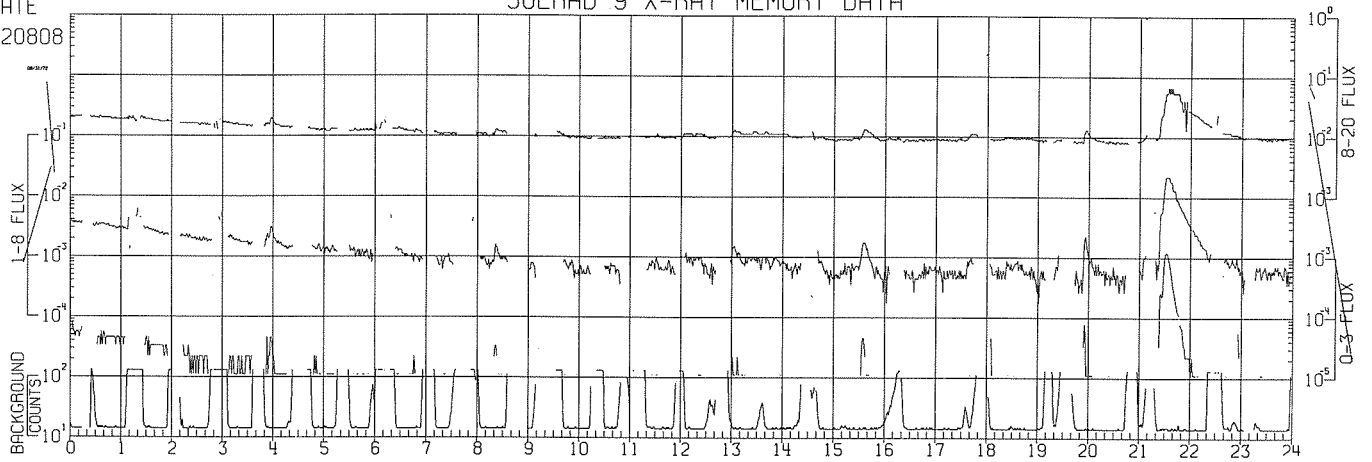


SOLRAD 10 STORED X-RAY DATA

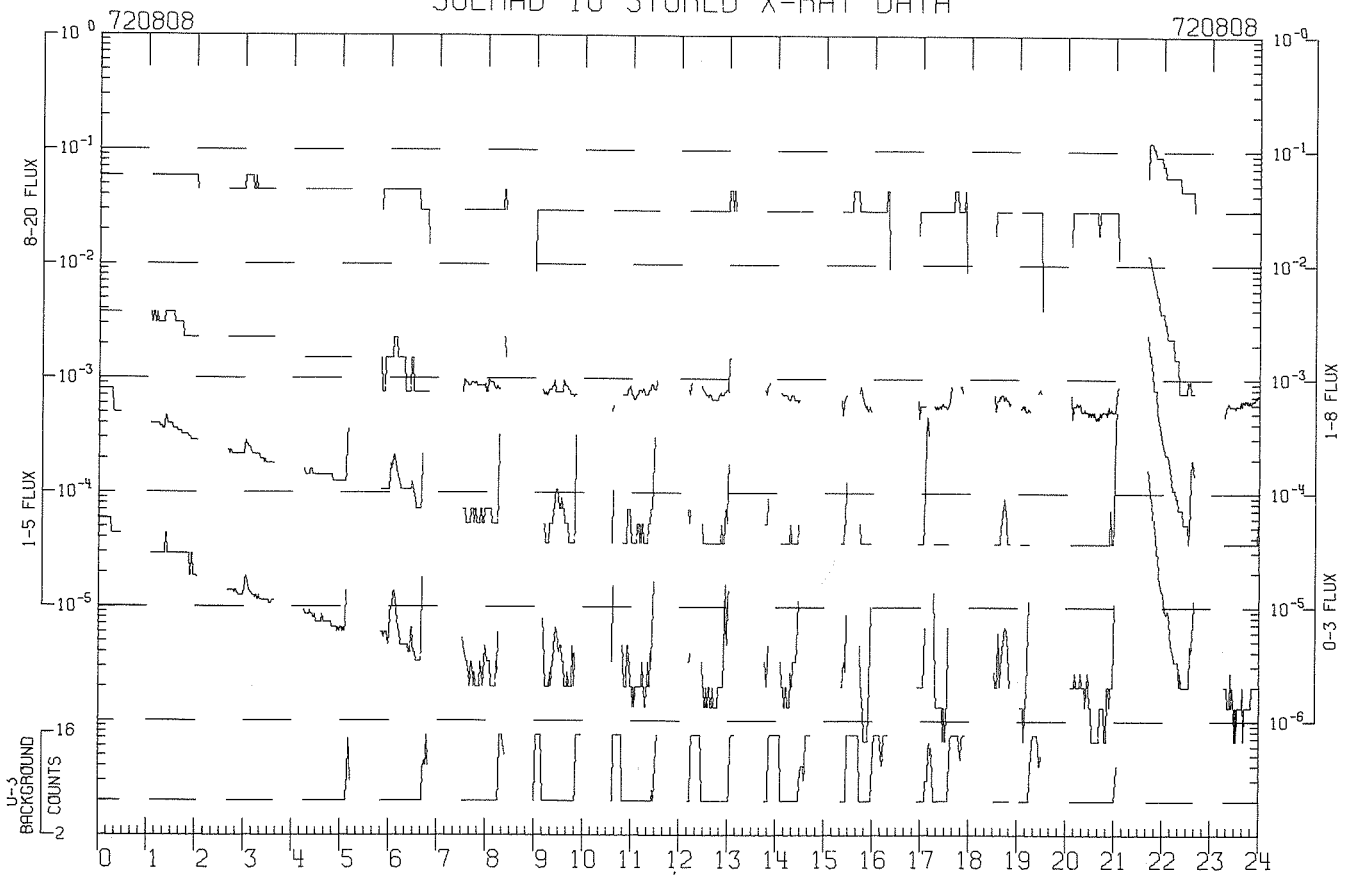


DATE
720808

SOLRAD 9 X-RAY MEMORY DATA

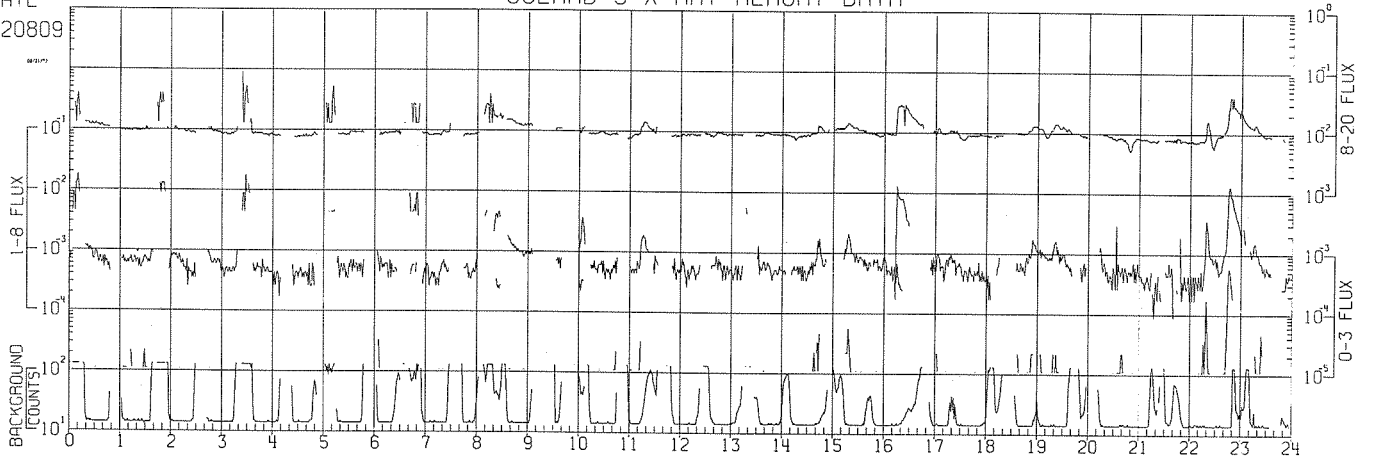


SOLRAD 10 STORED X-RAY DATA

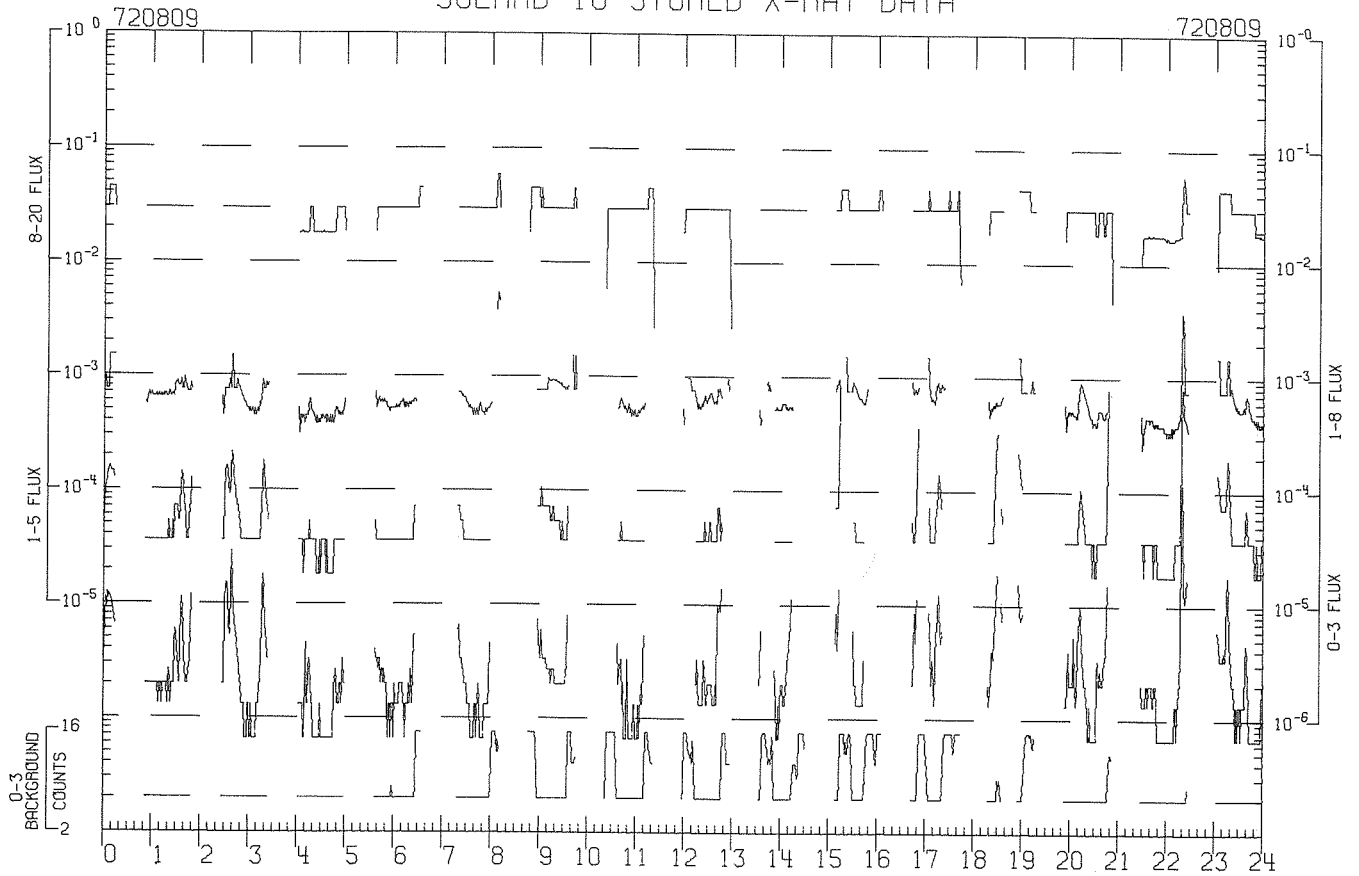


DATE
720809

SOLRAD 9 X-RAY MEMORY DATA

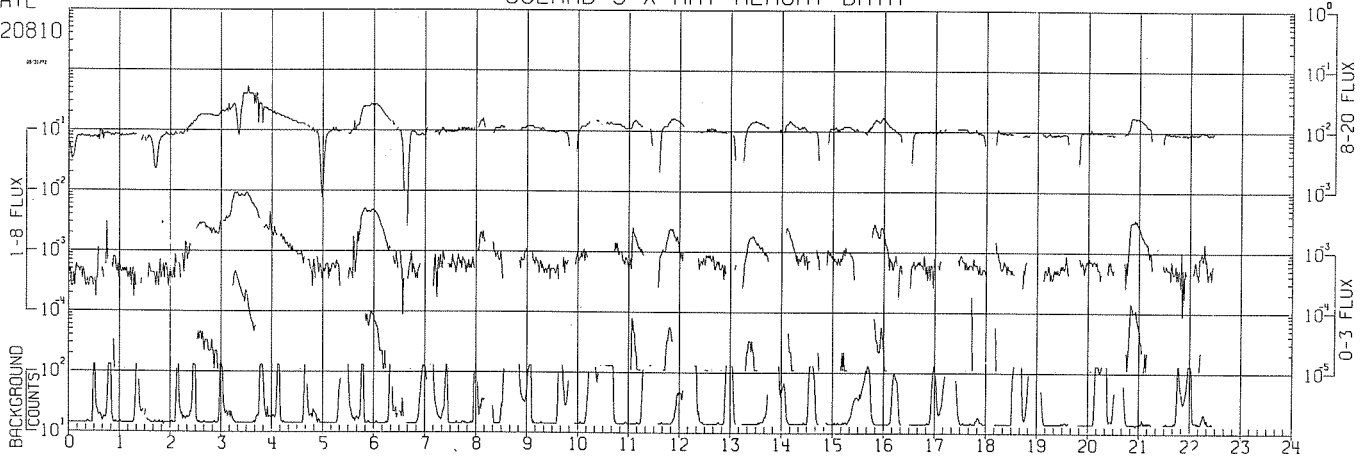


SOLRAD 10 STORED X-RAY DATA

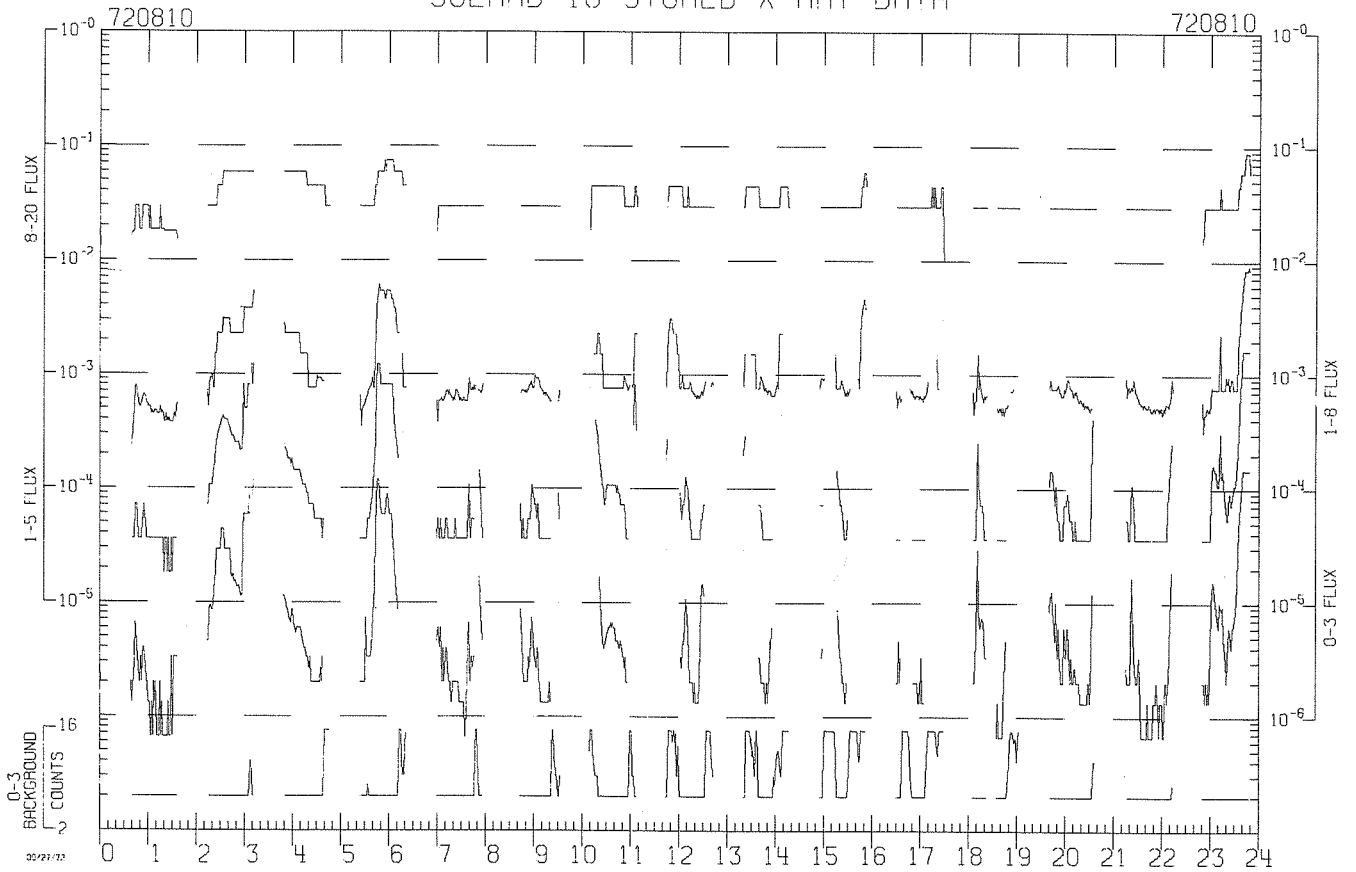


DATE
720810

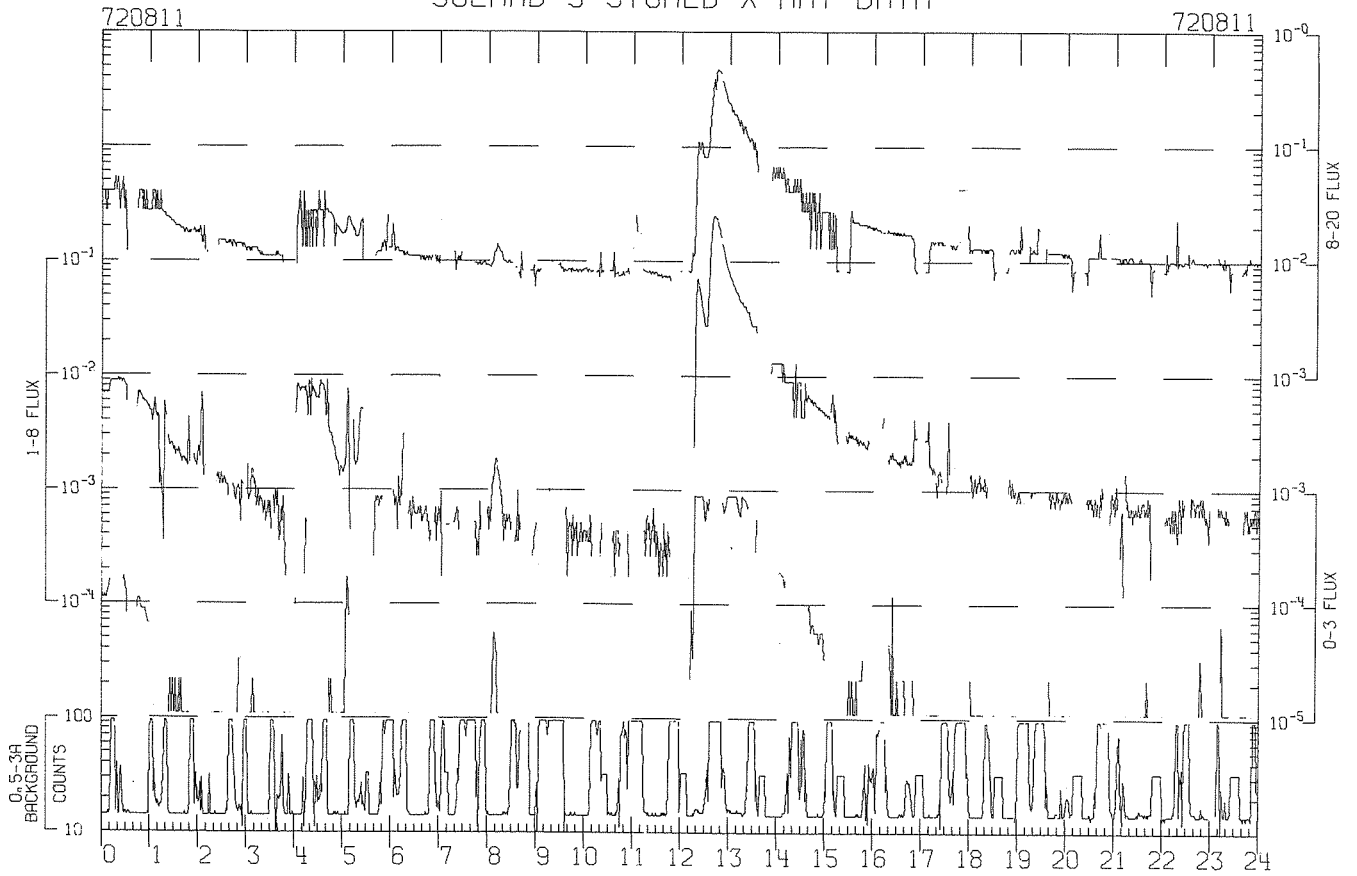
SOLRAD 9 X-RAY MEMORY DATA



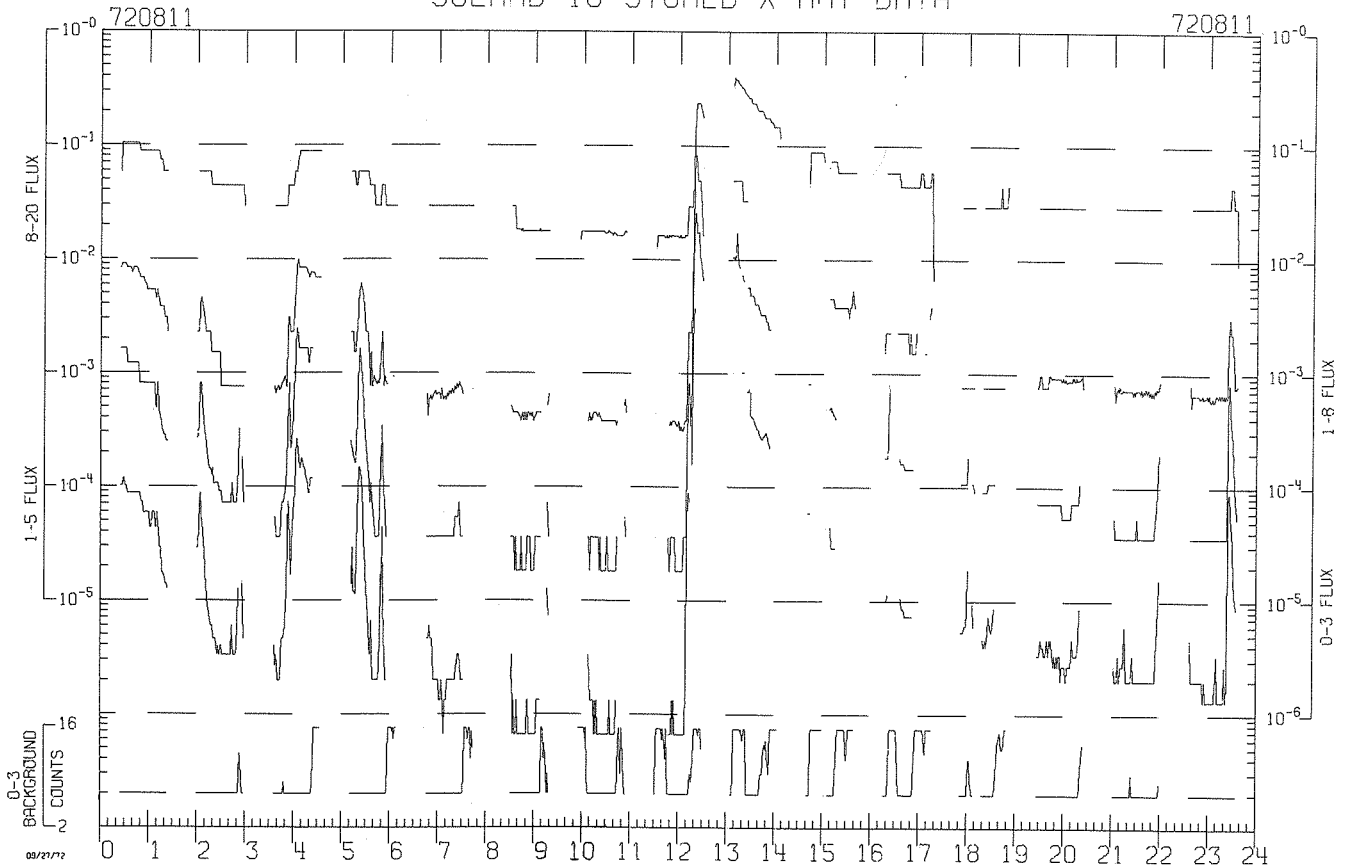
SOLRAD 10 STORED X-RAY DATA



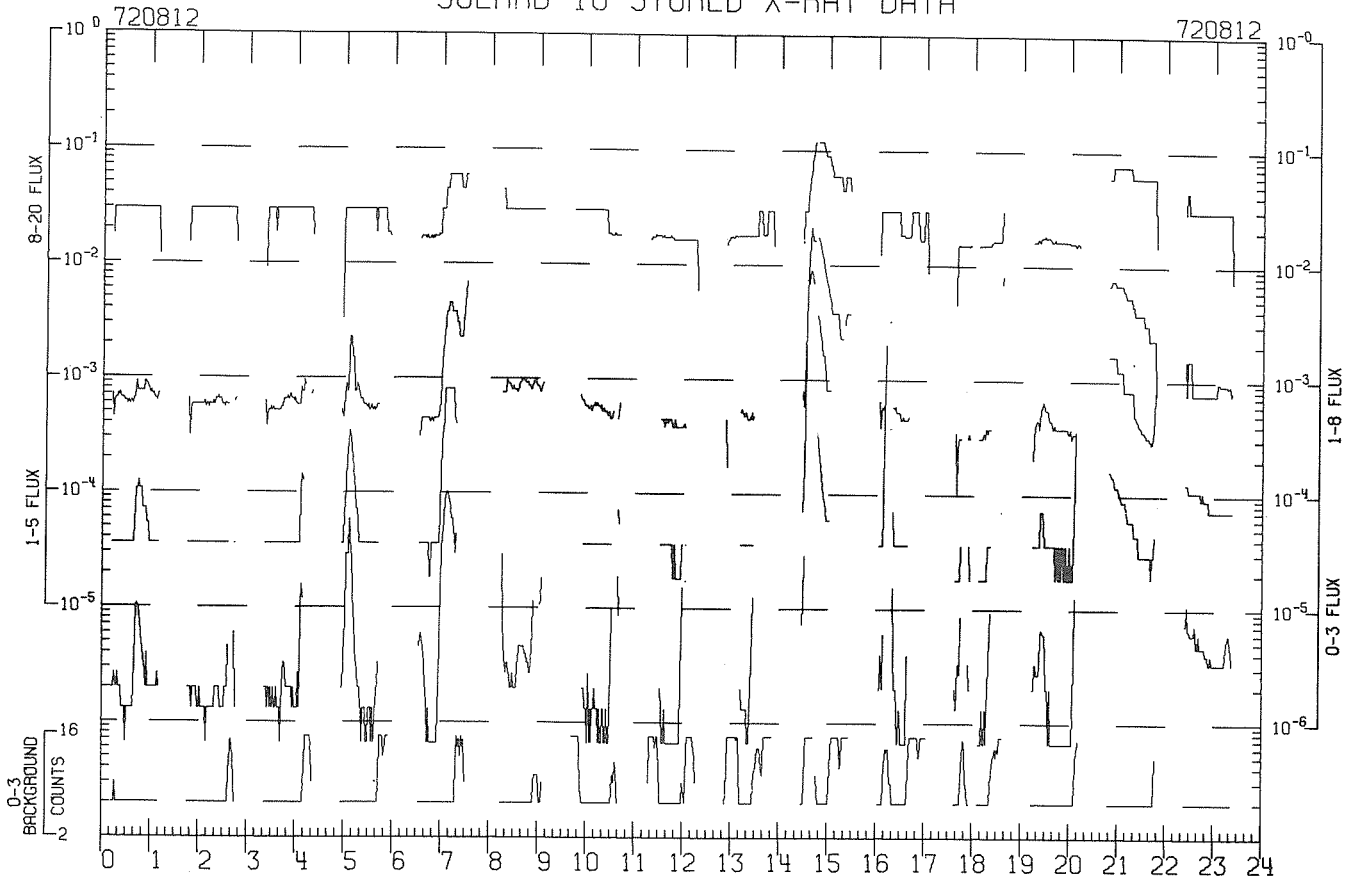
SOLRAD 9 STORED X-RAY DATA



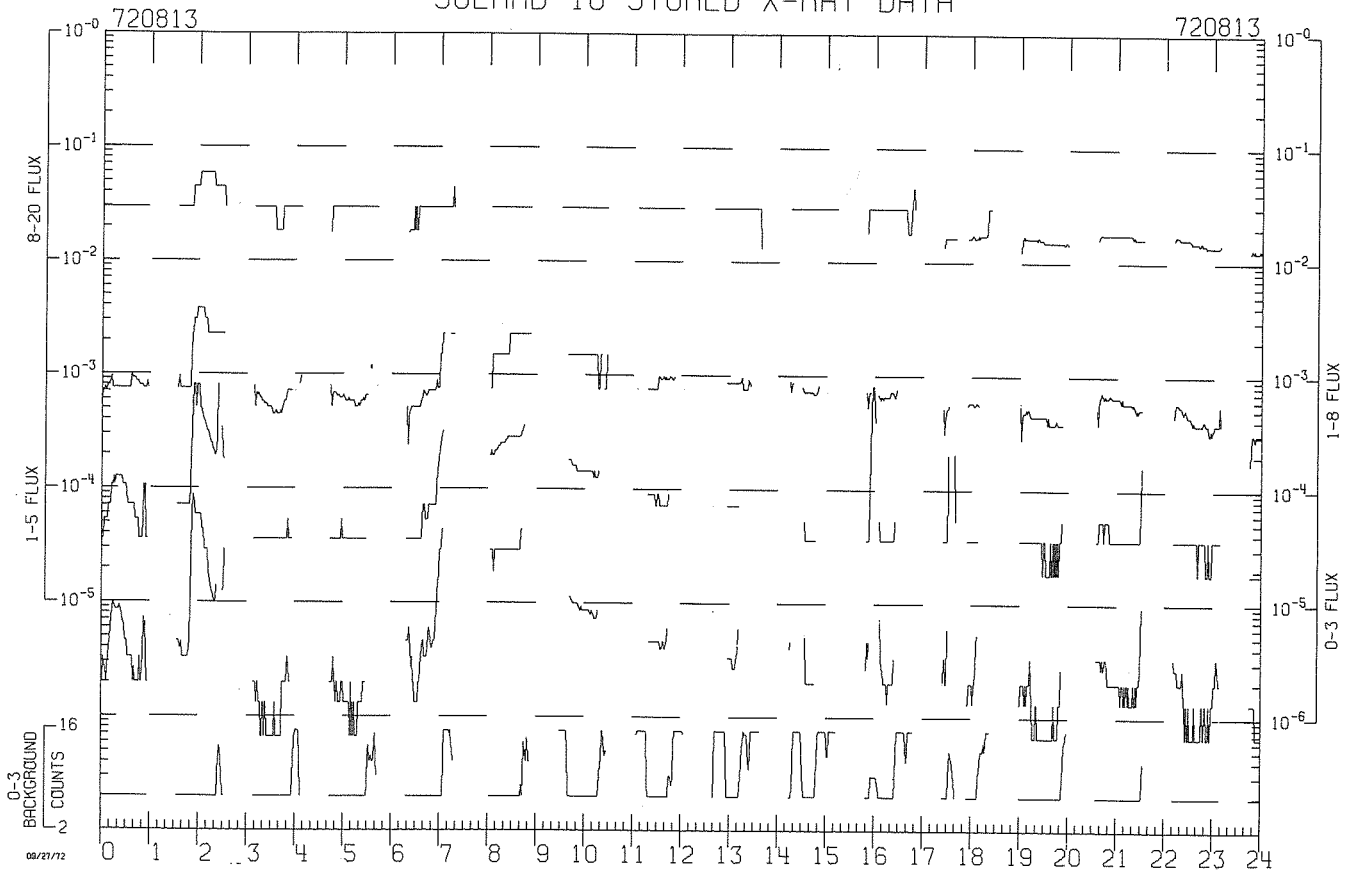
SOLRAD 10 STORED X-RAY DATA



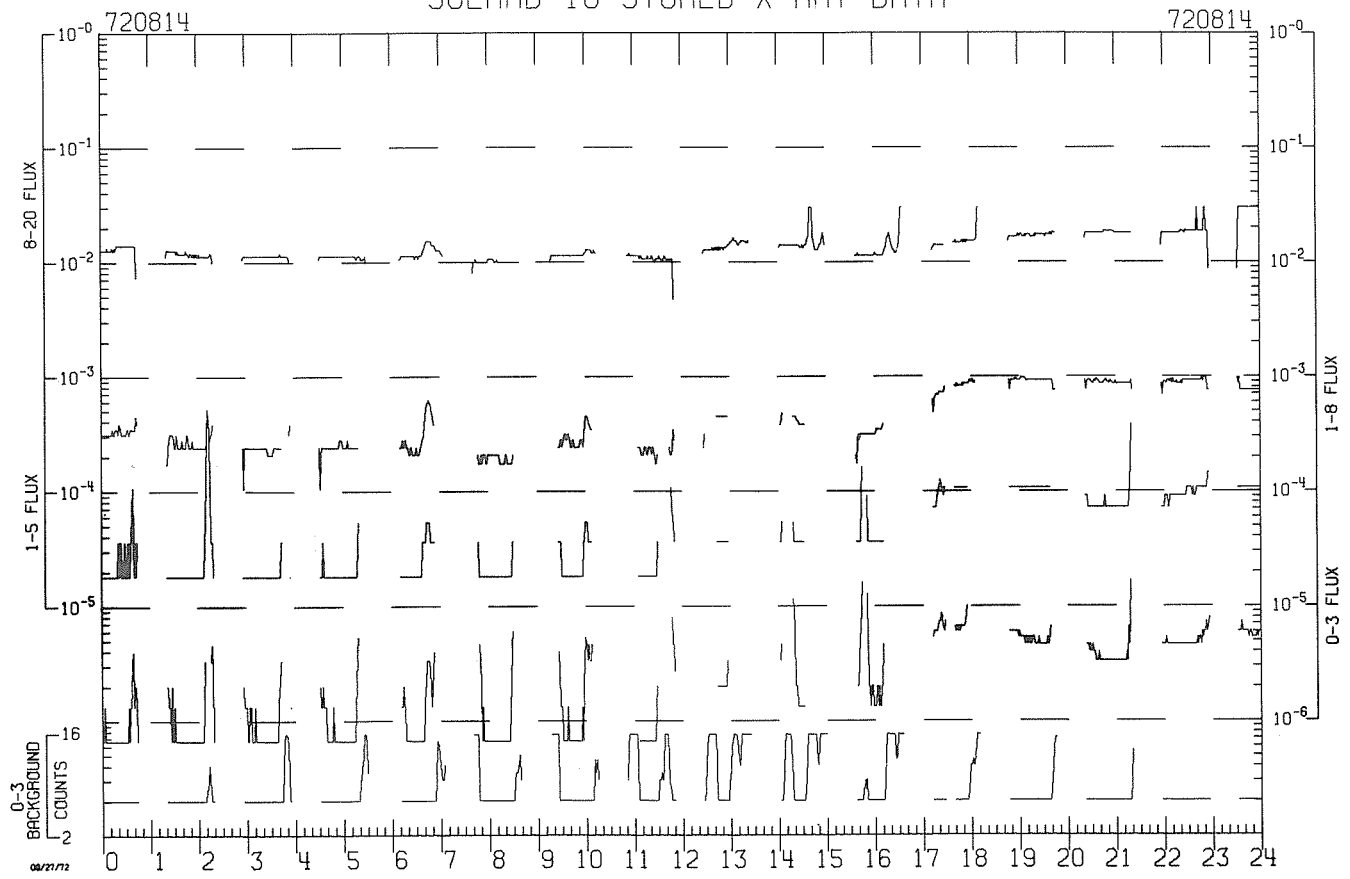
SOLRAD 10 STORED X-RAY DATA



SOLRAD 10 STORED X-RAY DATA



SOLRAD 10 STORED X-RAY DATA



Solar Flares Observed by the Hard X-Ray Spectrometer on Board
the ESRO TD-1A Satellite

by

H. F. van Beek, P. Hoyng and G. A. Stevens
Astronomical Institute
Space Research Laboratory
University of Utrecht
The Netherlands

The ESRO TD-1A satellite was launched March 12, 1972 into a near polar orbit. The orbital plane precesses 1° a day such that it will always be roughly perpendicular to the line connecting earth and sun. The Utrecht hard X-ray spectrometer is permanently sun-pointed and measures the solar radiation between 30 - 1000 keV in 12 logarithmically spaced energy channels. The time resolution is 1.2 sec for the four lowest energy channels and 4.8 sec for the other channels. The principal constituents of the instrument are a CsI crystal (effective area 5 cm^2 ; thickness 1.5 cm), photomultiplier and pulse height analyzer. Passive shielding has been applied in order to absorb Bremsstrahlung generated in the satellite; all charged particles that enter within the acceptance cone of the collimator of the instrument and that penetrate into the crystal, are also detected by two solid state detectors. Thus, events due to these particles can be rejected. Once every 38.4 sec the number of coincidences in the two solid state detectors is recorded during 4.8 sec, this number is called background (BG) and it is about equal to the number of incoming electrons with energies above $\sim 1.4 \text{ MeV}$. If necessary, it is used to correct the various photon channels for that (small) fraction of the satellite-generated Bremsstrahlung that still reaches the crystal.

The instrument includes an in-flight calibration mode. More details on the instrument are given by van Beek and De Feiter [1973] and by van Beek [1973].

During the 26 July - 14 August 1972 period, only real time data could be received. Table 1 summarizes the X-ray flares that have been reasonably covered and that, in addition, were visible against the channel background.

Table 1.

Observed X-ray Flares During The Period 26 July - 14 August 1972

imp.	OPTICAL FLARE				X-RAY FLARE	
	day August	beg. UT	max. UT	end UT	UT	
SN	1	0655		0733	0658 - 0700	
1B	2	0316	0410	0506	0313 - 0317 *	
					0326* - 0337	
SB	2	1838	1842	1859	1839 - 1841	
3B	4	0524	0634	0940	0621 - 0640*	
SB	7		0252		0251 - 0253	
3B	7	1500	1520	1700	1513:30* - 1522:30*	
					1524:50* - 1546	

* An asterisk indicates that the time mentioned corresponds to the beginning/end of real time observations while the flare was already/still visible. At the time of writing, we had not yet received all data; consequently, future extensions of this table are possible.

Discussion

Figures 1, 2 and 3 show the four best observed flares. In Figures 2 and 3 the background registration (BG) has been divided by a factor 4. As a consequence of the high solar activity, the channel boundaries on August 7 are slightly increased. In Figures 1, 2 and 3 the time (UT) mentioned corresponds to the zero of the time axis. The two big flares on August 4 and 7 consist of several (4 to 7) minor bursts with typical rise and decay times of 20 to 40 sec and a duration of $\sim 1 \text{ min}$. This phenomenon has been observed more often to occur in larger flares [Frost, 1969; Kane and Anderson, 1970; Parks and Winckler, 1971]. In addition, all four flares show a statistically significant fine structure down to 1.2 sec, the time resolution of the instrument. It is interesting to note that we have seen this fine structure in all our observations up to now. The upper limit to the decay time leads to a lower limit of the average proton density in the X-ray source region according to [Hoyng and Stevens, 1973]:

$$t_{1/2} = \frac{10^8 E_{\text{keV}}^{3/2}}{n_p} (2^{3/(2\gamma + 1)} - 1)$$

Taking $\gamma \sim 2.5$ and $E \sim 100 \text{ keV}$ we find $n_p \geq 3 \times 10^{10} \text{ cm}^{-3}$ for the large flares on August 4 and 7. It is clear that continuous and rapidly changing acceleration and injection of fast electrons occurred over the whole duration of all four X-ray flares.

Table 2

Parameters A_1 , γ_1 , A_2 and γ_2 and the position of the break, E_b , of the power law spectra which yield the best fit to the photon spectra measured during time intervals 1 through 10 of the August 4, 1972 flare (Figure 2)

Time interval	A_1	γ_1	A_2	γ_2	E_b (keV)
1	3.1×10^6	3.1	1.6×10^{10}	5.1	73
2	1.2×10^6	2.7	5.9×10^8	4.2	64
3	2.6×10^6	3.0	1.6×10^8	4.0	61
4	2.4×10^6	2.9	2.4×10^8	4.0	63
5	5.4×10^6	3.2	4.0×10^7	3.7	56
6	1.2×10^6	2.7	3.3×10^8	4.0	73
7	6.1×10^6	3.2	2.0×10^7	3.5	54
8	1.4×10^7	3.5	1.5×10^8	4.0	114
9	8.1×10^5	2.9	2.9×10^6	3.2	71
10	2.4×10^5	2.8	1.4×10^7	3.7	94

In Table 2 some spectral distributions are given for the August 4 flare. Surprisingly, it appeared that the observations fit very accurately a combination of two power law energy distributions ($I(E) = AE^{-\gamma}$ photons/sec.cm².keV). For ten selected time intervals the parameters A , γ_1 and A_2 , γ_2 (referring to the lower and higher energy part of the spectrum, respectively) are given in Table 2, together with the position of their intersection, E_b . In Table 2, the relative error of the values of A is ~4% and the absolute error in the values of γ is ~0.1; consequently, the E_b values are defined with the fairly high precision of about 5 keV. In Figure 4 three examples of measured pulse height distributions are given, together with the two component power law approximations. The occurrence of a break in the hard X-ray spectrum has been reported before [Frost, 1969; Frost and Dennis, 1971]. The E_b -values do not vary considerably with time; we remark that there is no clear steepening or flattening of the spectrum, as time progresses.

REFERENCES

- FROST, K. J. 1969 Rapid fine structure in a burst of hard solar X-rays observed by OSO-5, Ap. J., 158, L159-L163.
- FROST, K. J. and B. R. DENNIS 1971 Evidence from hard X-rays for two-stage particle acceleration in a solar flare, Ap.J., 165, 655-659.
- HOYNG, P. and G. A. STEVENS 1973 Interpretation of a hard solar X-ray Burst, Proceedings of the First Europ. Astron. Meeting, vol. 1, in press.
- KANE, S. R. and K. A. ANDERSON 1970 Spectral characteristics of impulsive solar flare X-rays ≥ 10 keV., Ap.J., 162, 1003-1018.
- PARKS, G. K. and J. R. WINCKLER 1971 The relation of energetic solar X-rays ($h\nu > 60$ keV) and high frequency microwaves deduced from the periodic burst of August 8, 1968 flare, Solar Phys., 16, 186-197.
- VAN BEEK, H. F. 1973 Development and performance of a solar hard X-ray spectrometer, Thesis.
- VAN BEEK, H. F. and L. D. De Feiter 1973 The hard solar X-ray spectrometer on board the ESRO TD-1A Satellite, Proceedings of the First Europ. Astron. Meeting, vol. 1, in press.

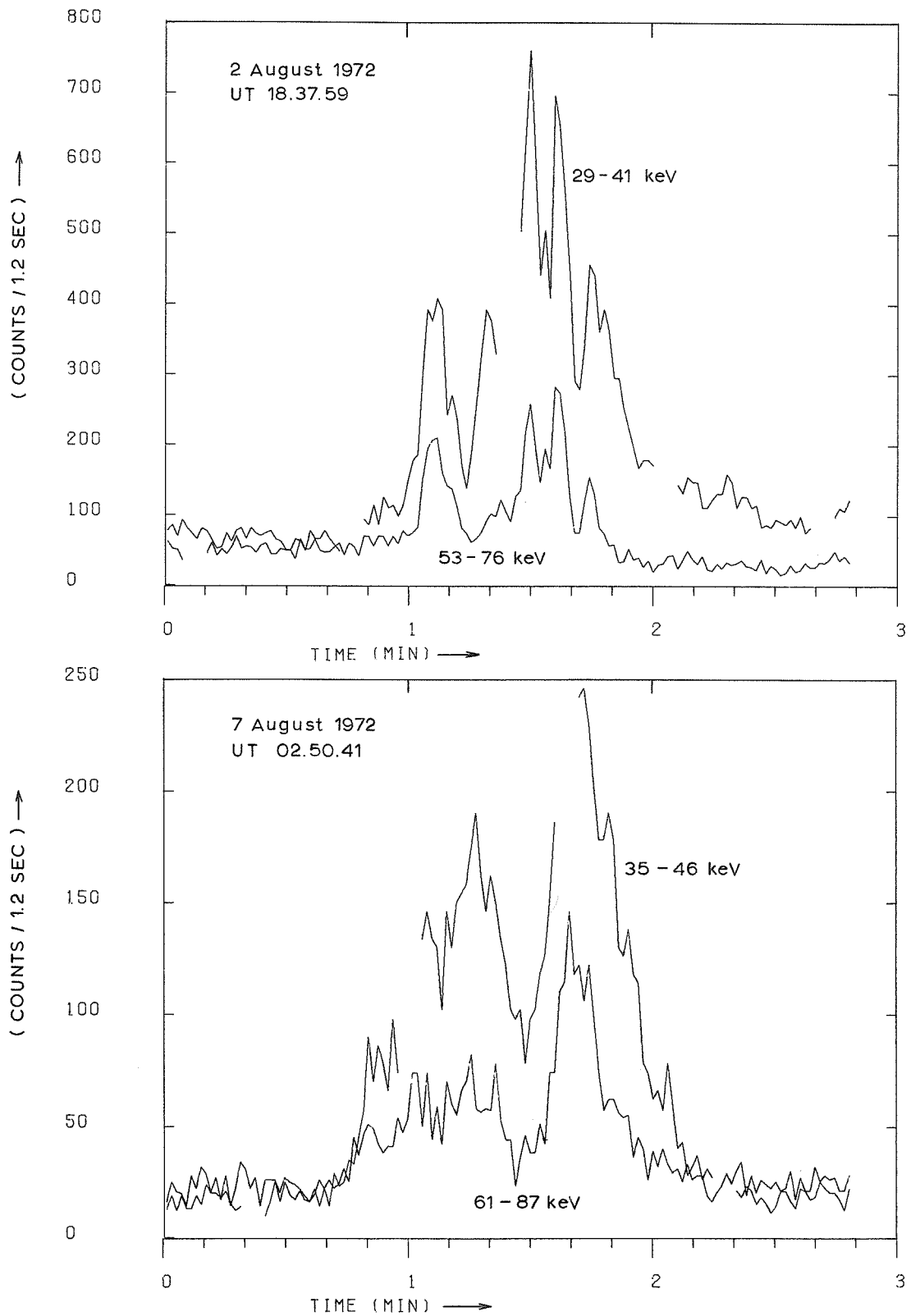


Fig. 1. Time profiles of two flares on August 2 and 7; shown are channels 1 and 3.

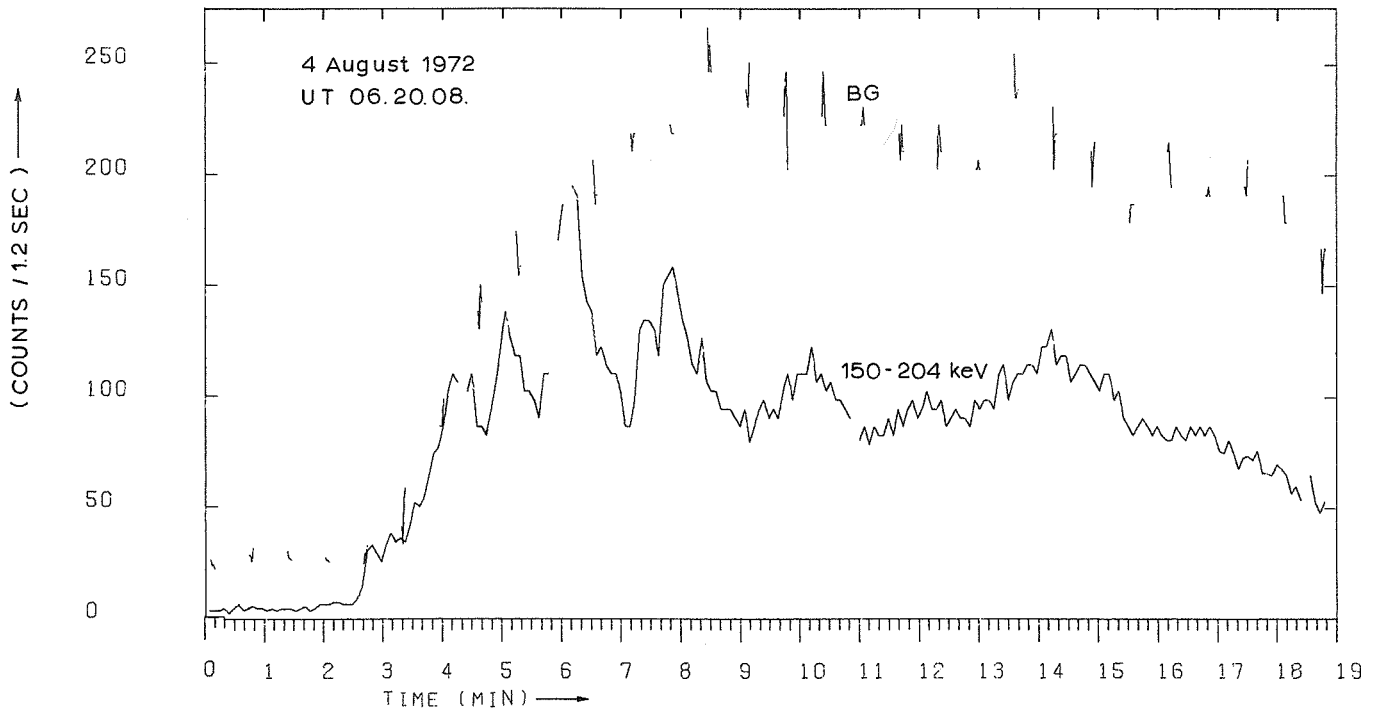
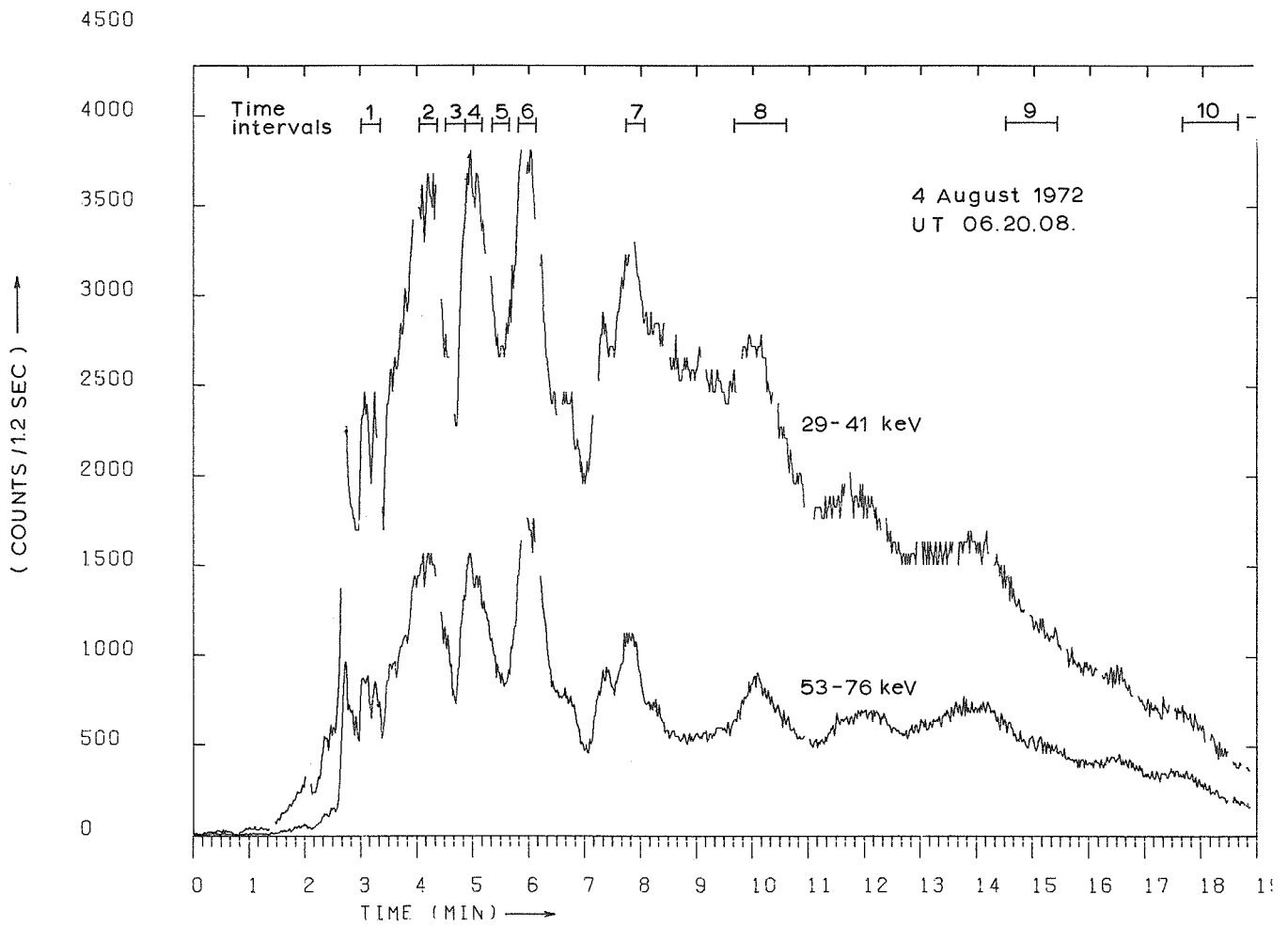


Fig. 2. Time profiles of the 3B August 4 flare; shown are the channels 1, 3, 6 and background.

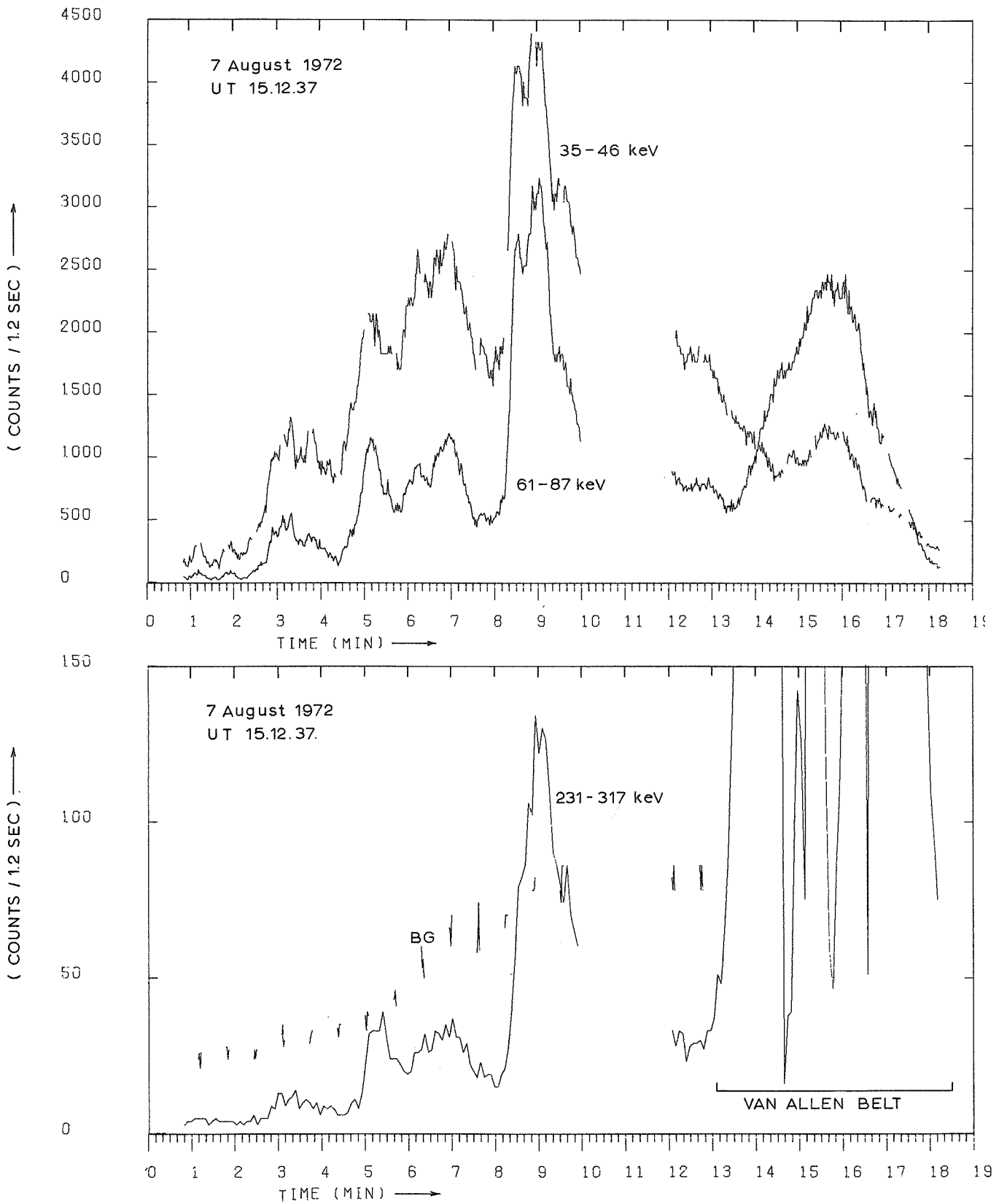


Fig. 3. Time profiles of the 3B August 7 flare; shown are the channels 1, 3, 7 and background.

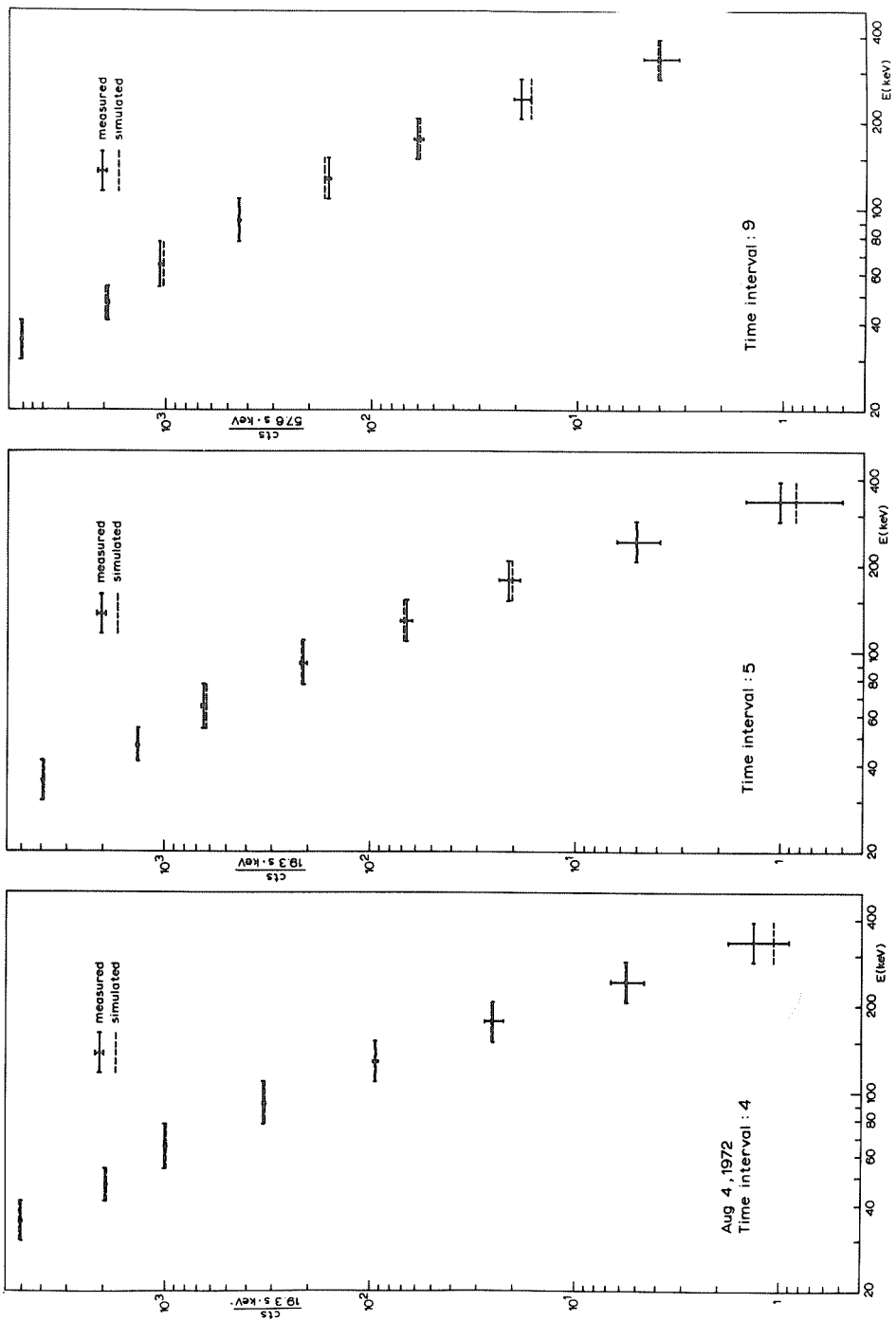


Fig. 4. Pulse height distributions measured during time intervals 4, 5 and 9 of the August 4, 1972 flare, showing the very good agreement of these distributions with those resulting from assumed combinations of two power law spectra defined by the parameters A_1 , γ_1 , A_2 and γ_2 and connected to each other at the break energy E_b . Vertical bars represent the statistical uncertainty in the measured values.

Gamma Ray Observations from OSO-7 (26 July to 14 August 1972)

by

E. Chupp*, D. Forrest, C. Reppin**, A. Suri, and C. Tsai
Department of Physics, University of New Hampshire
Durham, New Hampshire, USA

Introduction

The data presented in this report pertains to the hard x-ray and gamma ray emission from several of the larger flares that occurred in the interval 26 July to 14 August 1972. It was obtained from the University of New Hampshire's Gamma Ray Monitor on the OSO-7 satellite. The parameters of this instrument have been published [Higbie *et al.*, 1972]. Basically the gamma ray detector is a 7.6-cm by 7.6-cm NaI scintillator protected by 2- to 3-cm thick CsI shield. It accumulates two 400-channel pulse height spectra covering the energy range 0.3 to 8 MeV with a time resolution of 184 seconds. One spectrum is taken when the detector is pointing directly toward the sun (i.e., solar quadrant) and the other when the detector is pointed directly away from the sun (i.e., background quadrant). The x-ray detector measures the rates in four energy channels from 7.5 to 120 keV. It measures the full spectrum in the same two directions as above in 30 seconds. Some of the data contained here has been published earlier [Chupp *et al.*, 1973A].

Results

Figure 1 shows the rates versus time of the x-ray event associated with the 1B flare that occurred at ~ 1845 UT on 2 August 1972. To convert to a flux, one must divide by the 8 cm^2 area of the x-ray detector. The increase observed at ~ 1834 in the higher energy channels is due to trapped charged-particle effects at the spacecraft and is not associated with the flare. The saturation effect seen in the lowest energy channel is an instrumental effect. No gamma ray line emission was observed during this event.

Figure 2 shows the same rates for the event associated with the 2B flare that occurred at ~ 2050 UT on 2 August. Unfortunately, the OSO-7 spacecraft was eclipsed by the earth during the maximum of this event so that no data was obtained between ~ 2032 and 2108 UT. The postflare increase seen at ~ 2145 UT is real. This x-ray event seems to have been composed of several "bursts". The first, seen in Channels 1, 2 and 3, occurred at 2000. The second, seen in the same three channels, occurred at ~ 2025 and the last "burst" occurred at 2145 UT. Again no gamma ray line emission was observed at any time for this event.

Figure 3 shows the same time history for the event associated with the large 3B flare that occurred at ~ 0637 on 4 August 1972. Shown are rates in the four x-ray channels and the counting rate in the energy loss region 0.35 to 8 MeV as measured by the central gamma ray detector. Also shown for comparison is the time history of the 19,000 MHz radio burst from Slough, UK [NOAA Report No. UAG-21, November 1972]. The vertical dashed line shows the time (0632 UT) when the detector was eclipsed by the earth. When the spacecraft emerged from behind the earth at 0705 UT, the hard impulsive event was over and the soft x-ray event was in its decay phase.

Figure 4 shows the pulse height spectrum obtained from the central gamma ray detector during the time interval 0623 to 0632 UT. Indicated are spectra observed when looking toward the sun (solar quadrant) and when looking away from the sun (background quadrant). As can be seen, there was a definite increase in the energetic x-ray continuum. This excess was evident up to the maximum energy observed, 8 MeV. The intensity and spectra over the full energy range is not known at present because of unfolding difficulties; however, in the energy range 350 to 700 keV, the excess solar flux agrees with a power law shape with an index of ~ 3 and an intensity of 10^{-2} photons per $\text{cm}^2 \text{sec keV}$ at an energy of 400 keV. Also indicated in Figure 4 is the evidence for two of the four gamma ray lines that were observed from the sun in this same time period. The indicated lines are the 511 keV line from positron annihilation and the 2.23 MeV line from neutron capture by hydrogen. The other two were the 4.43 and 6.13 MeV lines from excited states of C^{12} and O^{16} . The time history of the emission of these lines although limited by the 180-second time resolution of the central detector and limited statistics, is consistent with the time history of the 0.35 to 8 MeV rate.

Figure 5 shows the time history of the event associated with the 3B flare that occurred at ~ 1534 UT on 7 August 1972. Shown are the rates in the four x-ray channels and the flux at 15,400 MHz observed at Sagamore Hill [Solar-Geophysical Data Report No. 342, February 1973]. Again note that the OSO-7 spacecraft was eclipsed during the maximum of the flare between 1500 to 1535 UT.

* Alexander von Humboldt Scholar and honorary Fulbright-Hayes Fellow at the Max-Planck Institute, Garching b. Munich, Germany.

** Presently on leave from the Max-Planck Institute, Garching b. Munich, Germany.

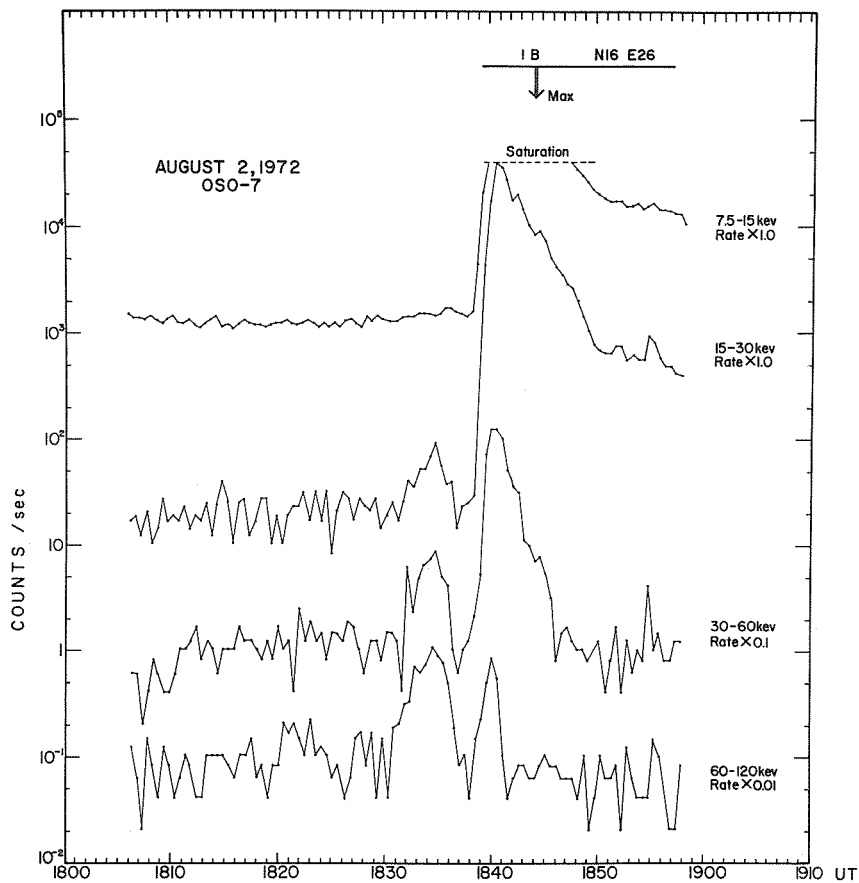


Fig. 1. The time history of the hard x-ray event associated with the 1B flare on 2 August 1972.

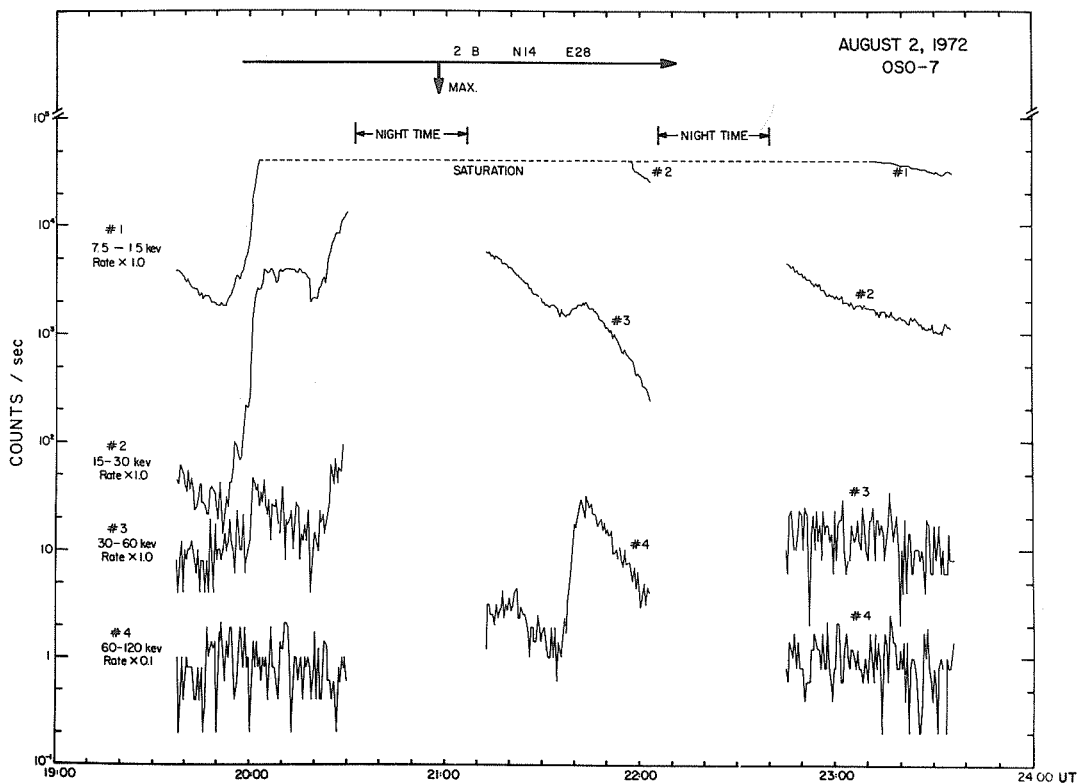


Fig. 2. The time history of the hard x-ray event associated with the 2B flare on 2 August 1972.

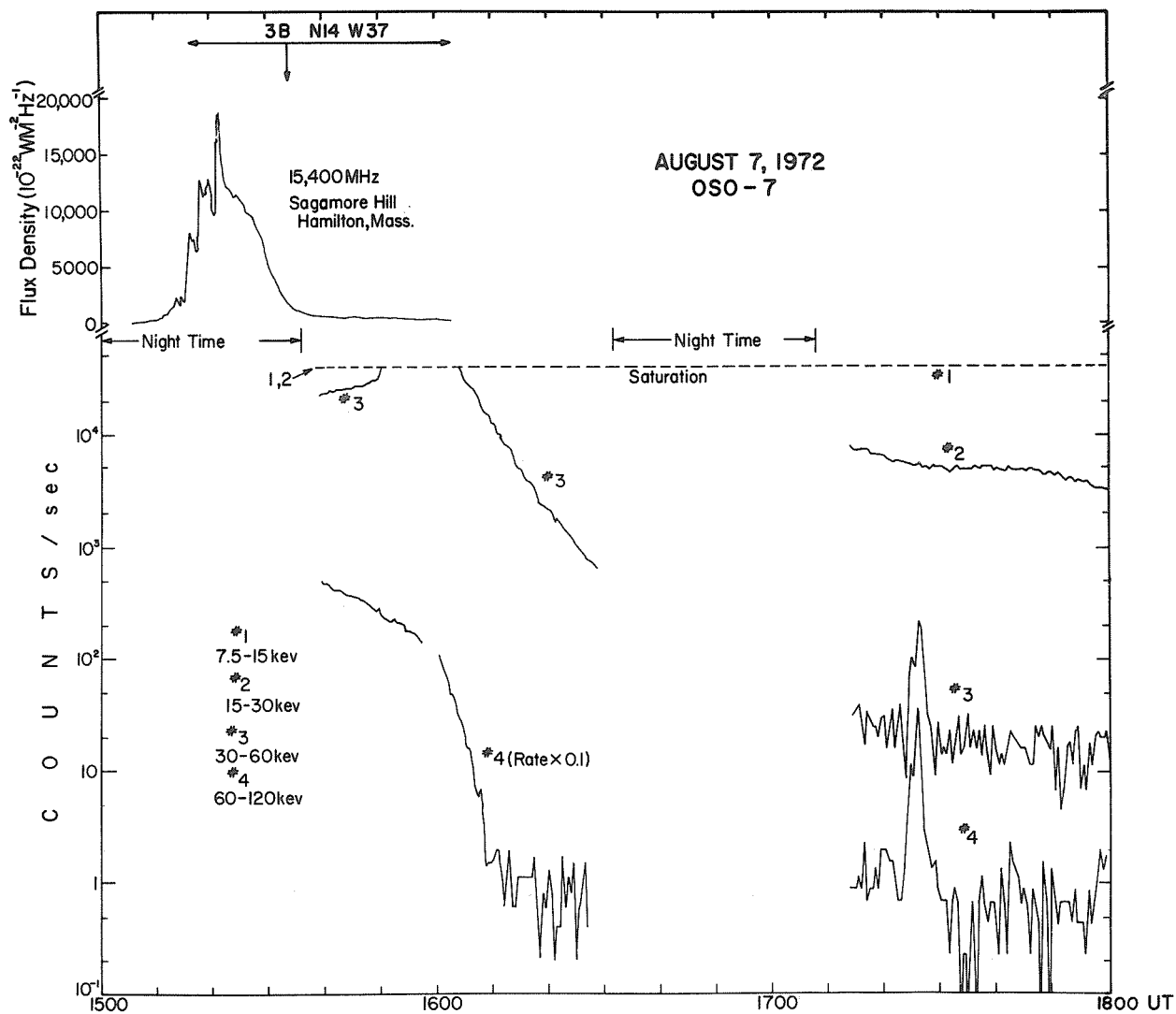


Fig. 5. The time history of the hard x-ray and radio event associated with the 3B flare on 7 August 1972.

The radio history indicates that the impulsive flash phase of the event was over by the time the OSO-7 came out from behind the earth and, in fact, no x-rays with energies greater than 120 keV were observed. However evidence for gamma ray line emission was observed at 511 keV and 2.23 MeV from 1538 to 1547 UT. The flux in these lines is given in Table I. Note that the increases seen in x-ray Channels 3 and 4 at ~1725 UT are due to local trapped charged particles and are not associated with the flare event.

Table I

Associated Flare and the time of Observations	Designations and Solar Flux at 1 AU Photons $\text{cm}^{-2}\text{sec}^{-1}$			
	0.5 MeV	2.2 MeV	4.4 MeV	6.1 MeV
3B ($\text{H}\alpha$) 4 Aug 1972 0624 - 0633 UT (Before $\text{H}\alpha$ Max)	$(7 \pm 1.5) \times 10^{-2}$	$(2.2 \pm 0.2) \times 10^{-1}$	$(3 \pm 1) \times 10^{-2}$	$(3 \pm 1) \times 10^{-2}$
3B ($\text{H}\alpha$) 7 Aug 1972 1538 - 1547 UT (After $\text{H}\alpha$ Max)	$(3.7 \pm 0.9) \times 10^{-2}$	$(4.8 \pm 1) \times 10^{-2}$	$< 2 \times 10^{-2}$	$< 2 \times 10^{-2}$

Interpretation

The results presented here represent the first clear evidence for energetic neutral nuclear secondaries produced in association with a solar flare. It has been shown earlier [Chupp et al., 1973B] that it is extremely unlikely that the gamma ray lines observed can be produced by thermonuclear reactions on the sun. The gamma ray lines observed and ratio of their intensities agree with theoretical predictions for the results from interaction of the energetic solar charged-particles interacting with the solar atmosphere [Lingenfelter and Ramaty, 1967]. Hence the time history that we have observed is either that of the acceleration of these energetic particles in the solar chromosphere or the dumping of a portion of the accelerated particles into the lower chromosphere or corona. The observation of the 511 keV and the 2.23 MeV line after the impulsive flash phase on 7 August is expected because some of the sources of positrons are radioactive nuclei with long half lives (i.e., C^{11} and N^{13}) and the absorption time for thermal neutrons in the photosphere is 100 to 200 seconds.

Acknowledgments

This work was supported by NASA under Contract Nas 5-11054 and Grant NGL 30-002-021.

REFERENCES

- CHUPP, E. L., 1973A Solar Gamma Ray Lines Observed during the Solar Activity of August 2 to August 11, 1972, Nature, 241, 333
D. J. FORREST,
P. R. HIGBIE,
A. N. SURI,
C. TSAI and
P. P. DUNPHY
- CHUPP, E. L., 1973B Gamma Ray Production in Solar Flares, Bull. Am. Phys. Soc.,
D. J. FORREST and 18, 100.
A. N. SURI
- HIGBIE, P. R., 1972 A Gamma Ray Monitor for the OSO-7 Spacecraft, IEEE Trans.
E. L. CHUPP, Nucl. Sci., NS-19, 606.
D. J. FORREST and
I. U. GLESKE
- LINGENFELTER, R. E. and 1967 High Energy Nuclear Reactions in Solar Flares, in High
R. RAMATY Energy Nuclear Reactions in Astrophysics, ed: B. S. P.
Shen, (New York: W. A. Benjamin Press), p. 99.

Particle Observations of the August 1972 Solar Events by Explorers 41 and 43

by

J. W. Kohl and C. O. Bostrom
The Johns Hopkins University
Applied Physics Laboratory
Silver Spring, Maryland

and

D. J. Williams
NOAA Environmental Research Laboratories
Boulder, Colorado

The data presented here is from the Solar Proton Monitoring Experiments on board Explorers 41 and 43 for the time period 2-12 August 1972.

Projections of the orbits of Explorers 41 and 43 onto the ecliptic plane, during the time of the observations of the August 1972 event, are shown in Figure 1. Direction markers are shown by the large arrowheads to indicate the paths of the satellites in their orbits. Heavy tick marks along the paths are shown at the beginning of a day - with the day of year indicated. Light tick marks along the paths are shown at 4-hour intervals. The projection of the bow shock and magnetopause are average values [Fairfield, 1971] and are shown here only as an aid to orientation and scaling. It can be seen that during the interval 2-12 August 1972 the orbit plane of Explorer 41 is in the late morning hours, local time, and Explorer 43 is in the early morning hours, local time. On 4 August (day 217), at the time of the peak fluxes, Explorer 41 is well into the magnetosphere and Explorer 43 is inbound toward the magnetosphere. Although it cannot be seen from the projections in Figure 1, it should be pointed out that the satellites are at high latitude, so data can be used deep into the magnetosphere without contamination by the radiation belts.

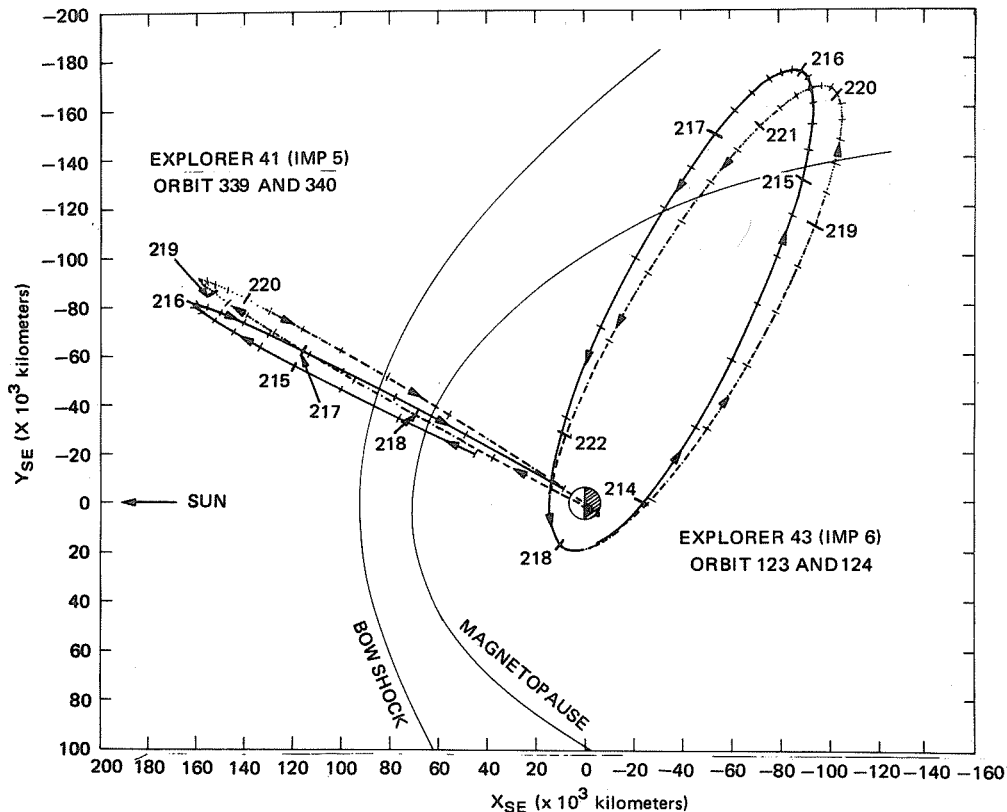


Fig. 1. Explorers 41 and 43 orbit projections onto the ecliptic plane for the period 1-9 August 1972 (days of year 214 to 222).

The integral fluxes of protons for energies >60 , >30 , and >10 Mev are presented in Figure 2 as hourly averages from 2-12 August 1972 with Explorer 41 data shown as solid lines and Explorer 43 data shown as points at the start of each hour. It is worthwhile mentioning at this point that: 1) data for $L < 10 R_E$ have been omitted, and 2) the $E_p > 10$ Mev channels have an efficiency of $\sim 25\%$ for electrons with $E_e > 700$ keV. Also shown on this Figure are solar flares and sudden commencements during this time interval - data for which were obtained from preliminary reports [Report UAG-21, Lincoln and Leighton, ed., 1972] and are subject to revision.

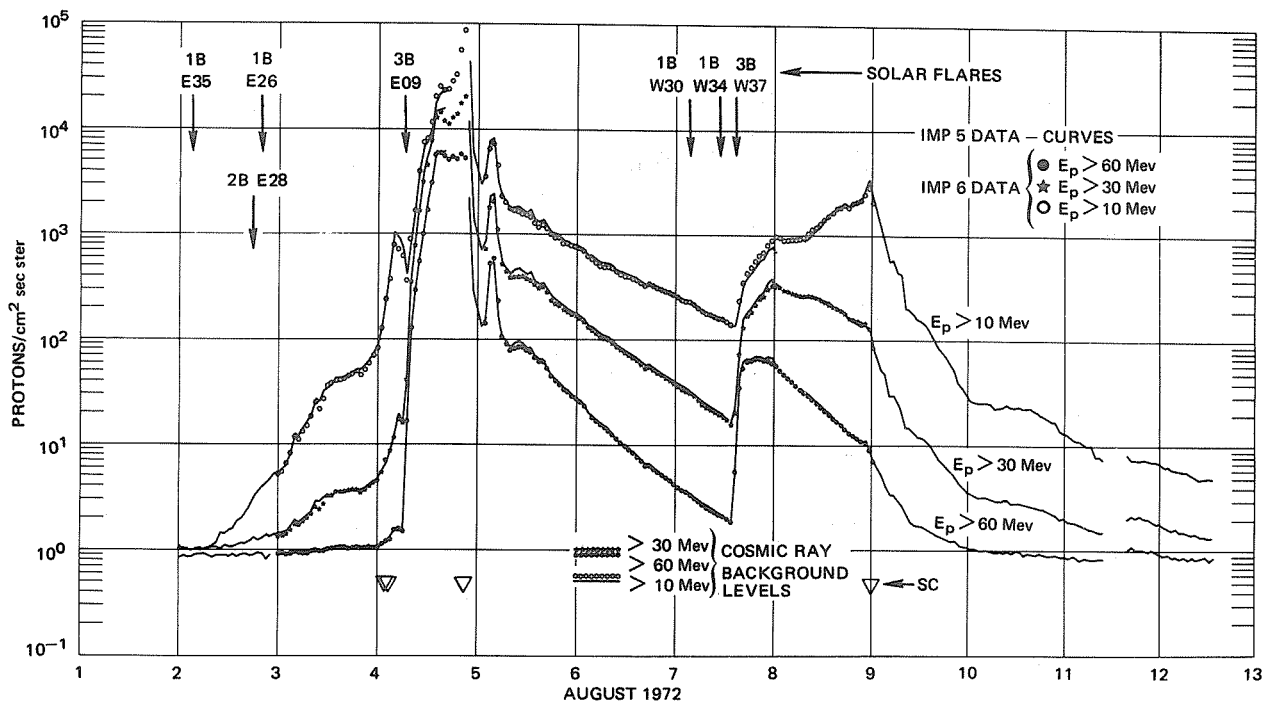


Fig. 2. Solar proton fluxes from the Solar Proton Monitoring Experiment (IMP 5 and 6) are given in hourly averages for energies >60 , >30 and >10 Mev for the period 2-12 August 1972. Explorer 41 data are solid lines; Explorer 43 data are discrete points at the start of each hour. Also indicated are solar flares and sudden commencements.

The presence of particles on 2 and 3 August is probably due to the small east hemisphere flares on 2 August. There is a gradual rise in all three channels which peak early on 4 August, about the same time as the sc's occur. Following a short decay, particles again begin arriving between 0700 and 0800 UT on 4 August - probably from the flare at solar longitude E09. The flux in all three channels continues to increase to peak values of 7.8×10^4 , 2.5×10^5 , and 1.1×10^6 protons/cm²sec ster for protons >60 , >30 , and >10 Mev, respectively - reached simultaneously at ~ 2200 UT on 4 August. At this time there is an sc followed by a rapid decline in particle fluxes which continues until approximately 0300 UT on 5 August when particles increase to a short plateau lasting until 0530 UT. This short increase is seen in both Explorers 41 and 43, with a time lag of ~ 10 minutes by Explorer 43. All channels then decay uniformly until 7 August. The integrated fluxes from ~ 0700 UT on 4 August to ~ 1500 UT on 7 August were 2.4×10^9 , 8×10^9 , and 2×10^{10} protons/cm² for protons >60 , >30 , and >10 Mev, respectively.

At approximately 1533 UT on 7 August, particle fluxes again begin to increase abruptly - most likely due to the 3B flare at longitude W38 at 1500 UT. The absolute increase is the same for all three channels, indicating a very hard spectrum. Peak fluxes for this event are 7×10^1 , 3.8×10^2 , and 3.5×10^3 protons/cm²sec ster for proton energies >60 , >30 , and >10 Mev, respectively. The integrated fluxes are less than for the 4 August event by a factor of 8.5 for the >10 Mev and a factor of 40 for the >60 Mev protons. Concurrent with an sc at ~ 0000 UT on 9 August there is a change in slope in the flux profiles leading to background values.

Particle fluxes from the differential channels of SPME on Explorers 41 and 43 are presented in Figure 3. The Explorer 41 data are hourly averages shown as solid lines for the proton energy range $1 < E_p < 10$ Mev and for the alpha energy range $1 < E_\alpha < 10$ Mev/nucleon. The Explorer 43 data are presented as hourly averages shown at the beginning of each hour. (The energy ranges for protons are

.21 < E_p < .56 Mev and 1 < E_p < 10 Mev, which were calculated from .56 < E_p < 2.2 Mev and 2.2 < E_p < 7.5 Mev channels to compare with Explorer 41). The Explorer 43 alpha particle energy range is 2 < E_α < 5 Mev/nucleon. The Explorer 43 proton channel, .21 < E_p < .56 Mev, is subject to electron contamination (with low efficiency) for electrons with E_e > .15 Mev. Perigee data (L < 10 R_e) have been omitted. Also shown in this Figure are solar flares and sudden commencements occurring in this time interval.

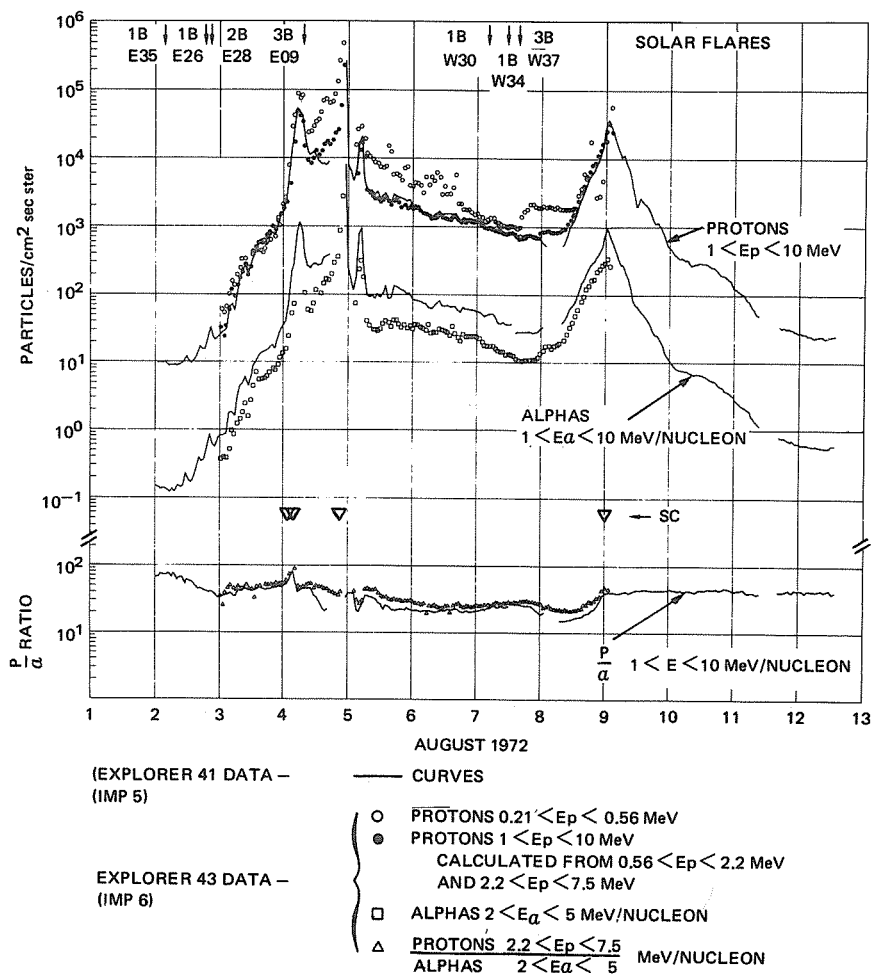


Fig. 3. Solar particle fluxes from the Solar Proton Monitoring Experiment (IMP 5 and 6) are given in hourly averages for energies >60, >30 and >10 Mev for the period 2-12 August 1972. Explorer 41 data are solid lines; Explorer 43 data are discrete points at the start of each hour. Also indicated are solar flares and sudden commencements.

In general, the flux profiles for the lower energy differential channels for protons and alphas are similar to the higher energy integral channels. The observed peak fluxes occurring late on 4 August were 2.8×10^5 protons/cm²sec ster for the 1-10 Mev protons, 8.3×10^3 alphas/cm²sec ster for the 1-10 Mev/nucleon alphas, 5.1×10^5 protons/cm²sec ster for the 0.21-0.56 Mev protons, and 2.8×10^3 alphas/cm²sec ster for the 2-5 Mev/nucleon alphas. The spike early on 5 August is again observed by both satellites in the lower energy ranges. The structure in the low energy proton channel on 5 and 6 August may be due to electron contamination in the magnetospheric tail or sheath region due to its finite efficacy for electrons. Electrons arriving soon after the flare are the cause of the sudden increase in the 0.21 - 0.56 Mev proton channel around the middle of 7 August and lasting to the middle of 8 August. Fluxes in the lower energy proton and alpha channels then gradually increase until at approximately 0000 UT on 9 August, coincident with a sudden commencement, the fluxes begin to decrease toward normal background levels.

Also shown in the lower profile of Figure 3 are the proton-to-alpha ratios from Explorer 41 in the 1-10 Mev/nucleon range (shown as a solid line) and from Explorer 43 in the 2-5 Mev/nucleon range (shown as hourly points). During the time interval shown, the ratios from the 2 satellites track fairly closely - allowing for the slightly different energy ranges - and remain in the range from 16 to 90. The differences near the end of 4 August and beginning of 8 August are probably due to magnetospheric effects seen by Explorer 41. It is interesting to note that after 9 August the proton-alpha ratio remains essentially constant even though the fluxes drop by approximately three orders of magnitude.

REFERENCES

- | | | |
|--|------|--|
| BOSTROM, C. O.,
J. W. KOHL,
R. W. McENTIRE and
D. J. WILLIAMS | 1972 | The solar proton flux - August 2-12, 1972, JHU/APL Preprint, November 1972. |
| FAIRFIELD, D. H. | 1971 | Average and unusual locations of the earth's magnetopause and bow shock, <u>J. Geophys. Res.</u> , <u>76</u> , 6700-6716. |
| KOHL, J. W. and
C. O. BOSTROM | 1972 | Observations of the August '72 solar events by the solar proton monitor on Explorer 41, <u>Trans. Am. Geophys. Un.</u> , <u>53</u> , No. 11. |
| LINCOLN, J. V. and
H. I. LEIGHTON | 1972 | Preliminary compilation of data for retrospective world interval July 26 - August 14, 1972, <u>World Data Center A for Solar-Terrestrial Physics, Report UAG-21.</u> |

by

R. P. Lin and K. A. Anderson
 Space Sciences Laboratory, University of California
 Berkeley, California 94720

ABSTRACT

We present observations of 18 to ~ 300 keV electrons and 29 to 2000 keV protons from the IMP-5 and IMP-6 spacecraft for the period 19 July - 14 August 1972.

The energetic particle observations presented here are from the University of California, Berkeley, experiments aboard the IMP-5 and 6 (Explorer 41 and 43) spacecraft.

IMP-5

The IMP-5 experiment consists of six thin mica window Geiger Mueller detectors, three of which are oriented parallel to the spin axis (P1, P2 and P3) and three perpendicular (E1, E2, E3). Two detectors, P2 and E2, observe the particle flux backscattered off a gold foil. Since the proton scattering efficiency is negligible compared to electrons, these detectors respond only to > 45 keV electrons. Two detectors, E1 and E3, also respond to solar X-rays since they view the sun on every spin. The energy ranges provided by each detector is given in Table 1. All the detectors are shielded against side wall penetration by ~ 2.5 g/cm² of copper and steel. Thus, ≥ 45 MeV protons and ≥ 4 MeV electrons are able to penetrate the side shielding and produce counts as well as much low energy particles entering the window.

Figure 1 shows the hourly average counting rate of each detector for the period of observation. To obtain fluxes simply divide the counting rate by the detector geometric factor given in Table 1.

The IMP-5 experiment was inadvertently turned off from 19 to 26 July. The large regular peaks are when the spacecraft enters the terrestrial trapped radiation. IMP-5's orbital plane is approximately perpendicular to the ecliptic plane and the apogee ($\sim 28.7 R_p$) is contained in the ecliptic plane. During the August events the apogee was located at $\sim 330 \pm 15^\circ$ ecliptic longitude.

Further information on the IMP-5 experiment is contained in Anderson and Lin [1970].

Table 1

IMP-5 DETECTOR CHARACTERISTICS

Detector Designation	Type of Detector	Sensitivity				Geometry Factor cm ² ster	Look Angle FWHM	Angle to Spin Axis
		Window	Electrons	Protons	X-ray			
P1	LND 705 GM tube	0.5 mg/cm ² mica	>18 keV	>0.25 MeV	None	2.7×10^{-2}	40°	0°
P2	LND 7041 GM tube in scatter configuration	1.5 mg/cm ² mica	>45 keV	---	None	6.3×10^{-2}	70°	0°
P3	LND 7041 GM tube with Al foil	3.0 mg/cm ² mica and 4.5 mg/Al	>80 keV	>1.5 MeV	None	0.75	70°	0°
E ₁	LND 7041 GM tube, thick window	13 mg/cm ² mica	>120 keV	>2.3 MeV	3-20 keV*	1.03	70°	90°
E ₂	LND 7041 GM tube in scatter configuration	1.5 mg/cm ²	>45 keV	---	None	6.5×10^{-2}	70°	90°
E ₃	LND 7041 GM tube with Al foil	2.7 mg/cm ² mica and 4.5 mg/Al	>80 keV	>1.5 MeV	1-20 keV*	0.86	70°	90°
IC	4" diameter spherical, Neher type integrating ionization chamber	210 mg/cm ² Aluminum skin	>0.7 MeV	>12 MeV maximum sensitivity ~ 17 MeV	≥ 20 keV	~ 80 cm ² omnidirectional	(Not operating during this period)	

*X-ray range -- 0.1% efficiency points

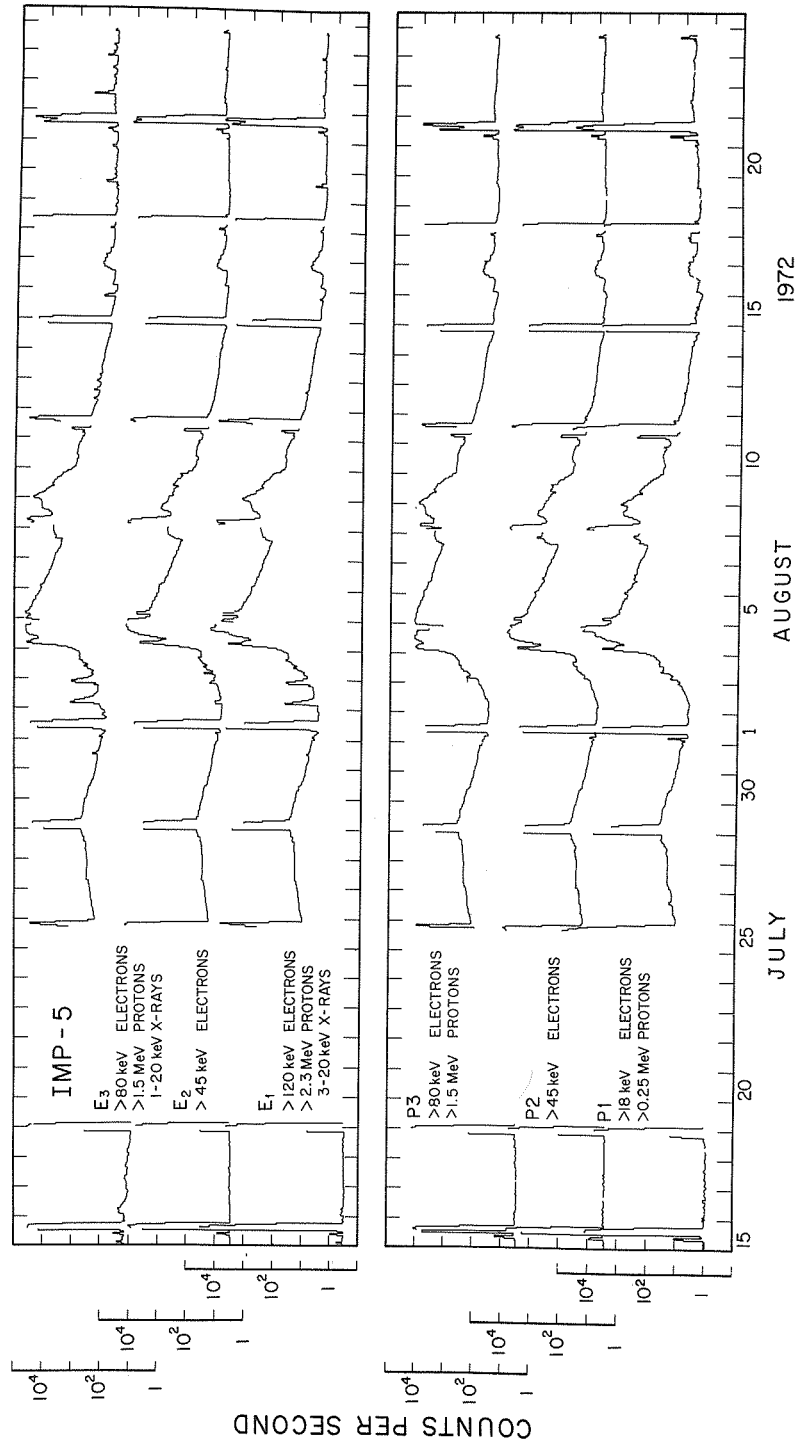


Fig. 1. Hourly average counting rate of the six Geiger Mueller detectors of the UCal IMP-5 experiment. To convert to flux ($\text{cm}^2 \cdot \text{sec} \cdot \text{ster}^{-1}$) divide count rate by the geometric factors given in Table 1.

The University of California experiment aboard the IMP-6 spacecraft consists of two semiconductor detector telescopes and two Geiger Mueller detectors. The two semiconductor detector telescopes are mounted on a thermally isolated cold plate in front of the package. This plate is covered with a special coating to provide a large emissivity/absorptivity ratio. Although the plate views the sun for a portion of each spin of the spacecraft, the equilibrium temperature of the plate ranges from -68°C at launch to $\sim -50^{\circ}\text{C}$ two years later. The surface barrier detectors used in the telescopes have optimal resolution and threshold noise characteristics below $\sim -20^{\circ}\text{C}$.

One telescope (P3) opens directly into space, has no foil covering, and consists of three elements: the first measures the energy of stopping particles and the third provides anticoincidence against penetrating particles. Because of the detectors' sensitivity to light, this telescope is pointed nearly parallel to the spin axis and is carefully collimated to eliminate scattered sunlight. P3 measures electrons from 18 keV to ~ 500 keV and protons from 29 keV to ~ 2 MeV. Pitch angle measurements of electron fluxes are provided by the second telescope, E1. Protons are eliminated from E1 by forcing all particles to backscatter off a curved gold foil before they can reach the detector. The collimation provides a $15^{\circ} \times 50^{\circ}$ aperture for E1, and its counting rate is sectorized into 16 angular sectors per spin at one energy threshold (~ 45 keV) and four sectors per spin at a higher energy threshold (~ 80 keV). Anticoincidence against penetrating particles is provided by the second detector.

The two Geiger Mueller detectors are similar to those flown on previous IMP spacecraft. Both have very thin (0.5 mg/cm^2) mica windows. One GM detector observes particles backscattered off a gold foil as in E1. Electrons >18 keV and protons >250 keV are detected by the open counter. The scatter counter responds only to electrons >18 keV. Table 2 summarizes the detector complement for the UCal experiment aboard IMP-6.

In order to take advantage of the high inherent energy resolution of the cooled surface barrier detectors in the P3 assembly the output is pulse height analyzed into 64 channels through the onboard computer (OBC). Only four broad energy channels are shown here, along with the E1 (>45 keV) and P1 counting rate. These are plotted in hourly averages in Figure 2.

The apogee is $\sim 31.2 R_E$ and the ecliptic longitude at apogee varies from -102° to -130° (toward dawn) during these observations. Much of the rapidly varying fluxes observed by P3 are ≤ 100 keV terrestrial upstream protons (see July 15-27). The large regular spikes are crossings of the terrestrial trapped radiation zones. Further information on the IMP-6 instrumentation is contained in Anderson and Lin [1972].

Table 2
IMP-6 DETECTOR CHARACTERISTICS

Detector Designation	Detector Type	Sensitivity		Geometric Factor cm^2ster	Look Angle FWHM	Angle to Spin Axis	Channels
		Electrons	Protons				
E1	Surface barrier semiconductor detector in scatter geometry; anticoincided against penetrating particles	47-350 keV	None	0.011	$15^{\circ} \times 50^{\circ}$	90°	47-350 keV electrons in 16 sectors per spin 80-350 keV electrons in 4 sectors per spin Coincidence Rate
P1	Open Geiger Müller detector with 0.5 mg/cm^2 mica window	>18 keV	>0.25 MeV	0.027	35°	$\sim 10^{\circ}$	---
P2	Geiger Müller detector with 0.5 mg/cm^2 mica window in scatter geometry	>20 keV	None	2.5×10^{-3}	35°	$\sim 10^{\circ}$	---
P3	Three element telescope made up of surface barrier semiconductor detectors, one for anticoincidence against penetrating particles	18-450 keV	29 keV 2 MeV	0.10	37°	$\sim 10^{\circ}$	deposited energy 18-38.5 keV 38.5-75.9 75.9-139 139-450 0.34-2.0 MeV protons 64 channel PHA 18-450 keV

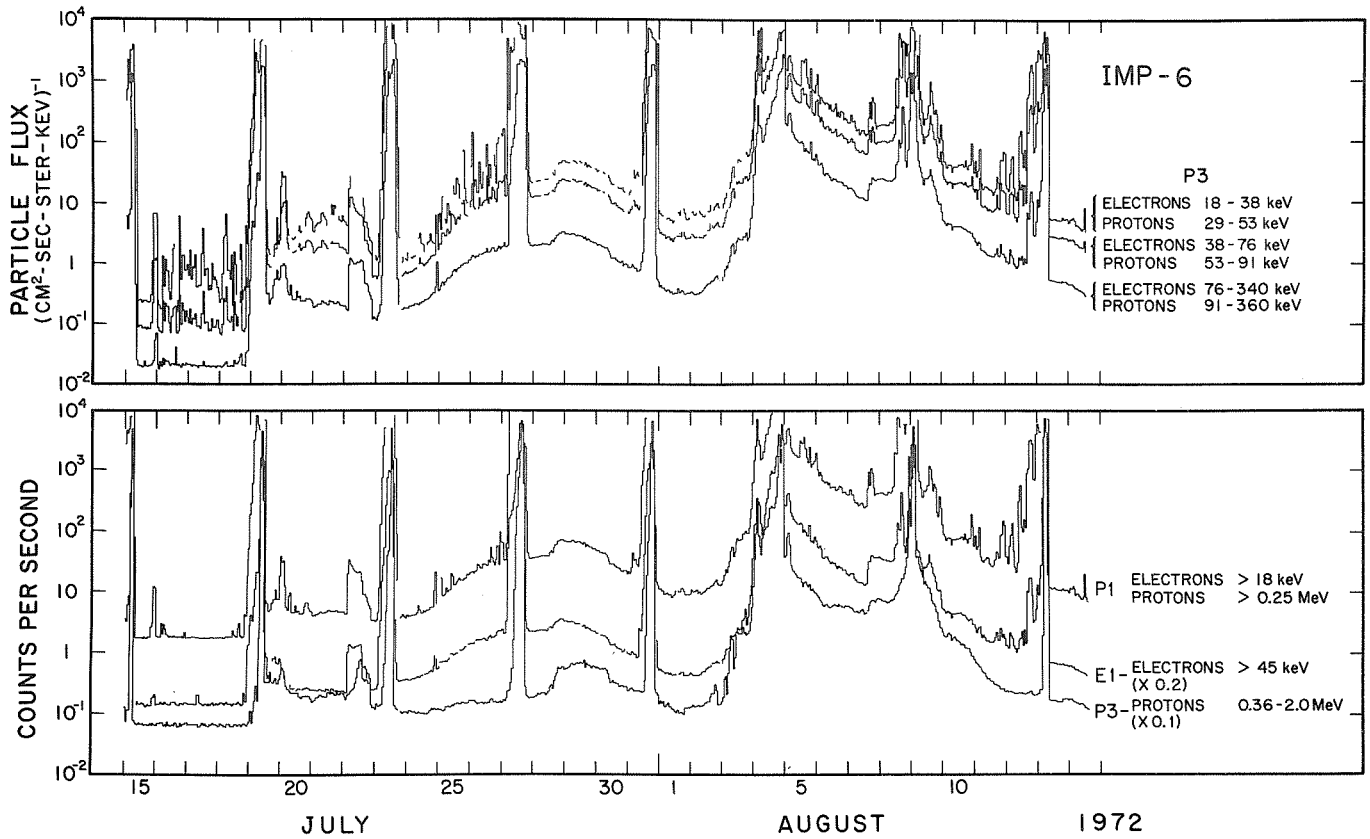


Fig. 2. Hourly average counting rates and fluxes measured by the detectors in the UCal IMP-6 experiment. Note that the E1 and P3 rates in the lower panel are multiplied by factors of 0.2 and 0.1 respectively. The particle fluxes may be obtained for the bottom panel by dividing by the geometric factors given in Table 2.

REFERENCES

ANDERSON, K. A. and R. P. LIN 1970

Information on the University of California Experiments in the Explorer 33 and 35 Satellites (Lunar Anchored IMP's) and the Explorer 34 and 41 Satellites (IMP's 4 and 5), UC Berkeley Space Sciences Laboratory Report, Series 11, Issue 89.

ANDERSON, K. A. and R. P. LIN 1972

First Year Report on the University of California Experiment on the Explorer 43 (IMP-6) Spacecraft, UC Berkeley Space Sciences Laboratory Report, Series 13, Issue 10.

Low Energy Interplanetary Particles during the August 1972 Events

by

L. J. Lanzerotti and C. G. MacLennan
Bell Laboratories
Murray Hill, New Jersey, 07974

The accompanying four Figures contain proton, alpha particle, and electron data measured at 1 A.U. during the period of large solar activity in McMath region 11976 in August 1972. The solar particle observations were made with a semiconductor detector telescope instrument [Lanzerotti *et. al.*, 1969] flown by Bell Laboratories on the Explorer 41 satellite. A more complete description and discussion of the data contained in the Figures is given in a paper by Lanzerotti and MacLennan [1974].

REFERENCES

LANZEROTTI, L. J., 1969
H. P. LIE, and
G. L. MILLER

A solar cosmic ray particle spectrometer with on-board particle identification, IEEE Trans. Nucl. Sci., NS16, 343.

LANZEROTTI, L. J. and 1974
C. G. MACLENNAN

Solar particle observations during the August 1972 event, Proc. 7th ESLAB Symp.: Correlated Interplanetary and Magnetosphere Observations, D. Reidel, Dordrecht-Holland.

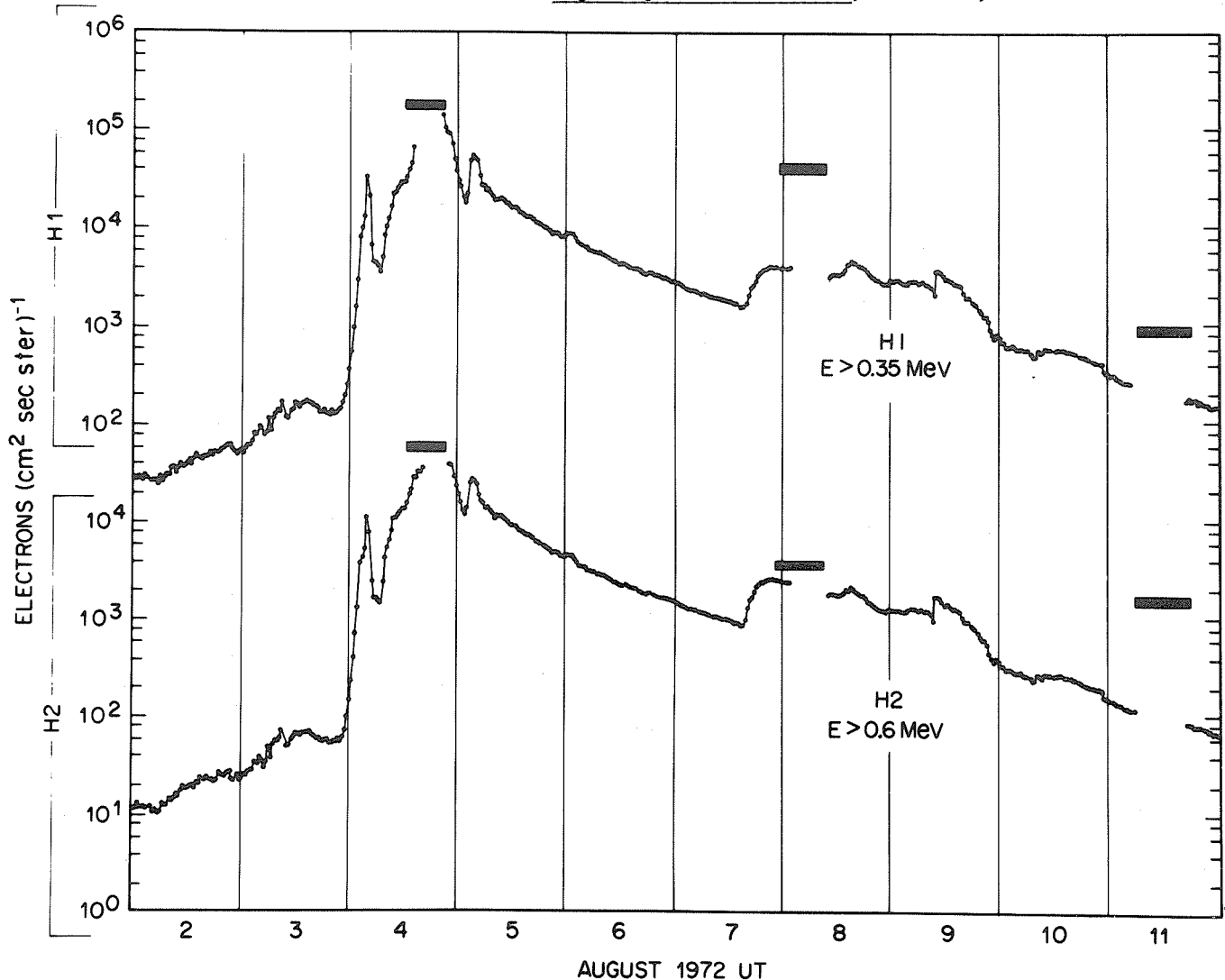


Fig. 1. Electron fluxes measured in two energy channels on Explorer 41 during the August events. The solid bars indicate passage of the space craft through the magnetosphere.

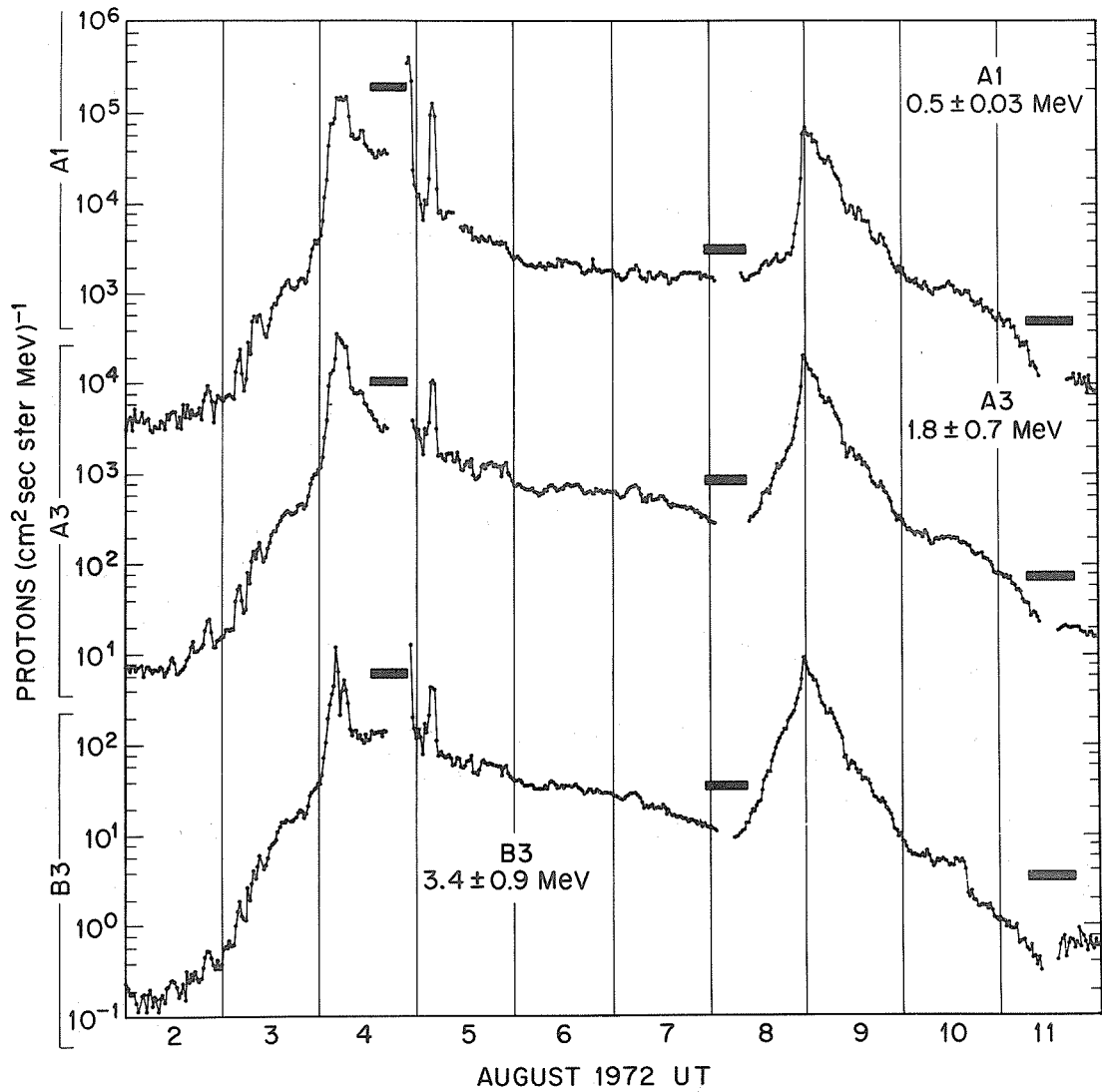


Fig. 2. Proton fluxes measured in three differential energy channels on Explorer 41 during the August events. These data show that the 7 August event was not observed at low energies until just prior to the interplanetary shock on 8 August.

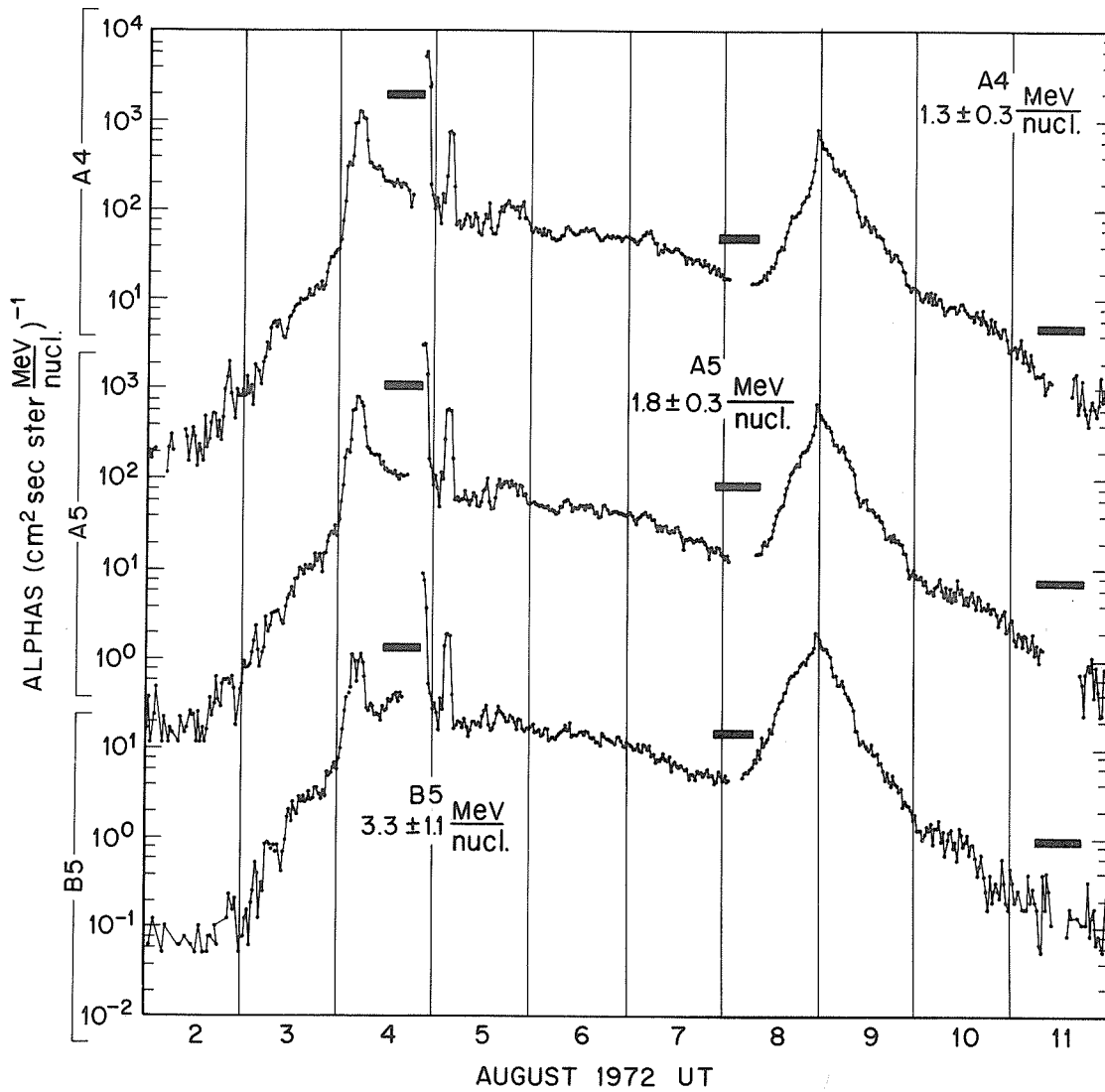


Fig. 3. Alpha particle fluxes measured in three differential energy channels on Explorer 41 during the August events.

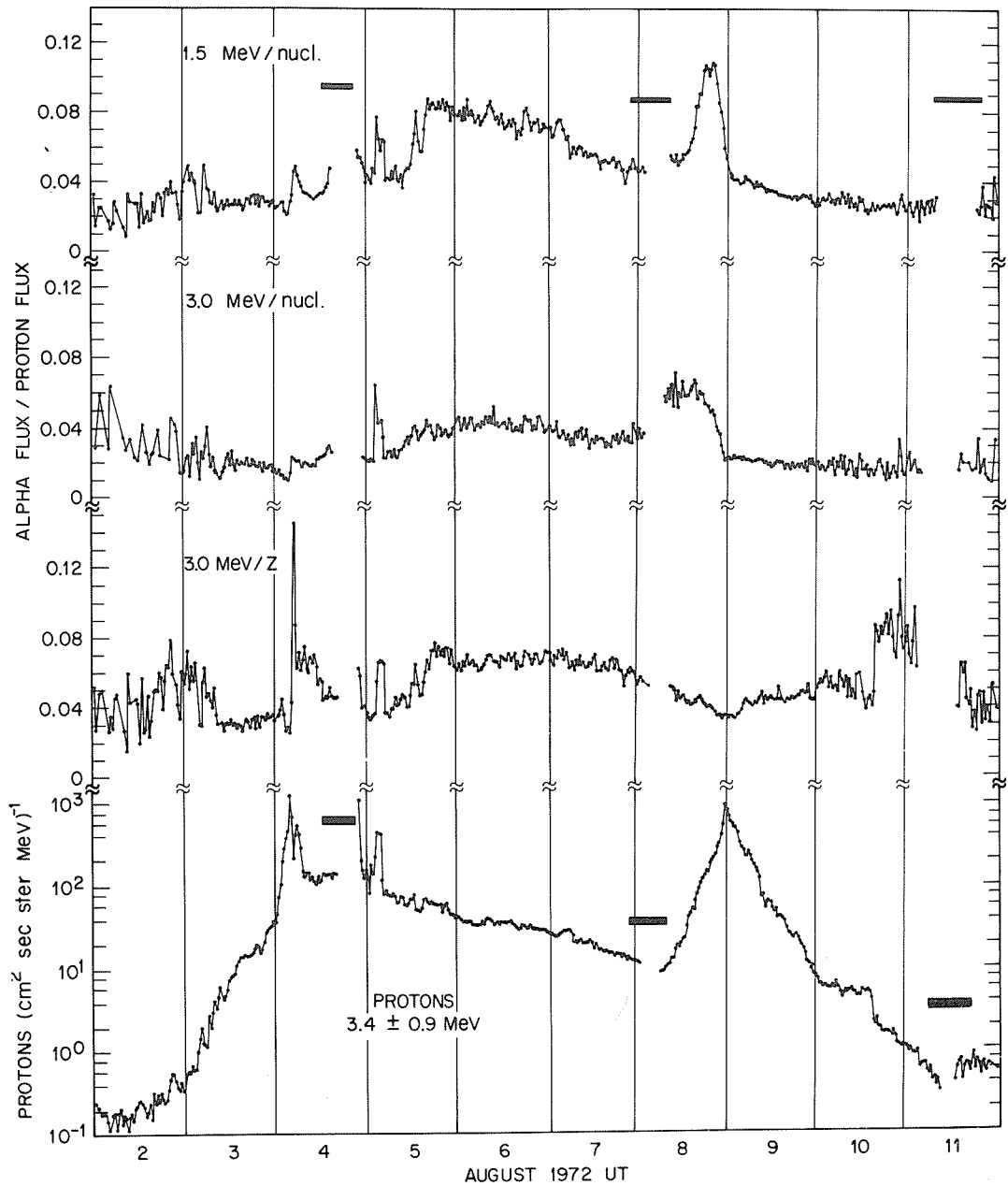


Fig. 4. Alpha-to-proton flux ratios during the August events. The ratios are plotted for equal velocity (MeV/nucleon) and equal energy per charge particles. Plotted at the bottom are the time-intensity fluxes of 3.4 ± 0.9 MeV protons.

MeV Electrons, Protons and Alpha Particles, August 2-13, 1972

by

V. Domingo, D. Köhn, D. E. Page, B. G. Taylor and K-P. Wenzel
Space Science Department (ESLAB)
European Space Research and Technology Centre
Noordwijk, The Netherlands

The HEOS-2 spacecraft, launched on January 31, 1972, is a spin stabilized satellite in a highly eccentric orbit having an apogee of 240,000 km at high Northern ecliptic latitude.

Here we report results of the measurements made by a solid state particle detector system oriented at 90 degrees to the spin axis. The detector system, described in detail by Köhn *et al.* [1972], is basically a two element telescope composed of a 500 microns thick surface barrier silicon detector, and a 6 mm thick lithium-drifted detector inside a plastic scintillator cup viewed by a photomultiplier and used in anticoincidence. The half opening angle of the detector system is 33°. The geometrical factor, which is slightly energy dependent, is about 1.1 cm² sterad.

The combination of two solid state detectors is used to differentiate between electrons, protons and alpha particles by the total energy versus energy loss method, and the pulse height from the thick detector is used to produce energy spectrum information in four levels. Table 1 lists the energy channels.

Table 1

<u>PARTICLES</u>	<u>ENERGY CHANNELS</u>				
	<u>ENERGY WINDOWS</u>				
electrons	0.45-0.76	0.76-1.18	1.18-1.77	1.77-3.5	MeV
protons and alpha particles	9.3-12.2	12.2-17.0	17.0-27.7	27.7-35.7	MeV/ Nucleon

The quoted energies are computed from energy loss data. Therefore in the case of the electrons, they must be taken only as rough estimates since internal scattering introduces serious distortions in the particle energy to energy loss conversion function.

In normal mode, spectral measurements are made every 128 seconds. When the experiment is switched to angular mode, it can produce four 90 degrees sector measurements for protons and alpha particles and eight for electrons every 512 seconds.

The August 1972 activity period is superimposed on a long period of high solar particle fluxes that extends for more than two solar rotations, from July 19 to September 15, 1972. In Figures 1 and 2 we show the 12-hour average count rate for protons of 9.3 to 35.7 MeV and for electrons of 0.45 to 3.5 MeV measured between July 14 and September 21.

Figures 3, 4 and 5 show the fluxes of electrons, protons and alpha particles respectively, each in four energy channels during the maximum activity period. The proton fluxes show evidence of saturation on August 4, from 1200 to 2340 UT. The electron measurements during the same period have been disregarded and must be considered as distorted during the period from 1000 UT August 8 to 1000 UT August 9 due to saturation and contamination effects introduced in the detector amplifier by the high proton fluxes. HEOS-2 was inside the magnetosphere on August 5, from 0300 to 1400 UT, and on August 10 from about 0100 to 2400 UT, and the crossing of the radiation belts can be seen in all three Figures. The bars at the top of the Figure indicate the starting times of all solar flares of importance greater than 1 N.

Figure 6 shows the fluxes of electrons, protons and alpha particles in the different energy channels, during the onset of the August 7 event. Table 2 lists the most likely arrival times for each particle channel. The electrons clearly arrived before the protons and alpha particles. Within the time and flux accuracy of our measurements it is not possible to observe any difference in the arrival times of the different electron energy channels.

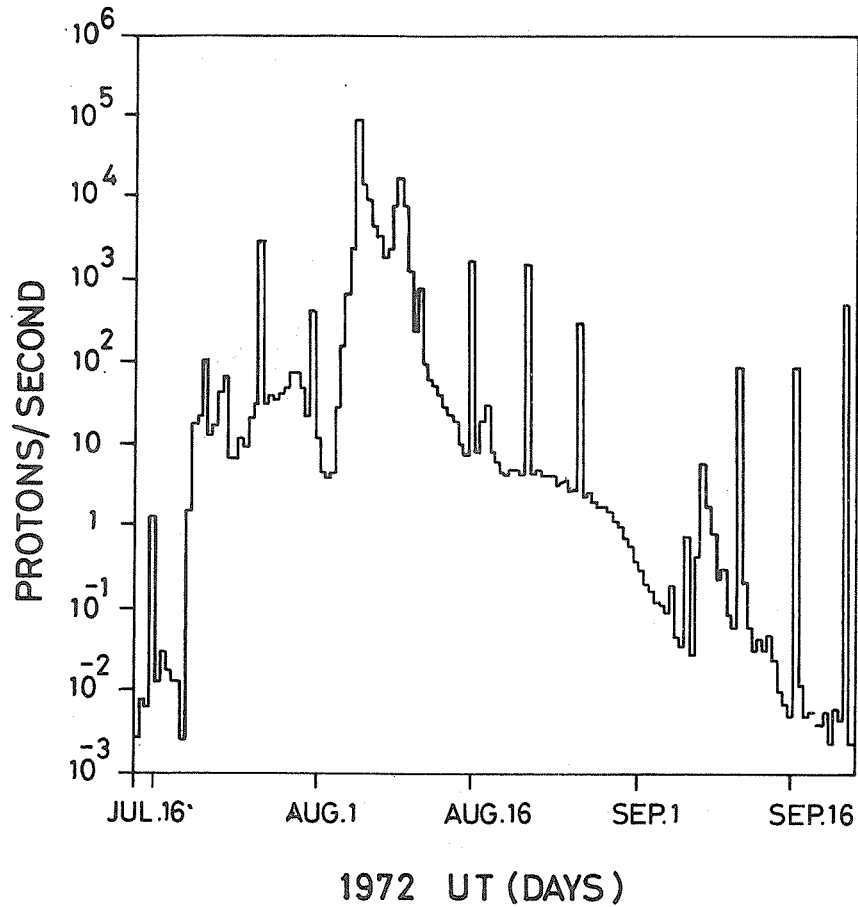


Fig. 1 Count rate of 9.3-35.7 MeV protons measured in HEOS-2 and averaged over 12-hour periods, from July 14 to September 21, 1972. The regular spikes every 5.2 days are produced by the crossing of the radiation belts.

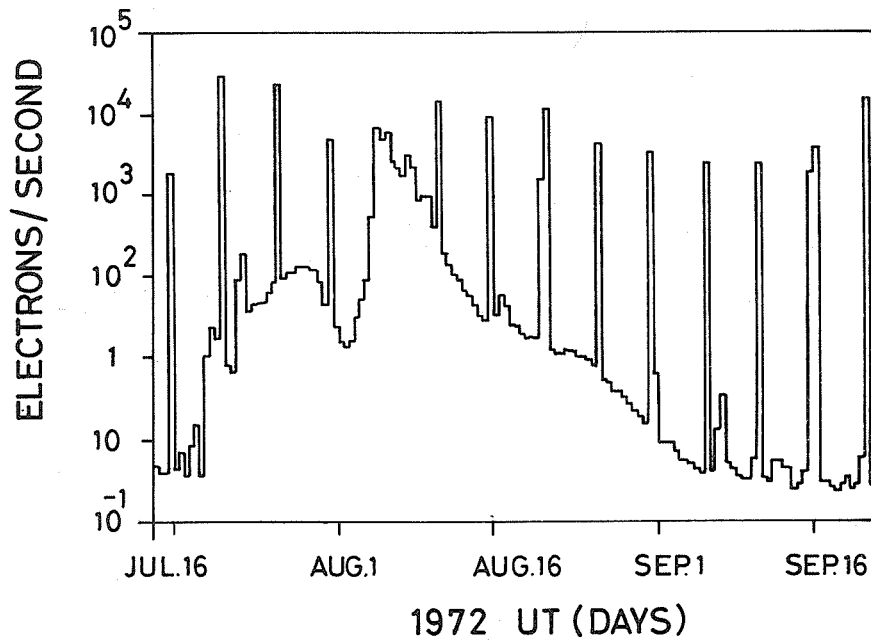


Fig. 2 Count rate of 0.45-3.5 MeV electrons measured in HEOS-2 and averaged over 12-hour periods, from July 14 to September 21, 1972. The regular spikes every 5.2 days are produced by the crossing of the radiation belts.

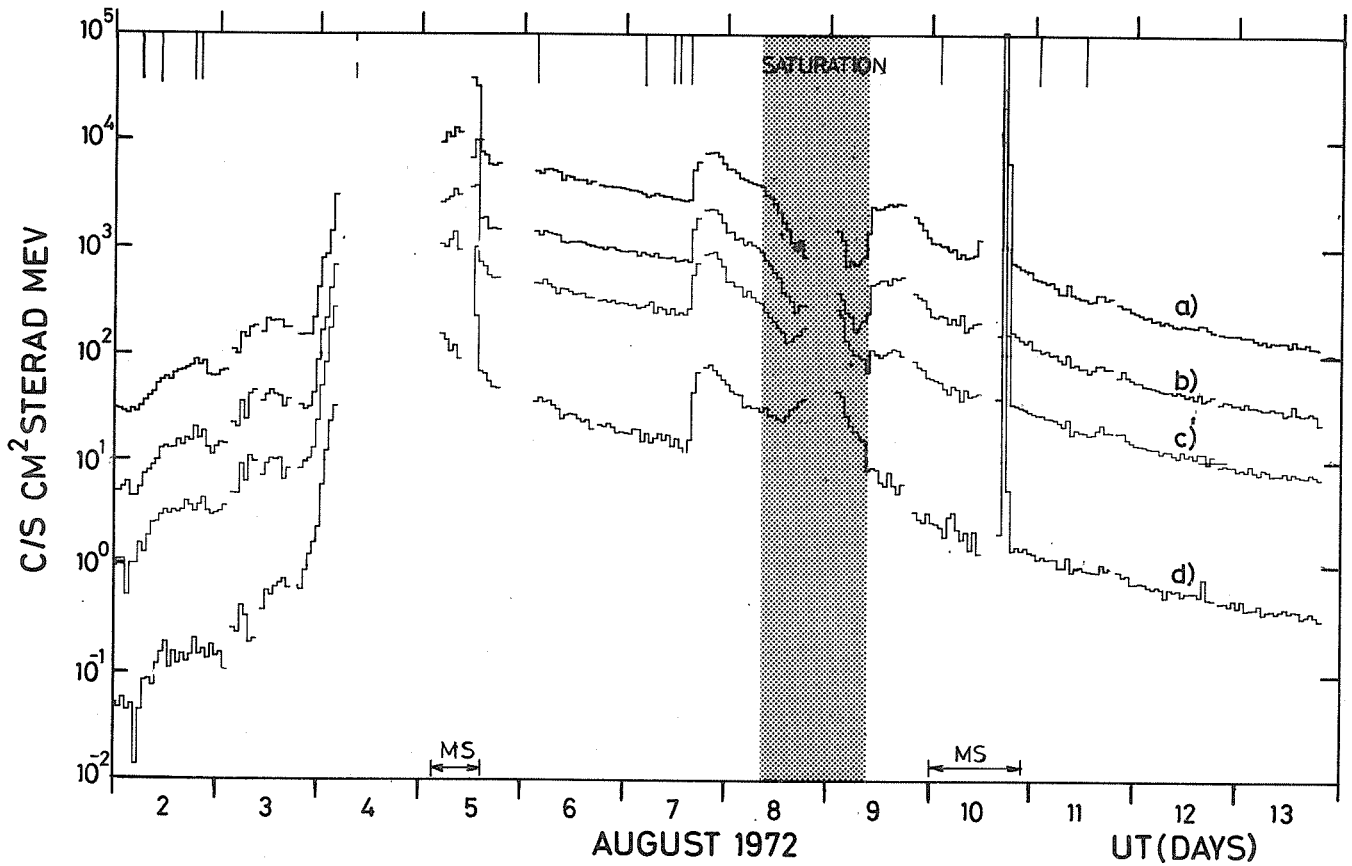


Fig. 3 Electron fluxes measured in HEOS-2 and averaged over one hour periods. Energy intervals are: a) 0.45-0.76 MeV, b) 0.76-1.18 MeV, c) 1.18-1.77 MeV, d) 1.77-3.5 MeV. (Used energy windows, geometrical factors and efficiencies are rough estimates.)

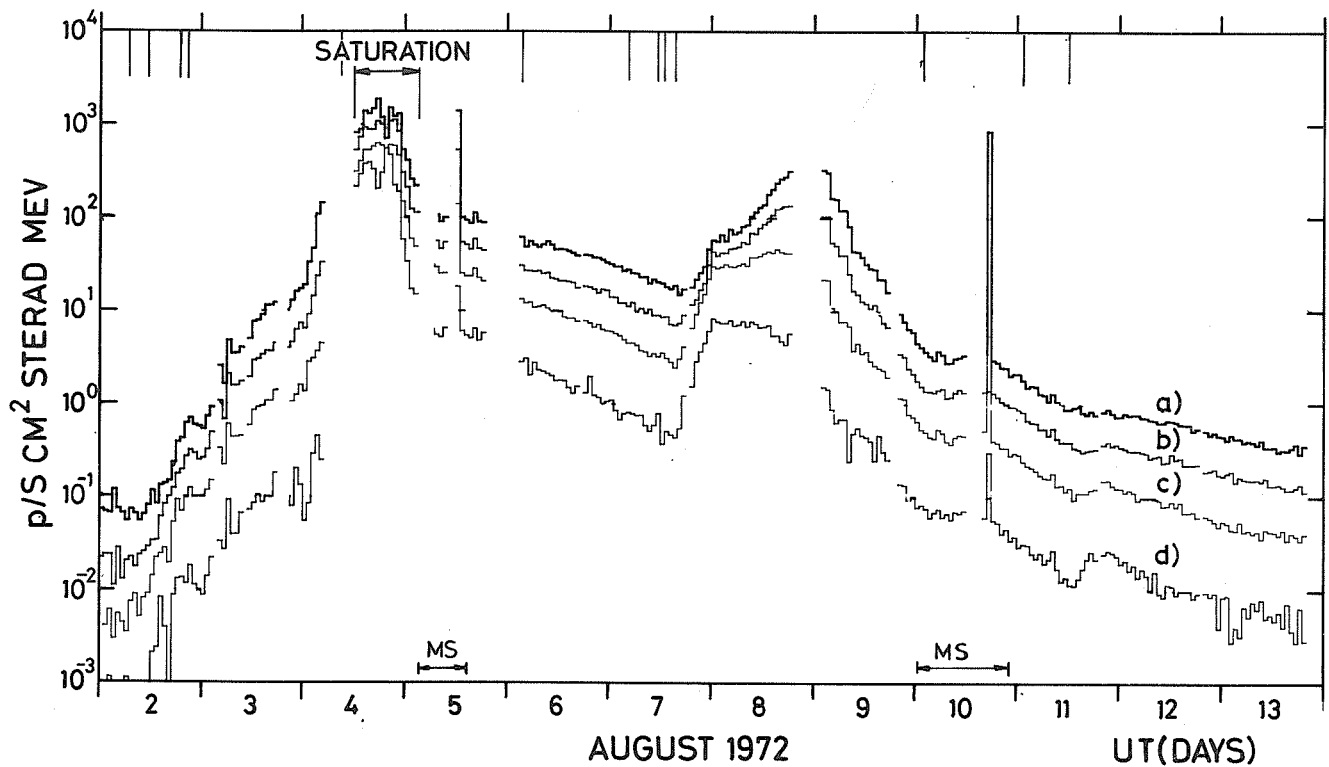


Fig. 4 Proton fluxes measured in HEOS-2 and averaged over one hour periods. Energy intervals are: a) 9.3-12.2 MeV, b) 12.2-17.0 MeV, c) 17.0-27.7 MeV, d) 27.7-35.7 MeV.

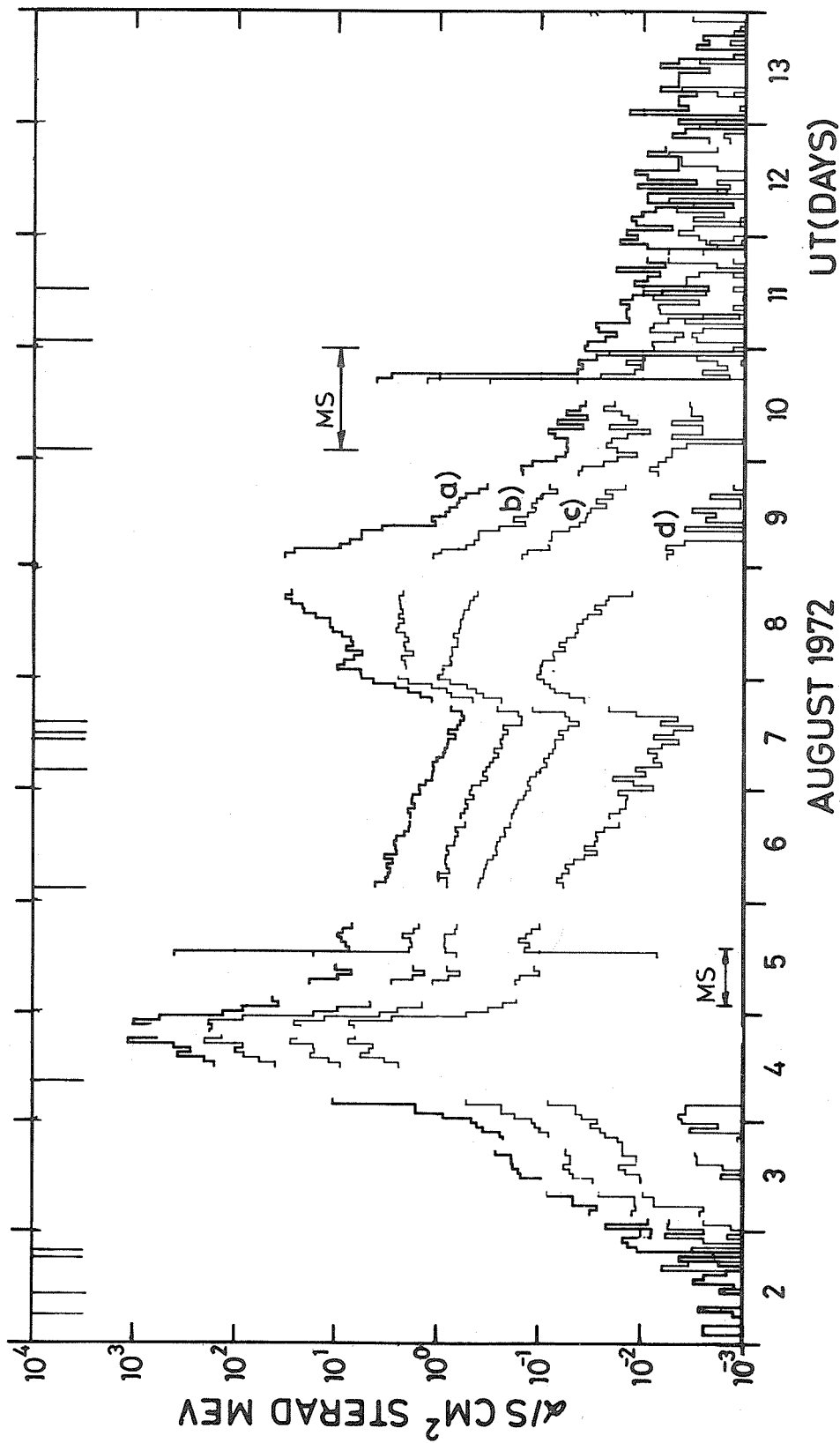


Fig. 5. Alpha particle fluxes measured in HEOS-2 and averaged over one hour periods. Energy intervals are:
 a) 9.3-12.2 MeV/nucleon, b) 12.2-17.0 MeV/nucleon, c) 17.0-27.7 MeV/nucleon, d) 27.7-35.7 MeV/nucleon.

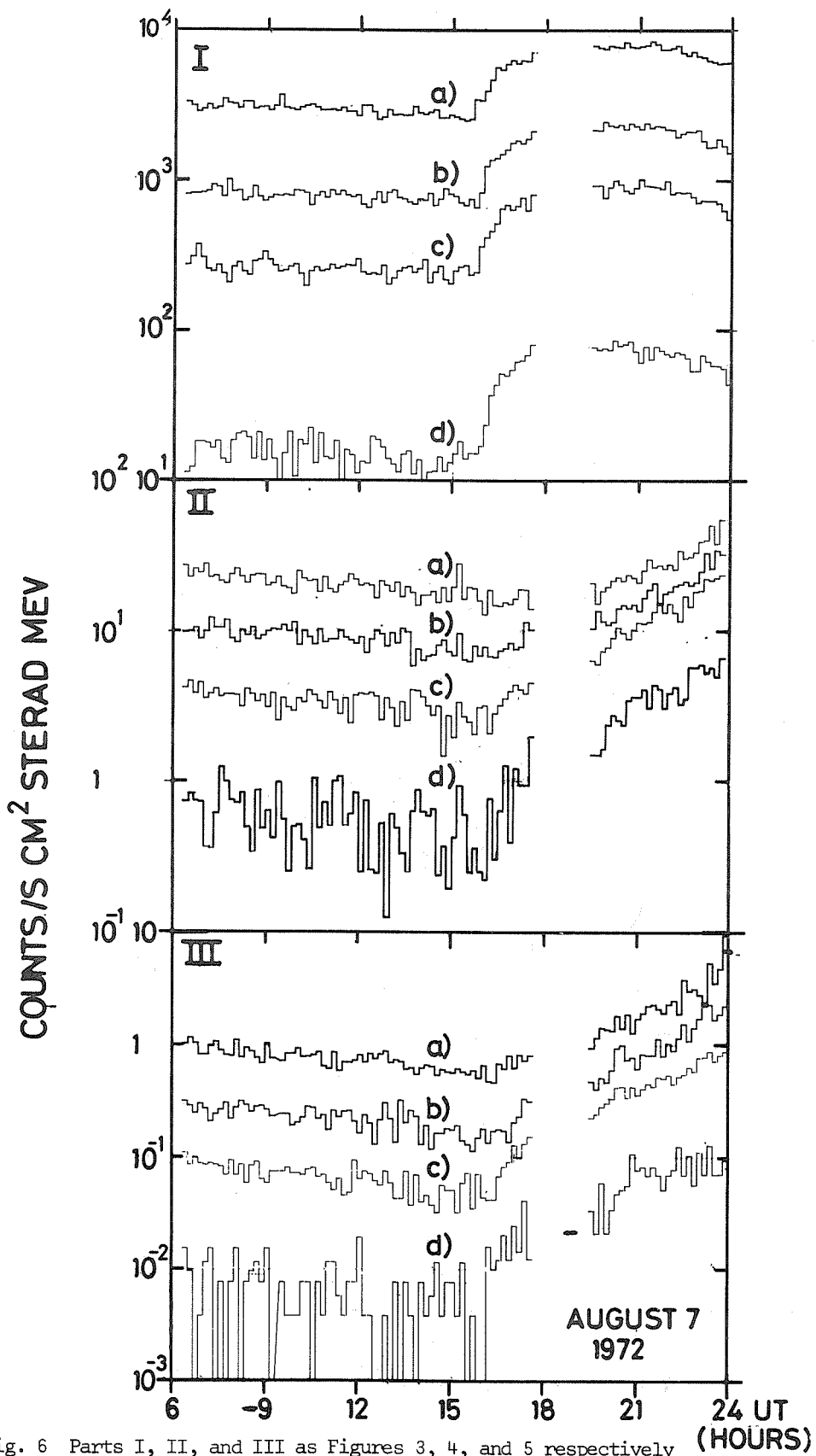


Fig. 6 Parts I, II, and III as Figures 3, 4, and 5 respectively with measurements averaged over 10 minutes periods.

Table 2

Arrival Time Observed in the Different Particle Channels
during the August 7, 1972 Solar Particle Event

Particle Channels	Arrival Time (UT)
Electrons	1550 ± 10
Protons 9.3-12.2 MeV	> 1700
12.2-17.0 "	1720 ± 10
17.0-27.7 "	1640 ± 10
27.7-35.7 "	1640 ± 20
α-particles	
9.3-12.2 MeV	1645 ± 15
12.2-17.0 "	1705 ± 15
17.0-27.7 "	1640 ± 15
27.7-35.7 "	1620 ± 15

REFERENCES

KÖHN, D.,
D. E. PAGE,
B. G. TAYLOR and
K-P. WENZEL

1972

Interplanetary Experiment (S204) for the HEOS-A2 mission.
ELDO/ESRO Scient. and Tech. Rev. 4, 19-57.

Proton and Alpha Particle Fluxes Observed Aboard OV5-6 in August 1972

by

G. K. Yates and L. Katz
Air Force Cambridge Research Laboratories
L. G. Hanscom Field, Bedford, Massachusetts

and

B. Sellers and F. A. Hanser
Panametrics, Inc., Waltham, Massachusetts

Satellite OV5-6 (International designation 1969-046B) measures solar fluxes of protons and alpha particles. The perigee is 16,341 km and the apogee is 112,196 km. Thus, for most of the time the instruments are outside the earth's magnetosphere. The data presented here do not include fluxes within this region. The orbit was described in greater detail in an earlier report in this series [Yates et al., 1971].

The proton-alpha particle detector on OV5-6 consists of two totally depleted silicon surface barrier detectors in a telescope configuration. The detectors each have a 2 cm² area and are separated by 2.54 cm. The outer one is 200 microns thick and the inner one 750 microns. The outer detector is shielded from light by 0.6 mil of aluminum foil. In the coincidence mode of operation, the telescope has a geometric factor of 0.52 cm²-sr, with a detection cone of 30° half angle. The average angle of detection is 17°. A coincidence is set by an energy loss window on the first detector and a threshold on the second detector. The resulting coincidences detect protons and alpha particles (principally) in the following ranges: protons 5.3 to 8 MeV, 8 to 17 MeV, 8 to 17 MeV, 17 to 40 MeV, and 40 to 100 MeV; alpha-particles 20 to 32 MeV, 32 to 68 MeV, and 68 to 100 MeV. The telescope cycles sequentially through these seven ranges, each range is counted and then read out. The complete cycle is completed in approximately two minutes. The telescope looks in the equatorial plane of the satellite.

The satellite spin axis is stable and is directed toward 0^h and 40^m RA and 32° declination in celestial coordinates. In August 1972 the sun appeared thirty-five degrees below (-35°) the satellite's equator. Since the spin period at this time was approximately 4.7 seconds, the telescope accumulated counts in a given particle energy range for approximately two satellite rotations.

The telescope also has a calibration or singles mode which allows some lower energy proton data to be obtained during high flux periods. Each coincidence count is followed by a single count from one of the detectors. The differential energy loss is measured in the 200 micron detector, and in the 750 micron detector the integral energy loss is measured. The detectors alternate in readout. Thus, each detector is read out once for each two coincidence count cycles (approximately 4 minutes) and each read out covers seven points. The singles mode count time is 1.8 seconds, and the detectors sweep out about 130° during the count time. For this mode the 200 micron detector has a geometric factor of 3.2 cm²-sr and provides information on protons in the energy ranges 1.25 to 1.41 MeV, 1.41 to 1.79 MeV, 1.79 to 2.71 MeV, 2.7 to 4.8 MeV, and 4.8 to 5.6 MeV. On 4/5 August 1972 the peak fluxes were so high that the 200 micron detector was saturated. During these periods the 750 micron detector, being shielded from protons below about 5 MeV, still operated reliably and thus singles mode counts from the 750 micron detector were used to measure the peak fluxes. The geometric factor for the 750 micron singles mode is 0.52 cm²-sr.

Figure 1 shows 30 minute averages of the data for selected energy intervals. Fluxes are given in particles /cm²-sec-sr-MeV; most gaps correspond to periods when the satellite was within the trapped radiation belt. Spectra at certain times during the event are shown in Figures 2, 3, 4 and 5. These include the calibration mode proton data averaged over spin to make it comparable to the coincidence mode data. The lower energy data have been corrected for the contribution by high energy protons and for background from a weak alpha source normally used to check the gain of the detector electronics. Where significant one sigma statistical uncertainties they are shown by vertical bars.

SOLAR PROTON EVENT AUGUST 2-11, 1972

DATA FROM OV 5-6

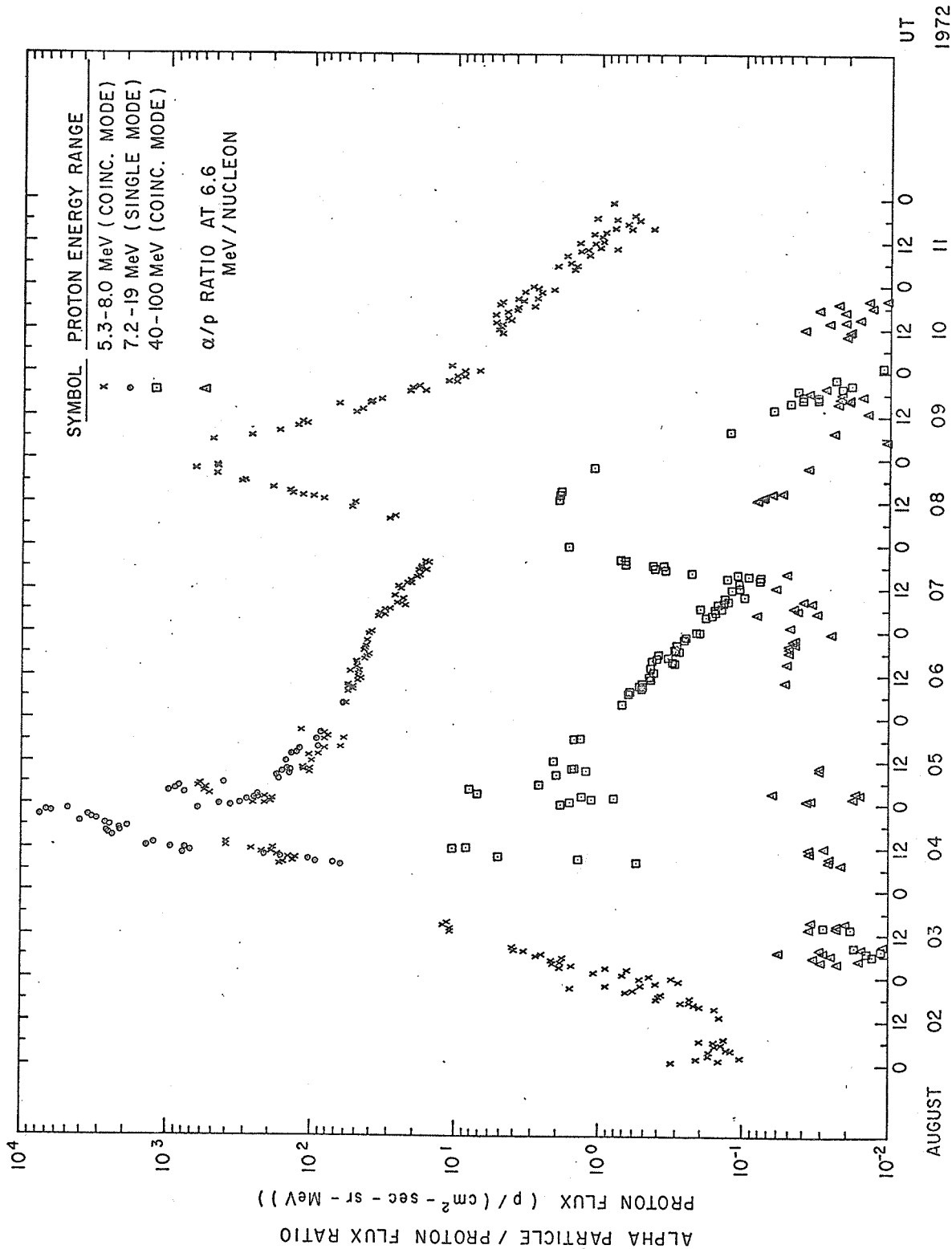


Figure 1 Proton Flux and Alpha-Particle/Proton Flux Ratio August 2-11, 1972.

OV 5-6 PROTON SPECTRA

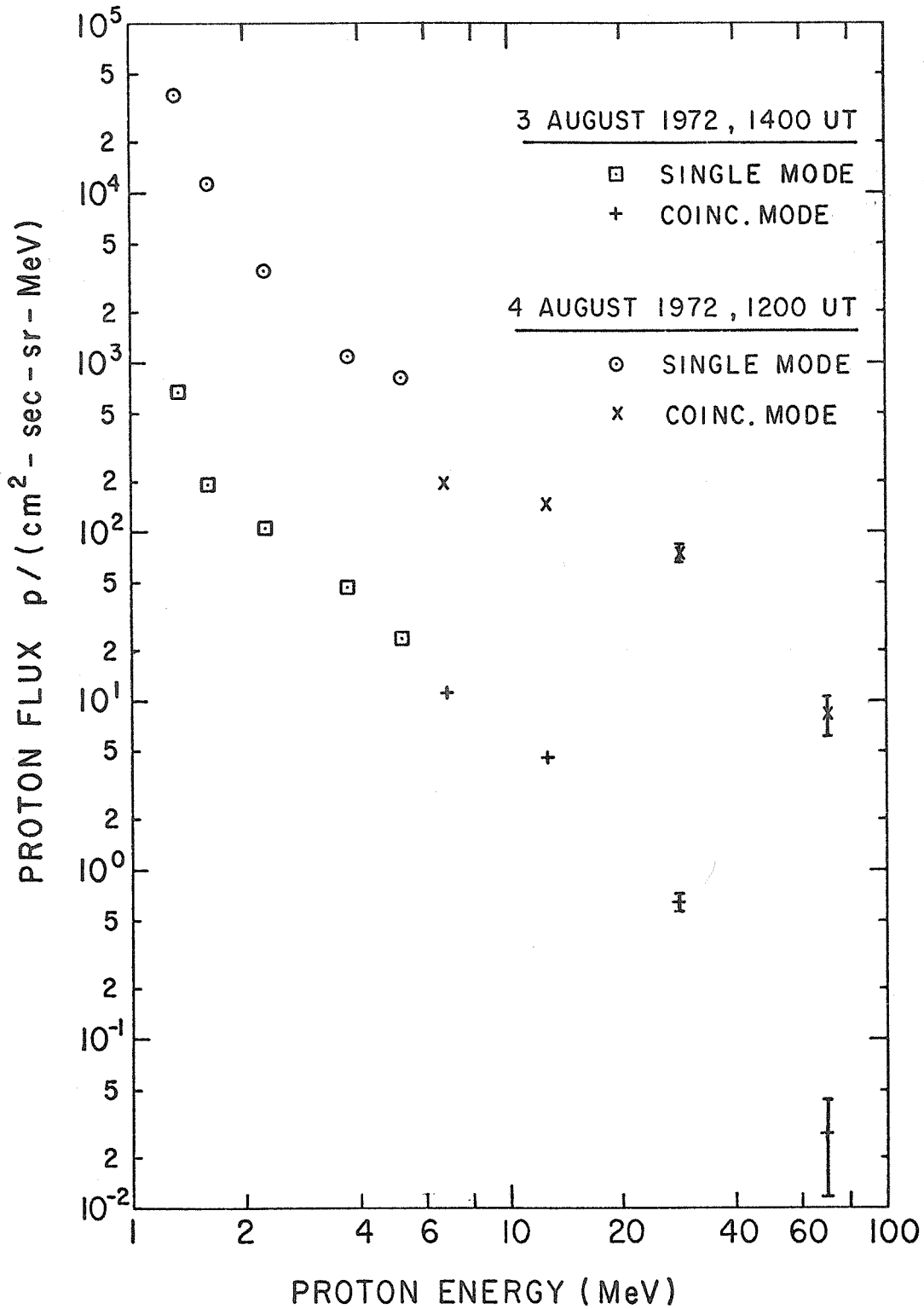


Figure 2

Proton Spectra August 3-4, 1972.

OV 5-6 PROTON SPECTRA

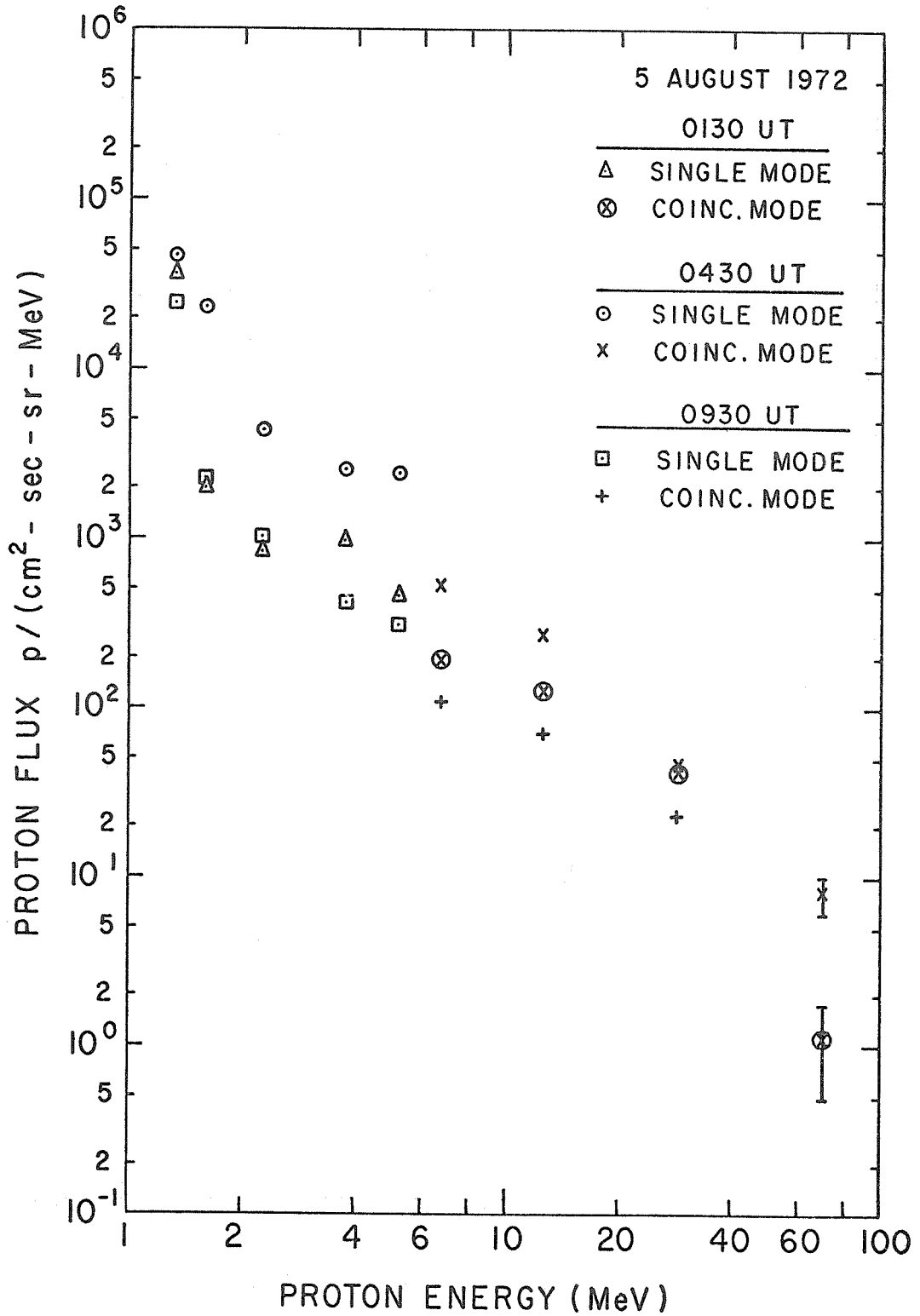


Figure 3

Proton Spectra August 5, 1972.

OV5-6 PROTON SPECTRA

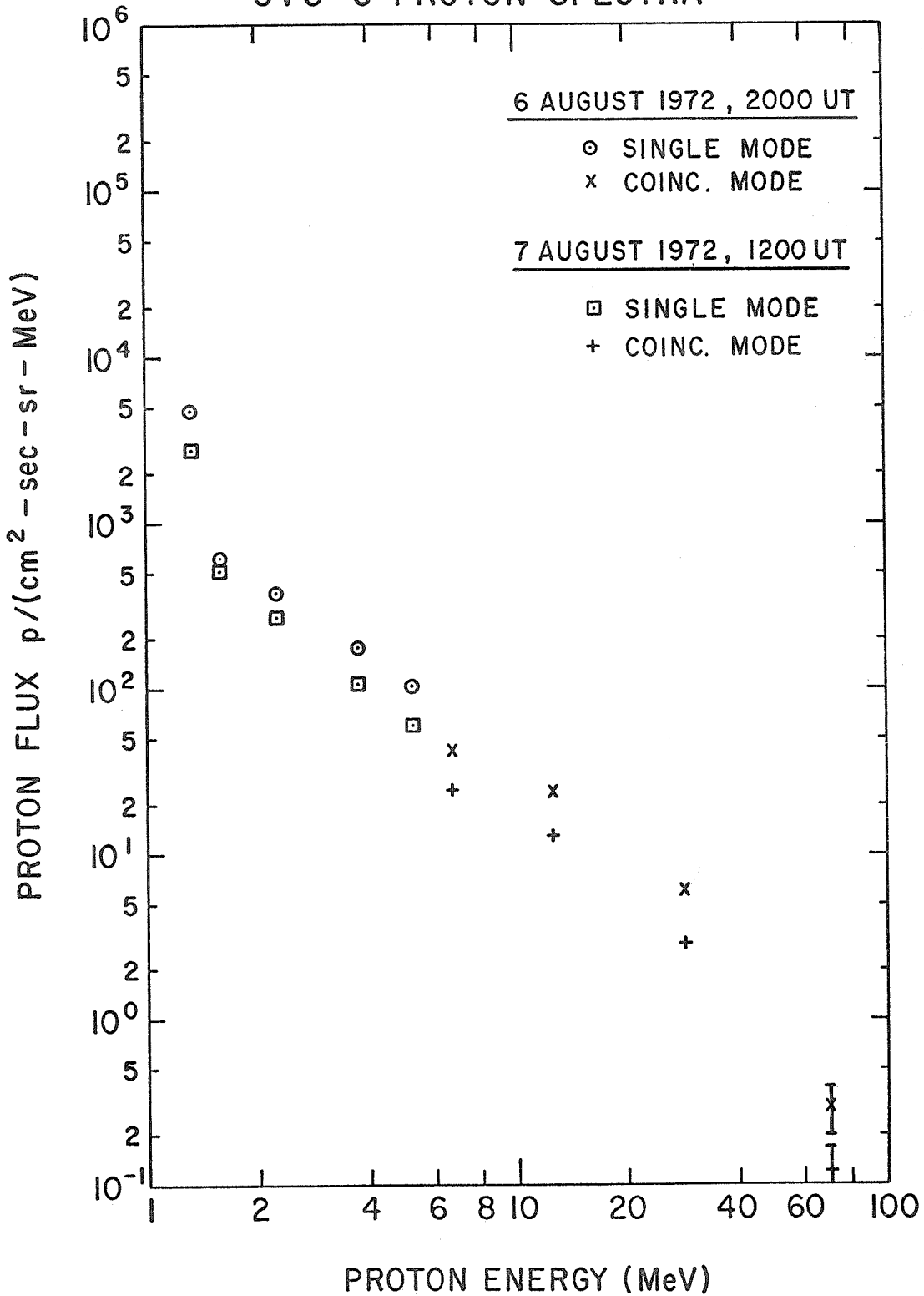


Figure 4

Proton Spectra August 6-7, 1972.

OV5-6 PROTON SPECTRA

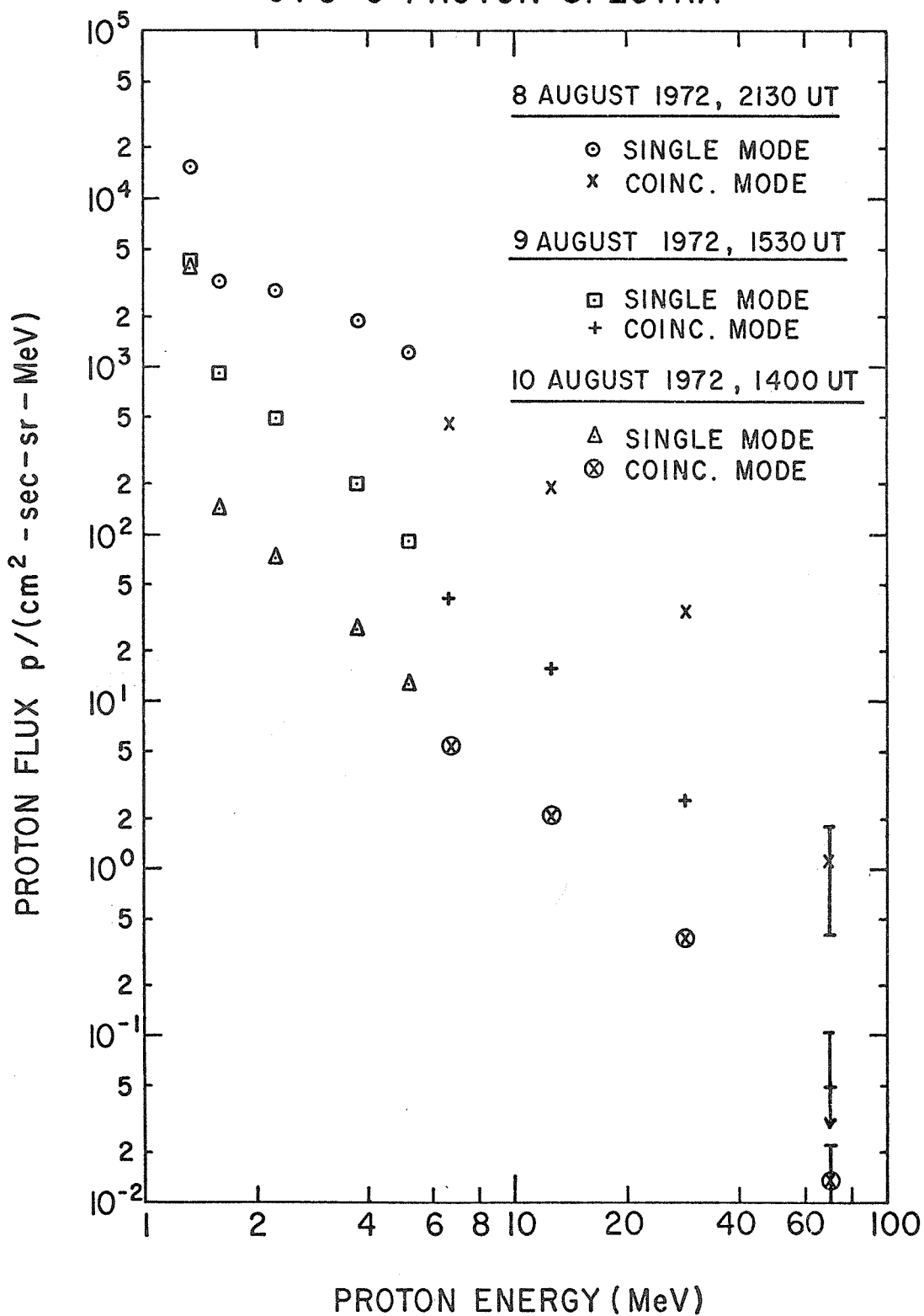


Figure 5

Proton Spectra August 8-10, 1972.

Energy Dependent Composition of Solar Flare Particles on 4 August 1972

by

P. B. Price, J. D. Sullivan and H. J. Crawford
Department of Physics
University of California
Berkeley, California 94720

A stack of Lexan polycarbonate sheet was exposed to solar flare particles for ~ 4 minutes in a rocket launched from Fort Churchill, Canada on 4 August 1972. Preliminary analysis of this data indicate:

1. At energies below ~ 10 Mev/nuc, the heavy elements are increasingly enriched relative to their abundances at high energies;
2. Tracks are observed of individual nuclei with Z up to 36 and energies ranging from ~ 1 to 40 Mev/nuc; and
3. The abundance ratio LiBeB/CNO at 25 Mev/nuc was no higher than ~ 0.01 .

REFERENCES

- | | | |
|--|------|---|
| BERTSCH, D. L.,
S. BISWAS,
C. E. FICHEL,
C. J. PELLERIN and
D. V. REAMES | 1973 | <u>Solar Physics</u> , in press. |
| PRICE, P. B.,
J. H. CHAN,
H. J. CRAWFORD and
J. D. SULLIVAN | 1973 | 13th International Cosmic Ray Conference, Denver,
paper 357. |
| SULLIVAN, J. D.,
H. J. CRAWFORD and
P. B. PRICE | 1973 | 13th International Cosmic Ray Conference, Denver,
paper 365. |

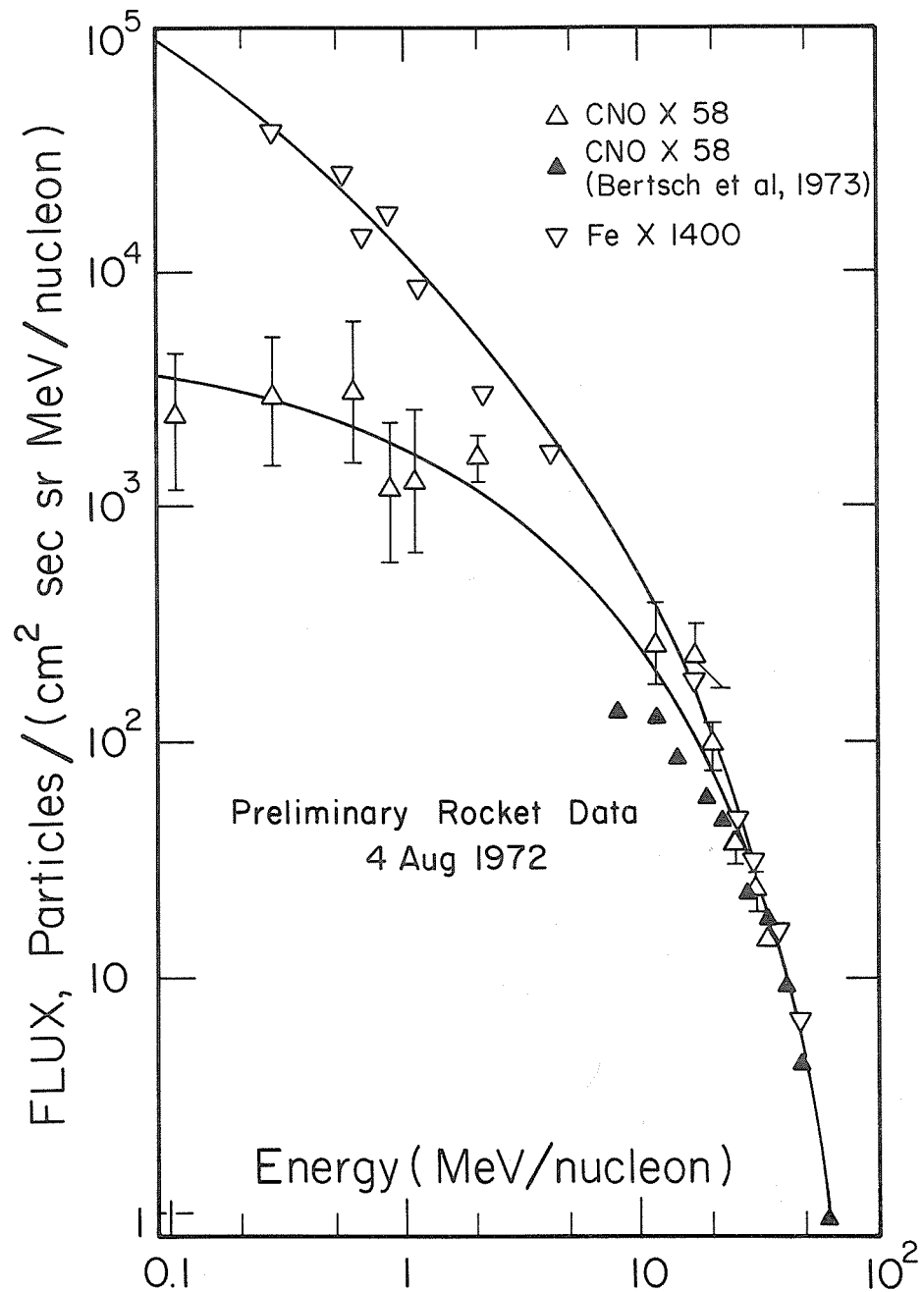


Fig. 1. Preliminary differential energy spectra of Fe and O measured with a Lexan stack on 4 August 1972 between 1914 and 1918 UT.

Lunar Surface Observations of the August, 1972 Solar Flare Activity

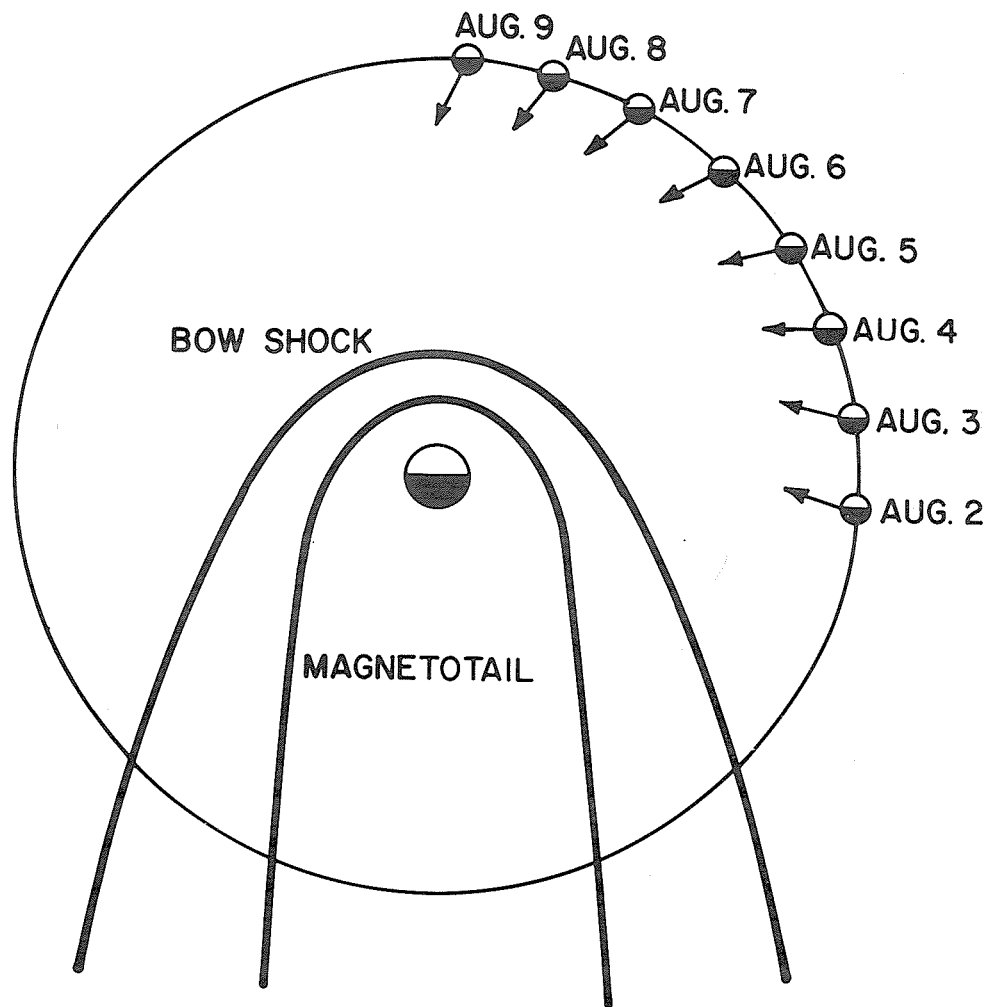
by

Patricia R. Moore, David L. Reasoner,
William J. Burke and Frederick J. Rich
Department of Space Science
Rice University
Houston, Texas 77001

Introduction

This paper reports on energetic particle fluxes observed at the lunar surface due to the solar flare activity of August, 1972. These particles were observed by the Charged Particle Lunar Environment Experiment (CPLEE), part of the Apollo 14 ALSEP system. The detector is an ion-electron spectrometer normally measuring particles with energies from 40 ev to 20 kev in 15 steps by using an electrostatic analyzer with 5 channels and stepped deflection voltages. For a more detailed description see O'Brien and Reasoner [1971] or Burke and Reasoner [1972].

Figure 1 shows the position of the moon relative to the magnetosphere during the time period in question. The instrument look directions are shown by the arrows.



CPLEE ECLIPTIC PLANE LOOK DIRECTIONS AUGUST, 1972

Fig. 1. Ecliptic plane projection of the lunar position for August 2-9, 1972. The look direction of Analyzer A (normal to the surface) is shown by the arrows.

Penetrating Particle Events

Figure 2 shows the counting rates of channel 1 at the deflection voltages of +0 (background), -35, and -350 volts for the period August 1-9, 1972. The negative deflection voltages of -35 and -350 normally correspond to channel 1 electron measurements with energies of 40 ev and 500 ev, respectively. The major flares of this time period are indicated by the arrows. However, during this period the counting rate in all data channels rose dramatically, up to 4×10^3 . As stated previously, the sign and magnitude of the deflection plate voltage determines the sign and energy range of the particles able to enter each of the five channels. However, for a given channel the deflection plate voltage made no significant difference in the counting rates, with the exception of the electron events described below. The differences in count rates between different channels were generally 10% or less. These data imply a large flux of particles penetrating the instrument case. The detailed geometry of the instrument is quite complex, but the principal shielding surfaces (the thermal plate, instrument case, electronics, etc.) are approximately equivalent to 3.2 mm of magnesium for stopping particles. Range-energy considerations set an approximate threshold of 20 Mev for protons, and correspondingly higher thresholds for heavier ions. The differences in count rates between different channels can be explained by the geometry of the instrument itself, with the lower-counting channels more effectively shielded.

The cosmic ray event of August 4 began at about 0800 UT, with a doubling of the background counting rate. The double-peaked maximum lasted from 1400 to 2230 UT August 4. A secondary peak was observed from 0320 to 0520 UT August 5. An exponential decrease in flux with a time constant of 17 hours was observed, followed by the second penetrating particle event starting at 1610 UT August 9. The background returned to normal values near 2000 UT August 9.

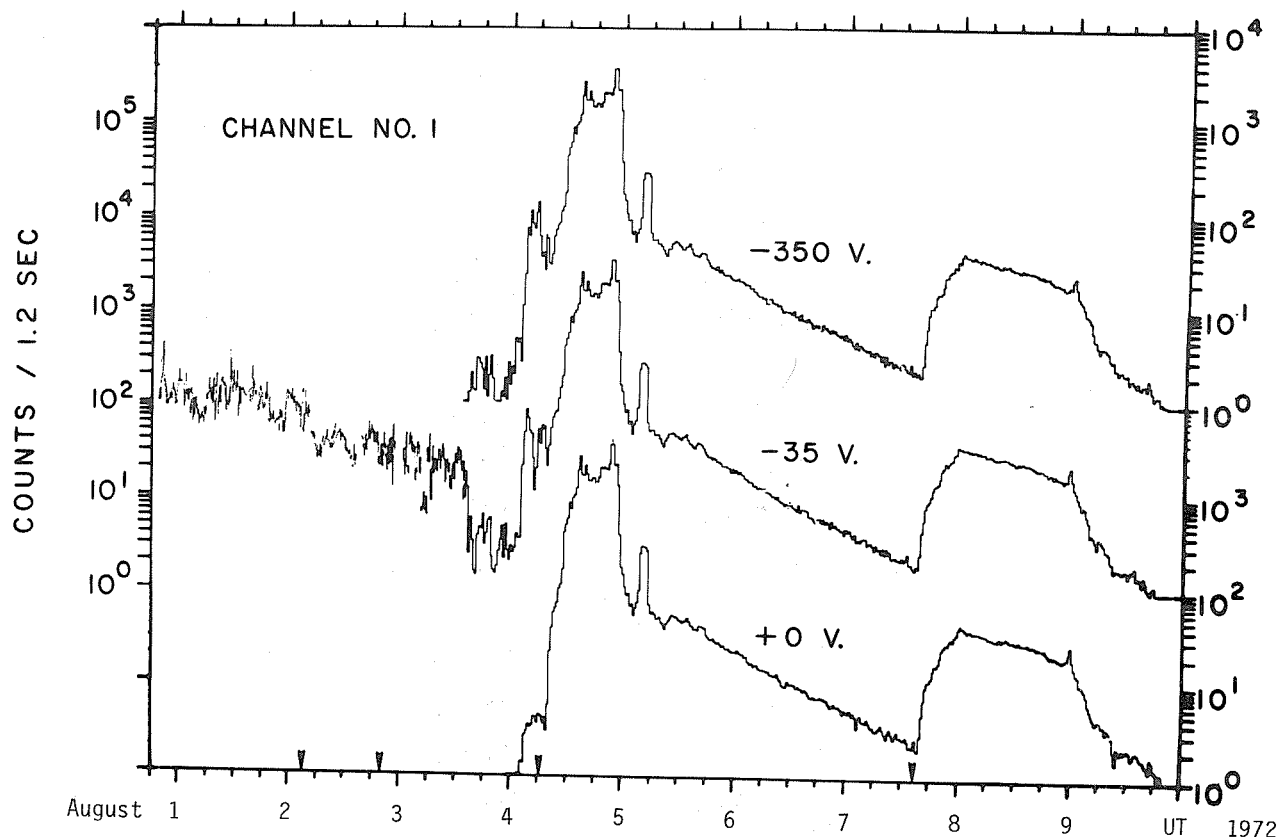


Fig. 2. Channel 1 count rate August 1-9, 1972. The deflection voltages of -350, -35, and +0 volts indicate 500 ev electrons, 40 ev electrons, and background, respectively. The major flares of the period are indicated by the arrows at 0316 and 2000 UT August 2; at 0620 UT August 4, and at 1530 UT August 7.

As the CPLEE instrument was not intended to measure penetrating particles, no calibration data is available on the sensitive area or efficiency. However, the best estimates of the geometric factor are $.03 - .1 \text{ cm}^2\text{-sr}$. Therefore, a peak counting rate of 3.7×10^3 counts/cycle (1 cycle = 1.2 seconds) corresponds to a maximum flux of $(3 - 10) \times 10^4 \text{ part/cm}^2\text{-sec-sr}$ or $(2 - 6) \times 10^5 \text{ part/cm}^2\text{-sec}$. The total flux for the August 4-6 event would then be $(4 - 13) \times 10^9 \text{ part/cm}^2$ and a factor of 18 less for the August 7-9 event.

Electron Events

Prior to the penetrating proton events, a period of electron flux enhancement occurred beginning at 0220 UT on August 4. Note in Figure 2 the enhancements of channel 1 at -35 and -350 volts relative to the background level (+0). Whereas the electron levels increased by an order of magnitude, the background channel enhancement was only 50% relative to the pre-event levels. This enhancement remained significant well into the penetrating proton event.

Sixteen-minute Time averages (49 cycles) of differential flux spectra for August 4 are plotted in Figure 3. Each point in the energy spectrum was determined by subtracting the average background

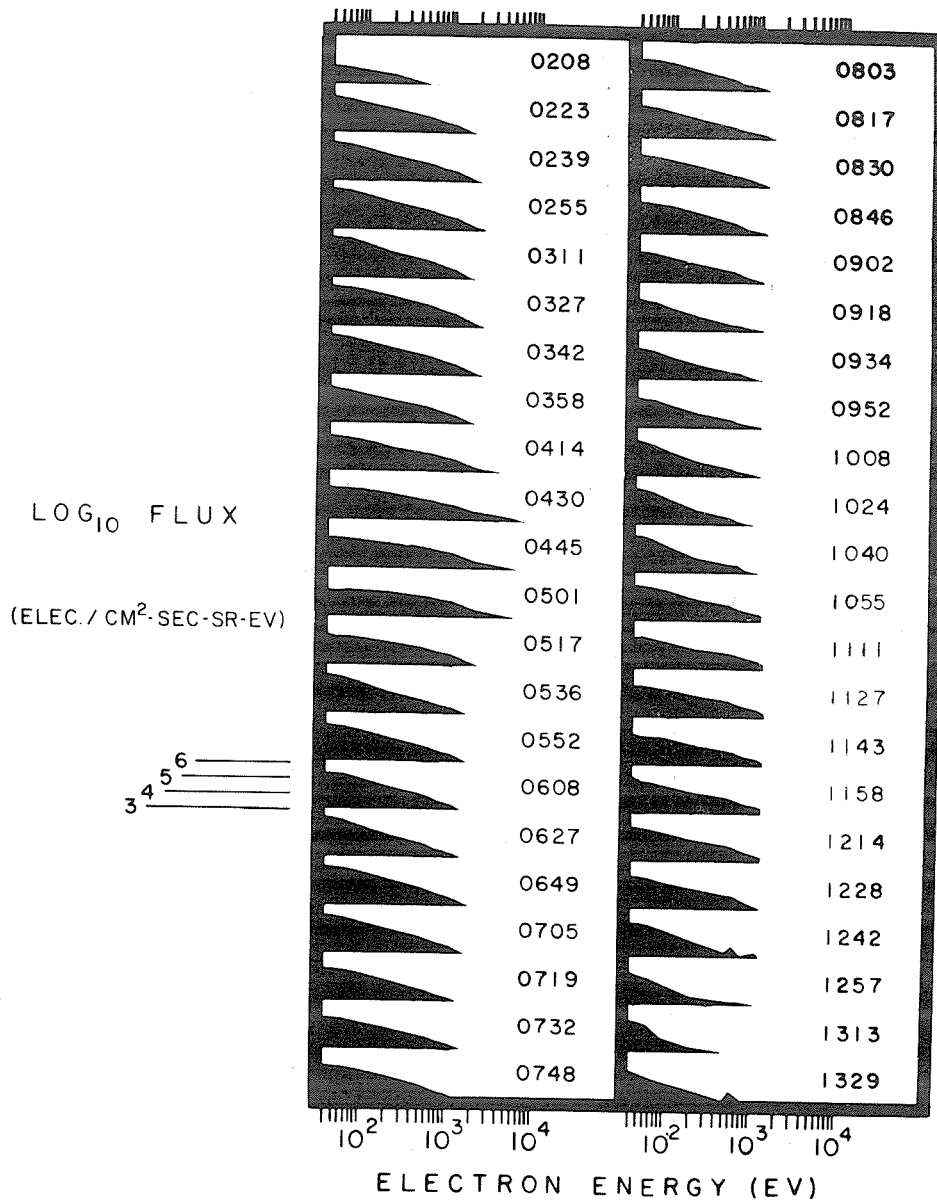


Fig. 3. Electron differential flux spectra, August 4, 1972.

count rate from the average data count rate for a given channel. Confidence levels of 99% in the majority of the 15 energy levels were required to accept any given spectrum. The density and directional flux of electrons with $E > 40$ ev reaching the lunar surface were also computed. The statistical considerations are discussed further in Appendix A. The spectra were, in general, quite variable, but showed two pronounced heating periods. Near the beginning of the event (0320 UT) the density was high ($.92/\text{cm}^3$), the directional flux was 5.6×10^7 part/ $\text{cm}^2\text{-sec-sr}$, and the temperature 170 ev. By 0500 UT the density had fallen to .36, the flux was 3.88×10^7 , and the temperature reached 541 ev. The spectrum cooled rapidly to a minimum temperature of 98 ev at 0530 UT ($n = .50$, $F = 2.2 \times 10^7$), then stabilized in temperature at about 150 ev from ~ 0600 to ~ 1040 UT. During this time the density decreased from .7 to .3, and the directional flux from 4 to 1.5×10^7 . A second heating event began at about 1100 UT. The temperature remained near 300 ev until around 1230 UT, when the density, total flux, and temperature declined rapidly. Loss of the significance criteria for the spectrum as a whole occurred at about 1345 UT, but certain energy levels showed sporadic significant flux enhancements until 1600 UT. As no significant electron fluxes were observed after the sharp decrease in penetrating radiation at 2400 UT, we hypothesize termination of the electron events between 1400 and 2400 UT August 4.

Conclusions

The time history of the penetrating particle events agrees quite well with that observed by other detectors outside of the magnetosphere: for example, Pioneer 9 [Lezniak and Webber, 1972], and others [Paulikas *et al.*, 1972]. The peak flux and exponential decay rates seem consistent with an energy threshold of 20 Mev, as higher energy particles exhibited a faster interflare decay rate [Bostrom *et al.*, 1972].

The heating mechanism for the electrons is uncertain. A solar source for hot interplanetary electrons has been discussed by Van Allen and Krimigis [1965]; however, in those cases a propagation time from the sun to the earth of about 40 minutes was determined. In the present data, however, there were no flares prior to the electron event within such a time period. We note that the electron event began simultaneously with a sudden commencement on earth, suggesting that the observed electrons were energized at the bow shock and subsequently propagated back upstream to the vicinity of the moon. This sort of process was postulated by Anderson [1969] based on observations of short-duration (30 - 150 seconds) enhancements of 40 to 45 kev electrons. If we postulate that the 1B flare at 0316 UT August 2 and the 2B flare at 2000 UT August 2 were responsible for the two electron heating events observed, then transit times of 47 and 39 hours or propagation velocities of 880 and 1000 km/sec are calculated for the flare-associated disturbances. While these velocities are certainly higher than reported average solar-wind velocities, they are plausible in consideration of the unique nature of the August, 1972 solar-flare events.

REFERENCES

- | | | |
|--|------|--|
| ANDERSON, K. A. | 1969 | Energetic Electrons of Terrestrial Origin behind the Bow Shock and Upstream in the Solar Wind, <u>J. Geophys. Res.</u> , <u>74</u> , 95-106. |
| BOSTROM, C. O.,
J. W. KOHL,
R. W. McENTIRE and
D. J. WILLIAMS | 1972 | The Solar Proton Flux - August 2-12, 1972, Johns Hopkins University Applied Physics Laboratory, Preprint. |
| BURKE, W. J. and
D. L. REASONER | 1972 | Absence of the Plasma Sheet at Lunar Distance during Geomagnetically Quiet Times, <u>Planet. Space Sci.</u> , <u>20</u> , 429. |
| KOHL, J. W. and
C. O. BOSTROM | 1972 | Observations of the August '72 Solar Events by the Solar Proton Monitor on Explorer 41, <u>EOS</u> , <u>53</u> , 1055. |
| LEZNIAK, J. A. and
W. R. WEBBER | 1972 | Pioneer 9 Cosmic Ray Observations During August 1972, <u>EOS</u> , <u>53</u> , 1054. |
| O'BRIEN, B. J. and
D. L. REASONER | 1971 | Charged Particle Lunar Environment Experiment, Apollo 14 Preliminary Science Report, <u>NASA Spec. Publ.</u> <u>272</u> , 193. |
| PAULIKAS, G. A.,
J. B. BLAKE and
E. F. MARTINA | 1972 | Energetic Solar Proton Observations 3-10 August 1972, <u>EOS</u> , <u>53</u> , 1055. |
| VAN ALLEN, J. A. and
S. M. KRIMIGIS | 1965 | Implusive Emission of ~ 40 kev Electrons from the Sun, <u>J. Geophys. Res.</u> , <u>70</u> , 5737. |

APPENDIX A

Statistical Considerations

Computation of the standard deviation of the flux is critical to evaluate the significance of low flux levels superposed on steadily rising background levels. The relevant equation is:

$$\bar{F} = \frac{\eta}{N} \sum_{i=1}^N (C_i - B_i) = \eta (\bar{C} - \bar{B})$$

Where \bar{F} is the average flux over N cycles, C_i and B_i the appropriate data count rate and background count rate, respectively, and η the appropriate multiplication factor.

Since $[\sigma(\eta)]^2 \ll [\sigma(C)]^2$, we may write

$$[\sigma(\bar{F})]^2 = \frac{\eta^2}{N^2} \sum_{i=1}^N ([\sigma(C_i)]^2 + [\sigma(B_i)]^2 + 2[\sigma(BC)]^2)$$

Assuming Poisson statistics,

$$[\sigma(C_i)]^2 = C_i \quad ; \quad [\sigma(B_i)]^2 = B_i$$

and assuming $[\sigma(BC)]^2$ small,

$$[\sigma(\bar{F})]^2 = \frac{\eta^2}{N^2} \sum_{i=1}^N (C_i + B_i) = \frac{\eta^2}{N} (\bar{C} + \bar{B})$$

Defining $X = (C - B)$, \bar{F} becomes $\eta\bar{X}$, and $[\sigma(\bar{X})]^2 = \frac{(\bar{C} + \bar{B})}{N}$.

The Student t statistic allows a computation of the significance of the net flux. The statistic is defined as

$$t(\bar{F}) = \frac{\bar{F}}{\sigma(\bar{F})} = \frac{\eta\bar{X}}{\eta \left(\frac{\bar{C} + \bar{B}}{N} \right)^{1/2}} = \frac{\bar{X}}{\sigma(\bar{X})} = t(\bar{X})$$

So we may work equally well with the statistics of the flux or the net counting rate X . We choose the latter for convenience.

A value of t greater than 2.5 implies that to the 99% confidence level \bar{C} and \bar{B} are not from the same parent population; averaging over many cycles (increasing N) decreases the time resolution but greatly increases the significance of the result. We see, therefore, for $\bar{C} = 810$, $\bar{B} = 790$, and $N = 49$, $t = 3.5$. This is an extreme example, as background levels did not rise that high until 1200 UT August 4. The criterion used for plotting the spectra (Figure 3), therefore, was 99% confidence level in each of the five lowest energy levels and in at least 60% of all energy levels.

Penetrating Solar Flare Particle and Solar Wind Observations
in the Lunar Night, August, 1972

by

René A. Medrano, John W. Freeman, Jr.,
H. Kent Hills and Richard R. Vondrak
Department of Space Science
Rice University
Houston, Texas 77001

ABSTRACT

Penetrating particles and solar wind-energy ions associated with the flare activity of early August, 1972 have been detected by the Apollo 12, 14 and 15 ALSEP-SIDE detectors during the lunar night. The penetrating particles are believed to be solar cosmic ray protons, with energies ≥ 20 Mev and ≥ 50 Mev, that penetrated the shielding of the thermal-energy and solar wind-energy detectors, respectively. There are sharp enhancements in the solar cosmic ray flux on August 4 and 7. These are associated with two 3B solar flares. These solar events of August, 1972 represent the most intense (by over 3 orders of magnitude) penetrating particle events seen by the SIDEs. Early on August 5, a peculiar cosmic ray square wave of 2 hours duration was observed. It cannot be associated with any important solar flare feature. Before the onset of the cosmic ray event, solar wind-energy ions from unusual directions were detected. The main features of the solar wind-energy ions divide the events into two types. The first type corresponds to sporadic ion events with energy spectra narrowly peaked around 2750 ev and moving upstream in the solar wind. The second type corresponds to streams of ions with unusually broad energy spectra that extend beyond the upper energy channels (3.5 kev) of the detectors.

Introduction

This report is concerned with penetrating solar cosmic rays originated by the impressive chain of solar flares in the first half of August, 1972. We also report observations of solar wind streams from directions up to 77° from the usual bulk flow direction before the onset of the penetrating particles. The data used in this paper come from the Rice University Suprathermal Ion Detector Experiments (SIDEs) which are part of the ALSEP scientific packages left on the lunar surface by the astronauts of Apollos 12, 14 and 15.

None of these instruments point directly to the Sun when outside the geomagnetic tail. Therefore they do not observe solar wind ions except when the interplanetary plasma is very disturbed [Medrano et al., 1972]. However, there are reports of observations of ions moving in upstream directions in the solar wind [Lindeman, 1971; Freeman, 1972]. Interpretations of these observations range from the particle ejection from the bow shock, to accelerated thermal ions of lunar origin.

The Experiment

The Suprathermal Ion Detector Experiment consists of the Mass Analyzer (MA) and the Total Ion Detector (TID). Details of the experiment have been published in other works [Freeman et al., 1970; Hills and Freeman, 1971; Hills et al., 1972]. We will mention here only the relevant features of the instrument.

The TID determines the energy/charge of ions in the energy range from 10 ev up to 3500 ev in 20 steps. The energy discrimination is provided by a pair of cylindrical parallel plates connected to a stepped power supply. The detection of the discriminated ions is performed by a funnel-type channel-electron-multiplier. The field of view of the detector is a square solid angle of approximately 6° on each side and the look direction is 15° from the local vertical.

The MA is designed to give the mass per unit charge of the detected ions. Mass discrimination is obtained for ions with energies up to 48.6 ev. The particle detection, as in the case of the TID, is made by a funnel-type channel-electron-multiplier. The MA field of view and look direction are similar to the TID. Except for the penetrating particle data, this part of the experiment is irrelevant for the purpose of this report since it operates in the thermal energy region. All the SIDEs on the three Apollo missions are of the same basic design.

Cosmic rays contribute to the background counting rate of the SIDE particle detectors. The usually low flux does not affect appreciably the accuracy of the plasma measurements. There are other comparatively more important sources that contribute substantially to the background of the particle detectors during the lunar day. Most of these are temperature dependent and arise from detector and electronic noise. Shortly after local sunset, most of the detector background counts are attributed to cosmic rays. Two of the six detectors are exceptions and retain high noise backgrounds during the lunar night.

Now we consider the shielding of the detectors against penetrating particles. The shielding surrounding the detectors is much the same for all three SIDE instruments. For a particular detector, the shielding varies according to the direction of penetration. Due to the different and sophisticated composition of the material from which SIDE was built, the shielding from a particular direction is very hard to determine accurately. In order to determine the minimum energy required for a proton to reach each detector other than through the normal ion flight path we chose the shortest paths (in gm/cm²) from the exterior to a particular detector. From some selected paths we estimate the following minimum proton energies:

$$E_{MA} \approx 25 \text{ Mev}; \quad E_{TID} \approx 50 \text{ Mev}$$

where E_{MA} - minimum proton energy to reach the channel-electron-multiplier of the Mass Analyzer

E_{TID} - minimum proton energy to reach the channel-electron-multiplier to the Total Ion Detector.

In the data that is presented we have simplified the notation. Solar proton fluxes with energies ≥ 25 Mev and ≥ 50 Mev have been labeled MA and TID, respectively.

The ALSEP sites of all of the SIDEs were past their local sunsets on August 4, 1972. The times of the local sunsets, along with the ALSEPs selenographic coordinates, and the look direction of the detectors with respect to the local vertical, for all three Apollo missions are shown in Table 1. Also given are the angular distances from the terminator at the beginning and the end of the early August observations. As one can see in Table 1, Apollo 12 and 14 ALSEPs are not too far from each other and, in global terms, both can be considered to be at the same location as compared to the location of Apollo 15 which is about 1000 km away.

Although all three instruments were constructed identically, they are deployed on the Moon's surface with different orientations. As we said, the detectors of 12 and 14 are within 180 km of one another, but their look directions are opposite. The Apollo 12 SIDE looks to the west and 14 to the east, both 15° from the zenith which is roughly in the ecliptic plane. The 15 instrument is in a high northern latitude and is tilted by 26° toward the south such that the detectors look direction still includes the ecliptic plane. As a consequence of the deployment configuration, the total flux of penetrating particles at any given time might be different for each instrument if the flux is not isotropic.

Table 1

General detector deployment characteristics for ALSEP-SIDEs on Apollos 12, 14 and 15

	Apollo 12	Apollo 14	Apollo 15
Time of the local sunset	0348 UT Aug. 4	1706 UT Aug. 3	2338 UT Aug. 1
ALSEP selenographic coordinates	Latitude	3.2°S	26.10°N
	Longitude	23.4°W	17.5°W
Detectors look direction in the Ecliptic Plane	15°W	15°E	15°E
Angular distance from terminator at 0800 UT, Aug. 4	1.6°	7.3°	26.2°
Angular distance from terminator at 1200 UT, Aug. 9	64.6°	71°	92.3°

We made an attempt to determine an in-flight calibration of the omnidirectional geometric factor G for the case of penetrating particles for both detectors. Two independent determinations gave different values of G . The first used data from ATS-1 during a distinguishable solar proton event, and the second used a data compilation of the galactic cosmic radiation made by Comstock *et al.* [1972]. In the first case we have compared the solar proton omnidirectional flux (in particles per cm² sec) measured by ATS-1 with the corresponding background counts registered by our detectors; in this case we found that $G = 1.2 \pm 0.8$ cm². In the second case we made an approximate integration of the differential energy spectrum of the galactic cosmic radiation measured by several authors [see references in Comstock, *et al.*, 1972] and we compared it with the long time average of the detectors' backgrounds when they were on the dark side of the Moon. This method gives the result: $G = 0.3$ cm².

Since for the first case the ATS-1 detector provides no information on proton fluxes above 70 Mev, the calculated G based on this data exceeds the actual value by an unknown amount. It is also possible that the data supplied by the ATS-1 satellite may not represent exactly the real fluxes because of sensor degradation problems that have been noticed by the investigators [Lincoln and

Leighton, 1972]. From the two results obtained for the geometric factor we favor the one that uses the galactic cosmic ray flux since its determination includes compilation of data from independent measurements. In any case our penetrating particle data in counts per second should be regarded as the order of magnitude of the real particle fluxes in particles per cm^2 sec.

In what follows, a distinction will be made between ions observed by the TID with energies between 10 ev and 3500 ev, and particles with energies ≥ 25 Mev and ≥ 50 Mev which are able to penetrate the shielding of the MA and TID detectors, respectively. The first kind of particles correspond to ions in the solar wind, and the events that fall in this category will be called ion events. The second type of particles correspond to solar cosmic ray particles released in the solar flares, and observations of these will be called penetrating particle or solar cosmic ray events.

Solar Wind Plasma Observations

As we said earlier, none of our detectors point directly towards the solar wind when the Moon is in interplanetary space. Figure 1 shows the look direction of all SIDE detectors on Apollo 12, 14 and 15 at the beginning of the penetrating particle event early on August 4, 1972. We also indicate the end of the solar cosmic ray event with the look direction of the detectors on August 9. Notice that during the days of observation the look directions of the detectors were not in position to observe normal solar wind ions.

Starting early on August 3, and almost throughout the whole day, Apollo 14's TID detected sporadic energetic ion events with durations of several minutes. The frequency of occurrence of these sporadic events increased late on August 3. These ion events detected by the Apollo 14 instrument are characterized by narrowly-peaked spectra with a maximum occurring at energies of 2500 ev or more. Sometimes the peak energy moved toward higher energies in one single event with a few

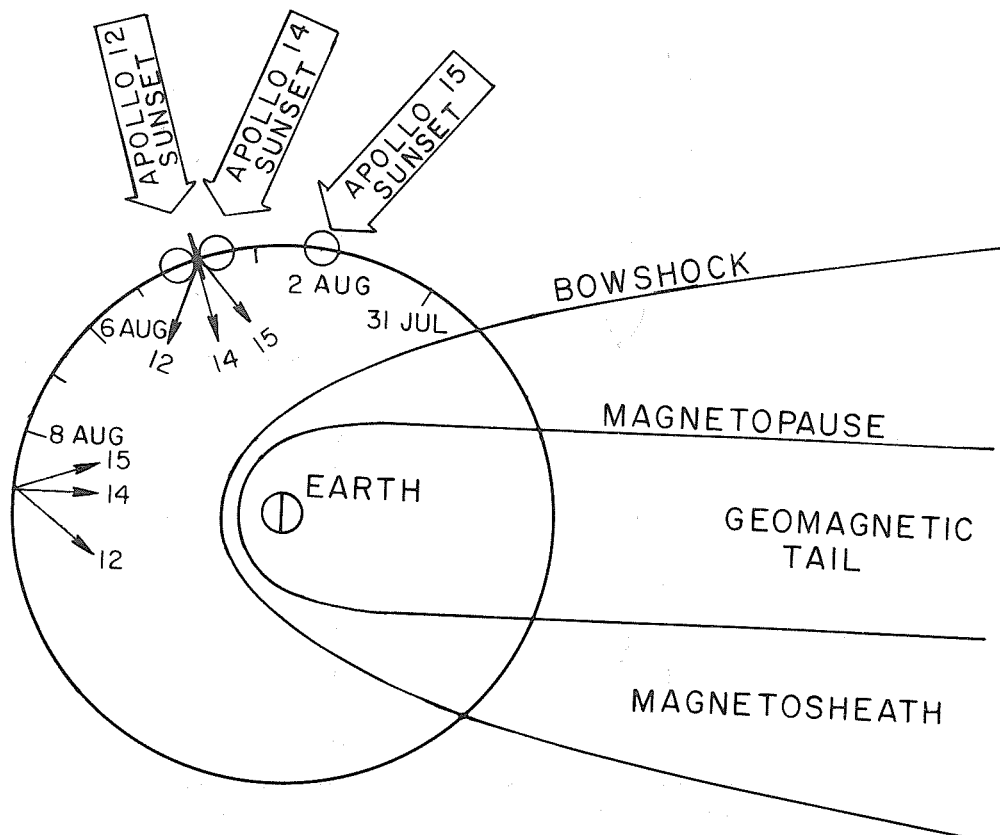


Fig. 1. Lunar orbit and the positions of the Moon at the local sunsets of Apollos 12, 14 and 15. The data reported in this paper were obtained between the two positions where the detector look directions are indicated. The geomagnetic cavity is shown for reference.

minutes duration. Six successive spectra of this type are shown in Figure 2. The sequence is identifiable by the Roman numerals at the top of each spectrum. All differential fluxes are given in number of ions per cm^2 sec ster ev. Every spectrum has the same scale range. Notice the narrow energy dispersion of the spectra and the consistent motion of the maxima toward higher energies. Occasional points in the low energy part represent only the stochastic character of the background which has not been subtracted in our example. A single count in a low-energy channel indicates a relatively high differential flux since the channel widths are proportional to the center energies. The look direction of the detector for this particular event was -80° from the Sun's radial direction. (Positive angles are defined in the ecliptic plane, counterclockwise towards sunset from the Sun's radial direction which is nearly the same as the downstream direction of the solar wind).

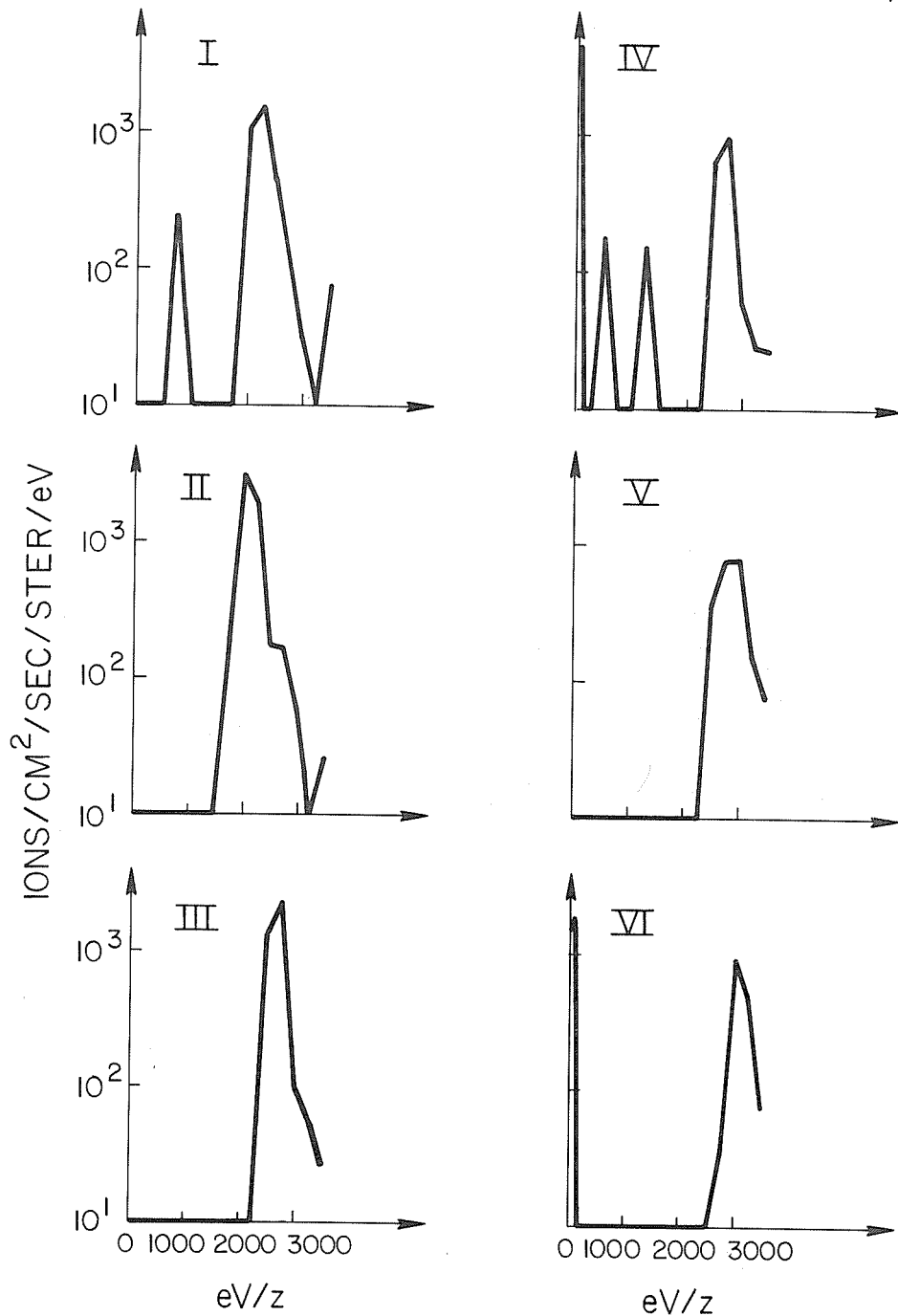


Fig. 2. Apollo 14 TID data. Sequence of differential energy spectra with the peak energy moving toward higher energies. The look direction of the detector is -80° from the Sun's radial direction. The sequence begins at 0609 UT and ends at 0612 UT on August 3.

The detector look direction for the Apollo 14 instrument changed from -80° to -71° from the Sun's radial direction during the occurrence of the sporadic ion events. In this same period the similar detector on Apollo 12 was looking at directions from -116° to -108° from the Sun's radial direction and did not detect any distinct ion event. The Apollo 15 TID was exhibiting a high background at this time, so no useful information was obtained by this detector.

If the interplanetary magnetic field lines were exhibiting the classical spiral shape, they could connect the bow shock with the direction of the Apollo 14 detector. In this manner it is possible to attribute the sporadic ion events observed by the Apollo 14's TID to protons ejected from the bow shock. Asbridge *et al.* [1968] and more recently Lindeman *et al.* [1971] have reported similar observations.

On August 4, starting at 0529 UT, Apollo 12's TID observed streams of ions with unusually broad spectra. Figure 3 shows a typical distribution function of ions observed just before the onset of

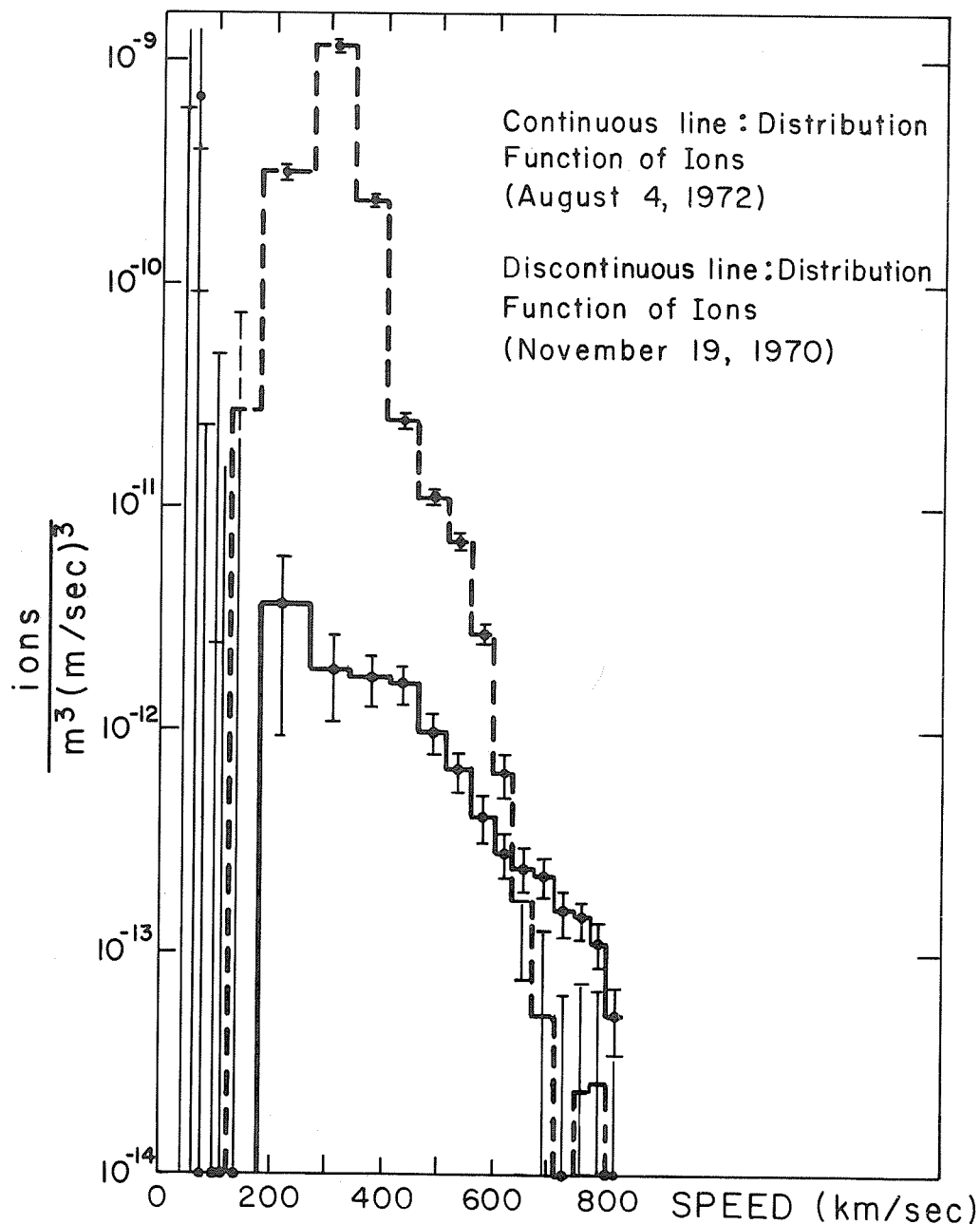


Fig. 3. Distribution function of ions observed by the Apollo 12 TID. The spectrum with continuous line corresponds to ions just before the penetrating particle event. The spectrum of another interplanetary disturbance (discontinuous line) detected at a similar location in the lunar orbit is shown for comparison.

the penetrating particles. The computed bulk speed and temperature for this distribution, assuming only protons with a Maxwellian distribution, are 510 km/sec and 3.2×10^6 K. Since significant points in the distribution seem to go beyond the energy limit of our detector, and because of the uncertain contribution of massive elements, the computed bulk speed and temperature are only apparent values. The look direction of the detector at this time was -103° from the Sun's radial direction. For sake of comparison, in the same graph we have plotted the distribution function of a shock wave-deviated solar wind on November 19, 1970 [Medrano, 1971]. The spectrum of reference was measured while the detector (the Apollo 12 TID) was pointing at -153.4° from the Sun's radial direction.

The particle spectra observed by the Apollo 12 TID are much broader than the recurrent ion spectra reported by Lindeman [1971] at the same part of the orbit during quiet times. We then conclude that the ions measured by the Apollo 12 instrument may be part of the shock wave particles associated with the August 2 flare (2000 UT) reported by Armstrong *et al.* [1972].

Penetrating Particle Observations

Starting at 0730 UT on August 4, the counting rates of all the detectors in all three Apollo experiments began to increase appreciably. The enhancement in the counting rate was independent of the mass or energy channel, indicating that these were penetrating particles. No spectrum of any sort was distinct in any detector from then on until the end of the cosmic ray event. Plots of averages over 145 sec (1 SIDE cycle) are displayed as a function of time in Figure 4. Graphs corresponding to Apollos 12, 14 and 15, each one containing plots of the MA and TID, are displayed in Figure 4 for 3 consecutive days. Each day's data are confined in a column of blocks containing all three experiments. The ordinates represent the logarithm of the counts/sec which is nearly the same as the omnidirectional flux of penetrating particles in number of particles per cm^2 sec. The MA of Apollo 12, like the TID of Apollo 15, was operating with a high background at this time. Therefore, information from these two detectors should be regarded as representing only the relative change in particle flux.

According to our minimum energy estimation, plots with the label MA represent fluxes of protons with energies ≥ 25 Mev. Likewise, plots with the label TID represent fluxes of protons with energies ≥ 50 Mev. Notice that at 0730 UT on August 4, the flux of the penetrating particles was enhanced substantially and it surpassed three orders of magnitude within seven hours. Associated with this enhancement, there was a 3B flare which began at 0530 UT [Lincoln, *et al.*, 1972], allowing a transit time of 2 hours.

One of the most interesting features in the penetrating particle event is shown on August 5 (Figure 4) between 0310 UT and 0507 UT. At 0259 UT a quick precursor spike occurred that lasted seven minutes. This was followed by a square wave flux enhancement that started at 0310 UT with a sharp rise time of 8.5 minutes, and a stepped decrease at 0459 UT with a decay time of also 8.5 minutes. The duration of the square wave was almost two hours. There was no outstanding solar flare reported that can be associated with this interesting event.

Pioneers 9 and 10, which were both at 50°E from the Sun-Earth line but at 0.8 AU and 2.1 AU, respectively, did not observe the square wave [Lezniak and Webber, 1972; Webber *et al.*, 1972; W. R. Webber, personal communication]. However, experiments onboard spacecraft operating in the vicinity of the Earth [Kohl *et al.*, 1972; Paulikas *et al.*, 1972; Bostrom *et al.*, 1972], and on the Moon's surface [Moore *et al.*, 1972; Medrano *et al.*, 1972], observed the passage of this peculiar cosmic ray event.

Figure 5 is a continuation of Figure 4. As can be seen, another important enhancement began at 1547 UT August 7. Although the related solar flare was again of 3B importance, the flux magnitude of this second burst is less strong than the one on August 4. The flare associated with this last event started at 1500 UT which allows a transit time of 47 minutes. Consequently, the diffusion process of these solar protons has to have been much quicker than for the first event on August 4.

Summary

The particles observed by the ALSEP-SIDEs of Apollos 12, 14 and 15 can be divided into two categories. The first category consists of ions within the energy range of 10 ev to 3500 ev. Meaningful ion observations in this energy range are called ion events. These ion events occurred before the onset of particles that fall in the second category. Particles of the second type correspond to penetrating particles of minimum energies (assuming they are all protons) 25 Mev and 50 Mev that are required to penetrate the shielding and reach the detectors of the MA and TID, respectively.

Sporadic energetic ion events were detected by the Apollo 14 instrument while its look direction changed from -80° to -71° from the Sun's radial direction. The spectra of these ions are characterized by a narrow dispersion in energy, with a maximum around 2750 ev. In this same period the similar detector on Apollo 12 was looking at directions -116° to -108° from the Sun's radial direction and did not detect any distinct ion event. These energetic ions are probably protons ejected from the bow

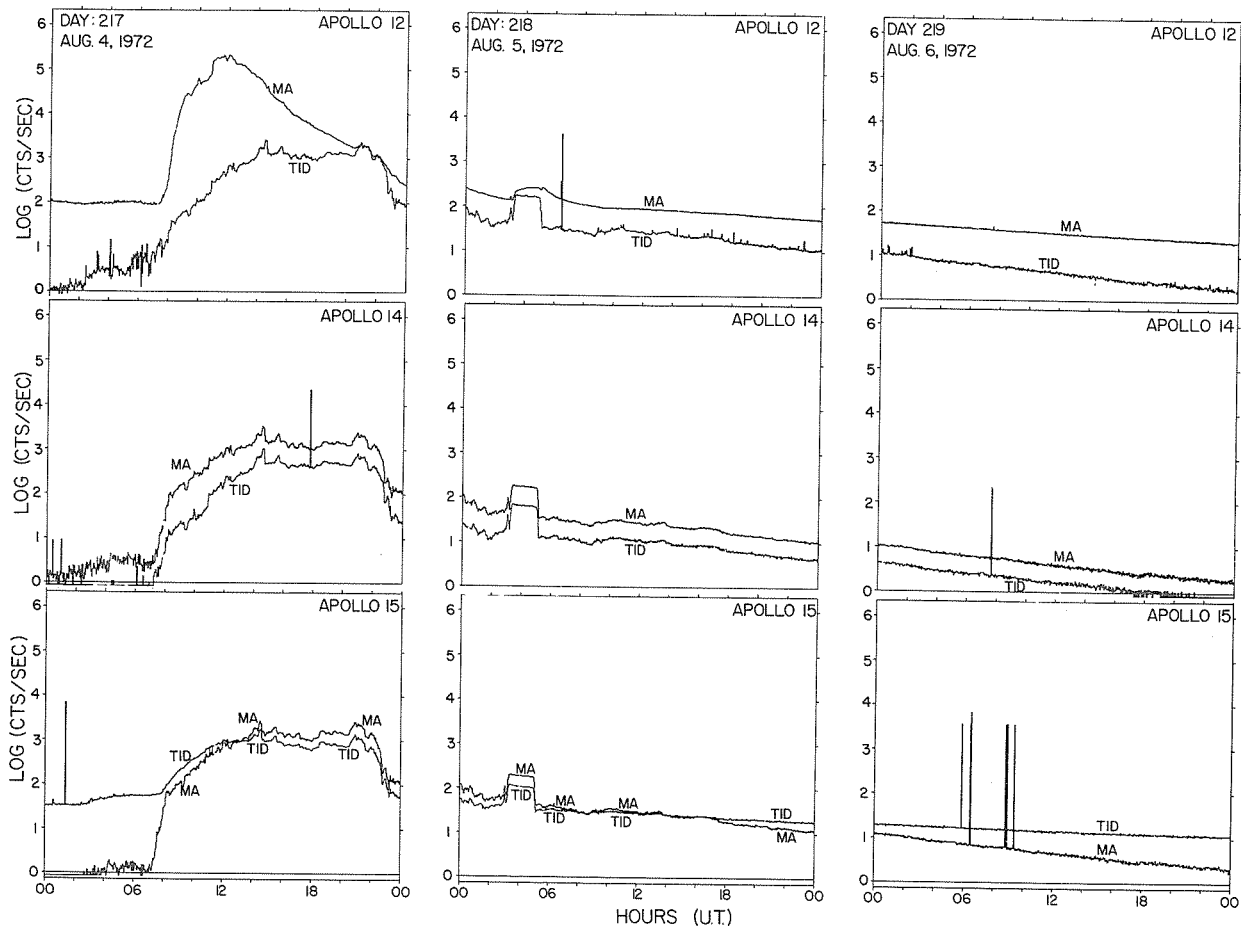


Fig. 4. Time history of the penetrating particle event. Every row of blocks displays 3 days of data from each Apollo experiment. The counts/sec, plotted on a logarithmic scale, very nearly represent also the omnidirectional flux in particles $\text{cm}^{-2} \text{sec}^{-1}$. MA and TID represent protons with energies ≥ 25 Mev and ≥ 50 Mev, respectively.

shock. Such events are not uncommon at this location in the lunar orbit. Similar phenomena have been reported by Asbridge *et al.* [1960], Montgomery *et al.* [1970], and Scarf *et al.* [1970].

Consistent spectra of ions with a very broad energy distribution were detected by the Apollo 12 SIDE detector early on August 4. The frequency of occurrence of these ion events of short duration (\sim minutes) increased before the onset of the penetrating particles. The detector look direction of the Apollo 12 instrument at that time was -105.4° from the Sun's radial direction. Significant data points in our highest energy/charge channel (3.5 kev) imply that the energy spectrum extended beyond this limit. Therefore, the computed bulk speed from a characteristic spectrum (510 km/sec) should represent only a lower limit. Estimation of temperatures is somewhat more complicated due to the contribution of heavier elements, although there are no distinguishable secondary peaks in the spectra. It is concluded that these ions correspond to solar wind ions that were disturbed by the shock wave that reached the earth early on August 4.

Solar protons with energies greater than 25 Mev and 50 Mev have been detected on the night side of the Moon. The first particle event started two hours after the importance 3B flare on August 4. The second particle onset took place only 47 minutes after the start of the 3B flare on August 7. The diffusion of the particles in the second event was much quicker than the first one, although the event was not as strong as the first at the back side of the Moon (the Moon was approaching new Moon on August 7, as can be seen in Figure 1).

The most interesting part of the solar cosmic ray event consists of a square wave particle enhancement early on August 5. The duration of this square wave was about 2 hours. It was preceded by a precursor spike of only 7 minutes duration. No significant solar flare can be associated with this enhancement. It appears that the square wave did not involve the space 50°E from the Earth-Sun line as revealed by the Pioneers 9 and 10 data (W. R. Webber, personal communication). This may imply that the propagation of the cosmic ray square wave had been confined within a narrow angle in space.

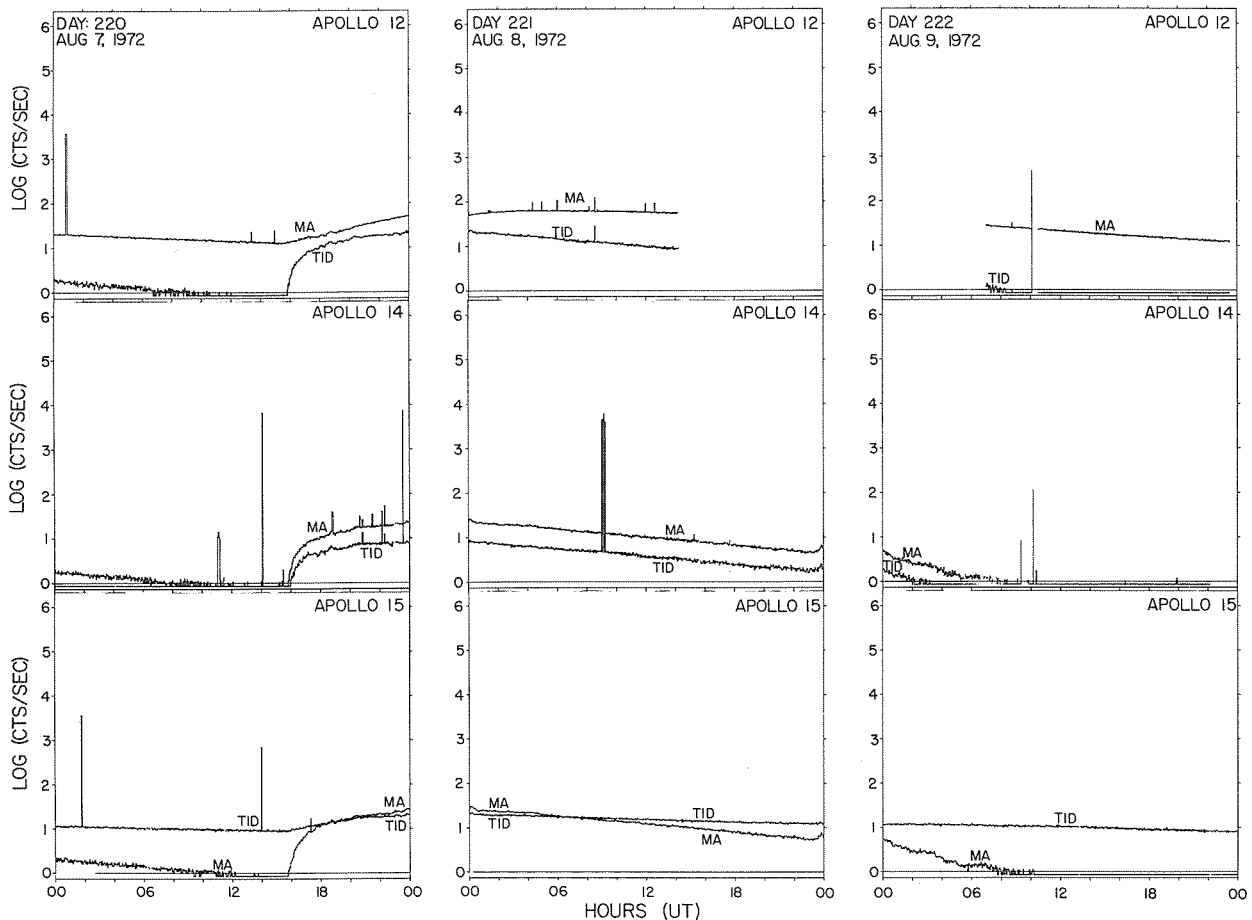


Fig. 5. Continuation of Figure 4.

During the period of the solar flares, strong active magnetic field gradients on the Sun have been reported by Livingston [1972; W. C. Livingston, personal communication]. Along with the active field gradients, strong hydromagnetic activity should be expected and may be associated with the production of the square wave. If the square wave particles were directly ejected from the Sun, the particle coherence observed at the Moon could represent a useful test case for comparing models of diffusion processes.

Acknowledgments

We have benefited from discussions with Drs. Paulikas and Bostrom in the 1972 Fall Meeting of the AGU. We thank Dr. W. C. Livingston for sending to us his unpublished solar magnetograms.

One of us (René A. Medrano) has been partially supported by the Instituto de Pesquisas Espaciais (São José dos Campos, S. P., Brasil).

This research has been supported in part by NASA under contract NAS 9-5911.

REFERENCES

- | | | |
|---|------|--|
| ARMSTRONG, J. W.,
W. A. COLES,
J. K. HARMEN,
S. MAAGOE,
B. J. RICKETT and
D. G. SIME | 1972 | The Solar Wind Velocity during August 1-5, 1972, <u>EOS</u> ,
<u>53</u> , 1957 (abstract). |
| ASBRIDGE, J. R.,
S. J. BAME and
I. B. STRONG | 1968 | Outward flow of protons from the Earth's bow shock,
<u>J. Geophys. Res.</u> , <u>73</u> , 5777. |

- BOSTROM, C. O., 1972 The Solar Proton flux-August 2-12, 1972, Johns Hopkins University, preprint, 1972.
J. W. KOHL,
R. W. McENTIRE and
D. J. WILLIAMS
- COMSTOCK, G. M., 1972 Cosmic-ray source and local interstellar spectra deduced from the isotopes of hydrogen and helium, Astrophys. J., 173, 691.
K. C. HSICH and
J. A. SIMPSON
- FREEMAN, J. W., Jr. 1972 Energetic Ion Bursts on the Night Side of the Moon, J. Geophys. Res., 77, 239.
- FREEMAN, J. W., Jr., 1970 Suprathermal Ion Detector Experiment (Lunar Ionosphere Detector), Apollo 12 Preliminary Science Report, NASA SP-235, 83.
H. BALSIGER and
H. K. HILLS
- HILLS, H. K. and 1971 Suprathermal Ion Detector Experiment (Lunar Ionosphere Detector), Apollo 14 Preliminary Science Report, NASA SP-272, 175.
J. W. FREEMAN, Jr.
- HILLS, H. K., 1972 Suprathermal Ion Detector Experiment (Lunar Ionosphere Detector), Apollo 15 Preliminary Science Report, NASA SP-289, 12-1.
J. C. MEISTER,
R. R. VONDRAK and
J. W. FREEMAN, Jr.
- KOHL, J. W. and 1972 Observations of the August '72 solar events by the solar proton monitor on Explorer 41, EOS, 53, 1055 (abstract).
C. O. BOSTROM
- LEZNIAK, J. A., and 1972 Pioneer 9 Cosmic Ray Observations during August 1972, EOS, 53, 1054 (abstract).
W. R. WEBBER
- LINCOLN, J. V. and 1972 Preliminary Compilation of Data for Retrospective World Interval July 26 - August 14, 1972, World Data Center A for Solar-Terrestrial Physics, Report UAG-21, 101.
H. I. LEIGHTON
- LINDEMAN, R. A., 1971 Recurring Ion Clouds at the Lunar Surface, EOS, 52, 340 (abstract).
J. W. FREEMAN, Jr. and
H. K. HILLS
- LINDEMAN, R. A. 1971 Recurring Ion Events at the Lunar Surface, M. S. Thesis, Rice University.
- LIVINGSTON, W. C. 1972 Solar Magnetic Fields of McMath 11976, EOS, 53, 1052 (abstract).
- MEDRANO, R. A. 1971 Solar Plasma Disturbance Observed by a Suprathermal Ion Detector on the Moon, M. S. Thesis, Rice University.
- MEDRANO, R. A., 1972 Fine Structure of a Solar-flare-associated Shock Wave, EOS, 53, 508.
J. W. FREEMAN, Jr. and
R. R. VONDRAK
- MEDRANO, R. A., 1972 Penetrating particles on the night side of the Moon associated with the August 1972 solar flares, EOS, 53, 1056 (abstract).
J. W. FREEMAN, Jr. and
H. K. HILLS
- MONTGOMERY, M. D., 1970 Vela 4 Plasma Observations near the Earth's Bow Shock, J. Geophys. Res., 75, 1217.
J. R. ASBRIDGE and
S. J. BAME
- MOORE, P. R., 1972 Effects of the August, 1972 Solar Flares Observed on the Lunar Surface, EOS, 53, 1056 (abstract).
D. L. REASONER and
W. J. BURKE

- PAULIKAS, G. A., 1972 Energetic Solar Proton Observations 3-10 August 1972,
J. B. BLAKE and EOS, 53, 1055 (abstract).
E. F. MARTINA
- SCARF, F. L., 1970 Direct Correlations of Large Amplitude Waves with
R. W. FREDRICKS, Suprathermal Protons in the Upstream Solar Wind,
L. A. FRANK, J. Geophys. Res., 75, 7316.
C. T. RUSSELL,
P. J. COLEMAN and
M. NEUGEBAUER
- WEBBER, W. R., 1972 Pioneer 10 Cosmic Ray Observations during August 1972,
E. C. ROELOF, EOS, 53, 1054 (abstract).
F. B. McDONALD,
B. J. TEEGARDEN and
J. H. TRAINOR

Radio Scintillation Measurements of the Solar Wind following
the Flares of August 1972

by

J. W. Armstrong, W. A. Coles, J. K. Harmon, S. Maagoe,
B. J. Rickett and D. G. Sime

University of California, San Diego
La Jolla, California 92037

Observations.

Since April 1972 we have been making daily observations of the solar wind, by observing the interplanetary scintillation (IPS) of several radio sources. The intensity variations are cross-correlated and velocities are deduced from the time shifts between our three 74 MHz antennas, which are separated by baselines of about 90 km [Armstrong and Coles, 1972]. As discussed by Coles and Maagoe [1972], two velocity estimates are made representing the range of velocities contributing to the scintillation pattern. The "peak" velocity is obtained from the time-shifts for maximum correlation; the "mean" velocity is from the average of the shifts at half the maximum. Both velocities are estimated under a radial assumption.

The scintillation pattern is the weighted sum of the scattered signals from along the line-of-sight to the radio source. Most of the scintillation comes from a dominant scattering region, defined by the half power width of the weighting function. The regions are shown in Figure 1 projected onto the solar equatorial plane, for the radio sources in use on August 7, 1972. The ticks mark the peak of the weighting functions with the heliographic latitudes indicated. The "mean" velocity is an average over the scattering region centered on the location of the tick; the "peak" velocity estimates (conservatively) the maximum velocity present in the region; ΔV is defined as the difference "peak" minus "mean" velocity, estimating a range of velocities in the region. In quiet conditions we find $\Delta V \lesssim 50$ km/s and ΔV increasing with latitude [Coles and Maagoe, 1972].

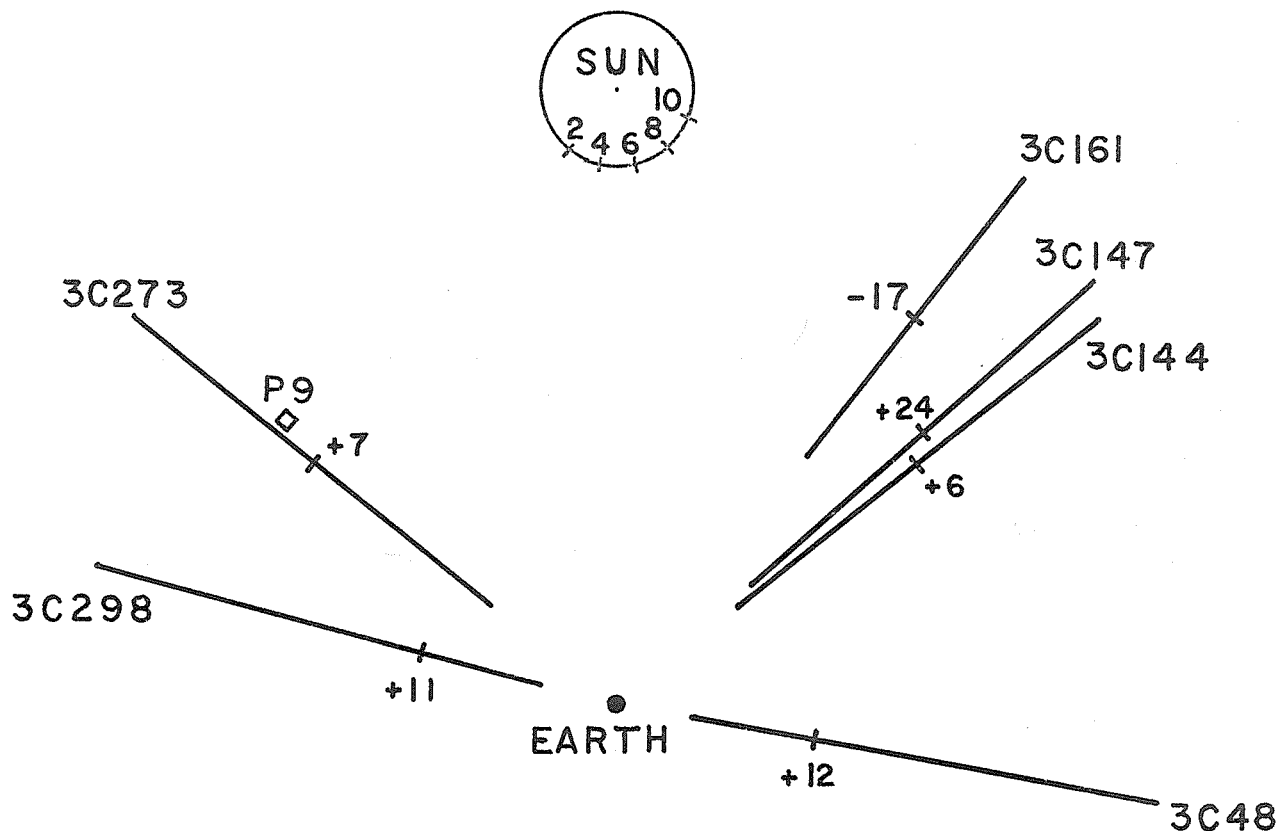


Figure 1. The location of the scattering regions on August 7th, 1972. The position of the active region is shown for the indicated dates in August.

The measurements made in August 1972 are given in Table I and Figure 2. As well as the spatial average discussed above, each observation is the average over about one hour centered on the time given. The mean velocity and ΔV are given, with error estimates derived from the self-consistency of the results for the three baselines. ΔV has no significance when it is negative or of similar magnitude to the error. The data gaps are largely due to interference from the very active sun via antenna side-lobes. The velocities from Pioneer 9 are also shown in Figure 2 [Report UAG-21, World Data Center A for Solar-Terrestrial Physics].

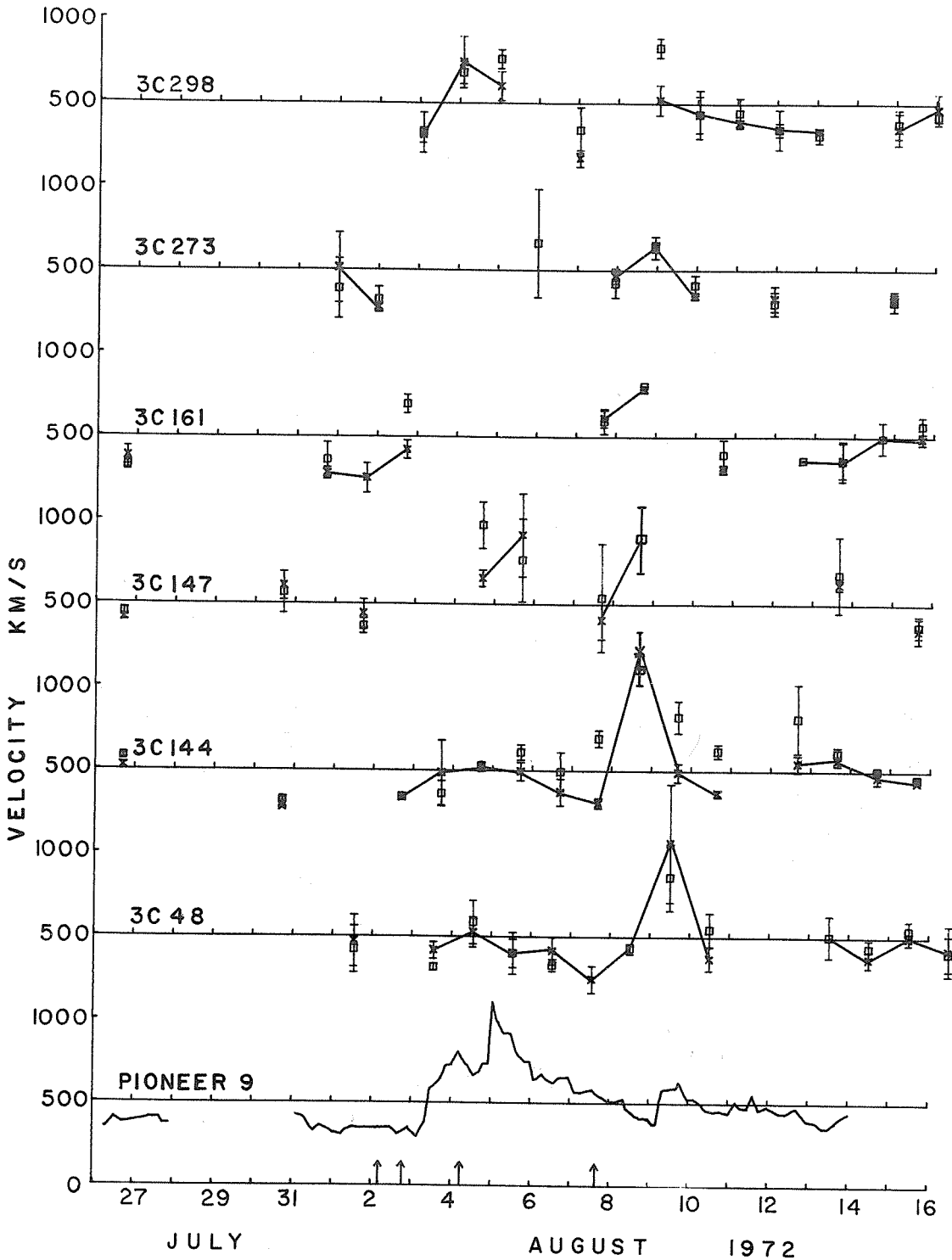


Figure 2. The "mean" IPS velocities (crosses) are joined by lines for consecutive UT dates. The "peak" velocities are shown as squares.

TABLE I

SOURCE	1972 MONTH/DAY/UT HRS.	\bar{v} (km/s)	ERROR (\pm km/s)	Δv (km/s)	LATITUDE (degrees)	DISTANCE (A.U.)
3C273	7/26/00	378	133	-132	5	0.88
3C147	7/26/17	410	16	35	33	0.70
3C144	7/26/17	524	24	58	5	0.65
3C161	7/26/18	380	58	-53	-30	0.63
3C147	7/30/17	606	88	-41	31	0.74
3C144	7/30/17	276	5	48	5	0.70
3C161	7/31/18	280	37	82	-25	0.67
3C273	7/31/24	513	211	-125	5	0.83
3C273	8/01/24	275	25	46	5	0.82
3C48	8/01/13	472	157	-48	12	1.07
3C147	8/01/17	441	86	-75	29	0.76
3C161	8/01/18	251	91	60	-24	0.68
3C144	8/02/17	336	7	8	5	0.73
3C161	8/02/18	420	58	278	-23	0.69
3C298	8/03/02	306	46	17	10	0.99
3C48	8/03/13	417	54	-102	12	1.07
3C144	8/03/17	486	199	-126	6	0.74
3C298	8/04/02	743	150	-63	10	0.98
3C48	8/04/13	527	90	62	12	1.08
3C147	8/04/17	657	53	319	27	0.78
3C144	8/04/17	521	27	13	6	0.75
3C298	8/05/01	603	88	158	10	0.98
3C48	8/05/13	401	126	0	12	1.08
3C147	8/05/17	915	252	-148	27	0.79
3C144	8/05/17	495	58	118	6	0.76
3C48	8/06/13	415	81	-83	12	1.09
3C144	8/06/17	370	83	127	6	0.77
3C298	8/07/01	174	51	167	10	0.97
3C48	8/07/13	246	84		12	1.09
3C147	8/07/17	407	117	137	26	0.81
3C144	8/07/16	306	34	393	6	0.79
3C161	8/07/17	613	52	-18	-20	0.73
3C273	8/07/23	466	47	-45	6	0.76
3C48	8/08/12	566	505	-133	12	1.10
3C144	8/08/16	1220	115	-50	6	0.80
3C161	8/08/17	786	20	20	-19	0.74
3C273	8/08/23	635	68	6	6	0.75
3C298	8/09/01	522	90	309	10	0.96
3C48	8/09/12	1069	355	-207	12	1.10
3C144	8/09/16	493	59	336	6	0.81
3C73	8/09/23	345	21	65	6	0.74
3C298	8/10/01	437	111	0	11	0.96
3C48	8/10/12	372	72	177	12	1.10
3C144	8/10/16	369	22	253	6	0.82
3C161	8/10/17	308	28	89	-17	0.75
3C298	8/11/01	389	22	57	11	0.95
3C273	8/11/23	331	75	-29	7	0.72
3C298	8/12/01	346	41	-1	11	0.95
3C144	8/12/16	549	52	269	6	0.83
3C161	8/12/17	390	192	-26	-16	0.77
3C298	8/13/01	336	13	-24	12	0.94
3C48	8/13/12	300	150	396	12	1.12
3C147	8/13/16	620	30	64	22	0.86
3C144	8/13/16	569	31	44	6	0.84
3C161	8/13/17	364	105	-9	-15	0.78
3C48	8/14/12	371	51	66	12	1.12
3C144	8/14/16	465	43	41	6	0.85
3C161	8/14/17	760	437	-262	-15	0.79
3C273	8/14/23	318	61	10	7	0.68
3C298	8/15/01	350	96	32	12	0.93
3C48	8/15/12	497	38	51	12	1.12
3C147	8/15/16	345	79	28	21	0.87
3C144	8/15/16	437	8	21	6	0.86
3C161	8/15/17	490	38	82	-14	0.79

Interpretation.

The flares of August 02/02^h UT and 02/22^h UT ejected material at high speed, from McMath region 11976, which had slowed to about 650 kms/s when observed at 03/12^h UT by Pioneer 9 (0.77 A.U.) and at 04/01^h UT for 3C298 (0.95 A.U.). This material reached the earth early on the 4th causing a geomagnetic storm; it had reached 3C48 and 3C144 by midday on the 4th giving 500 km/s velocities. The location of the active region on the sun is indicated in Figure 1 for a sequence of dates (0^h UT) in August. It is clear that the propagation time for the ejected material was considerably longer in directions away from the flare normal.

The 3B flare at 04/06^h UT provided fresh violent injection into the solar wind, which met with little decelerating resistance, causing the 1100 km/s velocity observed by Pioneer 9 at 05/00^h UT and probably caused the large geomagnetic storm starting at 04/22^h UT. The propagation time to the earth yields a velocity of 2700 km/s, which may be confirmed by the velocities above 2000 km/s, reported by Gruenwaldt et al. [1972] from the HEOS satellite. Our observations did not detect any high velocities on the 4th or 5th. However each source is only observed every 24 hours and the expansion of a shock front at 2500 km/s would have passed the scattering regions by the observing times of August 4th and 5th. The level of scintillation on the 5th and 6th was surprisingly low, indicating low turbulent densities. It seems that the whole region was cleared very rapidly by the sweeping action of successive blast waves from the outbursts of the 2nd and 4th. This idea is supported by the very low electron content observed by Croft [1972] between the earth and Pioneer 9 during August 5-7.

The sun was then relatively quiet until the 3B flare on 07/15^h UT. We observed increases in velocity to 1200 km/s from 3C144 at 08/16^h UT (0.8 A.U., +6° latitude), and to 800 km/s from 3C161 at 08/17^h UT (0.76 A.U., -19° latitude), and 1000 km/s from 3C48 at 09/12^h UT (1.11 A.U., +12° latitude). This outburst caused a geomagnetic storm starting at about 09/00^h UT and an increase from 376 to 585 km/s measured by Pioneer 9 on 09/07^h UT. The active region was 37°W of the earth's meridian, and 80°W of the Pioneer 9 meridian at the time of the flare, but the scattering regions for 3C144, 3C161 and 3C147 were roughly aligned with the flare normal. As with the August 4th flare, the material was ejected at very high speed near the flare normal, but spread more slowly in the direction of Pioneer 9 at 80° from the flare normal. The picture is qualitatively similar to the blast wave model of Hundhausen and de Young [1971] and a detailed comparison is in progress.

This work was supported by the Atmospheric Sciences Section of the National Science Foundation under Grant GA 20591.

REFERENCES

- | | | |
|---|------|--|
| ARMSTRONG, J. W. and
W. A. COLES | 1972 | Analysis of three-station interplanetary scintillation, <u>J. Geophys. Res.</u> , <u>77</u> , 4602. |
| COLES, W. A. and
S. MAAGOE | 1972 | Solar-wind velocity from IPS observations, <u>J. Geophys. Res.</u> , <u>77</u> , 5622. |
| CROFT, T. A. | 1972 | Wide variations in solar wind density on August 3-14, 1972, (SPR 34) <u>Trans. AGU</u> , <u>53</u> , 1057. |
| GRUENWALDT, H.
M. D. MONTGOMERY and
H. ROSENBAUER | 1972 | Extreme solar wind conditions observed after the activity related to McMath region, (SPR 39) <u>Trans. AGU</u> , <u>53</u> , 1058. |
| HUNDHAUSEN, A. J. and
D. S. DE YOUNG | 1971 | Two-dimensional simulation of flare-associated disturbances in the solar wind, <u>J. Geophys. Res.</u> , <u>76</u> , 2245. |

THE DISTRIBUTION OF SMALL-SCALE IRREGULARITIES IN THE SOLAR PLASMA

DURING JULY 26 - AUGUST 14, 1972

Z. Houminer *

Mullard Radio Astronomy Observatory,
Cavendish Laboratory, Cambridge, England.

Daily observations of a large number of scintillating sources over long periods of time indicate the presence of enhanced scintillation sectors which corotate around the sun [Houminer and Hewish, 1972]. These sectors are aligned along the spiral magnetic field and usually persist for one solar rotation or longer. Houminer and Hewish [1972] have shown that enhanced scintillation sectors lead high solar wind velocity streams and can be associated with enhanced plasma density regions detected by spacecraft.

Occasionally scintillation activity is noted which cannot be fitted into the corotating sector model. This activity can be related to shock fronts associated with solar flares [Wiseman and Dennison 1972, Houminer 1973]. It should be noted, however, that such events are relatively rare [Houminer 1973] and that the bulk of the scintillation variations are accounted for by long-lived corotating structure.

In this note we describe the morphology of enhanced scintillation sectors both before, and after the unusual solar activity, together with short-lived scintillation activity which may be associated with solar flares, observed during the period July 26 - August 14, 1972. In order to monitor the large scale structure of the solar wind a grid of about 30 radio sources was observed daily at transit with the 81.5 MHz array in Cambridge. These observations have been carried out since January 1971 [Houminer and Hewish 1972].

The positions of the lines of sight to the various sources on August 3 are shown in Fig. 1. At the beginning of the period only one scintillation sector was present in the interplanetary medium and its position on July 26 is shown in Fig. 2a. The position of the sector was determined by observing the times at which it produced enhanced scintillation for radio sources lying in different directions as discussed by Houminer and Hewish [1972]. This particular sector was present in the solar wind during the previous five solar rotations.

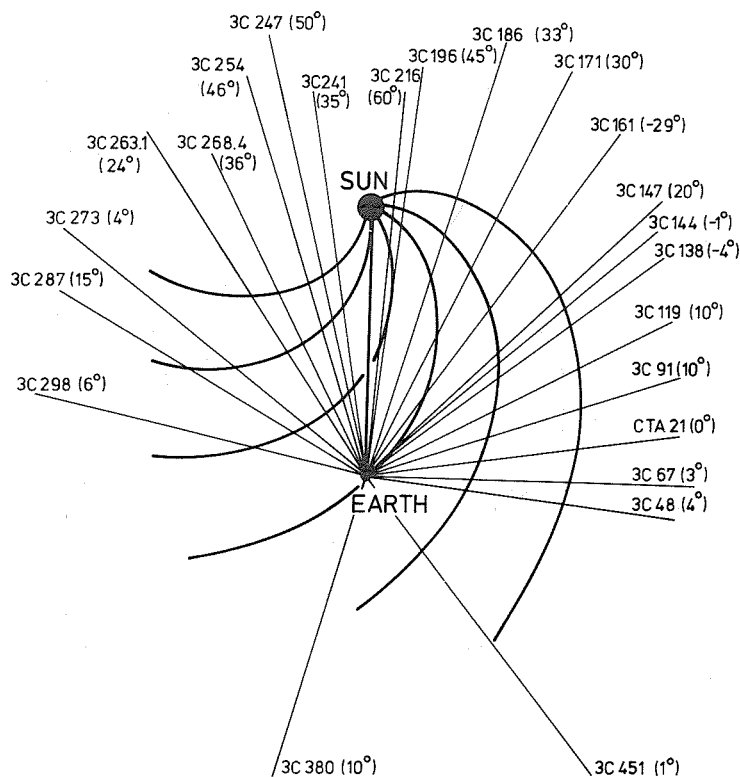


Fig. 1 The grid of sources observed on August 3, 1972. The numbers in brackets denote the heliocentric latitude of the point of closest approach along the line-of-sight.

* Permanent address: The Radio Observatory, National Committee for Space Research,
P.O. Box 4655, Haifa, Israel.

On August 3 and 4, large enhancements in scintillation index were observed for many sources with lines of sight east and west of the sun. The observed time lags between the scintillation enhancements for the various sources were consistent with a nearly spherical expansion of the region causing the enhanced scintillation. Thus the observed enhancements may be due to a shock wave associated with a solar flare [Houminer 1973]. Several relatively strong flares (1B-2B) occurred during August 1 and 2, which were associated with McMath plage region 11976 situated at N14° E30°-45° on the solar surface. It is significant that sources with lines of sight east of the sun showed much larger increases in scintillation index (100-300%) than sources with lines of sight west to the sun (50-100%). The shape of the shock front on August 3, as deduced from the scintillation observations is shown schematically in Fig. 2b. From the time lag between enhancements for the various sources the velocity of the shock front is estimated to be between 700-1300 km/sec.

Very large solar flares (3B-4B), all associated with the same McMath plage region 11976, occurred on August 4 and 7. However, there is no indication that a shock wave producing enhanced scintillation was associated with these flares. Though no shock wave was observed, there was evidence that a corotation scintillation sector may have originated from the same plage. region, giving sequential increases in the scintillation index for the various sources. The position of the scintillation sectors on August 8 is shown in Fig. 2c. The sector marked B was again observed one solar rotation later, together with sector A. The position of the scintillation sectors on September 5 (one solar rotation later) is shown in Fig. 2d.

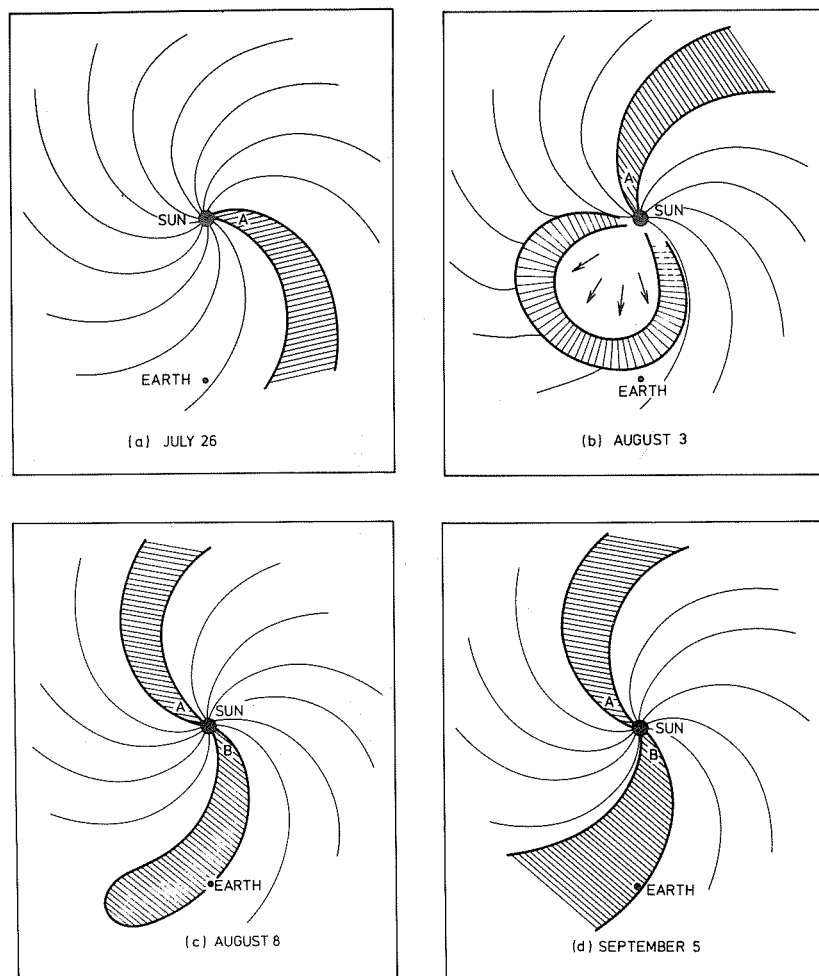


Fig. 2 The proposed large scale structure of the solar plasma during July 26-Aug. 14, 1972.

REFERENCES

- Houminer, Z. and Hewish, A. 1972 Long-lived sectors of enhanced density irregularities in the solar wind. Planet. Space Sci., 20, 1703.
- Houminer, Z. 1973 Flare associated shock waves observed by interplanetary scintillation. To be submitted to Planet. Space Sci.
- Wiseman, M. and Dennison, P.A. 1972 Flare induced shocks and corotating streams in the interplanetary medium. Proc. A.S.A., 2, 79.

The August 1972 Events; Pioneer 9 Plasma Wave Observations

by

Frederick L. Scarf

Space Sciences Department
TRW Systems Group
Redondo Beach, California 90278

A very preliminary inspection of the data for the giant storms of August 1972 shows that extremely valuable information was recorded on Pioneer 9, and this note contains a brief description of some of the electric field wave observations in terms of this initial analysis.

The trajectory of Pioneer 9 for this interval is described elsewhere. The point of interest is that Pioneer was near perihelion in August of 1972. Last year, Scarf and Siscoe [1971] analyzed some early data and showed that when disturbances were detected near 0.75 AU, the largest response generally appeared in the broadband (100 Hz) channel, with low wave levels being measured in the narrowband 400 Hz channel (a more comprehensive report by Scarf, Green, and Burgess [1973] verifying this result will be published shortly). The large earth-Pioneer 9 range shown here has some additional implications. In August 1972 the spacecraft was generally tracked at eight bits/sec, and at this rate the wave experiment has one word or 6 bits per seven-and-a-half minutes for each measurement channel. Figure 1 shows some of the actual wave data, along with isolated samples of the B-field magnitude (roughly one value per hour), and half-hour ranges of the peak solar wind speed. All of these measurements were derived from the real time teletype link being operated at NASA Ames Research Center.

The top panel in Figure 1 is the equivalent 100 Hz wave level derived from one step (#5) in our broadband pulse analysis scan. The second panel is the 400 Hz \pm 30 Hz wave level, and there are eight 400 Hz points for every one of these broadband data points. It can be seen that the wave instrument detected a long-lived enhancement in plasma wave turbulence level, starting on August 3, in association with the very large B-values. As anticipated for these near-perihelion measurements, the peak 400 Hz wave levels are low and the peak broadband wave levels are high, in comparison with the characteristic 1 AU storm values.

Figure 1 shows some interesting wave, particle, and field associations. The first event at 0430 UT on August 3 was apparently weak. Although the wind speed, V, initially jumped by 90 km/sec (300 to 390) and B then rose to 20 γ , no significant change in plasma wave turbulence level was noted. However, near 1130 UT on August 3, the main shock (V from 380 to 580 km/sec, B up to 95 γ [Colburn *et al.*, 1972]) was encountered and this did produce a very significant enhancement in wave activity. There is some evidence that simultaneous (but less clear) changes in B, V, and ϕ (wave) near 2220 UT on August 3 and 0145 UT on August 4 may have been connected with detection of reverse shocks, but further analysis is needed. However, it does appear fairly certain that the brief enhancement in B and in wave levels at the end of the 4th and the beginning of the 5th is connected with detection of a forward-reverse shock pair.

The shock on the 9th day of August (V from about 370 to 550 km/sec) is not shown here -- in terms of electric field wave levels it again appeared to produce relatively small changes. Moreover, we do not show the 30 kHz wave levels -- this channel gave no significant signals throughout the event.

Figure 2 shows the 1130 UT (August 3) shock on an expanded time scale. Here some points are missing from the teletype data, but they should be filled in when the Pioneer Project tapes are processed. It should also be noted that the top panel of Figure 2 now contains reduced data from all available broadband pulse height steps, 1 through 5; the dashed line connects sequences when the pulse height analyzer setting was high enough to exclude all ambient waves (steps 6,7,8).

Wolfe *et al.* [1972] and Mihalov *et al.* [1972] have discussed the potential importance of plasma turbulence effects for the August event. Local wave-particle interactions may account for some of the changes in wind characteristics observed as the storm propagated from Pioneer 9 to Pioneer 10. Moreover, it has been noted that plasma turbulence terms are likely to be of importance with respect to the Rankine-Hugoniot relations. The August event also provides an excellent opportunity for the wave experimenters to analyze the wave modes in the solar wind frame; the rapid and large excursions in B, N, and V mean that f_c^- and f_p^+ repeatedly swept through the channel frequencies, while variable Doppler effects were occurring. Further analysis of the August 1972 events will involve correlation studies with the complete ARC magnetometer and plasma probe observations. The magnetometer measurements will give the local gyrofrequency in the rest frame of the wind. From fully reduced plasma probe data the instantaneous ion plasma frequency (i.e., from the density), and the ion acoustic phase speed (from the temperature) can be computed. The solar wind velocity vector data can be used to evaluate the Doppler shift and thus identify the excited wave modes. This complete analysis should then indicate the extent to which enhanced plasma wave turbulence determines or modifies the dynamical properties of the solar wind during a major disturbance of this type.

* f_c^- = electron cyclotron frequency

f_p^+ = ion plasma frequency

PIONEER 9, TELETYPE DATA, 8 BITS/SEC TELEMETRY RATE

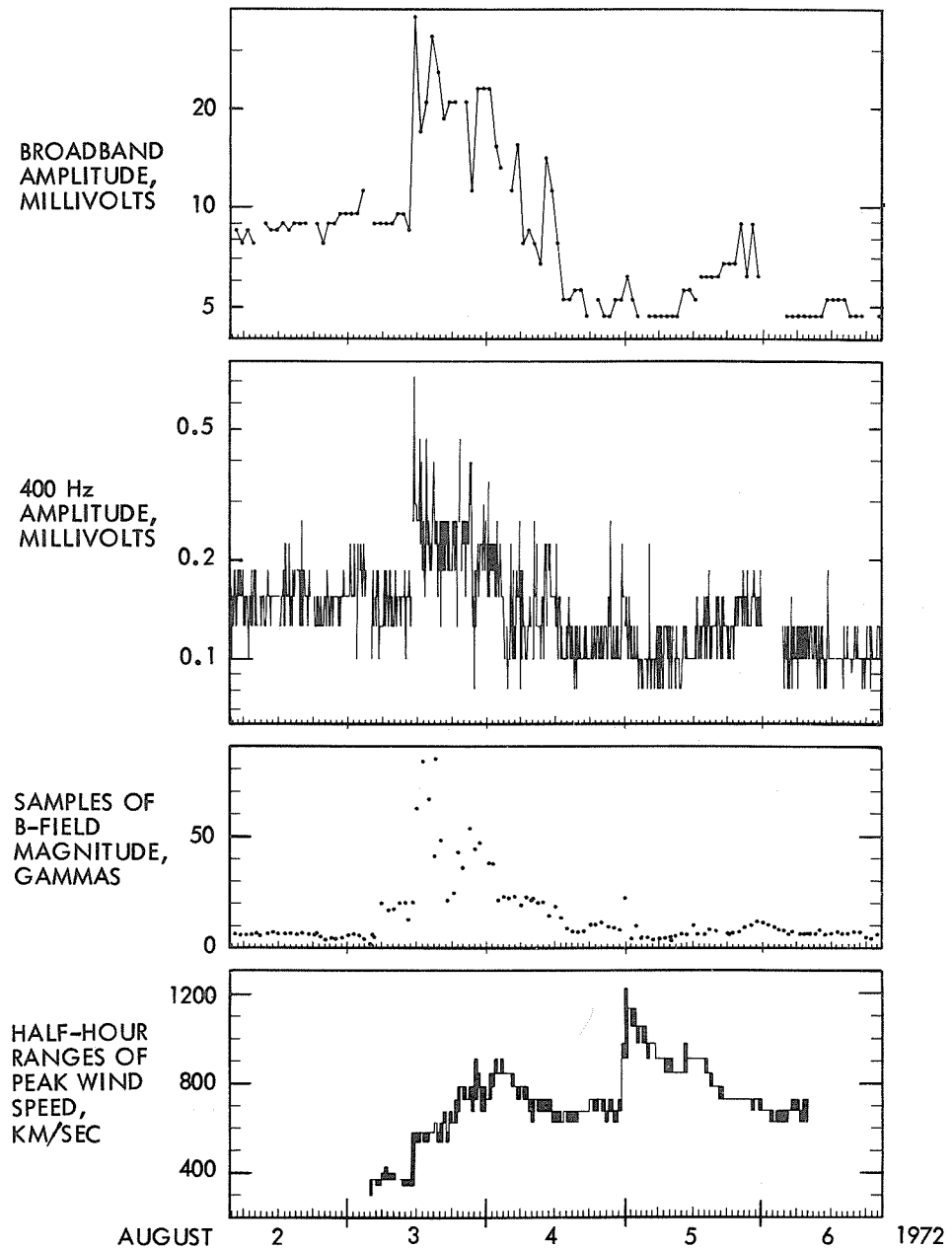


Fig. 1. Plasma wave data from Pioneer 9 for the period August 2-6, 1972. Also shown are interplanetary magnetic field measurements and peak solar wind speed values.

PIONEER 9
AUG. 3, 1972

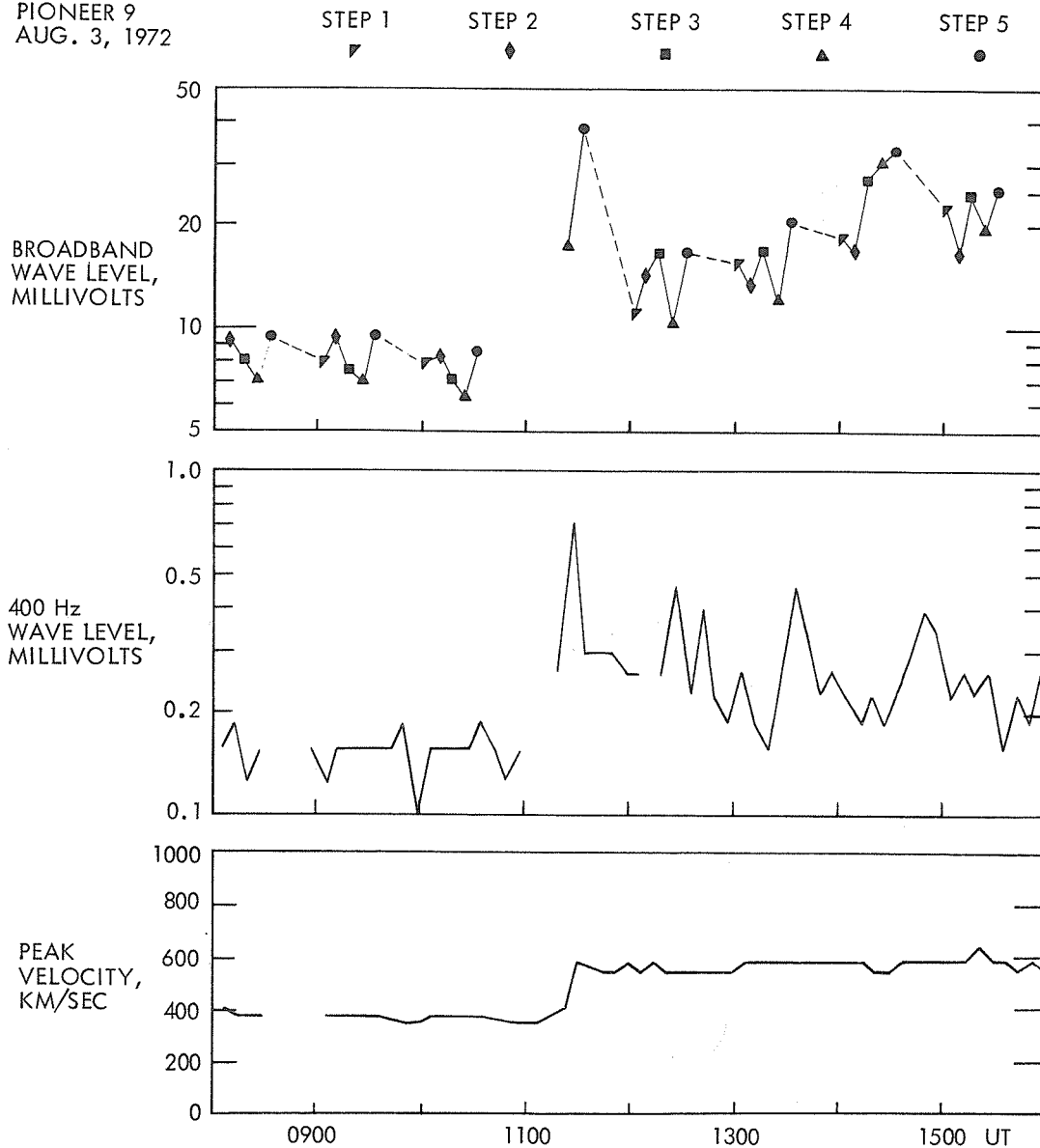


Fig. 2. August 3 data from Figure 1 presented on an expanded time scale.

REFERENCES

- | | | |
|--|------|---|
| COLBURN, D. S., B. F. SMITH and C. P. SONETT | 1972 | Pioneer 9 magnetic field observations during the solar storm of early August 1972, <i>EOS</i> , <u>53</u> , 1058. |
| MIHALOV, J. D., et al. | 1972 | Studies of interplanetary shocks during August 1972 using radially aligned Pioneer spacecraft, <i>EOS</i> , <u>53</u> , 1057. |
| SCARF, F. L. and G. L. SISCOE | 1971 | The Pioneer 9 electric field experiment: Part 2, Observations between 0.75 and 1.0 AU, <i>Cosmic Elect.</i> , <u>2</u> , 44. |
| SCARF, F. L., I. M. GREEN and J. S. BURGESS | 1973 | The Pioneer 9 electric field experiment: Part 3, Radial gradients and storm observations, <i>Cosmic Elect.</i> , in press. |
| WOLFE, J. H., H. COLLARD, D. MCKIBBIN and J. MIHALOV | 1972 | Preliminary interplanetary solar wind profile for the August 2-7, 1972 solar events, <i>EOS</i> , <u>53</u> , 1057. |

Solar Wind Density Variations Observed on A Long Path During August 1972

by

Thomas A. Croft
Center for Radar Astronomy
Stanford University
Stanford, California 94305

ABSTRACT

The average solar wind electron density was measured on a path about 100 million km long, extending inward and behind the earth during August 1972. Abrupt temporal variations were observed in the week beginning August 3, and the measurements taken during a particularly active 10-hour period are described in detail here for the first time. A summary of the observations taken from May through September is given in order to place this discussion in perspective.

Over this long path, the electron density reached 38/cc for a brief period on August 3. This is a very high value for such a long path, implying the localized regions must have experienced much higher densities. Following this about 2-3 days later, the entire path was virtually empty of plasma with the average of under 1/cc, implying in turn that localized regions must have had even lower densities. This report, coupled with a recent JGR letter [Croft, 1973] provides a detailed report on the observations made by the Stanford dual-frequency experiment aboard Pioneer 9 during this period.

1. Introduction

During early August 1972, the dual-frequency experiment of Pioneer 9 was in operation at frequent intervals, primarily because Pioneer 9 and Pioneer 10 were then aligned upon the same radial from the sun. By good fortune, this was also a time when the solar wind was unusually active and, as a consequence, we have obtained some definitive records of the average solar wind density along the path from earth to Pioneer 9.

This sequence of observations was reported by the author at the special 1972 Fall AGU meeting which was devoted to this specific period of solar activity. At that time, a report was prepared describing the provisional data then available [Croft, 1972]. At the time of those reports, the final data form was not available because NASA had not yet had time to process the magnetic tapes acquired by the Deep Space Net receivers. Later, when a portion of those tapes became available, an improved version of the report was published as a JGR letter [Croft, 1973]. Since that time, it has proven feasible to process data from the interval when the electron density was highest; that is, the ten-hour period on August 3-4. These data were unusually difficult to decipher because our transmitting antenna experienced intermittent failures in tracking the spacecraft. In this report, we concentrate on a description of that one day's events.

Further slight improvements in the quality of the data will be derived from a more careful analysis of the ionospheric component of the electron content which in turn is derived from Faraday rotation measurements of signals from geostationary satellites. At the time of this writing, we have used as a basis for calculations only the Faraday rotation observations obtained at Stanford. A more accurate ionospheric content calculation will be made possible through a careful analysis of the similar observations obtained by other stations in the western United States. Any such improvements will be slight, when considered on the scale of the events described here. In a sense, this report (coupled with the JGR letter) can be considered to provide the best possible representation of the dual-frequency observations in early August 1972.

2. Description of Experimental Operation

When VHF radio waves propagate through the interplanetary medium, the free electrons along the path cause a decrease in the group velocity and a corresponding increase in the phase velocity. The magnitudes of both these changes are nearly proportional to the number density of the electrons. As a consequence, a signal which propagates over a long distance undergoes a slight additional delay due to the electrons while at the same time its wavefronts are advanced beyond their free-space positions. When considering the total effect along a path, it is found that the group delay and phase advance are each proportional to the electron content (that is, to the average density along the path multiplied by the path length). The phase advance cannot be measured directly, but one can observe the radio frequency of the signal at the end of its travel and this will be found to vary with respect to rate of change (the time derivative) of the electron content. The group delay difference and the radio frequency shift due to the electrons are both extremely small so that it is not feasible to measure them directly. However, the effects are

less at higher frequencies so that the experimenter can transmit a pair of signals at different frequencies and it is then possible to measure the difference between the two group delays and the two doppler shifts. Koehler [1968] gives a good description of our implementation of this approach.

To work with Pioneer 9, we transmit two signals from Stanford via a 46-meter dish. These signals are at 50 and 423 MHz, with the specific frequencies numerically selected so that they differ precisely in the ratio 2/17, although we find it necessary to add a small fixed offset of roughly 100 cycles which serves to facilitate the receiver lock and which also makes it possible to use a one-way counter in the spacecraft data processor. From the difference of the two doppler shifts, we obtain a measurement of the time rate of change of the electron content. This is integrated to produce a plot of electron content vs time which is reproduced in Figure 1 for the August 3-4 period.

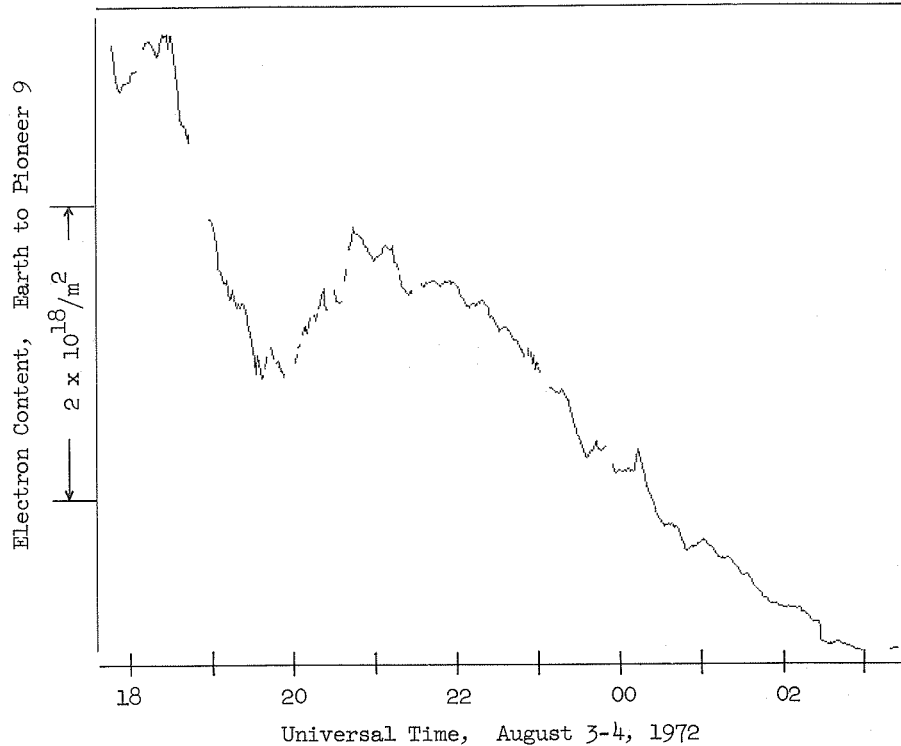


Fig. 1. Electron content as determined from the relative radio frequencies of the two signals arriving at the spacecraft. Since only the rate of change of content can be sensed by this method, the curve represents time integration with an unknown constant of integration; as a consequence, each curve segment can be vertically displaced as needed to match other observations.

The group delay measurement is more straightforward in a theoretical sense, but in implementation it is more complex. To reach the great distances involved, we transmit as much as 400 kilowatts of the 50 MHz signal and 30 kilowatts of the 423 MHz signal. In order to permit measurement of the group delay without loss of the full duty cycle of our amplifiers, we have chosen to impress a phase modulation upon each of these signals. The frequency of the phase modulation may be either 7692 or 8692 Hz. To make the measurement, it is necessary to vary the phase of the modulation itself. This sometimes leads to semantic difficulties because we speak of the phase angle of the phase modulation. The "phase angle" described is that between the two audio frequency sine waves which are then used to modulate the radio frequency phase angle.

Although the dual-frequency experiment can operate well when the spacecraft are as far away as 2 AU, it is necessary at such great distances to process the group delay data by a somewhat indirect approach which was never visualized when the equipment was designed or even when it was operated at closer distances. The indirect approach exploits the operational characteristics of a phase meter on the spacecraft which is used to measure relative phase angle of the modulation of the two signals after their transit through the solar wind. This method has been described previously [see Figure 2 of Landt and Croft, 1970]. In order to provide the reader with a full understanding of the events on August 3 and 4, it is necessary first to provide some understanding of the measurement method because this in turn provides the best avenue for understanding the degree of accuracy of the result.

The meter on the spacecraft reads an angle that varies between 0° and 360° and periodically places into the telemetry stream a six-digit binary number which represents that phase. The six-bit word is equivalent to a decimal number between 0 and 63 and is chosen by the meter according to the logic illustrated in Figure 2. As the angle increases from 0° , the output number rises from about 43 to its highest value which corresponds to a phase angle near 60° . Thereafter, with an increase in the phase angle, the meter output decreases at a nearly linear rate until it reaches its lowest value at a phase angle near 240° . Thereafter the meter output again continues to rise and it repeats this operation exactly for each multiple of 360° . The horizontal axis of Figure 2 could be labeled in terms of electron content along the radio path, provided that the frequency of the modulation is specified. For 7692 Hz, one full cycle of differential modulation corresponds to an electron content of $2.43 \times 10^{18}/\text{m}^2$; for the modulation of 8692 Hz, one turn corresponds to $2.15 \times 10^{18}/\text{m}^2$. When spacecraft are beyond a distance of about 100 million kilometers, the electron content may often exceed these values and therefore the phase angle difference between the modulations on the two signals may exceed 360° many times over. The two modulation frequencies were provided for the express purpose of making it possible to determine the number of full rotations of the differential modulation.

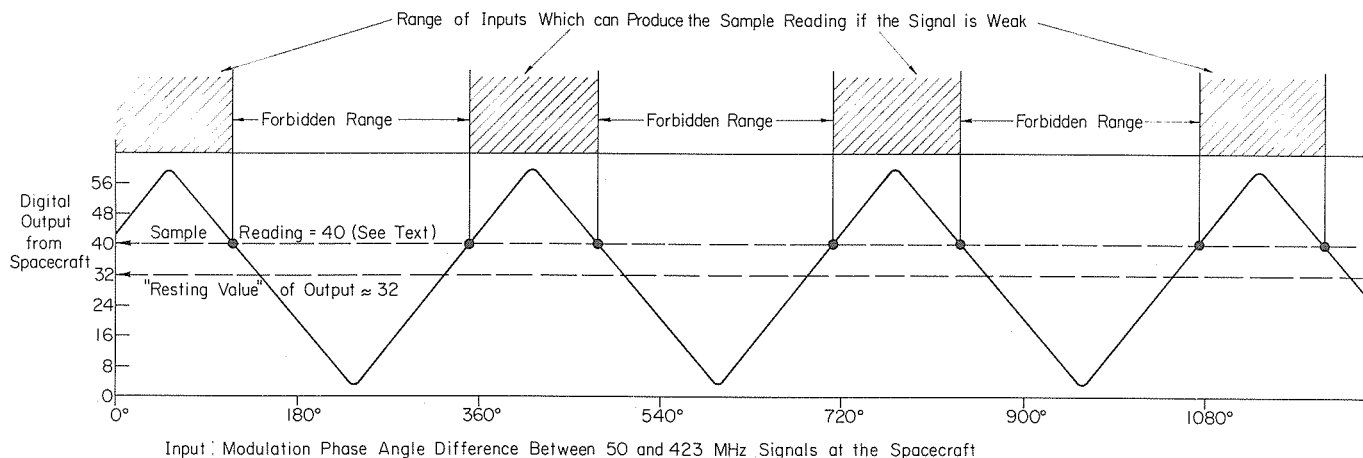


Fig. 2. The strong-signal response characteristic of the modulation phase meter on Pioneer 9. The measured phase angle is proportional to the electron content of a column from earth to the spacecraft. [From Landt and Croft, 1970].

When the signal from earth to the spacecraft is weak, then operation of the meter on the spacecraft changes in such a way that the sawtooth output (as shown in Figure 2) is degraded to a nonlinear form more nearly like a sinusoid, but it is fortunately true that the sinusoid continues to cross through the resting value of 32 (see the Figure) at the same phase angle as before. As the RF signals grow progressively weaker, the meter output progressively decreases in amplitude, but it still crosses the resting value of the same phase angle. For extremely weak signals, the meter output rests at 32. During operation the meter output contains a temporal fluctuation which has a standard deviation of one or two digits.

It is this sawtooth-sinusoid characteristic of the phase meter response which forms the basis for our processing of weak signals. As shown in Figure 2, we are able to specify forbidden ranges which are associated with any particular output from the spacecraft phase meter. In the example shown, it is seen that a digital readout of 40 is received from the spacecraft and this is associated with several forbidden ranges, one for each cycle of differential modulation phase angle. Except for a small amount of noise which is superimposed on all the output readings, the sum of our knowledge about the conditions in interplanetary space is represented by the forbidden ranges. We cannot derive any information concerning the location of the correct modulation phase angle within the various possible ranges of inputs which are not forbidden, because we have no way to determine the exact form of the sawtooth-sinusoid response at any given time. It remains true that all possible response curves lie between the sawtooth and the resting value, so the forbidden zones remain regardless of the RF signal strength.

The data processing thus involves a deduction process in which one gathers together all recoverable data from the spacecraft phase meter and considers all the forbidden ranges as a family. This information is coupled with the doppler information which was shown in Figure 1 and an attempt is made to infer a single solution for the electron content as a function of time during the observing period. The family of forbidden ranges for the August 3-4 observing interval are plotted in Figure 3. Each measured phase angle is used to calculate all the associated forbidden ranges between an electron content of zero and $10^{19}/\text{m}^2$. A single reading from the spacecraft leads to a set of vertical co-linear lines on this representation of the data. Some of these lines are drawn dotted to signify that the output from the spacecraft was within two digits of the resting value and therefore may be an indication only that the dual frequency signals were not reaching the spacecraft with enough strength to operate the instrument.

When the signal is strong, at shorter distances, then there is less noise impressed on the output from the spacecraft and also the phase meter response is very close to the linear sawtooth representation shown in Figure 2. In these circumstances, the ground crew at the transmitter site continually monitors the electron content and inserts a controlled phase angle difference between the transmitted signals in order to keep the spacecraft-measured phase angle on a linear portion of the curve. On most days, for spacecraft within 200 million km of earth, it has been possible to maintain real-time control over the output so that the use of the forbidden zone plots such as Figure 3 has not been necessary. When the signals can be kept strong enough to maintain the straight-line response of the phase meter, then the group delay measurement yields a very accurate representation of the electron content of the solar wind. This was the case on later days in August and an excellent example of such clean data is to be found in the JGR letter [Croft, 1973].

3. Analysis of the Data for August 3-4

Roughly speaking the data analysis concerns an attempt to fit the integrated doppler data of Figure 1 to the group delay data of Figure 3 by shifting the various doppler curves vertically in order that they might fit along the gaps in the forbidden zones without crossing far into any one zone. In addition, consideration is given to several other data forms which are available. For example, the signal amplitude is measured by the spacecraft and telemetered back to earth occasionally, as is the loop stress which is a measure of the ease with which the receiver is able to maintain its lock on the signal. Also, as the transmitter undergoes changes in the modulation phase angle, there is a transient response in the subsequent reaction of the spacecraft to the abrupt change in the received phase angle, and this requires great care in processing due to the critical timing of events. The greatest weakness in the data is probably the unreliability of the integrated doppler (Figure 1). Unlike the group path measurement, one can never tell when the difference-frequency counter is unlocked and running free. Sometimes an obvious out-of-lock condition is easily detected as, for example, that which occurred at 0225 UT when the doppler curve in Figure 1 is seen to undergo an abrupt downward translation. When this portion of the curve is fit to the forbidden zones, it is found that a very close agreement is obtained if the downward excursion is ignored and, therefore, we may conclude that the trend was instrumental, due to a loss of lock. In contrast, it can be seen that the short upward excursion and subsequent fall in the integrated rate which occurs at 0020 UT was probably a true measurement of a change in the interplanetary electron content, because the forbidden zone plot contains the same transient. These identifiable events are exceptionally clear; in the usual case, one must regard the counter with suspicion unless the integrated doppler data happens to agree in shape with the form of the forbidden zone pathways.

In Figure 4, the best fit of the counter data to the forbidden zone is shown together with the measurement of the electron content of the ionosphere. This should be compared with Figure 4 of Croft [1973] which was the provisional form based upon the real-time observations which are less accurate. The first half of this sequence was much less definitive than the second half because of the aforementioned difficulty in keeping the transmitting antenna aimed at the spacecraft. The large number of dotted lines which occur at about 2100 UT results from the fact that the antenna was misdirected so that the signal missed the spacecraft and consequently the spacecraft phase meter was resting near 32. During this time interval, we freely allow the content curve to cross the dotted forbidden zones. In addition, we allow the content curve to cross a forbidden zone which is solid at 2010 UT because it was a transient value representing a change in state of the phase meter shortly after the modulation phase angle was manually changed. In several locations along the curve, it is seen that there is an excellent agreement between the shape of the integrated rate curve and the shape of the edges of the forbidden zones. This is the expected form of the data when the signal is strong and it is considered to be the best evidence obtainable that our content curve is a correct inference from the data.

Although Figure 4 is carried up only to 10^{19} electrons/m², the calculation was carried twice as high and no other reasonable content curve could be found. The reader who wishes to make calculations based upon these data should carefully review the preceding discussions of the measurement method, because they bear upon the tolerance for error in the solution shown. For example, in the time interval near 1900 - 2000 UT, there is wide range of allowed solutions which would be compatible with the data. The solution shown could be lowered almost 5×10^{17} electrons/m² and it would still be compatible with the observed parameters. We have represented it as shown because this particular solution is not only compatible with the data but represents the least temporal variation of the possible solutions.

During the last three hours of the measurement, the integrated doppler data matches the forbidden zones except that the doppler data have a trend for a more rapid decrease than does the open passage among the forbidden zones. This decreasing trend in Doppler data is thought to be attributable to intermittent short losses of spacecraft receiver lock, combined with an observed tendency of the free-running spacecraft counter to run in that direction which causes an apparent decrease in content. During this period of observation the spacecraft telemetry system was being operated at its lowest rate, so that the doppler difference was continually integrated but read out of the spacecraft only once each 56 seconds. As a result, there was adequate opportunity for the spacecraft receivers to go unlocked for a few seconds without causing a marked degradation in the telemetered data. Periodic short unlockings such as this, coupled with the trend for the data processing counter to run in one preferred direction, could account for this type of disagreement between the doppler and group delay observations.

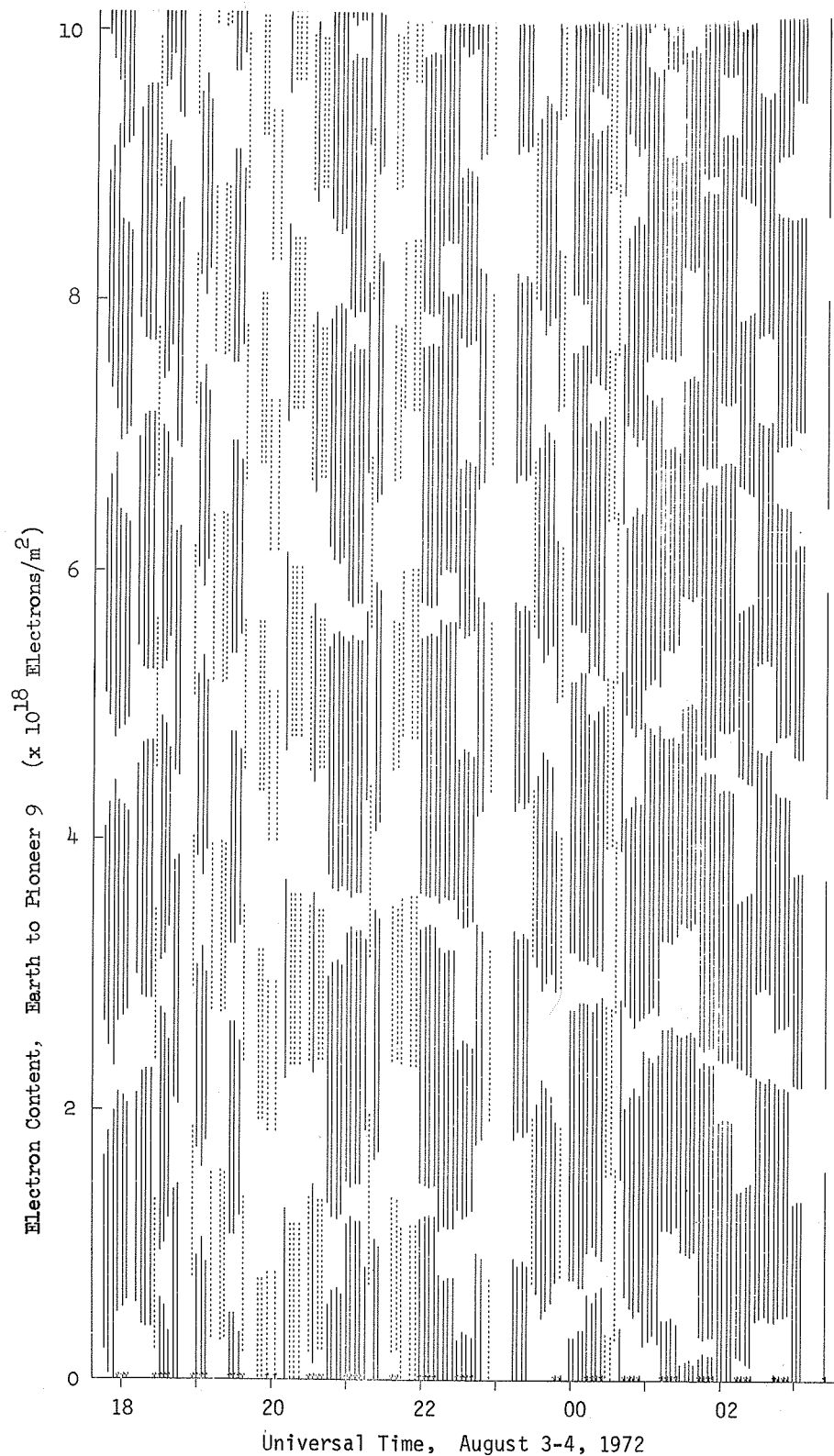


Fig. 3. Each set of co-linear vertical lines represents the forbidden zones derived from a single telemetry readout of the modulation phase meter. The entire plot summarizes our knowledge of the electron content derived from the measured group delay of radio signals on the path. The curve of true content cannot cross a forbidden zone and therefore it must lie in the open regions among the lines.

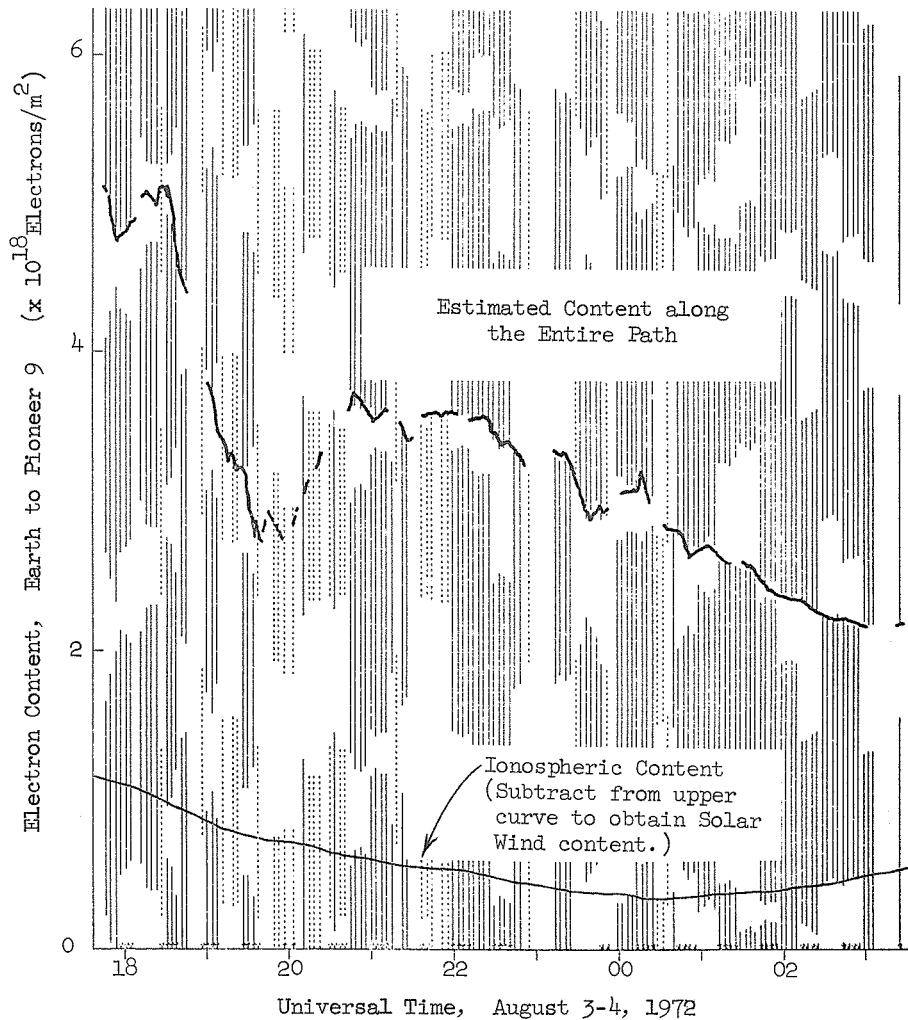


Fig. 4. A blending of doppler and group delay data from Figures 1 and 3 to determine the content-time curve on the path. Since a considerable portion of the observed electrons lie in the earth's ionosphere, this region is observed by means of Faraday rotation measurements of signals for geostationary satellites with the result as shown by the lower curve. The solar wind content is the difference between the two curves, and the spatially-averaged density of the wind is this content divided by the path length, 111 million km yielding values as high as 38/cc.

4. Some Perspective on this Observation

Figures 5 and 6 are added here for the convenience of the reader, having been extracted from Croft [1973]. Figure 5 shows the track of Pioneer 9 over a four and one-half month period and Figure 6 shows the measured electron content during this same period. The interval of observations displayed in Figure 4 is seen to be one of unusually high electron content. In Figure 6, the electron content from earth to the spacecraft has been normalized to 1 AU making use of an assumption that the electron number density varies in inverse proportion to the square of the distance from the sun. This removes from the overall picture a trend toward decreasing content which would otherwise be apparent, and which is attributable solely to the ever-increasing distance of the radio path from the sun during this four and one-half month period. In addition to the unusual activity on August 3-4, the events of the following week were marked by a unique appearance of extremely low density which reached a minimum on August 6. This minimum has been described in the aforementioned JGR letter. The events as depicted during the week following August 3rd are in good agreement with other observations of the solar wind during this period and many fruitful comparisons of the measurements taken by various experimenters are currently underway.

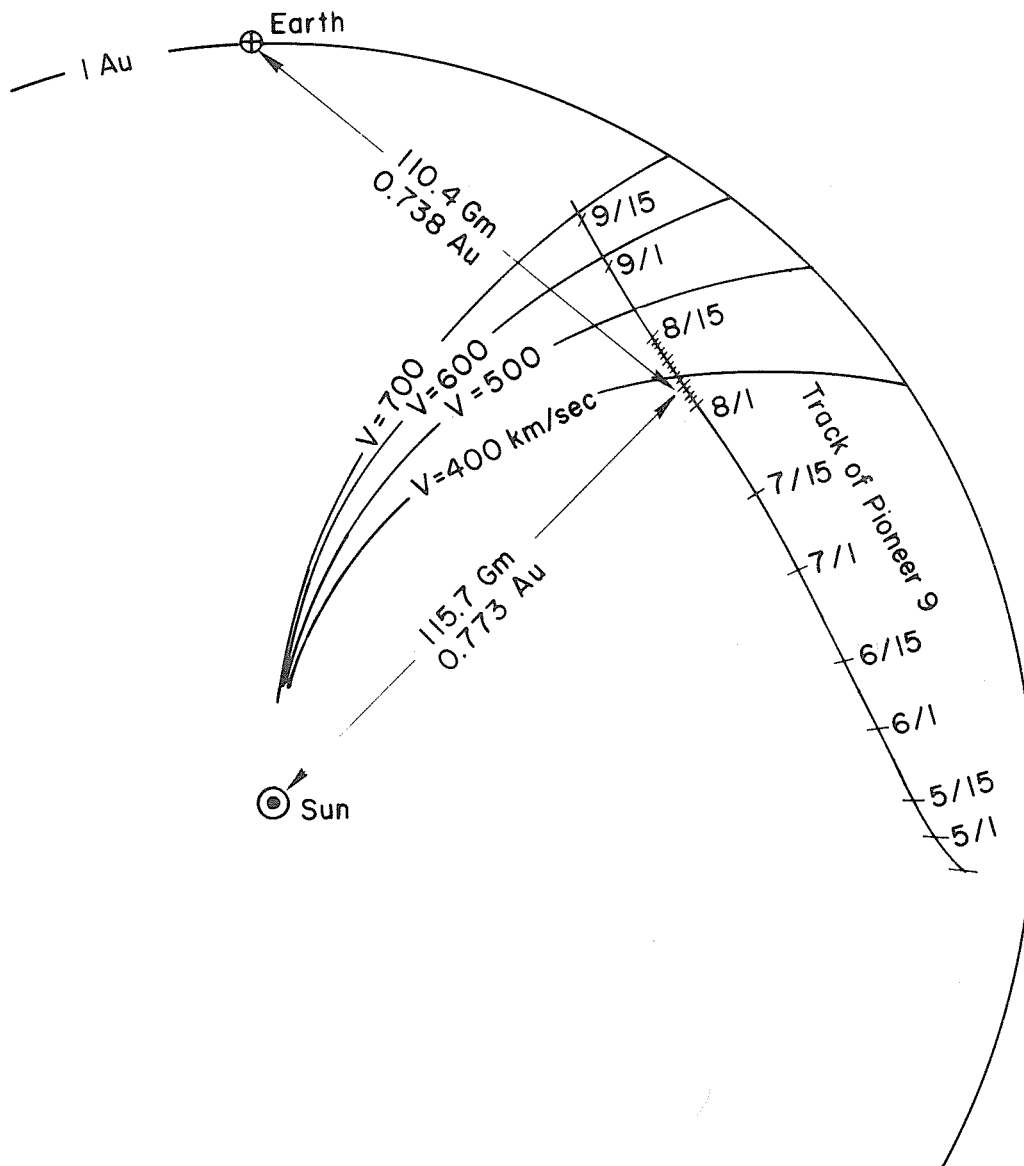


Fig. 5. The path of Pioneer 9 projected onto the ecliptic plane and shown in a frame that rotates with the earth. [From Croft, 1973].

REFERENCES

Croft, T. A.	1973	Traveling Regions of High Solar-Wind Density Observed in Early August, 1972, letter to <u>J. Geophys. Res.</u> , to be published.
Croft, T. A.	1972	Traveling Regions of High Density Observed in the Solar Wind on August 3 and 9, 1972, Scientific Report No. 7, SEL 72-059 <u>Stanford Electronics Laboratories</u> , Stanford University, November 1972.
Koehler, Richard L.	1968	Radio Propagation Measurements of Pulsed Plasma Streams from the Sun Using Pioneer Spacecraft, <u>J. Geophys. Res.</u> , <u>73</u> , 4883-4894.
Landt, J. A. and T. A. Croft	1970	Shape of a Solar Wind Disturbance on July 9, 1966, Inferred from Radio Signal Delay to Pioneer 6, <u>J. Geophys. Res.</u> , <u>75</u> , 4623-4630.

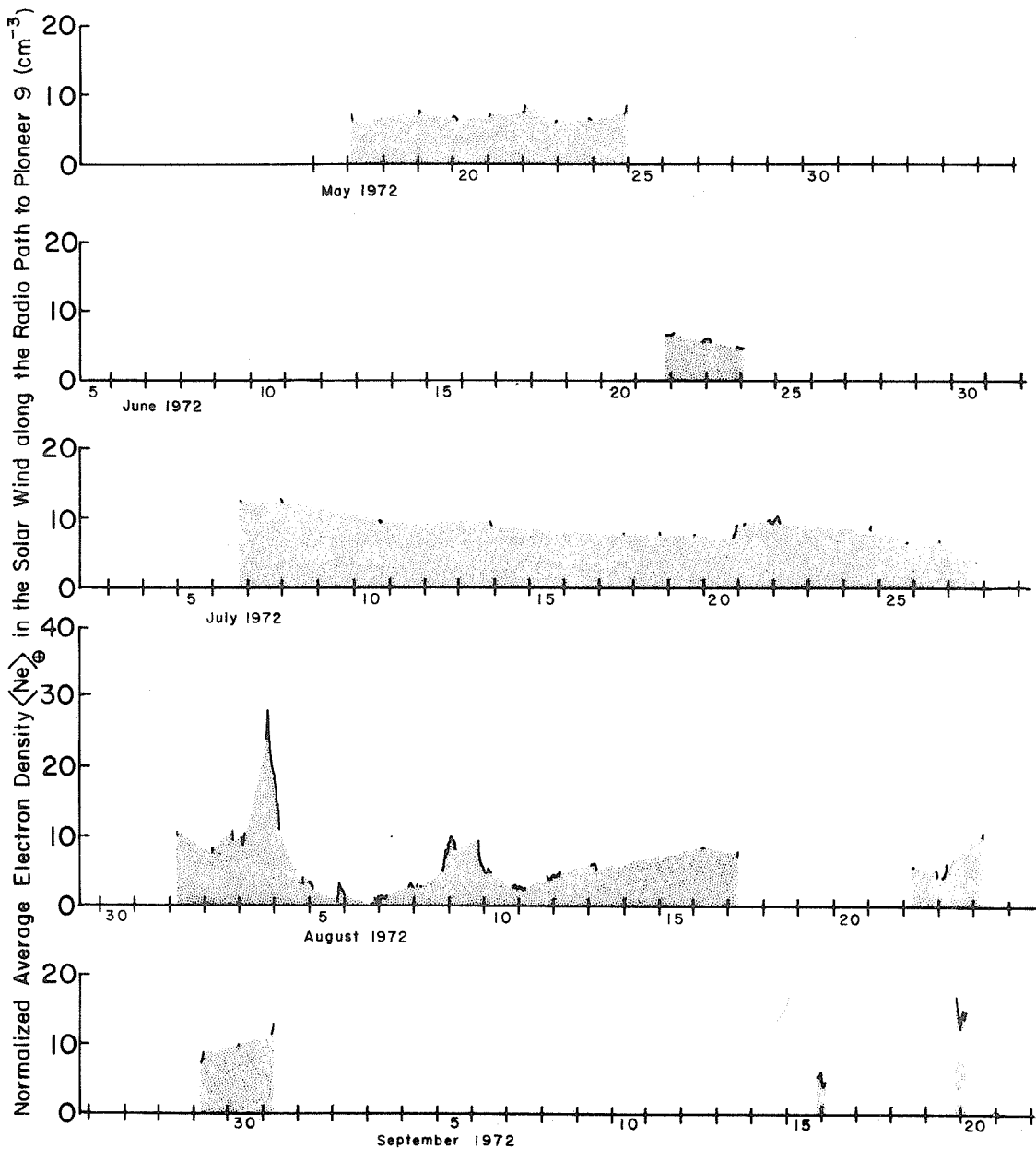


Fig. 6. The average density of the solar wind along the radio path from earth to Pioneer 9, displayed by solar rotations so that those times corresponding to the same Carrington longitude of the sun's central meridian are vertically aligned. These observations (the short dark line segments only) are drawn from our real-time data and are provisional. At each instant, the density has been normalized to 1 AU assuming $1/R^2$ spreading in order to eliminate slow trends due to the changing earth-spacecraft distance. [From Croft, 1973].

VLF Emissions and Whistlers Observed in Japan for the August 1972 Events

by

Tadanori Ondoh
Radio Research Laboratories
Tokyo, Japan

and

Yoshihito Tanaka
Research Institute of Atmospheric
Nagoya University
Toyokawa, Japan

Whistler-triggered emissions and a narrow band hiss (Figures 1a - 1c) were observed by ISIS 2 during the main phase (0732 - 0749 UT, $K_p = 7-$) of a geomagnetic storm on August 9, 1972 over Japan. This VLF observation period is shown by an upward arrow in Figure 2c. Whistler-triggered emissions were detected only below $L = 2.87$ (Invariant latitude, $\Lambda = 53.8^\circ$). A narrow band hiss with center frequency of 3.1 - 3.6 kHz and bandwidth less than 600 Hz lasted for 37 seconds between $L = 2.94$ ($\Lambda = 54.3^\circ$, 07h46m46s UT) and $L = 3.21$ ($\Lambda = 56.1^\circ$, 07h47m23s UT). The center frequency increases gradually with latitude from 3.1 kHz to 3.6 kHz. It is rare that the narrow band hiss is observed down to such a low latitude as $\Lambda = 54.3^\circ$.

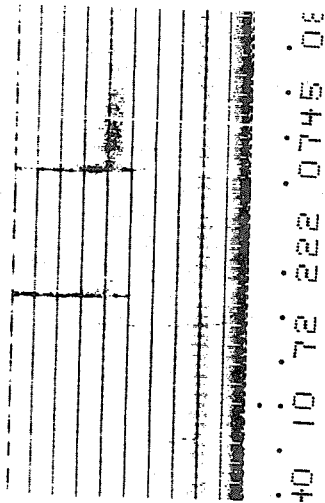
This narrow band hiss is very similar to that observed outside the plasmopause in a quiet period, and most whistler-triggered emissions occur inside the plasmopause. Taylor and Walsh [1972] also observed a narrow band VLF hiss just outside the light ion plasmopause (near 60° dipole latitude at $K_p = 1+$) and many whistlers inside it around an altitude of 1200 km. So the observation of narrow band hiss at $\Lambda = 54.3^\circ$ suggests a movement of the plasmopause toward lower latitudes during the main phase of geomagnetic storm. Hence it seems likely that the plasmopause lay around $L = 2.94$ ($\Lambda = 54.3^\circ$) on the evening side (1717 LT) during the main phase (0747 UT) of the August 9 geomagnetic storm. Rycroft and Thomas [1970] obtained an empirical relation of $L_p = 5.64 - (1.09 \pm 0.22) \sqrt{K_p}$ between the plasmopause location and K_p for the summer night using $N(h)$ data of Alouette I. Substituting $K_p = 6.5$ for $K_p = 7-$, we have $L_p = 2.86 \pm 0.56$ ($\Lambda = 53.8^\circ$) from the above relation. This coincides approximately with the plasmopause location of $L = 2.94$ estimated from the low latitude end of the narrow band hiss.

Figures 2a - 2c show, respectively, time variations of foF2 (thick solid line) at Wakkanai (geomag. lat. N35.3, long. E206.0), whistler occurrence rate (average number per minute) at Moshiri (N34.3, E206.7) and K-index at Memambetsu (N34.0, E208.4) observed for August 3 - 13, 1972, where a thin solid line of Figure 2a represents the monthly median of foF2 at Wakkanai in August 1972. The whistler observation at Wakkanai in this period was continuously conducted during two minutes at every ten minutes (XXh00m - 02m, 10 - 12m, 20 - 22m, 30 - 32m, 40 - 42m, and 50 - 52m). So the whistler occurrence rate in Figure 2b indicates average numbers per minute observed for 36 minutes per three hours. Most whistlers observed at Moshiri for August 3 - 13 were short whistlers propagating from the southern hemisphere. Peaks of the whistler occurrence rate at Moshiri occurred about 8 - 15 hours behind corresponding peaks of the K-index at Memambetsu for August 3 - 13 as a large foF2 decrease (ionospheric storm) began at Wakkanai about 11.5 hours after the sc of August 4 at 0119 UT. The whistler occurrence rate at Moshiri increased suddenly at 1500 UT on August 5 when the foF2 decrease at Wakkanai was greatest, and the whistler increase continued even during the daytime till 2100 UT on August 6.

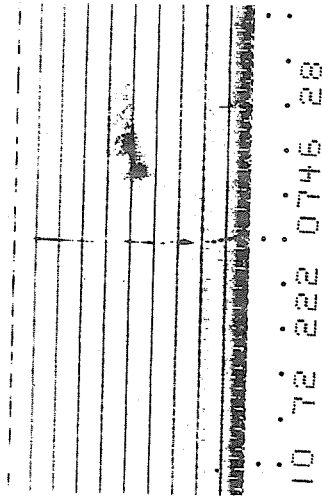
Also, during the period of August 4 - 10, the whistler occurrence rates increased generally for 2100 - 0900 LT when the diurnal variation of foF2 showed low values and some appearances of spread F. Thus, the whistler occurrence rate increased during periods of low ambient electron density for August 4 - 10. Field-aligned irregularities of whistler ducts and spread F may be represented by $\Delta N/N$, where N denotes the ambient electron density and ΔN the irregularity. Since $\Delta N/N$ becomes large for low values of N , the whistler duct may be apt to be formed at times of small ambient electron density such as an ionospheric storm or early morning. Hence, it is concluded that abnormal increases of the whistler occurrence rate for August 4 - 10 were caused by formation of many whistler ducts associated with redistribution of the ionization in the disturbed plasmasphere.

Large foF2 increases above the monthly median for 0600 - 0900 UT (1500 - 1800 LT) August 4 and for 0900 - 1200 UT (1800 - 2100 LT) August 9 occurred about 9 hours after sc's at 0119 UT, August 4 and 0037 UT, August 9, respectively, but no evident increase of the whistler occurrence rate occurred for these periods. No VLF emission was observed at Moshiri and Hiraio (N26.2, E206.3) for August 4 - 13.

(a)



(b)



Figs. 1a, 1b. Whistler-triggered emissions observed by ISIS 2 at 07h45m15s UT ($L = 2.42$, $\Lambda = 48.47^\circ$, $H = 1383$ km) and at 07h46m35s UT ($L = 2.87$, $\Lambda = 53.79^\circ$, $H = 1386$ km) on August 9, 1972. Solid points at bottom show "second" marks and the ordinate shows the frequency marks at 1 kHz intervals. Noises below about 800 Hz are due to an interference of the sounder receiver because of the mixed command mode (C1).

(c)

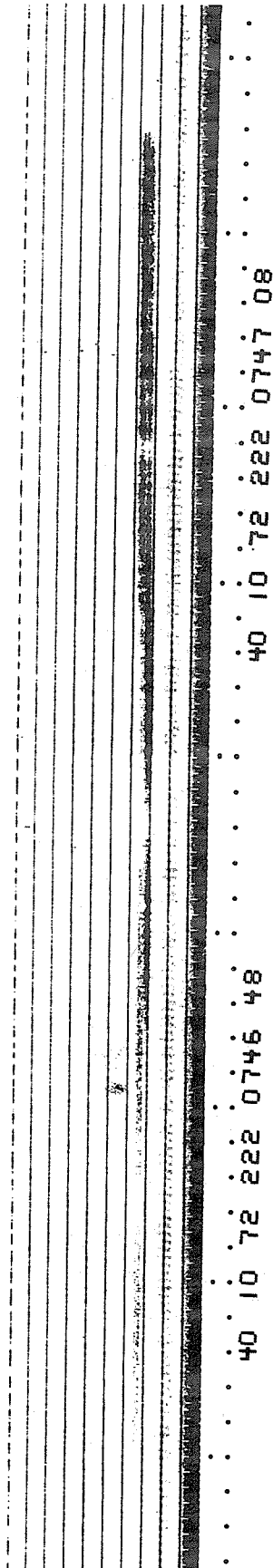


Fig. 1c. Narrow band hiss with center frequency of 3.1 - 3.6 kHz observed between 07h46m46s UT ($L = 2.94$, $\Lambda = 54.32^\circ$, $H = 1386$ km) and 07h47m23s UT ($L = 3.21$, $\Lambda = 56.09^\circ$, $H = 1388$ km) on August 9, 1972.

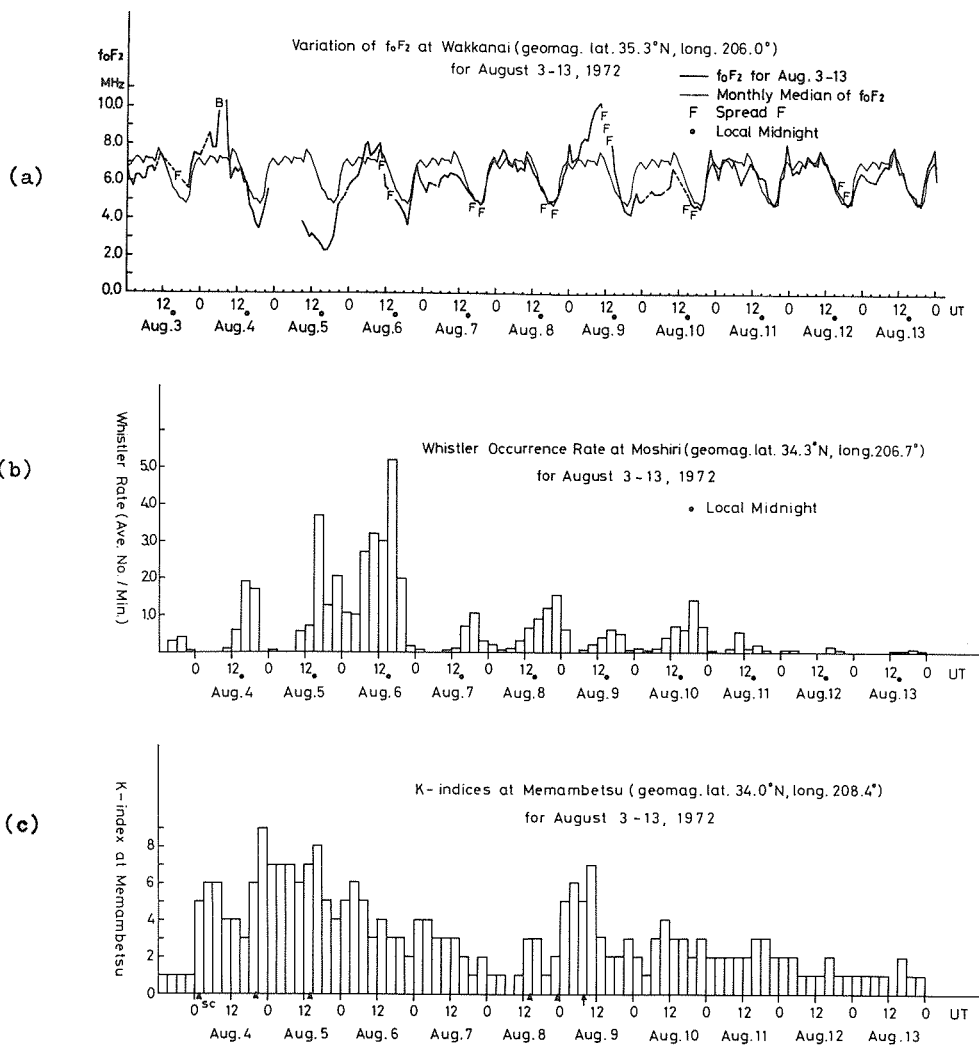


Fig. 2a. Time variation of f_oF_2 for August 3 - 13, 1972 (thick line) and August monthly median of f_oF_2 (thin line) observed at Wakkanai (geomag. lat. $N35.3$, long. $E206.0$).

Fig. 2b. Time variation of whistler occurrence rate (average number/minute) observed at Moshiri ($N34.3$, $E206.7$) for August 3 - 13, 1972.

Fig. 2c. Time variation of K-index observed at Memambetsu ($N34.0$, $E208.4$) for August 3 - 13, 1972.

REFERENCES

ONDOH, T., 1972
M. NAGAYAMA and
R. NISHIZAKI

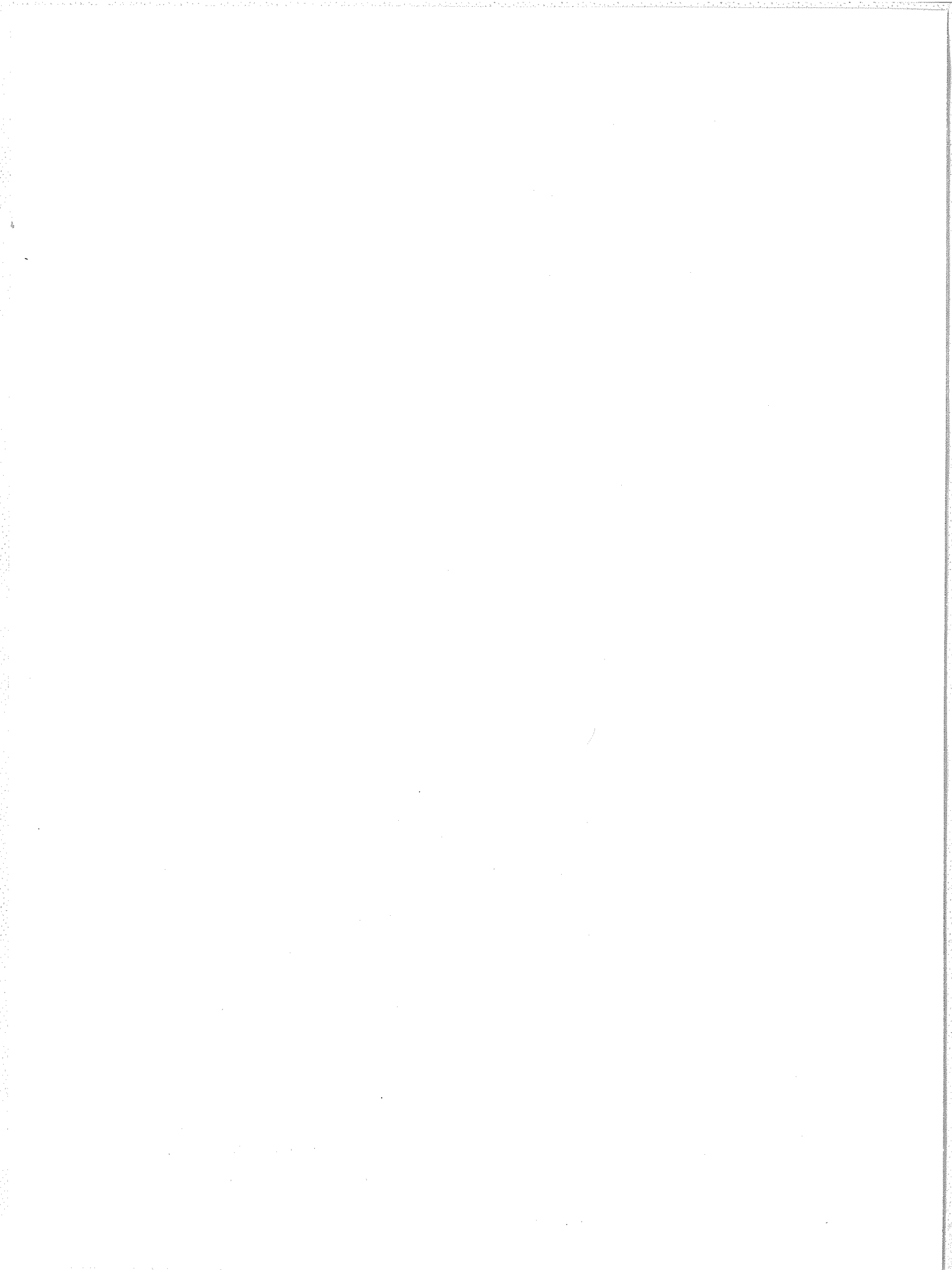
VLF emissions observed by ISIS-2 during the geomagnetic storm of August 9, 1972, Rept. Ionos. Space Res. Japan, **26**, 285 - 286.

RYCROFT, M. J. and 1970
J. O. THOMAS

The magnetospheric plasmopause and the electron density trough at the Alouette 1 orbit, Planet. Space Sci., **18**, 65 - 80.

TAYLOR, Jr., H. A. and 1972
W. J. WALSH

The light-ion trough, the main trough, and the plasmopause, J. Geophys. Res., **77**, 6716 - 6723.



5. COSMIC RAYS

Summary on page 8.

For basic data and indices for this section and others, see Appendix I for Table of Contents to Report UAG-21.

For data papers presented or published elsewhere which contain additional information on cosmic ray observations and the other categories included in this report, see Appendix II.

For additional data held by WDC-A for STP, see Appendix I.

Asymptotic Directions for Selected High Latitude Stations Appropriate
for the August 1972 Ground Level Cosmic-Ray Events

by

M. A. Shea and D. F. Smart
Air Force Cambridge Research Laboratories
Bedford, Massachusetts

The emission of relativistic cosmic rays from the sun is a relatively rare event providing an unique opportunity to study the propagation of these particles through the interplanetary medium. During the unusual period of solar activity in August 1972, two ground-level cosmic-ray increases (GLE) were detected by neutron monitors at various locations on the earth. The first GLE had an onset time of ~ 1300 UT on 4 August; the second had an onset time of ~ 1530 UT on 7 August.

In order to utilize the ground-level event data for detailed analyses of solar particle propagation, it is necessary to determine the amount of geomagnetic bending these particles undergo once they pass from the interplanetary medium through the magnetopause into the magnetosphere to the earth. The recent work of Gall *et al.* [1968] have shown that the external magnetic sources controlling the fields in the magnetosphere can have an effect on the amount of geomagnetic bending of cosmic-ray particles with rigidities less than a few GV. This effect, which is a function of local time, is most significant for particles arriving at high latitude stations. Consequently, it is important to consider both the internal and external sources in the model of the magnetosphere being used for the tracing of cosmic-ray trajectories for high latitude stations. This is particularly important for the study of the direction of the solar particle flux observed by ground-level cosmic-ray sensors located at a geomagnetic cutoff rigidity of ~ 1 GV [Shea and Smart, 1970a; Smart *et al.*, 1971]. In this paper we present the results of cosmic-ray trajectory calculations detailing the approach directions for a selected set of high latitude cosmic-ray stations. These calculations have been made for the local mean solar time of each station corresponding to 1300 UT and 1600 UT for the events on 4 and 7 August, respectively.

The quiescent magnetospheric model used for these calculations is described in detail by Shea and Smart [1972]. Briefly, it is based on the model derived by Williams and Mead [1965] and contains magnetic fields of both internal and external origin. The cosmic-ray trajectory calculations were restricted to the domain of the earth's magnetic cavity (i.e. the magnetosphere) represented by a boundary generated by a surface of revolution about the earth-sun line composed on the day side by a hemisphere of radius 13.9 earth radii centered at -3.5 earth radii and extended into a truncated cone whose generators form an angle of 15.3 degrees with the earth-sun line. Within this domain the magnetic field at any point in the magnetosphere is considered to be composed of an internal field (\vec{B}_{int}) represented by the Gaussian expansion with IGRF coefficients [IAGA Commission 2, Working Group 4, 1969] and an external field (\vec{B}_{ext}) as developed by Williams and Mead [1965]. Perturbations of the geomagnetic field or any possible contributions due to ring currents are not included in this model.

The magnetic field at any point inside the magnetosphere is given by the equation

$$\vec{B}_{total} = \vec{B}_{int}(R, \Theta, \Phi) + \alpha \vec{B}_{ext}(r, \theta, \gamma)$$

$$\vec{B}_{ext} = \vec{B}_s(r, \theta, \gamma) + \vec{B}_{cs}(r, \theta, \gamma).$$

The internal field is expressed in geocentric coordinates, R, Θ, Φ , while the Williams and Mead external field, symmetric with respect to the geomagnetic equator and the noon-midnight meridian, is computed in geomagnetic coordinates (r, θ, γ) . γ is the local time measured in degrees which corresponds to the angle in geomagnetic coordinates between the meridian of the anti-solar point and the meridian of the current particle position. The expressions for the external sources were limited to two terms since this limitation generates a magnetopause which nearly coincides with the boundary as described previously, [Gall *et al.* 1969]. A tail

configuration of $R_1 = 10$ earth radii and $R_2 = 40$ earth radii (the inward and outward termination points of the neutral sheet in the tail, respectively and \vec{B}_{CS} (the tail field associated with the current sheet) adjusted to $40 \mathcal{V}$ was utilized.

The cosmic-ray trajectories were calculated in the following manner. For each station the differential equation describing the motion ($\dot{\vec{r}} = (q/m) \vec{r} \times \vec{B}$) of a charged particle of mass m and charge q in the previously described magnetic field was solved at selected rigidities by using the Runge-Kutta integration method (see McCracken *et al.* [1962] for details of this process). In these calculations the step length employed in the Runge-Kutta process was about 1/100 of the distance traversed during a Larmor gyration. The particles were started at an altitude of 30 km in the radial (vertical) direction with the calculations for each station made at the local mean solar time corresponding to the particle increase. The asymptotic directions of approach were calculated at the position where (1) the orbit penetrated the magnetopause or (2) the orbit extended into the magnetospheric tail to a distance greater than 20 earth radii. Orbits that intersected the solid earth, or failed to reach an allowed solution by 100,000 iterative steps were declared "forbidden".

The asymptotic cones of acceptance for relativistic solar protons (0.90-10.0 GV) for selected high latitude stations appropriate for 1300 UT (the approximate onset time of the 4 August solar particle increase) are shown in Figure 1. The center of the world map has been

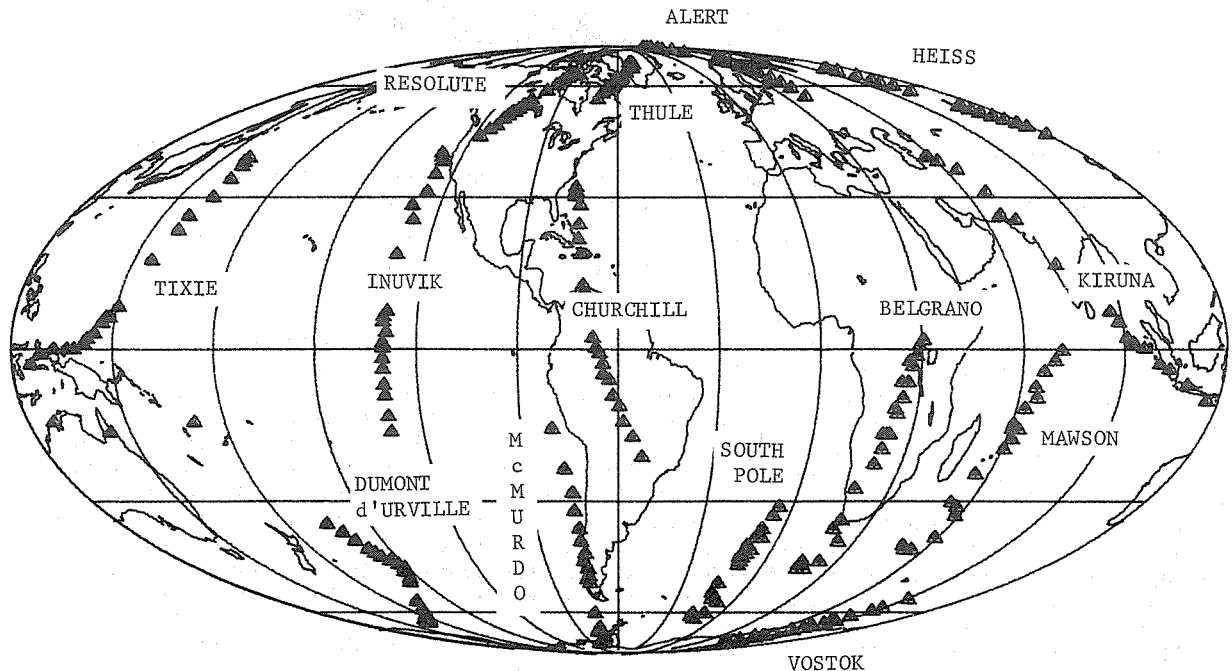


Fig. 1. Projection on a world map asymptotic directions for selected stations as calculated for 1300 UT. The map is centered about the theoretical Archimedes spiral path (45° West of the earth-sun line). Latitudes and longitudes are indicated at 30 degree intervals.

selected as the longitude along which the average theoretical Archimedes spiral angle is directed toward the earth. For a highly anisotropic flux the high latitude stations with their asymptotic directions nearest to the Archimedes spiral direction looking into the sun (assumed direction of particle flow) would record the earliest onsets and maximum flux during the anisotropic phase of the event. Figure 2 illustrates the asymptotic cones of acceptance for

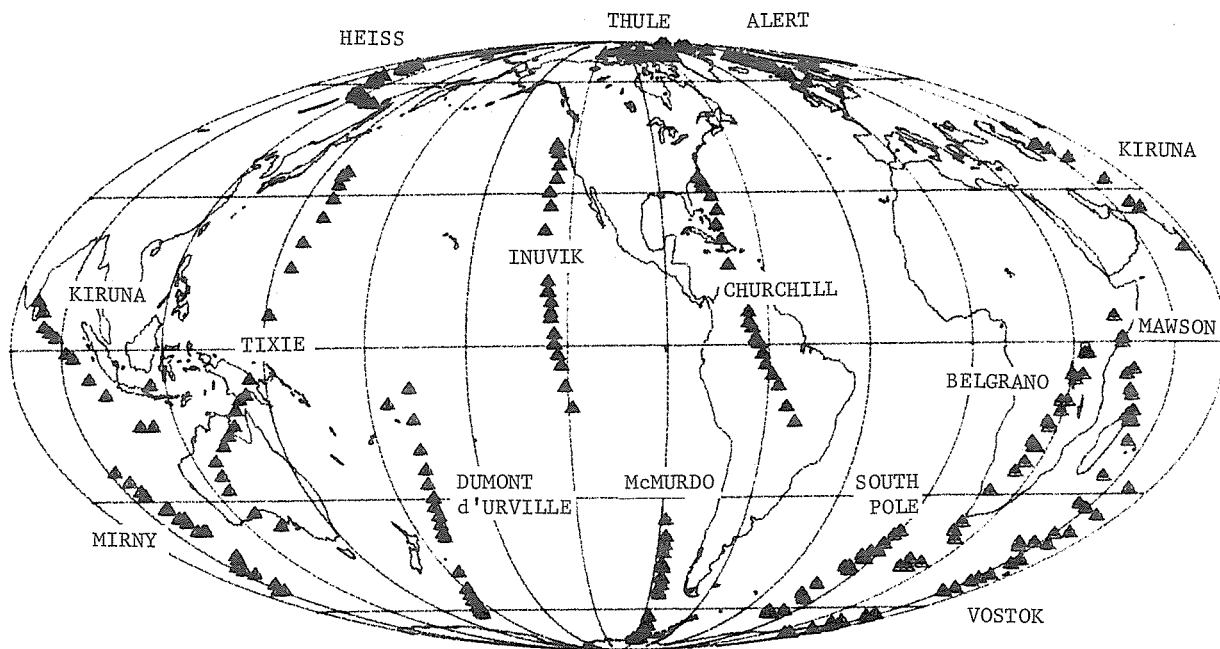


Fig. 2. Projection on a world map asymptotic directions for selected stations as calculated for 1600 UT. The map is centered about the theoretical Archimedes spiral path (45° West of the earth-sun line). Latitudes and longitudes are indicated at 30 degree intervals.

relativistic solar protons for selected high latitude stations appropriate for 1600 UT corresponding to the approximate onset time of the 7 August event.

The following tables contain the asymptotic directions of approach for selected high latitude neutron monitors. Negative asymptotic longitudes indicate that the particle trajectory does not cross the Greenwich meridian. Longitude values larger than 360 degrees are indicative of a large longitudinal drift of the particle as it traverses the magnetic cavity. The notation "R" and "F" mean a re-entrant or failed orbit respectively. All calculations were made for the local mean solar time of the station corresponding to the particle increase. These asymptotic directions can be compared with those given by Shea and Smart [1972] for 00 UT and 21 UT as these calculations have all been made with respect to the local mean solar time for each station. However, care should be used in utilizing the asymptotic directions given by Shea and Smart [1970b] for 11 UT as these calculations were made for the geomagnetic time for each station. For those stations where the geomagnetic and local solar times are within ~ 30 minutes, the calculations are essentially comparable; however, care must be taken in utilizing these published asymptotic directions for stations such as Alert, Vostok, McMurdo, South Pole and Mawson where there is a difference of as much as 7 hours between geomagnetic and local solar times.

REFERENCES

- | | | |
|---|------|--|
| GALL, RUTH,
JAIME JIMENEZ, and
LUCILLA CAMACHO | 1968 | Arrival of low-energy cosmic rays via the magnetospheric tail, <i>J. Geophys. Res.</i> , 73 , 1593-1605. |
| GALL, RUTH,
SILVIA BRAVO,
JAIME JIMENEZ, and
ADOLFO OROZCO | 1969 | Modelos del campo-geomagnetico para el estudio de la propagación de la radiación cósmica, <i>Anales del Instituto de Geofisica, U.N.A.M.</i> , 14 , 1-22. |

- IAGA COMMISSION 2,
WORKING GROUP 4 1969 International geomagnetic reference field
1965.0, J. Geophys. Res., 74, 4407.
- McCRACKEN, K. G.,
U. R. RAO, and
M. A. SHEA 1962 The trajectories of cosmic rays in a high simu-
lation of the geomagnetic field, Mass. Inst.
Technology Tech. Rept. 77, August 1962.
- SHEA, M. A., and
D. F. SMART 1970a The effect of the asymmetric magnetosphere on
the response of high-latitude neutron monitors
to solar particle events, Acta Physica, Academiae
Scientiarum Hungaricae, 29, Suppl. 2 (Proceedings
of the 11th International Conference on Cosmic
Rays, Budapest 1969), 539-543.
- SHEA, M. A., and
D. F. SMART 1970b Asymptotic directions of approach appropriate
for the high energy solar proton event of
November 18, 1968, Data on Cosmic Ray Event of
November 18, 1968 and Associated Phenomena, UAG-9,
World Data Center A, 68-80.
- SHEA, M. A., and
D. F. SMART 1972 Cosmic-ray trajectory calculations for selected
high latitude stations appropriate for the solar
cosmic-ray events in 1971, Data on Solar-Geophy-
sical Activity Associated with the Major Ground
Level Cosmic Ray Events of 24 January and 1 Sep-
tember 1971, World Data Center A for Solar-Ter-
restrial Physics Report No. UAG-24, 154-170.
- SMART, D. F.,
M. A. SHEA, and
P. J. TANSKANEN 1971 A determination of the spectra, spatial aniso-
tropy, and propagation characteristics of the
relativistic solar cosmic-ray flux on November 18,
1968, 12th International Conference on Cosmic Rays,
Hobart, Conference Papers (University of Tasmania
2, 483-488.
- WILLIAMS, D. J., and
G. D. MEAD 1965 Nightside magnetosphere configuration as obtained
from trapped electrons at 1100 kilometers,
J. Geophys. Res., 70, 3017-3029.

ALERT, CANADA

Geographic Latitude = 82.50 N
 Geographic Longitude = 62.33 W
 UT = 1300 LT = 0851

Rigidity (GV)	Asymptotic	
	LAT	LONG
10.00	82	-10
9.00	82	-8
8.00	83	-2
7.00	82	7
6.00	81	13
5.00	80	13
4.00	79	21
3.00	77	25
2.00	72	34
1.90	71	34
1.80	71	34
1.70	70	36
1.60	69	36
1.50	68	36
1.40	67	37
1.30	65	37
1.20	64	38
1.10	62	38
1.00	60	38
0.90	57	39

RESOLUTE, CANADA

Geographic Latitude = 74.69 N
 Geographic Longitude = 94.91 W
 UT = 1300 LT = 0640

Rigidity (GV)	Asymptotic	
	LAT	LONG
10.00	66	-90
9.00	65	-92
8.00	65	-93
7.00	64	-93
6.00	64	-94
5.00	62	-95
4.00	61	-98
3.00	59	-101
2.00	55	-105
1.90	54	-106
1.80	54	-107
1.70	53	-107
1.60	53	-108
1.50	52	-109
1.40	51	-110
1.30	50	-111
1.20	49	-112
1.10	48	-114
1.00	46	-115
0.90	44	-117

THULE, GREENLAND

Geographic Latitude = 76.55 N
 Geographic Longitude = 68.84 W
 UT = 1300 LT = 0825

Rigidity (GV)	Asymptotic	
	LAT	LONG
10.00	70	-49
9.00	70	-51
8.00	70	-52
7.00	70	-50
6.00	70	-49
5.00	68	-51
4.00	68	-53
3.00	66	-55
2.00	64	-58
1.90	63	-59
1.80	62	-61
1.70	62	-61
1.60	62	-61
1.50	61	-63
1.40	61	-64
1.30	60	-65
1.20	59	-66
1.10	58	-68
1.00	57	-69
0.90	56	-71

VOSTOK, ANTARCTICA

Geographic Latitude = 78.47 S
 Geographic Longitude = 106.87 E
 UT = 1300 LT = 2007

Rigidity (GV)	Asymptotic	
	LAT	LONG
10.00	-75	52
9.00	-75	58
8.00	-74	63
7.00	-72	63
6.00	-71	58
5.00	-72	56
4.00	-70	65
3.00	-71	66
2.00	-67	71
1.90	-68	71
1.80	-67	75
1.70	-65	76
1.60	-66	75
1.50	-65	79
1.40	-64	78
1.30	-63	82
1.20	-62	82
1.10	-60	85
1.00	-58	88
0.90	-56	90

DUMONT D'URVILLE, ANTARCTICA

Geographic Latitude 66.67 S
Geographic Longitude = 140.02 E
UT = 1300 LT = 2220

Rigidity (GV)	Asymptotic	
	LAT	LONG
10.00	-65	170
9.00	-64	171
8.00	-64	173
7.00	-63	175
6.00	-62	178
5.00	-61	181
4.00	-60	186
3.00	-57	193
2.00	-50	204
1.90	-49	205
1.80	-48	207
1.70	-46	208
1.60	-46	207
1.50	-45	206
1.40	-44	204
1.30	-42	203
1.20	-41	201
1.10	-40	200
1.00	-38	197
0.90	-36	194

McMURDO, ANTARCTICA

Geographic Latitude 77.85 S
Geographic Longitude = 166.72 E
UT = 1300 LT = 0007

Rigidity (GV)	Asymptotic	
	LAT	LONG
10.00	-76	277
9.00	-76	277
8.00	-75	279
7.00	-74	284
6.00	-71	286
5.00	-68	283
4.00	-66	286
3.00	-61	285
2.00	-51	287
1.90	-50	286
1.80	-49	286
1.70	-46	287
1.60	-44	286
1.50	-42	286
1.40	-39	286
1.30	-37	285
1.20	-32	284
1.10	-28	284
1.00	-23	282
0.90	-15	280

MIRNY, ANTARCTICA

Geographic Latitude = 66.55 S
Geographic Longitude = 93.00 E
UT = 1300 LT = 1912

Rigidity (GV)	Asymptotic	
	LAT	LONG
10.00	-55	84
9.00	-54	86
8.00	-53	88
7.00	-50	89
6.00	-49	86
5.00	-50	85
4.00	-48	90
3.00	-48	90
2.00	-44	92
1.90	-45	92
1.80	-45	94
1.70	-44	95
1.60	-43	94
1.50	-44	96
1.40	-42	97
1.30	-43	98
1.20	-42	98
1.10	-42	101
1.00	-42	103
0.90	-41	105

HEISS ISLAND, USSR

Geographic Latitude = 80.33 N
Geographic Longitude = 57.80 E
UT = 1300 LT = 1651

Rigidity (GV)	Asymptotic	
	LAT	LONG
10.00	68	95
9.00	67	96
8.00	66	98
7.00	64	100
6.00	63	99
5.00	62	98
4.00	60	102
3.00	58	102
2.00	54	107
1.90	54	107
1.80	54	108
1.70	53	109
1.60	52	109
1.50	52	110
1.40	51	111
1.30	50	112
1.20	49	114
1.10	48	115
1.00	47	116
0.90	46	118

SOUTH POLE, ANTARCTICA

Geographic Latitude = 89.98 S
 Geographic Longitude = 0.00 E
 UT = 1300 LT = 1300

Rigidity (GV)	Asymptotic	
	LAT	LONG
10.00	-60	-18
9.00	-62	-18
8.00	-62	-15
7.00	-61	-10
6.00	-57	-10
5.00	-54	-16
4.00	-55	-14
3.00	-50	-16
2.00	-46	-11
1.90	-44	-12
1.80	-44	-13
1.70	-44	-12
1.60	-42	-10
1.50	-41	-11
1.40	-41	-10
1.30	-38	-10
1.20	-38	-8
1.10	-36	-8
1.00	-34	-7
0.90	-32	-5

INUVIK, CANADA

Geographic Latitude = 68.35 N
 Geographic Longitude = 133.73 W
 UT = 1300 LT = 0405

Rigidity (GV)	Asymptotic	
	LAT	LONG
10.00	40	-128
9.00	40	-128
8.00	38	-127
7.00	35	-126
6.00	31	-127
5.00	28	-129
4.00	25	-128
3.00	19	-130
2.00	8	-129
1.90	6	-130
1.80	6	-130
1.70	4	-130
1.60	2	-130
1.50	0	-131
1.40	-2	-130
1.30	-4	-131
1.20	-7	-130
1.10	-10	-131
1.00	-13	-131
0.90	-17	-131

CHURCHILL, CANADA

Geographic Latitude = 58.75 N
 Geographic Longitude = 94.09 W
 UT = 1300 LT = 0644

Rigidity (GV)	Asymptotic	
	LAT	LONG
10.00	32	-76
9.00	31	-76
8.00	30	-75
7.00	28	-74
6.00	24	-73
5.00	21	-74
4.00	18	-73
3.00	12	-72
2.00	3	-68
1.90	1	-68
1.80	0	-68
1.70	-1	-67
1.60	-3	-66
1.50	-5	-65
1.40	-7	-64
1.30	-9	-63
1.20	-12	-61
1.10	-14	-59
1.00	-18	-57
0.90	-21	-54

MAWSON, ANTARCTICA

Geographic Latitude = 67.60 S
 Geographic Longitude = 62.88 E
 UT = 1300 LT = 1712

Rigidity (GV)	Asymptotic	
	LAT	LONG
10.00	-40	50
9.00	-42	51
8.00	-42	54
7.00	-39	58
6.00	-33	58
5.00	-30	54
4.00	-32	56
3.00	-24	55
2.00	-20	60
1.90	-17	61
1.80	-15	60
1.70	-16	60
1.60	-15	63
1.50	-11	63
1.40	-12	63
1.30	-9	65
1.20	-8	65
1.10	-4	67
1.00	-3	69
0.90	0	71

SYOWA, ANTARCTICA

Geographic Latitude = 69.03 S
 Geographic Longitude = 39.60 E
 UT = 1300 LT = 1538

Rigidity (GV)	Asymptotic	
	LAT	LONG
10.00	-30	32
9.00	-32	32
8.00	-33	34
7.00	-32	38
6.00	-26	41
5.00	-18	39
4.00	-19	38
3.00	-8	42
2.00	0	46
1.90	0	48
1.80	4	50
1.70	8	51
1.60	8	51
1.50	9	54
1.40	15	57
1.30	15	58
1.20	21	64
1.10	23	67
1.00	29	75
0.90	35	88

GOOSE BAY, CANADA

Geographic Latitude = 53.33 N
 Geographic Longitude = 60.42 W
 UT = 1300 LT = 0858

Rigidity (GV)	Asymptotic	
	LAT	LONG
10.00	20	-23
9.00	20	-23
8.00	20	-22
7.00	19	-19
6.00	15	-15
5.00	8	-14
4.00	7	-12
3.00	-2	-5
2.00	-10	7
1.90	-11	11
1.80	-14	14
1.70	-14	16
1.60	-15	19
1.50	-17	25
1.40	-18	29
1.30	-19	36
1.20	-19	44
1.10	-19	58
1.00	-15	75
0.90	12	148

TIXIE BAY, USSR

Geographic Latitude = 71.55 N
 Geographic Longitude = 128.90 E
 UT = 1300 LT = 2136

Rigidity (GV)	Asymptotic	
	LAT	LONG
10.00	39	160
9.00	38	160
8.00	37	160
7.00	35	162
6.00	30	161
5.00	27	159
4.00	24	159
3.00	17	155
2.00	8	150
1.90	7	149
1.80	6	147
1.70	5	147
1.60	4	145
1.50	3	143
1.40	2	141
1.30	0	138
1.20	0	136
1.10	-1	132
1.00	-1	128
0.90	-3	125

KIRUNA, SWEDEN

Geographic Latitude = 67.83 N
 Geographic Longitude = 20.43 E
 UT = 1300 LT = 1422

Rigidity (GV)	Asymptotic	
	LAT	LONG
10.00	39	56
9.00	39	57
8.00	38	60
7.00	36	63
6.00	31	66
5.00	26	66
4.00	25	69
3.00	17	74
2.00	8	86
1.90	5	89
1.80	2	91
1.70	2	92
1.60	0	96
1.50	-3	100
1.40	-4	103
1.30	-8	110
1.20	-10	116
1.10	-14	128
1.00	-16	143
0.90	-15	171

APATITY, USSR

Geographic Latitude 67.55 N
 Geographic Longitude = 33.33 E
 UT = 1300 LT = 1513

Rigidity (GV)	Asymptotic	
	LAT	LONG
10.00	38	68
9.00	38	70
8.00	37	72
7.00	34	75
6.00	29	78
5.00	24	78
4.00	23	82
3.00	14	87
2.00	3	101
1.90	0	104
1.80	-2	106
1.70	-3	108
1.60	-5	112
1.50	-8	117
1.40	-10	122
1.30	-13	130
1.20	-15	138
1.10	-17	154
1.00	-11	166
0.95	0	167
0.90	11	172

GENERAL BELGRANO, ANTARCTICA

Geographic Latitude 77.97 S
 Geographic Longitude = 38.80 W
 UT = 1300 LT = 1025

Rigidity (GV)	Asymptotic	
	LAT	LONG
10.00	-45	15
9.00	-46	16
8.00	-47	18
7.00	-45	22
6.00	-39	24
5.00	-34	19
4.00	-36	19
3.00	-28	19
2.00	-22	21
1.90	-20	23
1.80	-17	22
1.70	-16	21
1.60	-16	23
1.50	-12	24
1.40	-12	23
1.30	-10	26
1.20	-7	25
1.15	-7	26
1.10	-4	28
1.05	-2	27
1.00	-2	29
0.95	2	29
0.90	2	30

OULU, FINLAND

Geographic Latitude = 65.00 N
 Geographic Longitude = 25.40 E
 UT = 1300 LT = 1442

Rigidity (GV)	Asymptotic	
	LAT	LONG
10.00	32	62
9.00	32	64
8.00	31	66
7.00	28	70
6.00	23	73
5.00	17	74
4.00	15	78
3.00	4	87
2.00	-6	106
1.90	-8	110
1.80	-11	115
1.70	-12	120
1.60	-13	125
1.50	-15	135
1.40	-15	144
1.30	-14	158
1.20	0	163
1.15	8	166
1.10	19	175
1.05	23	188
1.00	-10	209
0.99	-35	206
0.98	-21	332
0.97	-4	258
0.96	-23	348
0.95	6	87
0.94	R	R
0.93	1	186
0.92	-13	372
0.91	R	R
0.90	-28	220

SANAE, ANTARCTICA

Geographic Latitude = 70.30 S
 Geographic Longitude = 2.35 W
 UT = 1300 LT = 1250

Rigidity (GV)	Asymptotic	
	LAT	LONG
10.00	-16	9
9.00	-16	8
8.00	-17	8
7.00	-18	11
6.00	-14	17
5.00	-3	20
4.00	5	19
3.00	14	30
2.00	32	58
1.90	33	62
1.80	32	66
1.70	33	76
1.60	33	93
1.50	28	104
1.40	23	114
1.30	8	111
1.20	-12	130
1.19	-16	136
1.18	-20	147
1.17	-23	164
1.16	4	208
1.15	-4	365
1.14	3	137
1.13	-32	292
1.12	-28	282
1.11	-37	160
1.10	31	125
1.09	-35	182
1.08	-27	300
1.07	2	218
1.06	-32	159
1.05	-14	146
1.04	-20	168
1.03	R	R
1.02	0	151
1.01	-36	161
1.00	-1	365
0.99	R	R
0.98	R	R
0.97	1	258
0.96	-29	137
0.95	R	R
0.94	-18	284
0.93	-11	276
0.92	-10	227
0.91	R	R
0.90	R	R

DEEP RIVER, CANADA

Geographic Latitude = 46.10 N
 Geographic Longitude = 77.50 W
 UT = 1300 LT = 0750

Rigidity (GV)	Asymptotic	
	LAT	LONG
10.00	5	-42
9.00	4	-42
8.00	4	-40
7.00	2	-37
6.00	-3	-32
5.00	-10	-28
4.00	-13	-24
3.00	-22	-9
2.00	-22	23
1.90	-20	31
1.80	-17	41
1.70	-13	48
1.60	-7	58
1.50	6	80
1.40	24	115
1.30	-14	152
1.29	17	142
1.28	R	R
1.27	-23	199
1.26	-13	196
1.25	-20	281
1.24	0	174
1.23	R	R
1.22	6	178
1.21	25	424
1.20	-17	302
1.19	-39	194
1.18	4	298
1.17	13	165
1.16	-11	178
1.15	-2	183
1.14	-25	180
1.13	-31	289
1.12	0	352
1.11	-19	322
1.10	1	340
1.09	R	R
1.08	4	359
1.07	-8	294
1.06	6	400
1.05	1	331
1.04	-3	417
1.03	8	286
1.02	-20	244
1.01	-19	279
1.00	-22	160
0.99	-5	263
0.98	-17	290
0.97	-24	171
0.96	-3	281
0.95	R	R
0.94	R	R
0.93	16	144
0.92	R	R
0.91	R	R
0.90	R	R

SULPHUR MOUNTAIN, CANADA

Geographic Latitude = 51.20 N
 Geographic Longitude = 115.61 W
 UT = 1300 LT = 0518

Rigidity (GV)	Asymptotic	
	LAT	LONG
10.00	5	-96
9.00	4	-95
8.00	3	-93
7.00	-1	-90
6.00	-8	-86
5.00	-14	-85
4.00	-17	-80
3.00	-28	-68
2.00	-32	-32
1.90	-30	-22
1.80	-27	-14
1.70	-23	-7
1.60	-16	5
1.50	0	24
1.40	22	55
1.30	-3	149
1.29	6	152
1.28	-8	189
1.27	-19	157
1.26	R	R
1.25	R	R
1.24	-9	171
1.23	-9	334
1.22	-10	180
1.21	-31	168
1.20	-26	273
1.19	R	R
1.18	-28	175
1.17	-16	186
1.16	-15	291
1.15	-18	306
1.14	-11	348
1.13	R	R
1.12	-9	275
1.11	-14	276
1.10	R	R
1.09-0.90	R	R

KERGUELEN ISLAND

Geographic Latitude = 49.35 S
 Geographic Longitude = 70.22 E
 UT = 1300 LT = 1741

Rigidity (GV)	Asymptotic	
	LAT	LONG
10.00	-6	82
9.00	-6	83
8.00	-6	86
7.00	-3	90
6.00	4	93
5.00	14	94
4.00	15	97
3.00	33	109
2.00	32	143
1.90	30	147
1.80	24	155
1.70	13	160
1.60	5	159
1.50	-7	161
1.40	-44	173
1.39	-45	188
1.38	-33	209
1.37	-1	232
1.36	-5	247
1.35	-4	262
1.34	-1	278
1.33	4	301
1.32	10	351
1.31	-40	184
1.30	-2	348
1.29	25	113
1.28	10	130
1.27	-36	203
1.26	15	131
1.25	R	R
1.24	R	R
1.23	3	352
1.22	-18	182
1.21	-24	168
1.20	-20	191
1.19	-2	357
1.18	-24	165
1.17	-16	195
1.16	-15	240
1.15	-16	372
1.14	R	R
1.13	R	R
1.12	R	R
1.11	-11	309
1.10	-5	265
1.09	-6	157
1.08	-18	268
1.07	R	R
1.06	R	R
1.05	R	R
1.04	R	R
1.03	2	165
1.02	R	K
1.01	-28	164
1.00-0.90	R	R

MT. WASHINGTON, USA

Geographic Latitude = 44.30 N
Geographic Longitude = 71.30 W
UT = 1300 LT = 0815

Rigidity (GV)	Asymptotic		Rigidity (GV)	Asymptotic	
	LAT	LONG		LAT	LONG
10.00	1	-30	1.29	R	R
9.00	0	-29	1.28	-11	291
8.00	0	-28	1.27	R	R
7.00	-1	-24	1.26	-13	338
6.00	-6	-18	1.25	-8	277
5.00	-14	-11	1.24	9	156
4.00	-16	-6	1.23	-11	376
3.00	-22	17	1.22	R	R
2.00	-6	63	1.21	R	R
1.90	0	75	1.20	-4	326
1.80	13	95	1.19	R	R
1.70	27	125	1.18	R	R
1.60	18	156	1.17	-21	344
1.59	12	158	1.16	R	R
1.58	2	160	1.15	-13	321
1.57	-12	161	1.14	R	R
1.56	-41	195	1.13	R	R
1.55	6	131	1.12	F	F
1.54	22	68	1.11	R	R
1.53	-26	192	1.10	F	F
1.52	-5	174	1.09-1.00	R	R
1.51	-14	229			
1.50	0	204			
1.49	R	R			
1.48	R	R			
1.47	6	274			
1.46	-28	344			
1.45	6	185			
1.44	1	191			
1.43	10	391			
1.42	-27	288			
1.41	-5	365			
1.40	6	170			
1.39	-18	186			
1.38	R	R			
1.37	-12	303			
1.36	-28	189			
1.35	-20	347			
1.34	-11	217			
1.33	-12	198			
1.32	-3	421			
1.31	-6	296			
1.30	0	379			

ALERT, CANADA

Geographic Latitude = 82.50 N
 Geographic Longitude = 62.33 W
 UT = 1600 LT = 1151

Rigidity (GV)	Asymptotic	
	LAT	LONG
10.00	81	-20
9.00	81	-19
8.00	81	-16
7.00	81	-10
6.00	80	-5
5.00	79	-6
4.00	78	-2
3.00	76	-1
2.00	72	5
1.90	71	4
1.80	71	4
1.70	70	5
1.60	69	5
1.50	69	5
1.40	68	6
1.30	66	5
1.20	65	6
1.10	64	6
1.00	62	5
0.90	60	5

RESOLUTE, CANADA

Geographic Latitude = 74.69 N
 Geographic Longitude = 94.91 W
 UT = 1600 LT = 0940

Rigidity (GV)	Asymptotic	
	LAT	LONG
10.00	67	-90
9.00	67	-92
8.00	67	-93
7.00	67	-93
6.00	66	-94
5.00	66	-96
4.00	65	-98
3.00	64	-101
2.00	63	-106
1.90	63	-107
1.80	63	-108
1.70	63	-109
1.60	62	-110
1.50	62	-111
1.40	62	-112
1.30	62	-113
1.20	62	-115
1.10	61	-117
1.00	61	-119
0.90	60	-121

THULE, GREENLAND

Geographic Latitude = 76.55 N
 Geographic Longitude = 68.84 W
 UT = 1600 LT = 1125

Rigidity (GV)	Asymptotic	
	LAT	LONG
10.00	72	-51
9.00	72	-52
8.00	73	-53
7.00	73	-52
6.00	73	-50
5.00	72	-53
4.00	72	-57
3.00	71	-60
2.00	72	-66
1.90	71	-66
1.80	71	-69
1.70	72	-71
1.60	72	-71
1.50	71	-74
1.40	72	-75
1.30	71	-77
1.20	72	-80
1.10	71	-84
1.00	71	-87
0.90	71	-92

VOSTOK, ANTARCTICA

Geographic Latitude = 78.47 S
 Geographic Longitude = 106.87 E
 UT = 1600 LT = 2307

Rigidity (GV)	Asymptotic	
	LAT	LONG
10.00	73	52
9.00	72	56
8.00	71	60
7.00	68	60
6.00	67	56
5.00	68	54
4.00	65	60
3.00	63	60
2.00	56	62
1.90	56	62
1.80	55	64
1.70	52	64
1.60	52	63
1.50	50	65
1.40	47	64
1.30	46	66
1.20	43	65
1.10	39	66
1.00	35	67
0.90	29	67

DUMONT D'URVILLE, ANTARCTICA

Geographic Latitude = 66.67 S
 Geographic Longitude = 140.02 E
 UT = 1600 LT = 0120

Rigidity (GV)	Asymptotic	
	LAT	LONG
10.00	-62	169
9.00	-61	170
8.00	-60	171
7.00	-59	173
6.00	-58	175
5.00	-56	177
4.00	-53	180
3.00	-49	183
2.00	-40	188
1.90	-38	189
1.80	-37	190
1.70	-35	190
1.60	-33	191
1.50	-30	191
1.40	-28	192
1.30	-24	192
1.20	-20	193
1.10	-15	193
1.00	-8	192
0.90	-11	186

McMURDO, ANTARCTICA

Geographic Latitude = 77.85 S
 Geographic Longitude = 166.72 E
 UT = 1600 LT = 0307

Rigidity (GV)	Asymptotic	
	LAT	LONG
10.00	-76	269
9.00	-76	268
8.00	-76	269
7.00	-75	274
6.00	-72	277
5.00	-69	273
4.00	-68	274
3.00	-63	273
2.00	-56	274
1.90	-55	273
1.80	-54	273
1.70	-53	274
1.60	-51	273
1.50	-50	273
1.40	-48	273
1.30	-46	272
1.20	-44	273
1.10	-42	273
1.00	-39	272
0.90	-36	272

MIRNY, ANTARCTICA

Geographic Latitude = 66.55 S
 Geographic Longitude = 93.00 E
 UT = 2100 LT = 0312

Rigidity (GV)	Asymptotic	
	LAT	LONG
10.00	-54	87
9.00	-53	90
8.00	-51	92
7.00	-48	93
6.00	-47	91
5.00	-48	91
4.00	-45	97
3.00	-44	99
2.00	-37	98
1.90	-38	100
1.80	-37	101
1.70	-35	98
1.60	-35	97
1.50	-34	99
1.40	-32	96
1.30	-32	98
1.20	-30	94
1.10	-28	95
1.00	-27	94
0.90	-24	92

HEISS ISLAND, USSR

Geographic Latitude = 80.33 N
 Geographic Longitude = 57.80 E
 UT = 1600 LT = 1951

Rigidity (GV)	Asymptotic	
	LAT	LONG
10.00	68	99
9.00	68	101
8.00	66	103
7.00	65	105
6.00	63	104
5.00	63	104
4.00	62	109
3.00	60	111
2.00	57	117
1.90	57	117
1.80	57	118
1.70	56	120
1.60	56	120
1.50	56	122
1.40	55	124
1.30	55	125
1.20	54	128
1.10	54	130
1.00	54	133
0.90	53	136

SOUTH POLE, ANTARCTICA

Geographic Latitude = 89.98 S
 Geographic Longitude = 0.00 E
 UT = 1600 LT = 1600

Rigidity (GV)	Asymptotic	
	LAT	LONG
10.00	-61	-15
9.00	-62	-15
8.00	-63	-11
7.00	-62	-7
6.00	-58	-6
5.00	-55	-12
4.00	-56	-9
3.00	-52	-12
2.00	-49	-6
1.90	-47	-7
1.80	-47	-8
1.70	-48	-6
1.60	-46	-5
1.50	-45	-6
1.40	-45	-4
1.30	-43	-4
1.20	-43	-2
1.10	-42	-3
1.00	-40	-1
0.90	-38	0

INUVIK, CANADA

Geographic Latitude = 68.35 N
 Geographic Longitude = 133.73 W
 UT = 1600 LT = 0705

Rigidity (GV)	Asymptotic	
	LAT	LONG
10.00	42	-128
9.00	41	-128
8.00	40	-127
7.00	37	-126
6.00	33	-127
5.00	31	-129
4.00	28	-127
3.00	22	-128
2.00	12	-126
1.90	11	-127
1.80	10	-127
1.70	9	-126
1.60	6	-125
1.50	5	-126
1.40	3	-124
1.30	0	-124
1.20	-2	-123
1.10	-4	-122
1.00	-8	-121
0.90	-12	-120

CHURCHILL, CANADA

Geographic Latitude = 58.75 N
 Geographic Longitude = 94.09 W
 UT = 1600 LT = 0944

Rigidity (GV)	Asymptotic	
	LAT	LONG
10.00	33	-76
9.00	33	-76
8.00	32	-75
7.00	30	-74
6.00	26	-73
5.00	23	-74
4.00	21	-72
3.00	15	-71
2.00	6	-67
1.90	5	-67
1.80	4	-66
1.70	3	-65
1.60	1	-64
1.50	0	-64
1.40	-2	-62
1.30	-4	-61
1.20	-7	-59
1.10	-9	-57
1.00	-12	-55
0.90	-16	-51

MAWSON, ANTARCTICA

Geographic Latitude = 67.60 S
 Geographic Longitude = 62.88 E
 UT = 1600 LT = 2012

Rigidity (GV)	Asymptotic	
	LAT	LONG
10.00	-41	51
9.00	-42	53
8.00	-42	57
7.00	-39	61
6.00	-34	60
5.00	-32	56
4.00	-34	60
3.00	-26	54
2.00	-20	54
1.90	-16	53
1.80	-14	50
1.70	-16	51
1.60	-14	52
1.50	-9	49
1.40	-11	49
1.30	-6	48
1.20	-6	47
1.10	0	44
1.00	2	44
0.90	5	42

SYOWA, ANTARCTICA

Geographic Latitude = 69.03 S
 Geographic Longitude = 39.60 E
 UT = 1600 LT = 1838

Rigidity (GV)	Asymptotic	
	LAT	LONG
10.00	-31	32
9.00	-33	32
8.00	-34	35
7.00	-33	39
6.00	-28	42
5.00	-21	38
4.00	-22	37
3.00	-13	38
2.00	-7	38
1.90	-8	39
1.80	-5	38
1.70	0	35
1.60	-2	36
1.50	1	36
1.40	10	30
1.30	8	31
1.20	17	25
1.10	18	23
1.00	28	29
0.90	37	37

GOOSE BAY, CANADA

Geographic Latitude = 53.33 N
 Geographic Longitude = 60.42 W
 UT = 1600 LT = 1158

Rigidity (GV)	Asymptotic	
	LAT	LONG
10.00	21	-23
9.00	21	-23
8.00	21	-22
7.00	20	-19
6.00	16	-15
5.00	10	-14
4.00	8	-12
3.00	0	-5
2.00	-8	8
1.90	-9	12
1.80	-12	15
1.70	-13	17
1.60	-13	21
1.50	-15	27
1.40	-16	31
1.30	-17	40
1.20	-17	49
1.10	-16	65
1.00	-11	86
0.90	11	101

TIXIE BAY, USSR

Geographic Latitude = 71.55 N
 Geographic Longitude = 128.90 E
 UT = 1600 LT = 0036

Rigidity (GV)	Asymptotic	
	LAT	LONG
10.00	36	158
9.00	34	158
8.00	33	158
7.00	30	159
6.00	25	159
5.00	20	156
4.00	16	156
3.00	7	152
2.00	-7	145
1.90	-9	143
1.80	-10	141
1.70	-12	140
1.60	-15	138
1.50	-17	134
1.40	-20	132
1.30	-23	127
1.20	-25	125
1.10	-29	124
1.00	-33	126
0.90	-36	131

KIRUNA, SWEDEN

Geographic Latitude = 67.83 N
 Geographic Longitude = 20.43 E
 UT = 1600 LT = 1722

Rigidity (GV)	Asymptotic	
	LAT	LONG
10.00	40	56
9.00	40	57
8.00	40	60
7.00	37	63
6.00	32	65
5.00	28	65
4.00	27	68
3.00	18	72
2.00	10	82
1.90	7	84
1.80	4	85
1.70	4	86
1.60	3	89
1.50	-1	92
1.40	-3	94
1.30	-6	98
1.20	-9	102
1.10	-15	108
1.00	-15	112
0.90	-7	116

APATTY, USSR

Geographic Latitude = 67.55 N
 Geographic Longitude = 33.33 E
 UT = 1600 LT = 1813

Rigidity (GV)	Asymptotic	
	LAT	LONG
10.00	39	68
9.00	39	69
8.00	38	72
7.00	36	75
6.00	30	76
5.00	26	76
4.00	24	79
3.00	16	82
2.00	5	90
1.90	2	90
1.80	-2	92
1.70	-3	92
1.60	-6	94
1.50	-9	96
1.40	-7	96
1.30	-6	100
1.20	-6	104
1.10	-5	110
1.00	-3	116
0.95	-2	120
0.90	0	124

GENERAL BELGRANO, ANTARCTICA

Geographic Latitude = 77.97 S
 Geographic Longitude = 38.80 W
 UT = 1600 LT = 1325

Rigidity (GV)	Asymptotic	
	LAT	LONG
10.00	-46	16
9.00	-47	16
8.00	-48	19
7.00	-46	23
6.00	-41	25
5.00	-36	20
4.00	-38	20
3.00	-30	20
2.00	-25	24
1.90	-23	26
1.80	-20	25
1.70	-20	24
1.60	-20	26
1.50	-16	27
1.40	-16	26
1.30	-14	29
1.20	-11	28
1.15	-11	30
1.10	-8	31
1.05	-7	31
1.00	-6	33
0.95	-3	33
0.90	-3	35

OULU, FINLAND

Geographic Latitude = 65.00 N
 Geographic Longitude = 25.40 E
 UT = 1600 LT = 1742

Rigidity (GV)	Asymptotic	
	LAT	LONG
10.00	32	62
9.00	32	63
8.00	32	65
7.00	29	69
6.00	24	72
5.00	18	72
4.00	16	75
3.00	5	82
2.00	-7	95
1.90	-11	98
1.80	-13	101
1.70	-11	102
1.60	-9	104
1.50	-9	110
1.40	-7	114
1.30	-4	119
1.20	0	126
1.15	1	130
1.10	2	138
1.05	5	145
1.00	4	154
0.99	3	157
0.98	3	160
0.97	2	165
0.96	2	170
0.95	-2	176
0.94	-11	181
0.93	-22	187
0.92	-23	208
0.91	-32	272
0.90	-7	142

SANAE, ANTARCTICA

Geographic Latitude = 70.30 S
 Geographic Longitude = 2.35 W
 UT = 1600 LT = 1550

Rigidity (GV)	Asymptotic	
	LAT	LONG
10.00	-16	9
9.00	-17	8
8.00	-18	8
7.00	-19	11
6.00	-15	16
5.00	-4	19
4.00	4	18
3.00	13	28
2.00	33	50
1.90	34	54
1.80	33	56
1.70	36	63
1.60	36	77
1.50	30	82
1.40	25	85
1.30	6	90
1.20	-10	87
1.15	-32	97
1.14	-40	116
1.13	-7	158
1.12	11	258
1.11	3	377
1.10	-25	267
1.09	11	174
1.08	-22	392
1.07	-3	99
1.06	-17	386
1.05	-29	120
1.04	-21	239
1.03	9	383
1.02	-16	401
1.01	-12	143
1.00	2	180
0.99	3	220
0.98	-2	211
0.97	-18	129
0.96	-8	210
0.95	3	172
0.94	-2	217
0.93	R	R
0.92	-21	255
0.91	25	398
0.90	5	171

DEEP RIVER, CANADA

Geographic Latitude = 46.10 N
 Geographic Longitude = 77.50 W
 UT = 1600 LT = 1050

Rigidity (GV)	Asymptotic	
	LAT	LONG
10.00	6	-42
9.00	5	-42
8.00	4	-40
7.00	3	-36
6.00	-2	-32
5.00	-10	-28
4.00	-12	-23
3.00	-21	-8
2.00	-21	27
1.90	-19	36
1.80	-16	46
1.70	-11	54
1.60	-5	65
1.50	8	81
1.40	29	81
1.30	-17	130
1.29	0	197
1.28	-22	130
1.27	-20	131
1.26	-19	135
1.25	-20	144
1.24	14	219
1.23	8	190
1.22	3	227
1.21	1	200
1.20	1	164
1.19	-32	325
1.18	-8	282
1.17	-7	262
1.16	-9	194
1.15	2	125
1.14	8	183
1.13	7	104
1.12	-11	271
1.11	-4	283
1.10	R	R
1.09	16	112
1.08	-8	233
1.07	R	R
1.06	-20	260
1.05	R	R
1.04	-17	219
1.03	-14	309
1.02	-22	133
1.01	-4	326
1.00	R	R
0.99	R	R
0.98	R	R
0.97	R	R
0.96	R	R
0.95	-19	312
0.94	R	R
0.93	R	R
0.92	1	232
0.91	R	R
0.90	R	R

SULPHUR MOUNTAIN, CANADA

Geographic Latitude = 51.20 N
 Geographic Longitude = 115.61 W
 UT = 1600 LT - 0818

Rigidity (GV)	Asymptotic	
	LAT	LONG
10.00	6	-95
9.00	5	-94
8.00	4	-92
7.00	0	-89
6.00	-7	-86
5.00	-14	-84
4.00	-17	-79
3.00	-28	-66
2.00	-32	-27
1.90	-30	-16
1.80	-26	-6
1.70	-21	2
1.60	-12	17
1.50	11	44
1.40	32	84
1.30	2	147
1.29	R	R
1.28	-15	360
1.27	-4	256
1.26	-15	374
1.25	-4	152
1.24	-8	374
1.23	-4	239
1.22	-32	131
1.21	2	172
1.20	2	231
1.19	-22	108
1.18	-11	106
1.17	-17	286
1.16	R	R
1.15	-11	341
1.14	-9	273
1.13	-6	159
1.12	-4	203
1.11	-8	225
1.10	R	R
1.09	R	R
1.08	-8	226
1.07	-17	283
1.06	R	R
1.05-0.90	R	R

KERGUELEN ISLAND

Geographic Latitude = 49.35 S
 Geographic Longitude = 70.22 E
 UT = 1600 LT = 2041

Rigidity (GV)	Asymptotic	
	LAT	LONG
10.00	-4	79
9.00	-4	79
8.00	-4	81
7.00	0	84
6.00	8	87
5.00	17	87
4.00	18	88
3.00	30	102
2.00	22	129
1.90	19	132
1.80	13	139
1.70	3	145
1.60	-5	145
1.50	-14	148
1.40	-12	188
1.30	-18	251
1.29	-15	265
1.28	-1	363
1.27	11	360
1.26	27	100
1.25	6	206
1.24	9	245
1.23	-14	215
1.22	5	200
1.21	R	R
1.20	R	R
1.19	R	R
1.18	R	R
1.17	-3	376
1.16	-18	383
1.15	R	R
1.14	-2	184
1.13	-7	248
1.12	-8	373
1.11	R	R
1.10	-42	136
1.09	R	R
1.08	R	R
1.07	4	375
1.06	R	R
1.05	R	R
1.04	R	R
1.03	R	R
1.02	F	F
1.01	R	R
1.00-0.90	R	R

MT. WASHINGTON, USA

Geographic Latitude = 44.30 N
 Geographic Longitude = 71.30 W
 UT = 1600 LT = 1115

Rigidity (GV)	Asymptotic	
	LAT	LONG
10.00	1	-30
9.00	1	-29
8.00	0	-28
7.00	-1	-24
6.00	-6	-17
5.00	-13	-11
4.00	-16	-5
3.00	-22	18
2.00	-5	65
1.90	0	75
1.80	10	82
1.70	31	94
1.60	16	132
1.59	9	135
1.58	0	138
1.57	-12	141
1.56	-30	144
1.55	-11	247
1.54	22	63
1.53	7	200
1.52	-3	232
1.51	8	229
1.50	13	228
1.49	R	R
1.48	R	R
1.47	-5	248
1.46	10	119
1.45	-8	150
1.44	5	239
1.43	-33	149
1.42	-5	215
1.41	2	242
1.40	-5	138
1.39	-8	157
1.38	-6	352
1.37	-10	223
1.36	-23	154
1.35	-9	237
1.34	-18	165
1.33	R	R
1.32	-5	119
1.31	R	R
1.30	-10	330
1.29	R	R
1.28	-11	166
1.27	-3	311
1.26	R	R
1.25	22	100
1.24	R	R
1.23	-12	259
1.22-1.18	R	R
1.17	-2	271
1.16-1.05	R	R

DURHAM, USA

Geographic Latitude = 43.10 N
 Geographic Longitude = 70.19 W
 UT = 1600 LT = 1117

Rigidity (GV)	Asymptotic	
	LAT	LONG
10.00	-2	-26
9.00	-2	-25
8.00	-2	-24
7.00	-4	-20
6.00	-8	-12
5.00	-16	-4
4.00	-18	4
3.00	-20	32
2.00	12	80
1.90	28	90
1.80	6	140
1.70	-2	174
1.69	14	117
1.68	12	227
1.67	R	R
1.66	R	R
1.65	10	231
1.64	0	342
1.63	5	170
1.62	-2	291
1.61	-6	320
1.60	12	384
1.59	-24	314
1.58	-10	171
1.57	-6	122
1.56	4	182
1.55	-5	151
1.54	-1	135
1.53	-24	334
1.52	12	218
1.51	-17	330
1.50	-18	339
1.49	R	R
1.48	-11	280
1.47	-12	273
1.46	R	R
1.45	R	R
1.44	R	R
1.43	R	R
1.42	-15	136
1.41	R	R
1.40	R	R
1.39	R	R
1.38	R	R
1.37	5	222
1.36	3	116
1.35-1.28	R	R
1.27	-13	337
1.26-1.15	R	R

SWARTHMORE, USA

Geographic Latitude = 39.90 N
 Geographic Longitude = 75.35 W
 UT = 1600 LT = 1059

Rigidity (GV)	Asymptotic	
	LAT	LONG
10.00	-9	-28
9.00	-10	-27
8.00	-10	-25
7.00	-11	-20
6.00	-16	-11
5.00	-22	3
4.00	-21	16
3.00	-7	56
2.90	-3	60
2.80	2	64
2.70	6	69
2.60	11	74
2.50	18	74
2.40	30	96
2.30	5	140
2.20	10	222
2.10	0	225
2.09	11	210
2.08	-4	315
2.07	-4	152
2.06	-1	162
2.05	-5	218
2.04	14	109
2.03	-22	265
2.02	-25	304
2.01	4	230
2.00	4	177
1.99	-2	158
1.98	-9	221
1.97	25	92
1.96	-15	314
1.95	R	R
1.94	R	R
1.93	R	R
1.92	-1	370
1.91	R	R
1.90	R	R
1.89	-9	143
1.88	R	R
1.87	-11	173
1.86	-4	359
1.85	6	191
1.84	-15	323
1.83	R	R
1.82	R	R
1.81	R	R
1.80	-11	175
1.79	R	R
1.78	R	R
1.77	R	R
1.76	R	R
1.75	-3	239
1.74-1.60	R	R

VICTORIA, CANADA

Geographic Latitude = 48.42 N
 Geographic Longitude = 123.32 W
 UT = 1600 LT = 0747

Rigidity (GV)	Asymptotic	
	LAT	LONG
10.00	-7	-98
9.00	-7	-97
8.00	-9	-94
7.00	-12	-89
6.00	-20	-82
5.00	-29	-75
4.00	-30	-64
3.00	-30	-24
2.90	-27	-20
2.80	-25	-17
2.70	-22	-12
2.60	-18	-5
2.50	-12	5
2.40	-1	19
2.30	16	38
2.20	30	72
2.10	-20	122
2.09	11	200
2.08	R	R
2.07	-15	228
2.06	-20	313
2.05	-1	122
2.04	0	218
2.03	R	R
2.02	-5	163
2.01	-8	144
2.00	22	81
1.99	-7	136
1.98	R	R
1.97	R	R
1.96	R	R
1.95	-7	251
1.94	-3	214
1.93	13	106
1.92	-13	296
1.91	R	R
1.90	8	405
1.89	-14	277
1.88	R	R
1.87	5	408
1.86	-5	238
1.85	-10	127
1.84	-14	310
1.83	-4	283
1.82	R	R
1.81	-2	232
1.80	14	78
1.79	5	352
1.78	R	R
1.77	4	182
1.76-1.65	R	R

Observations Relevant to the August 1972 Storm

by

P. J. Tanskanen, H. Kananen and K. A. Blomster
Department of Physics, University of Oulu
Oulu, Finland

Introduction

Some highlights of events associated with the giant storms of August 1972 are studied using data from both ground-level stations and satellites. Due to the complexity of the event emphasis is given here only on the most distinct and pronounced variations observed. For neutron monitor observations, only one hourly averages were available, thus limiting the determination of the onset times of the different events, accordingly. Interplanetary field conditions, solar wind velocities, and proton intensities for protons of energy $E > 13.9$ Mev were measured by Pioneer 9 [Lincoln and Leighton, 1972] at a location 0.77 A.U. from the sun, the earth-sun-spacecraft angle being between 43-48° east of the sun-earth line. In addition, data from proton experiments aboard Explorers 41 (outside the magnetosphere) and 43 (inside the magnetosphere) [Kohl et al., 1973; Bostrom et al., 1972] have been compared with ground-level observations. The various storm events will be discussed and analyzed in the same order they were observed.

A crude measure of the hardness of the primary energy spectrum is obtained simply by comparing the relative intensity changes of two nearby stations at different altitudes [Wilson et al., 1967]. We assume that an exponential attenuation law of the form

$$N = N_0 e^{-\alpha x}$$

can be applied, where N is the observed counting rate at an atmospheric depth x (m), N_0 the cosmic ray intensity at the top of the atmosphere, and α the attenuation coefficient. One can then write as an approximation, assuming an energy-independent attenuation for stations 1 and 2

$$\frac{\Delta N_1}{\Delta N_2} = e^{\alpha x}.$$

Here $x = x_2 - x_1$ = difference in altitude between the two stations. From this it can easily be inferred that the smaller the value of α the harder the energy spectrum. Among the stations from which data were available for this investigation, the following pairs can be formed for the study of the relative changes of the energy spectrum (see Table 1):

Mt. Washington/Durham	(α_1)
Sulphur Mt./Calgary	(α_2)
South Pole/Mc Murdo	(α_3)

FD-1/August 4

Although solar protons had been observed aboard Explorers 41 and 43 [Bostrom et al., 1972; Kohl et al., 1973] and Pioneer 9 [Lincoln and Leighton, 1972] as early as August 2 and 3 (Figure 1), the effect of an approaching shock front from the sun was not seen by neutron monitors until very early on August 4 (Figures 2 and 3) in conjunction with the sudden commencement at 0119 UT. On August 3 there was a sudden increase of solar wind velocity and a reversal of the interplanetary field direction from E 90° to W 110° taking place at 2215 and 2250 UT, respectively. From Table 1 and Figure 4 we can make following observations concerning FD-1.

1. Stations that "looked" into the direction of the sun or close to the "garden hose" direction registered an early decrease (0100-0200 UT).

2. Thule, "looking" north from the ecliptic plane is included among these stations probably due to a north-south asymmetry of the advancing "plasma cloud."

3. Stations "looking" away from the sun or south of the ecliptic plane registered the latest onsets.

4. Maximum decrease at sea-level and one of the latest onsets was recorded at Tixie Bay (7.5%, onset 0300-0400 UT).

TABLE 1

August 4 - 9 events as observed by neutron monitors.
R = rigidity, A = max. relative deviation (%).

Station (R)	Alt. (m)	AUG. 4						AUG. 5		AUG. 7		AUG. 9	
		FD-1		GLE-1		FD-2		"Recovery"		GLE-2		FD-3	
		onset (UT)	A(%)	onset (UT)	A(%)	onset (UT)	A(%)	onset (UT)	A(%)	onset (UT)	A(%)	onset (UT)	A(%)
Huancayo (13.5)	3400	1-2	3	11-12	~1	21-22	11.5	2-3	7	-	-	-	-
Rome (6.31)	60	1-2	4.5	14-15	~1	21-22	~17	2-3	10	-	-	-	-
Pic du Midi (5.36)	2860	1-2	4.5	15-16	<1	21-22	~24	1-3	15	?	?	?	?
Utrecht (2.76)	sl.	1-2	6	16-17	<1	21-22	~25	1-2	14	15-16	?	?	?
Kiel (2.29)	54	1-2	5.5	14-15	<1	21-22	~26	2-3	15	16-17	?	?	?
Leeds (2.20)	100	1-2	~6	15-16	<1	21-22	~25	2-3	13	15-16	?	?	?
Swarthmore (1.92)	80	3-4	~6.5	12-13	~1	21-22	23.5	2-3	10	15-16	?	?	?
Yakutsk (1.70)	105	3-4	~7	14-15	~1.5	22-23	~21	2-3	9.5	15-16	?	?	?
Durham (1.41)	sl.	2-3	~7	12-14	<1	21-22	22.5	2-3	9.5	15-16	?	?	?
Mt. Washington (1.24)	1900	2-3	~8	12-13	~5	21-22	26.4	2-3	11	15-16	?	?	?
Kerguelen (1.19)	sl.	1-2	~6.5	14-15	~5.5	21-22	25.3	2-3	15.5	15-16	?	?	?
Sulphur Mt. (1.14)	2283	3-4	~8	12-13	~13	21-22	28.5	2-3	13	15-16	?	?	?
Calgary (1.09)	1128	3-4	~7.5	12-13	~9	21-22	26.7	2-3	12	15-16	?	?	?
Oulu (0.81)	15	1-2	~6	13-14	6.5	21-22	25.4	2-3	~14	16-17	?	?	?
Kiruna (0.54)	400	1-2	~6.5	13-14	~8	21-22	27	2-3	14.5	16-17	?	?	?
Tixie Bay (0.53)	sl.	3-4	7.5	12-13	~6	21-22	~23	2-3	~11.5	15-16	?	?	?
Thule (<0.04)	260	1-2	6.5	13-14	~8	21-22	21.5	2-3	8.5	15-16	?	?	?
Dumont D'Urville (<0.05)	45	3-4	~6	14-15	~7.5	22-23	23	2-3	11	16-17	?	?	?
McMurdo (<0.05)	48	3-4	~8.5	12-13	~8	22-23	~26.7	2-3	~12.5	15-16	?	?	?
South Pole (<0.11)	2820	2-3	~9.5	12-13	~29.5	22-23	~35	2-3	~18	15-16	?	?	?

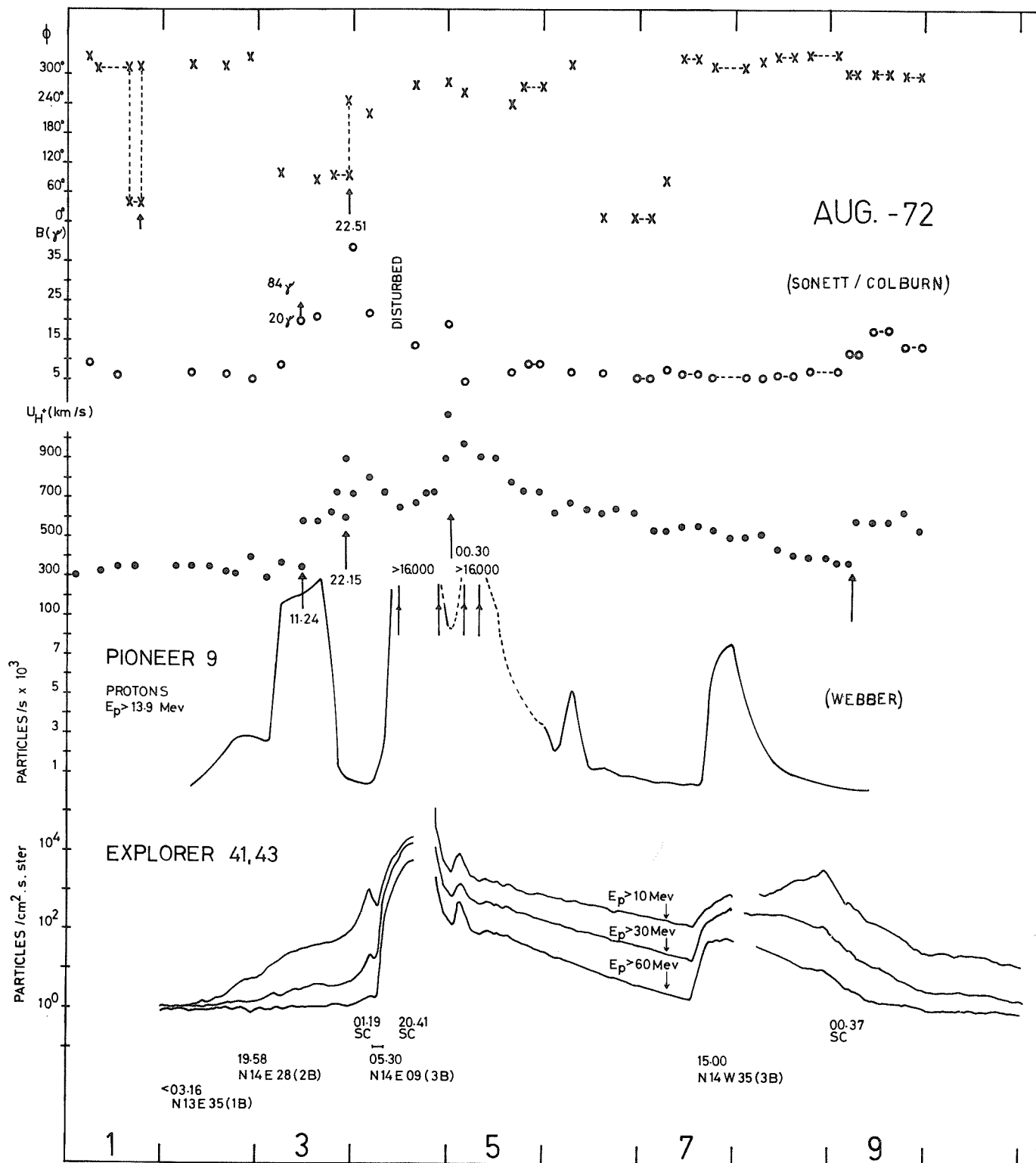


Fig. 1. Interplanetary magnetic field direction (ϕ), magnitude $B(\gamma)$, solar wind velocity U_{H^+} (km/s) and proton ($E_p > 13.9$ Mev) intensity registered by Pioneer 9. Proton intensities at energies $E_p > 10$ Mev, $E_p > 30$ Mev and $E_p > 60$ Mev registered by Explorers 41 and 43 (because of the very close resemblance between observations made aboard the two spacecrafts, they are represented by one single line).

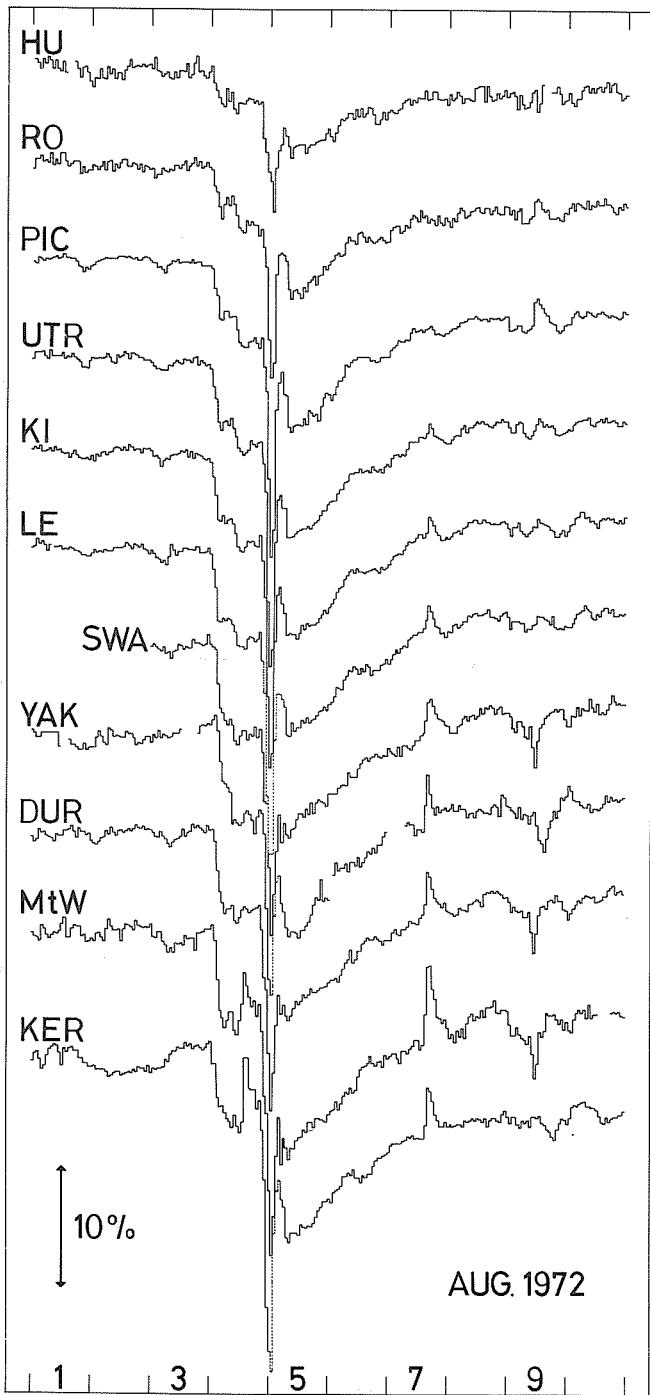


Fig. 2. Relative cosmic ray changes observed with neutron monitors at HU = Huancayo, RO = Rome, PIC = Pic du Midi, UTR = Utrecht, KI = Kiel, LE = Leeds, SWA = Swarthmore, YAK = Yakutsk, DUR = Durham, MtW = Mt. Washington and KER = Kerguelen during the August 1972 storm.

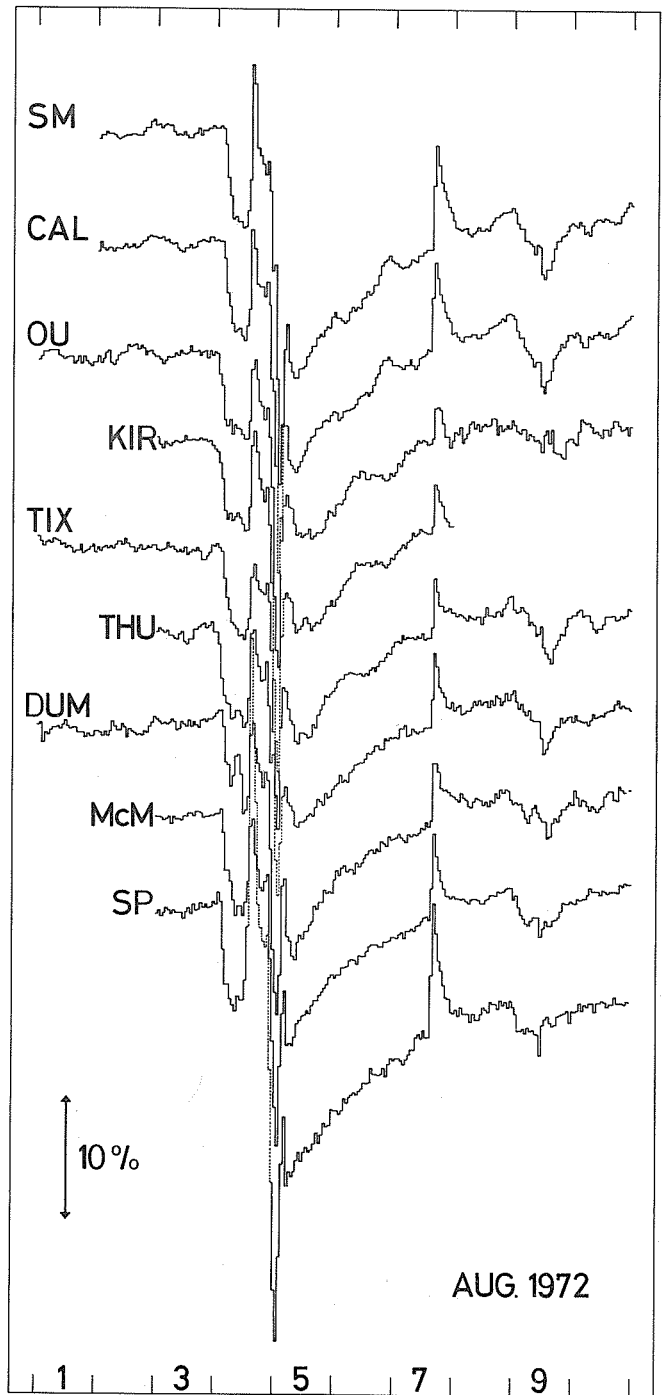


Fig. 3. Relative cosmic ray changes observed with neutron monitors at SM = Sulphur Mountain, CAL = Calgary, OU = Oulu, KIR = Kiruna, TIX = Tixie Bay, THU = Thule, DUM = Dumont D'Urville, McM = McMurdo, SP = South Pole during the August 1972 storm.

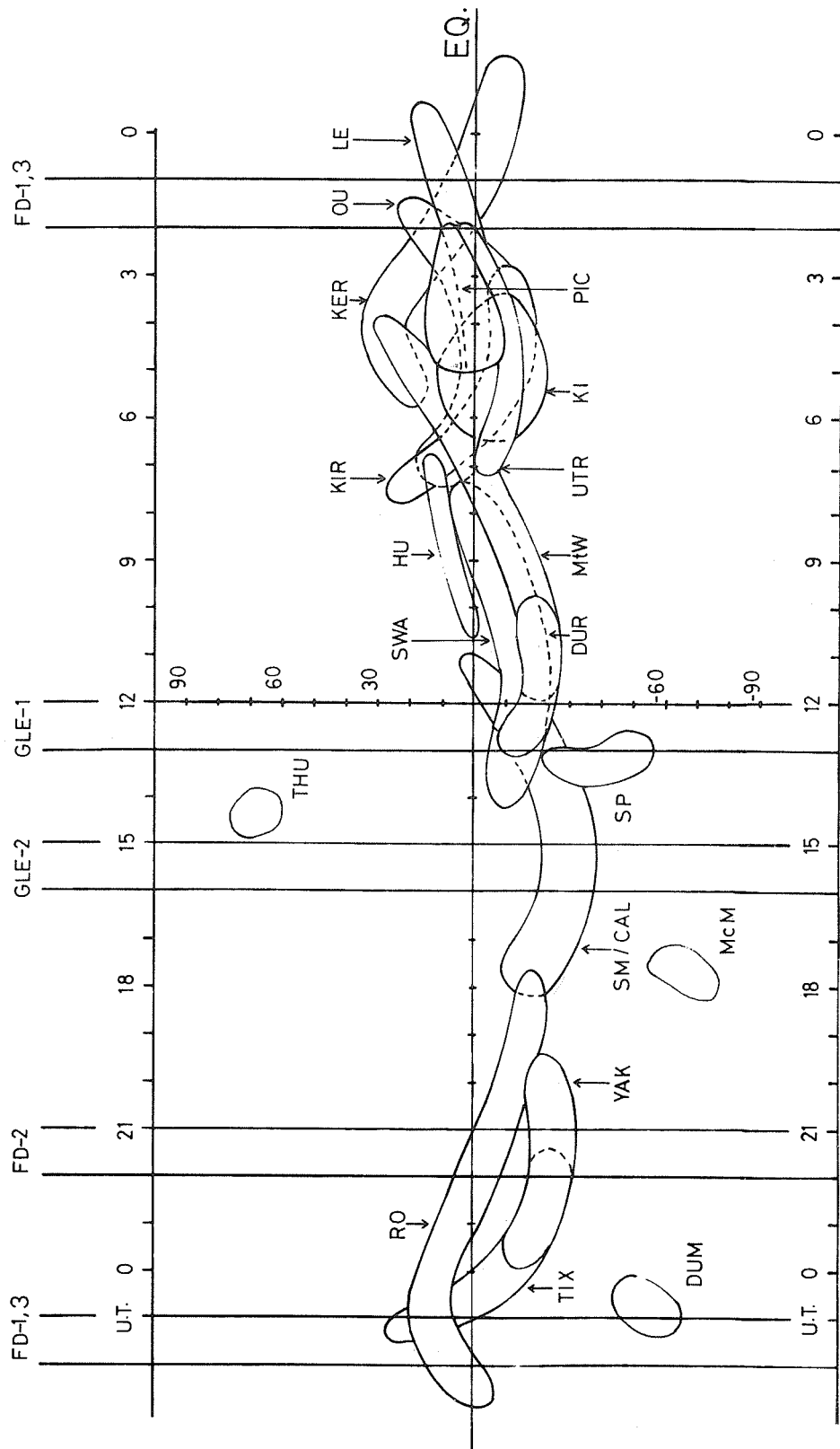


Fig. 4. Asymptotic directions of "viewing" calculated for the cosmic ray stations used in this study. The position of the sun at the earliest onsets are marked with the columns [McCracken et al., 1965].

5. If the decrease is attributed to a 2B flare that took place at 1958 UT on August 2 in a region N14, E28, and the sudden commencement recorded at 0119 UT on August 4 marks the arrival of the shock wave [McKinnon et al., 1972], one would obtain a solar wind velocity of about 1400 km/s. If, on the other hand, one considers the flare starting at 0316 UT at a location N13, E35 as the source of this disturbance, a delay-time of 46 hours would give a solar wind velocity of approximately 900 km/s. The value for the wind velocity recorded at Pioneer 9 was around 700-900 km/s.
6. When comparing the relative intensity decreases vs. rigidity (R), it is observed that stations with early onsets registered lower values of intensity changes than the stations with later onsets.

GLE-1/August 4

This proton event seems to correlate with the enormous intensity increase recorded at all three satellites and was probably caused by a 3B flare with coordinates N14, E09. The flare was observed at ~ 0530 UT and reached its maximum intensity at 0639 UT [McKinnon, 1972].

Summary of Ground Observations:

1. Early onsets (1200-1300 UT) at stations "viewing" in the direction of the sun or close to the "garden hose" direction. Delay from flare was around 7 hours.
2. There is a clear tendency for a time-delay to appear as a function of distance from an impact area.
3. The time difference between the onsets at Tixie Bay and Dumont D'Urville could be indicative of a slower diffusion in the north-south direction than in the east-west direction.

FD-2/August 4

This Forbush decrease which turned out to bring the counting rates of ground-level neutron monitors to the lowest level since July 1959, was probably connected with the same solar flare that caused the GLE-1 about 9 hours earlier. From Table 1 and Figures 2-4 the following facts can be deduced:

1. Earlier onsets at north-looking stations. Later onsets at McMurdo, South Pole, and Dumont D'Urville [Pomerantz and Duggal, 1972].
2. South-north anisotropy: McMurdo/Thule \approx 1.15 [Pomerantz and Duggal, 1973].
3. Stations "viewing" in the late morning - early evening sector and close to the ecliptic plane, namely, Tixie Bay, Yakutsk, Durham and Swarthmore, registered smaller relative decreases than stations looking in the early evening - late morning sector.
4. The solar flare probably responsible for this global disturbance started at 0530 UT and was located at N14, E09. The storm sudden commencement occurred at 2054 UT. This yields a solar wind velocity of about 2700 km/s which is over twice the magnitude of the solar wind velocity measured at Pioneer 9 (\sim 1150 km/s).

"Recovery Peak" and Subsequent Decrease/August 5

The intensity recovery after the large Forbush decrease FD-2 took place very quickly. Although this recovery can clearly be seen in all three satellite recordings available to us in this study (see Figure 1), we fail to find a flare responsible for this rapid recovery. We thus propose that this increase may have been caused by a combination of a flux of galactic particles and solar particles. In addition, the following observations can be made:

1. This "recovery peak" seems to have occurred simultaneously at all stations investigated.
2. Even though the onset was simultaneous there seems to be a tendency for stations "looking" in the late - morning - noon sector and in the ecliptic plane (Kerguelen, Oulu, Kiruna, Leeds, Kiel, Utrecht, Pic du Midi) to have recorded the largest increases.
3. The decrease following the "recovery peak" can be the result of an interruption of the particle-flow.
4. It is unlikely that a temporary lowering of cut-off rigidity due to a ring current effect, would have caused the observed intensity increase. This can be inferred from the fact that it was simultaneously observed outside the magnetosphere as well [Yoshida et al., 1968].

GLE-2/August 7

The recovery from the great storm was suddenly enhanced due to protons from a proton flare of importance 3B at a location N14, W37 starting around 1500 UT on August 7.

This event did not show any appreciable asymmetries although one might expect some, due to the favorable position of the flare. The time delay between the onset of the flare and the arrival of solar protons at the distance of the Explorers 41 and 43 where the onset can be observed at 1533 UT (Figure 1) was thus of the order of 30 min. This short time-delay could be indicative of:

1. Direct access of particles to the field lines leading in the direction of the earth.
2. Very little scattering of the particles along their path.

Since the absolute increases were approximately the same for all energy channels $E_p > 10$ Mev, $E_p > 30$ Mev and $E_p > 60$ Mev, the energy spectrum was relatively hard [Kohl et al., 1973].

Comparison of Energy Spectra for GLE-1, "Recovery Peak" and GLE-2

From a comparison of the calculated values for the attenuation coefficient α for the three increases GLE-1, "Recovery Peak" and GLE-2 as tabulated below one can draw the following conclusions:

Attenuation Coefficients $\alpha(1/m)$

	GLE-1	"Recovery"	GLE-2	Stations
α_1 (1/m)	0.85×10^{-3}	0.08×10^{-3}	0.33×10^{-3}	Mt. Washington/Durham
α_2	0.32×10^{-3}	0.07×10^{-3}	0.16×10^{-3}	Sulphur Mt./Calgary
α_3	0.47×10^{-3}	0.13×10^{-3}	0.16×10^{-3}	South Pole/McMurdo

- 1) The two events that have been classified as solar proton events show a considerably softer spectrum than the "recovery event."
- 2) Of the two proton events that latter one (GLE-2) had a harder spectrum than the former (GLE-1).
- 3) The hardness of the "recovery peak" would point towards galactic cosmic rays as the source of the event rather than solar protons though the existence of locally accelerated solar protons cannot be excluded fully.

FD-3/August 9

This Forbush decrease was observed to have started between 0000-0100 UT on August 9. The associated sudden commencement is reported to have occurred at 0037 UT.

The onset of the decrease as seen by neutron monitors was relatively gradual and does not show rigidity dependency, rather, there seems to be indications of some stations having recorded an intensity increase instead of a decrease (Rome, Pic du Midi). This increase bears resemblance to a solar proton increase. Of the available particle observations with satellites, it can be seen from Figure 1 that the proton intensity at Explorers 41 and 43 continued to remain quite high after the proton flare on August 7, whereas the proton intensity further away from the earth at Pioneer 9 had already decreased to a pre-increase level. There is some indication of a shock front passage at Pioneer 9 taking place between 0500-0700 UT on August 9, though the general behavior of the interplanetary magnetic field can be considered as fairly well ordered (Figure 1). The electron density along the radial path between the magnetosphere and Pioneer 9 shows a maximum on August 9 [Croft, 1972; Scarf, 1972].

Acknowledgements

The authors would like to express their gratitude to the following persons for kindly submitting us neutron monitor data for the events studied: Professors (Drs.) E. Bagge, N. P. Chirkov, S. P. Duggal, L. de Feiter, V. I. Ipatov, N. Iucci, S. Lindgren, J. A. Lockwood, A. A. Luzov, P. L. Marsdan, T. Mathews, M. G. Milleret, M. A. Pomerantz, J. A. Simpson, T. Thamyahpillai, N. L. Zangrilli. It is a great pleasure to thank several colleagues for useful correspondence and for sending us preprints of talks given at the December 1972 AGU meeting.

REFERENCES

- BOSTROM, C. O., 1972
 J. W. KOHL,
 R. W. McENTIRE and
 D. J. WILLIAMS
 The solar proton flux - August 2-12, 1972 (preprint, The Johns Hopkins University).
- CROFT, T. A. 1972
 Traveling regions of high density observed in the solar wind on August 3 and 9, 1972, Scientific Report No. 7, SEL 72-059, Stanford Electronics Laboratories, Stanford University, November 1972.
- KOHL, J. W., 1973
 C. O. BOSTROM and
 D. J. WILLIAMS
 Particle observations of the August '72 Solar events by Explorers 41 and 43 (preprint, The Johns Hopkins University).
- LINCOLN, J. V. and 1972
 H. I. LEIGHTON
 Preliminary Compilation of Data for Retrospective World Interval July 26 - August 14, 1972, World Data Center A for Solar-Terrestrial Physics, Report UAG-21, November 1972.
- McCRACKEN, F., 1965
 U. R. RAO,
 B. C. FOWLER,
 M. A. SHEA and
 D. F. SMART
 Cosmic Ray Tables Asymptotic Directions, Variational Coefficients and Cut-off Rigidities, IQSY Instr. Manual Nr. 10.
- McKINNON, J. A. 1972
 August 1972 Solar Activity and Related Geophysical Effects, NOAA Technical Memo ERL SEL-22.
- POMERANTZ, M. A. and 1972
 S. P. DUGGAL
 North-south anisotropies in the cosmic radiation, J. Geophys. Res. Lett., 77, 263-265.
- POMERANTZ, M. A. and 1973
 S. P. DUGGAL
 Record-breaking Cosmic Ray Storm stemming from Solar Activity in August 1972, Nature, 241, Feb. 2, 331-332.
- SCARF, F. L. 1972
 The August 1972 events; Pioneer 9 plasma wave observations (preprint 10472-6025-R0-00, Space Sci. Dept. TRW Systems Group).
- WILSON, B. G., 1967
 T. MATHEWS and
 R. H. JOHNSON
 Intercomparison of neutron monitors during solar-flare increases, Phys. Rev. Lett., 18, nr. 16, 675-676.
- YOSHIDA, S., 1968
 S.-I. AKASOFU and
 P. C. KENDALL
 Ring current effects on cosmic rays, J. Geophys. Res., 73, 3377-3394.

The Unprecedented Cosmic Ray Disturbances of Early August 1972

by

J. C. Dutt[†], J. E. Humble* and T. Thamyahpillai
Department of Physics, Imperial College
London SW7, England

This is a preliminary account of the severe and complex cosmic ray disturbances which were observed during the period 3 to 8 August 1972 following the occurrence of intense solar flares erupting chiefly in McMath plage region 11976. The cosmic ray disturbances include two solar proton events which were energetic enough to be recorded by ground-level neutron monitors but were otherwise un-spectacular showing at least three Forbush decreases of which the first and third did not exhibit any extraordinary properties. However, the second Forbush event was characterized not only by an exceptionally large amplitude but also by an extremely short onset phase so that the rate of depletion of intensity was the highest ever recorded since neutron monitor observations commenced. Also, the recovery rate was much more rapid than average. It is our purpose here to detail as many of the characteristics of these events as can be deduced from the meager data at hand so that this paper will be a precursor to much more detailed accounts which will follow when comprehensive data from the world-wide network of neutron and meson monitor stations become available.

The solar flares that initiated some of the above-mentioned cosmic ray disturbances occurred in McMath plage region 11976 on 2 August. Three bright flares were observed optically in H α to commence at 0316 UT (Importance 1B), 1838 UT (1B) and 2005 UT (2B). The shock fronts that are believed to have been created by these flares passed the earth (using sudden commencements, ssc, of geomagnetic storms as their signature) at 0119 UT (delay of 46 hours), 0220 UT (delay of 32 hours) and 2054 UT (delay of 49 hours) on 4 August. The shock fronts were also detected by the HEOS II satellite [P. C. Hedgecock, 1972] which was at a geocentric distance of 22 earth radii at the passage of the last of the shock fronts and which entered the magnetosheath shortly afterwards. It was the last of these shock fronts that produced an extremely large Forbush decrease at the earth. The strength of the interplanetary magnetic field behind this shock was measured by HEOS II to be over 45 gammas.

The passage of the three shock fronts was detected by Pioneer IX which was at a heliocentric distance of about 0.8 AU and whose direction made an angle of about 45° due east of the earth-sun line. The times of passage were 1124 and 2215 UT on 3 August and 0030 UT on 5 August. An examination of the delays involved shows that the speed of propagation was strongly dependent on the direction of travel. This is particularly marked in the case of the third shock which passed the earth 4 hours before it reached Pioneer IX at a distance of 0.8 AU ["Solar-Geophysical Data", 1972].

The hourly values of the cosmic ray intensity as recorded by neutron monitors at Kiel, Mawson, Oulu, Rome, Brisbane and Mt. Wellington and by meson telescopes at Hobart (vertical) and London (inclined at 45° to the vertical and pointing in the north and south directions) are plotted in Figures 1 and 2 for the period beginning at 1200 UT on 3 August and ending at 2400 UT on 7 August. The north-south asymmetry as measured by the difference in intensities between Thule and McMurdo is shown in Figure 3. Considering the events in temporal sequence, we note that the first event was a Forbush decrease (FD-1) which started at most stations after 0100 UT on 4 August. The onset phase of FD-1 was characterized by a strong equatorial anisotropy which is believed, at present, to have been strongly energy-dependent with a north-south asymmetry [Pomerantz and Duggal, 1973]. We have examined the equatorial anisotropy at low energies (mean energy \sim 5-10 Gev) by using high latitude neutron monitors which have fairly narrow viewing cones in the earth's equatorial plane [Mercer and Wilson, 1968; Hashim and Thamyahpillai, 1969]. The onset and the time of maximum depression of FD-1 were earliest at those stations which were looking in the inward direction along the average spiral interplanetary magnetic field at the earth's orbit. The only exception to this general picture was the Mt. Wellington neutron monitor which showed a higher intensity than the rest of the stations during most of the onset phase. The maximum depression of 7-8% in high latitude sea level neutron monitors was reached at about 1200 UT on 4 August. While the start of the decrease at low energies coincided with the arrival at the earth of two shock fronts in the interplanetary plasma, the situation was radically different at the higher energies to which meson monitors respond (mean energy is 20-50 Gev). The decrease started in the north telescope in London at about 2100 UT on 3 August (about 5 hours earlier than in neutron monitors) and a similar early start is visible in the south telescope at London. On the other hand the muon intensity at Hobart was above average between 0000 and 0500 UT on 4 August. The peak intensity at Hobart was 1.5% above the mean level. While the increase at Hobart which was viewing roughly in the sunward direction can be explained as a pre-increase, the early onset in the London telescopes which were looking roughly in the anti-sun direction is more difficult to interpret. The maximum depression in the muon telescopes was about 2 to 3%. Assuming that the modulation function follows a power law in rigidity, we estimate that the exponent in the power law is close to 1.0 ± 0.2 for this event.

[†] On leave from Atomic Energy Center, Dacca, Bangladesh.

* On leave from Department of Physics, University of Tasmania, Hobart, Australia.

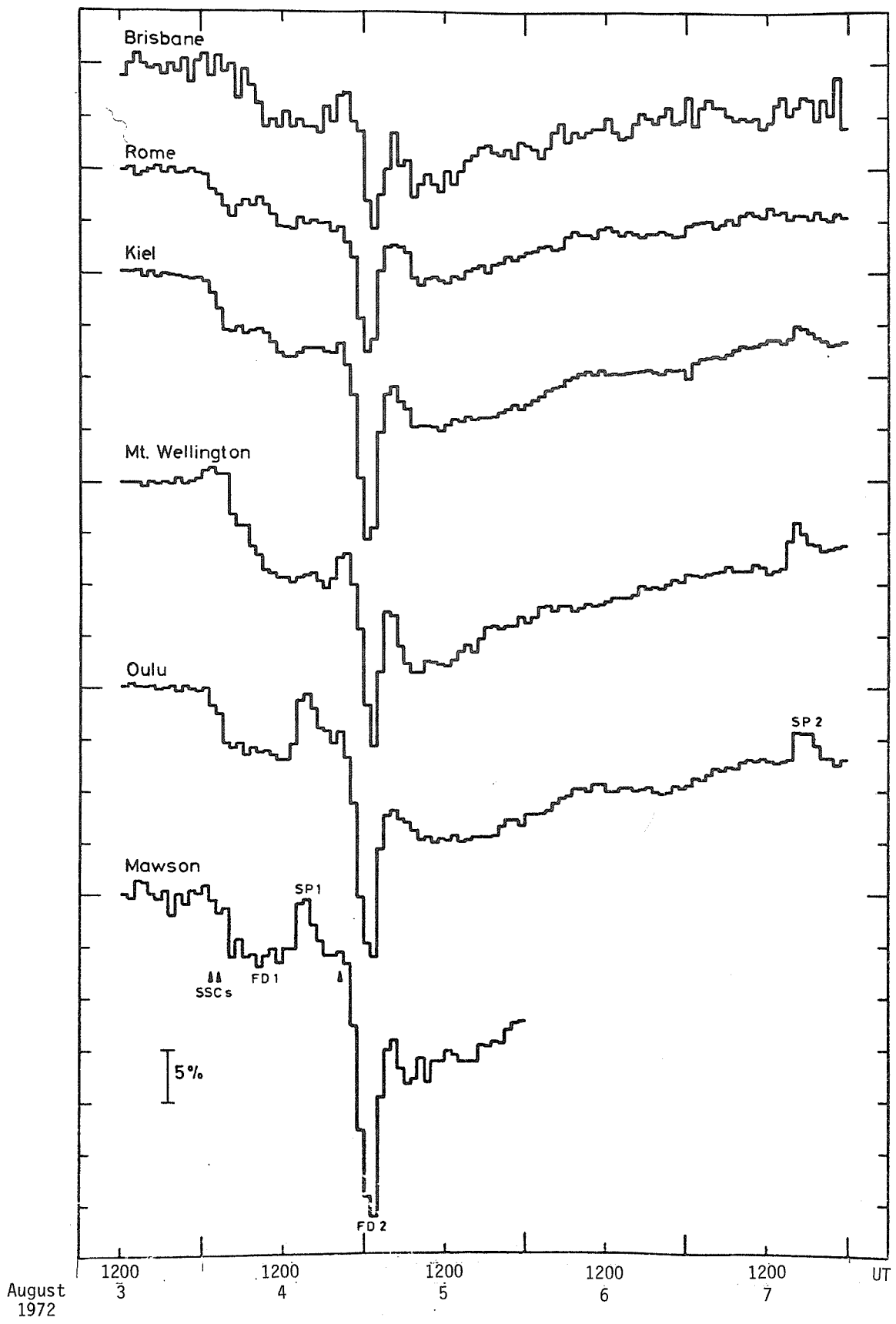
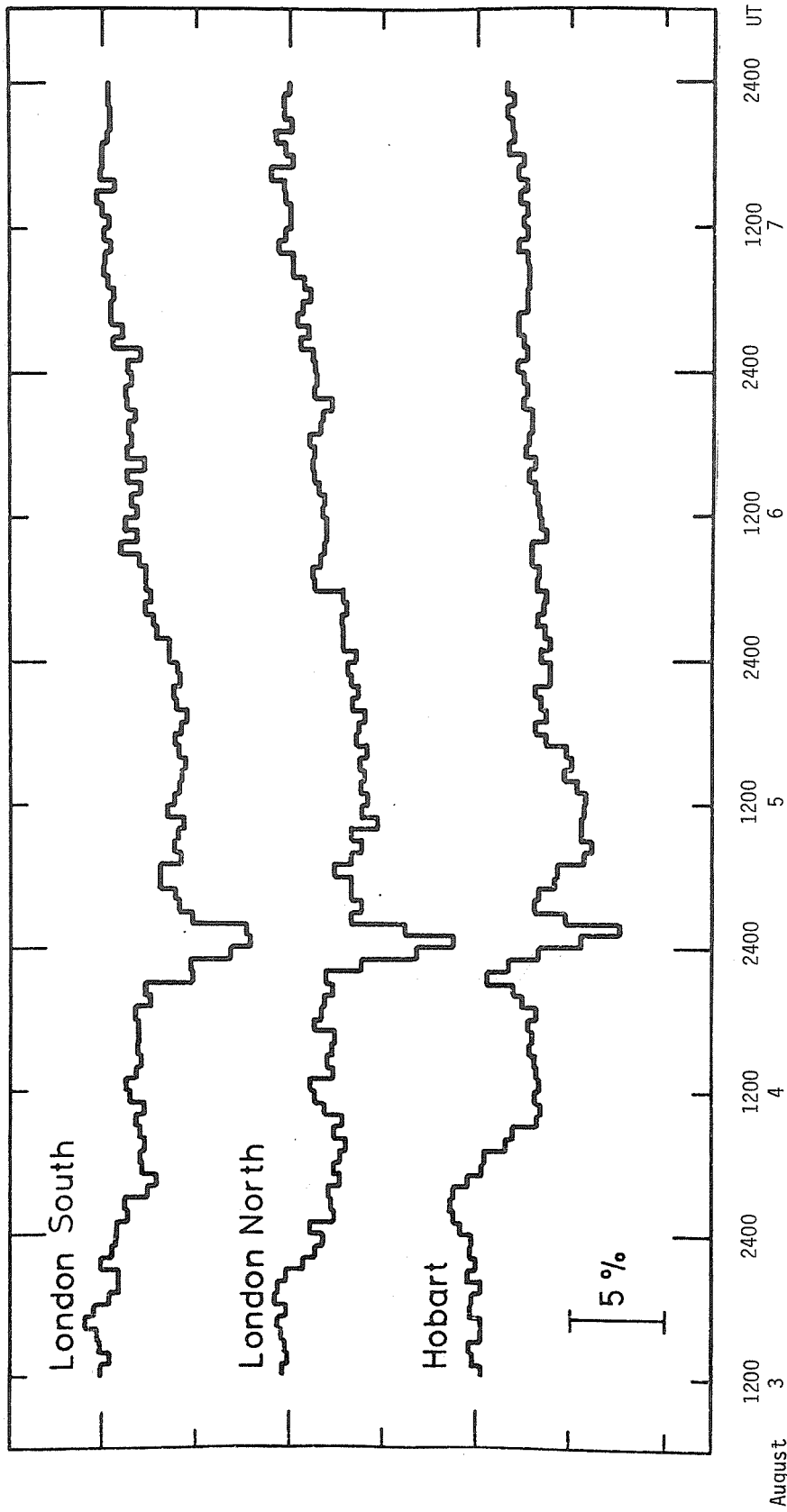


Fig. 1. The intensity variations measured during early August 1972 by neutron monitors at a number of different locations.



August 1972
 Fig. 2. The intensity variations measured by meson telescopes in London and Hobart. The telescopes at London were inclined at 45° to the vertical and were pointing in the north and south directions, while the Hobart telescope had its axis vertical.

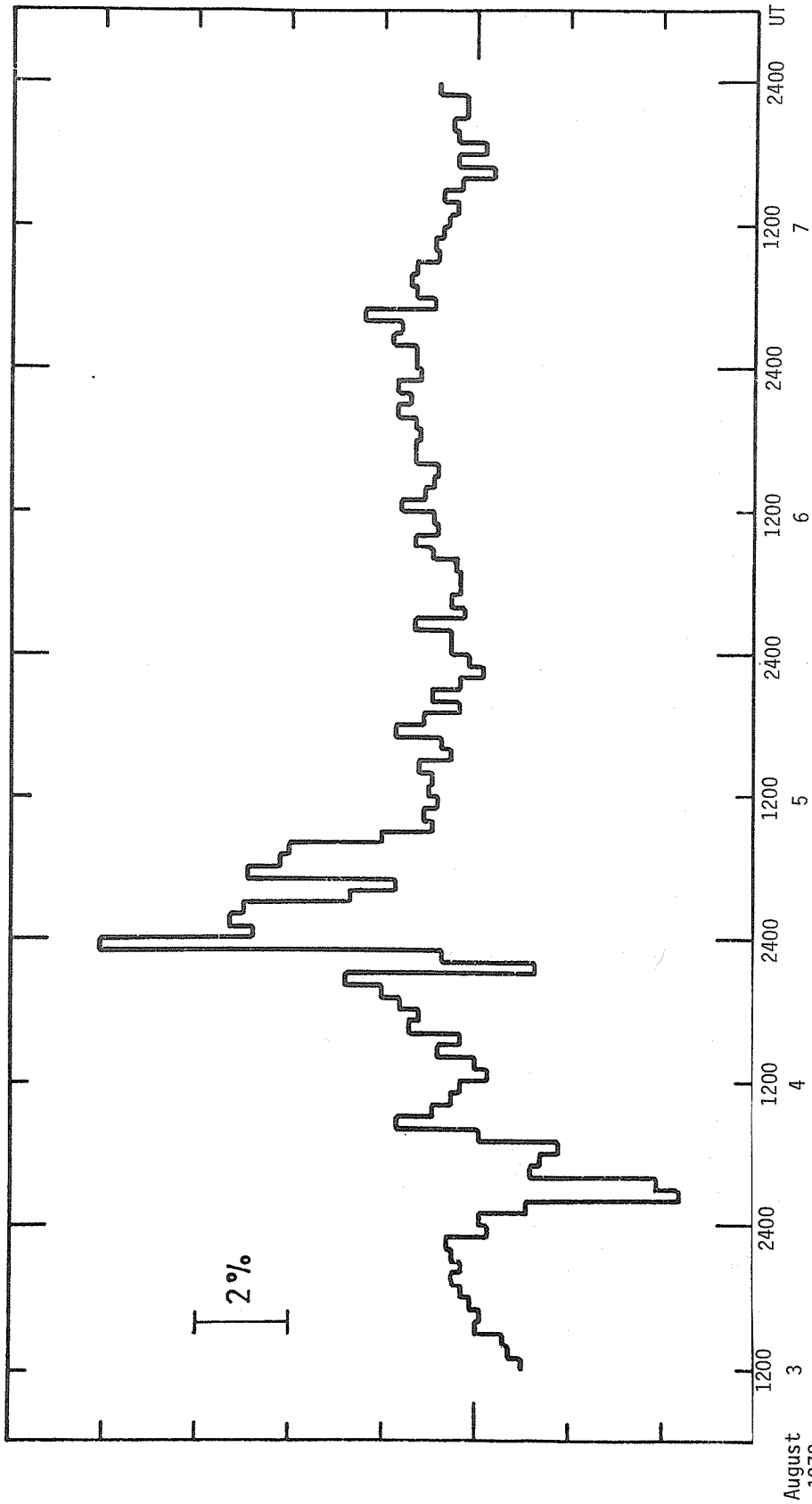


Fig. 3. The north-south asymmetry pertaining to the cosmic ray events of August 1972. The difference between the neutron intensity variations at Thule and McMurdo [M. A. Pomerantz, 1972] is shown.

There was also a marked north-south asymmetry associated with FD-1. While the neutron intensity at Thule, where the viewing cone points towards high northern latitudes, started decreasing between 0100 and 0200 UT, the intensity at McMurdo in the southern hemisphere did not start falling before 0300 UT. Also, the maximum depression was reached about 2 hours earlier at Thule than at McMurdo. This asymmetry is not surprising because the initiating flare of the shock fronts occurred at N13 heliollatitude. However, the maximum depression was about 1% larger in the southern direction than in the northern one.

Between 1300 and 1400 UT on 4 August, the neutron intensity at high latitude stations (quiet time threshold ≤ 1.0 GV) started rising because of the onset of a solar proton event (SP-1). This event can be identified as a solar proton increase without a slightest doubt when we take into consideration the dependence of the amplitude on the geomagnetic thresholds of the stations as well as the altitude dependence of the increase.

The proton intensity increased steadily until a maximum of 7 to 8% was reached at sea level stations between 1500 and 1600 UT on 4 August. The intensity died away gradually thereafter in a roughly exponential manner. At neutron stations with quiet time thresholds ≥ 1.8 GV and altitude < 1000 m the increase was too small (certainly less than 2%) to be disentangled from FD-1. As far as we can determine at present, SP-1 was a roughly isotropic event during both the increase and decay phases. It would be extremely difficult to determine the energy spectrum of the solar protons because the differential response function is not known accurately between 1.8 and 1.0 GV. The response function in this interval will depend strongly on the phase of the solar cycle, and the event occurred during the course of a severe geomagnetic storm so that the magnetic thresholds could have been lower than their quiet time values. In fact the only ground-level station at which an intermediate increase could have been observed is Durham, New Hampshire, U.S.A., and data from this station are not at hand at the time of writing. Towards the tail end of SP-1, pre-increases associated with the second Forbush decrease (FD-2) had started to occur and tend to complicate the picture.

There are some interesting features about identifying the solar flare which was responsible for SP-1 at the earth. There was a flare of importance 3B which erupted at about 0530 UT on 4 August and reached maximum intensity in H α at about 0640 UT. Protons were accelerated in this flare because the channel recording protons with energy > 14 Mev in Pioneer IX measured a substantial increase by 0800 UT. Yet the ground-level event involving protons of energy 1 Gev did not start till after 1300 UT on the same day. It is possible to explain this delay of about 8 hours by assuming that the solar protons were trapped behind a shock front which did not arrive at the earth until after 1300 UT. Mathews, Thambyahpillai and Webber [1961] have noted that the second solar proton increase on 12 November 1960 was roughly coincident with the arrival of a shock front which produced a Forbush decrease at higher energies. They have suggested that the second increase was due not to acceleration in a second flare, but to the trapping of the protons from the first flare behind the shock front. However, there is one important difference between the November 1960 event and SP-1. While the 1960 increase was extremely rapid, reaching maximum in a matter of minutes, SP-1 showed a very slow rise to maximum intensity. For this reason and also because there were no geophysical effects such as an ssc or a Forbush decrease at about 1300 UT on 4 August, we reject the explanation of delayed arrival and suggest that SP-1 was produced by a weak flare (importance -N) which started at 1305 UT on 4 August and reached maximum intensity around 1315 UT. The extreme steepness of the proton energy spectrum coupled with the slow rise to maximum lead us to this view. It is possible that protons from the weak flare were detected at ground level because the connection between the earth and the flare region via the interplanetary magnetic field was favorable.

Towards the end of SP-1 at about 2000 UT some stations, especially the polar stations Thule and McMurdo, saw an increase of neutron intensity. However, most stations with their viewing cones in the earth's equatorial plane did not see this increase and this rules out the possibility that SP-1 had a structure with a double maximum. It is suggested that Thule and McMurdo were seeing a pre-increase which preceded the large Forbush decrease FD-2. A pre-increase was observed in the equatorial plane in a narrow cone of directions with its axis pointing in the sunward direction. The behavior was similar at both low and high energies because the Hobart muon telescope looking in the sunward direction registered a pre-increase while the London north and south telescopes looking in a roughly opposite direction did not see an increase. The pre-increase is unusual in the sense that the equatorial variation was not intermediate between those in the north and south directions. Magnetic field measurements on board HEOS II show that the direction of streaming implied in the pre-increase was parallel to the interplanetary magnetic field at the relevant time.

As already mentioned, at 2054 UT on 4 August an ssc was registered signalling the arrival at the earth of a plasma shock front propagating away from the sun. The highest solar wind velocity ever measured in the Pioneer series was recorded by Pioneer IX in association with this shock front. Also the geomagnetic storm that followed the ssc was one of the severest recorded over 20 solar cycles. It is not surprising, therefore, that the Forbush decrease FD-2 which commenced at about the time of the ssc also had features without precedent in the history of neutron monitor recording.

Between the hours 2100 and 2200 UT many cosmic ray stations registered an intensity which was lower than that during earlier hours showing that FD-2 had already commenced. This commencement was highly anisotropic, exhibiting both a north-south asymmetry and an equatorial anisotropy. The depression at Thule was substantial during the first hour of the onset, while the intensity at McMurdo showed hardly any change from the previous hour. Thus, the onset was earlier from the northern direction. The equatorial anisotropy was such that the largest depressions were registered from a broad cone of directions centered along the anti-sun direction. This behavior was true not only at the lower primary energies to which neutron monitors respond but also at the higher energies monitored by muon telescopes. The start of FD-2 in the Hobart muon telescopes was delayed 2 hours with respect to the commencement in the London directional telescopes.

The onset phase of FD-2 lasted 5 hours or less at most stations, and there were north-south asymmetry as well as equatorial anisotropy throughout the onset phase. The maximum depression recorded at Thule (northern direction) was about 22% while that at McMurdo (southern direction) was about 27%. Most stations with viewing cones lying near the earth's equatorial plane registered intermediate depressions of about 25% with the exception of the Mawson neutron monitor which recorded a depression of nearly 32%. The large decrease at Mawson can be ascribed to the extreme narrowness of the viewing cone coupled with its being in a favorable position. The rate of decrease of intensity exceeded 4% per hour and is one of the highest known for Forbush decreases.

Because of the rapidity of the changes, the consideration of neutron counts in hourly groups tends to give too coarse-grained a picture of the variations and it would be desirable to confirm our conclusions by analyzing say 5 minute counts from various stations. Available evidence suggests, however, that the direction of maximum depression in the equatorial plane started off in the anti-sun direction but swung eastwards so that by the end of the onset phase the maximum depression was occurring along a direction 45° due west of the earth-sun line (inward direction of the average interplanetary magnetic field). The rate of recovery also was most rapid along the latter direction.

By comparing the decreases in high latitude neutron monitors and the muon telescopes in London, we find that if the modulation function can be assumed to follow a power law in rigidity, the exponent in the power law for FD-2 should have been 1.3 ± 0.2 .

After 0200 UT on 5 August, a rapid recovery started and the rate was so fast that about 3/4 the second decrease had been wiped out within 2 or 3 hours. The rapid fall in conjunction with the fast recovery give a negative pulse-like appearance to FD-2. Similar pulse-like decreases but of not such colossal amplitude as FD-2 have been observed on earlier occasions, particularly in July 1960 [Sandstrom, 1965] and December 1960 [Humble, 1968]. There were very strong directional anisotropies during this recovery phase. The intensity dropped again at many stations causing a hump-like structure in intensity-time diagrams. From the evidence at hand we can definitely rule out the possibilities that these humps were due either to solar protons or to changes in geomagnetic thresholds. We are inclined to interpret these humps as transient overshoots in the recovery phase. The possibility that a third Forbush decrease occurred during the recovery phase of FD-2 cannot be ruled out entirely, but there does not seem to be any evidence that a shock front that could have caused a Forbush event passed the earth at the relevant time.

As mentioned earlier, the early stages of the recovery phase of FD-2 were highly anisotropic, the differences between stations looking along the earth's axis and those viewing in the equatorial plane being very marked. The recovery was comparatively sluggish along both north and south directions, the increase up to the top of the hump being less than half the original decrease of FD-2. The recovery was much larger at some stations with equatorial viewing cones and the maximum recovery occurred at those stations viewing between the inward direction along the earth-sun line and the inward direction of the average spiral interplanetary field. The intensity dropped suddenly to a new low level along the south direction, while the drop to a lower level occupied several hours in the northern direction. The size of the hump varied also in those stations viewing in the equatorial plane, hardly any hump being observed at Swarthmore, while the humps in the Leeds, Oulu and Mt. Wellington data were very pronounced. After the end of the transient overshoot, the recovery was roughly isotropic and could be represented as an approximately exponential recovery to the pre-decrease level. This recovery proceeded smoothly until the start of a second solar proton event (SP-2) which occurred on 7 August.

After the occurrence of a 3B flare commencing at 1500 UT on 7 August, solar protons started arriving at the earth with a delay of less than $\frac{1}{2}$ hour. The proton intensity at stations with geomagnetic thresholds less than the atmospheric cut-off rose to a maximum of 5 to 6% and then decayed away over the next 5 or 6 hours. A measurable increase was observed at Kiel which has a quiet time threshold of about 2.3 GV. Thus, the rigidity spectrum of the solar protons of SP-2 was much less steep than that of SP-1. Apart from this, there were no unusual features about SP-2 that can be noticed.

Acknowledgements

We are very much indebted to those workers who communicated their neutron data promptly after our request for these. These include Professors D. E. Bagge, N. Iucci and P. J. Tanskanen and Drs. C. J. Hatton, D. Heristchi, M. A. Pomerantz and J. Skolnik. Data from Hobart, Mawson and Mt. Wellington were obtained by the University of Tasmania, assisted by grants from the Australian Research Grants Committee and the Antarctic Division, Department of Supply. Our thanks are due to Dr. P. C. Hedgecock for supplying interplanetary field and shock data from the HEOS II satellite.

REFERENCES

- | | | |
|---|------|---|
| HASHIM, A. and
T. THAMBYAHPILLAI | 1969 | <u>Planet. Space Sci.</u> , <u>17</u> , 1879. |
| HEDGECOCK, P. C. | 1972 | Private Communication. |
| HUMBLE, J. E. | 1968 | <u>Proc. Astron. Soc. (Aust.)</u> <u>1</u> , 146. |
| MATHEWS, T.,
T. THAMBYAHPILLAI and
W. R. WEBBER | 1961 | <u>Mon. Not. Roy. Astron. Soc.</u> , <u>123</u> , 97. |
| MERCER, J. B. and
B. G. WILSON | 1968 | <u>Canadian J. of Physics</u> , <u>46</u> , S849. |
| POMERANTZ, M. A. | 1972 | Private Communication. |
| POMERANTZ, M. A. and
S. P. DUGGAL | 1973 | Bartol preprint, in press. |
| SANDSTRÖM, A. E. | 1965 | <u>Cosmic Ray Physics</u> , North Holland. |
| | 1972 | <u>Solar-Geophysical Data</u> , 337 Part I, U. S. Department
of Commerce, (Boulder, Colorado, U.S.A. 80302). |

Remarkable Cosmic Ray Storm and Associated Relativistic Solar
Particle Events of August 1972

by

M. A. Pomerantz and S. P. Duggal
Bartol Research Foundation of The Franklin Institute
Swarthmore, Pennsylvania 19081

ABSTRACT

The greatest cosmic ray storm ever observed, that occurring in August 1972, displayed a complex and dynamic three-dimensional anisotropy which produced remarkable structure in the intensity profiles. The maximum depression of the galactic cosmic ray flux to about 50% of the pre-storm level was in a region located approximately 60° west of the sun-earth line.

Of the two ground level events (GLE) that overlapped the cosmic ray storm, the second on August 7 was highly anisotropic, and generally appeared to be "typical", in contrast with its highly unusual predecessor on August 4 that was characterized by an unusually steep spectrum (and, consequently, a relatively short absorption mean free path). Furthermore, the injection of relativistic solar particles appears to have occurred quite late, during the recovery phase of an Imp 3B flare rather than in the flash or explosive phase which has been either assumed or deduced to be the emission epoch in all other GLEs observed thus far.

Introduction

A record-breaking cosmic ray storm stemming from an outstanding solar activity center (sunspot group #331, McMath plage region #11976) was recorded by cosmic ray detectors on the earth's surface in August 1972 [Pomerantz and Duggal, 1973]. Two ground-level events (GLE) were observed with nucleonic intensity detectors during the course of this storm. One, a "typical" GLE, was recorded during the final recovery phase, whereas the other, highly unusual in several respects, was unambiguously evident at only a few polar stations where the intensity enhancement exceeded the pre-storm level. The anomalous relativistic solar particle event immediately preceded the onset phase of the Forbush decrease which reduced the primary galactic cosmic ray flux to 50% of the pre-storm intensity. Consequently, it is not surprising that it displayed atypical features.

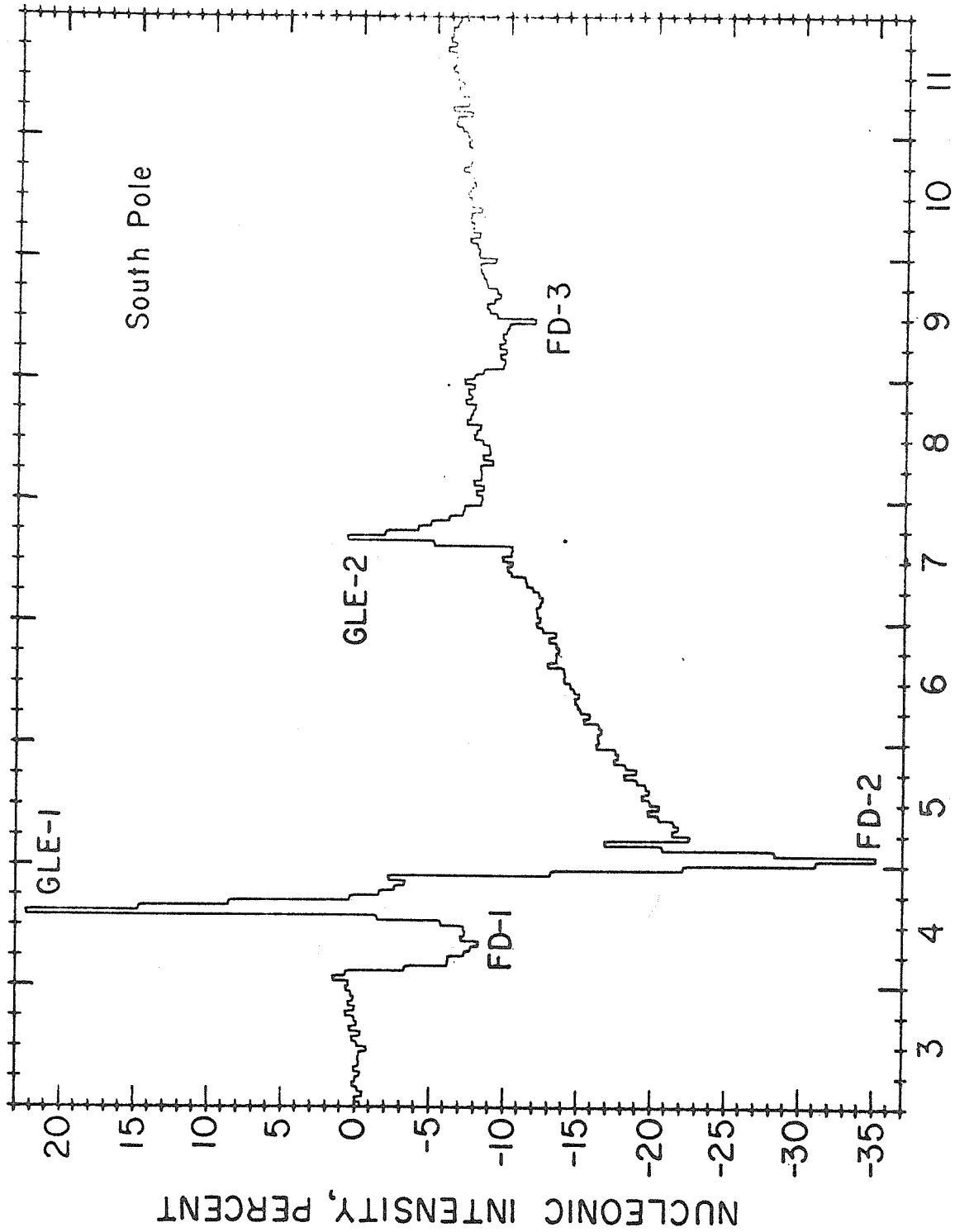
Observations and Discussion

Group 331, on its second passage across the visible disk of the sun, produced three H α flares commencing on August 2 before 0316 UT (1N-2N, N13, E35), at 1838 UT (1B, N14, E26) and at 1958 UT (2B, N13, E27) which were followed by the cosmic ray storm that started on August 4. Figure 1 shows that even when the data are averaged over hourly intervals, the nucleonic intensity profile as observed at South Pole (the only existing high altitude polar station) clearly manifests three Forbush decreases (FD) and two solar particle ground level events (GLE). The largest peak-to-valley fluctuation in the nucleonic intensity, $\sim 57\%$ in the hourly averages, was recorded there.

Ground Level Events

Pomerantz and Duggal [1973] have established that the increase during GLE-1, which was less spectacular at other stations than at South Pole, was produced by the influx of relativistic solar particles, rather than by other possible mechanisms. The increase, in hourly intervals, at several polar stations is shown in Figure 2. The maximum intensity was reached two to three hours after the onset, and the duration of the event was about eight hours. Since the total anisotropy during this event was not large, and the viewing directions of both Thule and McMurdo were far from the axis of symmetry, an analysis based upon existing theoretical models of the diffusion of relativistic particles is appropriate. The procedure initiated by Duggal and Pomerantz [1972] leads to the conclusion that the time of injection at the sun was approximately 1200 UT. Thus, it appears that the acceleration of relativistic particles occurred long after the optical maximum at 0635 UT of the Imp 3B solar flare (N14, E08) which commenced at 0620 UT August 4, 1972 in the McMath plage region #11976. The apparently abnormal time delay, originally noted in the preliminary report by Pomerantz and Duggal [1973], is confirmed, and poses a dilemma which remains to be resolved. In fact, the present analysis leads to the conclusion that, for the first time on record, relativistic particles were released very late in the recovery phase of a flare, rather than near onset or during the explosive or flash phase as has been either assumed or deduced in all past events (see, e.g. the excellent discussion of solar flare phenomena by Syrovatskii [1972]). It should be remarked that the comprehensive Flare Index of of the parent solar eruption, nominally never exceeding 15, was 17 in this case (H. D. Prince, private communication).

A subflare (-N) in this same region was also reported to commence at 1307 UT. Since the solar particles were clearly already reaching South Pole at this time, and since the calculated injection time is significantly earlier than the minor H α brightening, this subflare can be ruled out as the origin of the GLE. These considerations suggest that this and other time-related subflares might actually have been a consequence of the particle acceleration process.



AUGUST, 1972

Fig. 1 Nucleonic intensity during the record-breaking cosmic ray storm of August 1972, at South Pole, where the magnitudes of the Forbush decreases (FD) and ground level events (GLE) exceeded those at any other station.

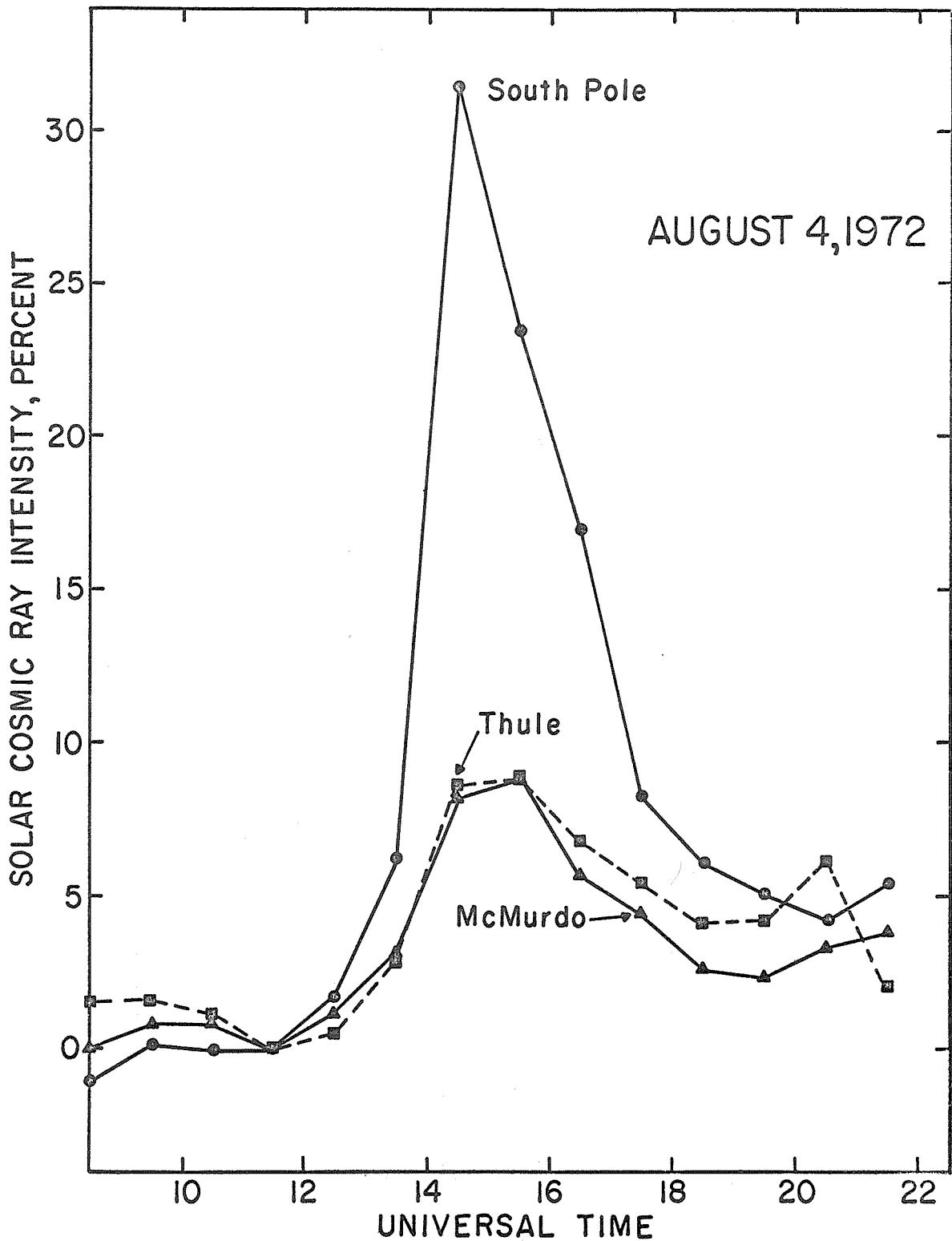


Fig. 2 Plot of nucleonic intensity arising from relativistic solar cosmic rays at several polar stations, expressed as hourly average percent above the pre-increase level during GLE-1 in Figure 1.

The fact that the ratio of the intensity increase at the high latitude mountain station, South Pole, to that at the corresponding sea level station, McMurdo, is the largest observed since the establishment of these stations more than ten years ago ($I_{sp}/I_{Mc} = 3.8$, compared to 2.1) bespeaks an usually steep spectrum. This is reflected in the fact that the atmospheric absorption length for the nucleonic component produced by the solar cosmic rays at about 1430 UT was abnormally small, i.e. $\sim 86 \text{ gm/cm}^2$, compared with the normal value of 104 gm/cm^2 [Baird et al., 1967].

A higher resolution plot (10 minute averages) of GLE-1 is shown in Figure 3. The maximum enhancement at South Pole was 68%, and the corresponding intensity ratio I_{sp}/I_{Mc} was ≈ 7.0 .

Although determination of the relativistic solar particle spectrum during the onset and the maximum phases of GLE-1 is complicated by anisotropic effects, the data recorded at a group of stations with threshold rigidities exceeding the atmospheric cutoff (near 1 GV) during the interval 1500-1600 UT on August 4, 1972 follow a straight line in the log-log plot shown in Figure 4.

In the primary power law spectrum deduced from this result, the value of the exponent is $\gamma = 6.6 \pm 0.5$, significantly steeper than during the succeeding two hours, when the spectral index, $\gamma = 5.2 \pm 0.5$, is consistent with the typical value determined by the identical procedure in earlier events ($\gamma \approx 5.0$).

The intensity profile (Figure 5) of the second ground level event (GLE-2) on August 7, 1972 was generally similar to those observed previously. At South Pole, the onset was around 1530 UT, roughly 45 minutes after the commencement of the solar flare of importance 3B at 1443 UT in sunspot region 331 (N14, W36). Flare maxima occurred at 1500 and 1527 UT, and the optical activity continued past 1730 UT. The comprehensive Flare Activity Index was 15. A small north-south asymmetry is evident around the maximum phase. This reflects the usual pitch angle distribution of solar particles [Maurer et al., 1973]. In fact, during the onset phase of this event the total anisotropy exceeded 70%. Contrary to GLE-1, in this case a significant nucleonic intensity increase was recorded at Swarthmore ($P_c = 1.9 \text{ GV}$) that persisted for more than four hours. During the period 1600 - 2000 UT on August 7 the value of the spectral index was $\gamma = 4.7 \pm .5$.

Forbush Decreases

A distinct north-south asymmetry occurred during the onset phase of FD-1 and throughout FD-2 (compare Thule and McMurdo in Figure 6), with minimum intensity in the Antarctic. The comparison of data from stations distributed over the earth has revealed that an exceedingly complex pattern of anisotropy prevailed. The dynamic character of the anisotropic modulation is exemplified in Figure 7. Here, the magnitude of the Forbush decrease FD-2 at various locations is indicated inside circles denoting the mean asymptotic directions of viewing at 2400 UT, according to trajectory calculations that take into account the currents both in the magnetopause and in the neutral sheet of the magnetospheric tail [Gall, 1968; Shea and Smart, 1972]. The epochs centered at 2330 UT August 4, and 0130 UT August 5, 1972, correspond to the onset and the minimum phases of the transient intensity diminution, respectively. Appreciable longitudinal and axial asymmetries are evident during both periods. The maximum modulation of the galactic intensity appears to have occurred somewhere near 60° west of the sun-earth line in the equatorial plane. Some apparent anomalies, such as the smaller decrease at Yakutsk with respect to neighboring stations, may reflect variations in asymptotic directions caused by magnetospheric phenomena.

In view of the appreciable anisotropy in the equatorial plane, the criteria for analyzing the north-south asymmetry by the procedure described previously [Pomerantz and Duggal, 1972] are not satisfied for this event, and further study of the three-dimensional anisotropy must be approached with great caution.

Following the minimum phase of FD-2, the cosmic ray intensity started to recover rapidly during the interval 0200 to 0500 UT, and roughly half of the depletion represented by FD-2 was wiped out in these three hours. At first glance, this pulse-like recovery may appear to have been caused either by the arrival of a new burst of relativistic solar particles, or by the acceleration of existing particles by interplanetary shocks. With respect to the first possibility, the analysis of data from 17 nucleonic intensity detectors has revealed that the observed rigidity spectrum was not indicative of the presence of solar particles. Furthermore, neither the spectral index nor the large anisotropies changed during the period 0500-0600 UT, immediately following the rapid recovery. These features are strikingly apparent in the comparison of the nucleonic intensities recorded at McMurdo and South Pole. In Figure 8, the ordinates represent the percentage increase (i.e. recovery) from the intensity minimum (0100-0200 UT). Throughout the entire interval 0200 - 0600 UT, the rates of intensity increase at the two stations were identical, that is, the intensity ratio I_{sp}/I_{Mc} remained equal to about 1.65 in marked contrast with the situation for solar particles described above. It should be remarked that there is no evidence in this Figure for the extension to high energies of the extra burst of 10-60 MeV protons recorded by Imp G satellite [Solar-Geophysical Data, 1973] between 0300 and 0500 UT.

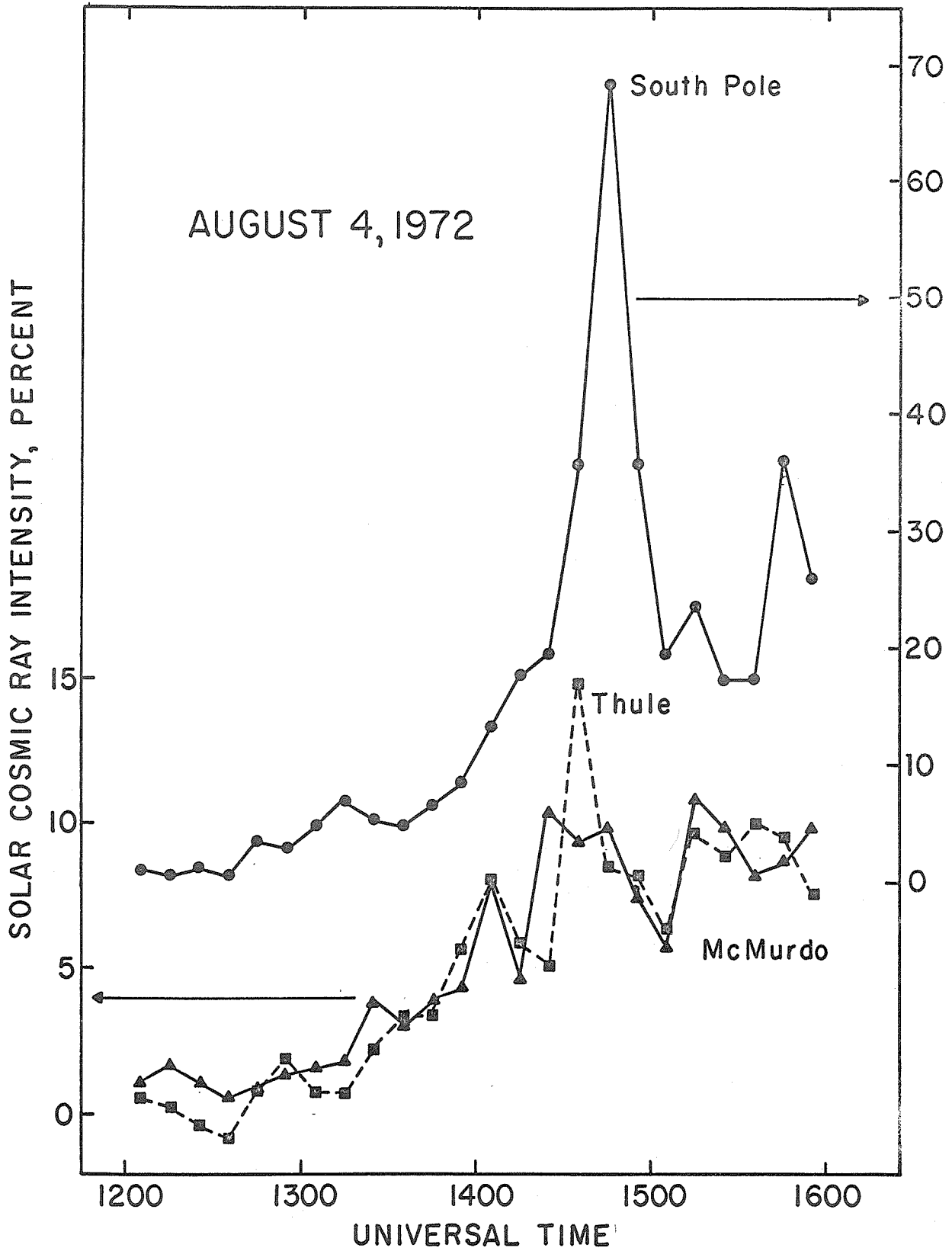


Fig. 3 Higher resolution plot (10 minute averages) showing the exceedingly steep spike during GLE-1 at the high altitude South Pole station.

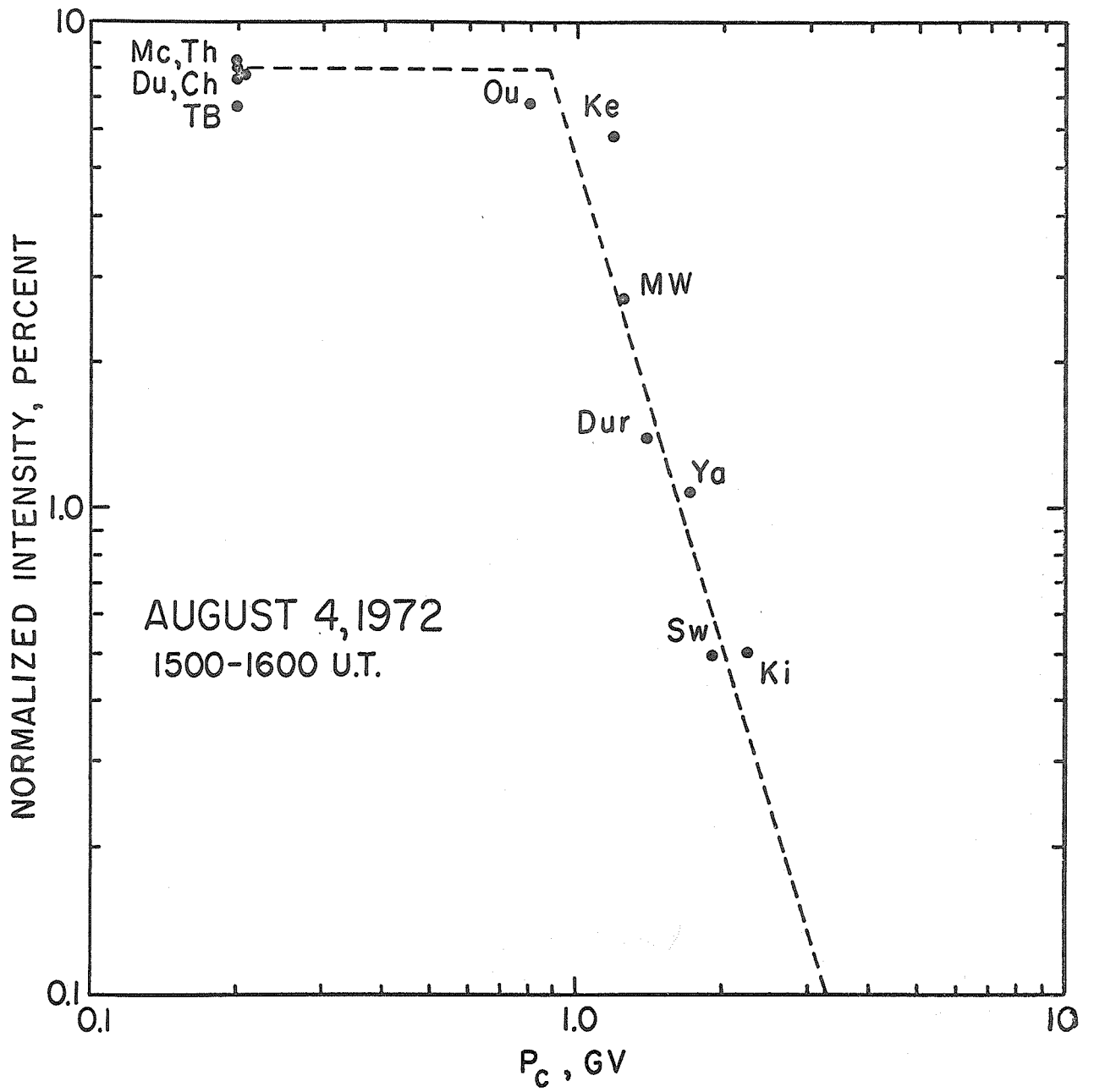


Fig. 4 Intensity vs. threshold rigidity during the hour immediately following the maximum of GLE-1.

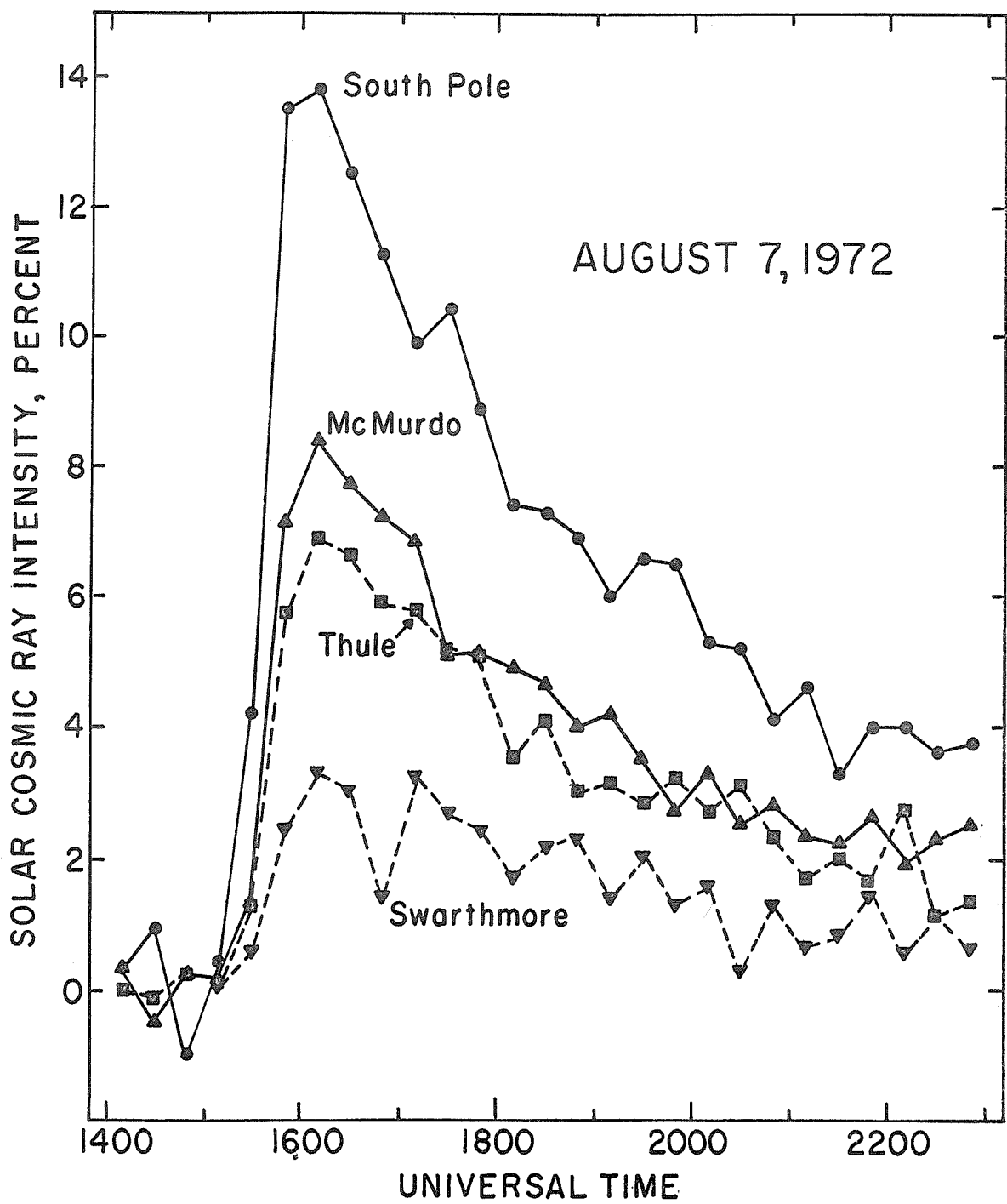


Fig. 5 The intensity profile of GLE-2 as observed at the Bartol network of stations.

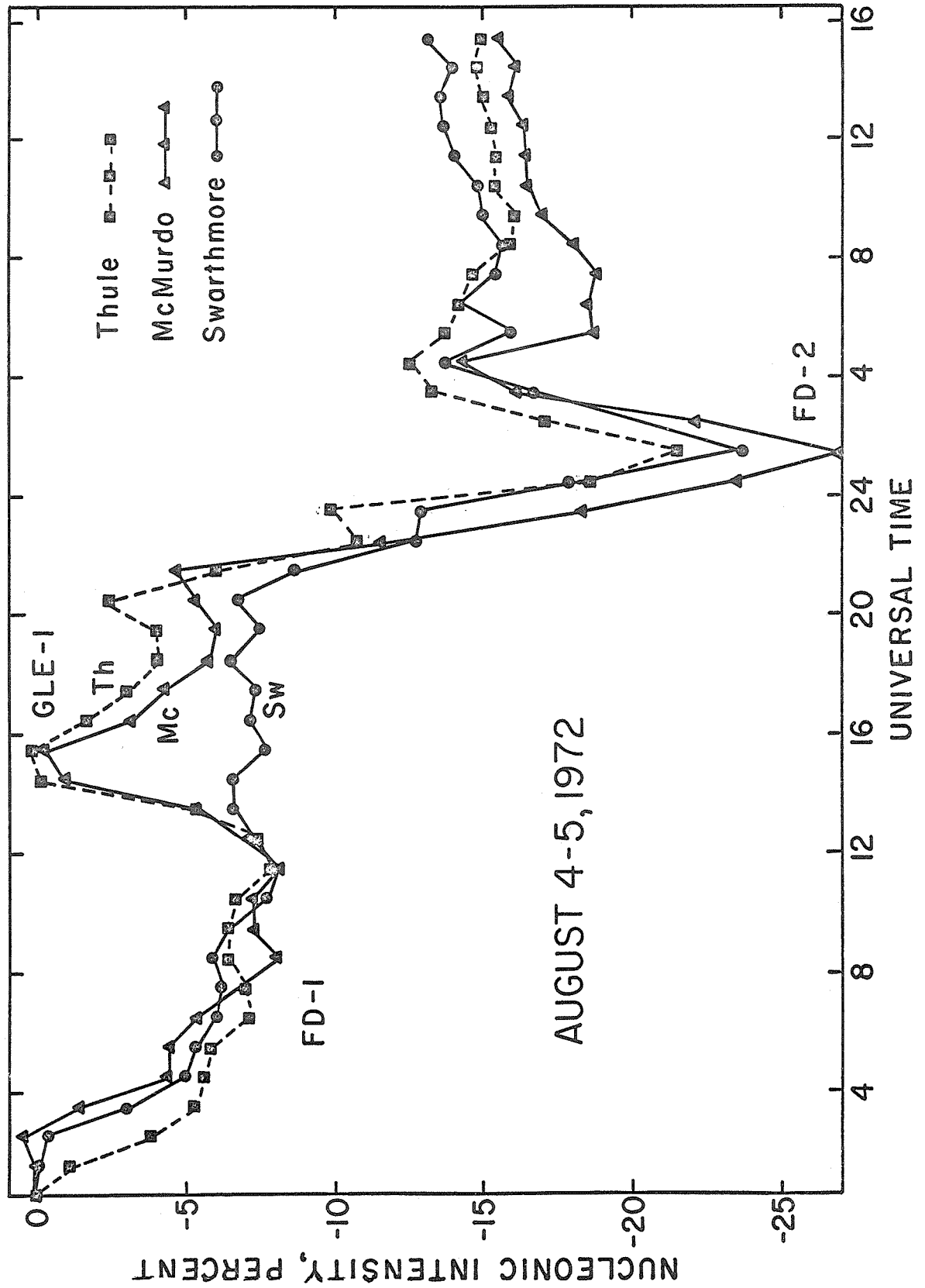


Fig. 6 Detailed comparison of the Forbush decreases FD-1 and FD-2 at three sea-level stations.

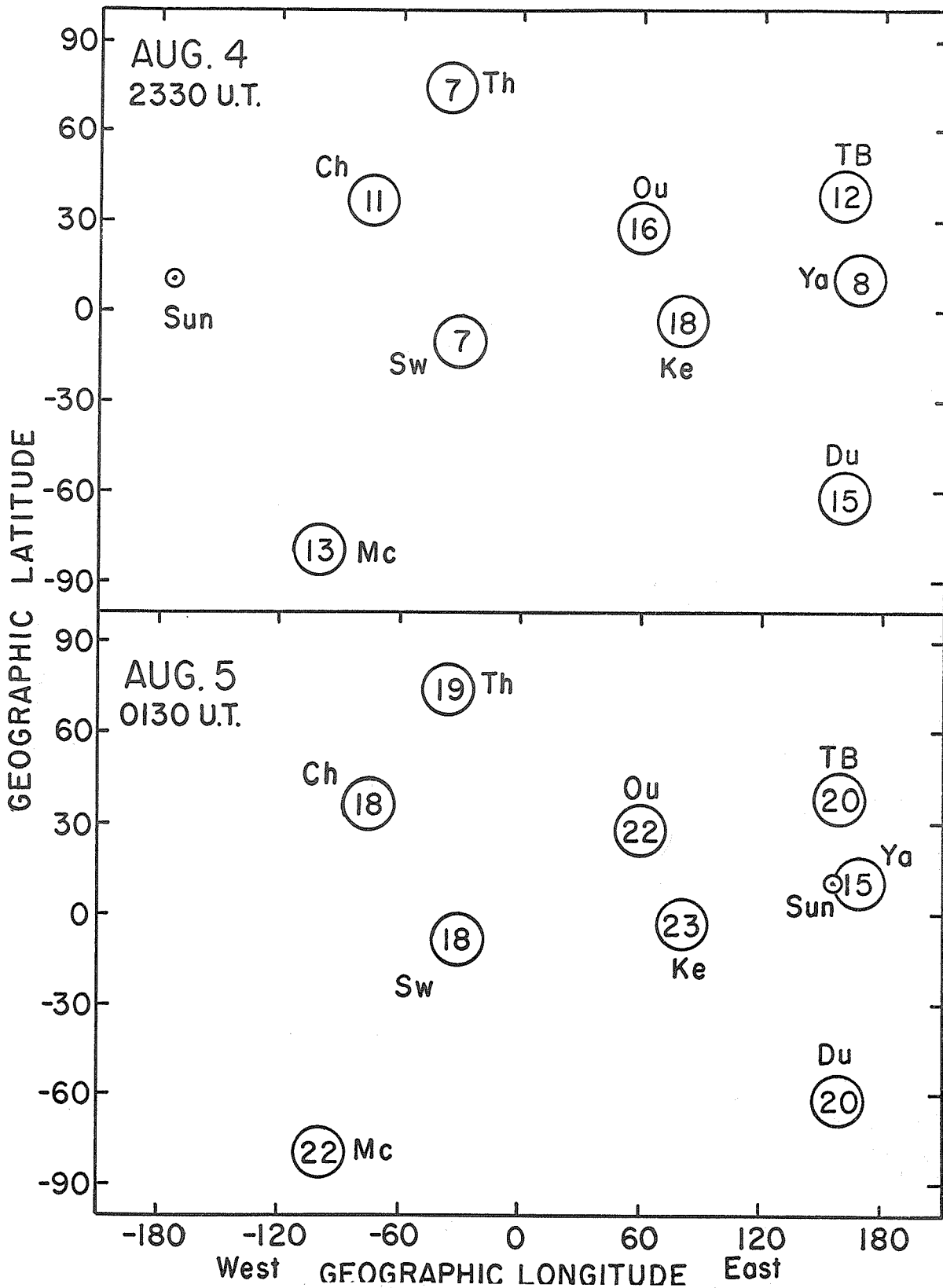


Fig. 7 Map of the celestial sphere, in geographic coordinates, showing the mean asymptotic direction of viewing and the corresponding magnitude of FD-2 at various stations during two hours representing the onset and minimum phases of this Forbush decrease when appreciable longitudinal and axial asymmetries are evident.

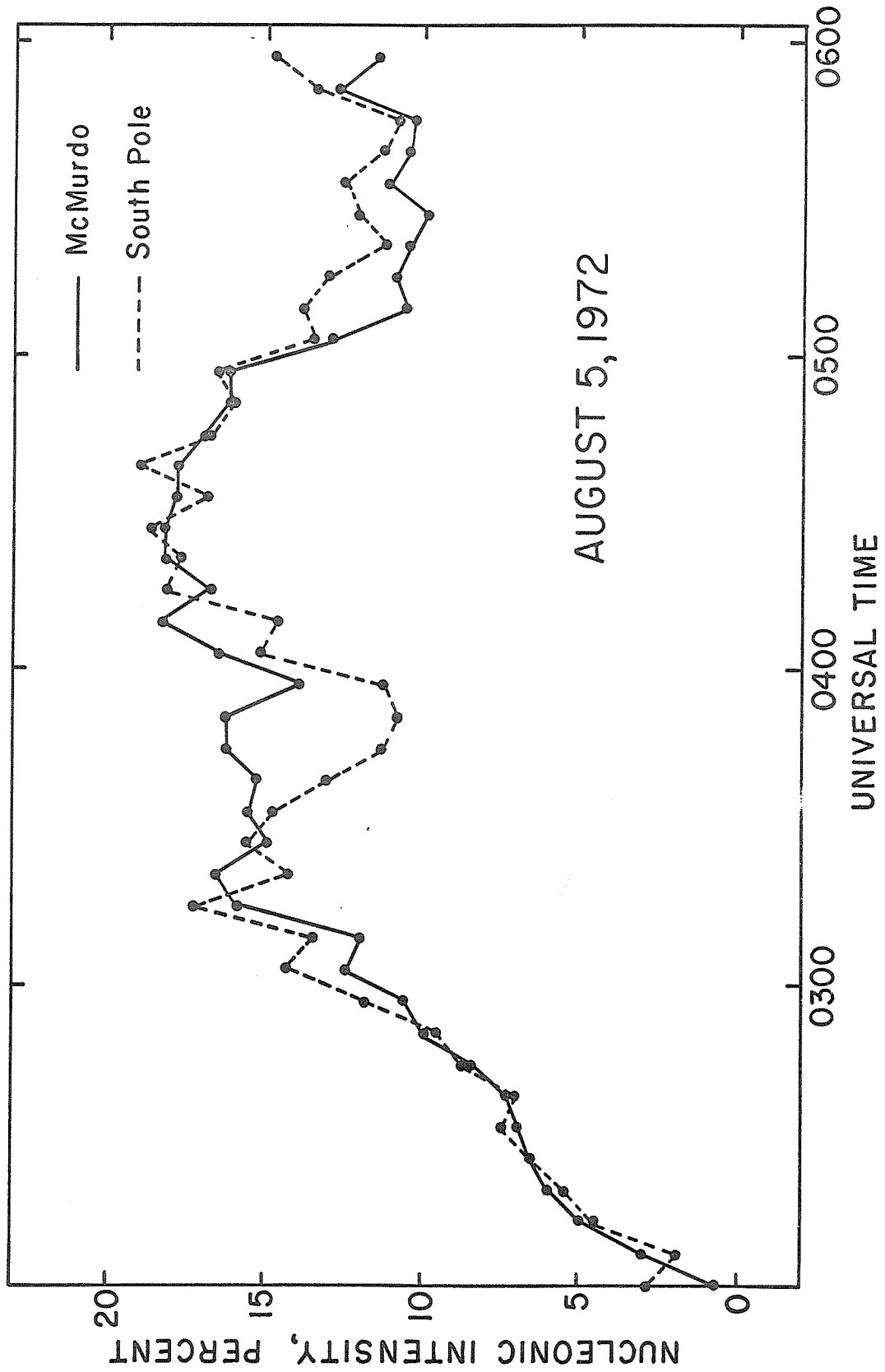


Fig. 8 Plot of the percentage increase (i.e. recovery) in six-minute intervals, from the intensity minimum (0100-0200 UT). The data has been normalized by dividing the South Pole values by 1.65.

Since the rapid recovery and the accompanying small spike were observed at polar stations (e.g. Figure 1) they can not be ascribed to geomagnetic threshold variations, but appear to manifest a discontinuity in the modulation of galactic cosmic rays. Such transient pulse-like structures are not an uncommon feature of cosmic ray storms.

Acknowledgements

We are indebted to Helen Dodson-Prince and Ruth Hedeman for their critical assessment of the vital statistics of the relevant flares, as cited in this paper, on the basis of reports emanating from a wide variety of sources.

This research was sponsored by the National Science Foundation and by the Air Force Cambridge Research Laboratories, Air Force Systems Command, under contract F19628-70-C-0190.

REFERENCES

- | | | |
|---|------|---|
| BAIRD, G. A.,
G. G. BELL,
S. P. DUGGAL and
M. A. POMERANTZ | 1967 | Neutron monitor observations of high-energy solar particles during the new cycle, <u>Solar Phys.</u> , <u>2</u> , 491. |
| DUGGAL, S. P. and
M. A. POMERANTZ | 1972 | Sectorial anisotropy of solar cosmic rays, <u>Solar Phys.</u> , <u>27</u> , 227. |
| GALL, R. | 1968 | Daily variation of the asymptotic directions of cosmic rays, <u>J. Geophys. Res.</u> , <u>73</u> , 4400. |
| MAURER, R. H.,
S. P. DUGGAL and
M. A. POMERANTZ | 1973 | Pitch angle distribution of solar flare particles in interplanetary space, <u>J. Geophys. Res.</u> , <u>78</u> , 29. |
| POMERANTZ, M. A. and
S.P. DUGGAL | 1972 | North-south anisotropies in the cosmic radiation, <u>J. Geophys. Res.</u> , <u>77</u> , 263. |
| POMERANTZ, M. A. and
S. P. DUGGAL | 1973 | Record-breaking cosmic ray storm stemming from solar activity in August 1972, <u>Nature</u> , <u>241</u> , 331. |
| SHEA, M. A. and
D. F. SMART | 1972 | Cosmic ray trajectory calculations for selected high latitude stations appropriate for the solar cosmic ray events in 1971, <u>World Data Center A for Solar-Terrestrial Physic, Report UAG-24</u> , 154. |
| SYROVATSKII, S. I. | 1972 | Solar flare time development: three phases, <u>Comments on Astrophys. and Space Phys.</u> , <u>IV</u> , 65. |
| | 1973 | <u>Solar-Geophysical Data</u> , 342 Part II, February 1973, U. S. Department of Commerce, (Boulder, Colorado, U.S.A. 80302 |

The Rigidity Dependence of Cosmic-Ray Variations
during the August, 1972 Solar Events

by

P.H. Stoker
Department of Physics
Potchefstroom University for C.H.E.
Potchefstroom, South Africa

The rigidity dependence of the cosmic ray variations during the August 1972 solar events may be studied with the South African neutron monitors at Sanae (Antarctica), Hermanus and Potchefstroom, having for 1973 vertical cutoff rigidities of 1.02 GV, 4.69 GV [Shea, 1971] and 7.05 GV [König, 1973] respectively. The data of the equatorial neutron monitor at Huancayo (13.10 GV) was also used to complete the latitudinal coverage in terms of cutoff rigidity. The cones of acceptances of these neutron monitors are in or close to the ecliptic plane. Although the asymptotic directions of the midlatitude neutron monitors at Hermanus and Potchefstroom follow the same line on the celestial sphere, the asymptotic directions of particles of the same rigidity do not coincide and time differences in the arrival of particles may complicate the study of the rigidity dependence of a cosmic ray intensity variation. However, by plotting the relative variation in counting rates of pairs of neutron monitors at different locations, a general picture of both the rigidity dependence and the difference in time of arrival of particles may be obtained.

In Figure 1 the hourly counting rates of these four neutron monitors are plotted as a percentage of the May, 1965 counting rates, for the period from 3 to 10 August, 1972. Three Forbush decreases (FD) and two ground level events (GLE) due to relativistic solar protons are indicated [Pomerantz and Duggal, 1973]. Obviously only the high latitude neutron monitor at Sanae has observed the two GLE's.

The FD-1 started at Sanae about two hours later and at Huancayo about one hour earlier than at Hermanus and Potchefstroom. All four stations have observed simultaneously the predecrease peak, PRE, preceding the FD-2. This predecrease peak is more obvious on plots of ten minute counting rates of the South African neutron monitors.* The FD-3 is not well defined at Sanae or at Huancayo, but is obvious on a plot of ten minute counting rates for the Sanae neutron monitor, indicating a 3 to 4 percent decrease. At Hermanus and Potchefstroom an increase in counting rate rather than a decrease has been observed.

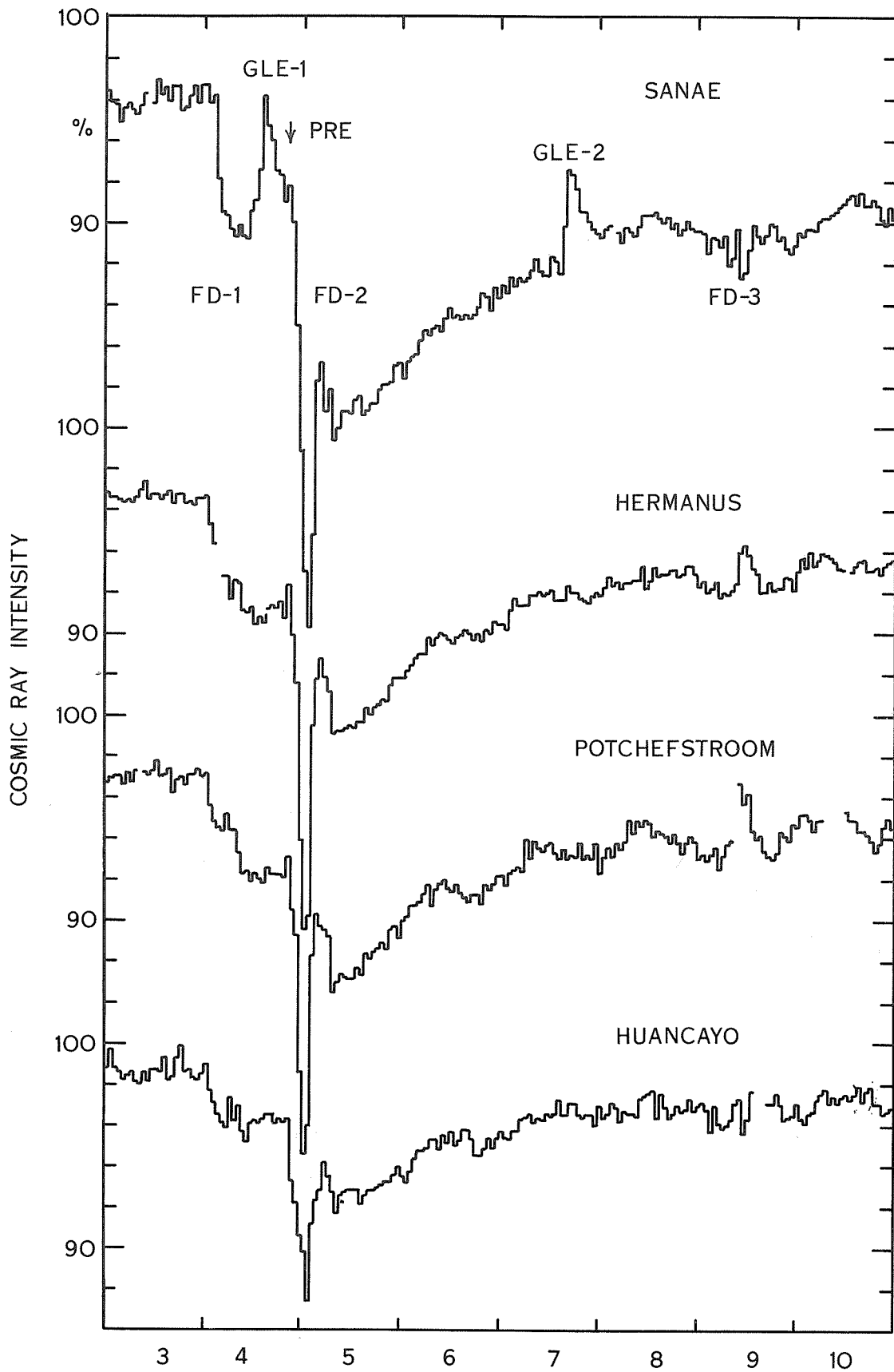
In Figure 2 the normalized daily average counting rates of pairs of these stations are plotted against each other for August, 1972, with the neutron monitor at the lower cutoff rigidity on the ordinate. The broken line represents the calculated relative counting rates for a modulation function proportional to P^{-1} , following Mathews *et al* [1971]. Apart from the contribution of GLE-1 at Sanae to the daily average counting rate on 4 August, the daily average counting rates of each pair of stations follow this modulation function very well.

In Figure 3 the normalized hourly counting rates are plotted for the same pairs of stations as in previous Figure, for the period 3 to 9 August. The later onset of FD-1 at Sanae is obvious from the position of the 0200 and 0300 hourly points of 4 August on the first graph. On this graph the GLE-1 and the effect of the negative going FD-3 at Sanae and positive going FD-3 at Hermanus, are also obvious for the hours 1100-1300 on 9 August. Furthermore, both the decreasing and recovery phases of FD-2 appear to lag behind in time at Sanae relative to Hermanus, from the time of GLE-1 until 0400 on 5 August. A slight time lag around the minimum of FD-2 is also obvious at Huancayo relative to Potchefstroom. Apart from these time differences and the effects of the GLE-1 and FD-3, the intensity variations appear to follow for the FD-1 and for both the decreasing and recovery phases of FD-2 a modulation very nearly proportional to P^{-1} , for primary cosmic rays in the rigidity range from about 2 to well above 13 GV.

REFERENCES

KONIG, P.J.	1973	<u>Private Communication</u>
MATHEWS, T., P.H. STOKER and B.G. WILSON	1971	<u>Planet. Space Sci.</u> , 19, 981
SHEA, M.A.	1971	<u>Conf. Pap. Int. Conf. Cosmic Rays</u> , 12th, 3 (MCD-95), 859
POMERANTZ, M.A. and S.P. DUGGAL	1973	<u>Nature</u> , 241, 331

* Tables of these 10-minute readings August 4-5, 1972 are available from World Data Center A for Solar-Terrestrial Physics.



AUGUST 1972

FIGURE 1

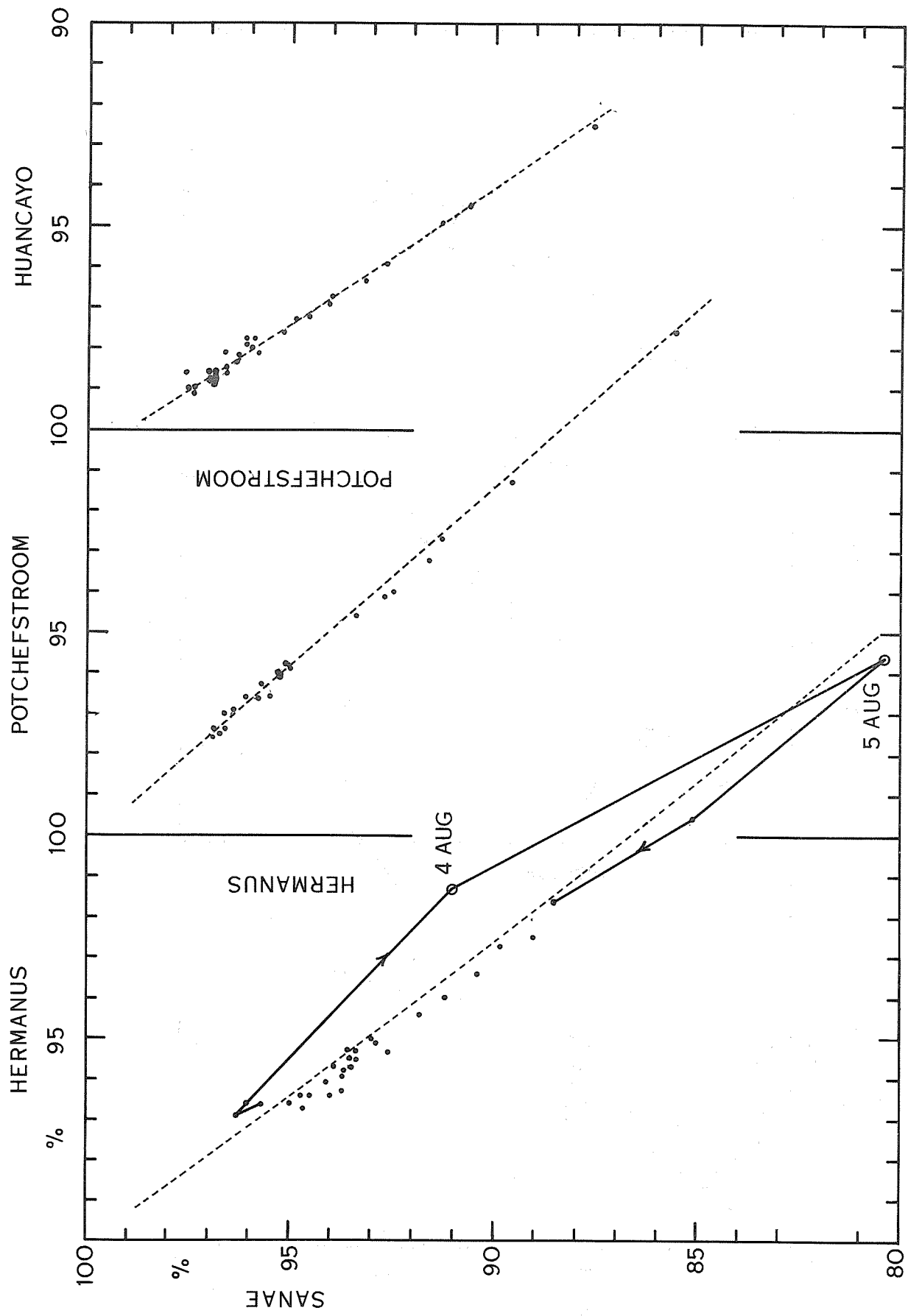


FIGURE 2

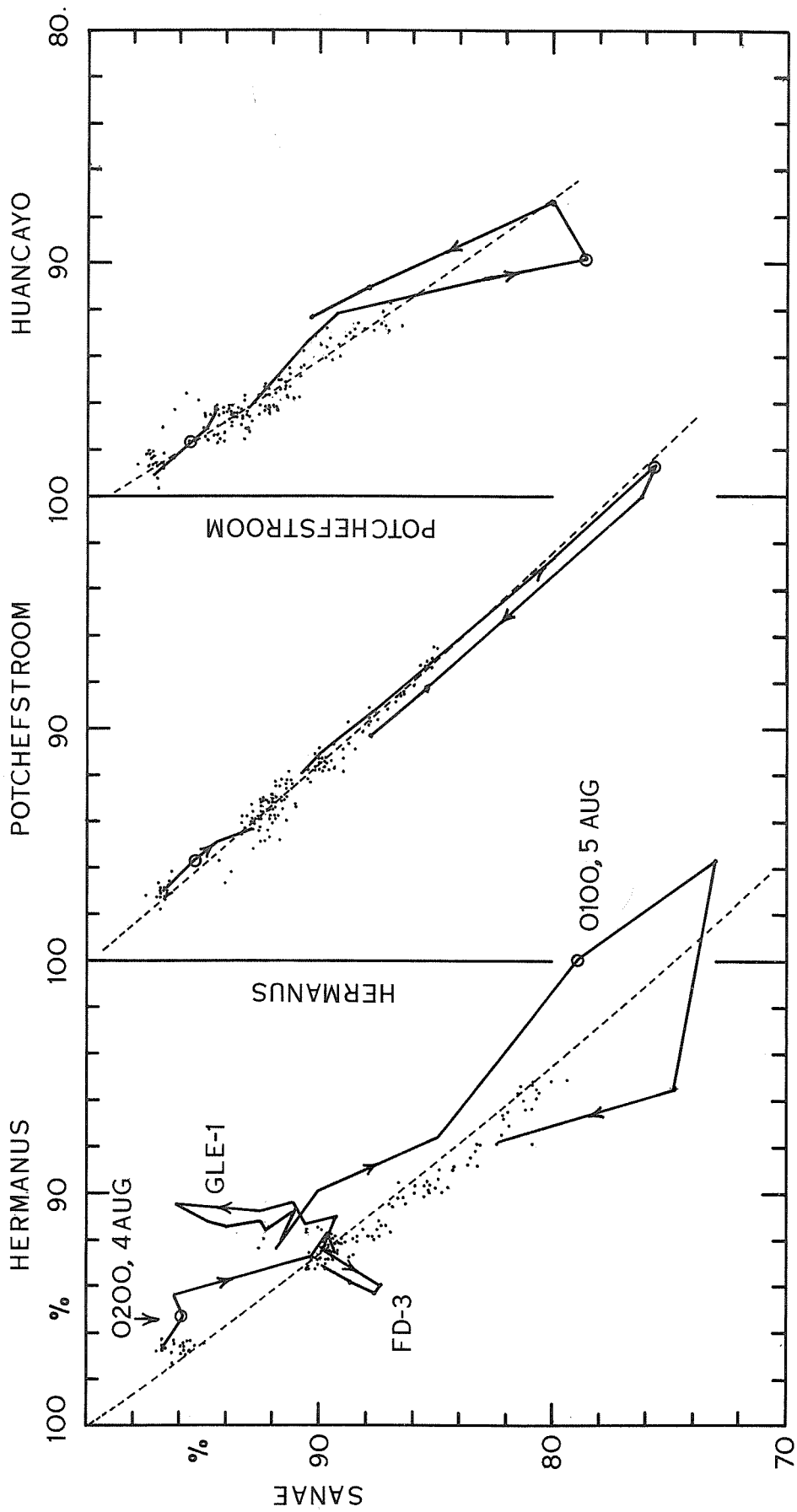


FIGURE 3

Three Dimensional Analysis of Cosmic Rays
during Forbush Decreases of August 1972

by

S. Yoshida* and N. Ogita**

*Geophysical Institute, University of Alaska
College, Alaska 99701

**Institute of Physical and Chemical Research
Yamato-Machi, Saitama, Japan

Introduction

The purpose of this brief note is to report preliminary results of our study on the first two Forbush decreases (FD-1, FD-2) during the August 1972 solar-terrestrial events. Figure 1 shows the ASY index [Kawasaki et al., this compilation] and the cosmic ray record from the South Pole station [Pomerantz and Duggal, 1972].

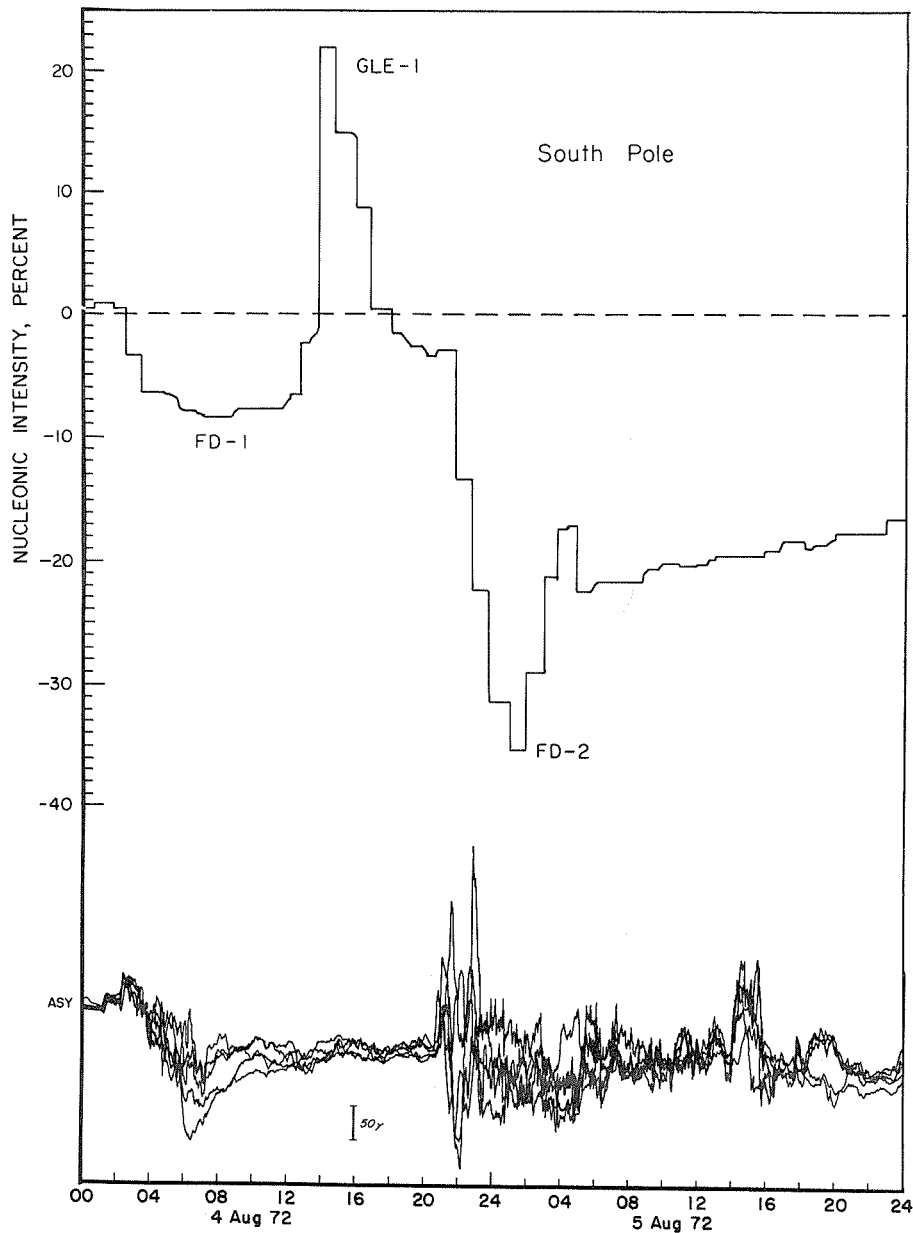


Fig. 1. Nucleonic intensity variations [Pomerantz and Duggal, 1972] and the ASY index [Kawasaki et al., 1973].

Our main interest is to examine how the two Forbush decreases and the associated anisotropy developed in interplanetary space, namely outside the magnetosphere. For this purpose, cosmic ray variations observed by seventeen neutron monitors distributed over the earth are examined by projecting the location of each monitor onto the solar-ecliptic coordinates along the asymptotic direction, corresponding to 9.5 GV particles; for details of the method of analysis, see Yoshida et al. [1971, 1973].

Figure 2 gives iso-variation contours of cosmic rays in interplanetary space. The sun-earth line in this coordinate system crosses the center of the contour maps. The longitude is measured with respect to the sun-earth line, east (positive) longitude being reckoned counter-clockwise and west (negative) longitude clockwise as viewed from the positive z-axis. The contours are obtained by using a computer.

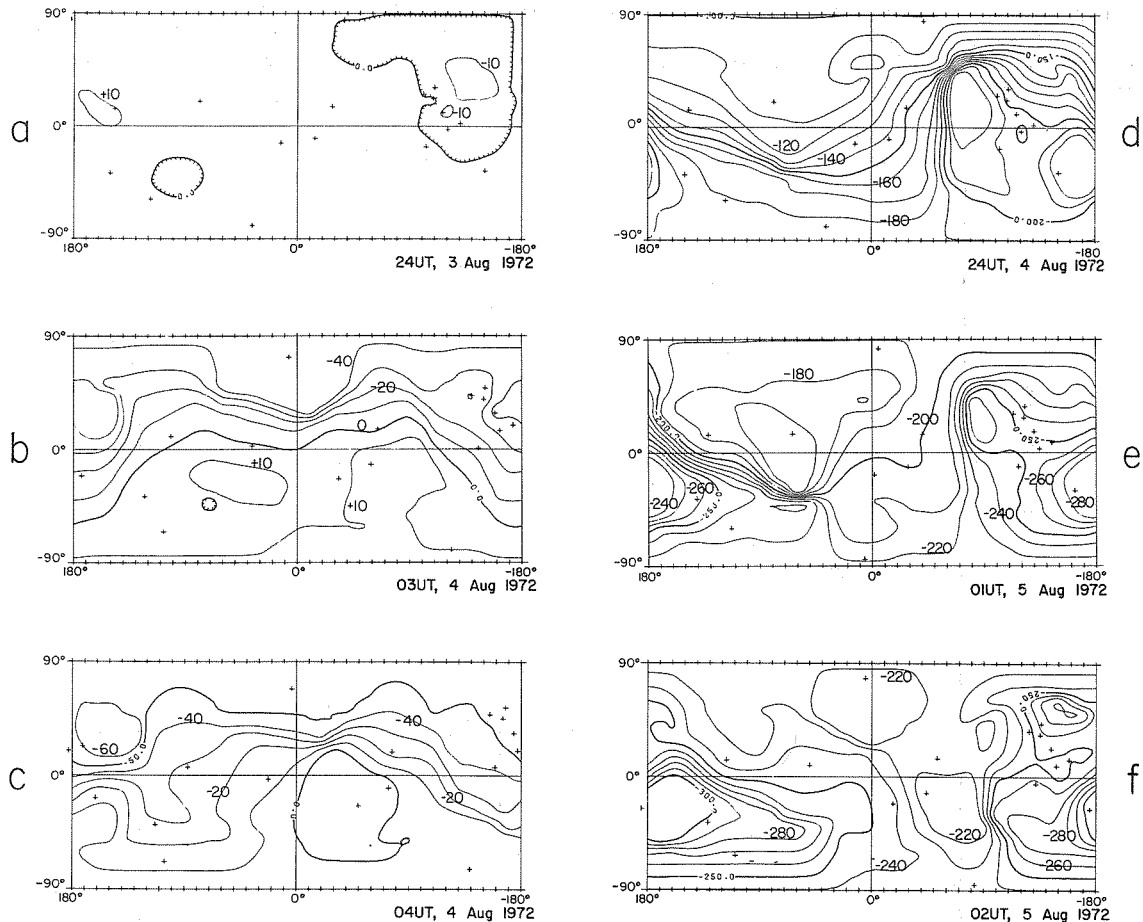


Fig. 2. The iso-variation contour maps during the first two Forbush decreases on the August 1972 solar-terrestrial events.

Before preparing such rectangular contour maps, polar plots are also constructed in order to accurately interpolate cosmic ray variations at the northern and southern poles in solar-ecliptic coordinates [see Yoshida et al., 1973]. The interpolated values thus obtained are included in obtaining the rectangular contour maps.

Figure 2a shows the contour map at 2400 UT on August 3, 1972. It provides the three dimensional anisotropy just prior to the onset of FD-1. Note that values for contour lines are given in units of 0.1%, namely +10=1%, -200 =-20%, etc.

FD-1

The first Forbush decrease began at about the time when the double sudden commencement (0119 and 0220 UT on August 4) occurred. Figures 2b and 2c show the contour maps at 0300 UT and 0400 UT on August 4. Both E-W and N-S anisotropies are clearly seen during the development of FD-1. The maximum depression was about 7%, and the amplitude of E-W anisotropy was 3.3% and that of N-S anisotropy -1.7%. The direction of the maximum flux was located at about +60° longitude and -10° latitude.

A very rapid growth of Forbush decrease began at about the time of storm sudden commencement (2054 UT) of the August 4, 1972 storm. Figures 2d, e and f show the contour maps at 2400 UT on August 4, 0100 and 0200 UT on August 5, respectively. Both E-W and N-S anisotropies grew considerably during the development of FD-2 reaching the maximum amplitude 4.1% for E-W and 4.0% for N-S. These values, together with the maximum depression of Forbush decreases, were the greatest ones ever recorded.

Acknowledgements

The work reported here was supported in part by a grant from the National Aeronautics and Space Administration, NGR-02-001-001 and in part by a grant from the National Science Foundation, Atmospheric Sciences Section, GA-29101 made to the Geophysical Institute, University of Alaska.

REFERENCES

- | | | |
|--|------|---|
| KAWASAKI, K.,
Y. KAMIDE,
F. YASUHARA and
S.-I. AKASOFU | 1973 | Geomagnetic Disturbances of August 4- 9, 1972, elsewhere this compilation. |
| POMERANTZ, M. A. and
S. P. DUGGAL | 1972 | Record-breaking cosmic ray storm stemming from the outstanding solar activity center in August, 1972, <u>Bartol Research Foundation of the Franklin Institute</u> , Preprint. |
| YOSHIDA, S.,
S. -I. AKASOFU,
N. OGITA and
A. OUTI | 1971 | Spherical harmonic analysis of world wide cosmic ray variations during geomagnetic storms, <u>J. Geophys. Res.</u> , <u>76</u> , 1. |
| YOSHIDA, S.,
N. OGITA,
S. -I. AKASOFU and
L. J. GLEESON | 1973 | Variations of three-dimensional anisotropy of cosmic-rays during Forbush decreases, <u>J. Geophys. Res.</u> (in press). |

The August 1972 Cosmic Ray Storm at High Rigidities

by

DEREK B. SWINSON

Department of Physics and Astronomy, The University of New Mexico
Albuquerque, New Mexico 87131

In this communication, observations of the effects of the August 4, 1972 cosmic ray storm by three large multidirectional underground mu-meson telescopes, using plastic scintillators [Regener et al., 1970], are reported. The telescopes are at Mt. Chacaltaya, Bolivia (16.31°S, 68.15°W), Embudo Cave, near Albuquerque, New Mexico (35.20°N, 106.41°W) and at Socorro, New Mexico (34.04°N, 106.56°W). The vertical depths underground are 25 m.w.e. at Bolivia, 40 m.w.e. at Embudo, and 80 m.w.e. at Socorro. The threshold rigidities for these underground telescopes are 17 GV for the Bolivia telescope, 30 GV for the Embudo telescope, and 52 GV for the Socorro telescope [Swinson, 1971]; these threshold rigidities (due to ionization loss in the atmosphere and in the overburden) have been determined according to the method of Ahluwalia and Ericksen [1971]. The counting rates for the three vertical-pointing mu-meson telescopes used here are 400,000 c/hour for the Bolivia and Embudo telescopes and 100,000 c/hour for the Socorro telescope.

In Figure 1 the pressure-corrected cosmic ray intensity recorded between the 3rd and 10th of August 1972 is displayed. Data from the Swarthmore neutron monitor, reproduced from the paper by Pomerantz and Duggal [1973], are compared with the intensities as observed by the three underground telescopes described above. The threshold rigidity for the Swarthmore neutron monitor is 1.9 GV (geomagnetic); the neutron monitor and the three underground telescopes all have asymptotic directions of viewing near the equatorial plane [Pomerantz and Duggal, 1973; Regener and Swinson, 1968].

The significant features of the storm are a Forbush decrease (FD-1) which began at 0130 U.T. on August 4, followed by a second Forbush decrease (FD-2) which began at 2130 U.T., leading quickly to the lowest intensity recorded; during the recovery an importance 3B flare on the sun, starting at 1500 U.T. on August 7, produced a ground level event (GLE) representing the arrival of relativistic solar protons beginning at about 1530 U.T. This was followed by a small Forbush decrease (FD-3) on August 9, after which the intensity gradually returned to the predecrease level [Pomerantz and Duggal, 1973].

The rapid decrease in intensity associated with FD-1 is evident on all three underground telescopes, as is the second decrease FD-2. All three underground telescopes reached their minimum intensity between 0300 and 0500 U.T. on August 5, somewhat later than the sharp minimum observed by the Swarthmore neutron monitor. The total reduction in intensity for the Swarthmore neutron monitor was 23.7% from a relatively constant predecrease intensity on August 3. The predecrease intensity for the three underground telescopes shows rather greater relative variation than is apparent in the case of the neutron monitor; however, taking an average intensity for August 3 as representative of the predecrease intensity the total reduction in intensity for the Bolivia telescope is 4.4%, with about 3% reduction at Embudo and about 1.5% reduction for Socorro. Because of the relatively lower counting rate of the Socorro telescope, and the higher threshold rigidity, FD-1 and FD-2 are less clearly resolved from the background; it seems apparent that the threshold rigidity for the Socorro telescope, 52 GV, is close to the upper limiting rigidity for the storm.

The ground level event (GLE) which was observed by the Swarthmore neutron monitor on August 7 is also evident, although to a lesser extent, at the Bolivia telescope; it is, however, indistinguishable from the statistical fluctuations in the intensity observed at Embudo and Socorro. The third Forbush decrease, FD-3, is quite evident at Bolivia and Embudo, and to a slight extent also at Socorro.

From these observations it is possible to assign an upper limiting rigidity of 60 to 65 GV to the cosmic rays affected by this remarkable storm, and an upper limiting rigidity of 20 to 25 GV to the solar protons contributing to the GLE on August 7 resulting from the importance 3B solar flare.

ACKNOWLEDGEMENTS

I am indebted to M. A. Pomerantz and S. P. Duggal for providing a preprint of their results. The work was supported by the Atmospheric Sciences Section, National Science Foundation, under grant GA-30591.

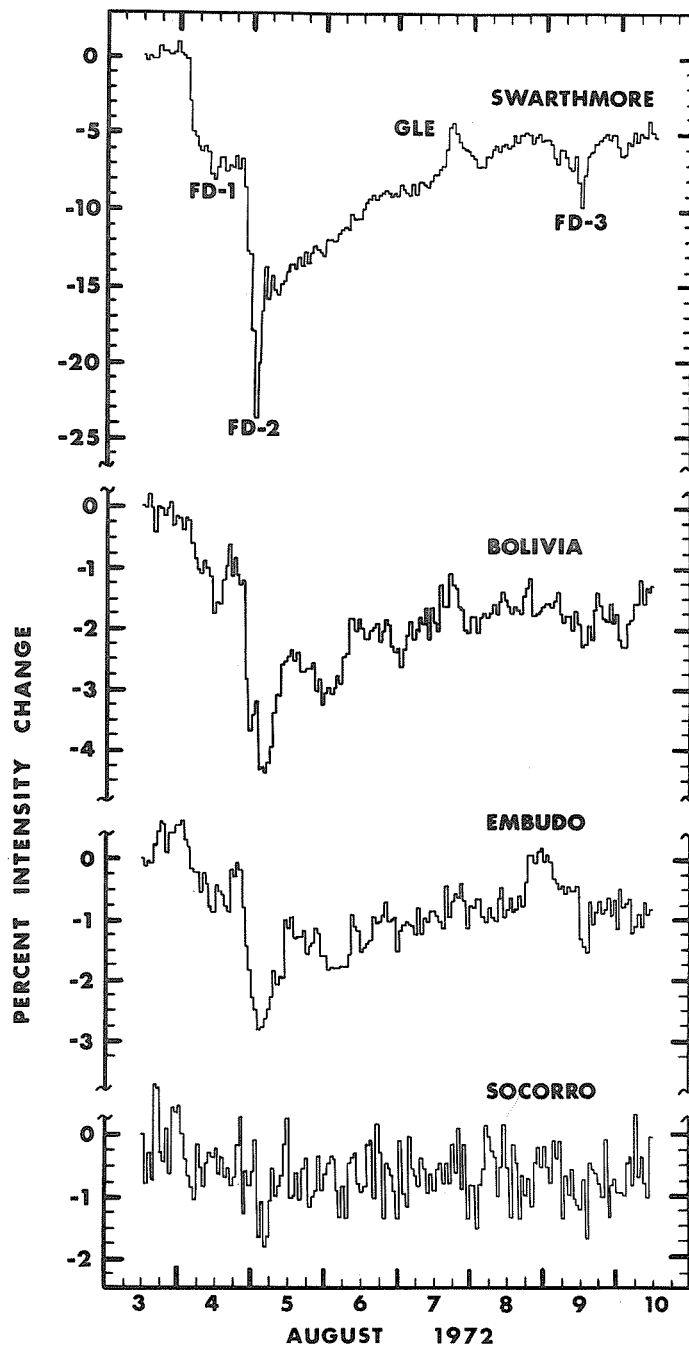


Fig. 1. The pressure-corrected cosmic ray intensity in Universal Time for the Swarthmore neutron monitor, and the Bolivia, Embudo and Socorro underground mu-meson telescopes.

REFERENCES

- | | | |
|---|------|---|
| AHLUWALIA, H. S. and
J. H. ERICKSEN | 1971 | Coupling functions applicable to the underground meson telescopes, <i>J. Geophys. Res.</i> , 76 , 6613. |
| POMERANTZ, M. A. and
S. P. DUGGAL | 1973 | Record-breaking cosmic ray storm stemming from solar activity in August 1972, <i>Nature</i> , 241 , 331. |
| REGENER, V. H. and
D. B. SWINSON | 1968 | Variation with solar cycle of the diurnal variation of cosmic rays underground, <i>Can. J. Phys.</i> , 46 , S784. |
| REGENER, V. H., D. B.
SWINSON, J. H. ERICKSEN
and H. S. AHLUWALIA | 1970 | The solar diurnal variation of cosmic rays underground since 1958, <i>Acta Phys. Acad. Sci. Hungaricae</i> , 29 , Suppl. 2, 133. |
| SWINSON, D. B. | 1971 | Solar modulation origin of 'sidereal' cosmic ray anisotropies, <i>J. Geophys. Res.</i> , 76 , 4217. |

Energy-Dependent Phenomena of Muons and Nucleons in August 1972

by

Robert L. Chasson
Department of Physics and Astronomy
University of Denver
Denver, Colorado 80210

ABSTRACT

- (1) The maximum primary rigidity of solar flare particles detected at earth on 7 August 1972 lay between 3 and 10 GV.
- (2) A daily wave with maximum at 1300 hours Local Time prevailed for particles of rigidity between 10 and 50 GV during the Forbush decrease recovery period 5-8 August 1972.

Introduction

A global picture is beginning to emerge of the interplanetary field and particle situation responding to the solar disturbances of August 1972. In this development of understanding it is evident that ground-based cosmic ray observations remain the only means by which propagation and modulation of extremely high energy particles may be studied. From the data available it is apparent that there are serious gaps in global coverage by muon monitors, particularly as one wishes to achieve more precise spectral and demographic information about the particles affected by such disturbances. There is potentially a great deal to be learned about off-ecliptic propagation of solar plasma and its entrained magnetic fields by studying storm-time effects on the muon progeny of galactic primaries; such particles reflect primary populations with median rigidities several times larger than those responsible for nucleonic recordings, and they are, therefore, the only existing realistic probes of modulation conditions lying some tenths of an AU off the ecliptic plane.

In this paper we shall refer to various features of the August 1972 events by using the notation of Pomerantz and Duggal [1973]. We propose to establish two particular points; namely (1) the maximum primary rigidity of the solar flare particles detected at earth during GLE-2 on 7 August lay between 3 and 10 GV, and (2) for at least four days following the Forbush decrease event FD-2 on 5 August an interplanetary process prevailed which caused a daily variation in the primary galactic radiation lying in the approximate rigidity range from 10 to 50 GV and with a direction of maximum at approximately 1300 LT.

Solar Cosmic Rays (GLE-2) of 7 August 1972

Examination of Table 1 will reveal that GLE-2 was evident at all neutron monitor stations up to the geomagnetic cut-off of 2.9 GV (Denver) but not above this value. None of the muon detectors (with cut-offs ranging from atmospheric to 52 GV) showed the increase. Thus we infer that the upper limiting rigidity of the solar flare particles detected as GLE-2 lay between 3 and 10 GV; this conclusion is sustained by the lack of a flare spike at higher cut-off neutron monitor stations such as Rome, Brisbane, and Buenos Aires, with uncertainty of the absolute upper limit being imposed by anisotropy of the short-lived particle injection as seen at earth.

This upper limit is considerably smaller than that of Swinson [1973], where he placed the value at 20-25 GV. His estimate was entirely reasonable, however, in light of the data then available to him. We wish to emphasize the importance of more precisely setting the upper limit, which is of crucial importance if a satisfactory model of the solar flare particle emission process is to be devised, taking into account all known solar surface data and knowledge of the time sequence of changing magnetic fields and chromospheric structures.

Post FD-2 Daily Wave

It is quite evident from Figure 1 that on Days 218-221 (5-8 August) a pronounced daily wave (amplitude approx. 0.7%) was observed for the Denver muons but not for the nucleonic component; this wave is superimposed upon the recovery from the Forbush decrease of early 5 August and terminated upon the occurrence of FD-3 on 9 August. There was some skepticism about the reality of this high energy modulation phenomenon when it was first reported [Chasson et al., 1972], but substantiating data have since become available, which are summarized in Table 1. (Application of available Denver upper-air data in an attempt to make a finer correction of the muon data did not yield any sensible change of the simple pressure-corrected trace shown in Figure 1).

The wave is absent for all neutron monitors except for those with cut-offs above 10 GV, and it is present for those meson telescopes which are sensitive to the progeny of primaries somewhat above 10 GV. Table 2 is a distillation of the data, which also contains evidence that the interplanetary mechanism responsible for the daily variation may lie close to the ecliptic. There is no way of

Table 1

Evidence of GLE-2 and post FD-2 daily wave from various stations in approximate ascending order of effective minimum rigidity observable by each detector.

Station	P_c (GV)/alt.	Detector/ Effective Cutoff	GLE-2 evident?	Post FD-2 daily wave evident?	Reference
Thule	0. 0/s. 1.	NM/atm	yes	no	8
McMurdo	0. 0/s. 1.	NM/atm	yes	no	8
Gen. Belgrano	0. 8/s. 1.	NM/atm	yes	no	3
Oulu	0. 8/s. 1.	NM/atm	yes	no	2
Calgary	1. 1/1128 m.	NM/atm	yes	no	7
Sulfur Mtn.	1. 1/2283 m.	NM/atm	yes	no	7
Mt. Wellington	1. 9/725 m.	NM/atm	yes	no	2
Hobart	1. 9/s. 1.	MT/atm	no	no	2
Swarthmore	1. 9/s. 1.	NM/atm	yes	no	8
Kiel	2. 3/s. 1.	NM/2. 3GV	yes	no	2
London *	2. 7/s. 1.	MT/2. 7	no	no	2
Denver	2. 9/1600 m.	NM/2. 9	yes	no	1
Denver	2. 9/1600 m.	MT/2. 9	no	yes	1
Rome	6. 3/s. 1.	NM/6. 3	no	no	2
Brisbane	7. 2/s. 1.	NM/7. 2	no	uncertain	2
Buenos Aires	10. 6/s. 1.	NM/10. 6	no	yes	3
Tokyo	11. 4/s. 1.	NM/11. 4	no	yes	6
Mt. Norikura	11. 4/2770 m.	NM/11. 4	no	uncertain	6
Chacaltaya **	13. 1/5220 m.	MT/17	no	yes	9
Embudo **	4. 4/2622 m.	MT/30	no	uncertain	9
Socorro **	4. 7/1677 m.	MT/52	no	no	9

* N and S inclined pair

** Underground

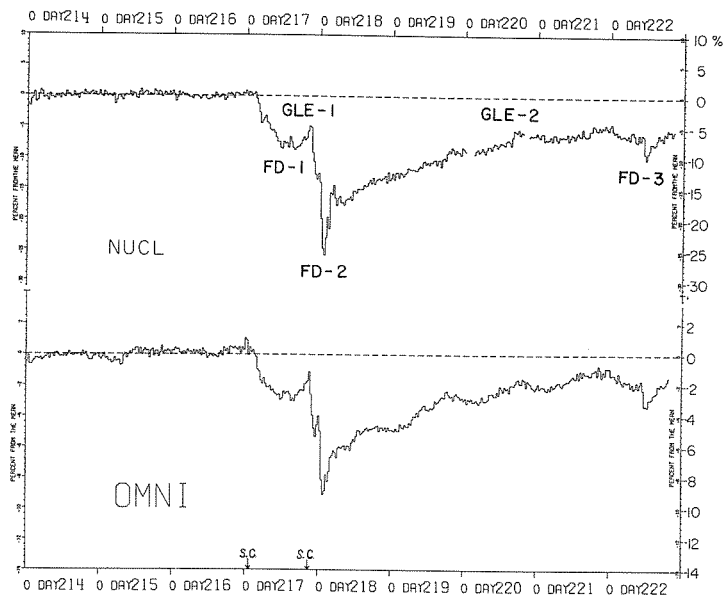


Fig. 1

Nucleonic and omnidirectional muon variations at Denver 1-9 August 1972. (Day 214 is 1 August.) Local time of maximum of the post FD-2 daily wave in muons is ~ 1800 UT. Direction of maximum is ~ 1300 LT for 35 GeV particles. Data are corrected for pressure.

Table 2

Data from selected stations delineating the post FD-2 daily wave according to asymptotic latitude of arrival of 35 GV primaries and corresponding direction of the maximum of the wave (*Data for Socorro and Embudo are estimated from curves for Sacramento Peak [Hatton and Carswell, 1963]. The Socorro asymptotic latitude value is for 55 GV).

Station	Detector/ Effective cutoff	Asymp. lat. for 35 GV	Post FD-2 daily wave evident?	Local time of max. (± 1 hr.)	Direction of max. (local time)
London	MT/2.7 GV	40 ⁰	no		
Rome	NM/6.3	28	no		
Socorro	MT/52	22*	no		
Denver	NM/2.9	21	no		
Denver	MT/2.9	21	yes	1100	1300
Mt. Norikura	NM/11.4	16	uncertain		
Tokyo	NM/11.4	15	yes	1100	1400
Embudo	MT/30	12 *	uncertain		
Chacaltaya	MT/17	-11	yes	1000	1300
Brisbane	NM/7.2	-15	uncertain		
Buenos Aires	NM/10.6	-21	yes	1000	1300
Hobart	NM/atm	-33	no		

concluding, however, that either asymptotic latitude or rigidity dominate in producing the observed order of the results. Further, for the four stations which more clearly show the wave, the direction in space of the maximum lies very close to 1300 LT (using Hatton and Carswell [1963] for 35 GV particles, a "representative" value for primaries yielding counts at these stations). Since the wave was clearly not seen in the Socorro trace (52 GV effective cut-off; see Swinson [1973]), we conclude that the effect was restricted to primaries in the 10-50 GV rigidity range, another example of modulation not experienced by the low-energy primary population (Gold *et al.* [1973], the Forbush predecrease).

Discussion

Pomerantz and Duggal [1973] have indicated that a north-south anisotropy prevailed during the period following FD-2, with the flux from the north being modulated less than that from the south (see also Dutt *et al.* [1972]). This condition implies a gradient of intensity from north to south, perpendicular to the ecliptic, and if one considers such a gradient in terms of the direction of a possible prevailing interplanetary magnetic field sector, one finds a diurnal maximum slightly to the east of the earth-sun line if the field is directed toward the sun. "Snapshot" data of the field direction for the period recorded aboard Pioneer 9 [Sonnnett and Colburn, 1972] show such a dominant field orientation, although the evidence is not conclusive in view of the disturbed nature of the interplanetary magnetic field regime during the period under examination. We therefore defer further remarks on this matter until more definitive information becomes available about the prevailing sector configuration. Additional quantitative studies are in progress regarding the spectral response of the post FD-2 daily wave.

Acknowledgements

This work was performed under National Science Foundation Grant No. 26528. The author is indebted to Professor Dennis S. Peacock for important discussions and George Crabbe for much help in data acquisition and reduction.

REFERENCES

- | | | |
|--|------|---|
| CHASSON, R. L.,
D. S. PEACOCK, and
R. E. GOLD | 1972 | EOS, Trans. Amer. Geophys. U., <u>53</u> , 1054. |
| DUTT, J. C.,
J. E. HUMBLE, and
T. THAMBYAHPILLAI | 1972 | Preprint. |
| GHIELMETTI, H.,
et al. | 1972 | Private correspondence. |
| GOLD, R. E., and
D. S. PEACOCK | 1973 | <u>J. Geophys. Res.</u> , <u>78</u> , 577. |
| HATTON, C. J., and
D. A. CARSWELL | 1963 | AECL-1824, Chalk River, August 1963. |
| MIYAZAKI, Y. | 1972 | Private correspondence. |
| POMERANTZ, M. A.,
and S. P. DUGGAL | 1973 | <u>Nature</u> , <u>241</u> , 331. |
| SONNETT, C. P., and
D. S. COLBURN | 1972 | Preliminary Compilation of Data for Retrospective World Interval July 26 - August 14, 1972, <u>World Data Center A for Solar-Terrestrial Physics, Report UAG-21</u> , 51. |
| SWINSON, D. B. | 1973 | <u>J. Geophys. Res.</u> , <u>78</u> , 1707. |

The Event of August 1972 Studied with Cosmic Rays at Magnetic Cut-off Rigidity of 8.72 GV

by

A. Apostolakis, H. Mavromichalaki and X. Moussas
University of Athens
Nuclear Physics Laboratory
104, Solonos Street (Chimion)
Athens 144-Greece

As in many other neutron monitor stations, a Forbush decrease starting on August 4, 1972 was also observed by the Athens 3-NM-64 station (at the cut-off rigidity of 8.72 GV). The maximum of the depression was 13.8% and occurred at 0100 UT August 5.

The event had some very characteristic features. Even at Athens with relatively high cut-off rigidity the depression was deep and lasted about five hours. It was followed by a relative increase in the intensity but again decreased, recovering normally after a few days.

To understand the structure of this event the relation between the neutron intensities measured at ground level and observations of the Solar Cosmic Radiation (SCR) measured by Pioneer IX was studied.

At the time of the event, Pioneer IX was at a radial distance of ~ 0.78 AU from the Sun and the Earth-Sun-probe (Pioneer IX) angle was $\sim 45^\circ$. SCR intensities with energies $E > 13.9$ Mev and solar wind velocities were measured.

Many authors [e.g., Charakhchyan, et al., 1961; Bryant, et al., 1962; Krimigis and Van Allen, 1966; Vernov, et al., 1972] have examined the influence of the SCR measured on satellites to the Galactic Cosmic Radiation (GCR) measured at satellites or ground level. In the present work, the satellite measurements were developed in time and space dynamically in order to map the SCR intensities vs. time. To simplify calculations the following assumptions were made:

1. The solar wind produced by three solar flares was azimuthally isotropic in the interplanetary space within the 45° angle defined by the Earth-Sun-probe positions.
2. The solar wind velocity was about the same in the region of the satellite and Earth.

The empirical relation of Vernov [1970] and the theoretical predictions of Parker [1963] for the variation of the solar wind velocity with the solar distance, were not used in these preliminary calculations.

The variation of the density, n_i , of the SCR of constant velocity, V_i , was found assuming the relationship:

$$n_i V_i r_i^2 = \text{constant}$$

where r_i is the distance from the Sun [e.g., Dessler, 1959]. This relation is valid when very little diffusion and loss of solar particles occur.

In Figure 1C are shown the estimated SCR intensities $P(r,t)$, as a function of r , measured in AU, and at time intervals of about 4 hours. The published SCR intensities in Lincoln, et al., [1972] were used for these. These intensities are given for time intervals ranging from 1.5 to 6.5 hours, which unfortunately introduces large uncertainties in evaluating exact profiles of the events. In Figure 1C there are shown 61 intensity curves in all, covering the time from 0000 UT, August 1 to 1900 UT, August 10. Due to the saturation of the counting system of Pioneer IX the maximum counting rate was 16380 particles/sec. This is indicated in the graph with a heavy, wavy line. It is noted that due to the different velocities of the solar plasma, shock waves of short time duration were formed near the Earth, particularly at midnight on August 4. The increased SCR intensity at the time of observation at the satellite was about 16 hours, whereas at the distance of the Earth the width of the shock wave was estimated to be about 8 hours. Because of this, the profile of this wave is known more accurately. The position of the Earth is shown in Figure 1C, indicated with the dashed line at 1 AU.

For direct comparison, the neutron counting rates of 8 stations of different cut-off rigidities, covering the range of 8.72 to 1.02 GV are shown in Figure 1B. In Figure 1A are shown the following:

- (a) the K_p index of the magnetic field, and
- (b) the SCR INTENSITY, $P(1,t)$, at the position of the Earth.

It is easily seen that there is a correlation between the observed Forbush decrease and $P(1,t)$ in amplitude but not in time. There seems to be a time difference between the estimated time of arrival of the shock waves and the observed Forbush decreases. This time difference is about 6 hours

and could be due to assumptions 1 and 2. It is very difficult without more data from other satellites to determine the predominate source of this time delay. The correlation of $P(1,t)$ advanced by ~ 6 hours and the ground level GCR intensities is rather good.

The small Forbush decreases of 0200 UT and 1200 UT on August 4 were related to the increased SCR intensity. The deepest Forbush decrease started at 2200 UT August 4 and lasted until 0300 UT August 5. The estimated (SCR) shock wave shows a very large increase between 0130 UT and 0930 UT of August 5, the amplitude of which, as has already been pointed out, is not known because of the saturation of the satellite counting system*.

T A B L E

STATION:	ATHENS	POTCHEFSTROOM	ROME	HERMANUS	UTRECHT	KIEL	LEEDS	SANAE
Geographic Latitude	38.00	-26.70	41.90	-34.42	52.06	54.33	53.82	-70.46
Longitude	24.73	27.10	12.52	19.22	5.07	10.13	358.45	357.51
CUT-OFF RIGIDITY (GV)	8.72	7.30	6.32	4.90	2.76	2.29	2.20	1.02
Date Time Aug. UT	DECREASE %							
4 0200	1.66	2.76	3.59	4.14	5.53	5.66	5.94	5.80
4 1200	3.73	5.53	5.25	6.77	8.29	8.29	8.15	
4 1500								0.00
4 2100	4.01	4.42	5.39	4.56	7.18	6.90	7.05	4.42
5 0100	<u>13.82</u>	<u>19.43</u>	<u>17.56</u>	<u>22.24</u>	<u>25.56</u>	<u>25.84</u>	<u>25.15</u>	<u>24.18</u>
5 0200	<u>12.71</u>	<u>17.96</u>	<u>16.30</u>	<u>21.42</u>	<u>24.18</u>	<u>24.73</u>	<u>25.15</u>	<u>26.94</u>
5 0400-0700	5.25	8.01	7.32	9.53	11.47	10.91	12.02	13.40
5 0800	8.29	10.50	10.50	13.26	14.92	15.06	15.47	17.27
ERROR	± 0.5	± 0.3	± 0.3	± 0.5	± 0.2	± 0.2	± 0.2	± 0.5

The relative increase in the flux observed at all stations (between 0400 UT and 0800 UT, August 5) following the main Forbush decrease coincides with an estimated decrease of SCR intensity. The Forbush decrease starting at 0800 UT occurs at about the time the second shock wave is at the distance of the Earth (taking into account the 6 hours difference). The estimated SCR intensity, $P(1,t)$, has almost gone to zero at about August 9. The GCR intensity, however, recovers much more slowly and approaches to normal values at about August 17. The traveling shock waves are expanding, constituting a long (0.7 ± 0.1) AU wave with rapidly diminishing intensity. This long wave is effecting the GCR intensity even when it is at a radial distance of (6.7 ± 0.5) AU. With the present data, it is very difficult to estimate this effect quantitatively by using Parker's theory. It is hoped that with more data from other satellites, it will be possible to estimate the spatial distribution of the SCR intensity and its traveling velocity more accurately. This work is in progress.

The authors would like to thank Prof. N. Iucci, Dr. B. O. Binder, Dr. L. D. de Feiter, Dr. C. J. Hatton and Dr. H. Moraal for the neutron monitor data of the Rome, Kiel, Utrecht, Leeds and Potchefstroom, Sanae and Hermanus. This work was supported by a NATO grant No. 489.

NOTE * The profile of Forbush decrease changes with the cut-off rigidity of the observing station. In particular the minimum of the GCR intensity shifts to later time as the cut-off rigidity of the station decreases. This could be due to an overspill of the observed increase of SCR of the large Importance 3B flare (N15, E09) which started at 0621 UT with maximum at 0638 UT and ends at 0852 UT.

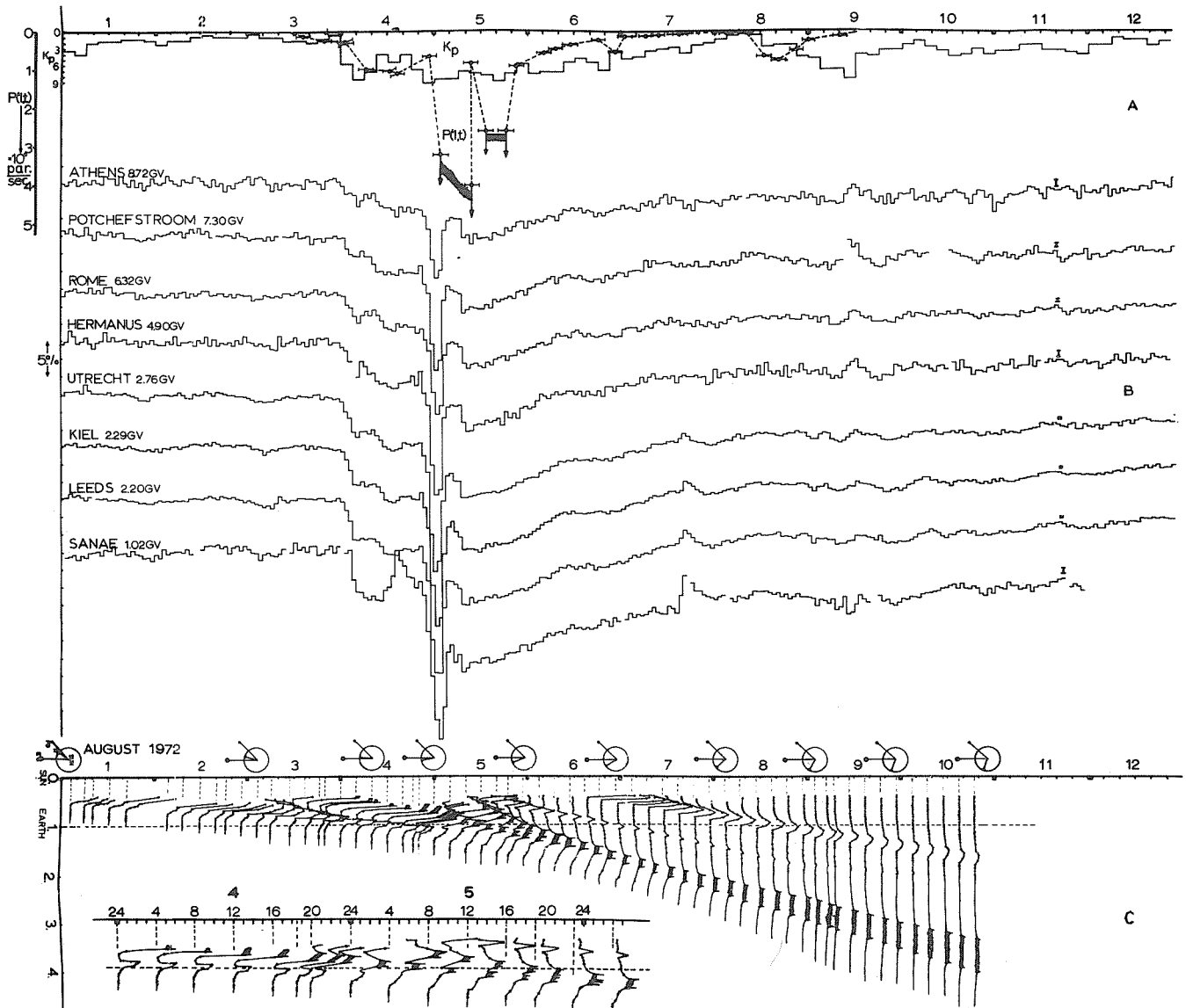


Fig. 1Aa. Estimated intensity of Solar Cosmic Rays (SCR), at the position of the Earth $P(1,t)$, derived from measurements of solar particles, with energy $E > 13.9$ Mev, made with Pioneer IX.
 1Ab. The K_p magnetic index.
 1B. The neutron monitor counting rates of 8 different stations, in increasing cut-off rigidities.
 1Ca. Estimated intensity curves of SCR at different time. The position of the Earth, $r=1$ AU, is indicated with a dashed line.
 1Cb. Along the time axis the relative positions of the Sun, Earth, Pioneer IX and the active region (McMath No. 11976) in the Solar equator are also shown.
 1Cc. The same as Ca during August 4 and 5, 1972 on an expanded time scale.

REFERENCES

- BRYANT, D. A., 1962
T. L. CLINE,
U. D. DESAI and
F. B. McDONALD
Explorer 12 observations of solar cosmic rays and energetic storm particles after the solar flare of September 28, 1961, J. Geophys. Res., 67, 4983.
- CHARAKHCH'YAN, A. N., 1961
V. F. TULINOV and
T. N. CHARAKHCH'YAN
Energy spectrum and time dependence of the intensity of solar cosmic ray protons, Zh.E.T.F., 41, 735, or Soviet Physics JETP, 13, 530 (1962).
- DESSLER, A. J. 1969
General applicability of solar wind and solar breeze theories, Comments on Astrophysics and Space Physics, 1, 31.
- KRIMIGIS, S. M. and 1966
J. A. VAN ALLEN
Observation of 500 keV protons in interplanetary space with Mariner IV, Phys. Rev. Letters, 16, 419.
- LINCOLN, J. V. and 1972
H. I. LEIGHTON
Preliminary Compilation of Data for Retrospective World Interval July 26 - August 14, 1972, World Data Center A for Solar-Terrestrial Physics, Report UAG-21, November 1972.
- PARKER, E. N 1963
Interplanetary dynamical processes, Interscience, New York.
- SHEA, M. A., 1968
D. F. SMART,
K. G. McCracken and
U. R. RAO
Supplement to IQSY instruction manual No. 10 cosmic ray tables, asymptotic directions, variational coefficients and cut-off rigidities, AFCRL-68-0030, SPECIAL REPORTS, No. 71.
- VERNOV, S. N. 1968
E. N. GORTCHAKOV,
YU. I. LOGATCHOV,
G. P. LYUBIMOV,
N. Y. PERESLEGINA,
B. A. TVERSKOY and
A. E. CHUDAKOV
Energetic solar particle propagation and the structure of interplanetary space, Can. J. of Phys., 46, S812.
- VERNOV, S. N., 1970
P. N. CHUDAKOV,
P. V. VAKULOV,
E. V. GORCHAKOV,
N. N. KONTOR,
YU. I. LOGACHEF,
G. P. LYUBIMOV,
N. V. PERESLEGINA and
G. A. TIMOFEEF
Propagation of solar and galactic cosmic rays of low energies in the interplanetary medium. ACTA PHYSICA, ACADEMIAE SCIENTIARUM HUNGARICAE, Suppl. 29, 459.
- VERNOV, S. N and 1972
G. P. LYUBIMOV
Low energy cosmic rays in interplanetary space, Dyer (ed), Solar terrestrial physics, 1970, part II, 92, D. Reidel Publishing Co., Dordrecht, Holland.

A Comparison of Recordings of the Forbush Effect
of the 4th August 1972
by Several Terrestrial Cosmic Ray Monitors

by

V. J. Kisselbach
Max-Planck-Institut für Aeronomie
Institut für Stratosphärenphysik
3411 Lindau/Harz, Germany

The Max-Planck-Institut für Stratosphere Physics at Lindau (N51.6, E10.1, 3.25 GV/c threshold rigidity) operates an 18-NM-64 Superneutron monitor, a meson coincidence device which responds to vertically incident mesons with a half angle of 45° , an oblique meson coincidence device inclined 15° south of the local zenith, and has access to the recordings of a 3-NM-64 superneutron monitor located on the Hafelekar at Innsbruck, Austria. The latter device was originally installed by this Institute.

The vertical meson device is located under the 18-NM-64 monitor and is thus shielded by an average of 13.7 cm Pb. The inclined telescope does not have an absorber and thus responds to both the classical soft as well as the hard component.

All devices were operating during the August 4, 1972 event.

Figure 1 shows a synoptic representation of the recordings of these instruments during the interval August 2 to 10, 1972. The data have been corrected for atmospheric pressure variations according to standard regression - correlation methods. No temperature variation corrections have been applied to the meson recordings since the size of the appropriate effects are roughly an order of magnitude smaller than the amplitude of the variations recorded during the interval.

The effect sets in at 0000 UT on August 4 for the neutron monitor and shielded meson devices. In the case of the unshielded meson device the onset time is about 10 hrs earlier, i.e. at 1400 UT on August 3. Apparently, the softer radiation causing the response of the unshielded device is affected by the primary agency causing the effect earlier than the harder components. In all registrations a slight increase in the intensity beginning at about 0500 UT on August 3 can be seen (pre-storm increase).

On the assumption that this pre-increase is an integral part of the overall effect, it follows that the actual onset time of the effect is about 0500 UT on August 3.

In attempting to describe the quantitative morphology of the effect one can speak of a first minimum at 0400 to 0500 UT on August 4. The respective amplitudes of this first minimum are

Lindau Neutrons	4.5%
Lindau Inclined Mesons	5.5%
Hafelekar Neutrons	5.0%
Lindau Shielded Mesons	2.8%

A second minimum in the neutron registrations occurs at about 1100 UT on August 4. Here the amplitudes of the Lindau and Hafelekar Neutrons are virtually identical, 7.2% and 7.3% respectively.

For the main maxima on August 5 at 0100 UT we have

Lindau Neutrons	24%
Lindau Inclined Mesons	12%
Hafelekar Neutrons	21.8%
Lindau Shielded Mesons	9.5%

The errors due to counting statistics for the respective devices are

Lindau Neutrons	$\pm 0.15\%$
Lindau Inclined Mesons	$\pm 0.28\%$
Hafelekar Neutrons	$\pm 0.17\%$
Lindau Shielded Mesons	$\pm 0.22\%$

During the recovery phase of the effect the pronounced diurnal variation on August 6 and 7 may be pointed out. There is further evidence of enhanced diurnal variation activity on August 9 and 10.

In particular, the Hafelekar neutrons show an increase setting in at 1000 UT on August 9.

Summarizing, the recordings of ground-based cosmic ray detectors operated by our institute during the August 4, 1972 event indicate that the event was, in the main, a typical Forbush type event, with a monotonic variation of the event amplitudes as a function of monitor rigidity response. An onset deviation is, however, apparent in the soft meson recordings. This deviation may be resolved if one places the true onset of the event at 0500 UT on August 3. The asymmetry of the recordings at 0000 UT on August 4, the presence of minima in the neutron recordings not evident in the meson registrations, and the high-altitude increase appearing only in the Hafelekar neutrons would seem to indicate that the primary modulation mechanism is not wholly isotropic.

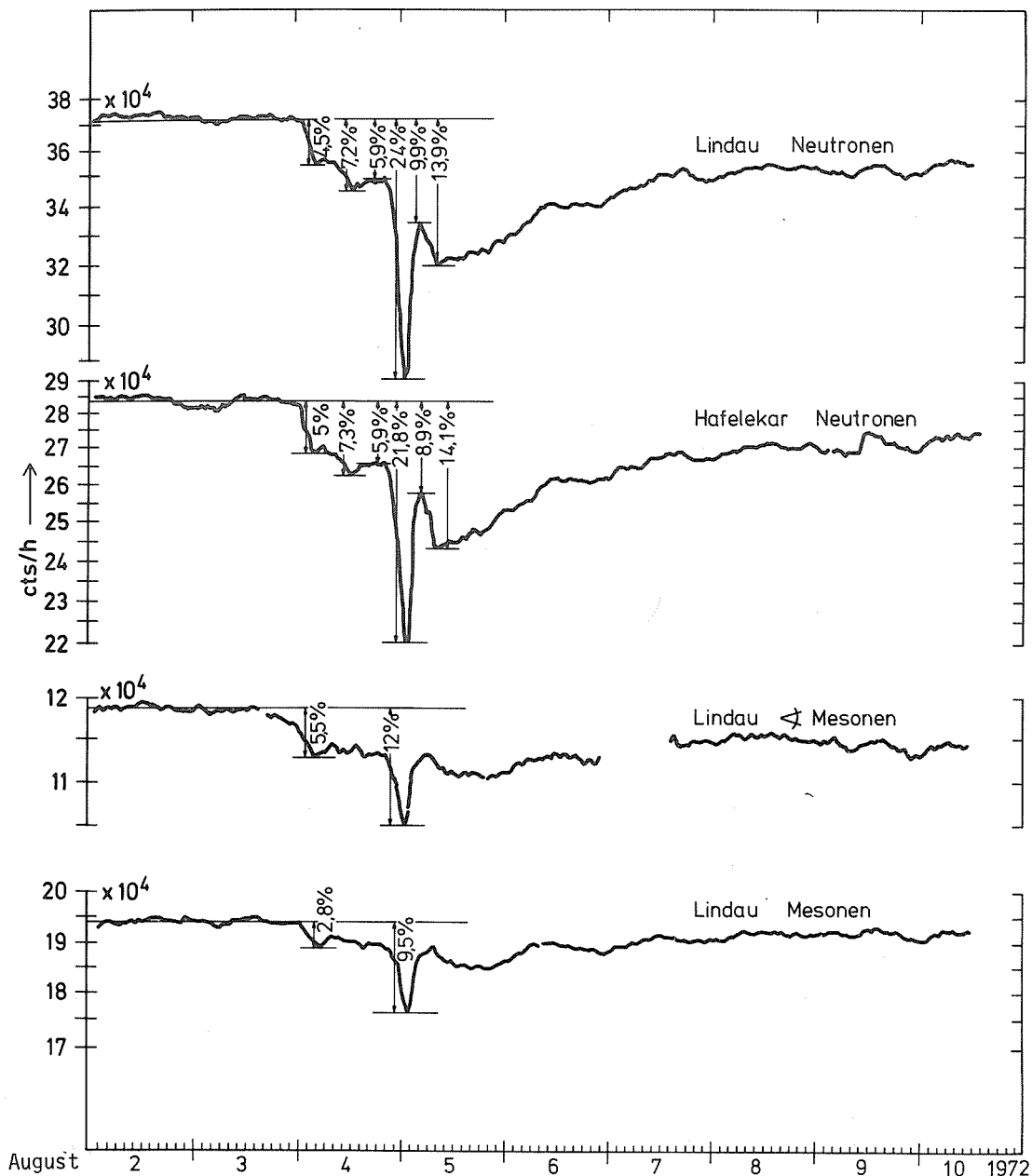


Fig. 1. Synoptic representation of recordings for August 2-10, 1972.

Solar Cosmic Ray Flares of August 4 to 9, 1972 as Measured in the Stratosphere

by

G. A. Bazilevskaya, Yu. I. Stozhkov,
A. N. Charakhchyan and T. N. Charakhchyan
Lebedev Physical Institute, The Academy of Sciences of the USSR
Institute of Nuclear Physics, Moscow State University
Moscow, U S S R

ABSTRACT

Experimental material obtained with stratospheric balloon measurements during the events of August 4 to 9, 1972 is presented: tables of solar proton intensity in the 100-600 Mev energy range. The measurements were taken in the Murmansk region (geomagnetic cut-off threshold $p_c=0.5$ GV) and in Antarctic (Mirny station, $p_c=0.04$ GV). A preliminary brief analysis is attempted.

Powerful solar chromospheric flares early in August, 1972 caused a cosmic ray intensity increase which was recorded with stratospheric balloons. The measurements were taken in the Murmansk region (geomagnetic cut-off threshold $p_c=0.5$ GV) and in the Antarctic (Mirny station, $p_c=0.04$ GV) using radiosondes which carried Geiger counters CTC-6 with 0.05 g/cm² steel walls. Particles were detected with a single counter and a two-counter telescope with 2 g/cm² Al interlayer. Energy was determined from stratospheric absorption assuming all the particles were protons.

The measurements are listed in the Table which indicates the date, time and location of observation and intensity of solar protons with kinetic energy above that specified.

Figure 1 shows the time dependence of the events under discussion for August 4 to 9, 1972. Solar proton intensity according to Pioneer 9 [UAG-21, 1972] and stratospheric data, neutron monitor data from Kiel and Apatity (data obtained from World Data Center B-2), and chromospheric flare data [UAG-21, 1972] are presented.

On July 29 the eastern part of the solar disk displayed a complex active region of enormous size (1000 millionths of the solar hemisphere). Three powerful flares occurred in this active region on August 2: 1B (0316 UT), 1B (1838 UT), 2B (2005 UT). The last flare probably caused the magnetic storm and Forbush decrease. A chromospheric flare of 2B class occurred on August 4 at 0621 UT in the same active region (N15, E09) and lasted for 2.5 hours. The flare caused powerful radio emission in the centimeter range. Solar cosmic rays with energy more than 100 Mev were generated during this flare, an unusual characteristic for the cosmic ray flare.

An extremely high cosmic ray flux of ≥ 200 Mev should be noted at first. The ≥ 200 Mev solar proton intensity detected by us was ~ 50 cm⁻²sec⁻¹ster⁻¹. This is the highest value for the present solar cycle. It can only be compared with the flux observed on November 15, 1960 when N_p (≥ 200 Mev) 15 cm⁻²sec⁻¹ster⁻¹ [Charakhchyan, 1964]. However, much softer solar proton spectra were observed in 1972.

The second feature of the event of August 4 is a very slow increase in the intensity which lasted about 10 hours. This is unusual considering the central position of the chromospheric flare on the solar disk. A similar slow increase was usually observed when the protons were generated in the flares located at the east edge of the solar disk. The increase of the solar proton flux in the low (Pioneer 9) and moderate (stratosphere) energy ranges started earlier than the increase of intensity at the neutron monitor, which is also surprising. Figure 2 shows the time profile of solar cosmic ray intensity according to stratospheric measurements and the Apatity neutron monitor data. The time is read from the moment of chromospheric flare beginning. If the particles are assumed to have arrived within a magnetic trap one has to admit that this trap was more effective for high energy particles. Such a phenomenon is observed for the first time.

Early on August 5 we have another increase of solar cosmic rays in stratosphere. The same was observed at Pioneer 9. It seems probable that another chromospheric flare caused this effect, yet there was no reference to such a flare in the literature. Perhaps it was missed due to poor solar patrol during the time from 2322 UT August 4 till 0112 UT August 5 [UAG-21, 1972]. An unusual sharp recovery of intensity at the neutron monitor (~ 0115 UT August 5) would be considered a result of the same flare if there had not been data of underground measurements [Krymski et al., 1972] which proved the modulation character of this phenomenon. Possibly the solar protons were affected by this mechanism of modulation too, and this is an alternative explanation of the solar proton intensity in the stratosphere increase on August 5.

TIME UT	>Energy Mev	$N_p(>E)$ $cm^{-2} sec^{-1} ster^{-1}$	TIME UT	>Energy Mev	$N_p(>E)$ $cm^{-2} sec^{-1} ster^{-1}$	TIME UT	>Energy Mev	$N_p(>E)$ $cm^{-2} sec^{-1} ster^{-1}$	TIME UT	>Energy Mev	$N_p(>E)$ $cm^{-2} sec^{-1} ster^{-1}$	TIME UT	>Energy Mev	$N_p(>E)$ $cm^{-2} sec^{-1} ster^{-1}$
August 4, 1972														
1. Mirny, single counter												15. Murmansk, single counter		
0758	265	0,34	I439	285	8,17	1833	455	1,04	0216	234	0,76	0805	250	0,08
0804	215	1,24	I442	270	13,27	1836	413	1,34	0229	170	2,30	0809	220	0,21
0808	190	2,67	I445	245	18,03	1839	375	1,77	0232	175	2,31	0811	200	0,53
0810	175	3,53	I448	225	27,56	1848	298	5,31	0240	230	0,74	telescope		
0820	127	11,64	I451	210	41,50	1851	280	7,03	0243	256	0,44	0805	257	0,07
0823	115	14,32				1854	256	10,17	0246	280	0,19	0809	225	0,18
0826	102	17,90	I508	235	48,99	1858	235	14,59	12. Murmansk, single counter *			0811	212	0,36
0829	86	24,22	I511	270	23,13	1900	225	20,48	0249	406	0,10	0814	197	0,58
0832	78	37,70	I514	297	11,23	9. Murmansk, single counter *			0252	375	0,16	16. Murmansk, single counter		
2. Murmansk, single counter			telescope *			2125	637	0,36	0255	337	0,23	I010	245	0,12
0812	290	0,22	I428	420	0,10	2128	585	0,57	0258	305	0,49	I018	190	0,65
0815	265	0,48	I432	373	0,52	2131	533	0,79	0301	285	0,63	I021	175	1,14
0818	240	0,76	I435	335	1,14	2134	500	0,84	0308	242	1,74	I024	162	1,33
0821	220	1,30	I438	300	1,82	2140	398	1,41	0311	220	2,36	I031	106	3,39
0824	205	1,93	I441	280	4,65	2143	368	1,91	0314	205	3,26	I034	86	4,72
0831	160	5,12	I444	260	6,62	2146	330	2,53	0317	190	7,65	I037	71	6,83
0834	149	6,31	I446	250	7,51	2149	303	3,08	0320	175	9,16	I040	59	9,76
3. Mirny, single counter			I448	240	10,98	2152	283	3,36	0322	172	16,77	I043	51	13,73
0950	440	0,08	I451	215	8,52**	2159	234	7,40	0333	129	33,00	telescope		
0954	375	0,21	I454	200	17,70**	2201	220	9,05	telescope *			I015	212	0,19
1000	305	0,73	I457	190	17,13**	2204	205	11,78	0258	315	0,12	I018	197	0,33
1004	270	1,19	I500	180	17,76**	2207	192	14,96	0301	292	0,17	I021	180	0,61
1007	250	1,56				2210	188	17,81	0303	275	0,36	I024	170	0,99
1010	235	2,16	I503	197	14,72**	2212	176	21,89	0306	265	0,43	I026	162	1,51
1012	220	2,61	I505	212	13,19**	telescope *			0308	250	0,67	I029	137	1,89
1022	170	10,47	I510	265	6,35	2143	370	0,09	0311	226	1,02	I031	118	2,46
1025	160	14,77	I513	290	4,73	2146	335	0,22	0314	213	1,79	I034	102	3,51
1028	147	19,70	I515	310	2,34	2149	310	0,31	0317	197	3,26	I037	86	4,82
1031	138	24,01	I517	342	0,97	2152	280	0,59	0320	185	5,35	17. Murmansk, single counter		
telescope			6. Murmansk, single counter *			2155	267	0,87	0322	180	7,25	I252	217	0,11
0957	345	0,15	I512	550	0,74	2158	240	1,01	0324	170	8,57	I301	185	0,88
0959	317	0,19	I515	497	1,15	2201	225	1,76	0327	157	12,25	I304	160	1,44
1001	300	0,34	I518	465	1,71	2204	215	2,56	0330	148	20,08	I307	147	2,52
1004	280	0,69	I520	437	2,21	2207	200	3,12	13. Murmansk, single counter *			I310	139	3,77
1007	255	0,98	I522	405	0,48	2210	198	5,57	0448	482	0,16	I319	102	7,66
1010	242	1,48	I524	385	0,69	2212	185	7,14	0451	437	0,24	I322	90	13,50
1012	225	1,71	I526	350	4,29	2214	175	12,73	0454	375	0,33	telescope		
1014	212	3,26	I529	325	8,00	2217	170	19,96	0501	295	0,73	I255	223	0,18
1017	200	4,03	I532	297	11,64	August 5, 1972			0504	270	0,86	I258	205	0,27
1020	185	5,12	I542	220	47,15	10. Murmansk, single count *			0507	242	1,15	I301	190	0,48
1022	175	7,08	telescope *			0058	290	0,25	0510	213	1,53	I304	174	0,90
1025	160	9,10	I518	470	0,17	0101	265	0,52	0520	155	2,85	I307	165	1,69
1028	158	9,80	I520	445	0,34	0104	250	0,78	0523	142	4,67	I310	145	2,40
4. Murmansk, single counter *			I522	405	0,48	0106	230	0,96	0525	133	4,15	I313	138	3,14
I247	550	0,09	I524	385	0,69	0115	173	3,25	telescope *			I315	132	3,93
I253	450	0,32	I526	357	1,32	0118	156	4,65	0454	380	0,12	I317	122	5,47
I256	398	0,56	I529	330	2,81	0121	141	6,27	0457	350	0,15	I320	112	6,78
I259	365	0,86	I532	310	5,78	0124	132	8,74	0459	330	0,16	I323	106	7,95
I302	338	1,23	I538	265	9,2**	0127	121	10,66	0501	300	0,29	18. Murmansk, single counter		
I304	317	1,61	7. Mirny, single counter			0058	297	0,11	0504	275	0,41	I513	250	0,14
telescope *			I621	650	0,32	0101	275	0,18	0507	250	0,70	I515	230	0,17
I256	405	0,06	I624	588	0,58	0104	257	0,24	0510	220	1,13	I523	180	1,03
I259	370	0,15	I627	530	0,71	0106	237	0,28	0513	201	1,62	I526	170	1,80
I302	340	0,32	I632	450	1,21	0109	212	0,71	0516	185	1,88	telescope		
5. Mirny, single counter *			I635	390	2,06	0112	192	1,18	0518	180	1,89	I515	237	0,06
I419	575	0,20	I638	347	2,58	0115	180	2,13	0520	170	2,52	I517	215	0,10
I423	500	0,52	I641	315	3,34	0118	170	3,18	0523	152	3,19	I520	200	0,18
I428	412	1,19	8. Murmansk, single counter			0121	150	4,01	0525	143	3,17	I523	191	0,39
I432	367	1,96	I821	665	0,14	0124	141	6,27	14. Mirny, single counter			I526	175	0,68
			I824	625	0,30	0127	131	8,09	0810	230	0,33			
			I830	505	0,70	11. Mirny, single counter			0813	210	0,69			
						0123	256	0,34	0815	197	0,93			

* The data from single counter and telescope disagree.
 ** The result may be underrated due to overflow of registers.

TIME UT	>Energy Mev	$N_p(>E)$ $cm^{-2} sec^{-1} ster^{-1}$
19. Murmansk, single counter		
I737	I92	0,22
I740	I75	0,42
I743	I55	0,84
I746	I38	1,18
I754	I08	3,13
I757	94	4,97
I759	84	6,76

telescope		
I740	I80	0,20
I743	I65	0,42
I746	I48	0,66
I749	I35	1,14
I753	I28	1,62
I755	I20	2,02
I757	I10	2,77
I759	I01	3,65

20. Murmansk, single counter		
2I29	208	0,13
2I38	I65	0,57
2I41	I46	0,99
2I44	I34	1,56
2I47	I23	2,25
2I50	I14	3,27

telescope		
2I34	I92	0,09
2I36	I80	0,13
2I38	I70	0,19
2I41	I56	0,36
2I44	I43	0,64
2I47	I34	0,96
2I50	I24	1,38

August 6, 1972		
21. Murmansk, single counter *		
0642	I85	0,16
0645	I68	0,32
0648	I56	0,43
0650	I44	0,53

telescope *		
0650	I50	0,03

22. Mirny, single counter *		
0702	205	0,06
0714	I42	0,42
0717	I27	0,49
0720	II5	0,75

telescope *		
0712	I65	0,08
0715	I47	0,11
0718	I33	0,18
0721	I22	0,28

23. Murmansk, single counter		
I018	I55	0,15
I029	I03	1,71
I031	94	1,96

telescope		
I018	I65	0,06
I020	I50	0,13
I023	I36	0,24
I026	I24	0,42
I029	II6	0,69
I031	I09	0,87

TIME UT	>Energy Mev	$N_p(>E)$ $cm^{-2} sec^{-1} ster^{-1}$
24. Murmansk, single counter and telescope		
I610	I45	< 0,03

25. Murmansk, single counter		
I841	I56	0,08
I844	I46	0,09
I852	I03	0,23
I855	90	0,56
I858	78	1,03
I901	69	1,59

telescope		
I846	I41	0,05
I849	I28	0,08
I852	II7	0,17
I855	I06	0,28
I858	94	0,42
I901	88	0,69

August 7, 1972		
26. Murmansk, telescope		
0325	I36	0,10
0328	I31	0,14
0330	I25	0,18
0332	II7	0,21
0335	I09	0,32
0338	I00	0,46
0341	94	0,63
0344	89	0,80

27. Mirny, single counter		
0350	I85	0,04
0352	I75	0,07
0404	I22	0,17

28. Mirny, single counter *		
0620	I65	0,05
0625	I43	0,06
0629	I27	0,09
0632	II5	0,13
0635	94	0,16

telescope *		
0630	I33	0,03
0634	II9	0,07

29. Murmansk, single counter *		
I010	220	0,06
I019	I55	0,12
I022	I40	0,19
I025	I25	0,28
I028	II3	0,37
I031	I06	0,50

telescope *		
I033	I09	0,06
I036	99	0,17

30. Murmansk, single counter and telescope		
I323	I40	< 0,03

August 8, 1972		
31. Mirny, single counter		
0404	340	0,12
0408	302	0,19
0415	250	0,30
0418	230	0,39
0421	210	0,51
0424	192	0,67

TIME UT	>Energy Mev	$N_p(>E)$ $cm^{-2} sec^{-1} ster^{-1}$
32. Mirny, single counter *		
0427	I75	0,87
0429	I70	1,05

0748	420	0,06
0751	390	0,07
0754	368	0,10
0804	292	0,16
0808	265	0,21
0811	250	0,26
0814	230	0,34
0827	I75	0,69
0830	I77	0,72
0833	185	0,72
0836	192	0,60
0841	200	0,57

telescope *		
0806	281	0,08
0811	252	0,12
0814	237	0,17
0817	223	0,21
0820	208	0,27
0824	192	0,35
0827	I80	0,43

0830	I85	0,44
0833	192	0,43
0836	I97	0,38
0839	210	0,37
0842	213	0,28
0845	215	0,28
0848	225	0,21
0851	240	0,17
0854	242	0,14

33. Murmansk, single counter		
0803	375	0,09
0806	345	0,12
0809	325	0,17
0812	300	0,18
0815	280	0,26
0818	260	0,31
0821	235	0,40
0824	220	0,51
0827	205	0,67
0830	190	0,89
0833	I75	1,14
0836	I65	1,55
0839	I53	1,98
0842	I42	2,70

34. Murmansk, single counter *		
I024	390	0,06
I027	365	0,09
I038	280	0,19
I041	260	0,22
I044	235	0,27
I047	225	0,32
I049	210	0,41

telescope *		
I041	265	0,08
I044	240	0,10
I047	235	0,18
I049	220	0,21
I052	210	0,30

TIME UT	>Energy Mev	$N_p(>E)$ $cm^{-2} sec^{-1} ster^{-1}$
35. Murmansk, single counter *		
I421	385	0,05
I427	310	0,07
I430	282	0,11
I433	256	0,13
I436	242	0,16
I444	I85	0,31
I447	I70	0,43
I450	I53	0,52
I459	I08	1,25

telescope *		
I443	201	0,11
I447	I75	0,21
I450	I60	0,37
I453	I48	0,53
I456	I39	0,82
I458	I29	1,03

36. Murmansk, single counter *		
2I59	357	0,03
2202	338	0,04
2206	310	0,04
2215	245	0,06
2218	230	0,07
2221	212	0,10

2224	220	0,10
2227	225	0,08
2230	242	0,06

telescope *		
2221	220	< 0,03

August 9, 1972		
37. Murmansk, single counter *		
0107	321	0,05
0116	245	0,07
0119	220	0,10
0122	205	0,14
0125	I90	0,14
0128	I75	0,19
0140	II8	0,43
0143	I06	0,56

telescope *		
0125	I97	0,04
0128	I80	0,09
0131	I65	0,11
0134	I49	0,14
0137	I39	0,19
0140	I29	0,23
0143	I20	0,33

38. Mirny, single counter		
0446	208	0,04
0456	I60	0,12
0459	I47	0,19
0504	I38	0,23

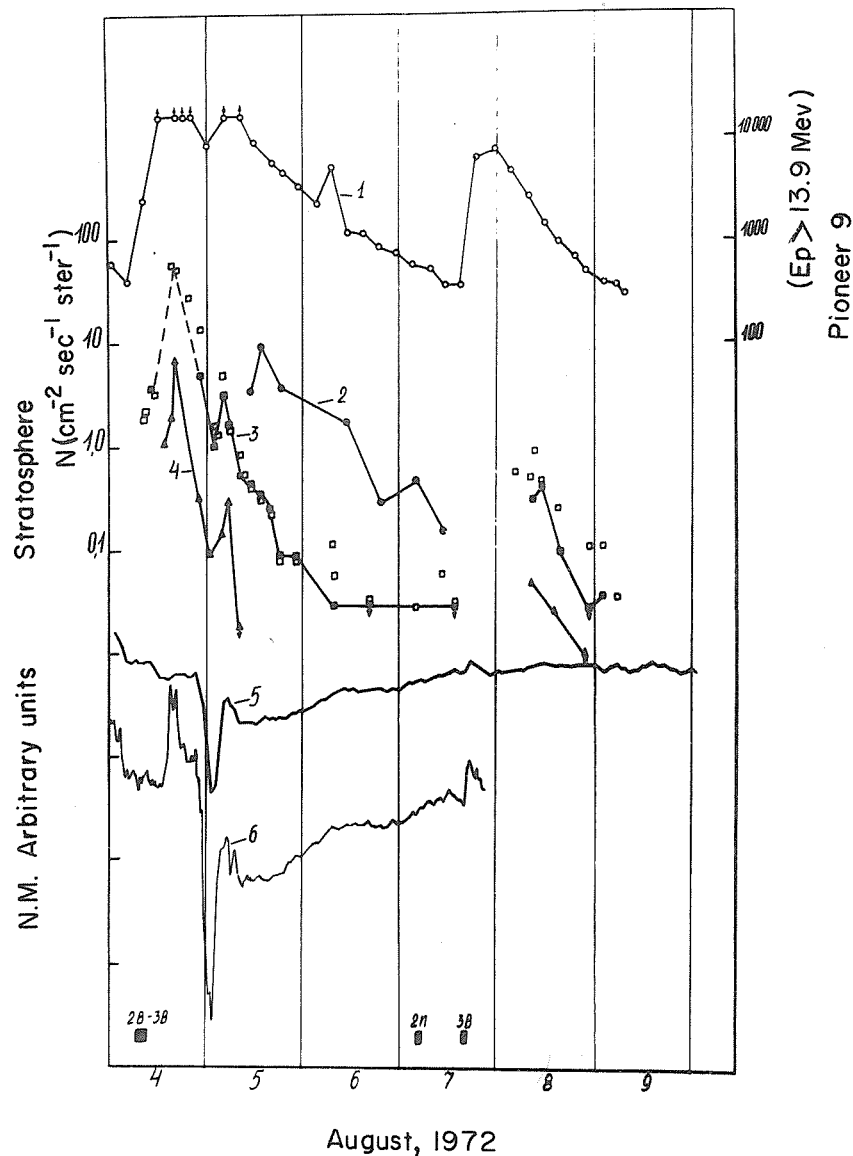


Fig. 1. Time dependence of cosmic ray intensity on August 4 to 9, 1972.

1. Solar proton flux with $E > 13.9$ Mev as measured by Pioneer 9.
2. Solar proton intensity with $E \geq 100$ Mev in the stratosphere.
3. The same for $E \geq 200$ Mev (light squares are the single counter data, solid squares are the telescope data).
4. The same for $E \geq 300$ Mev.
5. Data of neutron monitor at Kiel.
6. Data of neutron monitor at Apatity.

Stratospheric data for Murmansk and Mirny do not separate as they coincide.

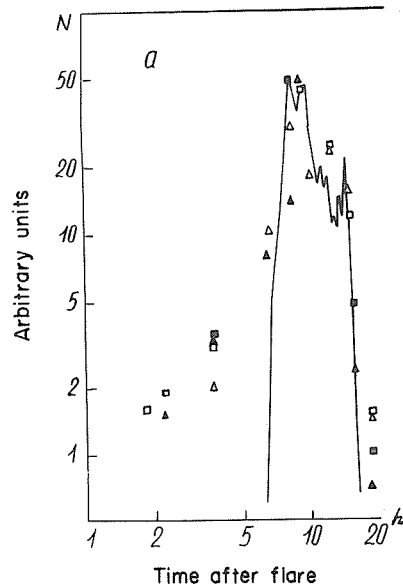


Fig. 2. Time profile of proton fluxes in the flare of August 4.
 Solid line is neutron monitor data, squares and triangles
 are stratospheric ones for $E \geq 200$ Mev and $E \geq 300$ Mev,
 respectively.

Another feature of the cosmic ray intensity in the stratosphere on August 4 to 9, 1972 is the fact that in our measurements the data of the single counter and the telescope disagree in certain periods. Such flights are labelled with asterisks in the Table. In such a case proton intensity should be determined according to telescope data only. At that time a flux of short-path particles was generated in stratosphere. They were possibly the secondary γ -rays created in the nuclear reactions of the solar protons with air nuclei [Hofmann and Winckler, 1963]. However the analysis is not performed yet.

REFERENCES

- | | | |
|--------------------------------------|------|--|
| CHARAKHCHYAN, A. N. | 1964 | <u>Uspekhi Fiz, Nauk</u> , <u>83</u> , 35. |
| HOFMANN, D. J. and
J. R. WINCKLER | 1963 | <u>J. Geophys. Res.</u> , <u>68</u> , 2067. |
| KRYMSKI, G. Ph. <u>et al.</u> | 1972 | Report at Cosmic Ray Conf. at Apatity, in press. |
| | 1972 | Preliminary Compilation of Data for Retrospective
World Interval July 26 - August 14, 1972. <u>World Data
Center A for Solar-Terrestrial Physics Report UAG-21.</u> |

Cosmic Ray Variations on August 1-14, 1972 from
Data of Neutron Supermonitors in Siberia and Far East

by

N. P. Chirkov, A. M. Novikov, I. S. Samsonov, A. A. Upolnikov
Institute of Cosmophysical Research and Aeronomy
Yakutsk Branch, Siberian Department of the USSR Academy of Sciences
Yakutsk, USSR

and

A. A. Luzov, A. V. Sergeyev and Yu. A. Kurchenko
Siberian Institute of Terrestrial Magnetism
Ionosphere and Radio Wave Propagation
Siberian Department of the USSR Academy of Sciences
Irkutsk, USSR

V. N. Nikolayev
Institute of Geophysics and Tectonic
Far-East Scientific Center of the
USSR Academy of Sciences
Khabarovsk, USSR

V. L. Yanchukovsky
Institute of Geology and Geophysics
Siberian Department of the USSR Academy of Sciences
Novosibirsk, USSR

G. G. Todikov
North-East Complex Research Institute
Far-East Scientific Center of the
USSR Academy of Sciences
Magadan, USSR

In early August 1972, a complex of events in cosmic ray intensity variations was observed. In Figure 1, data of neutron supermonitors of the Siberian net of cosmic ray stations for August 1-14, 1972 are presented. In Table 1, station coordinates and threshold rigidities are given.

Table 1

No.	Station	Geographic Coordinates		P (Bv)
		Latitude	Longitude	
1.	Tixie Bay	N71.5	E128.9	0.52
2.	Norilsk	69.3	88.1	0.60
3.	Yakutsk	62.0	129.7	1.85
4.	Magadan	60.1	151.0	2.16
5.	Novosibirsk	54.8	83.0	2.85
6.	Irkutsk	52.4	104.0	3.74
7.	Khabarovsk	48.5	135.2	5.55

Cosmic ray variations in early August 1972 were associated with great flares on the Sun observed during the same period. In Table 2 chromospheric flares of importance 1 and larger for the period of August 1-7, 1972 are presented (see Lincoln *et al.* [1972] and "Solar-Geophysical Data" [1973]). In Figure 1 these flares and their duration are noted by arrows. All the flares presented in Table 2 were observed in a single active region McMath 11976. Geomagnetic storms are noted by triangles in Figure 1.

For ease of analysis one can divide the observed cosmic ray variations into several effects discussed below.

1. The first Forbush decrease began at 0200 - 0300 UT on August 4 and according to high-latitude station data its amplitude was 7-8%. In a paper by Krymsky *et al.* [1973] it is found the energy spectrum of this Forbush decrease to have a form $\delta D(\epsilon)/D(\epsilon) \sim \epsilon^{-\gamma}$, where $\gamma = 0.8 \pm 0.1$, i.e., this Forbush decrease is typical. We assume that the first Forbush decrease was associated with the chromospheric flares observed on August 1. We obtain values of the order of 650 km/sec for the mean solar wind velocity.

2. The first cosmic ray increase began at 1415 UT on August 4 and reached its maximum (11%) in 30 minutes according to 5-minute data of the Tixie Bay neutron monitor station. The increase was detected only by high-latitude neutron monitors. The amplitude dependence on rigidity P of the data of Figure 1 is of a form $A(P) \sim P^{-\gamma}$, where $\gamma = 2.5 \pm 0.1$. By all signs, this increase was due to a solar cosmic ray flare and was possibly associated with a chromospheric flare of importance SB which was observed at 1306 - 1342 UT on August 4.

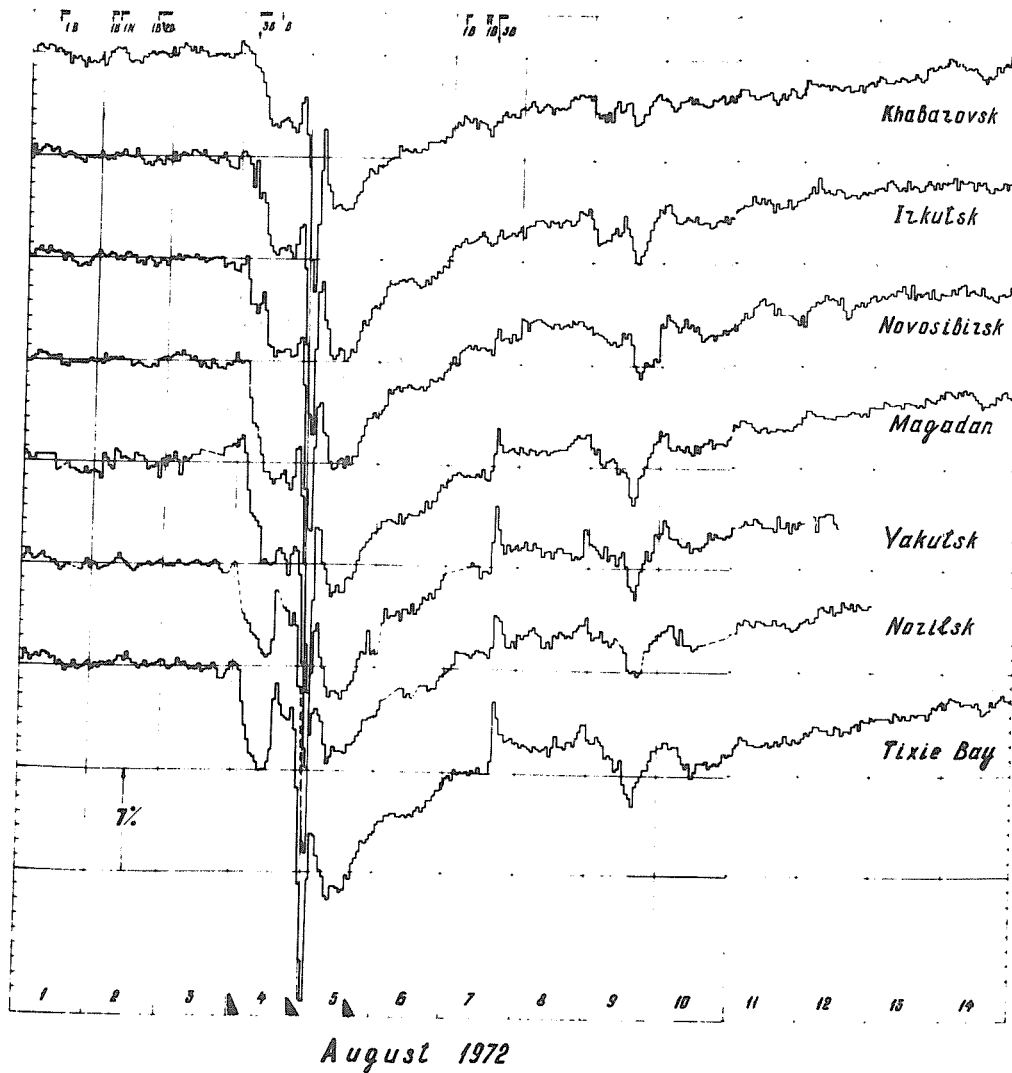


Fig. 1. Cosmic ray variations on August 1-14 according to data of neutron supermonitors at Khabarovsk, Irkutsk, Novosibirsk, Magadan, Yakutsk, Norilsk and Tixie Bay.

Table 2

No.	Date Aug. 1972	Onset (UT)	End (UT)	Maximum (UT)	Coordinates Lat. Long.		Importance
1.	1	0858	1012	0925	N12	E46	1N
2.	"	1135	1207	1147	13	46	1N
3.	2	0336	0608	0355	12	34	3N
4.	"	0605	0710	0620	14	34	1N
5.	"	1839	1857	1844	14	26	1B
6.	"	1958	2336	2058	14	28	2B
7.	"	2248	0111	2248	12	25	1B
8.	4	0617	0855	0640	14	08	3B
9.	"	0740	1000	0751	13	08	2B
10.	7	0349	0444	0359	14	W30	1B
11.	"	1055	1144	1103	15	34	1N
12.	"	1200	1232	1204	13	34	1B
13.	"	1449	1721	1534	14	37	3B

3. The second cosmic ray intensity increase began at 2000 UT and reached its maximum at 2200 UT on August 4. The largest amplitude (3 - 4%) was observed at high-latitude stations. The increased amplitude is weakly dependent upon rigidity P.

4. The second Forbush decrease began at 2300 UT on August 4, reached its maximum in 4 hours and had abnormally large amplitude. In the Tixie Bay neutron monitor station data, the second Forbush decrease amplitude was 23% (0200 UT on August 5); a typical cosmic ray intensity decrease at this time is of order 16%. As it is evident from the paper by Krymsky et al. [1973] cosmic rays up to energies 50 - 60 Bev undergo modulation. The second Forbush decrease energy spectrum had the form $\delta D(\epsilon)/D(\epsilon) \sim \epsilon^{-\gamma}$, where $\gamma = 1.1 \pm 0.1$, i.e., the second Forbush decrease was softer than the first one. The second Forbush decrease was apparently connected with chromospheric flares observed on August 2 and accompanied by the immense streams of radio waves and X-rays. The mean solar wind velocity is of the order of 640 or 850 km/sec depending on which flare was associated with the magnetic storm with onset at 2053 UT on August 4. According to the Tixie Bay station data, 75-80 minute cosmic ray intensity variations with amplitudes up to 2-3% were observed between the first and the second Forbush decreases.

5. The third cosmic ray intensity increase began at 0300 UT on August 5 and reached its maximum in 3 hours. The largest amplitudes of order 10-11% were observed at high latitudes. The increased amplitude is almost independent of rigidity P.

6. The third Forbush decrease of cosmic ray intensity began at 0600 UT on August 5. The largest decrease was 5-6%. Krymsky et al. [1973] showed that the energy dependence of the third Forbush decrease had a form $\delta D(\epsilon)/D(\epsilon) \sim \epsilon^{-\gamma}$, where $\gamma = 0.5 \pm 0.1$, i.e., it had the hardest Forbush decrease. Energies up to 100 - 120 Bev underwent modulation.

7. According to 5-minute data of the Tixie Bay station, the solar cosmic ray flare on August 7 began at 1540 UT and reached its maximum in 50 minutes. The solar cosmic ray flare was associated with a chromospheric flare of importance 3B observed from 1455 to 1725 UT. The dependence of the flare amplitude on rigidity had a form $A(P) \sim P^{-\gamma}$, where $\gamma = 1.8 \pm 0.1$.

Forbush decreases of cosmic ray intensity in the early part and at the end of August 4 were associated with solar wind shock fronts reaching the Earth as indicated by geomagnetic storms and Dst-variations observed during these periods on August 4.

The magnetic storm for August 5 is not presented in the storm list. However, from the Dst-variations, one can assume that a magnetic storm occurred at 1600 UT on August 5. We obtain a solar wind velocity equal to 1200 km/sec. From magnetograms for August 4-5 it is evident that the geomagnetic field was strongly disturbed on August 4-5. Therefore, we can consider the magnetic storm at the end of August 4 and the following Earth's magnetic field disturbances in the first half of August 5 to be caused by a shock wave of a complicated structure. Then, apparently, one can understand the whole complex of phenomena in cosmic ray variations during August 4-5. One can assume that the first Forbush decrease was connected with shock waves from chromospheric flares which took place on August 1. The second Forbush decrease was caused by shock waves from chromospheric flares during the early part and at the end of August 2. One can assume that a shock wave from one of the flares at the end of August 2 caught up to a shock wave from one of the flares during the early part of August 2. A structure generated as the result of the interaction of shock waves in the form of a compression and a discharge could have caused the abnormal decrease of cosmic ray intensity at 0200 UT on August 5. The focussing of cosmic rays by a shock wave front could have caused the cosmic ray intensity increase at the end of August 4 before the Forbush decrease. It is very likely that the cosmic ray increase which occurred in the middle of August 4 was a product of the interaction of shock waves in the space. The distance from the Sun where the interaction occurred was of the order 1.3×10^8 km.

A sharp cosmic ray increase after 0200 UT on August 5 was apparently caused by a compression of cosmic rays by the third shock wave which arrived on August 5 and which caused the third Forbush decrease.

REFERENCES

KRYMSKY, G. F., 1973
A. I. KUZMIN,
V. I. KOZLOV,
I. S. SAMSONOV,
G. V. SKRIPIN,
V. A. FILIPPOV,
G. V. SHAFER,
N. P. CHIRKOV and
I. A. TRANSKY

Yavleniya v kosmicheskikh luchakh v avguste 1972 goda.
Izvestiya AN SSSR, seriya fizicheskaya, v pechati

LINCOLN, J. V. and
H. I. LEIGHTON

1972

Preliminary compilation of data for retrospective world interval July 26 - August 14, 1972. World Data Center A, Upper Atmosphere Geophysics Report UAG-21.

1973

Solar-Geophysical Data, 342, Part II, US Department of Commerce, (Boulder, Colorado, USA 80302).

Data of the Events of August 1972 from the Cosmic Ray Installation Complex in Yakutsk

by

V. A. Filippov, A. I. Kuzmin, A. N. Prikhodko, I. S. Samsonov,
G. V. Skripin, G. V. Shafer, A. A. Upolnikov
Institute of Cosmophysical Research and Aeronomy, Yakutsk Branch
Siberian Department of the USSR Academy of Sciences, Yakutsk, USSR

In early August, 1972, a number of unusual and interesting events in cosmic rays were observed. In Figure 1, 15-minute data of two neutron monitors for the interval 1500 UT August 3 to 0300 UT August 8, 1972 are presented. Both of the monitors consisting of 6-SNM-15 counters (barometric coefficient is -0.65% /mb with a counting rate of $N = 160,000$ count/hour) are located in Yakutsk ($\psi = N62, \lambda = E129$) in a building with a shield thickness of 42 g/cm^2 . The second one consisting of 12-SNM-15 counters (barometric coefficient is -0.68% /mb with a counting rate of $N = 420,000$ count/hour) are located in Oktyomtsy, 60 km south of Yakutsk ($\psi = N61.5, \lambda = E129$) in a building with a shield thickness 2 g/cm^2 .

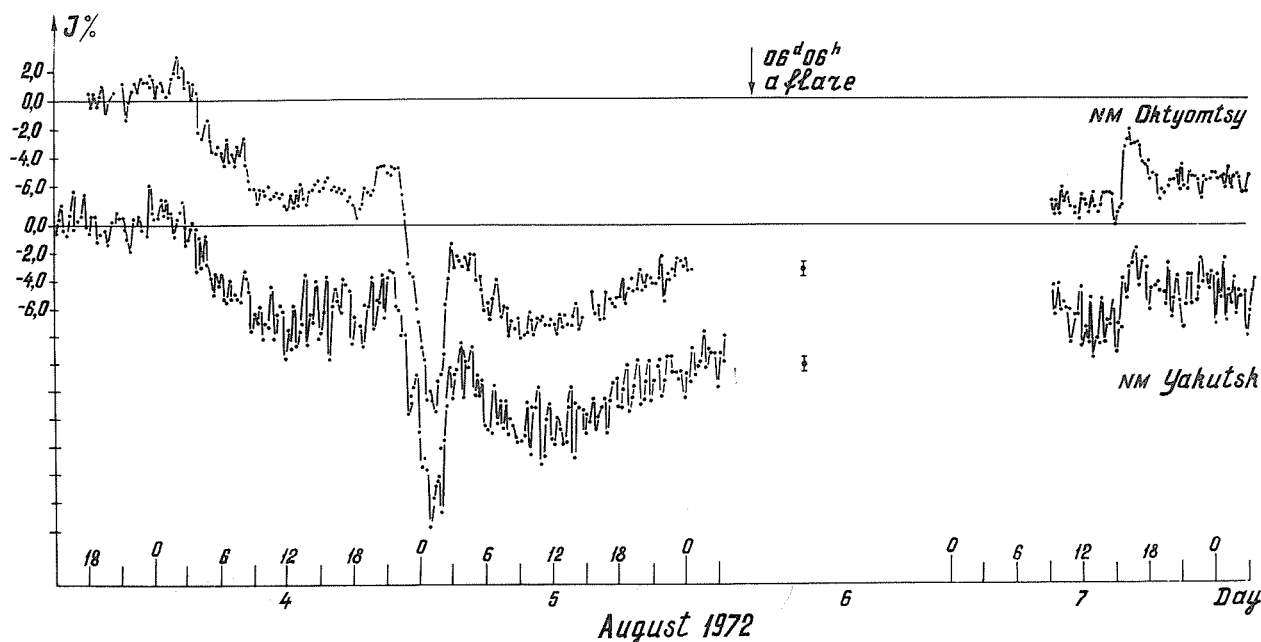


Fig. 1. 15-minute values of cosmic ray component in per cent for the interval 1500 UT on 3 August to 0300 UT on August 8, 1972 for Yakutsk and Oktyomtsy.

In Figure 2, the hourly values of neutron intensities at Yakutsk and Oktyomtsy and of meson intensities registered by several semicubical telescopes in Yakutsk oriented vertically (Z) and located on the Earth's surface and underground at depths 7, 20 and 60 m.w.e. are presented. Data of the Yakutsk ionization chamber ASK-1 having a volume of 1000 liters filled with argon at 10 atm and shielded with 12 cm of lead are also given. Times of chromospheric flare onsets on the sun are marked by arrows.

In Figure 3, the hourly values of muon intensities registered by azimuthal telescopes at Yakutsk on the Earth's surface and underground at 7 and 20 m.w.e. are given. The telescopes are inclined at an angle of 30° from the zenith, three pointing toward the north and three toward the south.

From Figures 1-3, it is evident that from August 3 to August 8, 1972, complicated events in cosmic rays associated with powerful flares on the Sun were observed. Events with unusually sharp intensity decreases and increases were observed by all the installations up to 20 m.w.e., where the primary mean energy is about $E = 70\text{-}100\text{ Gev}$; these events were less noticeable at a depth 60 m.w.e. ($E = 200\text{-}280\text{ Gev}$).

One can expand the whole complex of events into a series of effects, the characteristics of which are given in Table 1. Here, an estimate of the statistical accuracy of the detectors (σ) and the minimum energy of primary cosmic rays determined from the initial coordinate of a coupling coefficient function curve are presented.

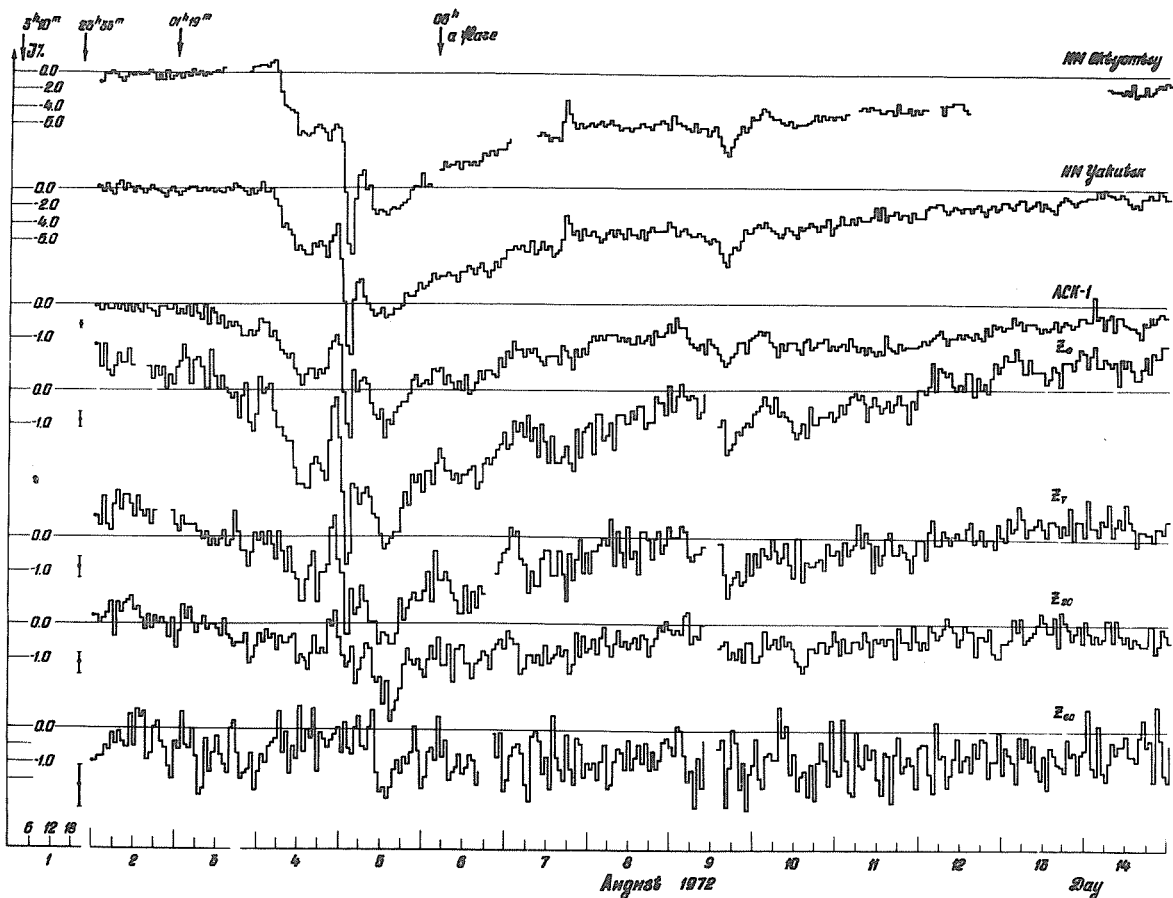


Fig. 2. Hourly values of neutron intensity recorded at Yakutsk and Oktyomtsy and those of meson intensity at Yakutsk from the data of the ionization chamber ASK-1 and a complex of semi-cubical telescopes oriented vertically (Z) and located on the Earth's surface and underground at depths 7, 20 and 60 m.w.e. during August 2-14, 1972.

1. The situation before the first Forbush decrease: 0500 UT August 3 - 0300 UT August 4. The counting rate on August 2 at all depths and inclinations was fairly stable; thus, the average value of this day was used as the zero level and all the following data were normalized to this level. On August 3, the neutron component intensity was comparable with the normal intensity level. On August 4 from 0100 to 0300 UT a neutron intensity increase of 3% was observed. However, prior to this period, the meson detectors registered an appreciable intensity decrease. Beginning at 0500 UT August 3, the muon intensity gradually decreased reaching its minimum value of $2.4 \pm 0.6\%$ on the Earth's surface at 2200 UT and also at 7 and 20 m.w.e.. This decrease was not caused by temperature effects since the largest correction for such an effect in the muon intensity on the Earth's surface at this time did not exceed 0.7%. At 0100 UT August 4, the muon intensity sharply recovered to near the initial level. Thus, the muon intensity gradually decreased and recovered sharply to the zero level just prior to the onset of the first Forbush decrease.

2. The initial phase of the first Forbush decrease began at 0400 UT and lasted till 1200 UT August 4. At 0800 UT, a short-period (01h 15 min) increase of neutron intensity to 2.7% was observed.

The ratios of the Forbush decrease amplitudes detected by the neutron monitor and telescopes at levels 7, 20 and 60 m.w.e. to the respective amplitude at sea level are 2.9; 0.67; 0.49; 0.2. Hence, it follows that one can approximate the energy spectrum of the Forbush decrease by the expression $E^{-0.8}$. Such a spectrum does not differ significantly from that found for the average of a large number of Forbush decreases.

3. An increase of intensity began at 1300 - 1500 UT August 4 and in three to four hours reached its maximum of 2% in the neutron monitor data and 1% in the data of the vertical telescopes at depths to 20 m.w.e.

Table 1
 Characteristics of August 1972 Solar Events

DETECTOR	E _{min} , Gev	Decrease 1		Increase 1		Decrease 2		Increase 2		Decrease 3		Increase 3		Decrease 3		A cosmic ray flare				
		Comment	Amp. %	Comment	Max. Amp. %	Comment	Amp. %	Comment	Max. Amp. %	Comment	Amp. %	Comment	Max. Amp. %	Comment	Amp. %	Comment	Max. Amp. %			
		Aug. 4 Hours UT																		
Oktyomtsy, NM	1.8	0.16	03	8.2	13	16	2.0	19	21	2.8	21	23.0	02	05	9.8	06	17.5	1500	1615	6.8
Yakutsk, NM	1.85	0.25	03	6.9	13 ^b	17	1.6	19	22	3.6	22	21.6	02	05	8.7	06	15.5	1500	1615	6.3
ASK-1	15.0	0.08	05	1.7	13	15	0.6	19	22	1.2	22	3.6	03	04	2.0	07	3.8			
Z ₀	5.0	0.22	03	2.6	14	16	1.0	20	22	2.0	22	6.0	02	06	2.4	08	5.4			
N ₀	6.0	0.42	03	3.3	13	16	1.0	19	22	2.2	22	4.9	02	06	2.4	06	3.0			
S ₀	6.0	0.42	03	3.4	13	15	0.8	18	22	1.8	22	5.3	02	06	2.0	06	3.0			
Z ₇	15.0	0.45	03	2.0	14	16	1.0	19	22	2.0	22	3.6	02	06	1.3	08	4.0			
N ₇	16.0	0.52	03	2.1				20	22	1.7	22	3.7	02	06	1.2	07	3.6			
S ₇	16.0	0.52	03	2.7	13	16	1.1	19	22	1.8	22	3.2	02	06	0.7	09	3.6			
Z ₂₀	34.0	0.45	04	1.0	14	16	1.0	19	22	1.3	22	1.6	02	07	0.5	09	3.0			
N ₂₀	36.0	0.52	02	1.2				19	22	1.3	22	0.6	02	07	0.8	07	2.7			
S ₂₀	36.0	0.52	04	1.8	13	16	1.4	19	21	1.0	22	1.4	02	06	0.5	06	3.0			
Z ₆₀	85.0	0.7	-	-	-	-	-	17	23	1.2	-	-	-	-	-	09	1.5			

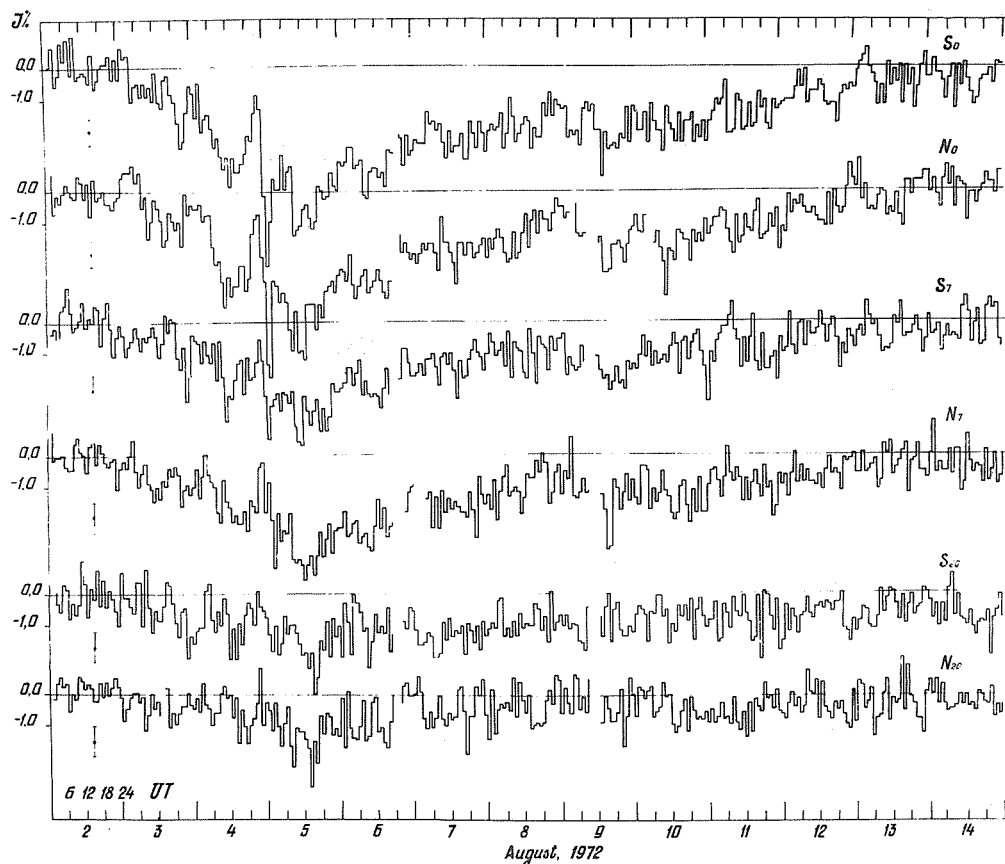


Fig. 3. Hourly values of muon intensity registered at Yakutsk by a complex of azimuthal telescopes on the Earth's surface and underground at depths 7 and 20 m.w.e. inclined at an angle of 30° to the north (N) and the south (S) (N,S) from the vertical during August 2-14, 1972.

The northern-pointing telescopes did not detect this increase at all; the southern-pointing ones registered an increase of 1-1.5% at 7 and 20 m.w.e..

4. A second large increase of intensity began at 1900 - 2000 UT on August 4 and reached its maximum in 2h 30 min. The increase was noticeable to all depths up to 20 m.w.e. (1.3%). The increase was particularly distinct in the northern and vertical telescopes. The meson intensity at maximum recovery was nearly to the normal level. However, the neutron intensity did not recover to pre-storm values.

The two increases were not typical of those which occur during solar chromospheric flares. Beginning from 1957 the Yakutsk azimuthal telescopes have never heretofore detected such a large intensity increase. In this case, even at a depth 20 m.w.e., an intensity increase up to 1.3% was observed. These facts are evidence for some new acceleration processes of particles in the interplanetary medium as compared with ordinary solar cosmic ray flares.

5. The second Forbush decrease began at 2200 - 2300 UT on August 4. This event was unique in that there was both a decrease and an increase during a comparatively short period of time. The event lasted 6-7 hours. It had an abnormally large value, reaching 23% in neutron intensity.

The relative amplitudes of the event at maximum are as follows:

$$NM / Z_0 ; Z_7 / Z_0 ; Z_{20} / Z_0 ; Z_{60} / Z_0 = 3.9 ; 0.56 ; 0.34 ; 0.1.$$

The energy spectrum of this decrease is considerably softer than that of the first Forbush decrease and is satisfactorily approximated by form $\sim E^{-3.1}$.

6. A third intensity increase began at 0300 UT August 5 and reached maximum at 0600 UT. This maximum is somewhat different in meson intensity and two separate intensity peaks can be noted in some of the telescope data. This increase is also difficult to interpret in terms of solar cosmic rays, since it was observed in the high energy particles. Therefore, all three increases are

unusual and likely to be connected with interaction processes of particles with the interplanetary magnetic field.

7. A third cosmic ray intensity decrease was first observed in a neutron component at 0600 UT August 5 and in a meson component 2-3 hours later. This event was detected by all the instruments at Yakutsk.

Even at 60 m.w.e. it was equal to 1.5% which indicates a rather hard spectrum which can be approximated from the ratio of amplitudes at different levels (2.5 : 0.75 : 0.65 : 0.42) by form $E^{-0.5}$.

8. The recovery of the intensity to normal level was complete by August 12-13. However, prior to the recovery a number of events were noted. Substantial daily variations occurred early in the period. On August 7 there occurred another large solar cosmic ray flare which began at 1455 UT. Associated with this flare, the neutron intensity increase was 4% in Oktyomsky and 3.5% in Yakutsk.

The complicated events described above are connected with the active region No. 11976 on the sun which caused a number of great chromospheric flares on August 2, 4 and 7 [Lincoln et al., 1972]. A list of flares of importance larger than 1B is given in Table 2.

Table 2

Date of commencement Aug. 1972	Onset Time UT	Maximum phase UT	Coordinates		Importance
			lat.	long.	
2	0316	0410	N13	E35	1B
	0619	0739	15	35	1B
	1839	1844	14	26	1B
	1958	2058	14	28	2B
4	0530	0639	14	09	3B
7	1455	1536	14	W37	3B

The following sudden commencements were associated with the arrival of the shock fronts from some of these flares in the vicinity of the Earth: at 0119, 0220 and 2054 UT August 4 and at 2354 UT August 8 [Lincoln et al., 1972].

A preliminary interpretation of these events is given in Krymsky et al., [1972].

At 1800 - 2000 UT on August 3, before the first Forbush decrease, a substantial pre-decrease 1.5 - 2.4% was detected by the underground telescopes to depths up to 20 m.w.e.. This event appears to have been caused by the ejection of matter from the flare which at some later time acted as screen against high energy cosmic rays. If this was so, then the pre-decrease at the earth should have been anisotropic and in this case the largest effect should have been observed at the meson installations of the American and Canadian station groups. The largest effect at the crossed telescopes, as would be expected, was shown by southern-pointing installations which were more sensitive to the particles arriving along the ecliptic plane. The mechanism of such screening is not yet clear.

From a comparison of meson telescope data from Yakutsk, Hobart and London [Dutt et al., 1972], it can be noted that the first and the third decreases were strongly longitudinally dependent. Thus, the telescopes in Yakutsk and Hobart with similar longitudes show identical variations. The telescopes in London did not detect the first and the third maxima at all and the first and the third decreases were only slightly distinct. Hence, it may be concluded that the events which caused the first and the third decreases were anisotropic for the high energy particles registered by meson telescopes.

A deep and rather short-period decrease together with unusual increases prior to and after the decrease are associated with the formation of a piston shock wave in the interplanetary medium [Krymsky et al., 1972]. The peculiarity of a piston wave is its dual front structure. Between the fronts, a region of relative compression of the solar wind plasma and magnetic field occurs. Therefore, the magnetic field intensity can substantially exceed those values which are reached within the body of explosive waves.

The intensity increase at the fronts is connected with the "raking up" of cosmic rays. The decrease between the fronts is due to the matter expansion which, though small, is effective because of a small diffusion coefficient. Note that similar short-period Forbush decreases with the steep recovery fronts have been observed previously (July 1959; December 1966; November 1968 and others). These allow us to conclude that the modulation mechanisms similar to ones described by Krymsky et al., [1972] are characteristic for most Forbush decreases.

Detailed study of these complicated events in August 1972 using extensive experimental data will provide valuable information about the cosmic ray modulation mechanisms by the solar wind.

REFERENCES

- | | | |
|---|------|--|
| DUTT, J. C.,
J. E. HUMBLE,
T. THAMBYAHPILLAI | 1972 | The unprecedented cosmic ray disturbances of early August, 1972, (elsewhere this compilation). |
| KRYMSKY, G. F.,
A. I. KUZIM,
V. I. KOZLOV,
I. S. SAMSONOV,
G. V. SKRIPIN,
V. A. FILIPPOV,
G. V. SHAFER,
N. P. CHIRKOV and
I. A. TRANSKY | 1972 | Yavleniya v kosmicheskikh luchakh v Avguste 1972, Doklad na Vsesoyusnoi Konferentsii po kosmicheskim lucham, Apatity. |
| LINCOLN, J. V. and
H. I. LEIGHTON | 1972 | Preliminary Compilation of Data for Retrospective World Interval July 26 - August 14, 1972, <u>World Data Center A for Solar-Terrestrial Physics, Report UAG-21, November, 1972.</u> |

Note: World Data Center A for Solar-Terrestrial Physics holds tables of the August event data including: Neutron Monitor data from Yakutsk and Oktyomtsky, hourly and 15-minute values; Yakutsk semicubical telescope hourly data, vertical, at sea level and 7, 20 and 60 m.w.e. underground.

México City Cosmic Ray Observations during the Large Solar Events of August 1972

by

Oscar Troncoso Lozada
 Instituto de Geofísica, Universidad Nacional de México and
 Instituto Nacional de Energía Nuclear, México

Continuous cosmic ray hourly mean data recorded by the Mexico City neutron monitor, IGY type ($P_C = 9.5$ GV) from July 26 to August 14, 1972 are shown in Figure 1; World Data Center A for Solar-Terrestrial Physics holds the numerical table of data for this period. The gross features of the variations in intensity of the nucleonic component observed during the period reported are given in the Table 1. This reflects a variation in the solar activity during that period of time.

Comparison of cosmic ray charts from Calgary, Sulphur Mountain [Lincoln and Leighton, WDC-A, 1972], Mt. Norikura and Tokyo-Itabashi [WDC-C2, 1972], with our cosmic ray graph given in Figure 1 shows some interesting anisotropic features. After the first Forbush decrease on August 4, the cosmic ray intensity began to increase at Calgary and Sulphur Mountain at 1200 UT and reached the maximum at 1500 UT, six hours earlier than at the low-latitude stations of Mt. Norikura, Tokyo-Itabashi and Mexico City. Also at these three stations, no short-lived intensity increase was recorded on August 7 during the recovery phase. Since such an increase was detected by the high-latitude stations, it was most probably due to solar cosmic rays. Meanwhile, we are led to believe that the first anisotropic increase was produced by galactic cosmic rays. Suggestions concerning the modulating mechanism directly associated with the cosmic ray increase will be published once the experimental data are properly analyzed.

Table 1

FORBUSH DECREASE		COSMIC RAY INCREASE		PERCENTAGE DEPARTURES
Start	End	Start	End	(from the pre-event mean level)
UT	UT	UT	UT	%
04/0300	04/1600.			10.0
		04/1700	04/2100.	5.8
04/2200	05/0200			12.5
		05/0300	05/0700	10.2
05/0800	05/1400			4.3
		05/1800	x	Recovery time: approx. 10 days

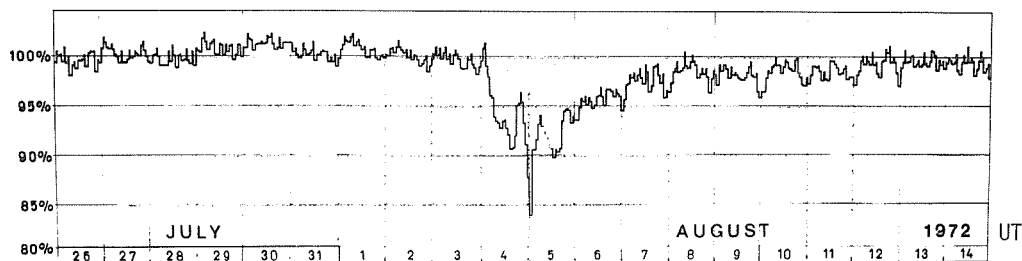


Fig. 1. Cosmic ray hourly mean data recorded by the Mexico City neutron monitor, July 26 - August 14, 1972.

REFERENCES

- LINCOLN, J. V. and H. I. LEIGHTON, WDC-A 1972 Preliminary Compilation of Data for Retrospective World Interval July 26 - August 14, 1972, World Data Center A, Upper Atmosphere Geophysics Report UAG-21, 116.
- WDC-C2 1972 World Data Center-C2, August 19, 1972.

Cosmic Ray Hourly Intensities During August 1 - 10, 1972

by

Y. Miyazaki, S. Kawasaki, M. Kodama, K. Murakami and M. Wada
Cosmic Ray Laboratory, Institute of Physical and Chemical Research
Kaga-1, Itabashi, Tokyo, Japan

and

L. S. Chuang
Department of Physics, Chinese University of Hong Kong
Shatin, N.T., Hong Kong

and

Y. Nakano
Physics Department, Hokkaido University of Education
Sapporo, Japan

We present here the hourly digital data of cosmic ray intensities recorded by our instruments in Japan and at Hong Kong in their graphical representations.* A brief description of each observation is given below.

Neutron Monitors

The graphs are plotted in natural logarithms of the respective counting rates. The difference between the linear and logarithmic scales becomes significant for large variations such as the one that occurred in the present case. For example, the difference between the daily average of August 3 and the hourly value at 0000-0100 UT on August 5 at Syowa is 33% or 0.33 in logarithmic value, whereas it is 28% if the value of August 3 is taken as the reference.

The pressure correction is carried out by

$$N_{\text{corr}} = N_{\text{obs}} \times \exp(-b(P - P_0))$$

where b is the barometer coefficient which is negative, and P_0 is the standard pressure to which N_{corr} is reduced.

Ionization Chambers

The percentage deviations from adequately set level are given in the tables. In the graphs, deviations from the average of August 2 and 3 are plotted. Variations equivalent to the atmospheric temperature variations are shown by circles at times of the radiosonde observations. SN and SC stand for solar noise outbursts and sudden commencements, respectively. Linear correction is applied for the barometric effect.

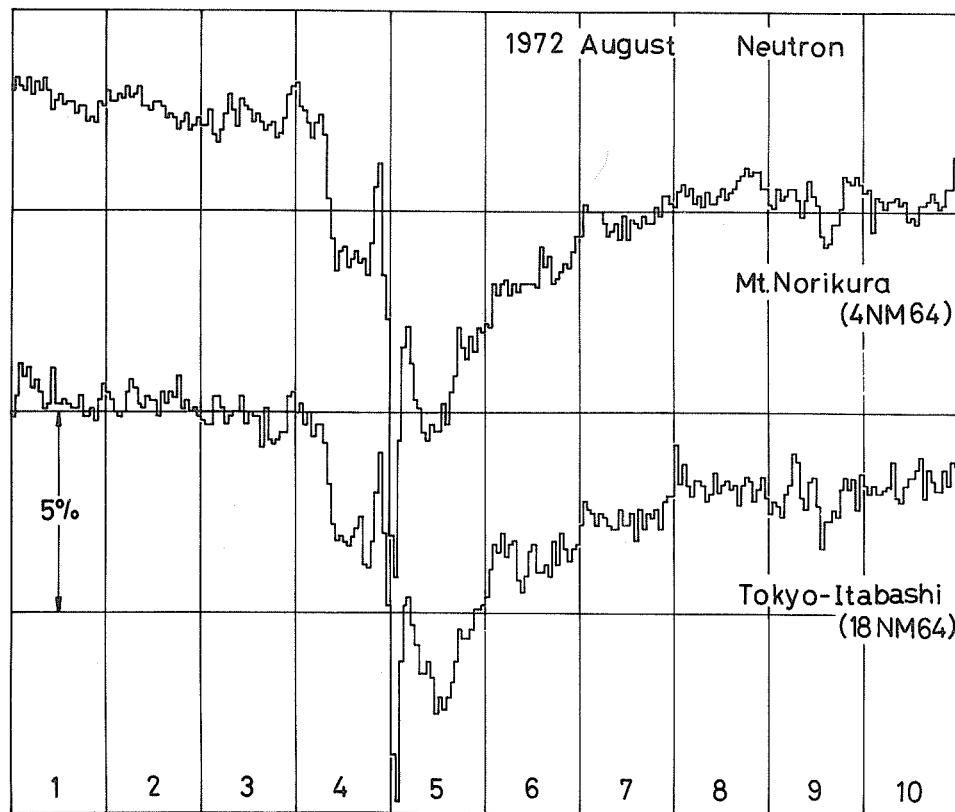
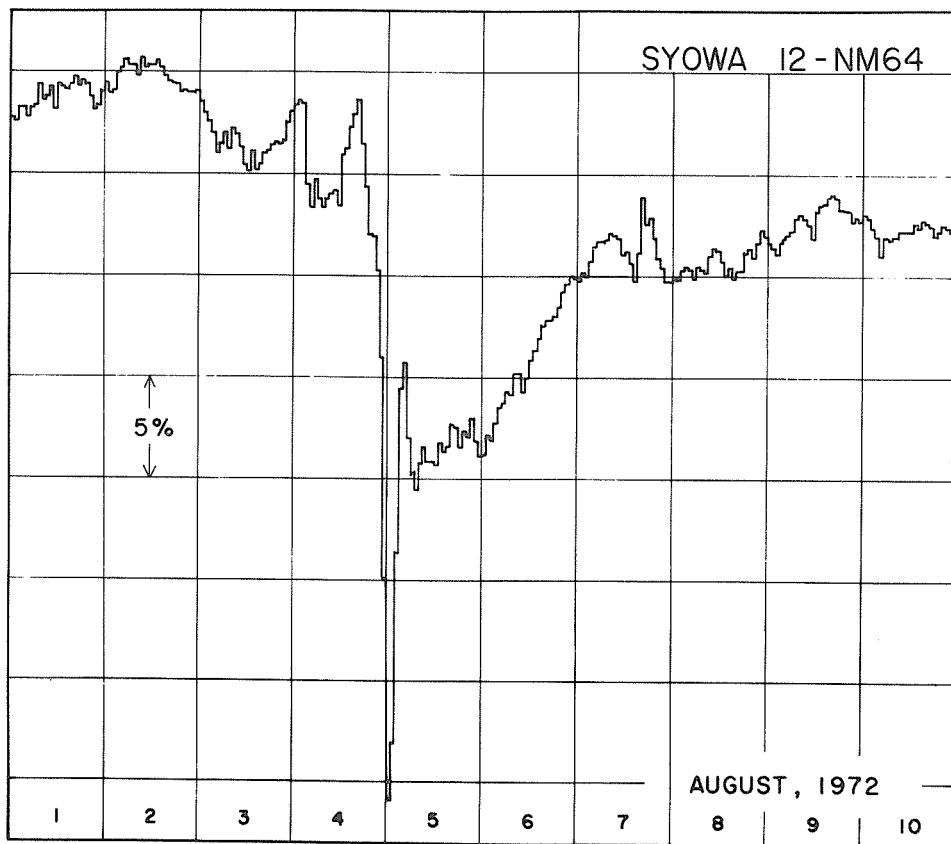
Underground Meson Telescopes

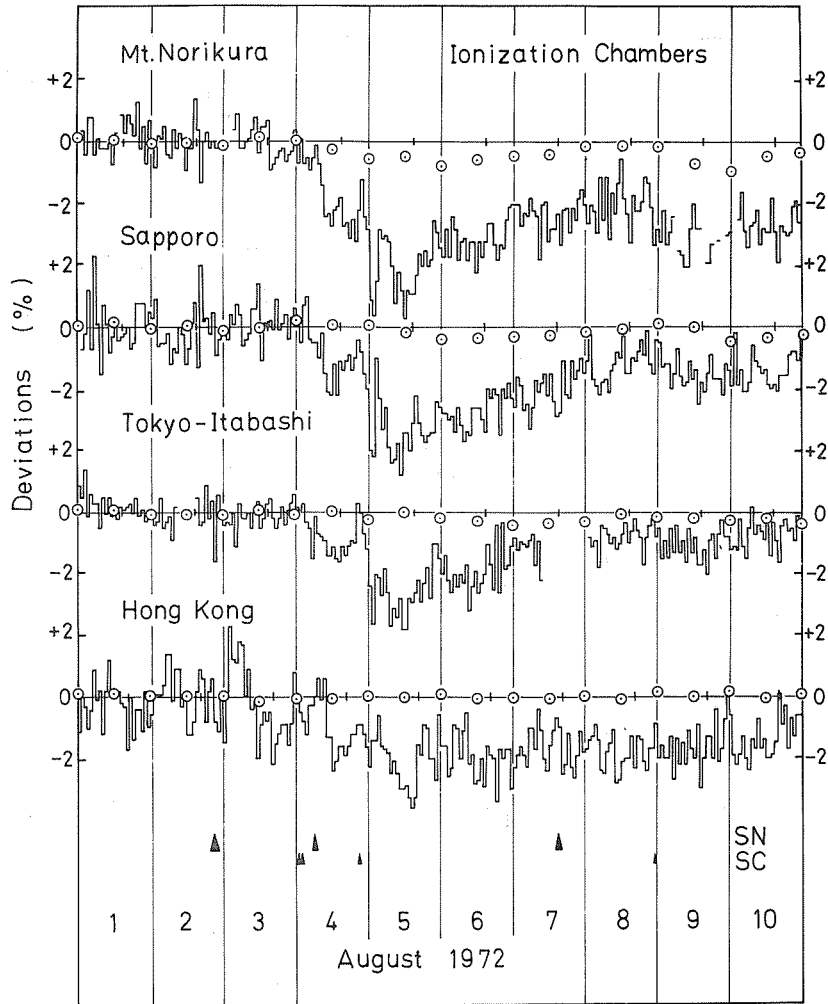
The data for the inclined directions are given only in graphical form. The data are not corrected for the atmospheric effect, which is not serious in the present case.

REFERENCES

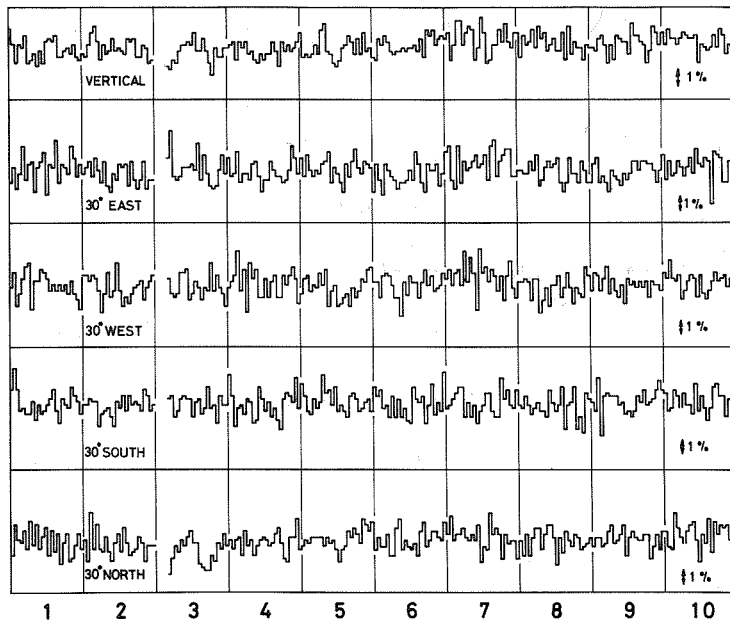
- | | | |
|----------------|------|--|
| CHUANG, L. S., | 1973 | August 1972 Cosmic Ray Event as Observed at Different Stations by Identical Ionization Chambers, <u>Sci. Papers I.P.C.R.</u> , <u>67</u> , 1-6 |
| S. KAWASAKI, | | |
| Y. NAKANO, | | |
| M. WADA and | | |
| Y. MIYAZAKI | | |

*Tables of these hourly readings August 1 - 10, 1972 are available from World Data Center A for Solar-Terrestrial Physics.





TAKEYAMA UNDERGROUND 1972 AUGUST



Multi-directional Meson Intensities at Mt. Norikura and Nagoya, August 1972

by

Y. Sekido, K. Nagashima, I. Kondo, H. Ueno, K. Fujimoto and Z. Fujii
Department of Physics, Nagoya University, Nagoya, Japan

The solar flares in early August 1972 produced various solar-terrestrial events. The Cosmic ray storm that started on August 4 was observed by multi-directional meson telescopes at Mt. Norikura and Nagoya (Table 1) [Nagashima, 1972; Shea, 1972]. Hourly averaged intensities for several components observed at Mt. Norikura and Nagoya are plotted in Figures 1 and 2, respectively. Figures 1a and 2a show time variations observed at vertical and 30° zenith angle, whereas Figures 1b and 2b show those observed at 49° (Mt. Norikura) and 55° (Nagoya) zenith angles. These components reflect cosmic ray variations in different rigidity ranges arising from differences in cut-off rigidities and effective atmospheric depths as well. Thus, it is possible to determine the rigidity dependence of the cosmic ray variation in a selected interval by comparing the amounts of intensity change of different components. Assuming a power law spectrum ($P \propto R^{-\gamma}$) for the rigidity dependence, the relative intensity change of various components were calculated for $\gamma = 0, -0.25, -0.5, -0.75, -1.0, -1.5$ and -2.0 and were compared with the observed intensity changes.

1. Differences between the daily mean intensities on August 1 and August 5 were chosen to denote the amount of the decrease of the cosmic ray intensity on a day-to-day basis. The rigidity dependence of this decrease was found to have the best fit with the power law spectrum for $\gamma = -0.75$ as shown in Figure 3. Even the decrease of the EEE component at Nagoya which has the highest effective rigidity (~ 200 GV) agrees with the theoretical calculation.
2. A short period increase (or recovery) of intensity was observed between 0200 - 0600 UT August 5 following the sharp minimum at 0000-0200 UT. An increase of low energy proton flux was observed by IMP 5 and 6 [Bostrom, 1972] almost in coincidence with this intensity change. Rigidity dependence of the intensity differences between the averages for 0300 - 0500 UT and 0000 - 0200 UT was found to have the best fit with the power law spectrum for $\gamma = 1.5$ as shown in Figure 4. This fact shows that this intensity change has much softer spectrum than the day-to-day variation.

REFERENCES

- | | | |
|----------------------|------|--|
| NAGASHIMA, K. et al. | 1972 | Three-dimensional cosmic ray anisotropy in interplanetary space, Part IV, - Origin of solar semi-diurnal variation <u>Rep. Ionos. Space Res. Japan</u> , <u>26</u> , 38. |
| SHEA, M. A. | 1972 | Ground-based cosmic ray instrumentation catalog, Air Force Cambridge Res. Lab., AFCRL-72-0411, <u>Air Force Surveys in Geophysics</u> , No. 243. |
| BOSTROM, C. O. | 1972 | Preprint, John Hopkins Univ., Md., USA |

Note: Neutron monitor data were provided by WDC-C2.

Table 1

Characteristics of Multi-directional Meson Telescope at Mt. Norikura and Nagoya

Component	Azimuth	Zenith	Cut-off Rigidity P_c (Gv)	Mt. Norikura			Nagoya		
				Counting Rate $N \cdot 10^6$ hr	Standard Error σ hr %	Barometric Coefficient -B %/mb	Counting Rate $N \cdot 10^6$ hr	Standard Error σ hr %	Barometric Coefficient -B %/mb
V		Vertical	11.5	6.3	0.04	0.29	2.7	0.06	0.12
N	North	30°	13.2						
E	East	30°	16.6						
S	South	30°	11.3	3.0	0.06	0.31	1.2	0.09	0.12
W	West	30°	9.4						
NE	North-East	39°	17.7						
ES	East-South	39°	14.9	1.5	0.08	0.32	0.57	0.13	0.12
SW	South-West	39°	9.3						
WN	West-North	39°	11.1						
NN	Far-North	49°	13.5						
EE	Far-East	49°	20.7						
SS	Far-South	49°	11.0	1.3	0.08	0.34	0.47	0.14	0.12
WW	Far-West	49°	9.4						
NNN	Three-North	55°	10.7						
EEE	Three-East	55°	23.4						
SSS	Three-South	55°	10.9	-	-	-	0.13	0.28	0.15
WWW	Three-West	55°	8.4						

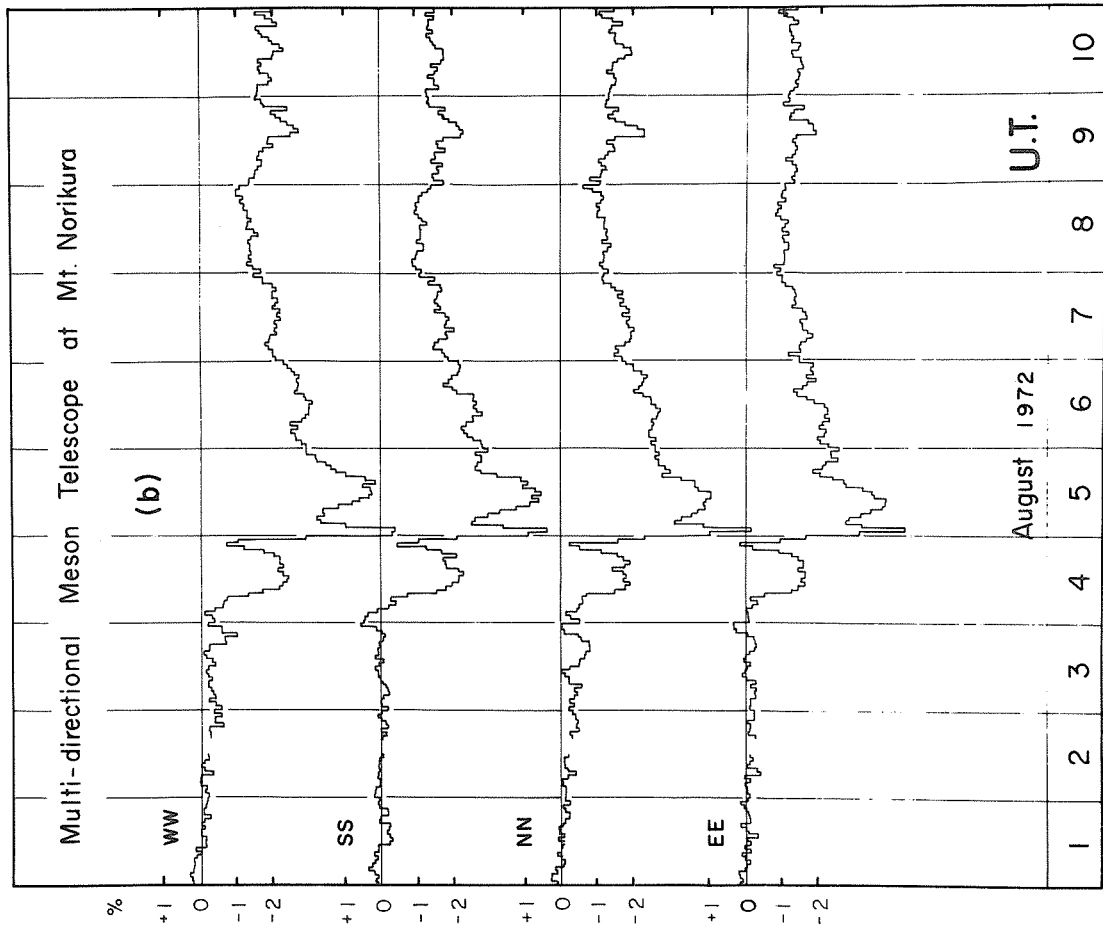
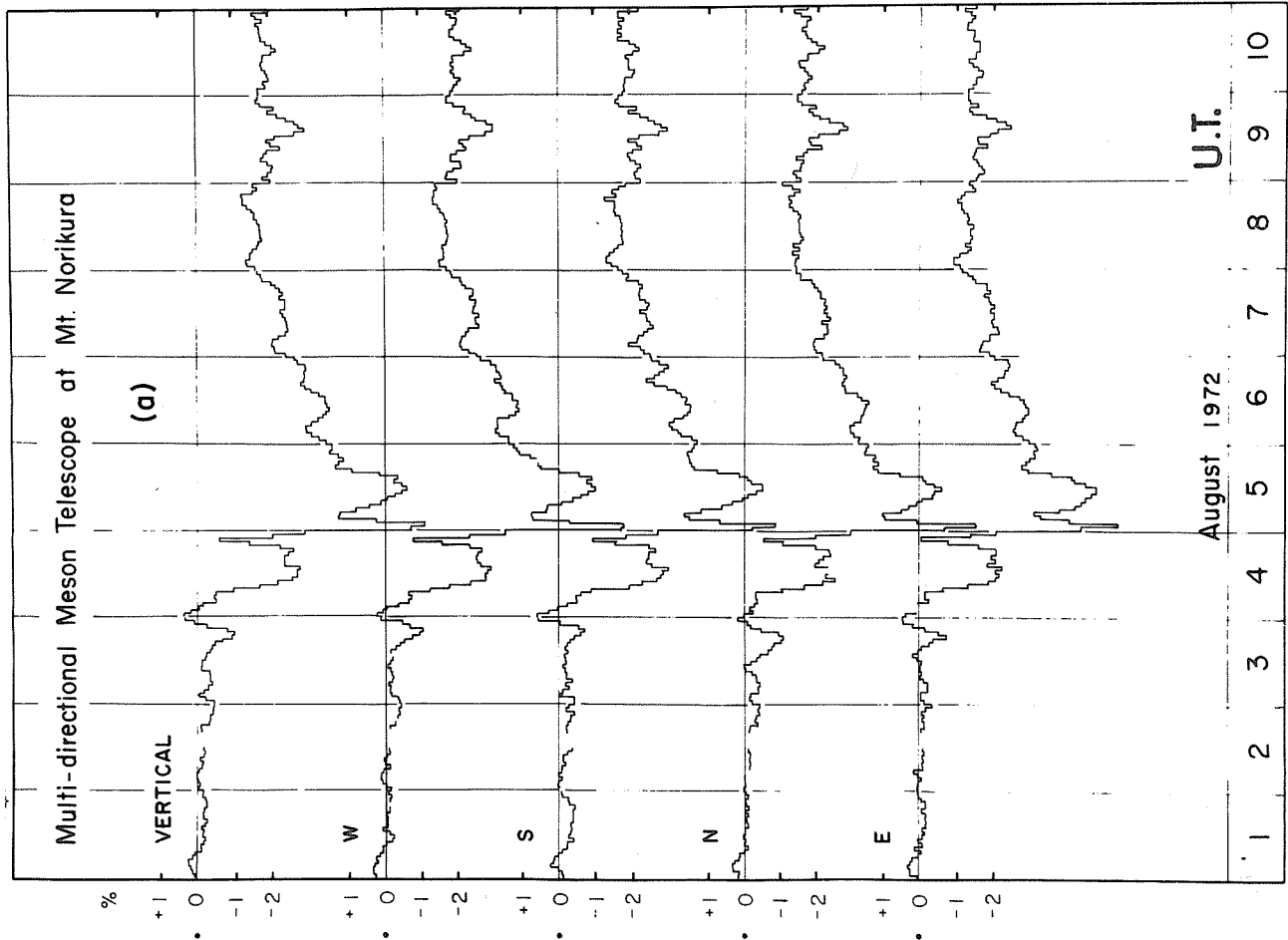


Fig. 1. Variations of cosmic ray intensities observed by the multi-directional meson telescope at Mt. Norikura corrected for the barometric effect. (a) and (b) show time variations observed at the vertical and 30° zenith angle and 49° zenith angle, respectively.

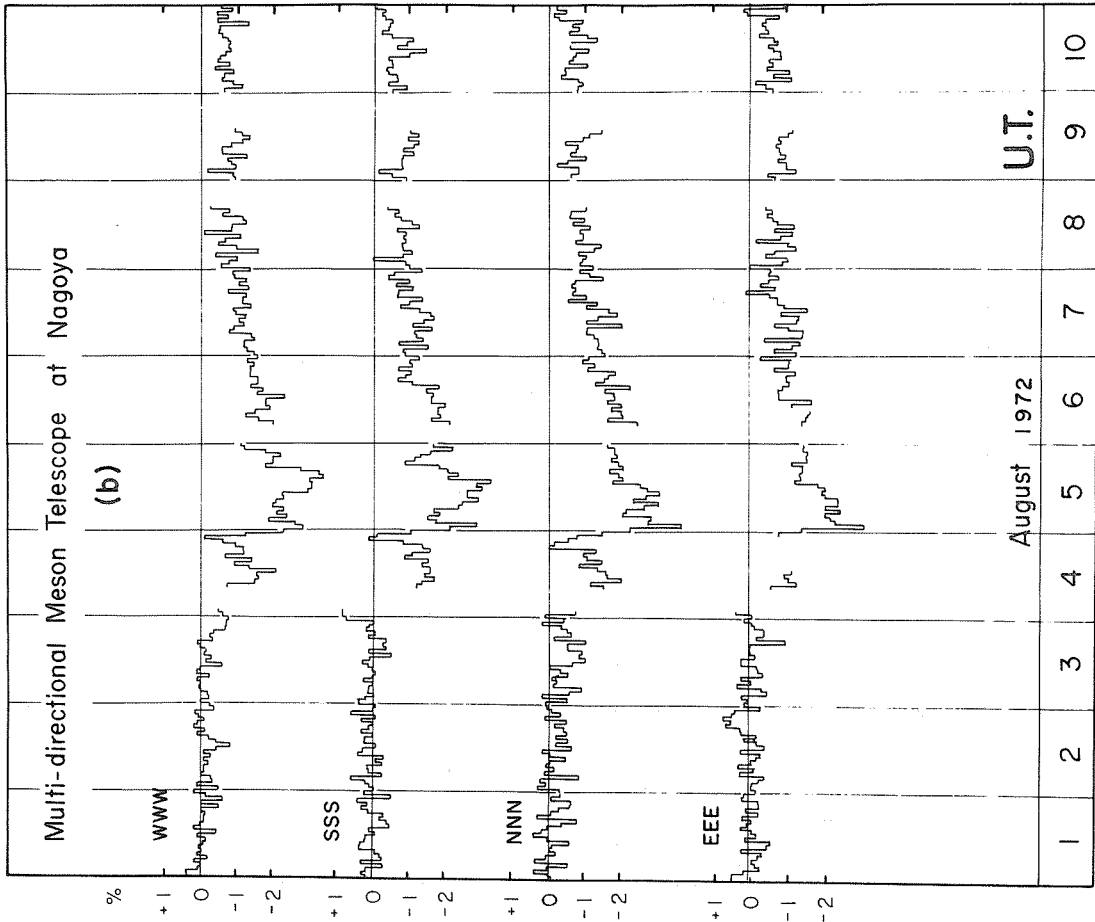
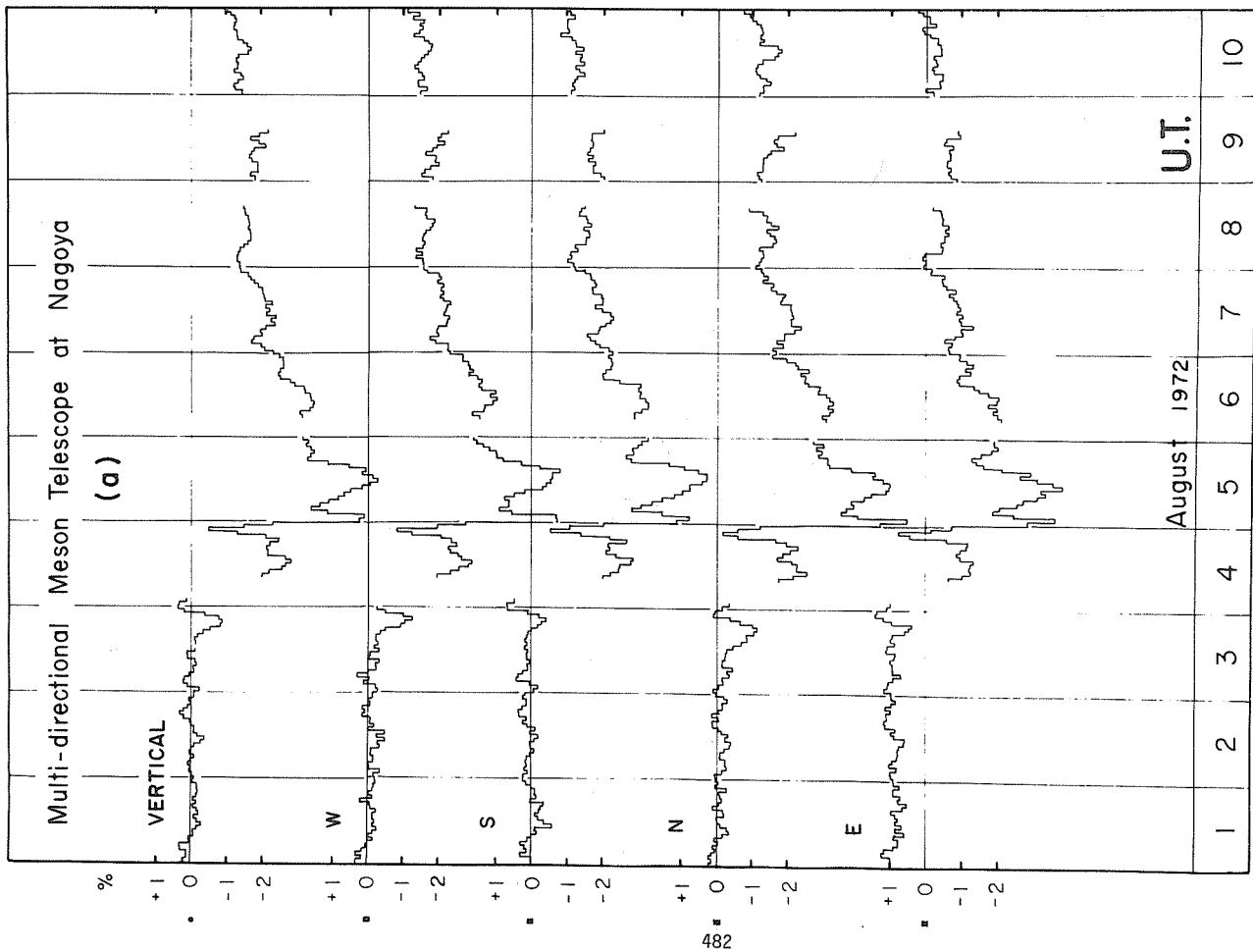


Fig. 2. Variations of cosmic ray intensities observed by the multi-directional meson telescope at Nagoya corrected for the barometric effect. (a) and (b) show time variations observed at the vertical and 30° zenith angle and the 55° zenith angle, respectively.

x K
 xx x S
 U C

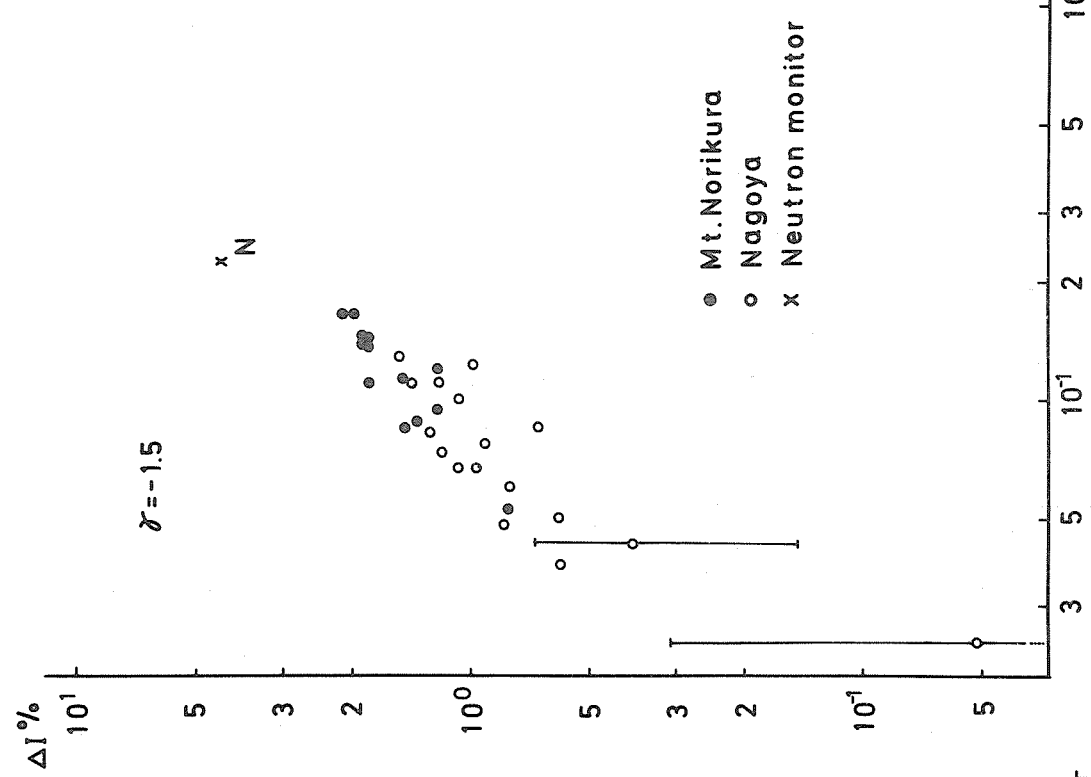


Fig. 4. Correlation between a short period increase on August 5 and expected relative intensity variation for $\gamma = -1.5$. The characters N, U, K, C and S denote neutron monitor data at Mt. Norikura, Uppsala, Kiel, Calgary and Sulphur Mountain, respectively.

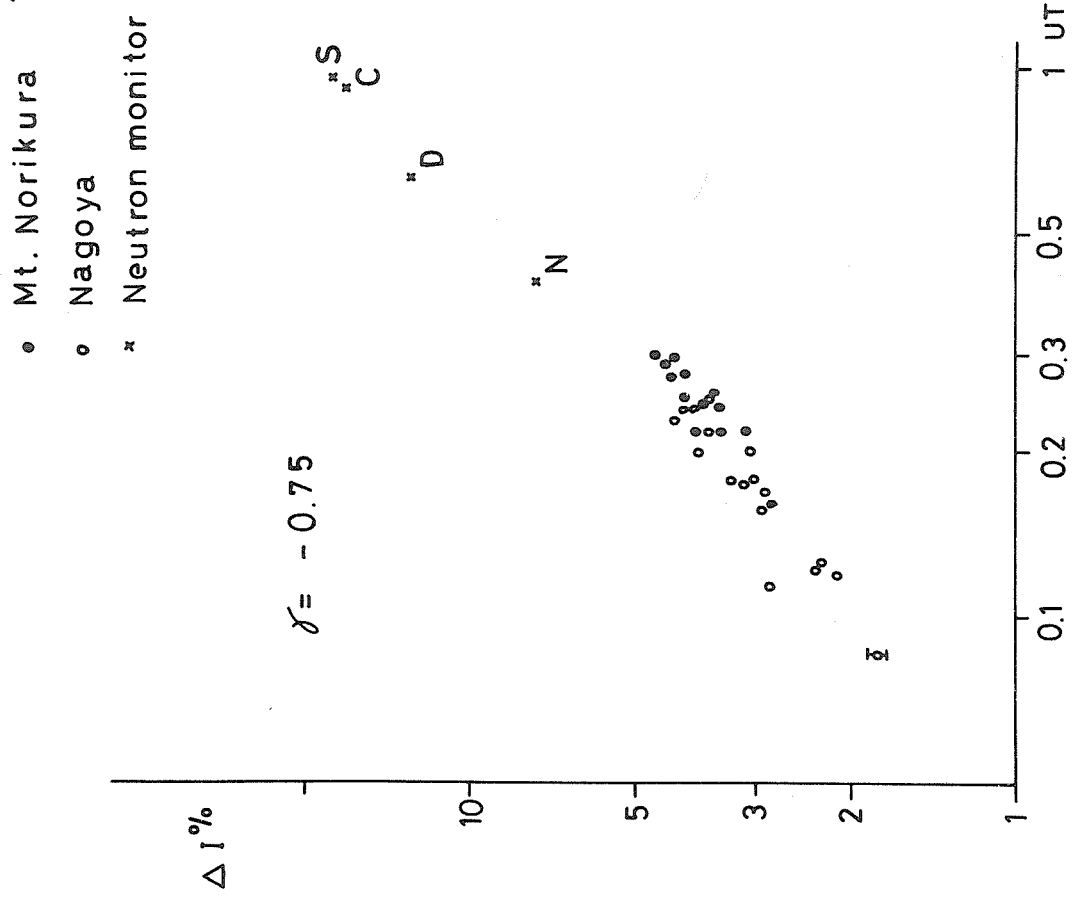


Fig. 3. Correlation between the decrease of the cosmic ray intensity on a day-to-day basis and expected relative intensity variation for $\gamma = -0.75$. The relative intensity variation were normalized to 1 at 10 GV. The characters N, D, C and S denote neutron monitor data from Norikura, Dallas, Calgary and Sulphur Mountain, respectively.

Cosmic Ray Neutron Intensity during the Interval
July 26 - August 14, 1972 at Morioka, Japan

by

Hachiro Takahashi and Toshimi Chiba
Department of Physics
Iwate University
Morioka, Japan

Abstract

A very sharp decrease of cosmic ray neutron intensity was observed early in August 1972 at Morioka, Japan. This paper gives the digital values of the observed neutron intensities. The minimum occurred at 0000-0200 UT on August 5 during the period concerned.

The Neutron Monitor

A Simpson's type neutron monitor was set up on the campus of Iwate University in May 1970 [Takahashi *et al.*, 1971; Chiba, 1971]. Its location is given in Table 1, together with that of the Morioka Local Meteorological Observatory, from which barometric data are supplied for pressure correction of the counting rates. The counting rate of the monitor was found to be 1197.0 ± 9.1 x8/hr, which was reduced to the value at barometric pressure 1000 mb.

Table 1. Location of observational station

Station	Geographic		Height	Cut-off rigidity
	Longitude	Latitude		
Iwate University	141°08' E	39°42' N	135.0 m	10.13 GV*
Morioka Local Meteorological Observatory	141°10' E	39°42' N	156.4 m	

* M. A. Shea: (Private communication).

Observational Results

The values of the cosmic ray neutron intensity observed at Morioka are shown in Figure 1 during the interval July 26 - August 14, 1972. It is clear from Figure 1 that the observed neutron intensities at 0000-0200 UT on August 5 indicate a decrease of about 10% from the normal level for the ten days prior to August 5.

REFERENCES

- | | | |
|--|------|---|
| TAKAHASHI, H., T. CHIBA
and N. YAHAGI | 1971 | Observation of Cosmic-Ray Neutron Intensity at Morioka, Part I. The Neutron Monitor, <u>Annu. Rep. Faculty of Education, Iwate Univ.</u> , <u>31</u> , 15-24. |
| CHIBA, T. | 1971 | Observation of Cosmic-Ray Neutron Intensity at Morioka, Part II. Barometric Pressure Effect, <u>Annu. Rep. Faculty of Education, Iwate Univ.</u> , <u>31</u> , 25-29. |

NOTE: World Data Center A for Solar-Terrestrial Physics holds the hourly tabulated neutron monitor data for Morioka for this period.

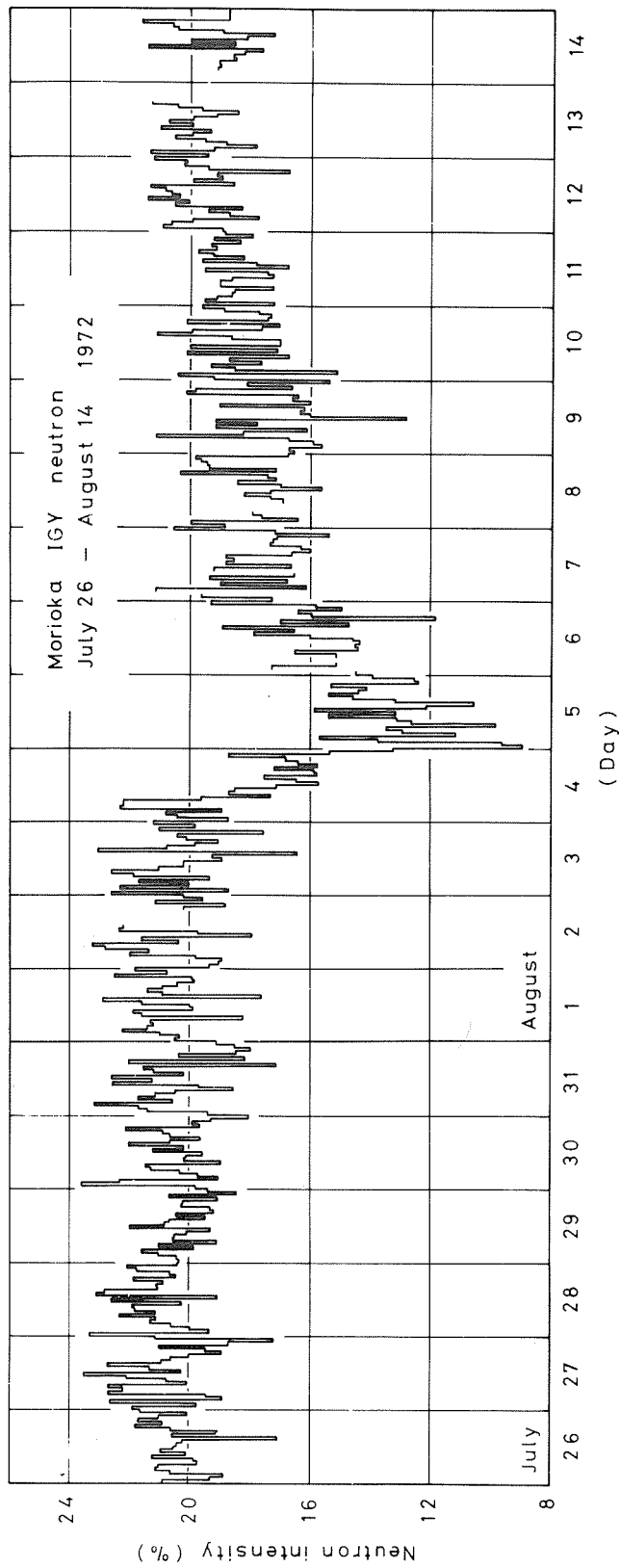


Fig. 1. Hourly values of cosmic-ray neutron intensity variation in unit of % during the interval July 26 - August 14, 1972 observed at Morioka.

Unusual Cosmic Ray Intensity Variations in August 1972

by

Prof. U. R. Rao
Chairman, Cosmic Ray & Radio Astronomy Group
Physical Research Laboratory
Navrangpura, Ahmedabad 380009, India

A variety of solar and terrestrial events, associated with the remarkable McMath plage region 11976, were observed during the early period of August 1972. These events have not only attracted the attention of the scientific community dealing with the solar-terrestrial relationships but also the public in general. Unusual cosmic ray intensity variations were also recorded during the period August 4-9, 1972. Figure 1 depicts the cosmic ray intensity variations (percentage deviation) for a network of equatorial neutron and meson monitors operated by Physical Research Laboratory, Ahmedabad, namely, Gulmarg neutron monitor, Ahmedabad super neutron monitor and Ahmedabad meson scintillation telescope.

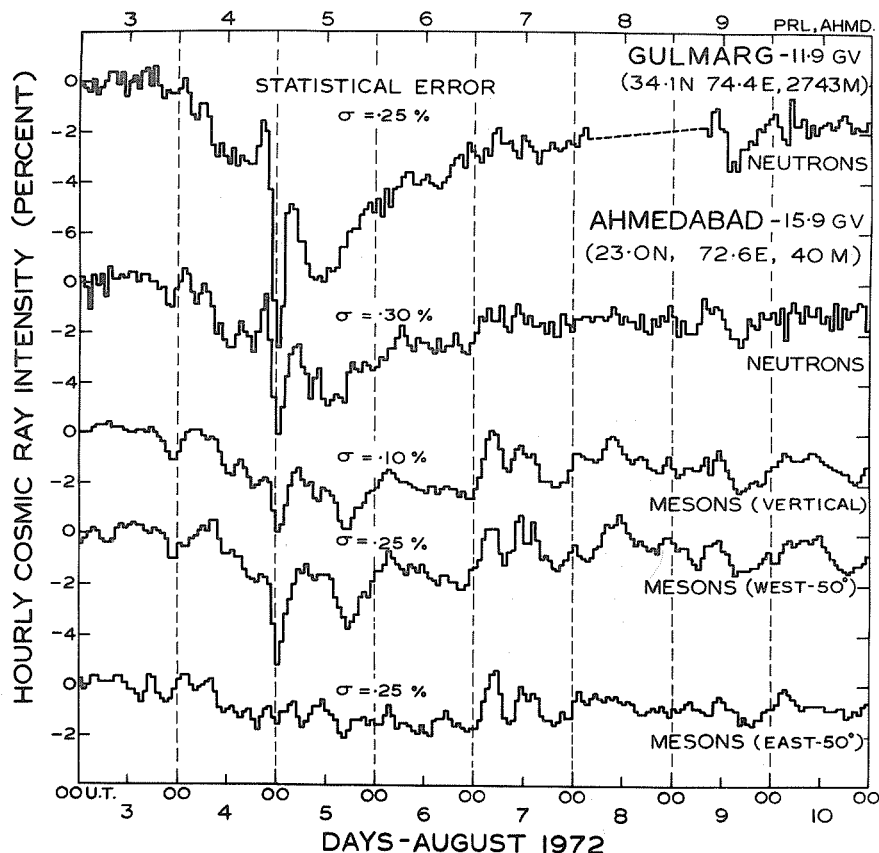


Fig. 1 Cosmic ray intensity variations are shown from a network of equatorial neutron and meson monitors for the period August 3-10, 1972.

Besides the spectacular and unusually large Forbush decrease observed during early hours of August 5, 1972, there were other cosmic ray variations of great importance. The unambiguous cosmic ray intensity increase on 4 August 1972 (2100-2200 UT), before the commencement of large Forbush decrease, is seen more prominently in equatorial monitors (high cut-off rigidity) as compared to the high latitude monitors, thereby indicating a positive exponent in the rigidity spectrum during this increase. A similar behavior is again observed on 5 August 1972 (0400-0600 UT) during the recovery phase of the Forbush decrease. This event is also accompanied with large anisotropies at higher rigidities. The chain of events during August 1972 are being analyzed in detail by the scientists in the Cosmic Ray and Radio Astronomy Group here and the preliminary results using the data from a large number of neutron and meson monitoring stations indicate the presence of intense, short-lived anisotropies of large magnitude throughout the event which have a bearing on the propagation and storage of relativistic particles near the sun. The detailed analysis of these events will be presented elsewhere.

Forbush Decrease of August 4, 1972

by

H. Razdan and M. M. Bemalkhedkar
High Altitude Research Laboratory
Navrangpura, Ahmedabad, India

Gulmarg Neutron Monitor
Geog. Long. 74.42°
Geog. Lat. 34.07°
Altitude 9000 feet

The Forbush decrease of August 4, 1972 is a two step decrease. With the Gulmarg neutron monitor (see Figure 1) the first decrease started at about 0200 UT August 4, 1972. The intensity reached $\cong 96\%$ level by 1000 UT and remained nearly constant till 1900 UT. A significant increase in the intensity of magnitude 1.7% was then recorded at 2100 UT which was followed by the main sharp decrease. The intensity reached its minimum of 89.4% level by 0100 UT August 5, 1972 resulting in a total decrease of $\cong 10.6\%$ with respect to intensity level on August 2, 1972. Immediately after, a sharp increase in intensity was again observed, reaching a level of 95.1% by 0400 UT, followed by a shower decay to 92.1% by 1200 UT on August 5, 1972. Thereafter, the intensity recovered continuously till August 8, 1972. Data during some hours on August 8 and 9, 1972 were not recorded due to camera failure. Another smaller Forbush decrease of about 2% was recorded on August 9, 1972 which reached its minimum at 1400 UT on the same day. The full recovery to 100% level was achieved on August 15, 1972.

No intensity increases were observed around 1600 UT on August 4, 1972 and at 1700 UT on August 7, 1972 which were observed at the high latitude neutron monitors.

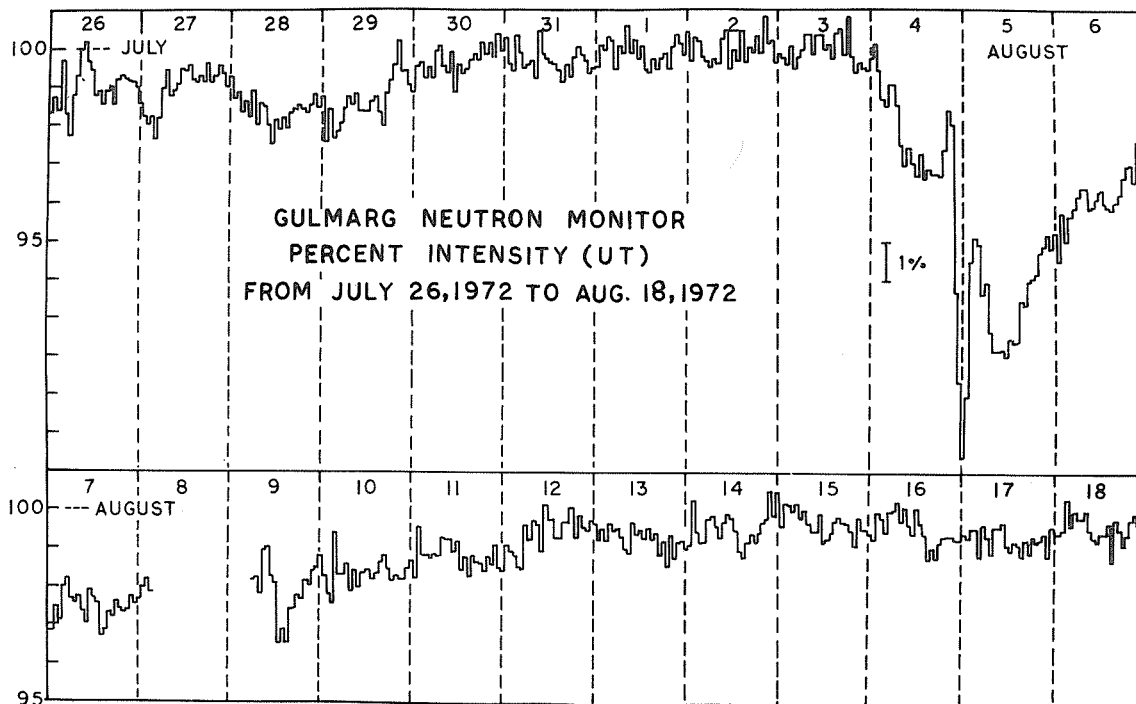
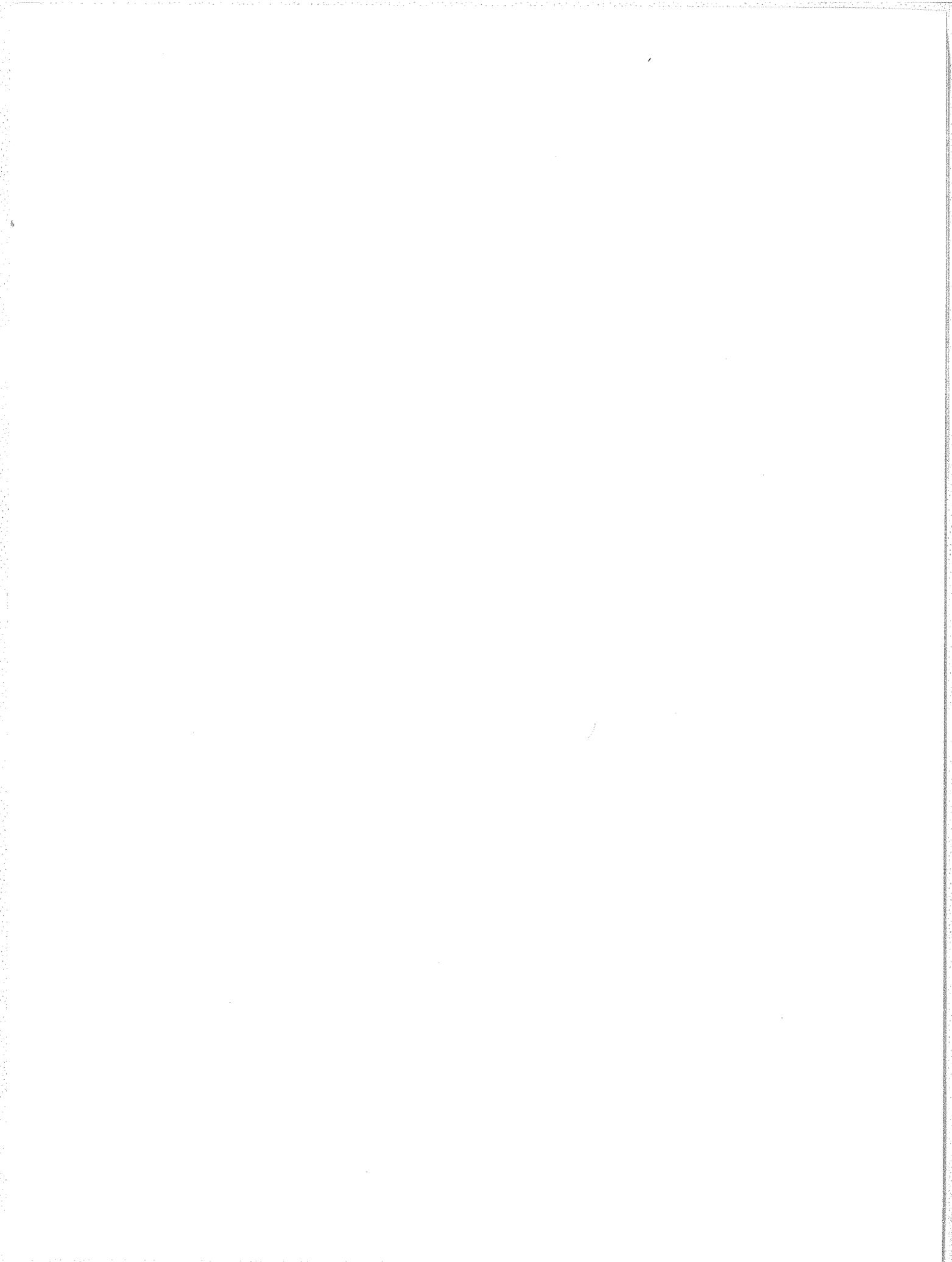


Fig. 1.* Gulmarg neutron monitor hourly data for July 26 - August 18, 1972.

*World Data Center A for Solar-Terrestrial Physics hold tables of the data shown in Figure 1. They were not reprinted here due to lack of space, but are available upon request.



6. IONOSPHERE

Summary on page 8.

For basic data and indices for this section and others, see Appendix I for Table of Contents to Report UAG-21.

For data papers presented or published elsewhere which contain additional information on ionospheric observations and the other categories included in this report, see Appendix II.

For Tables of hourly foF2 from 64 stations covering the period August 1-11, 1972, see Appendix I.

For plots of hourly foF2 and fmin from 8 stations covering the period July 26 - August 14, 1972, see Appendix I.

Overview of Solar Events and Related Auroral-Zone Geophysical Observations during the August 1972 Storm

by

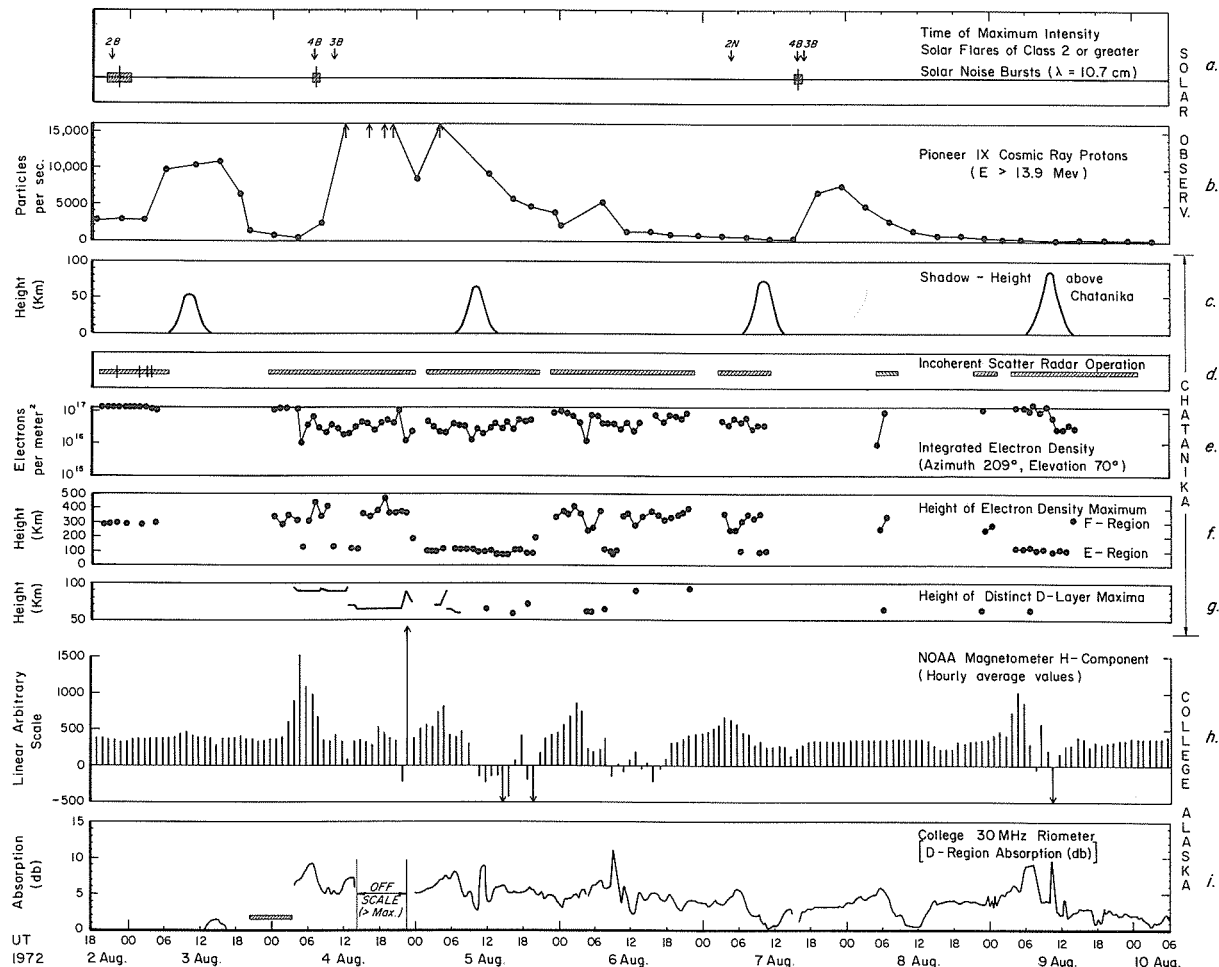
Robert D. Hunsucker
 Geophysical Institute, University of Alaska
 Fairbanks, Alaska 99701

The purpose of this brief report is to relate ionospheric data obtained in the auroral zone (College and Chatanika, Alaska) to solar events during the August 1972 storm. Figure 1 shows selected solar observations, incoherent scatter radar data, geomagnetic variations, and D-region absorption for the period 1800 UT 2 August until 0600 UT 10 August 1972. Plot a. in Figure 1 indicates the time of maximum intensity of solar flares of Class 2 or greater (arrows) and solar radio noise bursts at $\lambda = 10.7$ cm (shaded blocks). Figure 1b. shows the intensity of cosmic-ray protons of Energy > 13.9 Mev measured by the Pioneer IX satellite. Figure 1c., f., and g. illustrate measurements made by the Chatanika, Alaska, incoherent-scatter radar [Leadabrand, et al., 1972]. Figure 1d. shows the solar shadow height above Chatanika, indicating that the ionosphere above the D-region was sunlit all the time during the observations. The Chatanika radar operates at a frequency of 1290 MHz, and during the storm the following operating parameters were used:

- | | |
|---|--|
| Pulse power output = 3 MegaWatts | Beamwidth resolution = 1 to 3 km |
| Pulse lengths = 320 and 67 μ sec | Lower electron density threshold $\approx 10^4$ e l/cm^3 |
| Range resolution = 10 km | Antenna elevation = 70° |
| Antenna azimuths = 89°, 209°, and 329° geographic for 10 minutes at each azimuth. | |

Figure 1d. shows by shaded bars the periods when the Chatanika radar was operating. The vertical lines on August 2 - 3 indicate solar noise bursts at 1290 MHz.

During the most active part of the storm the decreases in electron density (integrated from h = 50 to 500 km) correlated quite well with positive geomagnetic H-component variations. Every D-layer absorption peak (Figure 1i.) was accompanied by either a thick, low E-layer or a distinct D-layer observed with the Chatanika radar, which agrees with results reported by Hunsucker, et al. [1972].



References

Hunsucker, R.D., H.F. Bates,
and A. E. Belon

1972

Observations of simultaneous auroral D
and E layers with incoherent-scatter
radar, Nature-Physical Science, 239,
102--104.

Leadabrand, R.L., M.J. Baron,
J. Petriceks, and H.F. Bates

1972

Chatanika, Alaska, auroral zone inco-
herent scatter facility, Radio Science,
7, 747--756.

Electron Density Variations at Chatanika, Alaska,
during the Storm of August 04-09, 1972

by

B. J. Watkins, H. F. Bates, A. E. Belon and R. D. Hunsucker
Geophysical Institute
University of Alaska
Fairbanks, Alaska 99701

The Chatanika Incoherent Scatter Radar [Leadabrand et al., 1972] was in operation before and during most of the storm of August 04-09, 1972. We present in Figures 1 through 8 electron density measurements at 110 and 350 km altitudes which are representative of auroral particle precipitation and F-region behavior, respectively. Electron density vs. height profiles are also illustrated on the Figures at approximately two hour intervals.

During the period of operation, the radar was used to make successive ten minute measurements in three different directions. The antenna was fixed at 70° elevation, then rotated 120° in azimuth each ten minutes. The 110 and 350 km density variations have been derived by plotting the ten minute average densities at successive antenna positions. Only those density vs. height profiles obtained at an antenna azimuth of 209° and elevation 70° are shown. At this orientation the radar antenna is nearly directed toward the magnetic zenith (azimuth 209°, elevation 76.5°).

All the data shown were derived from a radar pulse length of 67 μ s (10 km spatial resolution) except that for August 9 which used a pulse length of 320 μ s (48 km resolution).

The radar was operated the day before the storm onset and almost continuously during the storm period; however, no data are available for some periods, and a large gap occurs on August 7 and 8 because of instrumental problems.

Notable features on the vertical profiles during the period 1200 - 2300 UT August 4 (Figure 2) are the large D-region densities (at about 75 km altitude) associated with the solar proton event. It was during this period that the College riometer displayed maximum absorption (greater than 10dB) for the entire storm period.

Large fluctuations in the E-region densities were noted. Good examples of auroral E-layers can be seen in the density profiles at 1400 UT August 5 (Figure 4), and 0900 UT August 6 (Figure 6). At about 0400 UT (1600 LT) August 4 (Figure 1), the radar probably moved from beneath the auroral oval as evidenced by the sudden change of E-region densities; and subsequent to this time large variations were noted at altitudes 100 - 120 km until August 9. Unfortunately no darkness occurs during August at Chatanika, and no optical data on auroral behaviors are available. For the period 0000 - 0300 UT August 4 (i.e., prior to the onset of the storm) as shown in Figure 1 the F-region densities are large but have the same general shape as other quiet daytime density profiles obtained by the radar in the month of August. Subsequent to this period F-region densities were depressed for all the data obtained.

REFERENCE

- | | | |
|-------------------|------|--|
| LEADABRAND, R. L. | 1972 | Chatanika, Alaska, Auroral Zone Incoherent Scatter |
| M. J. BARON, | | Facility, <u>Radio Science</u> , 7, July. |
| J. PETRICEKS and | | |
| H. F. BATES | | |

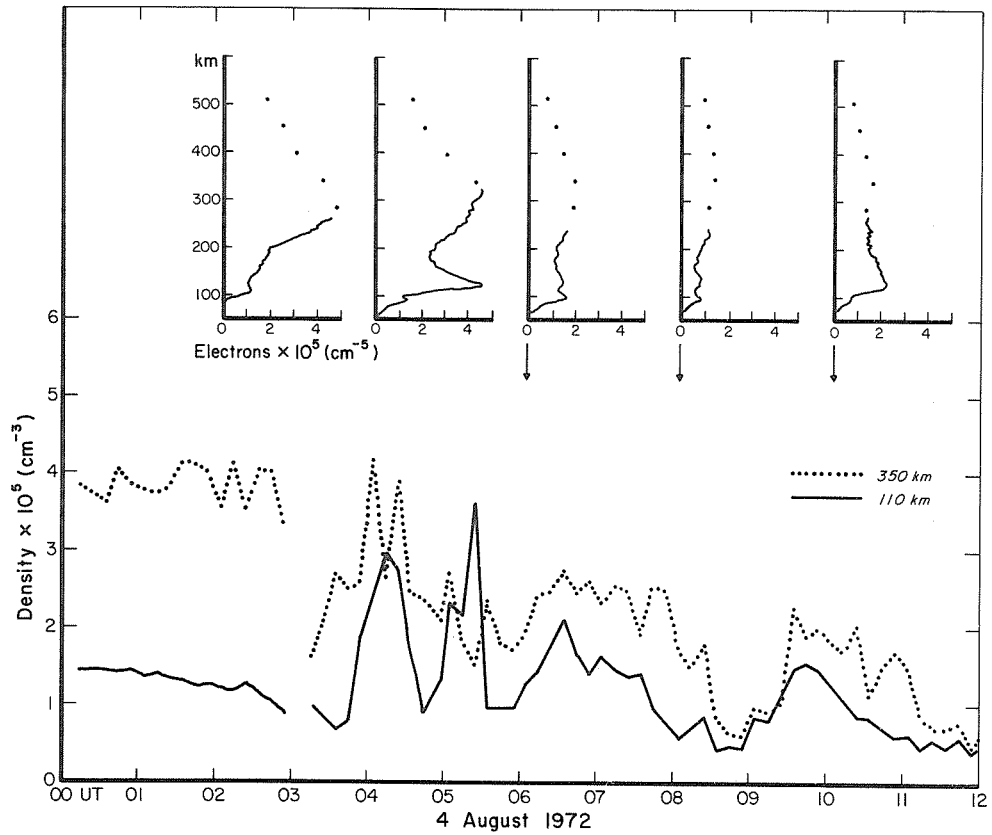


Fig. 1. Electron density variations at 110 and 350 km altitudes. Above these plots are shown electron density profiles at approximately two hour intervals.

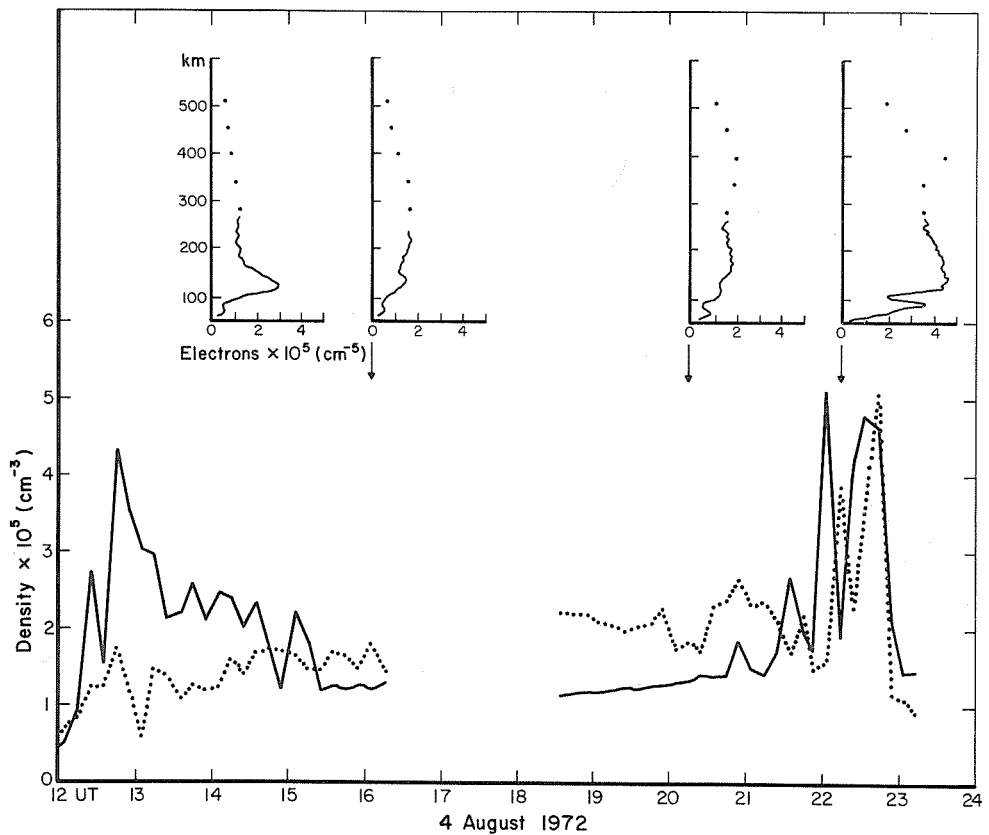


Fig. 2. Same as in Figure 1.

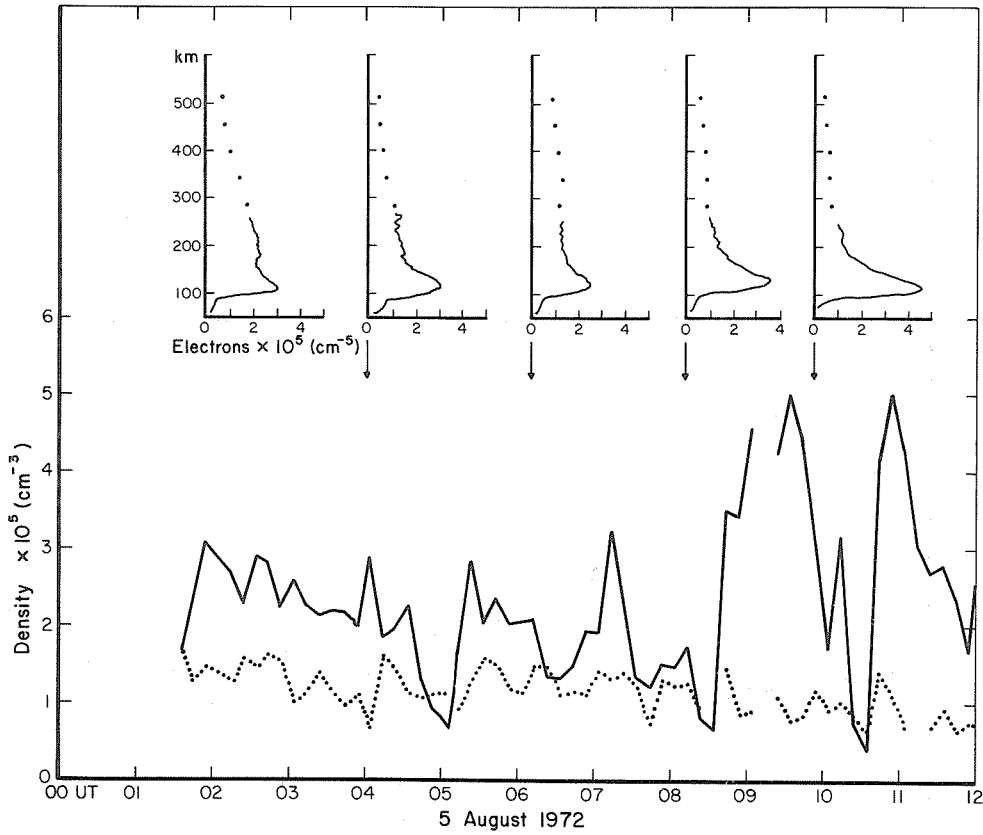


Fig. 3. Same as in Figure 1.

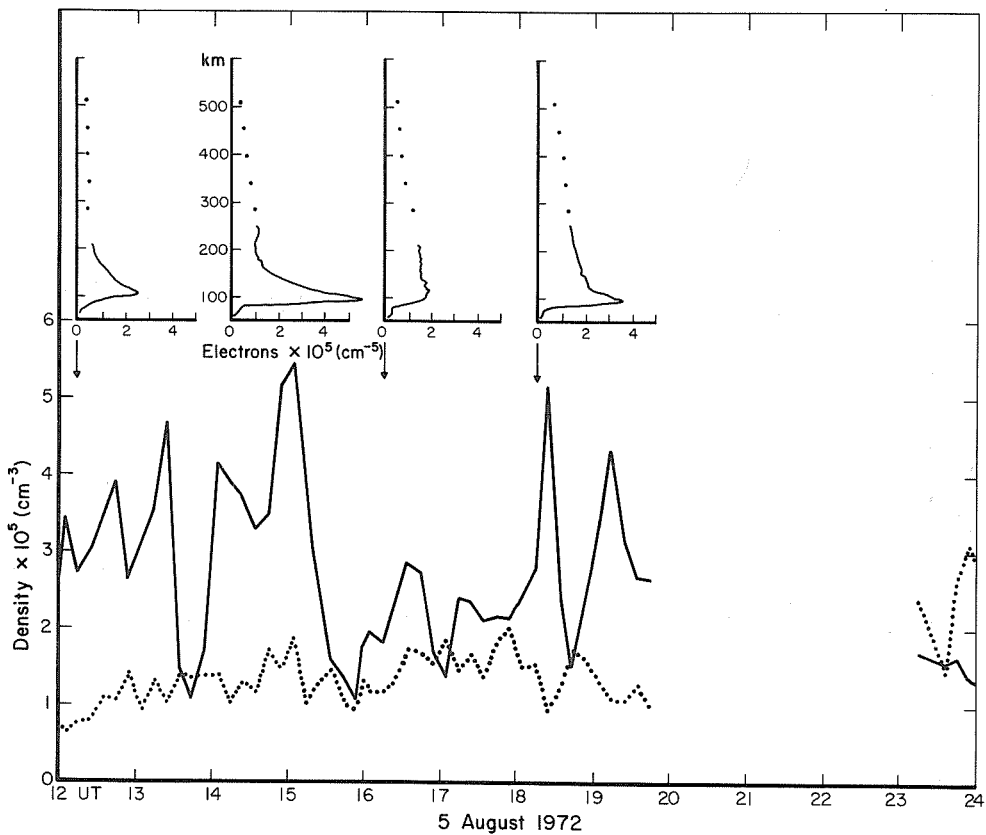


Fig. 4. Same as in Figure 1.

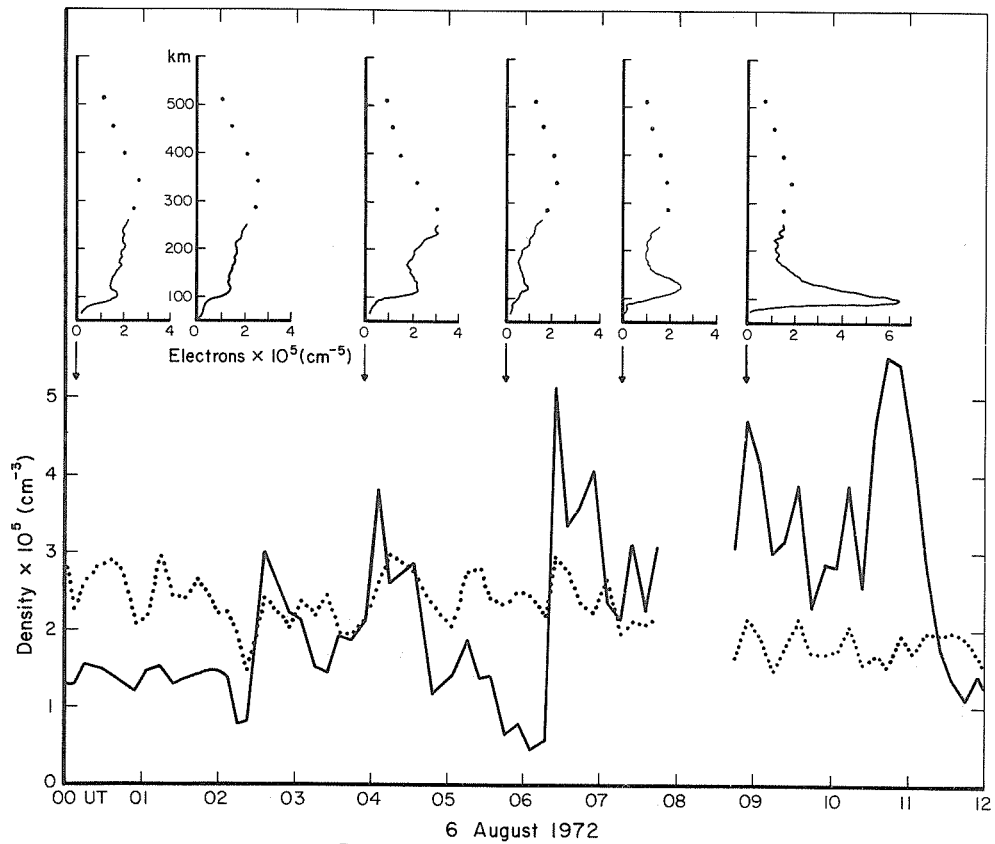


Fig. 5. Same as in Figure 1.

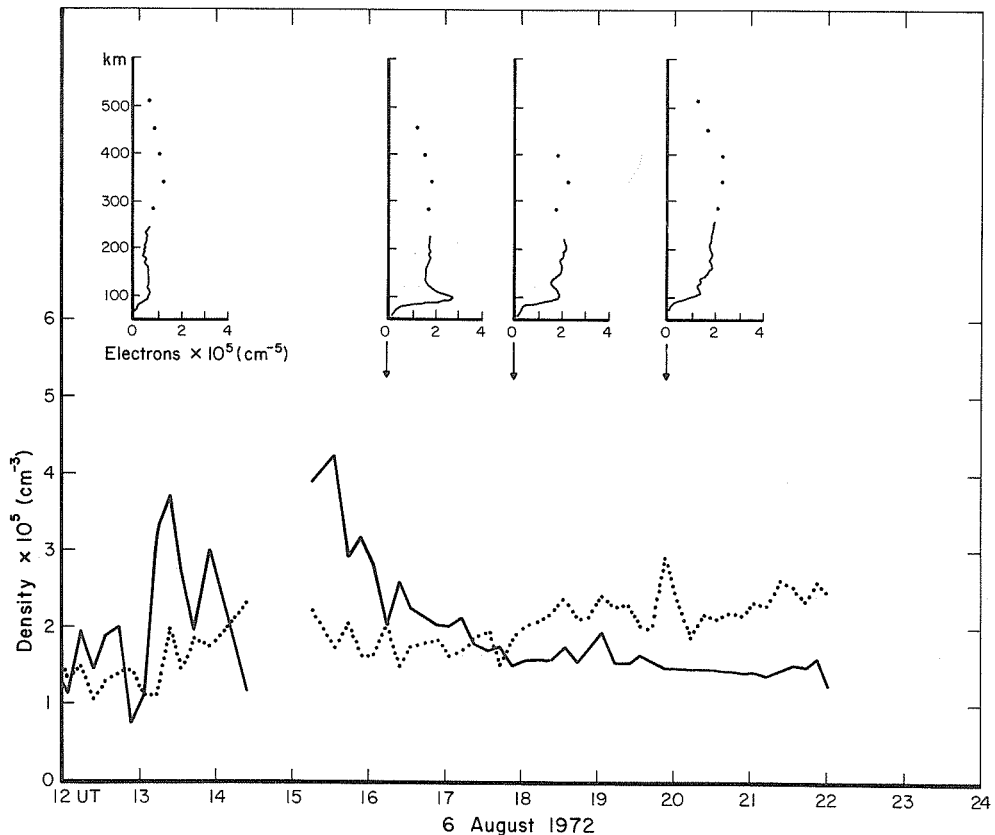


Fig. 6. Same as in Figure 1.

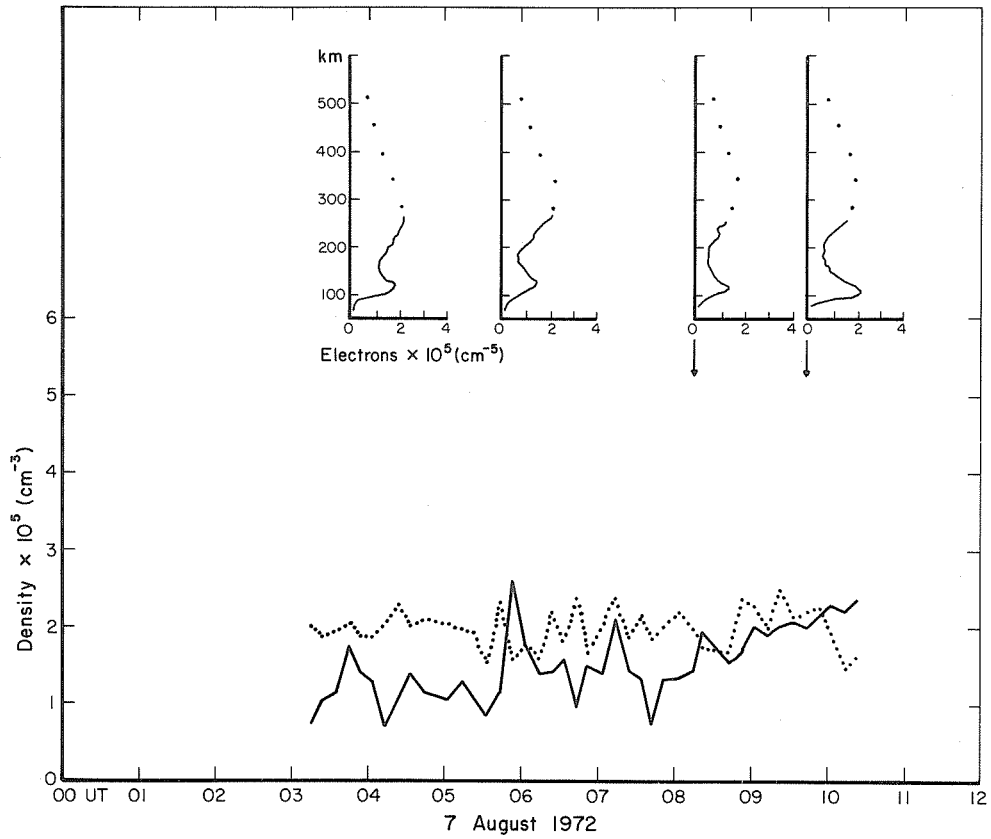


Fig. 7. Same as in Figure 1.

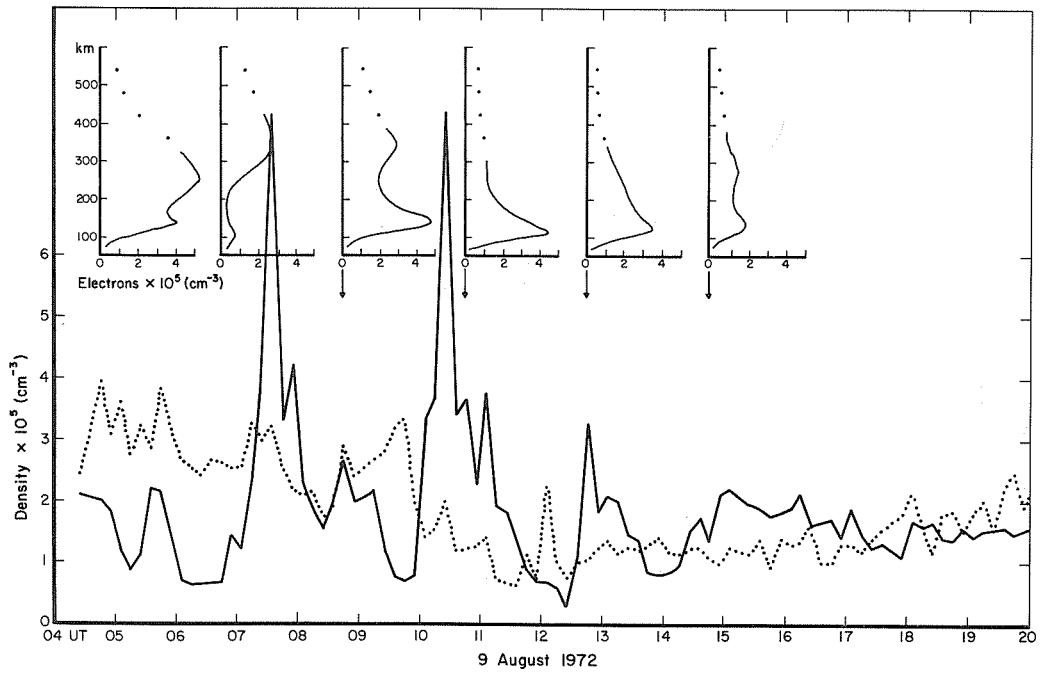


Fig. 8. Same as in Figure 1.

Millstone Hill Incoherent Scatter Observations

by

J. V. Evans
Lincoln Laboratory
Massachusetts Institute of Technology
Lexington, Massachusetts 02173

During the Retrospective World Interval, July 26 - August 14, 1972, the Millstone Hill (N42.6, W7.15) incoherent scatter radar [Evans and Loewenthal, 1964] was operated twice for periods of 24 hours: these were 1030 EST July 26 through 1100 EST July 27, and 0915 EST August 7 through 0915 EST August 8.

The measurements were essentially confined to the F-region (150-900 km) by the choice of the operating mode for the radar. The observations yielded the electron density distribution N_e with a height resolution of 15 km, and electron temperature T_e , ion temperature T_i and vertical drift V_d with a height resolution of 75 km. To gather all these data three separate experiments are undertaken requiring a total of 30 minutes observing time. Accordingly, in each 24 hour period some 48 altitude profiles of N_e , T_e , T_i , and V_d were obtained. The manner in which the measurements were made and the data reduction carried out has been described elsewhere [Evans et al., 1970].

Results for N_e , T_e , and T_i are presented in Figures 1a-c and 2a-c for the two days. These figures are contour diagrams showing the altitude variation of a given value of $\text{Log}_{10} N_e$, T_e , or T_i as a function of local time. Contours of $\text{Log}_{10} N_e$ are in 0.2 steps, while those for T_e and T_i are in 200°K and 100°K intervals, respectively. These results may be compared with the behavior reported for summer months in other years [Evans, 1967, 1970, 1973].

The measurements on July 26 commenced after a period (23-25 July) of anomalously low F-region electron density. This condition persisted into 26 July until about 1300 EST. The difference in the sunrise behavior of the electron density on 26 and 27 July is clearly evident in Figure 1a. The electron temperature appears to have been slightly higher than normal during this period of depressed electron density in the region 250-450 km (Fig. 1b), but the ion temperature seems to have changed little (Fig. 1c).

The measurements made on 7-8 August commenced a little before the onset of a class 3B flare (1500 UT). The flare raised the F-region electron density and electron temperature at all levels and has been the subject of an earlier paper [Mendillo et al., 1972]. One of the most striking features of the flare was the large upward flux of ionization established in the topside of the F-layer due to the rapid growth of the layer [Evans, 1971]. The electron and ion temperatures, together with the vertical drift velocity observed during the period surrounding the flare, are shown in Figure 3. In order to account for the upward fluxes observed at altitudes above 375 km (Fig. 3), it appears necessary to include the production of ionization at this and higher levels as the thermal expansion model [Evans, 1971] fails to predict such large velocities for the temperature changes observed.

REFERENCES

- | | | |
|--|------|---|
| EVANS, J. V. | 1967 | Mid-latitude F-Region Densities and Temperatures at Sunspot Minimum, <u>Planet. Space Sci.</u> , <u>15</u> , 1387-1405. |
| EVANS, J. V. | 1970 | Millstone Hill Thomson Scatter Results for 1965, <u>Planet. Space Sci.</u> , <u>18</u> , 1225-1253. |
| EVANS, J. V. | 1971 | Observations of F-Region Vertical Velocities at Millstone Hill, 1, Evidence for Drifts due to Expansion, Contraction, and Winds, <u>Radio Science</u> , <u>6</u> , 609-626. |
| EVANS, J. V. | 1973 | Millstone Hill Thomson Scatter Results for 1966 and 1967, <u>Planet. Space Sci.</u> , in press. |
| EVANS, J. V. and
M. LOEWENTHAL | 1964 | Ionospheric Backscatter Observations, <u>Planet. Space Sci.</u> , <u>14</u> , 915-944. |
| EVANS, J. V.,
R. F. JULIAN, and
W. A. REID | 1970 | Incoherent Scatter Measurements of F-Region Density, Temperatures, and Vertical Velocity at Millstone Hill, Lincoln Laboratory, Lexington, Mass., Tech. Report 477. |
| MENDILLO, M.,
J. A. KLOBUCHAR, and
D. H. CHUNG | 1972 | Ionospheric and Geomagnetic Observations During the August 72 Solar-Terrestrial Events, Presented at the Fall AGU Meeting, San Francisco. |

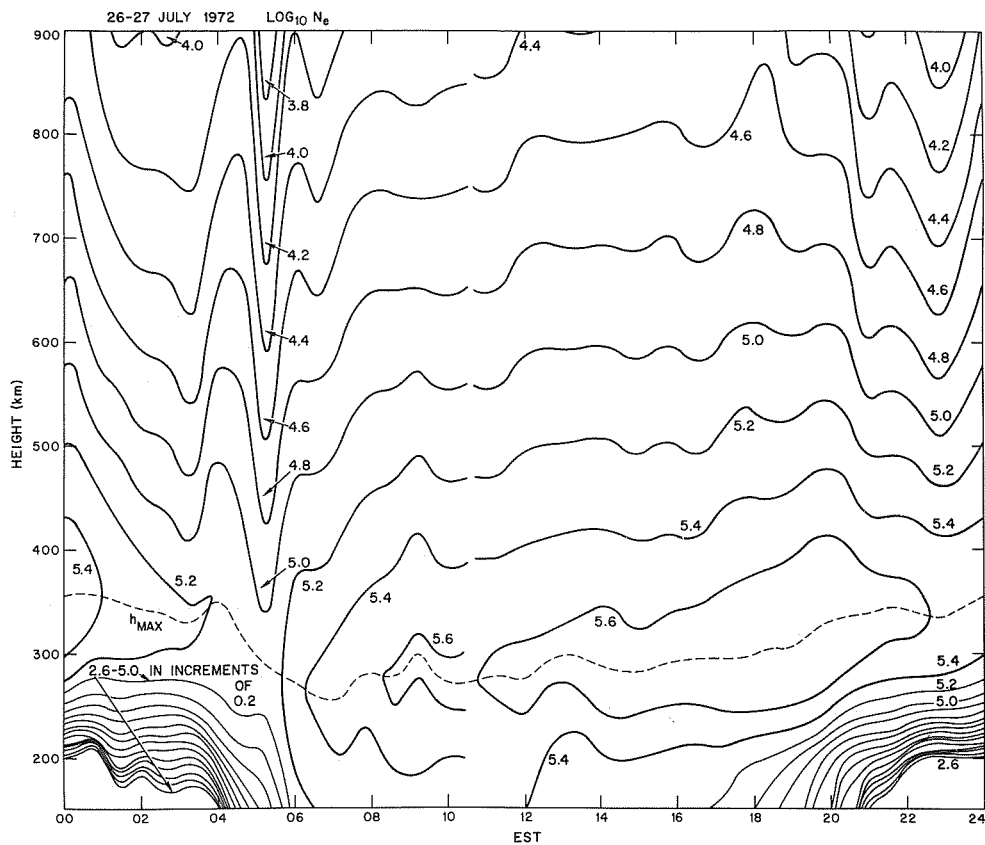


Fig. 1a. Electron density results obtained on 26-27 July 1972.

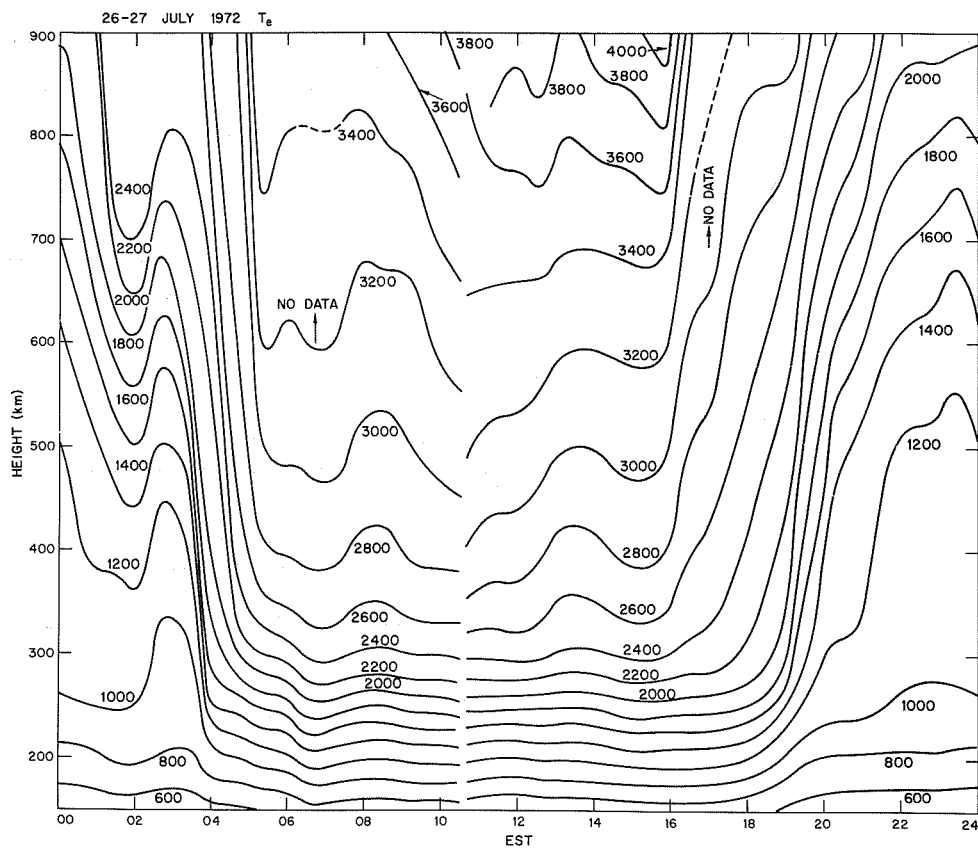


Fig. 1b. Electron temperature results obtained on 26-27 July 1972.

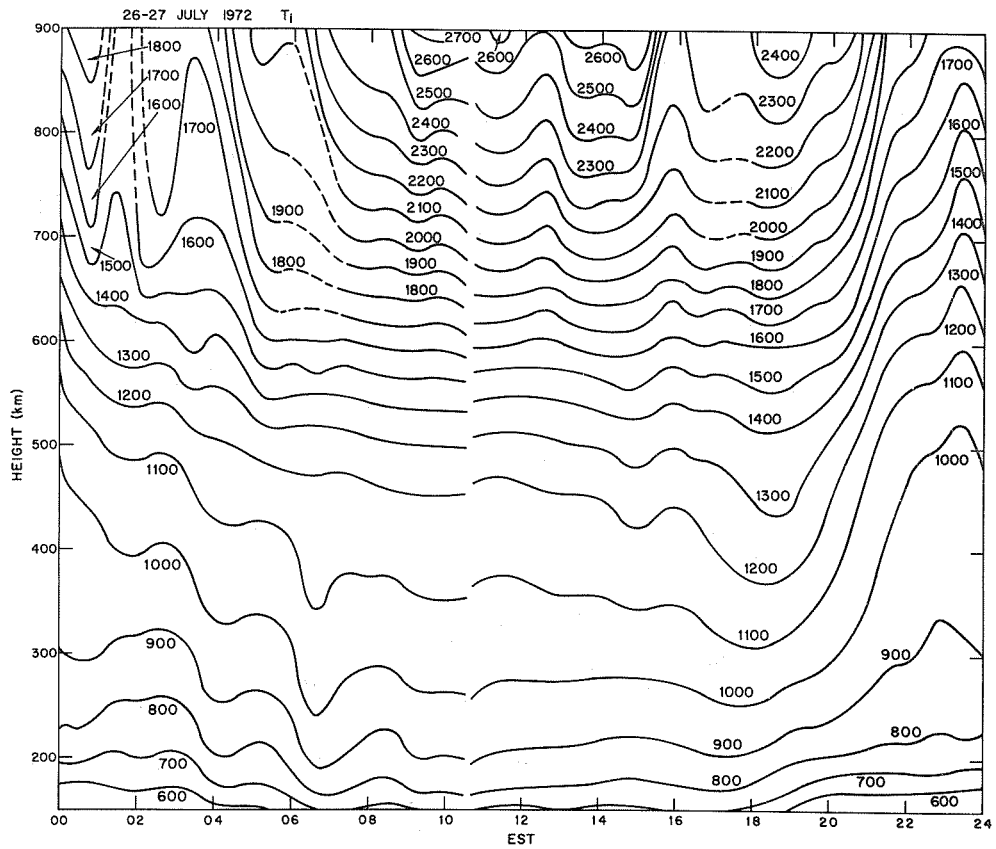


Fig. 1c. Ion temperature results obtained on 26-27 July 1972.

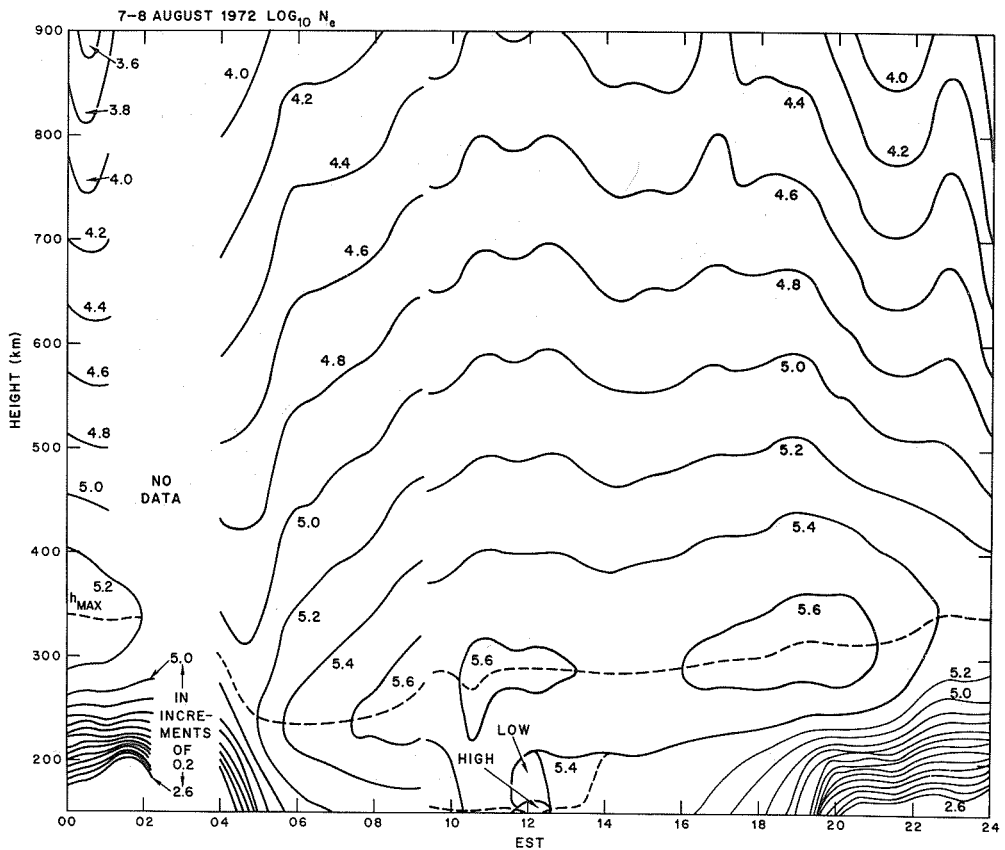


Fig. 2a. Electron density results obtained on 7-8 August 1972.

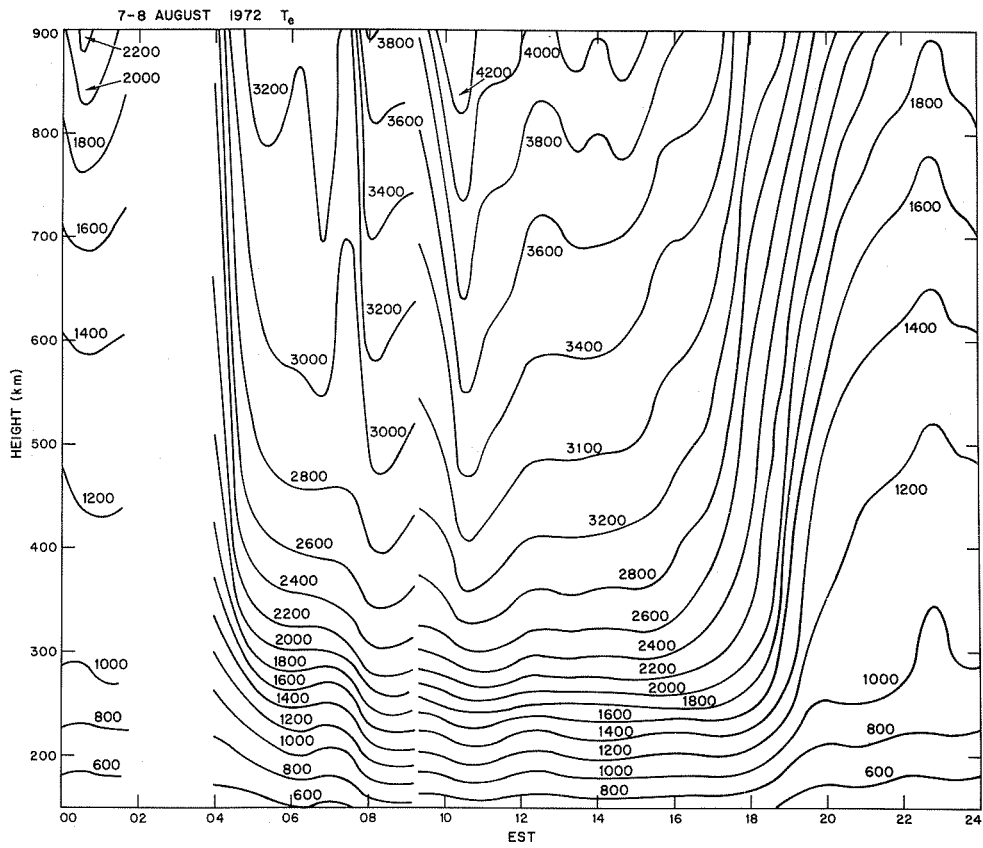


Fig. 2b. Electron temperature results obtained on 7-8 August 1972.

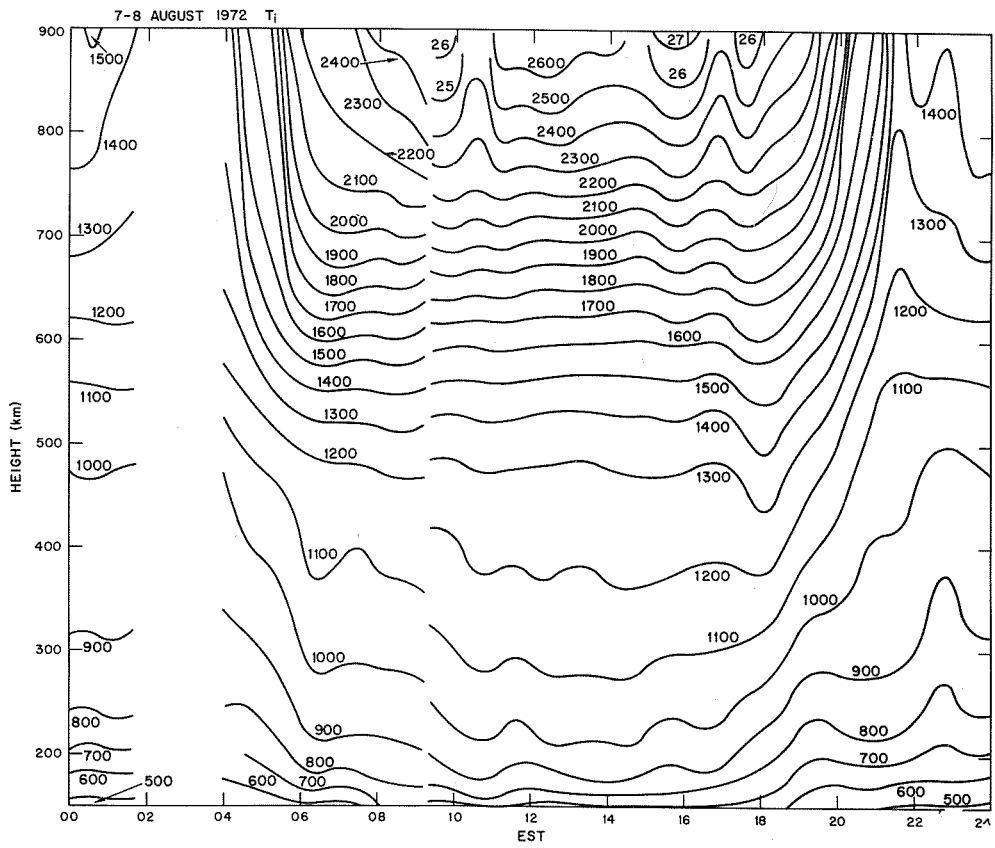


Fig. 2c. Ion temperature results obtained on 7-8 August 1972.

MILLSTONE HILL TEMPERATURE AND VELOCITY PROFILES ----- 7 AUGUST, 1972

START TIMES (U.T.)

START TIMES (U.T.)	IMP 3B FLARE	START	MAX
14:21	H α	UT = 1500	1530
14:55	10 cm	UT = 1500	1527
15:29		UT = 1500	
16:04		UT = 1500	
16:39		UT = 1500	

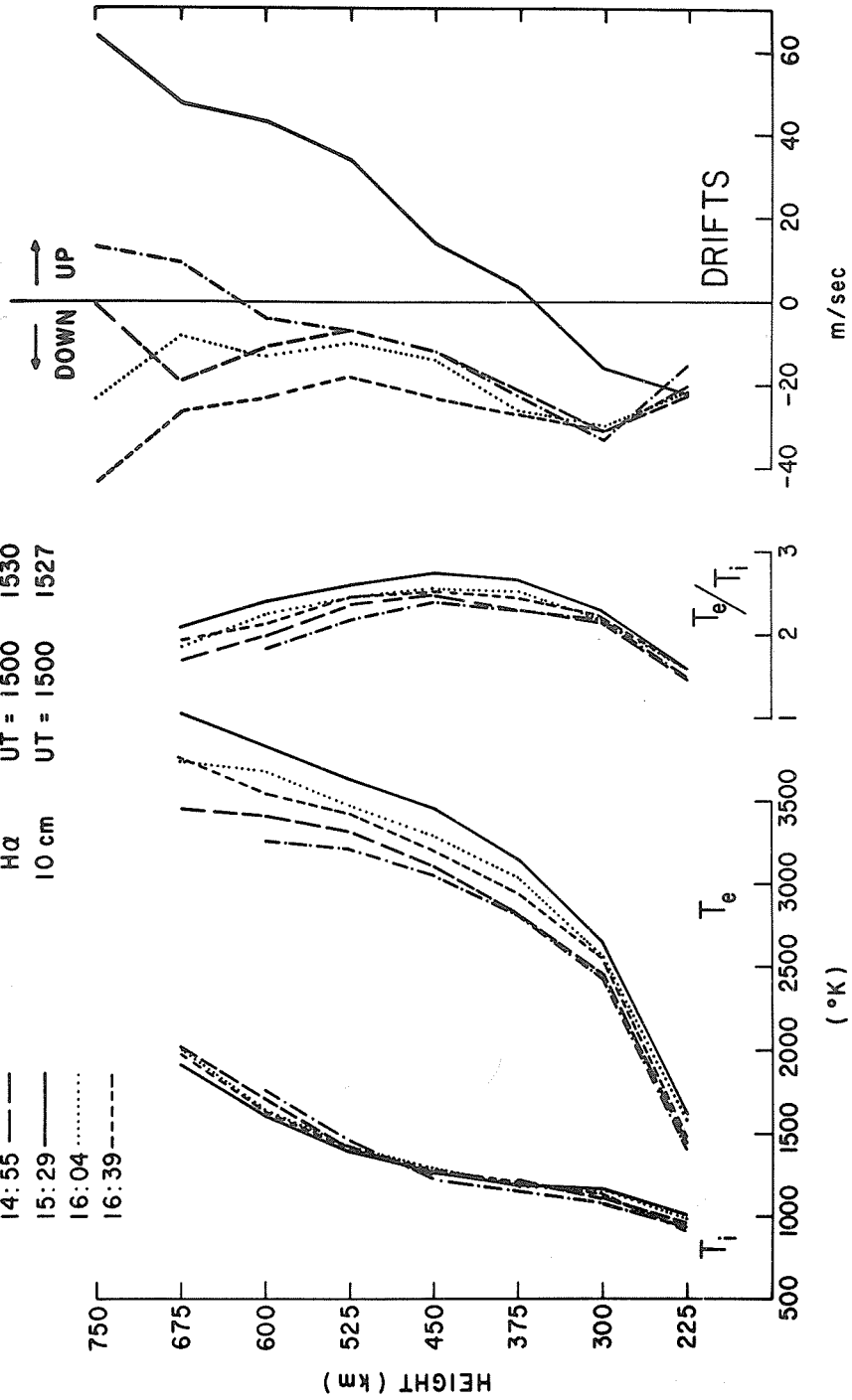


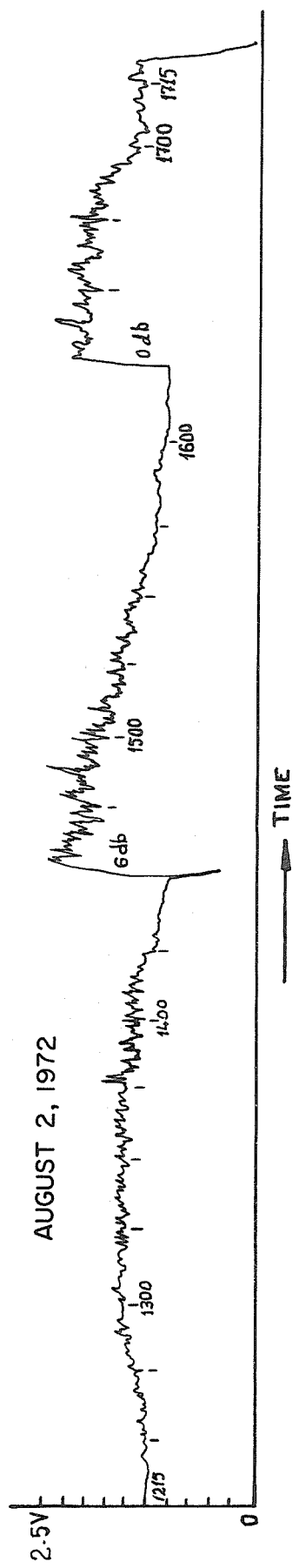
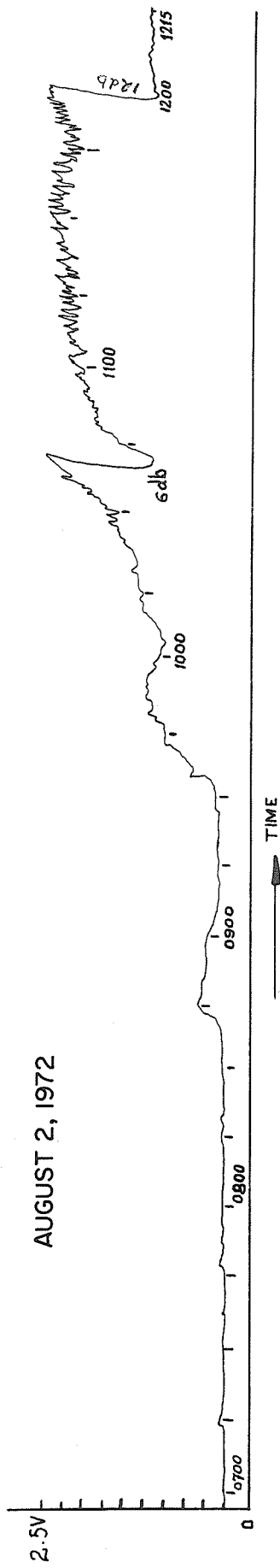
Fig. 3. Variation of electron temperature, ion temperature and vertical velocity during the class 3B flare that occurred on 7 August 1972 (commencing at 1500 UT).

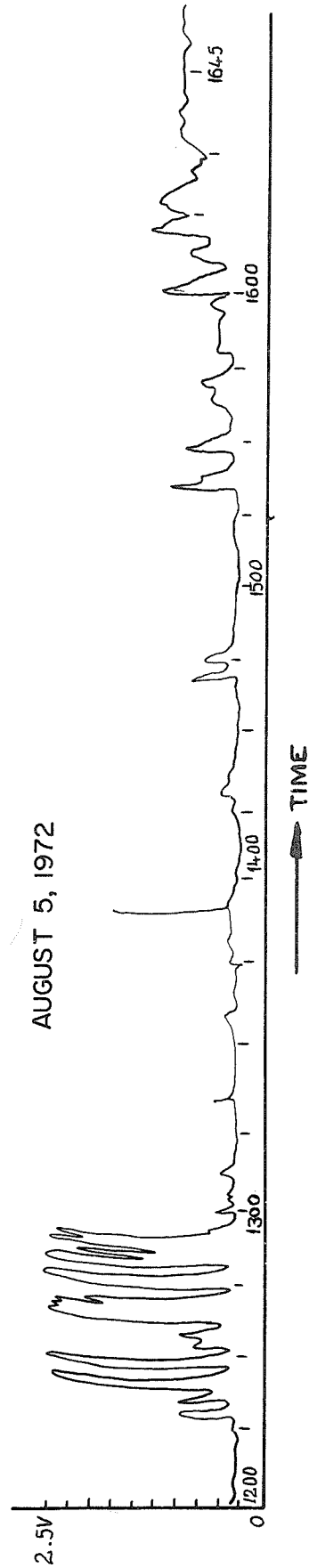
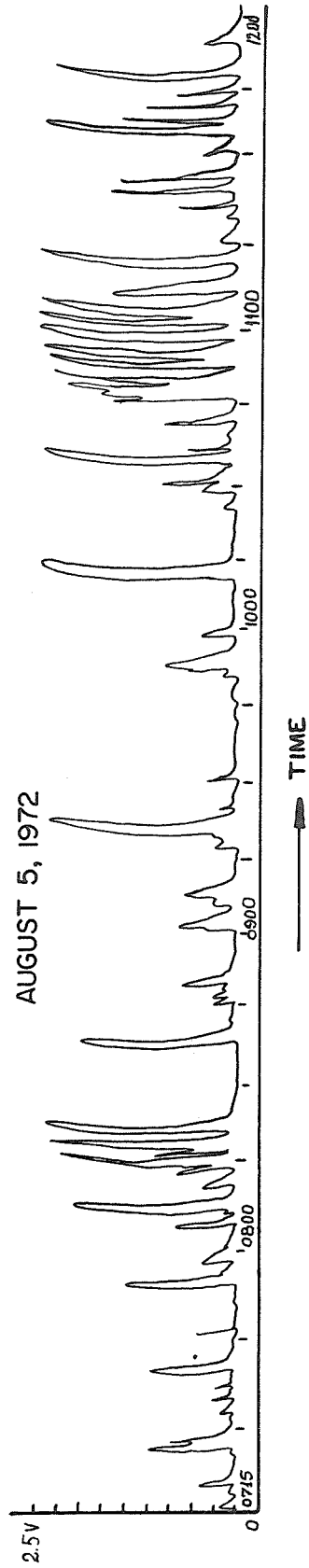
Data of the Radar Echoes from Electrojet Irregularities

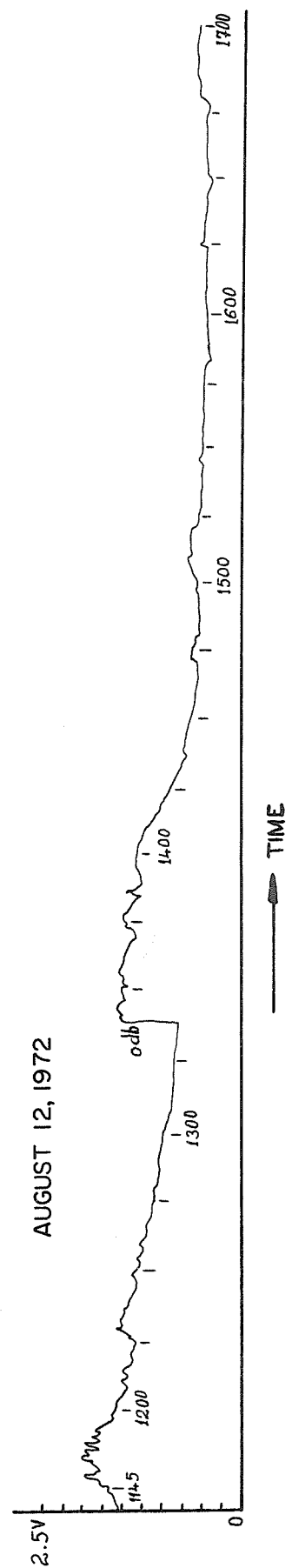
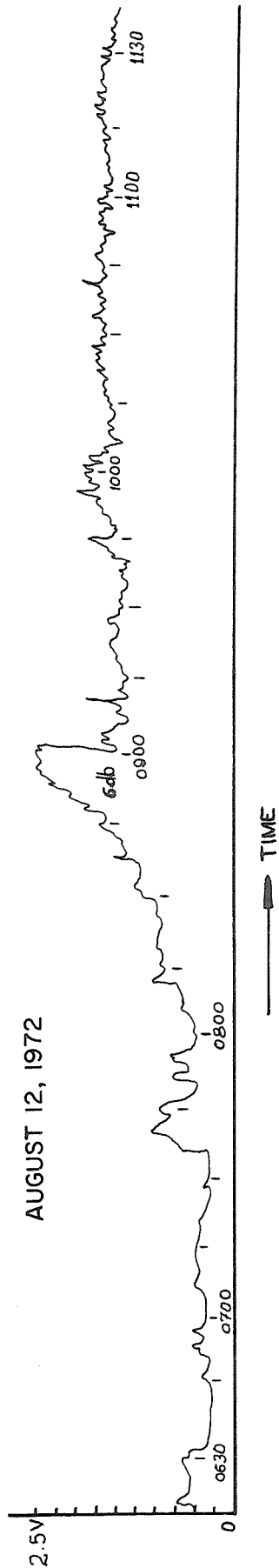
by

C. L. Jain
Space Physics Division
Vikram Sarabhai Space Centre
Trivandrum 695022, India

The records of the intensity of the scattered signal of the Coherent Back Scatter Radar operating on 54.95 MHz and installed at Thumba (dip -0.9 geographic latitude N 8.6 , geographic longitude E 76.9 for the days 2, 5 and 12 August 1972 are presented here. The signal corresponds to the height range of about 90 km.







Variations of Noon Electron Density at Wallops Island
July 31 - August 11, 1972, and Related Parameters

by

T. N. Gautier and L. R. Wescott
Environmental Data Service
National Oceanic and Atmospheric Administration
Boulder, Colorado 80302

The variations of electron density are shown as contours in Figure 1. In Figure 2, foF2, Kp, and SHmax for noon are plotted on the same day-of-the-month time scale. SHmax is the integrated electron density to Hmax, the height of maximum electron density. Noon Kp was obtained by averaging the 3-hour value just preceding with that just following noon. Figure 3 shows the noon ionograms for this period. Echo-like traces in the frequency range between about 0.3 and 0.5 MHz on several of these ionograms are believed to be spurious, as is the trace near the top on August 6.

Looking first at foF2 in Figure 2, the variation in the first four days (July 31-August 3) is within the normal range of fluctuation caused by traveling disturbances, but on the following four days foF2 is abnormally low, while Kp is high with a strong peak on August 5. The moderately low value of Kp on August 8 is accompanied by an immoderately high value of foF2. On the following day Kp is again high, and foF2 is quite low. On the next two days, August 10 and 11, foF2 is approximately normal. The variations of SHmax in this period is similar to that of foF2 (or Nmax). Though not shown on the graph, the storm-time trend of the noon values of foF1 is similar to that of foF2. Thus, the lowest values of noon foF1 are on August 5 and 9, the days of highest Kp.

In Figure 1, low Nmax, associated with high Kp, tends to be accompanied by low values of N at lower heights, as though the density decreased more or less proportionately at all heights, although there is some tendency for Hmax to decrease on the disturbed days. The indicated decrease of Hmax is especially marked on August 9, which is also the day of lowest foF2. On August 4, the day of next lowest Hmax, the F2-layer echoes are barely discernible in a very narrow frequency range between foF1 and foF2, a condition that also occurred on August 9.

The virtual blackout on the August 7 ionogram in Figure 3 was caused by the bright flare that began just after 1000 Wallops time and lasted until after noon.

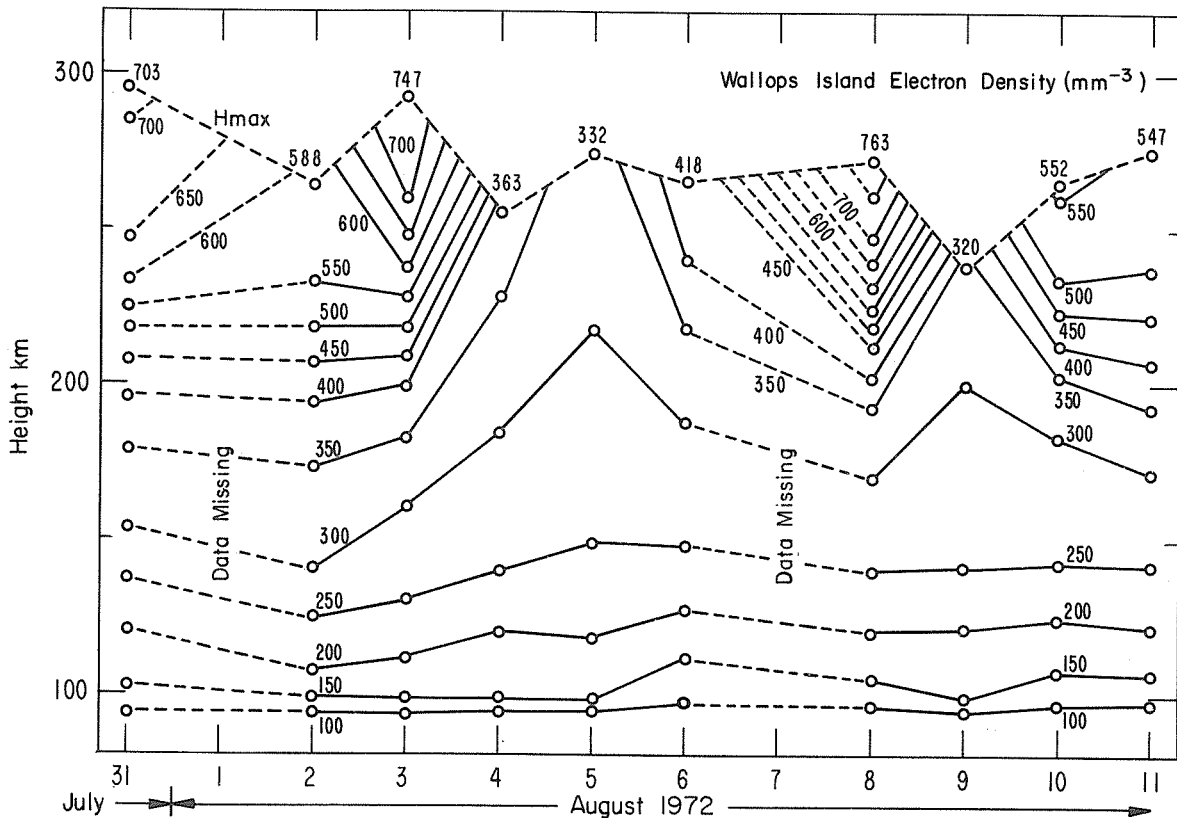


Figure 1. Noon electron density derived from Wallops Island ionograms, July 31 - August 11. Numbers on contours are electrons per cubic millimeter. H_{max} is the height of maximum electron density. Numbers at H_{max} are values of N_{max} , the maximum electron density.

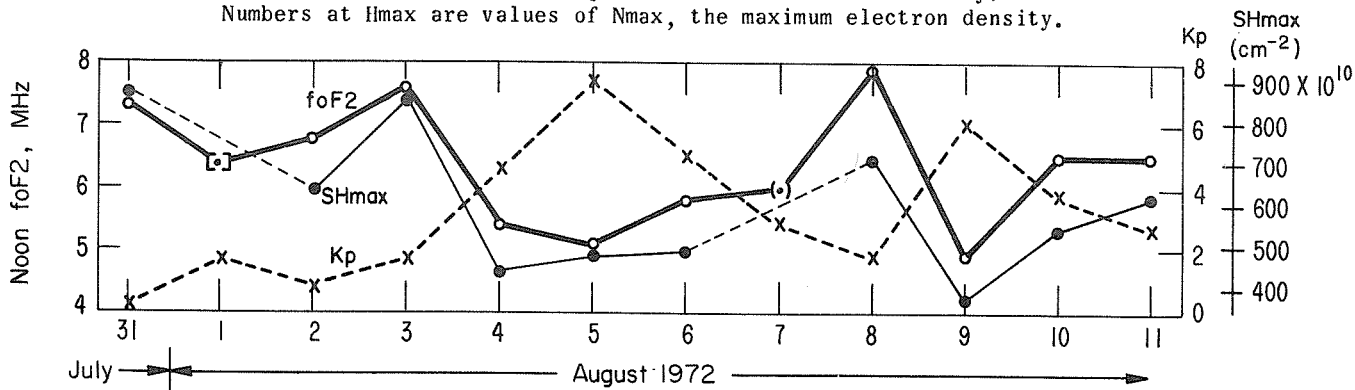


Figure 2. Noon foF2 and SHmax compared with the average of the 3-hour Kp values just preceding and just following noon. SHmax is the integrated electron density to H_{max} . Monthly median values of foF2 in July and August were about 6.5 MHz. The noon value of foF2 on August 1, shown in brackets, is the average of values at 1100 and 1300. The value for August 7, shown in parentheses, is uncertain.

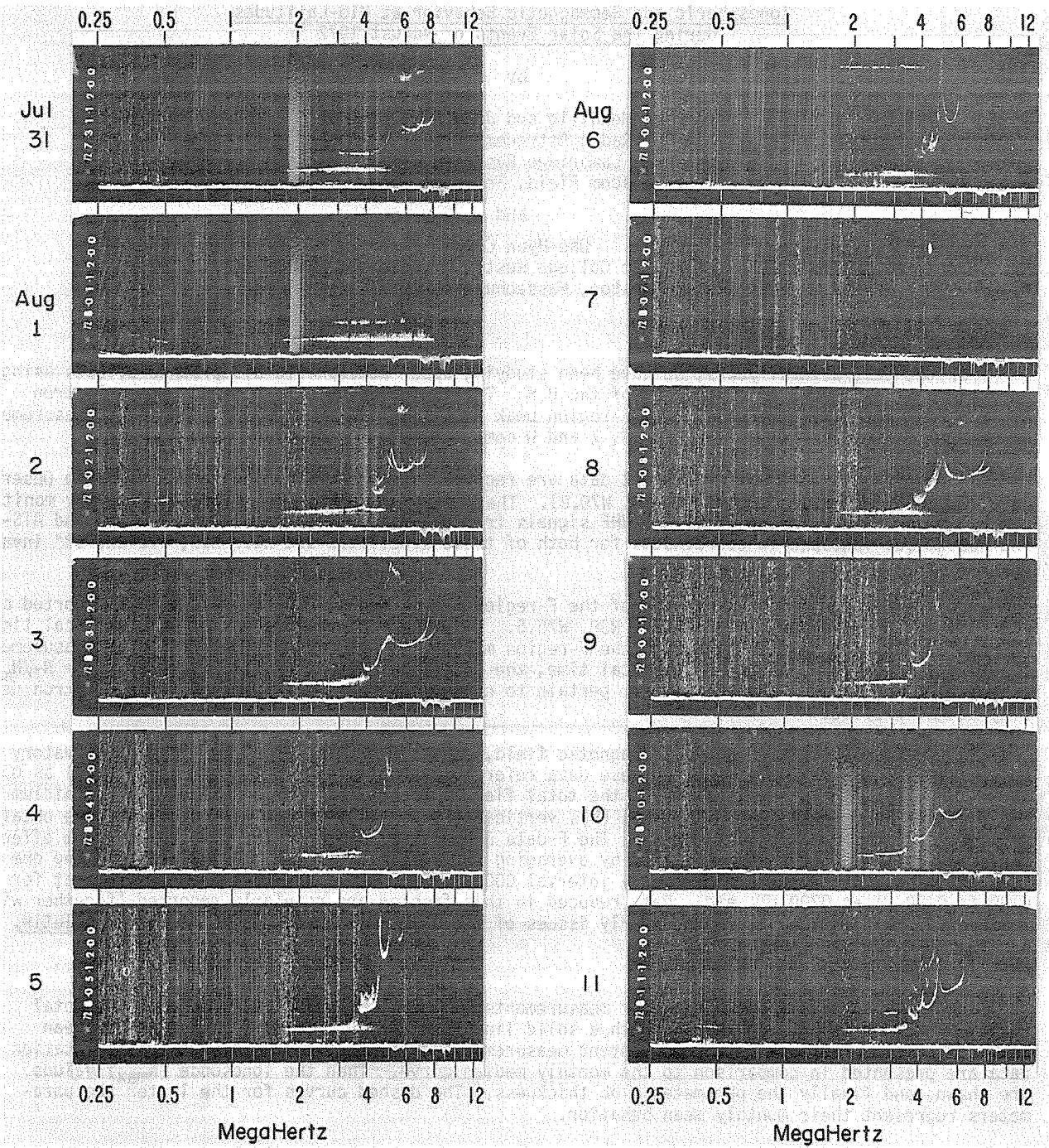


Figure 3. Noon ionograms, Wallops Island, July 31-August 11, 1972

Ionospheric and Geomagnetic Behavior at Mid-Latitudes
during the Solar Events of August 1972

by

Michael Mendillo and John A. Klobuchar
Radio Astronomy Branch
Air Force Cambridge Research Laboratories
L. G. Hanscom Field, Bedford, Mass. 01730

and

Dae-Hyun Chung
Boston College Weston Observatory
Weston, Massachusetts 02193

Introduction

For the past several years, we have been studying upper atmospheric disturbance effects using data taken at sites on the East Coast of the U.S. These measurements consist of total electron content (N_T) data, foF2 values of the F-region peak density (N_{max}) and geomagnetic field measurements of the total field (F) as well as the H, Z and D components.

Ionospheric total electron content data are recorded at the AFCRL's Sagamore Hill Radio Observatory in Hamilton, Massachusetts (N42.6, W70.8). These measurements are made by continuously monitoring the amount of Faraday rotation of the VHF signals from the geostationary satellites ATS-3 and ATS-5. The 400 km sub-ionospheric coordinates for both of these satellites are near N39, W70 and 53° invariant latitude.

Measurements of the peak density of the F-region are obtained from the foF2 values reported by the Wallops Island Ionospheric Station N38, W75.5. Using these hourly values of N_{max} in local time, one can examine the gross behavior of the F-region maximum at a location close to our N_T measurements. By selecting hourly values of N_T in local time, the additional parameter slab thickness ($\tau = N_T/N_{max}$) can also be monitored. Variations in τ pertain to changes in the overall shape of the electron density height profile.

As a means of monitoring the geomagnetic field, measurements taken at the Weston Observatory (N42.4, W71.3) are examined because these data refer to approximately the same L-shell (L=3) as our N_T measurements. At Weston, values of the total field intensity (F) are obtained from a rubidium vapor magnetometer while the horizontal (H), vertical (Z) and declination (D) components are obtained from standard observatory variometers. The F-data normally examined in our studies of storm effects consist of hourly mean values obtained by averaging the seven ten-minute readings made during one UT-hour. Thus, the mean for the hourly interval 0000 to 0100 UT is given at 0100 UT and that for 0100 to 0200 UT at 0200 UT, etc. Data reduced in this fashion are regularly reported (together with statistical information) in the quarterly issues of the AFCRL Geophysics and Space Data Bulletin.

Results

Figure 1 contains a summary of our measurements for the 3-8 August 1972 period. The total field (F) data are shown on the top with a solid line, the dashed line giving the monthly mean behavior. Next, the total electron content measurements obtained from the ATS-3 Faraday-rotation data are presented in comparison to the monthly median curve. Then the ionosonde (N_{max}) values are shown, and finally the parameter slab thickness. The dashed curves for the latter two parameters represent their monthly mean behavior.

The starting times of four solar flares are denoted by the letters A, B, C and D, and their corresponding geomagnetic sudden storm commencements (ssc's) by A', B', C' and D'. The ionospheric response to this series of storms was quite unspectacular in comparison to the behavior seen during a somewhat similar period in October-November 1968. There were none of the large enhancements in total content and total field which are so typical of the storm effects we normally see [Papagiannis et al., 1971]. Only on 4 August is this tendency apparent near the sunset period. Thus, while the disturbances were very large magnetically, they were unimpressive from an ionospheric point of view. This was probably due to the prolonged nature of the high level of activity (the N_{max} behavior suggests sustained heating effects), and also to the local times of the ssc's [see Mendillo, 1973].

By far the most interesting event during this period occurred in connection with the flare at 1500 UT on 7 August. This can be seen as a noticeable "jump" near 1015 EST in the ATS-3 total content values plotted in Figure 1. The VHF component of the solar burst interfered to some extent with the polarization measurements from ATS-3, but to a lesser extent with the ATS-5 measurements, made looking further to the west. Figure 2 contains an expanded version of the ATS-5 data together with the Weston H, D and Z magnetograms. The H and D traces show an extremely large solar flare

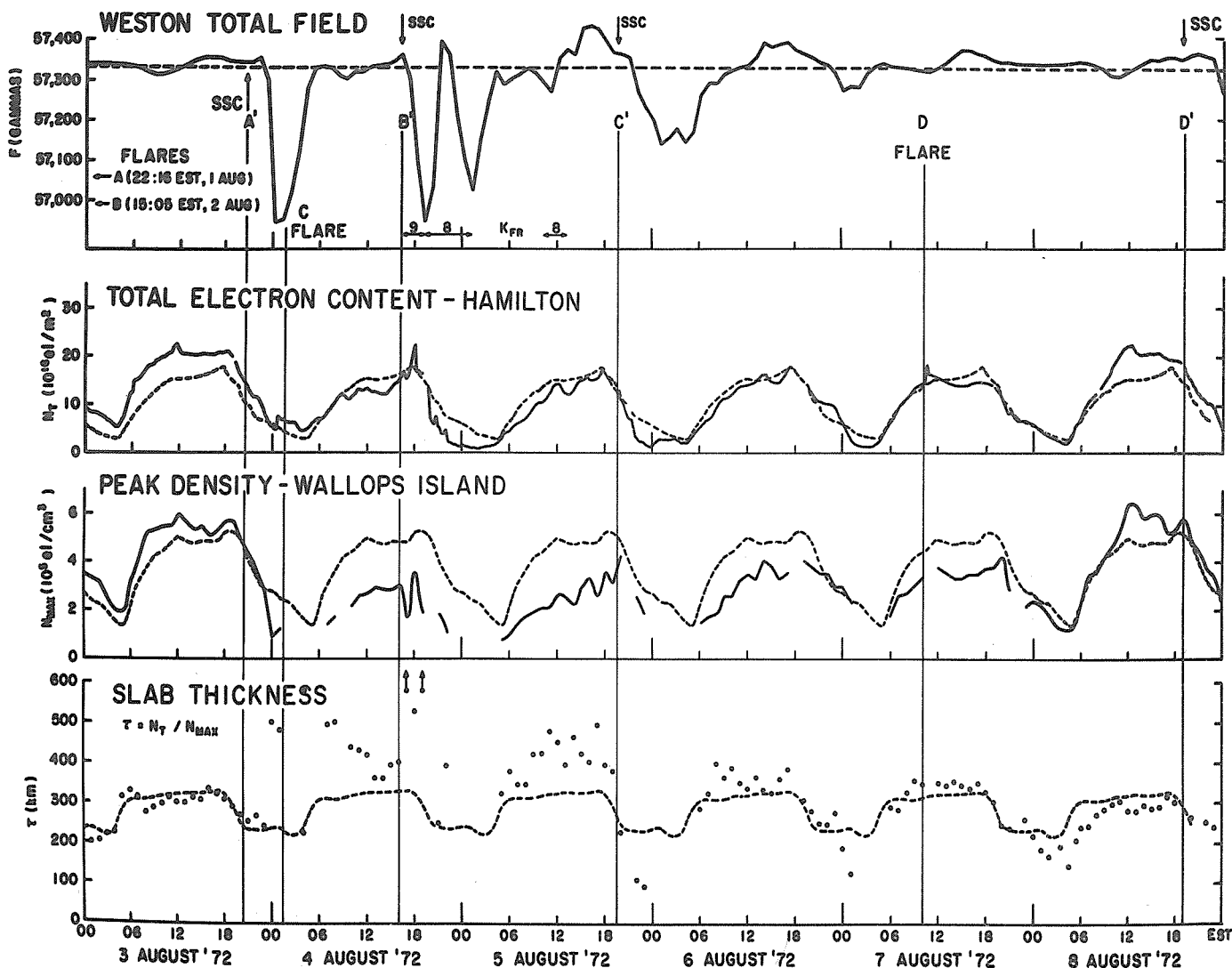


Fig. 1. Total field (F) data, total electron content, ionosonde (N_{max}) values, and slab thickness are illustrated for the period 3-8 August 1972, along with their monthly mean or median values.

effect (SFE) or magnetic crochet simultaneous with the sudden increase in total electron content (SITEC). In nearly five years of continuous operation, many SITEC events have been observed at Hamilton, but this is the largest one to date. The change in N_T was approximately 4.3×10^{16} el/m², which corresponds to nearly 30% of the pre-flare value. The maximum prior SITEC noted was 2.4×10^{16} el/m² (8%) which occurred during the flare at 1619 UT on 29 September 1968.

Geomagnetic flare effects at Weston (or any similar mid-latitude station) are typically less than 20 gammas in the horizontal component. During this event, observatories throughout the U.S. reported extremely large crochets (50-100 gammas). At Weston the effect was readily seen in the total field data as an abrupt decrease of about 20 gammas (depending on an estimate of the "no-flare" field, $53,330 \pm 5$ gammas). If one assumes a completely overhead current system, as Figure 2 suggests, then $\Delta F = \Delta H \cos I$, which is in agreement for these observations at $I=72^\circ$.

A large-scale study of the TEC flare increase is in preparation using data obtained from colleagues throughout the U.S., Europe and Africa. A second study of the ionospheric effects observed at the Millstone Hill incoherent scatter facility is also in preparation [Mendillo and Evans, 1973].

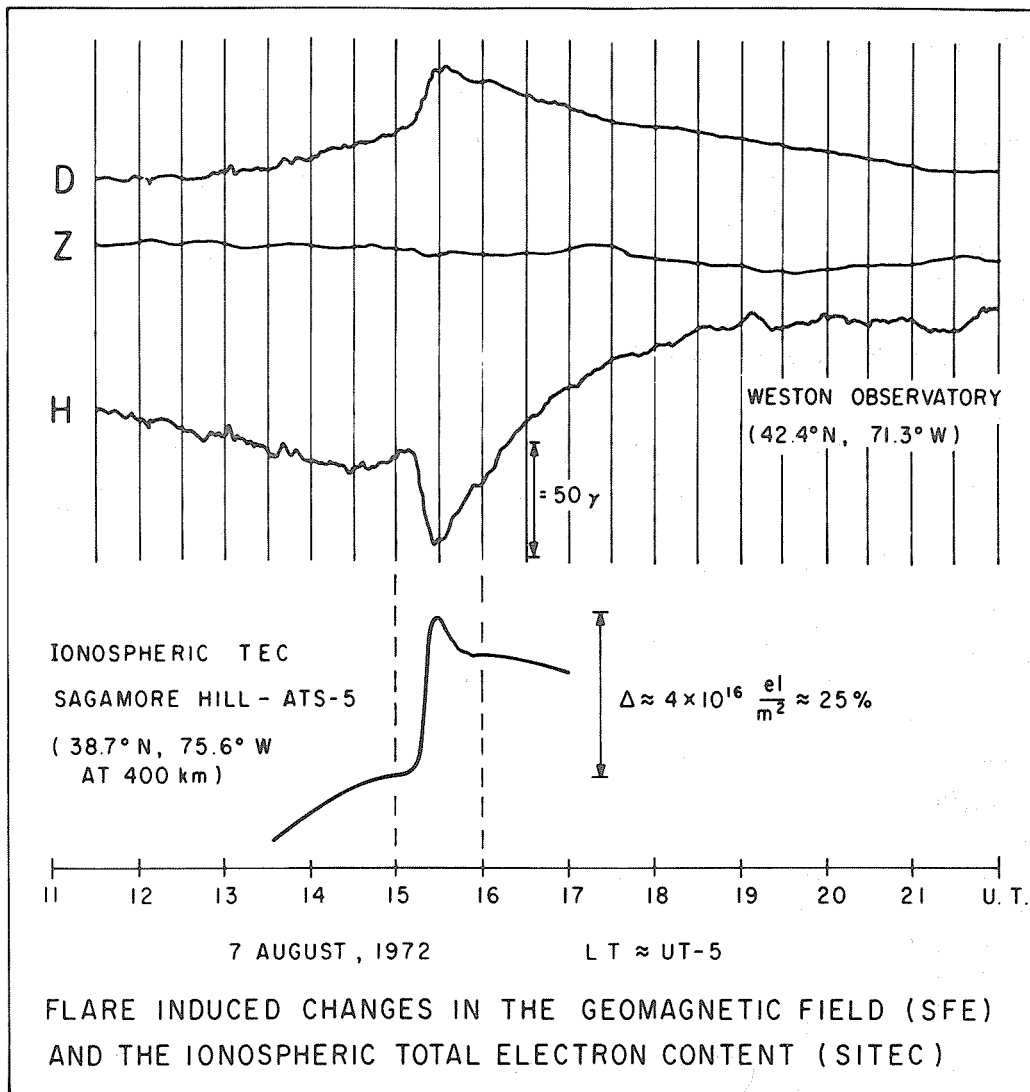


Fig. 2. Flare induced changes in the geomagnetic field (SFE) and the ionospheric total electron content (SITEC).

Acknowledgements

One of us (M.M.) wishes to acknowledge the support of the National Research Council/National Academy of Science Postdoctoral Research Associateship. The continued assistance of Miss Esther Rodriguez of the Weston Observatory is gratefully acknowledged.

REFERENCES

- | | | |
|---|------|---|
| MENDILLO, M. | 1973 | A study of the relationship between geomagnetic storms and ionospheric disturbances at mid-latitudes, <u>Planet. Space Sci.</u> , in press. |
| MENDILLO, M. and J. V. EVANS | 1973 | Incoherent scatter observations of the ionospheric response to a large solar flare, to be presented at the <u>URSI Commission III Conference on Incoherent Scatter</u> , 12-16 June, 1973, in Tromso, Norway. |
| PAPAGIANNIS, M. D., M. MENDILLO and J. A. KLOBUCHAR | 1971 | Simultaneous storm-time increases of the ionospheric total electron content and the geomagnetic field in the dusk sector, <u>Planet. Space Sci.</u> , <u>19</u> , 503-511. |

Total Electron Content of the Ionosphere over Lindau/Harz
by Dispersive Doppler Effect, July 26 - August 12, 1972

by

G. K. Hartmann, G. Schmidt and *A. Tauriainen
Max-Planck-Institut für Aeronomie
D-3411 Lindau/Harz, P.O. Box 20,
Federal Republic of Germany

*University of Oulu, Finland. On a Humboldt
scholarship at the MPI für Aeronomie.

Introduction

The importance of low orbiting satellites for the determination of the ionospheric electron content up to heights of 1,100 km has a new significance due to the recent use of geostationary satellites which now enable the determination of the total electron content up to heights of 36,000 km. Due to technical problems aboard the spacecraft Explorer 22 (S-66), the beacons which transmitted continuously for 4 years were switched off in 1969 [Schmidt, 1966; Schmidt and Tauriainen, 1970]. At the MPI discussions were started on whether the equipment should be and could be modified for receiving the beacons of other low orbiting satellites in order to determine the total electron content of the ionosphere with sufficient accuracy. The application of the group delay method, which will be in operation for the first time aboard the geostationary satellite ATS-F (launch date May 1974), yields the total electron content up to the height of the satellite (36,000 km) with an accuracy of 5% [Schmidt, 1970a]. If by means of actual simultaneous measurements, e.g., using beacons of low orbiting satellites, one can determine the total electron content up to 1,100 km height with roughly the same accuracy, one can expect to measure for the first time the exospheric electron content by means of beacons. It has to be assumed, however, that the content up to 36,000 km exceeds that up to 1,100 km by more than 5%.

System Description (US NNSS Satellites)

The navigation system of these satellites uses two coherent radio signals which are transmitted by the satellite (150 MHz and 400 MHz). This is done in order to eliminate the influence of the ionosphere on Doppler measurements. It is fairly simple with the well-known dispersive Doppler technique to process the satellite signals in such a manner that the regular vacuum Doppler effect can be eliminated, and that one obtains as a measurable quantity the influence of the ionosphere.

Table 1 displays the available satellites. The five NNSS satellites transmit continuously on 150/400 MHz. The transmitter frequencies of the NNSS satellites are allocated a few kHz below 150 and 400 MHz and are harmonically related to 49.996 MHz. The radiated power is 1.25 and 0.80 Watts. All these satellites are orbiting in nearly circular polar orbits in altitudes of \sim 1,100 km. The dumbbell satellite body has a gravity gradient altitude control with respect to its Z-axis. Magnetic rods with hysteresis produce a spin damping. Therefore, the satellite has no residual spin, and its antennas are always directed towards the earth. The information on the arrangements of the transmitting antennas is at this time incomplete. It is fairly obvious that the frequencies 150/400 MHz are radiated by a small cone antenna which is directed towards the earth. This antenna type has almost the same radiation pattern as a rod antenna that is directed towards the earth. The minimum of the radiation pattern which is vertical towards the earth can be measured during a zenith passage of a satellite.

Table 1

List of NNSS Satellites

Satellite (NNSS)	Inclination (°)	Period (min)	Apogee (km)	Perigee (km)	Transmitting Frequency (MHz)
30120 1967-34 A	90.2	106.4	1078	1052	150/400
30130 1967-48 A	89.6	106.9	1103	1072	150/400
30140 1967-92 A	89.2	106.7	1115	1040	150/400
30180 1968-012 A	89.9	106.9	1143	1029	150/400
30190 1970-67 A	90.0	106.9	1223	953	150/400

Faraday effect and dispersive Doppler effect measurements are feasible [Hartmann et al., 1972].

Dispersive Doppler effect

The dispersive Doppler effect is measurable as a phase difference between two channels at different frequencies:

$$\psi_{DD} = \frac{2\pi}{\omega_0} \left(\frac{1}{m_1} - \frac{1}{m_2} \right) \int N ds$$

$$m_1 = 3; m_2 = 8; \omega_0 = 5.3 \times 10^{-6} \text{ [Rad } m^2 s^{-1}]$$

For a determination of the total electron content up to 1,100 km the dispersive Doppler method and the Doppler-Faraday-hybrid method are applicable [Ebel *et al.*, 1969].

Remarks

The NNSS system yields the possibility to determine the ionospheric electron content fairly accurately (Figures 4 and 5). These satellites will be available throughout this decade. At the present time five satellites are orbiting. At our field station Gillersheim we have 30 - 36 passages per day with elevation angles $> 0^\circ$. About 20 of them have elevation angles $> 20^\circ$. Apart from time intervals when the satellite is overhead, Faraday measurements can be carried out. The information which is supplied by the satellite is sufficient for final data reduction and needs no additional information, e.g., as refined world maps (Explorer 22, 27). These results can be compared with signals from geostationary satellites.

Since the accuracy of the total electron content up to 1,100 km by NNSS satellites is much better than obtained by Faraday rotation measurements with signals of the geostationary satellite alone, a much better calculation of the exospheric electron content is possible.

Results

From July 26 to August 12, 1972, 86 dispersive Doppler recordings were evaluated. Figures 1 through 11 display the electron content as a function of geographic latitude ($I=I(\psi)$) as obtained with two different evaluation methods at Lindau (N51.62, E10.09). At the top of each graph the date and time (LT: local time \approx UT + 1 hour) is displayed. The first two digits represent the year, the next digits the month, and the last digits the day, e.g., 720726 represents July 26, 1972. Time is given in hours and decimal fractions of hours. LT 8.19 to 8.44 represents the time period of the satellite passage from 0800 hours and 11.4 minutes to 0800 hours and 26.4 minutes. Furthermore, the satellite whose signals were received are indicated and also the degree of distortion which was observed during the recording, e.g., SAT 130140 means satellite 30140, the preceding number 1 indicates slight distortions. A number 2 indicates strong distortions. Those cases were not used for calculating I. No preceding number indicates there were no distortions. The abscissa gives the geographic latitude and the ordinate the electron content (electrons m^{-2}). The crosses (1) and the open squares (2) distinguish the two different evaluation methods.

In 1971, 101 dispersive Doppler recordings of this July/August period were evaluated. In 39 cases dispersive Doppler recordings from 1971 and 1972 fell into the same 1 hour time interval and could be compared. Table 2 presents the results.

Conclusion

The most significant feature is that in the period from August 4 through August 7, 1972 the electron content is mostly lower than in the same period of 1971. Furthermore, $I=I(\psi)$ 1972 exhibits more cases with wave-like structures. All other days, apart from August 12, reveal that the mean $I(\psi)$ curves in 1972 were higher than in 1971, but they show no distinct differences in their principal behavior.

REFERENCES

- | | | |
|--|------|---|
| EBEL, A.,
G. K. HARTMANN,
R. LEITINGER,
G. SCHMIDT and
J. P. SCHÖDEL | 1969 | Zeitschrift für Geophysik, <u>35</u> , 373. |
| HARTMANN, G. K.,
K. OBERLÄNDER,
G. SCHMIDT and
J. P. SCHÖDEL | 1972 | Mitteilungen aus dem Max-Planck-Institut für Aeronomie,
Nr. 48, Springer Verlag, Berlin-Heidelberg-New York. |
| SCHMIDT, G. | 1966 | A.E.Ü. <u>20</u> , 374 |

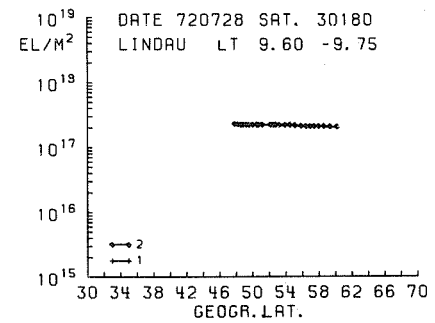
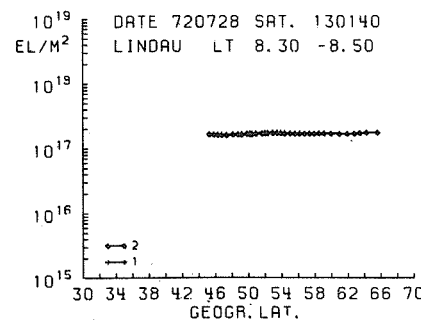
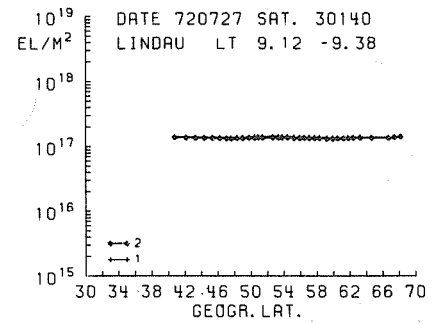
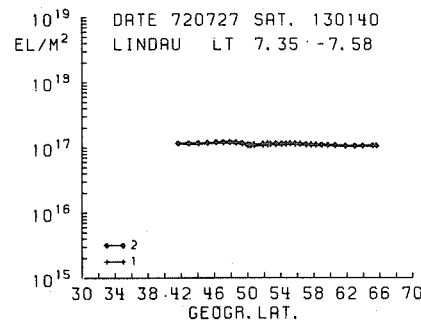
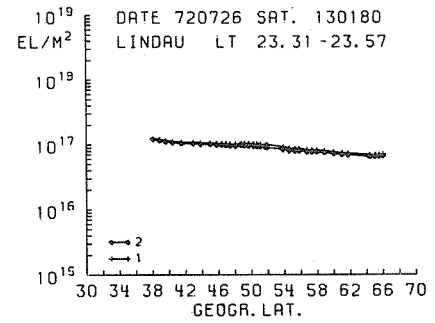
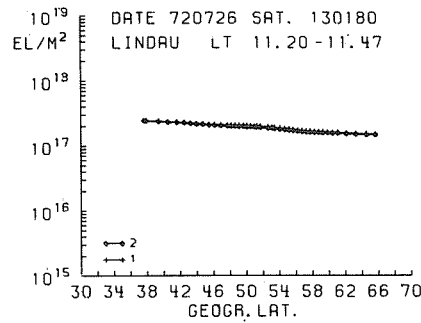
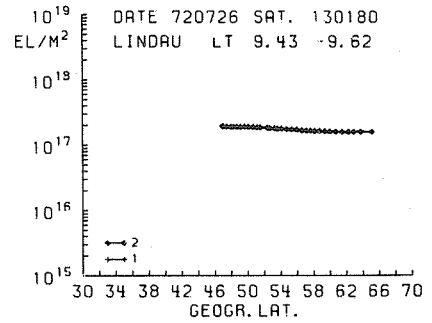
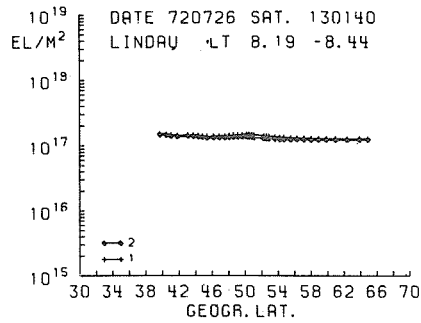


Fig. 1: $I=I(\psi)$

Table 2

Comparison of $I=I(\varphi)$ curves 1972 and 1971

Day	Time CET	I= $I(\varphi)$ increase towards north	decrease towards north	constant	Mean I(φ) compared with 1971			wave like structures	
					lower	equal	higher	1971	1972
720726	11.20		X			X			
720727	7.50		X			X			
720727	9.15			X		X			
720728	8.30			X			X		
720728	9.60		X				X		
720729	22.70	X				X			X
720730	7.30		X				X	X	
720730	9.80		X				X		
720730	11.50		X				X		
720730	14.90		X				X		
720730	16.30		X				X		
720731	3.00	X					X		X
720731	8.30			X			X		
720731	21.10			X			X	X	
720801	8.40		X				X		
720801	15.00		X			X			
720802	7.60			X			X		
720802	21.20			X			X	X	X
720803	6.70	X					X		
720803	7.70			X			X		
720804	11.00		X				X		
720804	13.47		X				X		
720804	19.00		X			≤ X			
720804	21.40		X			≤ X			
720804	23.20		X						X
720806	21.50		X			X			X
720807	8.00			X		X			
720807	10.30			X		X			
720807	14.30		X				X		
720807	15.50		X				X		
720807	19.70		X				X	X	
720807	20.70		X			X			
720808	7.20		X			X			
720808	14.70		X				X		
720808	19.30		X				X >>		
720809	8.20		X				X		
720809	14.20		X				X >>		X
720809	15.70		X				X		
720811	8.30		X				X		
720811	18.60		X				X		
720811	22.80		X			X			
720812	7.50	X				X			X
720812	19.00			X		X			

≤ and > indicates that the difference exceeds 40 %

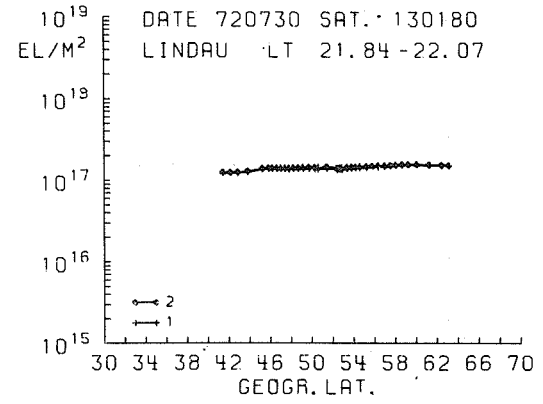
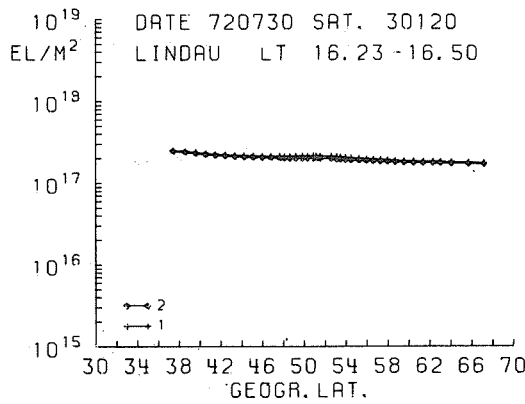
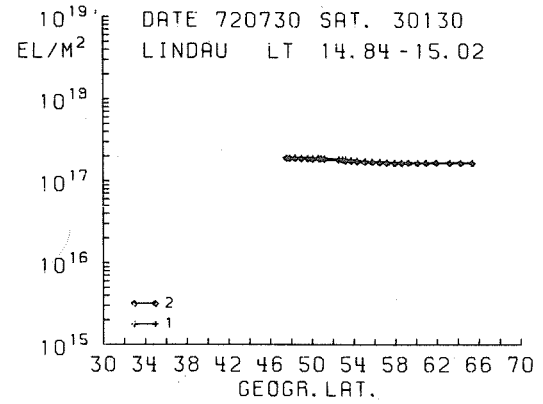
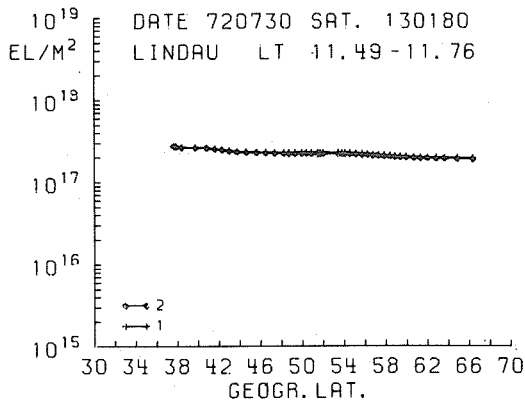
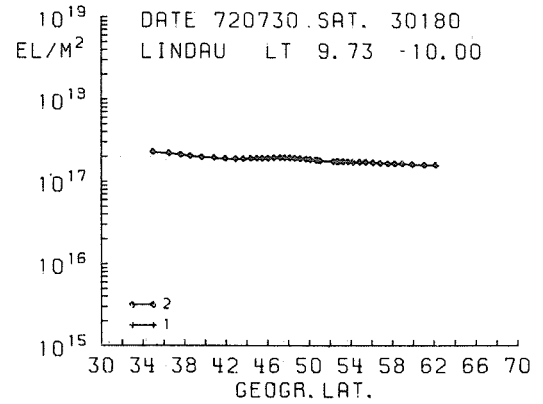
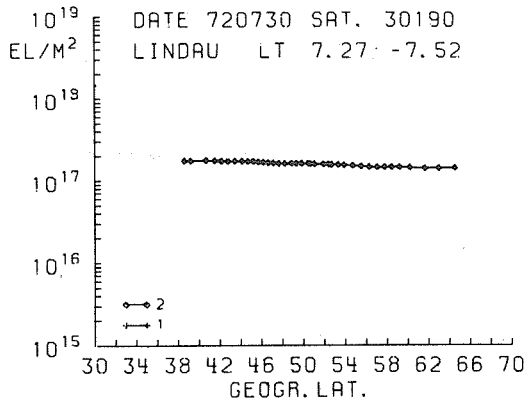
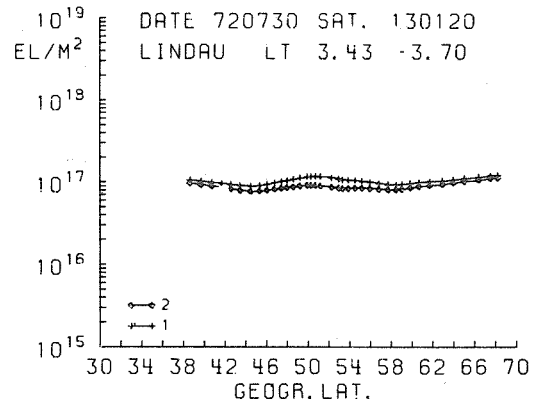
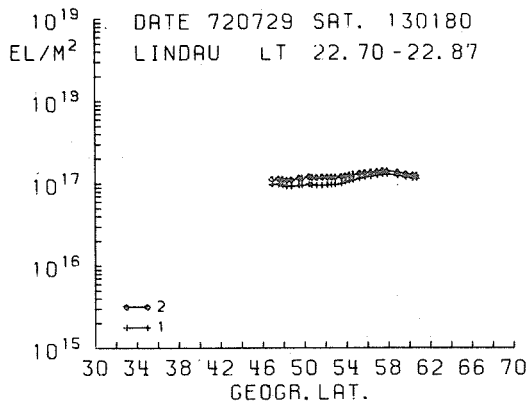


Fig. 2: $I=I(\varphi)$

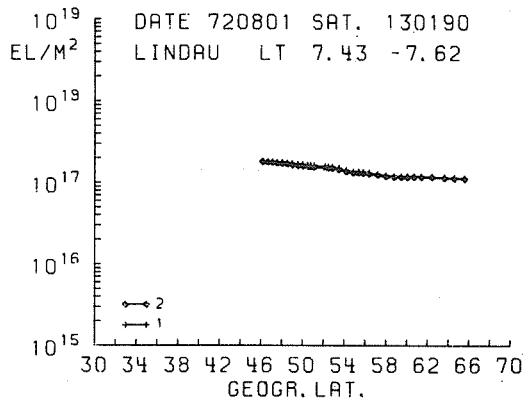
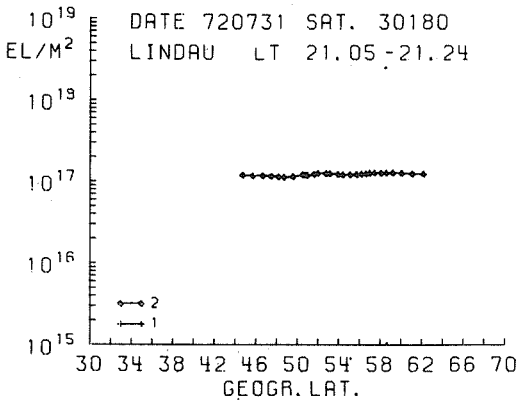
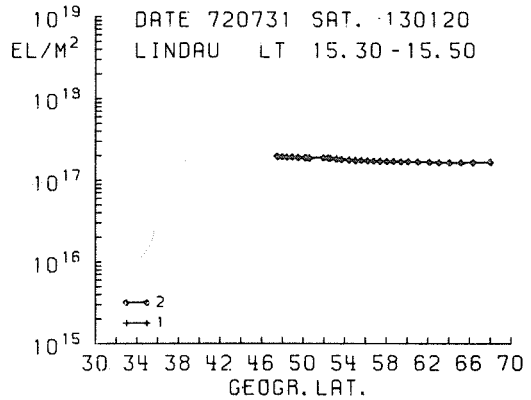
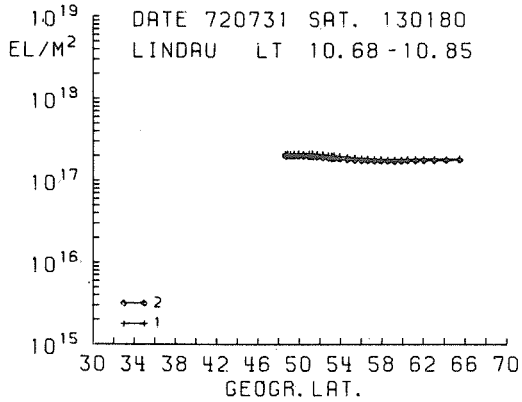
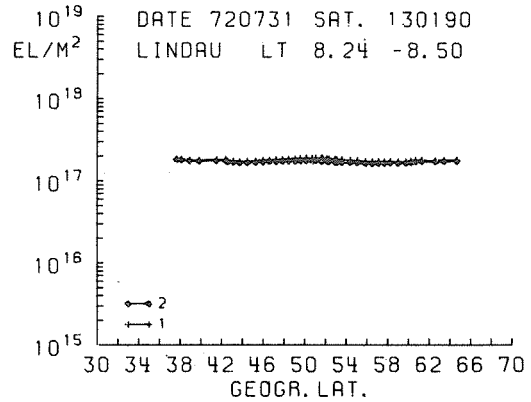
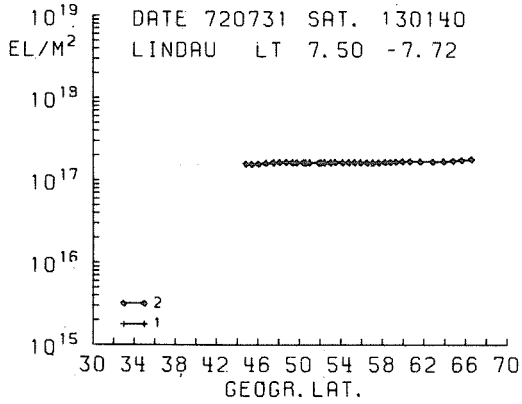
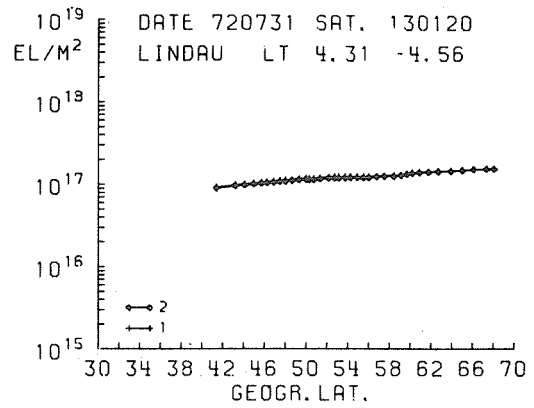
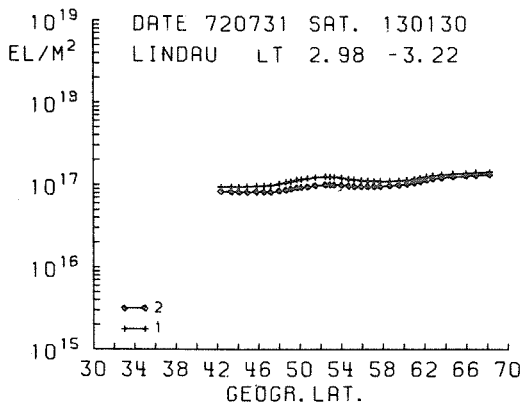


Fig. 3: $I=I(\varphi)$

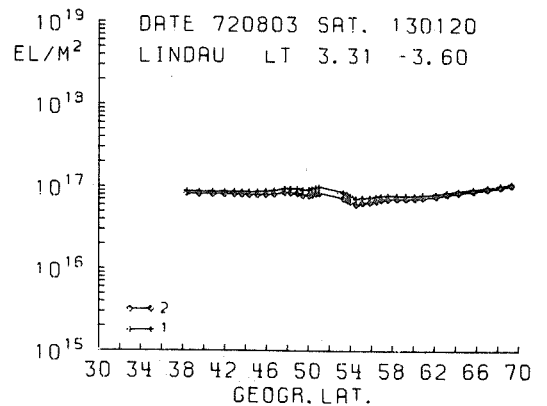
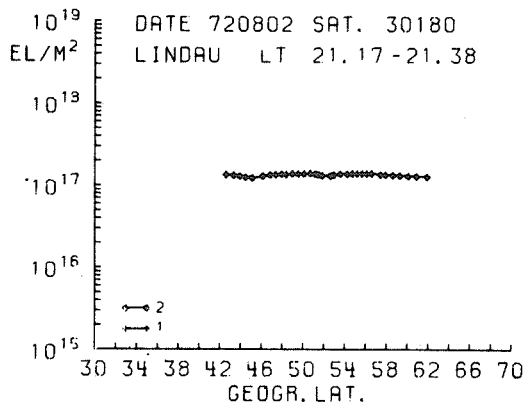
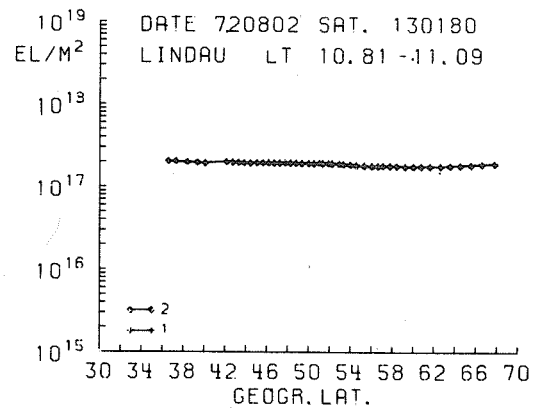
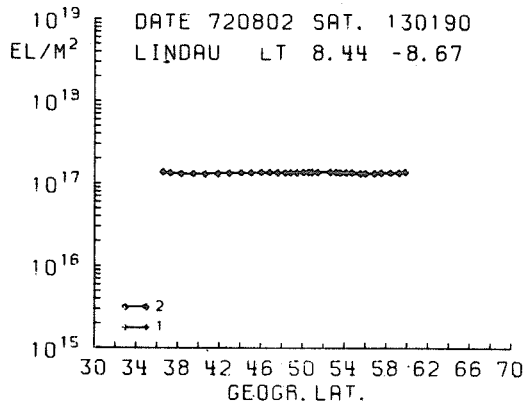
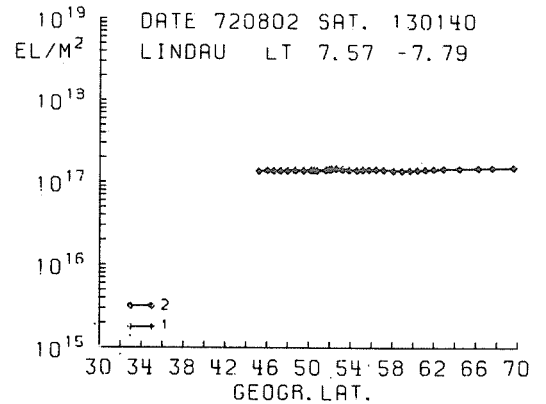
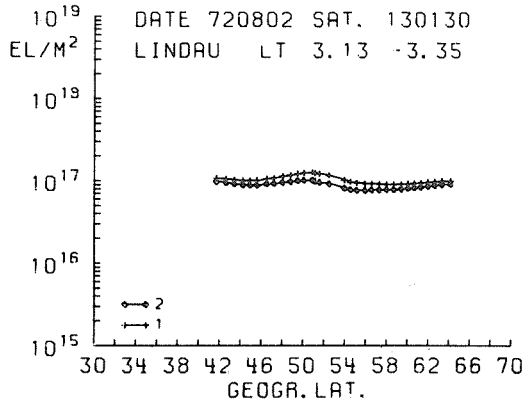
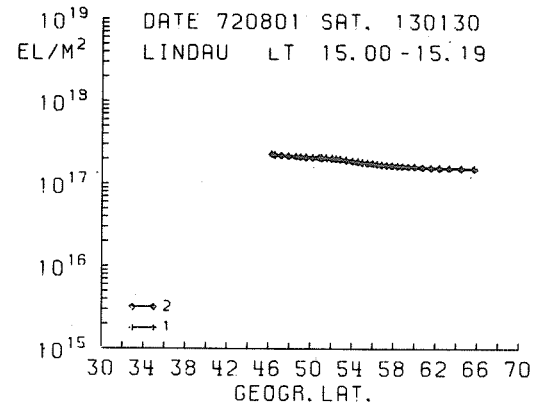
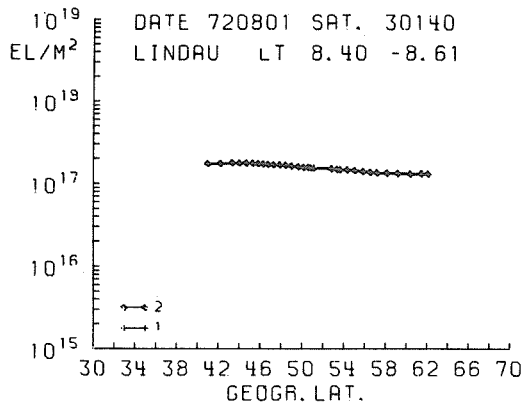


Fig. 4: $I=I(\varphi)$

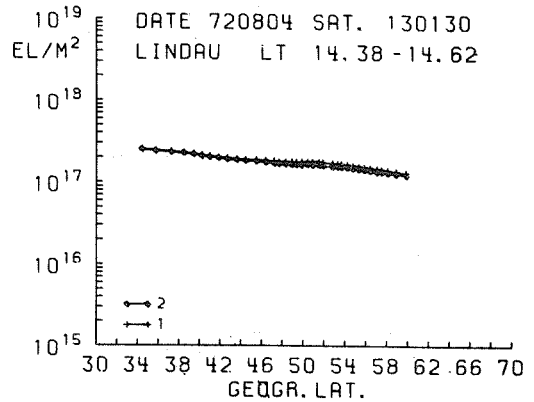
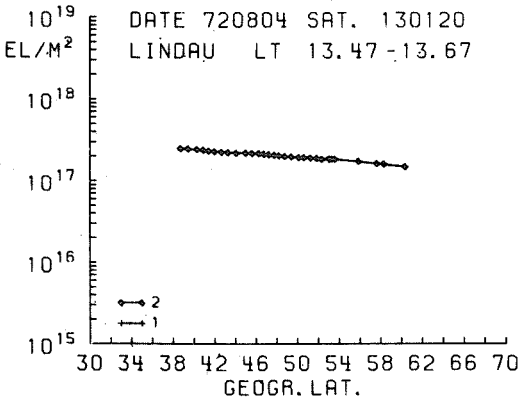
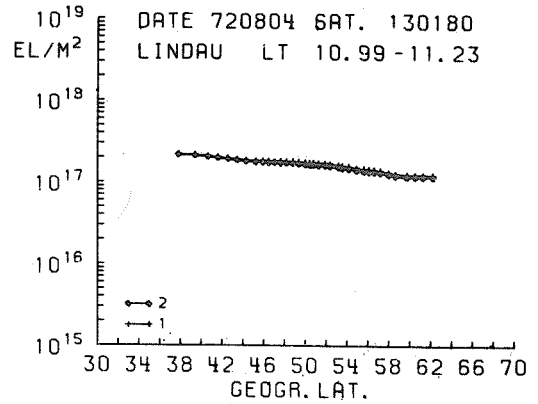
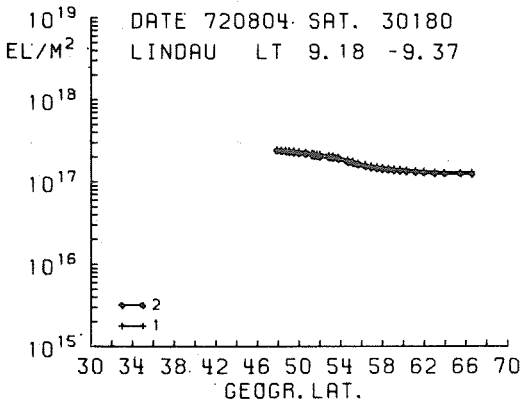
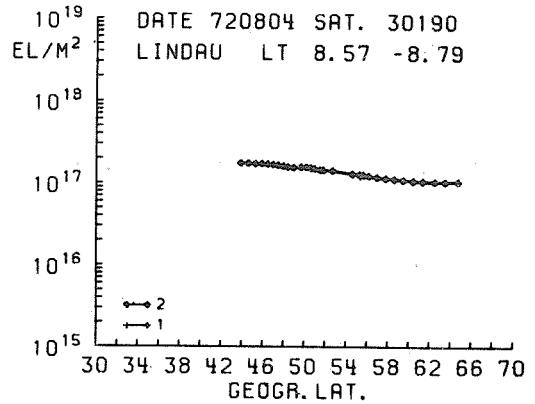
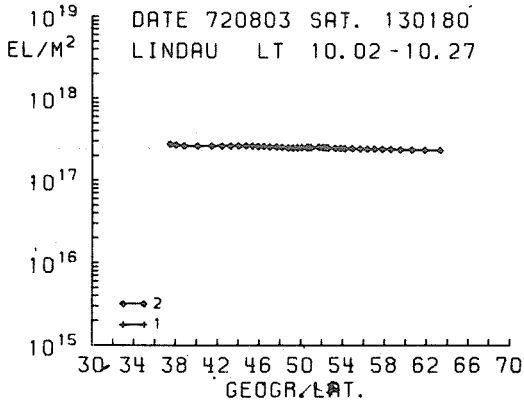
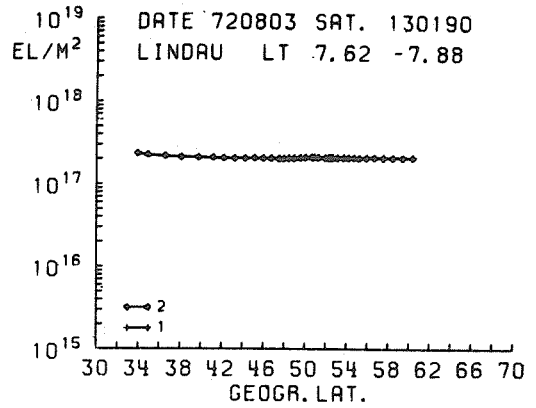
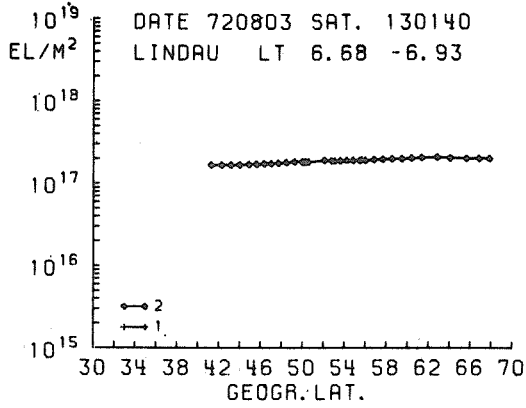


Fig. 5: $I=I(\psi)$

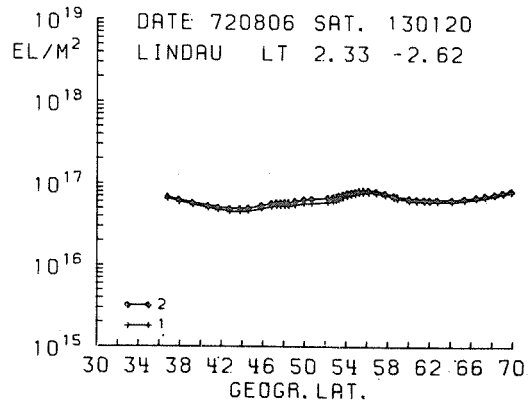
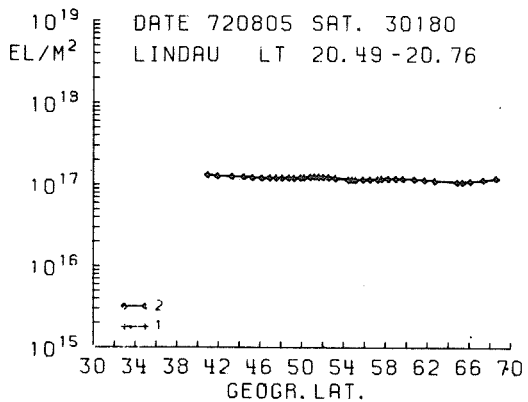
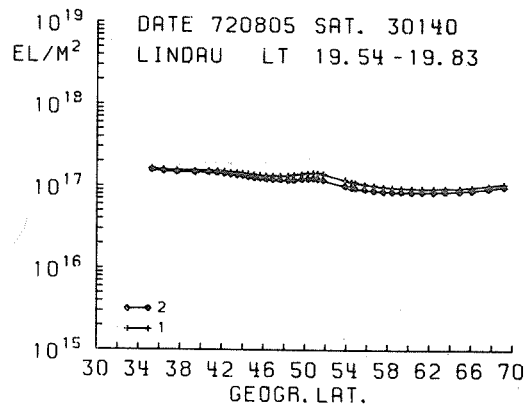
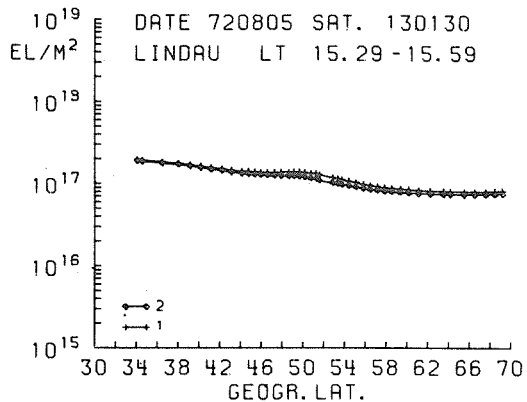
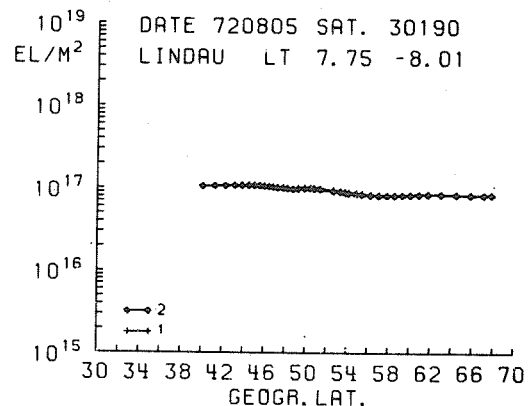
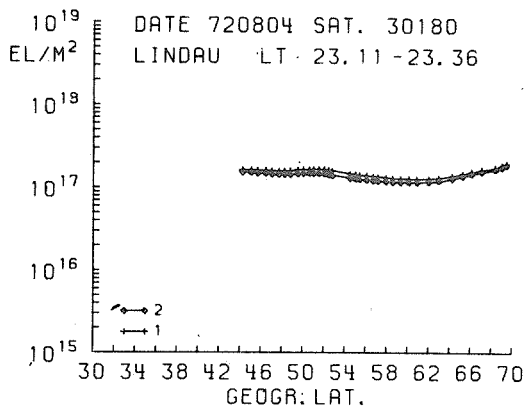
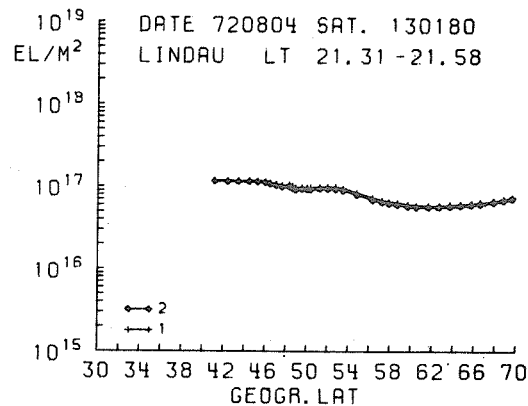
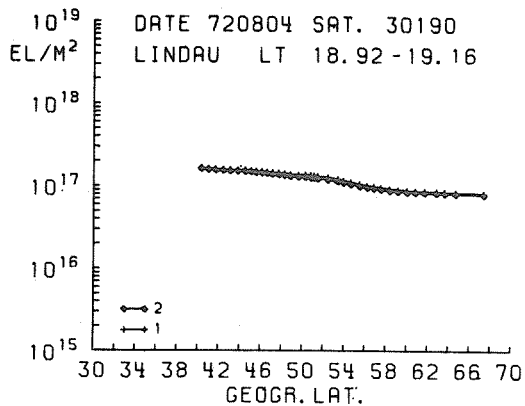


Fig. 6: $I=I(\psi)$

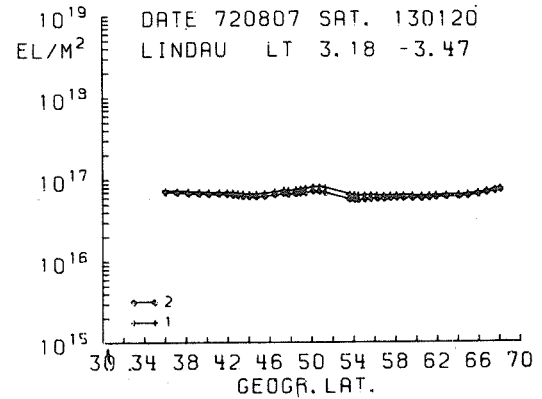
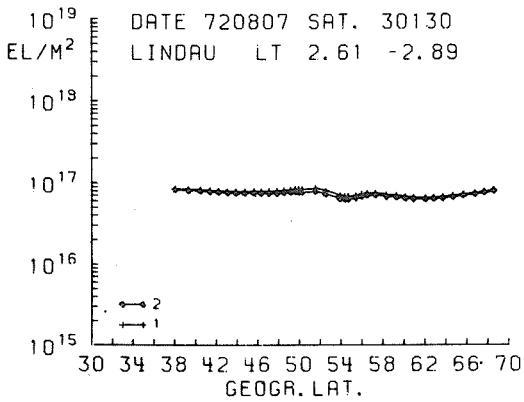
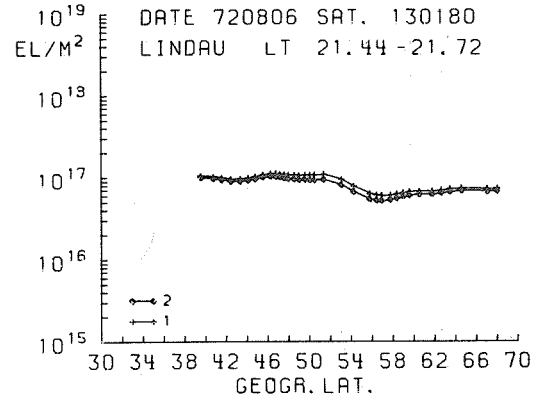
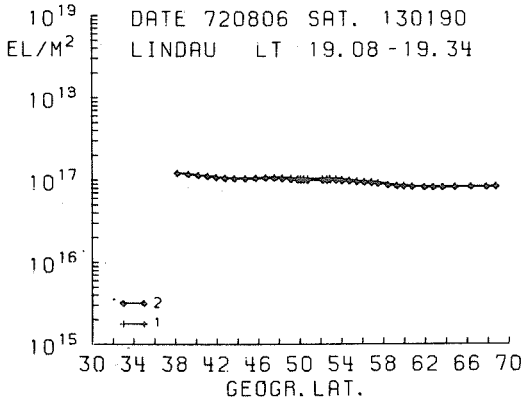
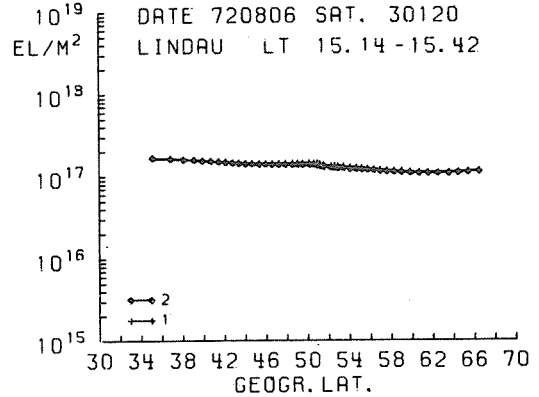
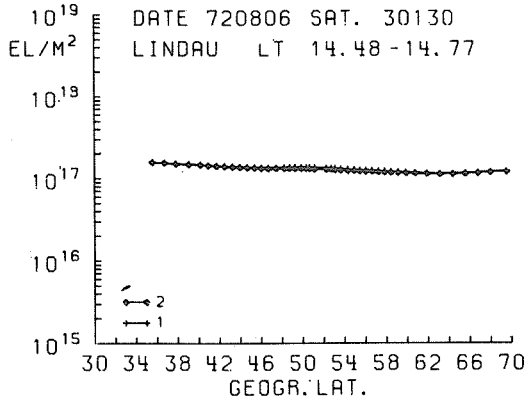
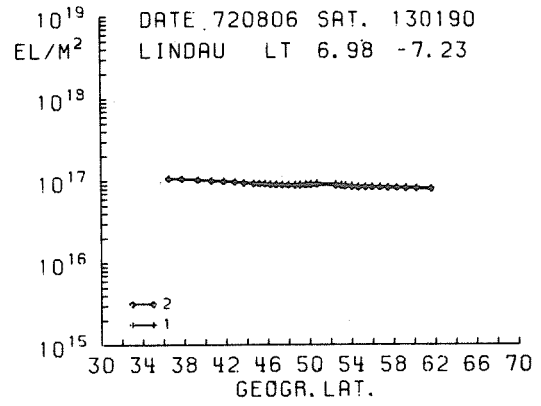
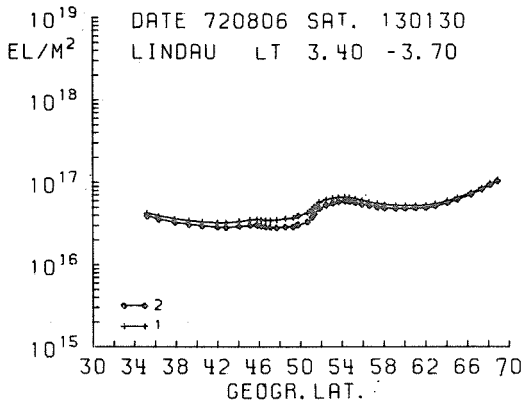


Fig. 7: $I = I(\varphi)$

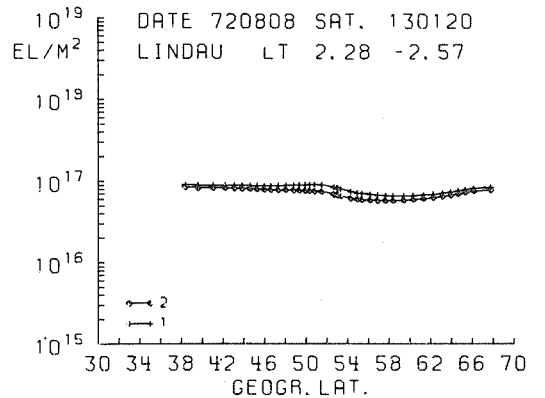
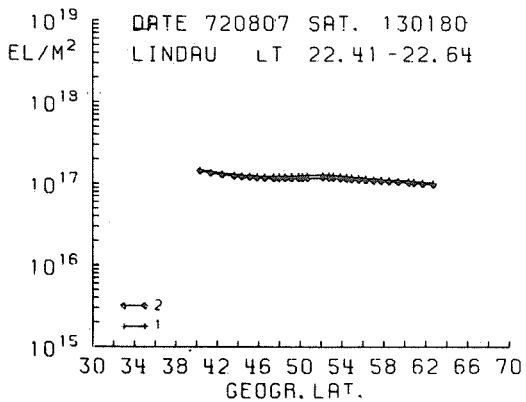
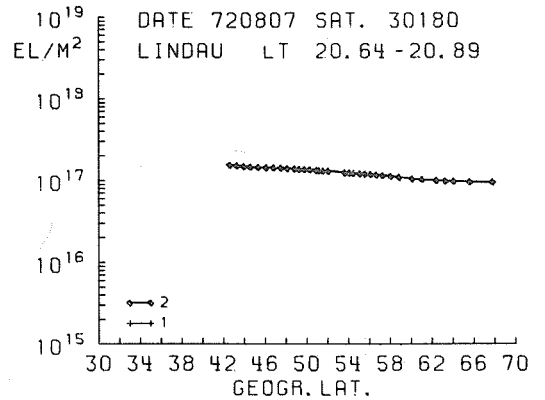
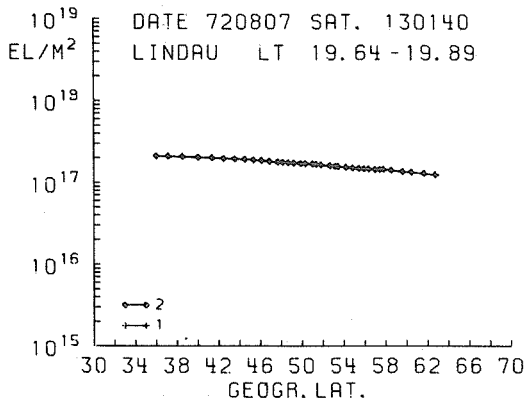
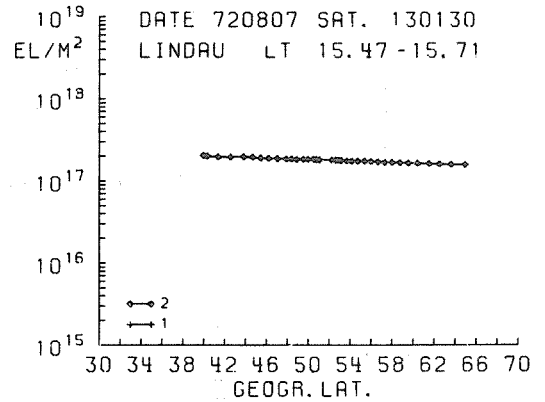
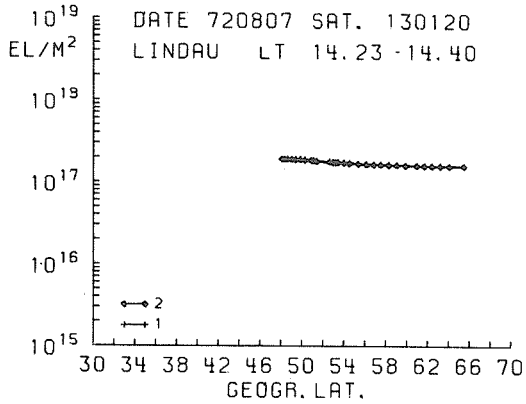
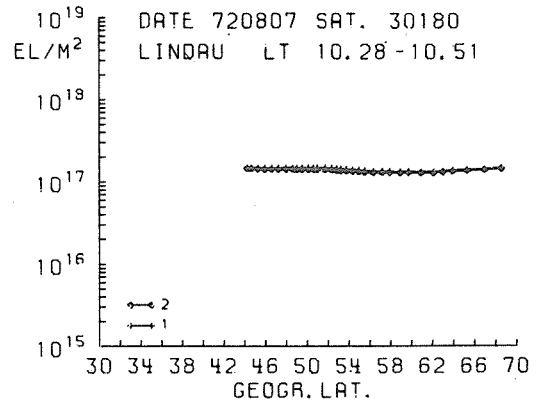
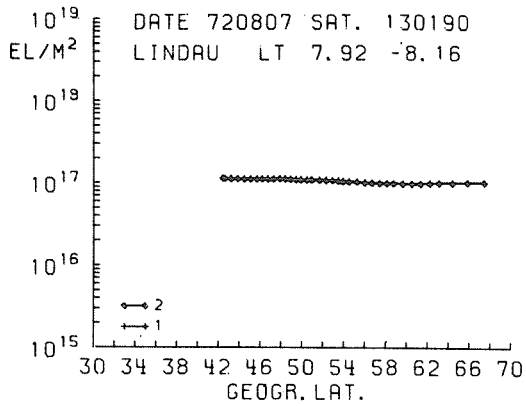


Fig. 8: $I=I(\varphi)$

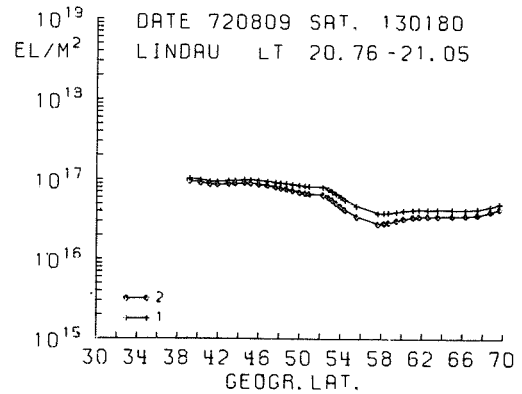
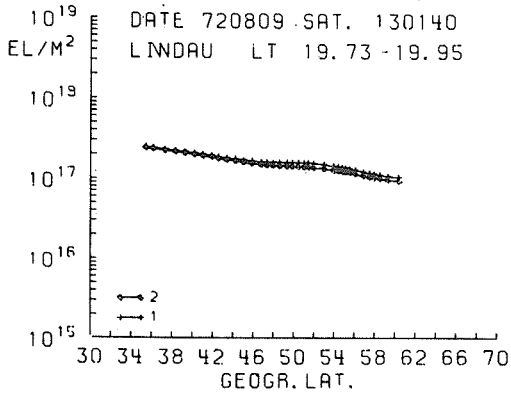
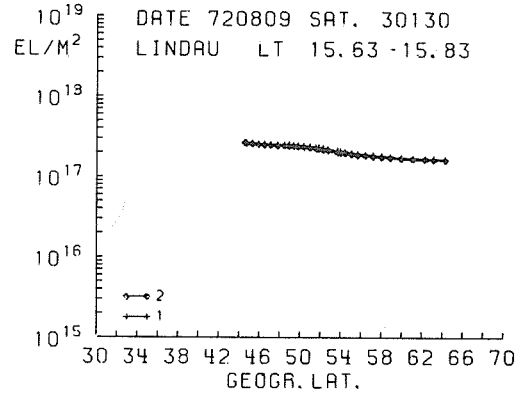
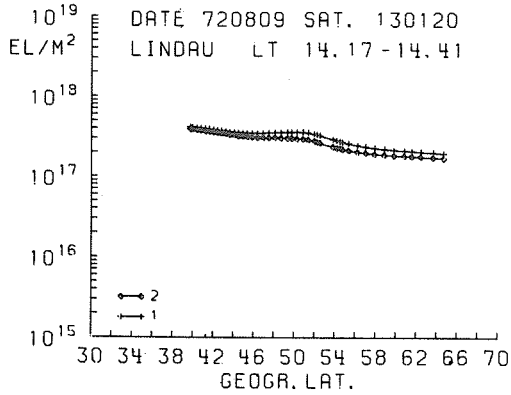
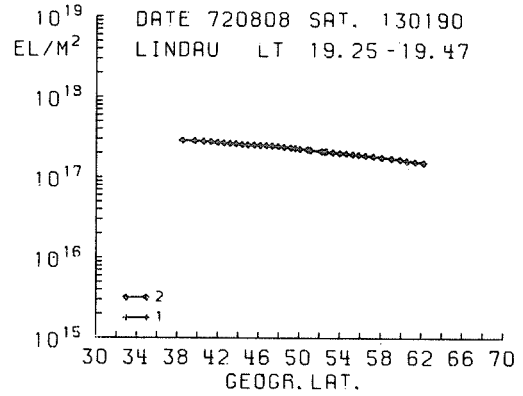
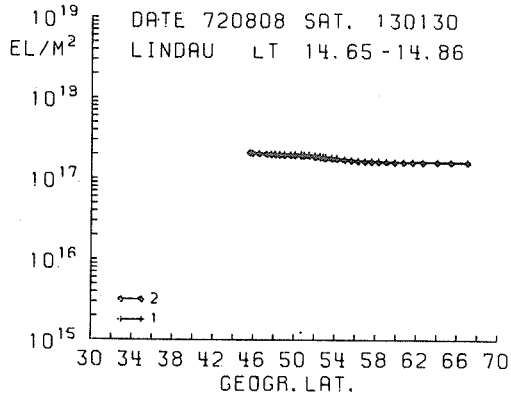
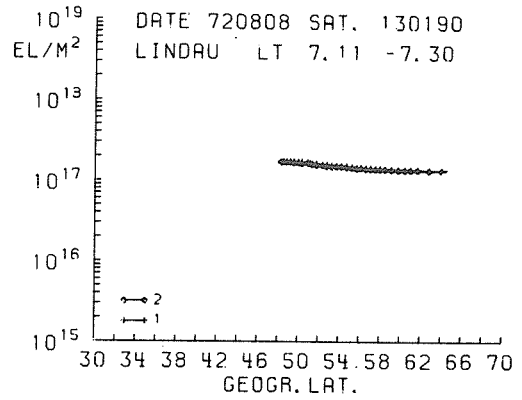
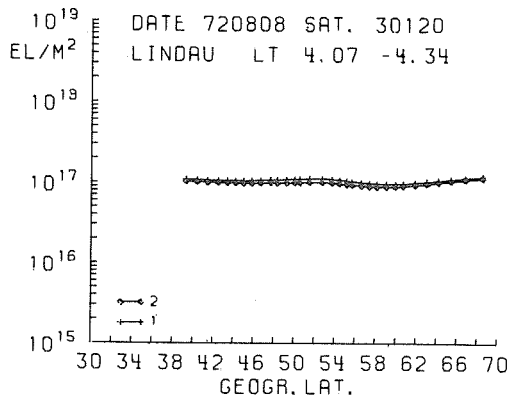


Fig. 9: $I=I(\varphi)$

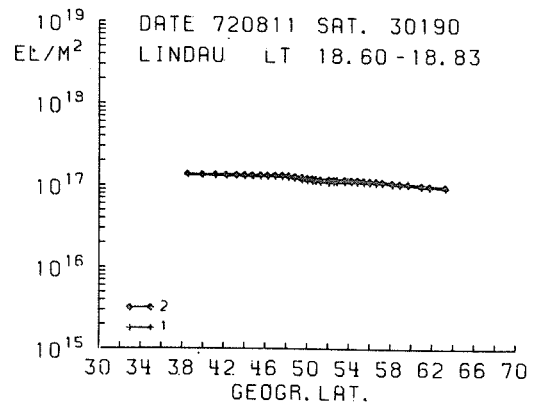
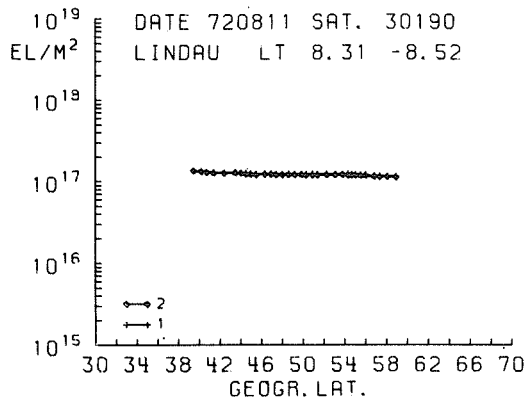
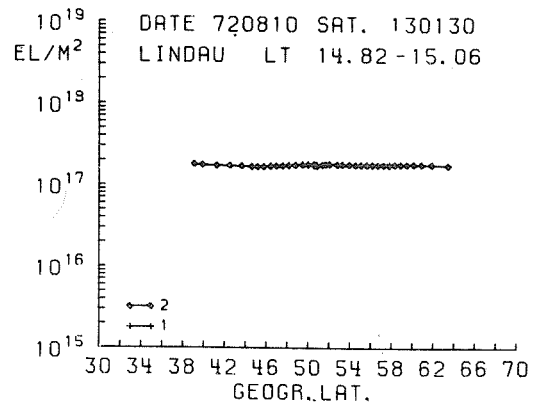
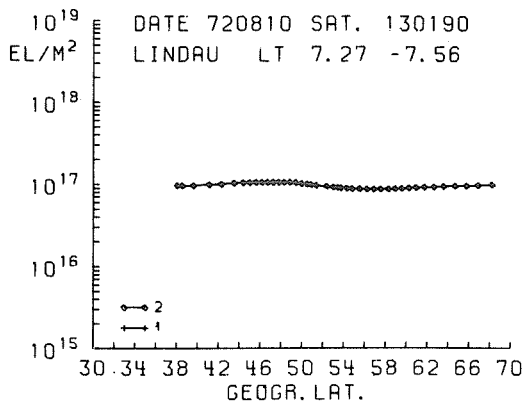
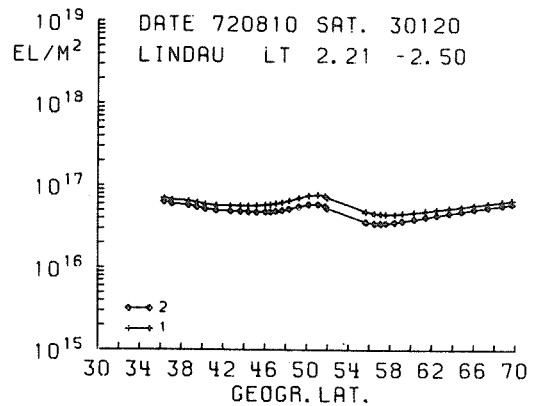
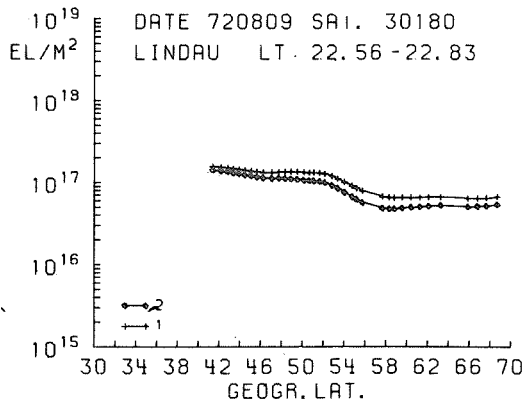
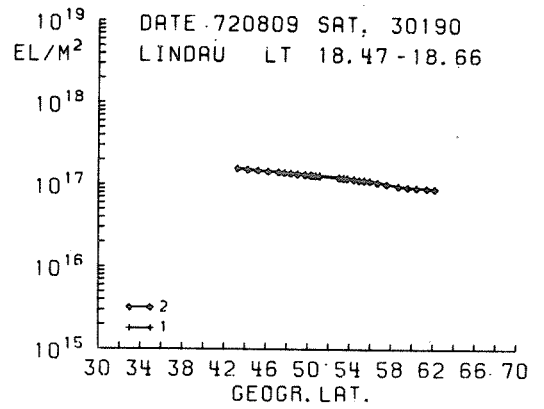
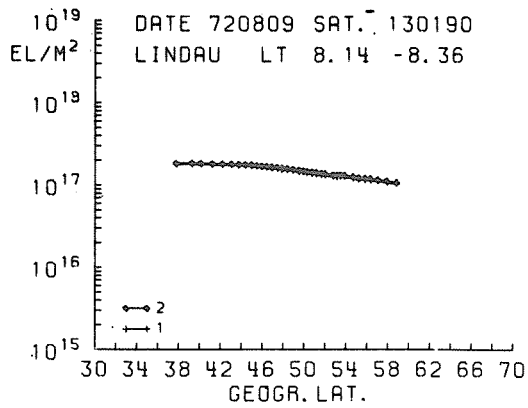


Fig. 10: $I=I(\varphi)$

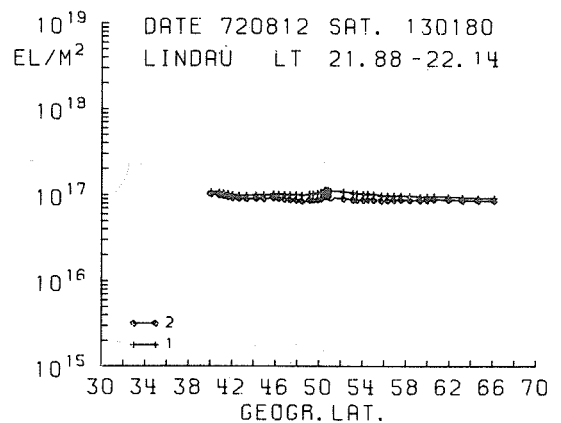
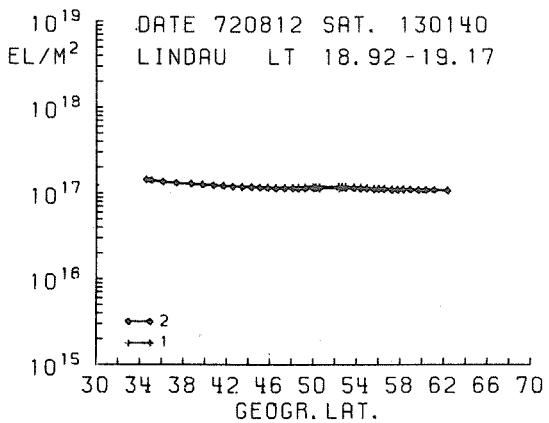
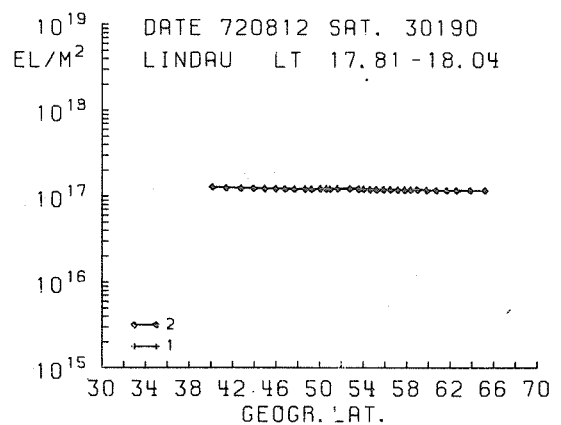
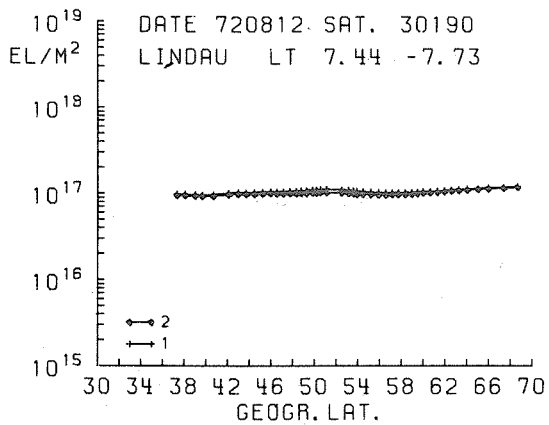
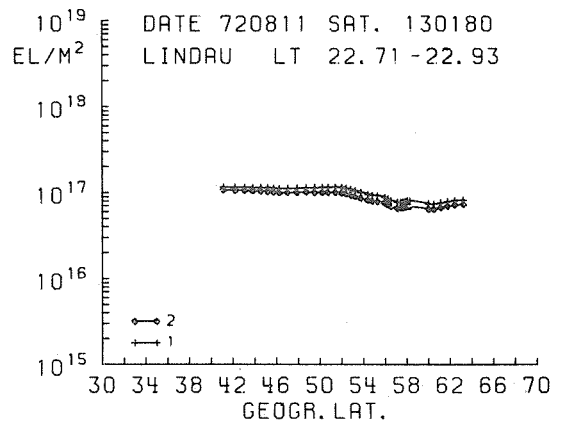
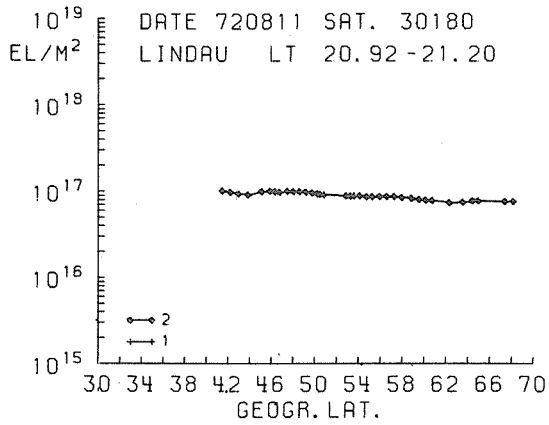


Fig. 11: $I=I(\varphi)$

Faraday Rotation Measurements of the Equatorial Ionosphere
for the Period July 26 - August 14, 1972

by

D. Yeboah-Amankwah and J. R. Koster
Department of Physics
University of Ghana
Legon, Accra, Ghana

This report covers measurements of the total electron content (TEC) of the equatorial ionosphere as a function of local time made at Legon (N5.63, W0.19; Dip angle - 8.47°), Ghana. The period covered is 26 July to 14 August, 1972.

The total electron content has been deduced from measurements on the Faraday rotation made on the 136-47 MHz radio signals from the transmitters located on the geostationary satellite ATS-C.

Measurements of the content were made at 10-minute intervals and the results have been tabulated, and also plotted in Figure 1. World Data Center A for Solar Terrestrial Physics holds the tables.

The mean ionospheric height was taken as 420 km, and this has been employed to compute the geomagnetic factor M which is required to convert the Faraday Rotation angle to electron content. There were periods of loss of data due to equipment malfunction. This is indicated by zero entries in the electron content.

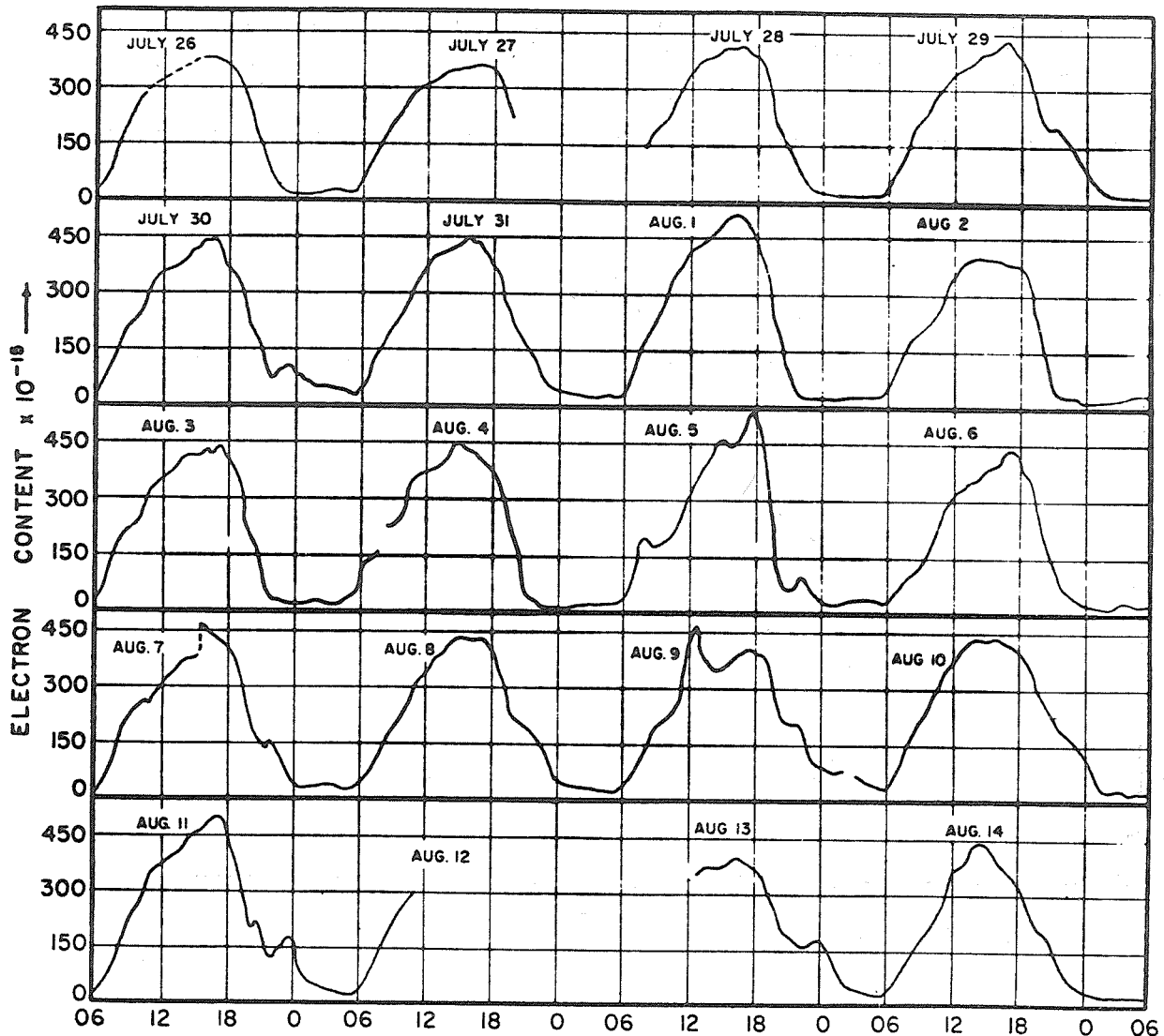


Fig. 1. Total electron content (TEC) of the equatorial ionosphere as a function of Local Time at Legon, Ghana for the period 26 July - 14 August, 1972.

Ionospheric Electron Content Data 2-8 August 1972
Observed at the NASA-Goddard Space Flight Center, Greenbelt, Maryland

by

S. Rangaswamy
Atlantic Science Corporation
9332 Annapolis Road, Lanham, Md. 20801

and

P. E. Schmid
Geodynamics Program Division
NASA-Goddard Space Flight Center
Greenbelt, Md. 20771

Introduction

During the period 2-8 August 1972, the 137.35 MHz signal from the NASA geostationary satellite ATS-3 was continuously monitored at the NASA Goddard Space Flight Center, Greenbelt, Md. (N39.0, W76.8). The Faraday rotation of the linearly polarized signal was measured by an electronic polarimeter and recorded continuously on a chart recorder running at the rate of 2 inches per hour. This note presents the electron content data deduced from the Faraday rotation observations during the period of geophysical disturbances associated with McMath region 11976.

Response of the Electron Content to the Solar Flare on 7 August 1972

Figure 1 shows the diurnal variation of electron content on 7 August 1972. The sudden increase in the electron content due to the occurrence of the solar flare at 1500 UT (1000 EST) can be seen in the Figure. The solar flare produced an increase of 4×10^{16} electrons per meter² within a period of 20 minutes. This was equivalent to a 20% enhancement of the ambient electron content.

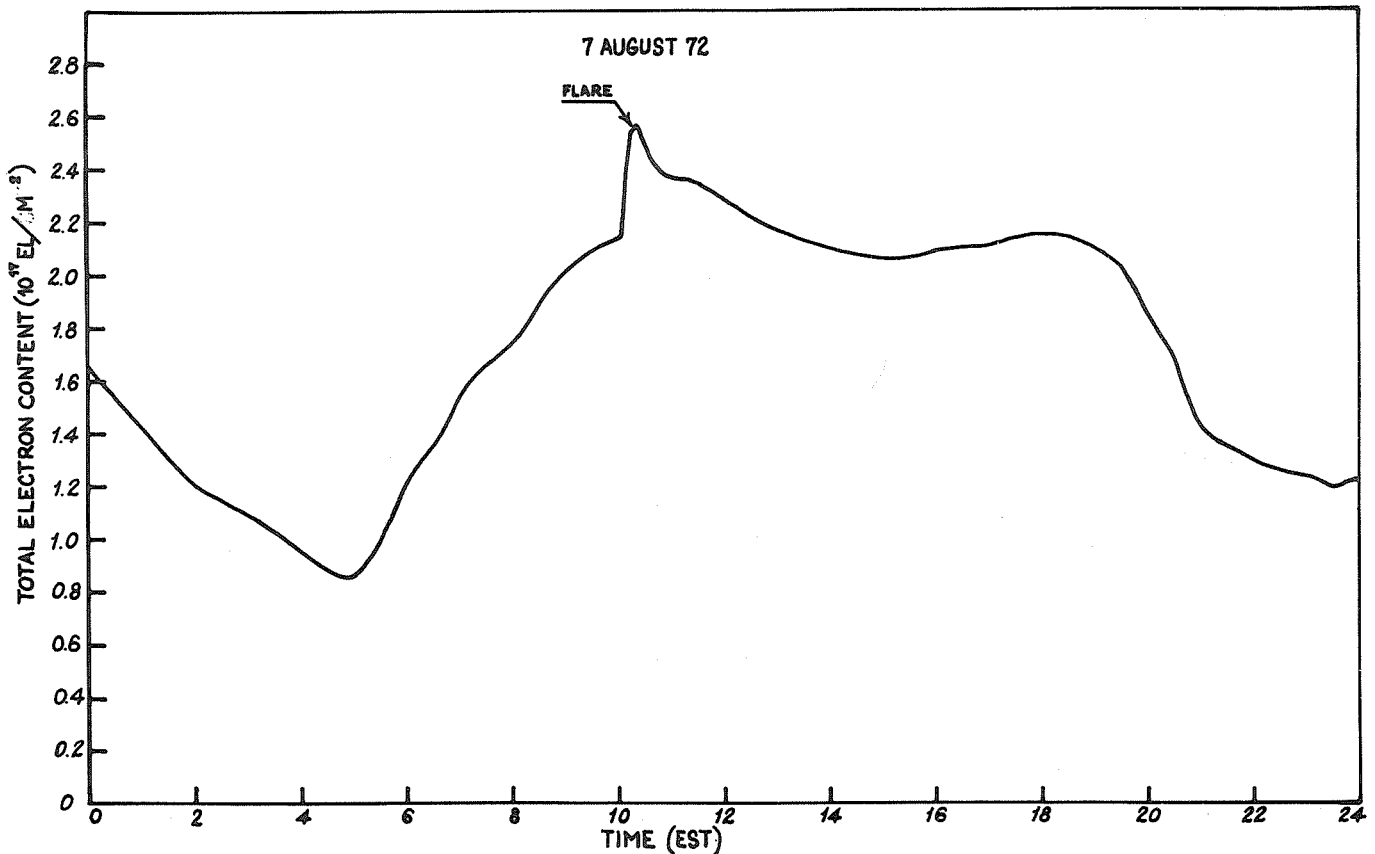


Fig. 1. Diurnal variation of electron content on 7 August 1972.

Response of the Electron Content to Geomagnetic Storms

The main effect of the geomagnetic storm was to reduce the electron content values below the quiet period values. In addition, quasi-sinusoidal oscillations of large amplitude were seen in the time variation of electron content and the thickness parameter (electron content/critical frequency of the F-region). These are plotted in Figure 2. The electron content on August 4 can be seen to be low except near the sunset period when there is a sudden increase. This post-sunset increase is characteristic of mid-latitude electron content during geomagnetic storms.

The thickness parameter data have intermittent breaks due to the non-availability of critical frequency data. The breaks are shown by dashed lines in Figure 2. The thickness parameter was enormously increased during the storm period, with values reaching double the magnitude of quiet day values. This enhancement of the thickness parameter is related to the heating of the neutral atmosphere during the geomagnetic storm.

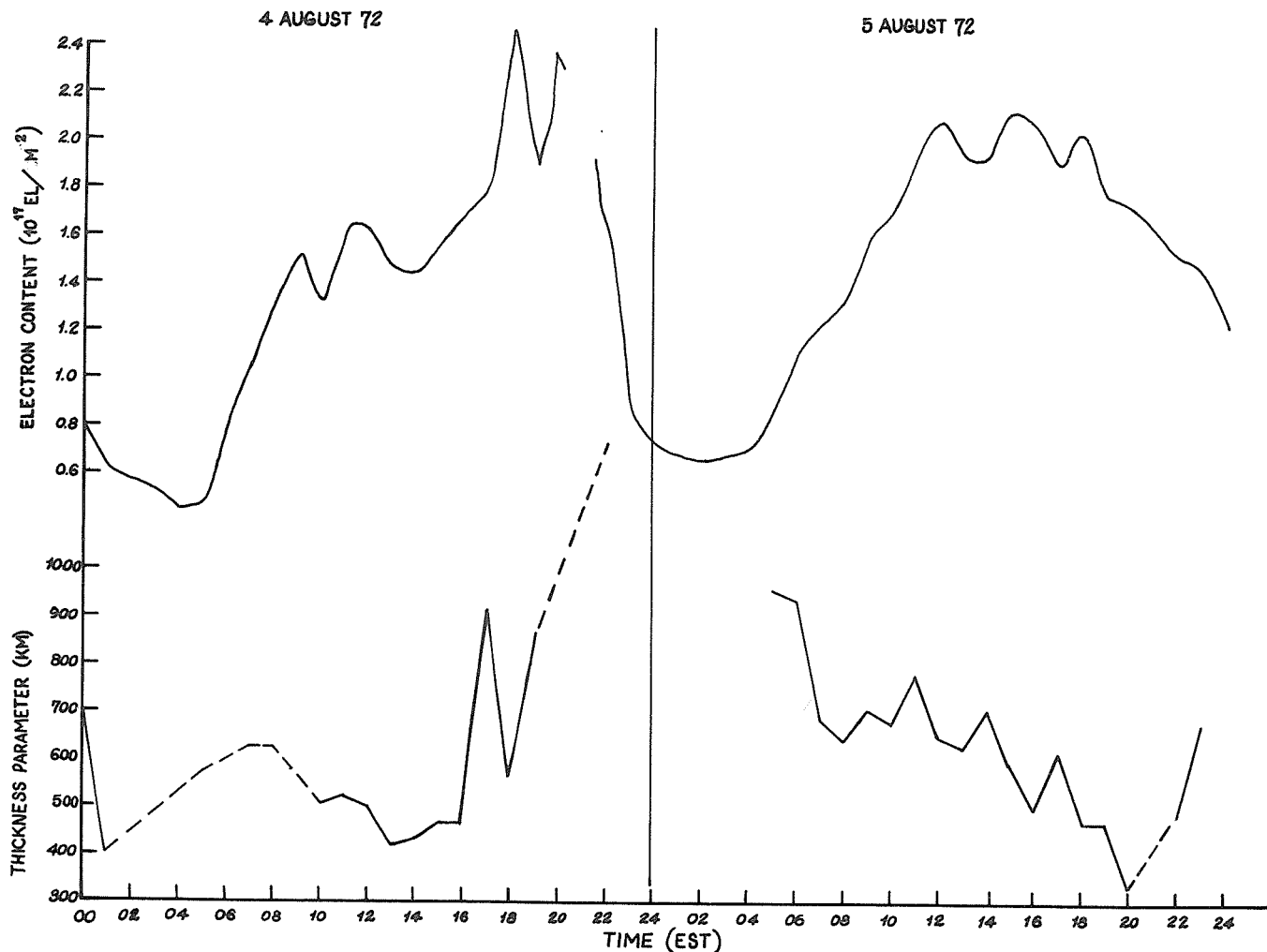


Fig. 2. Diurnal variation of electron content and the thickness parameter (electron content/critical frequency of the F-region) on 4 and 5 August 1972.

Table 1 gives the hourly tabulation of electron content data for the period 2-8 August 1972.

Table 1

Hourly Values of Electron Content (in units of 10^{17} electrons/meter²)
August 1972

Day	0	1	2	3	4	5	6	7	8	9	10	11
1												
2	1.115	0.858	0.768	0.720	0.526	0.622	0.974	1.289	1.626	1.789	1.989	2.118
3	1.184	1.122	0.986	0.834	0.731	0.744	1.230	1.703	2.112	2.265	2.430	2.524
4	0.784	0.616	0.560	0.536	0.447	0.482	0.789	1.074	1.307	1.520	1.332	1.628
5	0.741	0.692	0.671	0.687	0.710	0.865	1.123	1.233	1.344	1.622	1.705	1.972
6	1.235	0.742	0.764	0.773	0.731	0.891	1.190	1.328	1.610	1.851	1.986	2.118
7	1.635	1.418	1.214	1.107	0.950	0.858	1.219	1.552	1.735	1.997	2.133	2.366
8	1.273	1.250	1.146	1.010	0.918	0.969	1.329	1.683	1.920	2.258	2.594	2.880

Day	12	13	14	15	16	17	18	19	20	21	22	23
1												
2	2.171	2.205	2.230	2.272	2.409	2.451	2.535	2.309	1.782	1.523	1.362	1.275
3	2.646	2.567	2.449	2.366	2.247	2.266	2.289	2.175	1.761	1.593	1.363	1.268
4	1.615	1.469	1.455	1.566	1.691	1.824	2.462	1.890			1.609	0.875
5	2.099	1.954	1.961	2.141	2.091	1.924	2.039	1.777	1.738	1.637	1.517	1.481
6	2.153	2.163	2.373	2.162	2.078	2.217	2.234	2.130	1.828	1.678	1.640	1.684
7	2.281	2.171	2.093	2.063	2.096	2.112	2.153	2.092	1.837	1.423	1.288	1.259
8	3.092	3.083	2.969	2.854	2.757	2.586	2.575	2.519	2.115	1.798	1.710	1.659

Total Electron Content Measurements during July 26 - August 15, 1972

by

Elizabeth A. Essex
Division of Space and Theoretical Physics
La Trobe University
Bundoora, Victoria 3083, Australia

We present observations of the columnar electron content for the period July 25 - August 15, 1972. These observations were taken at Melbourne (geographic coordinates $S37.46^{\circ}$, $E144.93^{\circ}$) using the 137.35 MHz VHF beacon on the geostationary satellite ATS-1. Faraday rotation of the beacon signal was measured using the rotating antenna technique of Titheridge [1966]. ATS-1, located at $W149^{\circ}$, has an azimuth of $E75^{\circ}$ and elevation of approximately 10° from Melbourne. The geographic coordinates of the sub-ionospheric point are $S33.74^{\circ}$, $E158.94^{\circ}$. A mean ionospheric height of 400 km is assumed.

Figures 1a, b and c show a comparison of the total electron content N_f with slab thickness and magnetic K indices. The electron density was obtained from Canberra ionograms ($S35.30^{\circ}$, $E149.00^{\circ}$ geographic coordinates, -43.99 , 224.29 geomagnetic coordinates). The magnetic K indices were obtained from Toolangi observatory ($S37.53^{\circ}$, $E145.47^{\circ}$ geographic coordinates). Gaps in the data are due to a transfer in observatory location.

Perhaps the most interesting feature of the data is the sudden increase in electron content on August 4 (local time is UT + 10 hours). During the period of one hour (approximately 0900 hours August 5 local time) the electron content increased from $193 \times 10^{15} \text{ em}^{-2}$ to $371 \times 10^{15} \text{ em}^{-2}$ and just as quickly decreased to $229 \times 10^{15} \text{ em}^{-2}$. Such a rapid increase and decrease has not been observed previously at this location. The time of occurrence is also not in accord with previous storm observations as an increase usually occurs after midday at the earliest. On this particular occasion, the electron content remained below average for the rest of the day. There were two ssc associated with this event, on August 4 at 0119 UT and the other at 2055 UT. The large increase on August 5 at approximately 0900 local time followed the second ssc by about two hours. During the previous evening (local time) a dusk enhancement associated with the first storm sudden commencement had occurred.

The Canberra ionograms of August 4 were complicated for most of the day after 0900 local time by the existence of the G condition, i.e. the F2-layer was masked by the underlying F1-layer which had a higher maximum electron density. Hence the slab thickness is also complicated by this behavior. This type of behavior associated with storm conditions has also been noted by Fritz [1971]. It is difficult to offer an explanation for the behavior of the total electron content during this period. However, transport of ionization appears to be a feasible explanation.

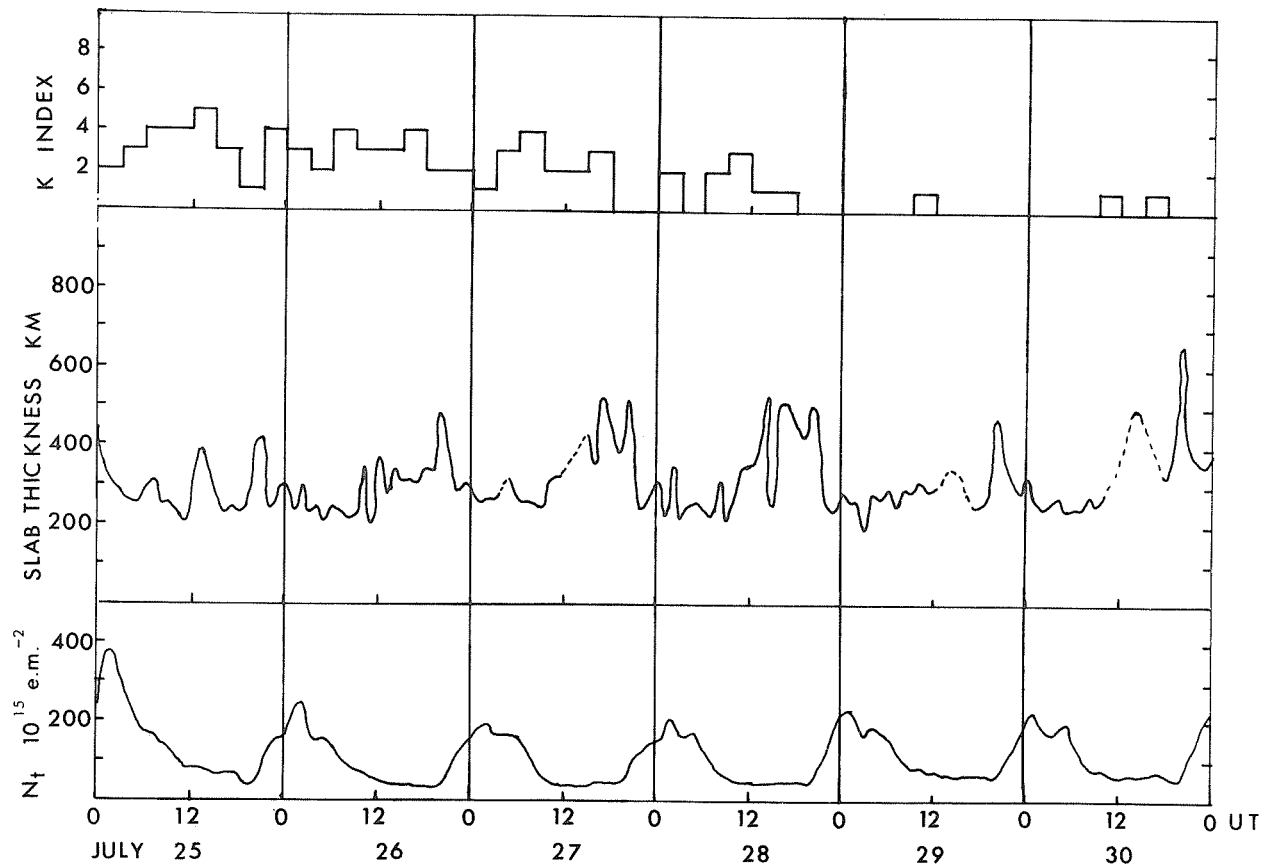
The day of August 9-10 (UT) shows a typical decrease in electron content below the average monthly value following the storm sudden commencement on August 8 at 2354 UT.

Acknowledgments

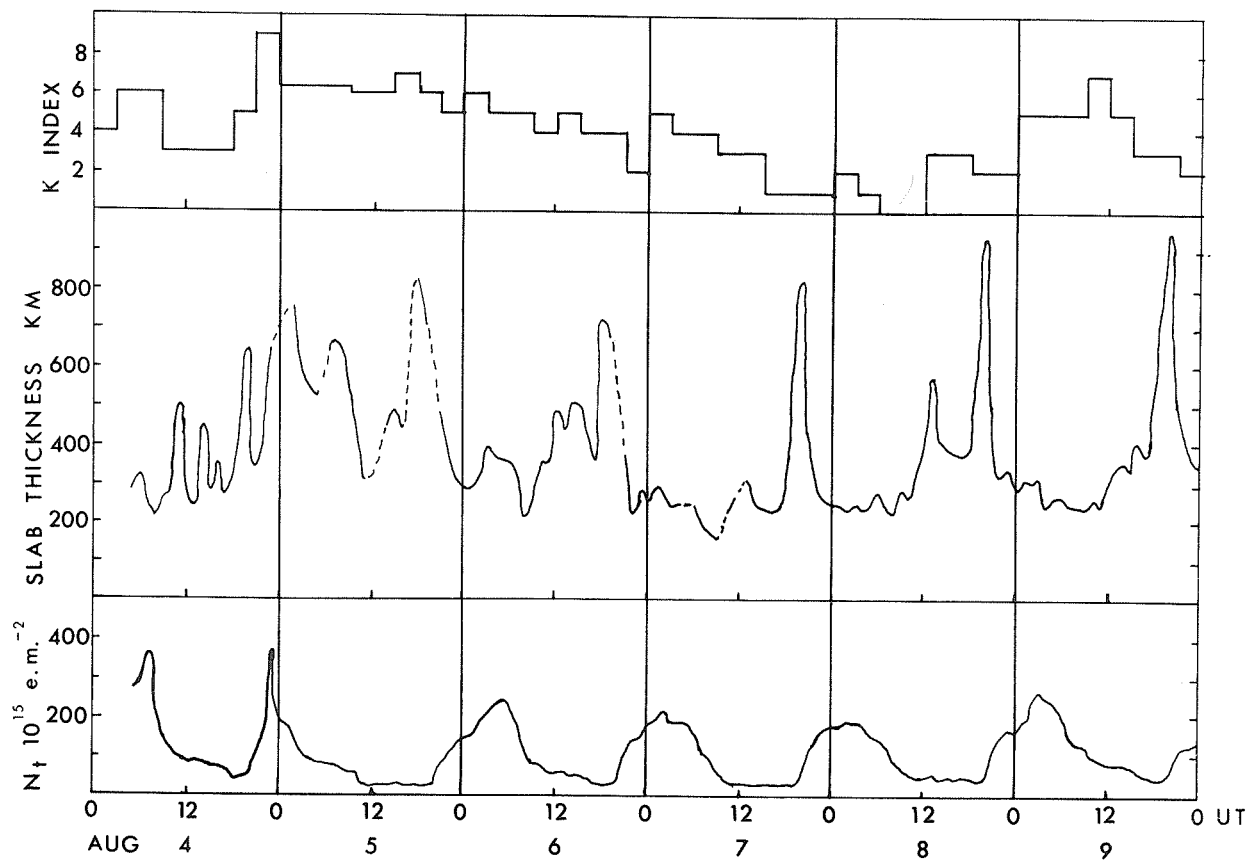
The K indices were supplied by the Bureau of Mineral Resources of the Department of Minerals and Energy, and the ionograms by the Ionospheric Prediction Service Division of the Department of Science. This work is supported by the Australian Radio Research Board.

REFERENCES

- | | | |
|-------------------|------|--|
| FRITZ, R. B. | 1971 | <u>Ionospheric structure during the Storm of March 8, 1970, World Data Center A, Upper Atmosphere Geophysics Report, UAG-12, Part II, 213.</u> |
| TITHERIDGE, J. E. | 1966 | Continuous records of the total electron content of the ionosphere, <u>J. Atmosph. Terr. Phys.</u> , <u>28</u> , 1135. |



(a)



(b)

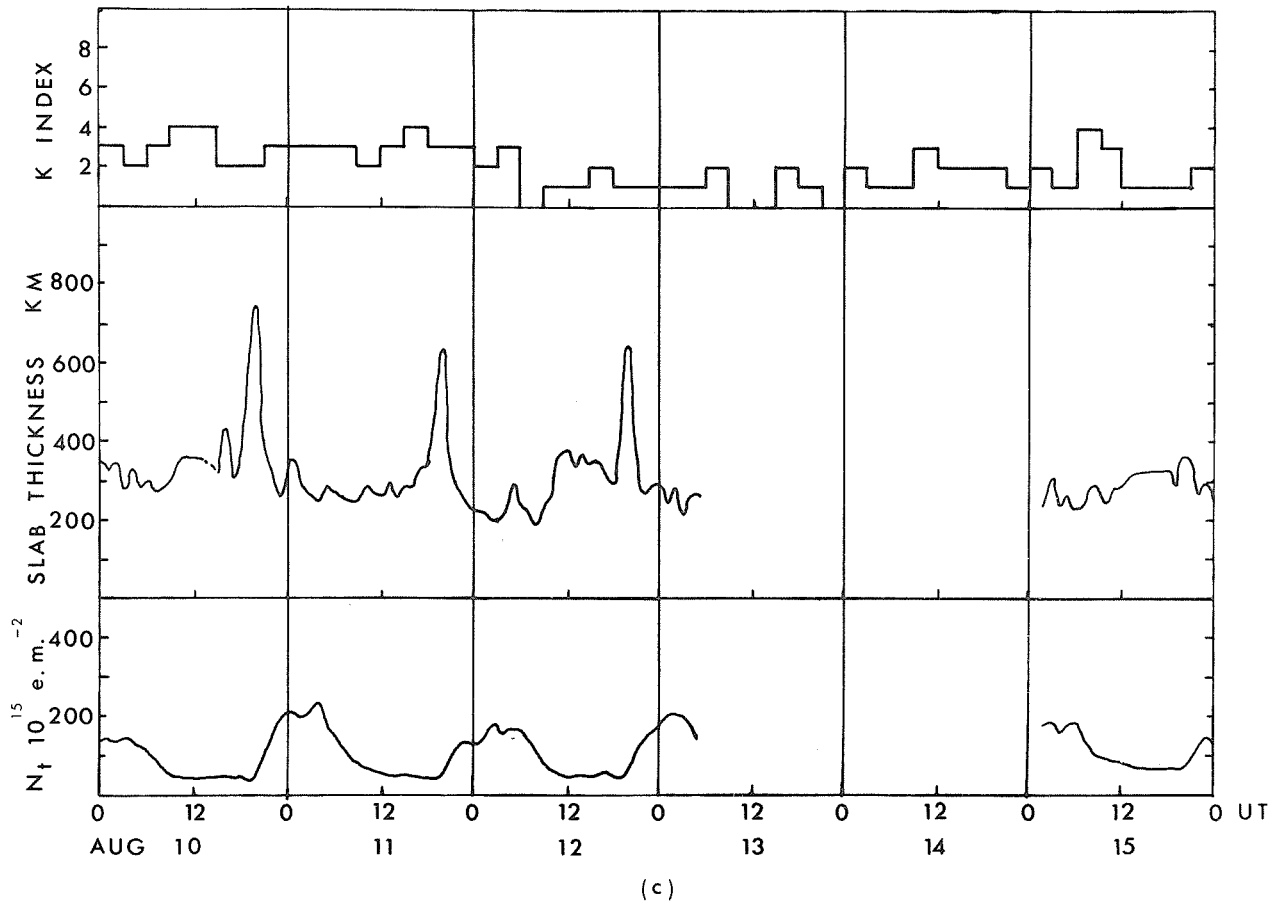


Fig. 1 Total electron content of N_t from the geostationary satellite ATS-1 as observed from Melbourne July 25 - August 15 compared with the three hour magnetic K indices from Toolangi and with the slab thickness calculated using ionograms from Canberra.

Satellite Scintillation Observations at Sagamore Hill, Mass. and
Narssarssuaq, Greenland during the Solar Events of August 3 - 10, 1972

by

Jules Aarons
Ionospheric Physics Laboratory
Air Force Cambridge Research Laboratory
L. G. Hanscom Field, Bedford, Mass. 01730

and

Eileen Martin
Emmanuel College
Boston, Mass. 02115

Introduction

Small scale F-layer irregularities (500m - 5km) have a high latitude morphology which schematically appears as Figure 1. The coordinates are local time and invariant latitude at 350 km. The equatorward edge of the magnetically quiet boundary of these irregularities expands during magnetic storms; the intensity of the irregularities also increases during these storms. However, the basic structure of the region is maintained. Therefore, the effect of an increase in magnetic activity which affects the scintillation occurrence pattern is determined by local time at the intersection of the ray path from the station to the satellite and the ionospheric height where the irregularities are situated, here assumed to be ~ 350 km. Using the method of scintillation analysis shown by Whitney et al. [1969], scintillation data from the time period August 3 - 10, 1972 was analyzed for the stations at Narssarssuaq, Greenland and the Sagamore Hill Observatory, Hamilton, Mass. The 254 MHz beacon of the LES-6 satellite was used for the measurements at both of these stations, and, in addition, the 136 MHz beacon of the ATS-3 and ATS-5 satellites was included in the data measurements made at the Sagamore Hill Observatory. The elevation angles and subionospheric intersection coordinates for these satellites are given in Table 1 below.

Table 1.

Sub-ionospheric Intersection at 350 km.

	Elevation Angle	Invariant Latitude	Geographic Latitude	Geographic Longitude
Sagamore Hill				
ATS-3	41.0°	53.3°	39.3°	-71.0°
ATS-5	29.5	53.2	39.2	-75.2
LES-6	30.9	52.8	39.2	-66.7
Narssarssuaq				
LES-6	20.7	62.9	54.4	-43.9

The data for this time period is seen as a classic case in point. A model of F-layer high latitude irregularities is now in process, a preliminary analysis of which has been presented by Aarons [1973].

Sagamore Hill

August 2 and 3 were magnetically quiet days and the scintillation rate was low, as can be seen in Figure 2. On August 4, shortly after local midnight, there is a sharp increase in K index, accompanied by a more pronounced diurnal peak of scintillation index (SI). August 5 is also a period of increase in magnetic activity and again the large peak of SI in the early morning hours is evident. On August 6, the magnetic index is in a disturbed condition, but not to the extent of the previous day. This diurnal peak after local midnight is somewhat smaller, but it is still larger than usual. As the magnetic index continues to fall on August 7 and 8, the scintillation index does the same until both are very low on August 8. The index becomes disturbed again on August 9, and the SI peak after local midnight is again exaggerated. Both magnetic index and the scintillation index fall on August 10.

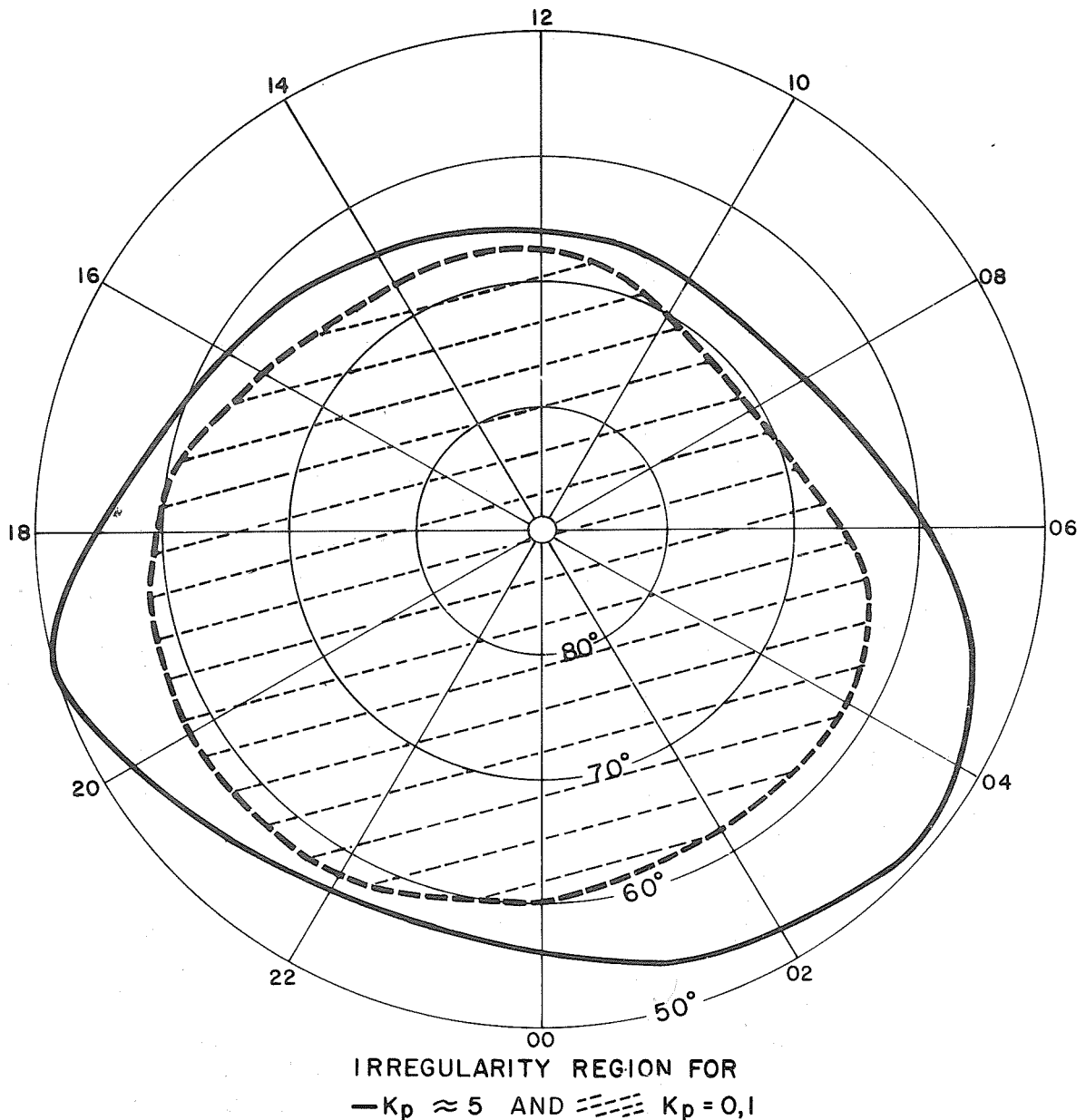


Fig. 1 Small scale F-layer irregularities at high latitudes

Narssarssuaq

The scintillation index at Narssarssuaq was high for most of this period, particularly for the days of August 4-6 (Figure 3), which as was noted earlier, was a magnetically disturbed period. The diurnal pattern is still seen, but the effect of the increased magnetic activity can be seen in the large scintillation index over a somewhat expanded time period around the usual peak.

REFERENCES

AARONS, J.	1973	A descriptive model of F-layer high latitude irregularities, AGARDograph No. 166, <u>Total Electron Content and Scintillation Studies of the Ionosphere</u> , Jules Aarons, ed., 59-70.
WHITNEY, H. E., C. MALIK and J. AARONS	1969	A proposed index for measuring ionospheric scintillation, <u>Planet. Sp. Sci.</u> , 17, 1069-1073.

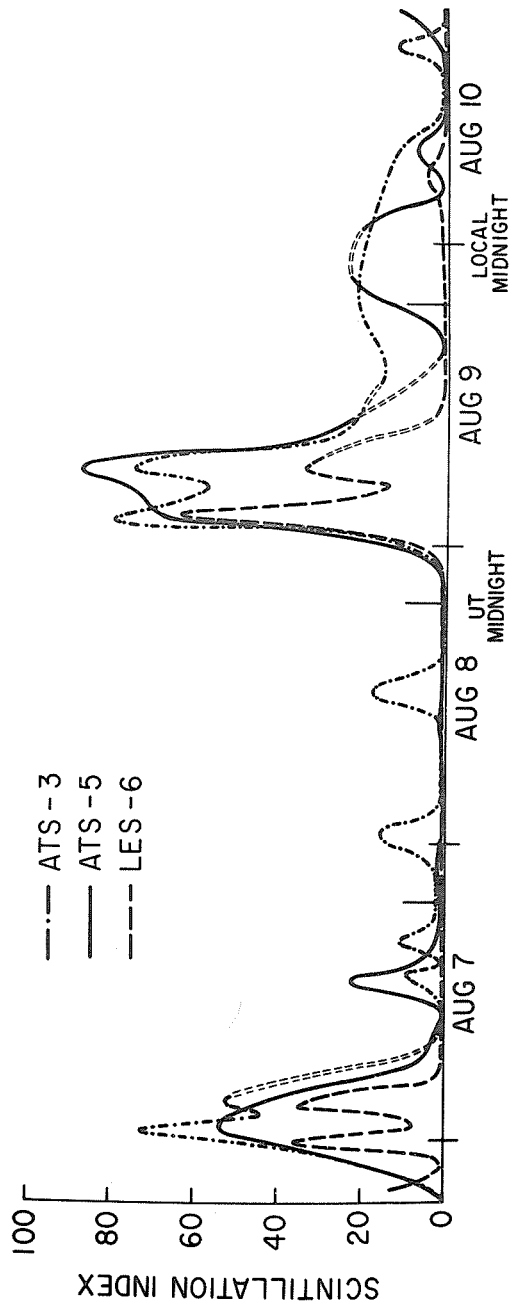
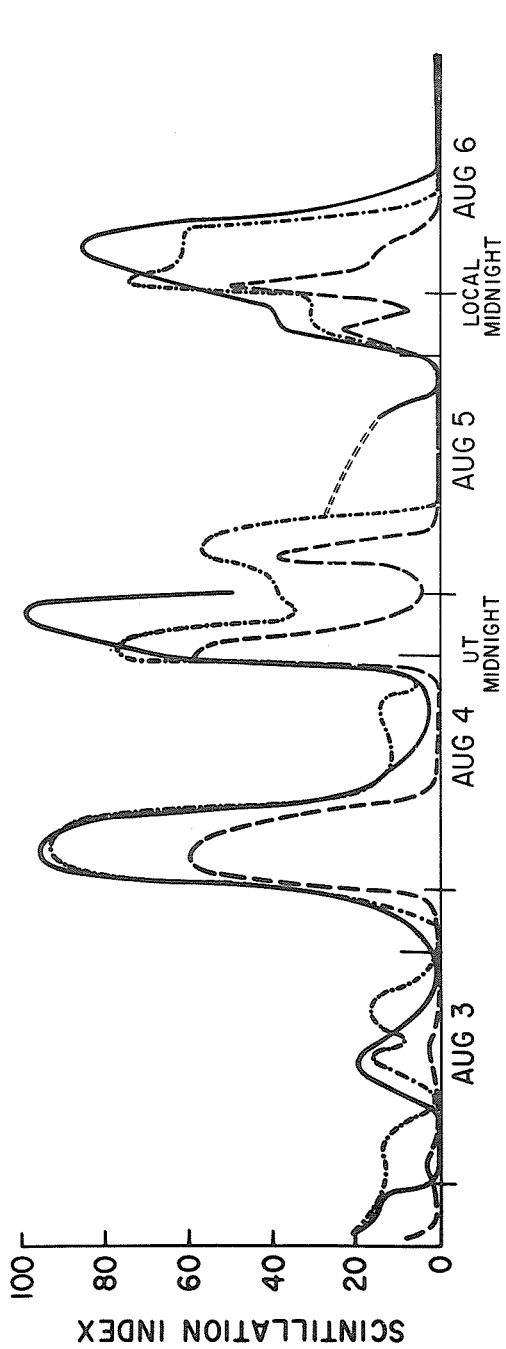
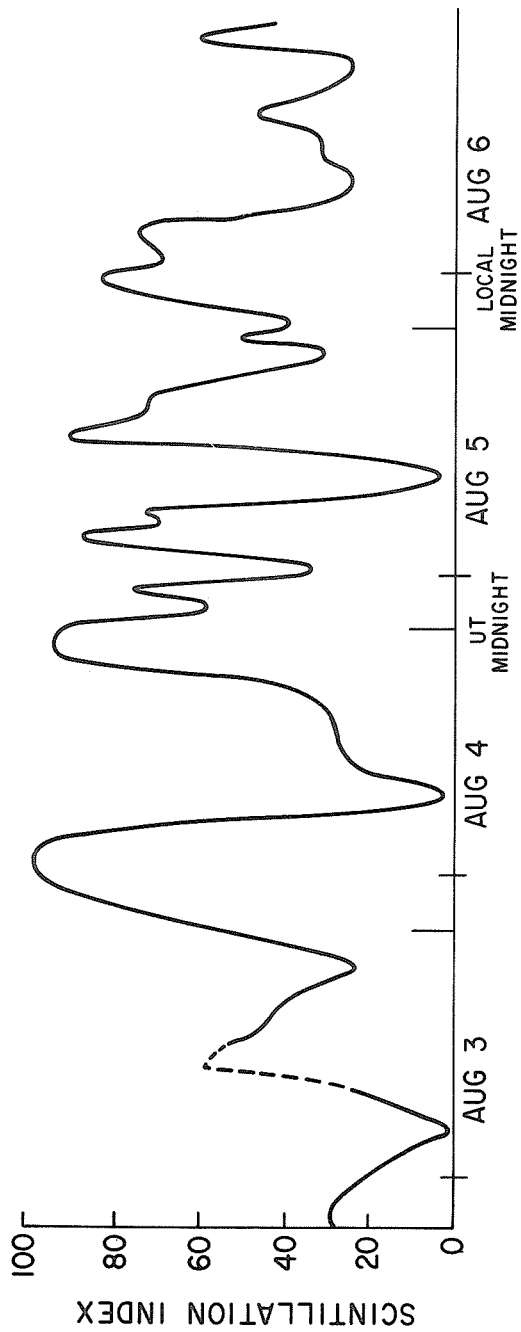


Fig. 2 Scintillation index for the Solar Events of August 3-10, 1972, as measured by the synchronous satellites ATS-3, ATS-5 and LES-6.



SCINTILLATION INDEX, NARSSARSSUAQ, GREENLAND FOR LES - 6

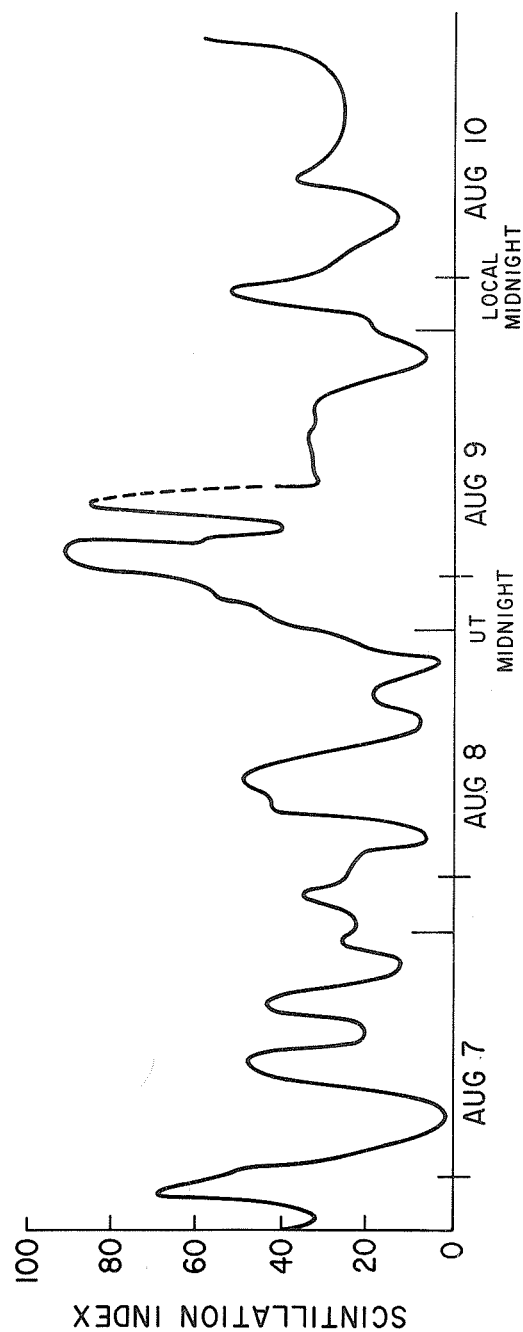


Fig. 3 Scintillation index for the Solar Events of August 3-10, 1972 as measured by the synchronous satellite LES-6.

Australian Ionospheric Observations during the Magnetic Storm of August 1972

by

D. G. Cole, L. F. McNamara and F. E. Cook
Ionospheric Prediction Service, Department of Science
Box 702, Darlinghurst, NSW, Australia

In Table 1 the characteristics of some ionospheric stations operated by the Ionospheric Prediction Service, Dept. of Science, are listed along with the storm parameters. The Magnetic storm began at 2056 UT, August 4, Figure 1, and displayed many small period oscillations. The Sydney magnetogram shows much the same form as that reported for Kakioka [1973]. The ionospheric storm disturbance can be seen in Figures 2 and 3 which display the foF2 percentage deviation from the 31 day median centered on the storm. The times used on these figures are those listed in Table 1, i.e. approximately local time is used. The symbol X in the vertical axes of the graphs denotes missing data.

The following are noticeable characteristics of the storm as observed by these stations:

1. The starting times of the storm observed by stations close to the same meridian increase with decreasing latitude.
2. The negative phase storm duration decreases with latitude.
3. At the local time of the two major solar flares reported before 8 August [Lincoln et al., 1972] there are significant positive increases in foF2 at Hobart (0600 UT August 3), Canberra (0600 UT August 3, 1700 UT August 4), Brisbane (0600 UT August 3, 1700 UT August 4), Townsville (1700 UT August 4).
4. The storm was particularly severe at Vanimo during the positive phase. Positive excursions from the median reached 96% at 0600 150°E time on August 5.

Figures 2 and 3 suggest that much of the effect of the August ionospheric storm took place during night-time hours. The only exceptions to this are Vanimo, Cocos Islands, and Hobart which all show effects throughout the day for a number of days.

At nighttime small changes in foF2 are greater, relative to the foF2 values, than during the day. There can be a greater range of foF2 variation near dawn and dusk because of delays in the foF2 rise caused by storms; but, in fact, during this storm there was little delay in the foF2 rise as can be seen from the f-plots in Figures 4-9.

Figures 4-9 also show the rise in the F-layer height that accompanied the foF2 disturbance. Total absorption showed on the ionograms of Mundaring at 0630-0645 UT, August 4 and at Hobart several times between 1745 and 2030 UT August 4 and at 0845-1045 UT August 5.

Es activity was high throughout the period from August 4 to August 6 (Figures 10 and 11), and the blanketing frequencies were often high.

The sensitivity of foF2 at Vanimo to the storm, as shown by the large positive excursions from the median value, was not expected. No such effect was found at Townsville or Cocos Islands, and it may have been caused by movements of the southern crest of the equatorial anomaly.

The assistance of Mr. T. Morgan and Mr. C. Mathers in this work is gratefully acknowledged.

REFERENCES

- | | | |
|--------------------------------------|------|--|
| Lincoln, J. V. and
H. I. Leighton | 1972 | Preliminary Compilation of Data for Retrospective World Interval July 26 - August 14, 1972, <u>World Data Center A, Upper Atmosphere Geophysics Report UAG-21</u> , November 1972. |
| Lincoln, J. V. and
H. I. Leighton | 1973 | <u>Solar-Geophysical Data</u> , 342 Part II, February 1973, U. S. Department of Commerce, (Boulder, Colorado, U.S.A. 80302) |

TABLE 1. Station details and the ionospheric storm characteristics

Station	Geographic Coordinates		Local Time Zone	Geomagnetic Latitude	Negative Phase Storm				Positive Phase		
					Start	End	Duration (Hours UT)	Max % Deviation	Start	End	Max % Deviation
HOBART	42.9S	147.3E	150 E	51.6S	4/0900	6/0600	45	66	2/1400	2/2200	65
CANBERRA	35.3S	149.0E	150 E	44.0S	4/1800	6/0500	35	59	2/1600	2/2200	53
SALISBURY	34.7S	138.6E	135 E	44.7S	4/1900	6/0100	30	58	4/0600	4/1400	58
MUNDARING	32.0S	116.2E	120 E	43.5S	4/1900	6/0200	31	60	4/0900	-	55
BRISBANE	27.5S	152.9E	150 E	35.7S	4/1800	5/2200	28	58	3/1100	3/1300	33
TOWNSVILLE	19.3S	146.7E	150 E	28.4S	4/2300	5/2100	22	44	4/0800	4/1900	56
COCOS IS.	12.2S	96.8E	90 E	23.3S	5/0000	5/1800	18	51	6/0800	6/1000	45
VANIMO	2.7S	141.3E	150 E	12.6S	5/0000	5/1200	12	58	2/1800	2/2100	29
									4/0600	4/1000	70
									4/1200	4/1800	52
									6/0500	6/1000	35
									4/0600	4/1000	44
									6/0500	6/1000	50
									3/1300	3/1500	41
									4/1200	4/1800	57
									6/0400	6/1800	68
									3/0900	3/1300	48
									4/1600	4/2300	96
									5/1300	6/0100 ?	48 ?
									6/1300	6/2200	48

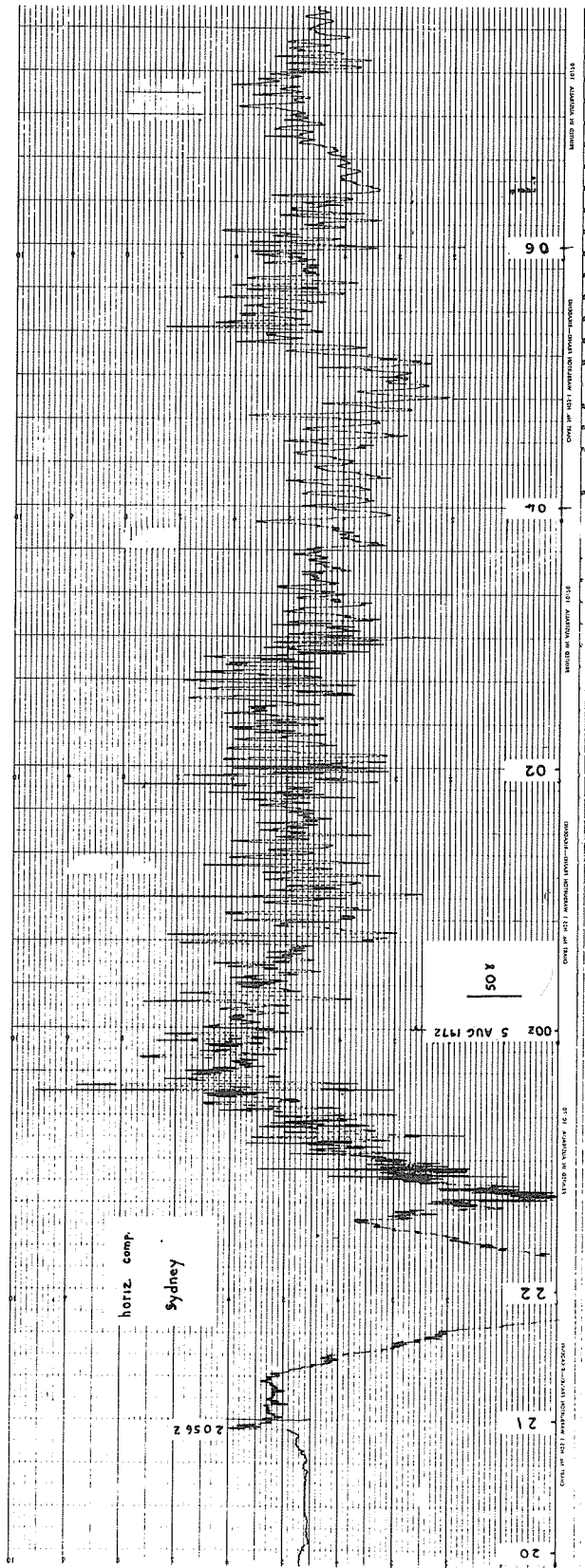


Fig. 1 VARIATION OF THE HORIZONTAL COMPONENT OF THE EARTH'S MAGNETIC FIELD

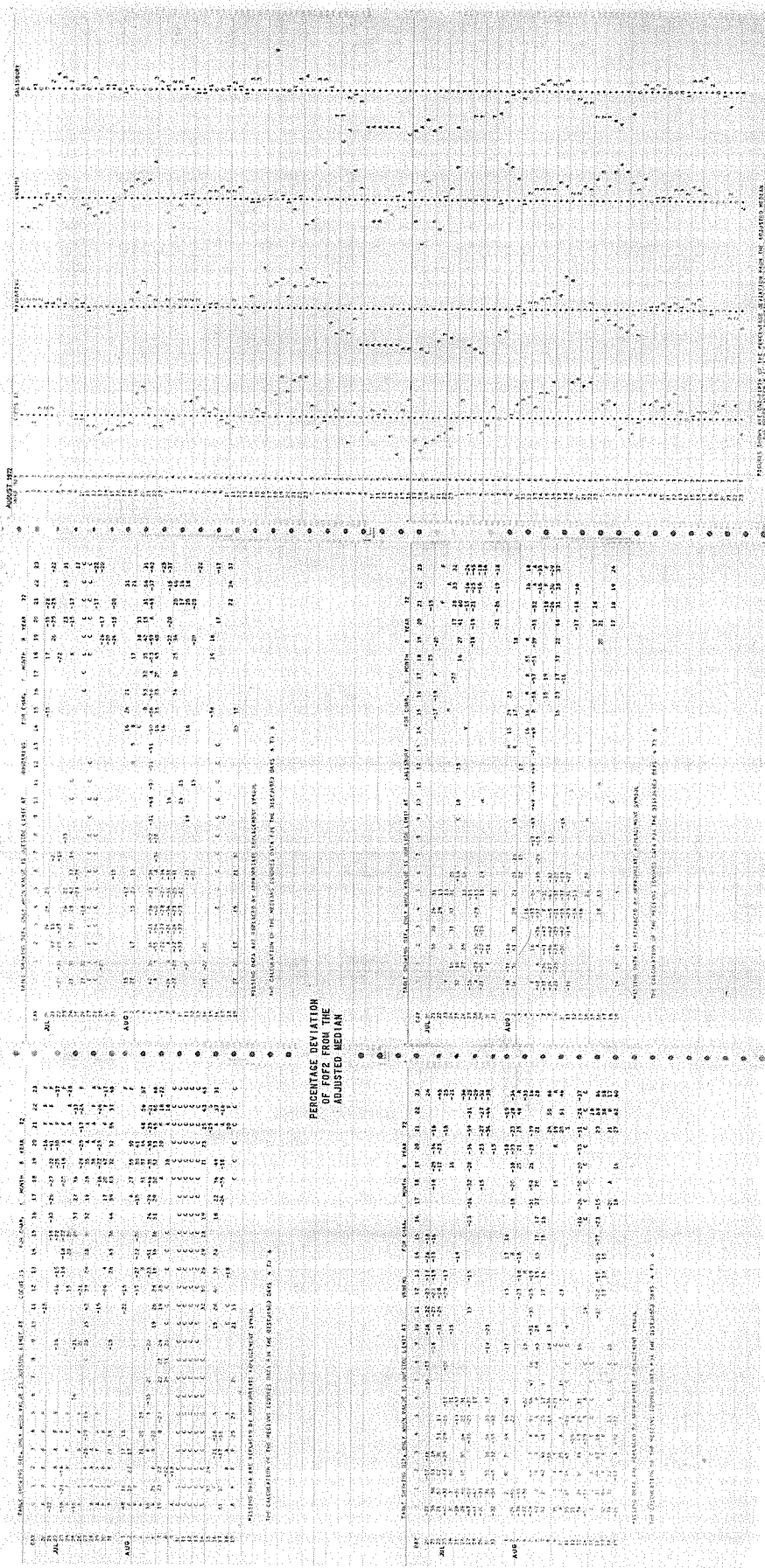


Fig.2 PERCENTAGE DEVIATION OF fOF2 FROM THE MEDIAN BASED ON THE 31 DAY PERIOD CENTRED ON AUGUST 4, BUT EXCLUDING AUGUST 4, 5 AND 6

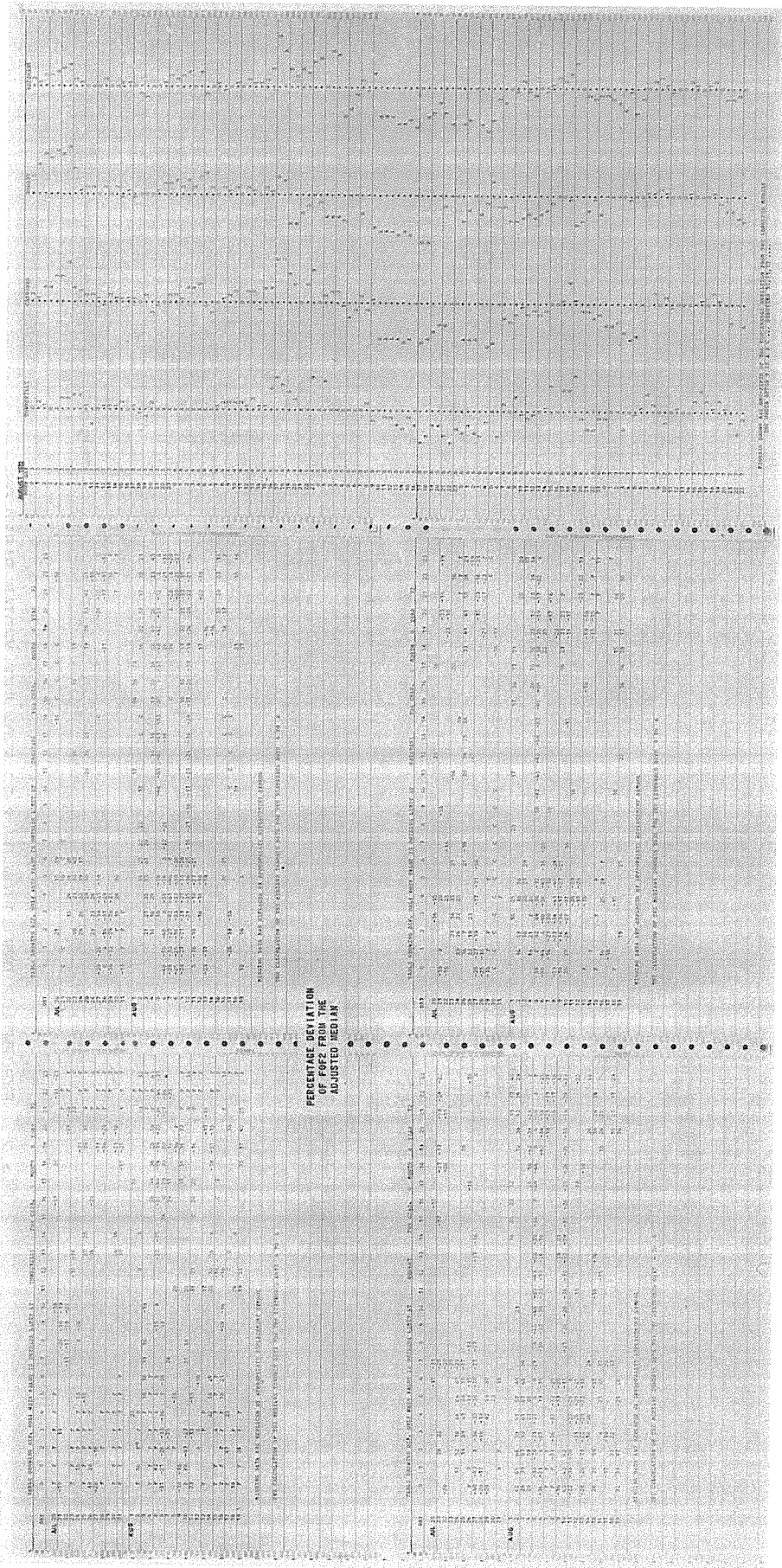


Fig.3 PERCENTAGE DEVIATION OF fof2 FROM THE MEDIAN BASED ON THE 31 DAY PERIOD CENTRED ON AUGUST 4, BUT EXCLUDING AUGUST 4, 5 AND 6

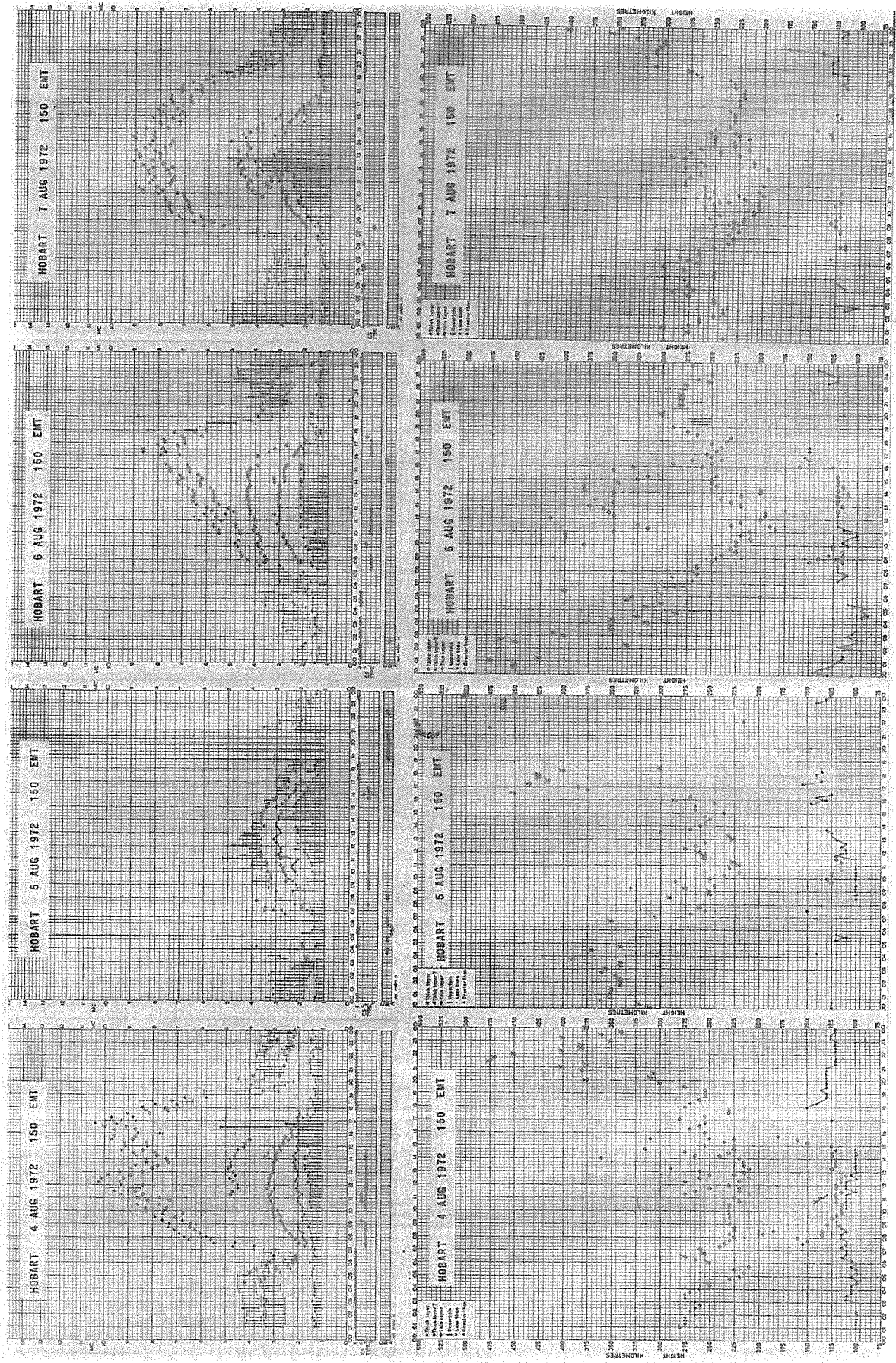


Fig. 4 f PLOTS AND h PLOTS FOR HOBART FOR AUGUST 4, 5, 6 AND 7 (150 E TIME)

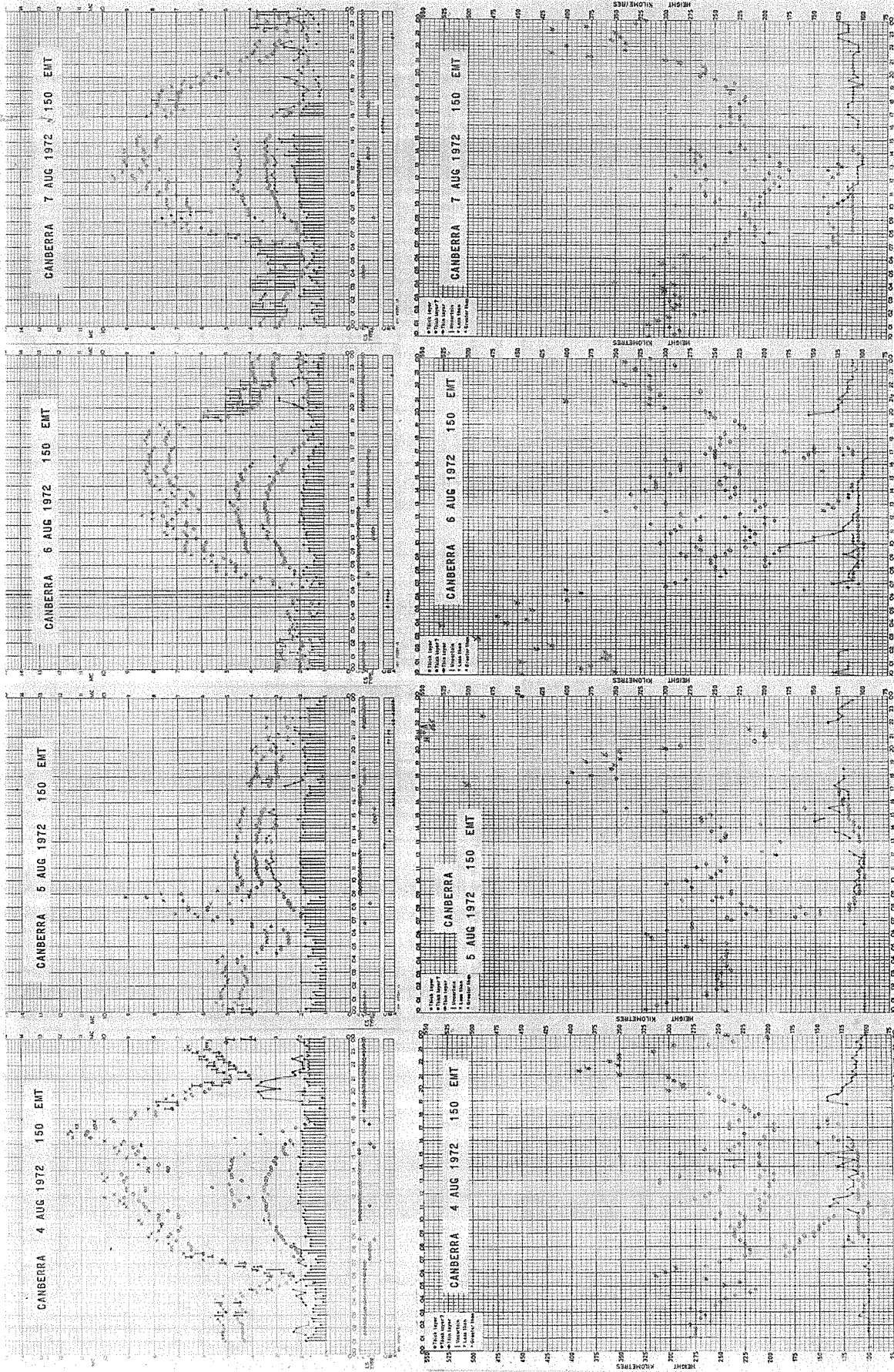


Fig.5 f plots and h plots for CANNBERRA FOR AUGUST 4, 5, 6 AND 7 (150°E TIME)

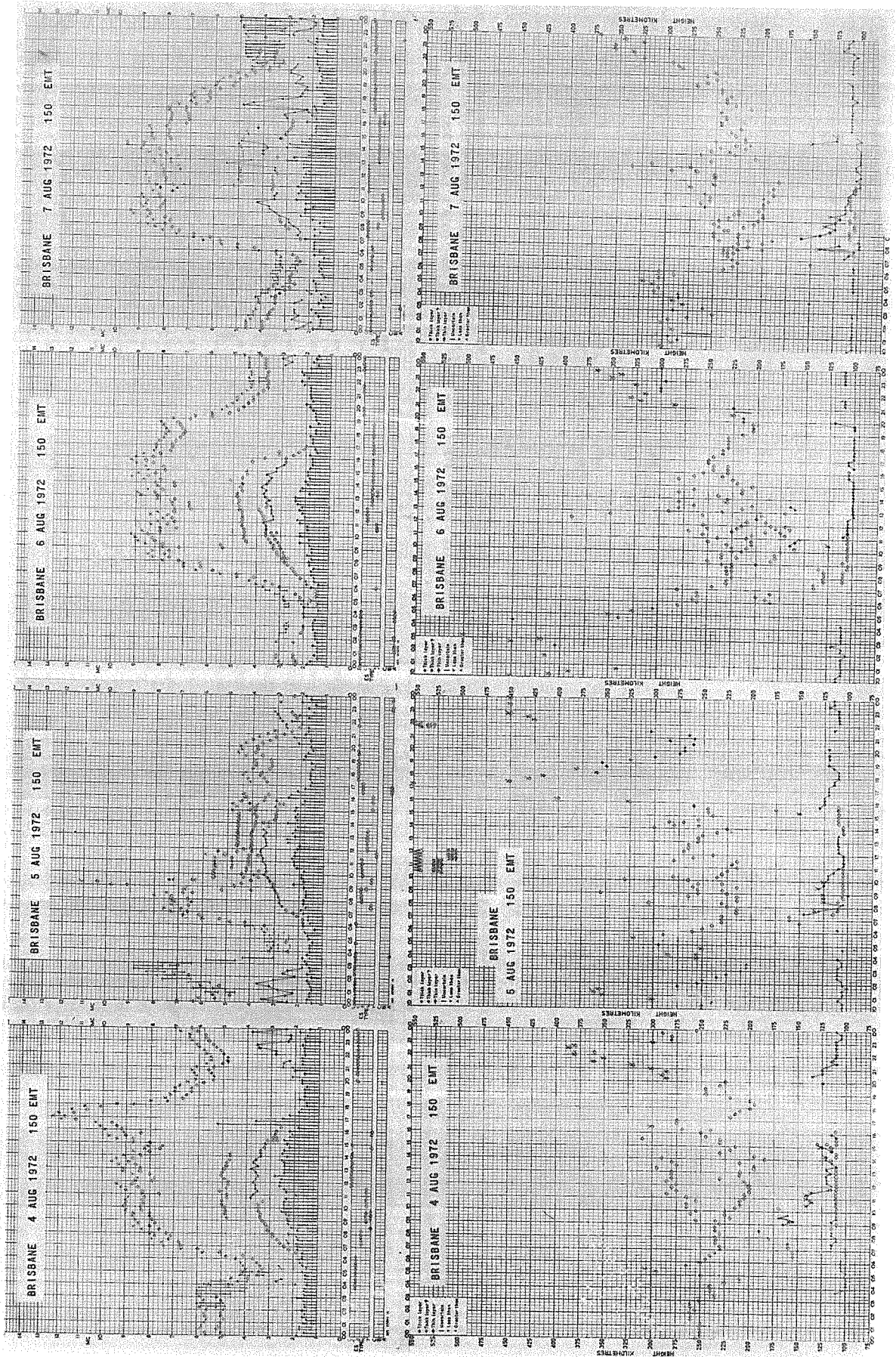


Fig. 6 f plots and h plots for BRISBANE FOR AUGUST 4, 5, 6 AND 7 (150 E TIME)

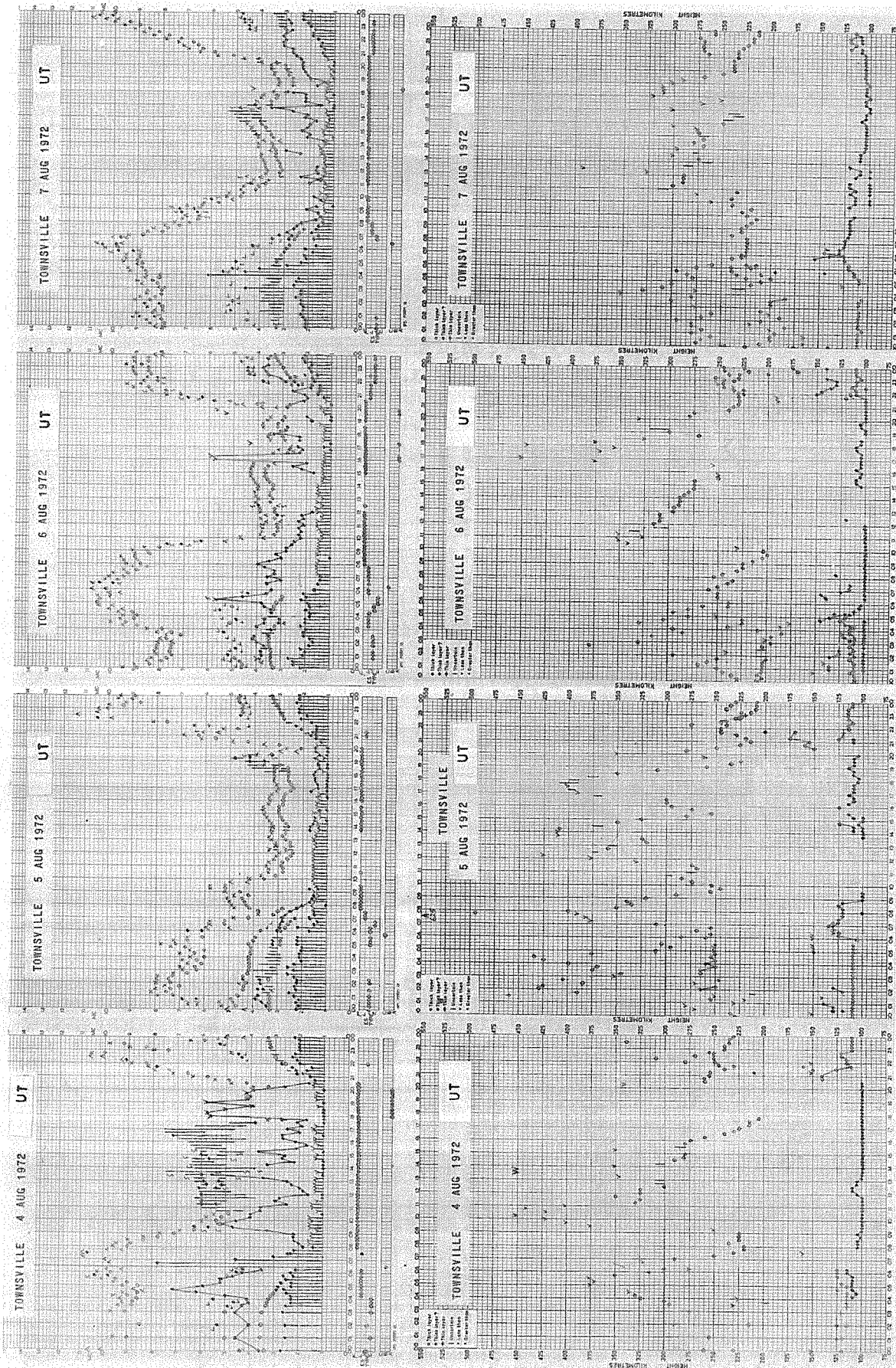


Fig.7 f PLOTS AND h PLOTS FOR TOWNSVILLE FOR AUGUST 4, 5, 6 AND 7 (UT)

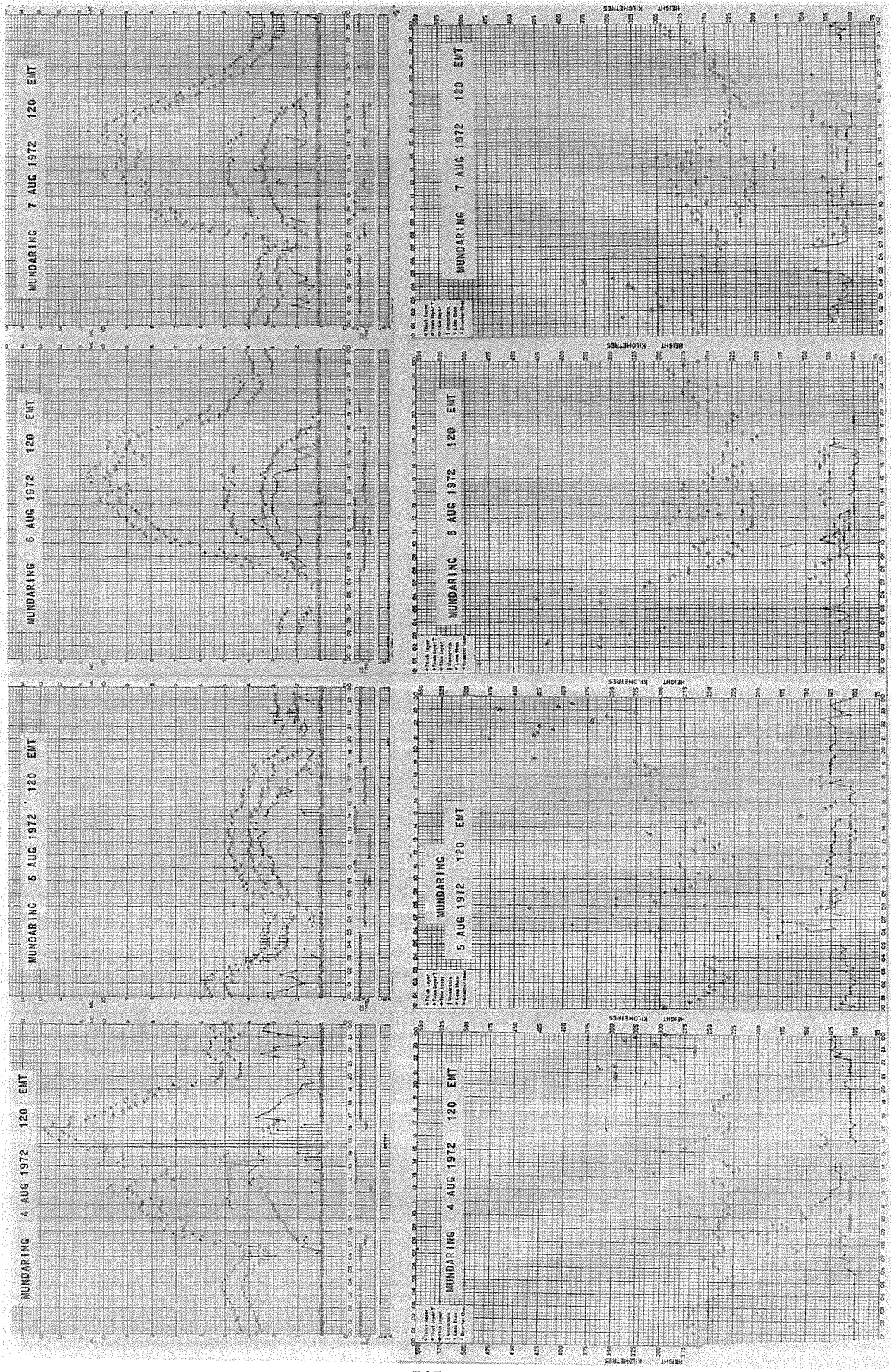


Fig. 8 f PLOTS AND h PLOTS FOR MUNDARING FOR AUGUST 4, 5, 6 AND 7 (120°E TIME)

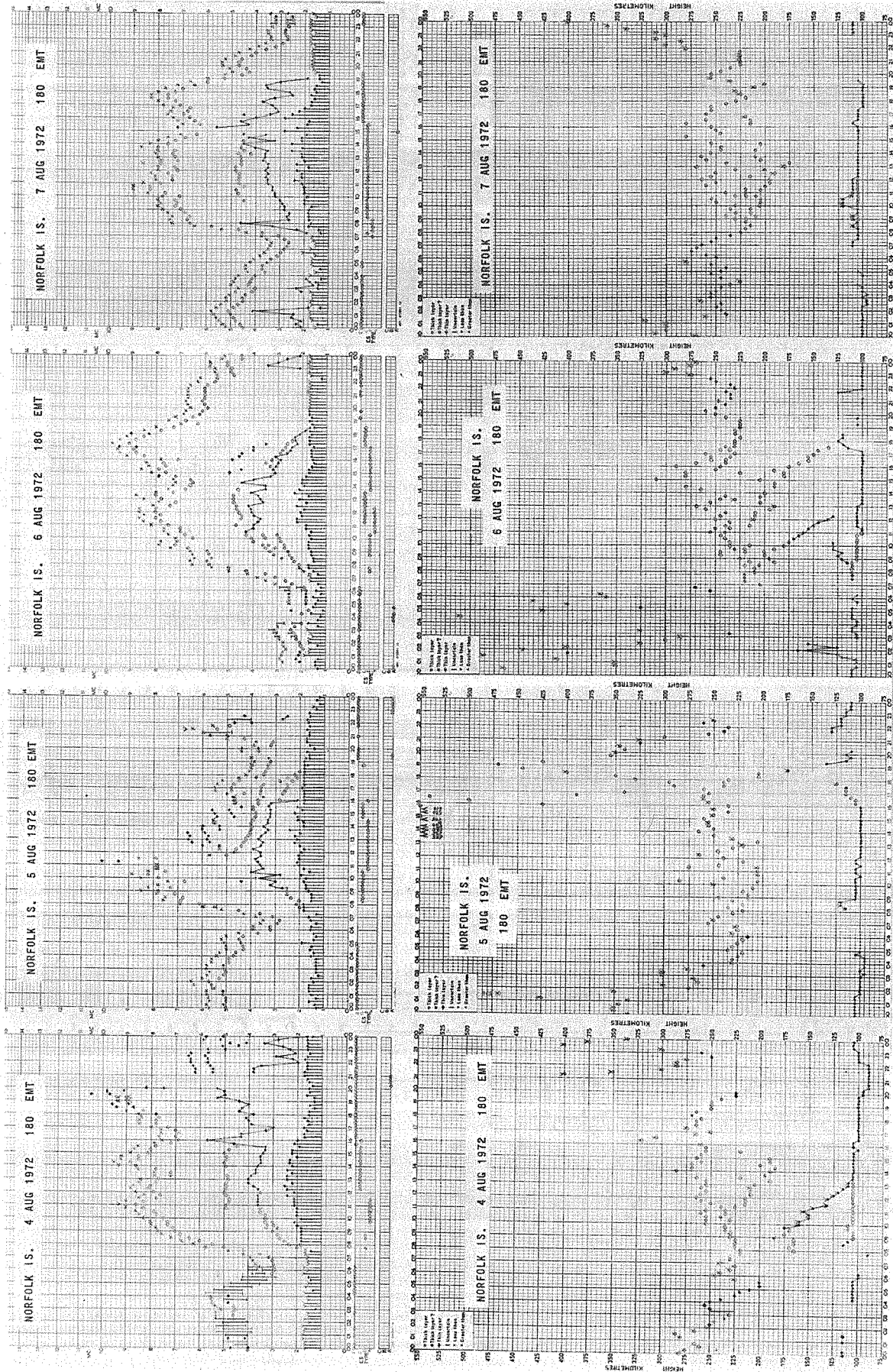


Fig. 9 f plots and h plots for NORFOLK IS. FOR AUGUST 4, 5, 6 AND 7 (180° E TIME)

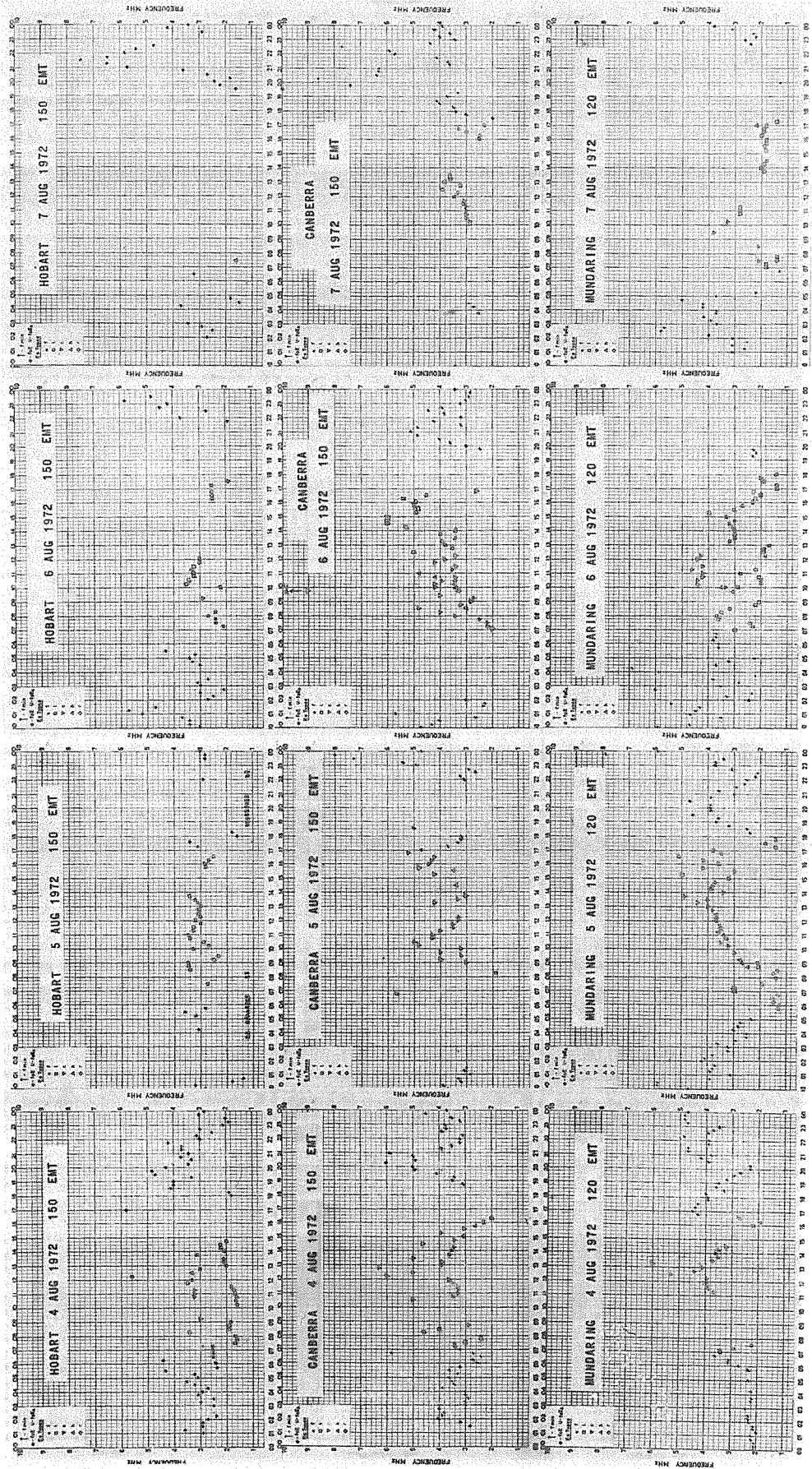


Fig.10 Es PLOTS FOR HOBART, CANBERRA AND MUNDARING FOR AUGUST 4, 5, 6 AND 7

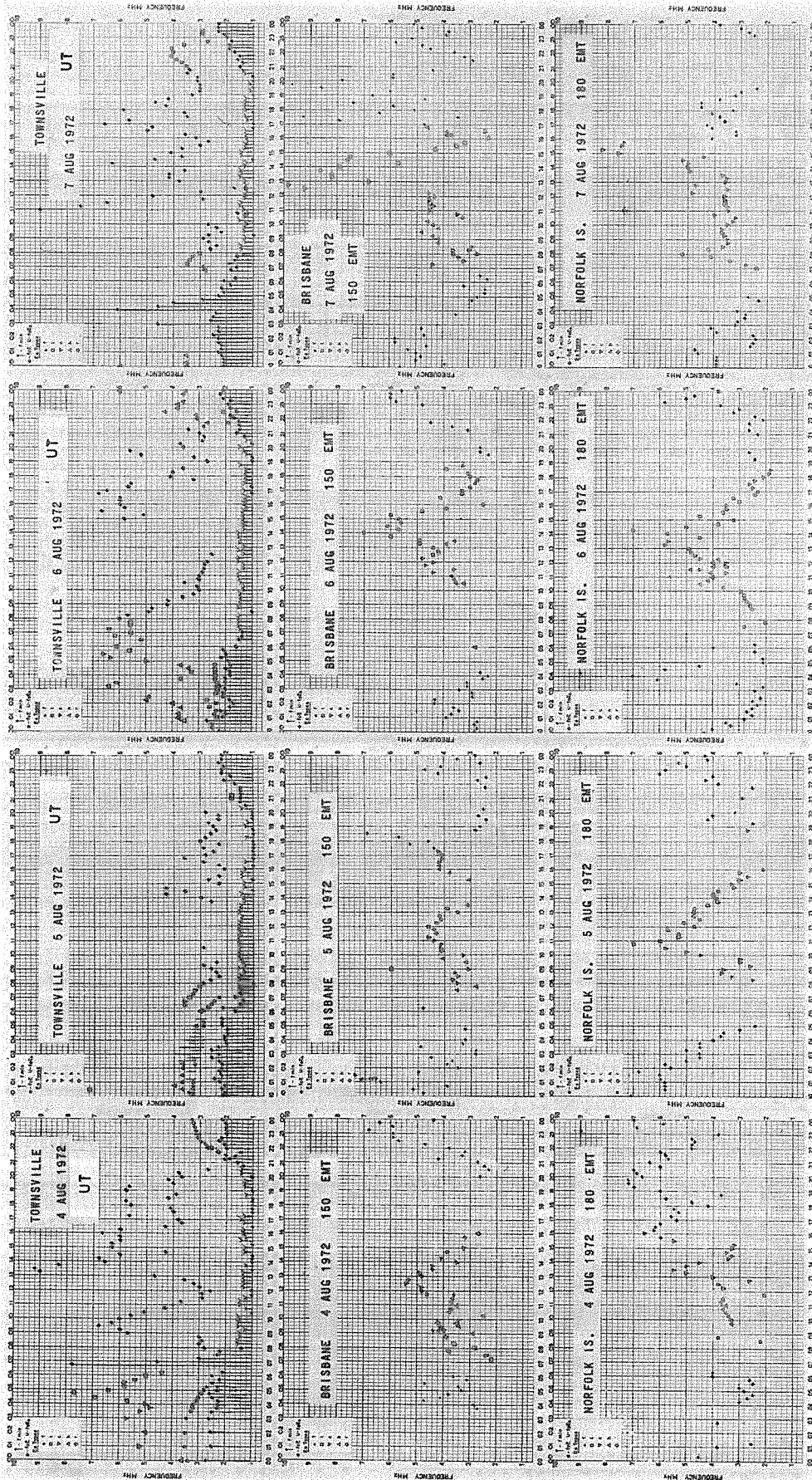


Fig.11 Es PLOTS FOR TOWNSVILLE, BRISBANE AND NORFOLK IS. FOR AUGUST 4, 5, 6 AND 7

Ionospheric and Geomagnetic Effects of The Solar-Activity Event in August 1972

by

R. A. Zevakina, E. E. Goncharova and L. A. Yudovitch
The Institute of Terrestrial Magnetism, Ionosphere and Radio Wave Propagation
of the USSR Academy of Sciences
Moscow, USSR

ABSTRACT

SID, PCA Es disturbances of F-region and geomagnetic field for August 1-14, 1972 are considered utilizing data from the stations listed in Table 3 and those in the Western hemisphere [Lincoln, et al., 1972]. Ionospheric and magnetic disturbances are compared with X-ray radiation, energetic protons and low-energy solar plasma during the flares. The parameters of particle fluxes in the ionosphere are determined by N(h) profile changes in Moscow.

At the end of July there appeared a very active region at the eastern limb of the solar disk, and during 1 - 11 August several scores of flares took place [Lincoln, et al., 1972]. Seven of them were accompanied by considerable increase of X-rays (Table 1). During the flares of 2, 4 and 7 August, besides X-rays, considerable increase of energetic proton flux and low-energy solar plasma was also observed (Table 2). As a result of this several intensive disturbances occurred in the ionosphere and magnetosphere of the Earth.

Table 1

Solar flare, solar X-ray, fmin and SID data

Date Aug. 1972	SOLAR FLARES				Loca- tion	Solar X-rays 10 ⁻⁴ erg/cm ² sec		Max fmin (MHz) during SID				SID*				
	Start (UT)	End (UT)	Dur. (min)	Int.		0.5-3A	1-8A	Moscow	Kiev	Ashkha- bad	Magadan	Khaba- rovsk	Start (UT)	End (UT)	Imp	No. of Sta.
1	0920	1215	175	1B	N13E45	16.9	326	2.6	2.0	2.2	1.4	2.3	0920	1010	2	10
													1135	1145	1	6
													1151	1220	1	4
2	0316	0506	118	1B	13 35			3.0	2.8	3.2	3.3	B	0312	0630	3	18
						71.2	179						0620	0709	1-	2
	0505	0800	175	2B	13 35			4.0	2.8	3.5	2.0	3.0	0740	0904	1-	2
													2000	2430	2	15
	1958	2336	214	2B	14 28	61.0	1470	1.0	1.6	1.2	2.8	2.3	2025	2230	2+	8
													0528	0907	1+	2
													0623	0947	3	22
4	0605	1158	358	3B	12.08	746	4560	B	B	B	2.8	B	0942	1057	1-	1
7	1505	1905	240	3B	16W35	895	4560	3.9	3.0	B	1.0	2.3	1505	1710	3+	37
													1217	1233	2-	21
11	1216	1320	64	3N	10 90	37.3	815	4.0	2.7	B	1.0	1.0	1233	1400	2	16

*[Lincoln et al., 1972]

Table 2

Times of Solar Flares and Sudden Commencements, Solar Wind
and Shock Wave Velocities, Proton Flux and Interplanetary Magnetic Field

Start of Solar Flares Date: Aug. 1972	UT	Time of sc Date: Aug. 1972	UT	SC H (γ) in Moscow	Delay of SC	Shock-wave velocity km/sec	Solar-wind velocity km/sec	Proton flux with energy > 3.9 Mev.	Interplanet. magn. field γ
2	0316	4	0119	24	46	900	585	215	6.6
2	1958	4	0220	45	30	1400	804	2980	5.2
4	0605	4	2054	189	15	2800	1130	>16380	19.2
7	1505	8	2354	48	33	1300	523	7660	7.8

We have considered ionospheric and magnetic disturbances on the basis of the data of Soviet stations (Table 3) and those in the western hemisphere [Lincoln, et al., 1972], and have compared them with other disturbances related to analogous flares for past years. Variation of the lower ionosphere was considered on the basis of parameters f_{min} , fEs , and riometer records; variation of the upper ionosphere was considered on the basis of parameters $\Delta foF2$ and $\Delta hpF2$. Figure 1 represents X-ray and proton variations [Lincoln, et al., 1972] causing some disturbances of the lower ionosphere, absorption (according to the data of riometer on 30 MHz in McMurdo), f_{min} and fEs through the network of stations (Table 3). It follows from Figure 1 that during all the flares an intensification of X-ray radiation within the range 1-8 Å caused the increase of ionization in the D-region manifested by the growth of absorption (f_{min}) on the day-side of the Earth. During the first flare 1 August at 0920-1215 UT the enhancement of X-rays and absorption was not great. On 2 August from 0316 to 0800 UT a sudden ionospheric disturbance (SID) was observed at all stations considered. In the evening of 2 August at 1958-2336 UT it was observed only at Heiss Island and Magadan where the ionosphere was illuminated. In the eastern hemisphere the most intensive SID was recorded on 4 August at 0605-1158 UT during which total absorption (B) was observed at all stations considered, excepting Magadan, where the sunset had already come. The most intensive flare was that of 7 August at 1505-1905 UT that caused a great SID even on the evening side of the Earth (in Moscow, Kiev, Ashkhabad). The flare of 11 August at 1216-1320 UT was followed by SID of moderate intensity. SIDs determined by f_{min} and some other methods are cited in Table 1. It follows from this Table that the most intense (importance 3+) was the SID on 7 August observed at most of the stations (37). The next by intensity (importance 3) is the SID of 4 August at 0623-0947 UT observed at 22 stations, and then the SID of 2 August at 0312-0612 UT with the importance 3 observed at 18 stations. Intensities of SID's are in full accord with the variation of X-ray energies.

Table 3

List of Soviet Stations Providing Data for the August Events

No.	Station	Geographic		Geomagnetic		L-Value
		Lat	Long	Lat	Long	
1.	Heiss Is.	N80.62	E58.05	N71.3	E156.1	9.8
2.	Murmansk	68.95	33.05	64.1	126.5	5.3
3.	Leningrad	59.95	30.70	56.3	117.3	3.2
4.	Moscow	55.47	37.32	50.8	120.5	2.5
5.	Kiev	50.45	30.50	47.3	112.2	2.1
6.	Ashkhabad	37.93	58.36	30.6	133.5	1.4
7.	Magadan	59.55	150.80	50.2	211.5	2.4
8.	Khabarovsk	48.52	135.12	37.9	200.1	1.6

The second important event of the flares observed in August in the lower ionosphere was the polar cap absorption (PCA). It started on 3 August at 0700 UT in Godhavn ($\phi = N79.9^\circ$), at 0800 UT in Narsarsuaq ($\phi = N71.3^\circ$), and at 1100 UT in Heiss Island ($\phi = N71.3^\circ$). At the same latitudes in the southern hemisphere at McMurdo ($\phi = S79.0^\circ$) the PCA started 18 hours later (at 0100 UT on 4 August) and had its maximum on 4 August at 0100-0400 UT (7 dB) and at 1400-2300 UT (12.5dB). On 5 August, the intensity of the PCA decreased considerably from 3 dB in the morning down to 1 dB in the evening; and on 6 August, from 1 dB in the morning down to 0.5 dB by the end of the day. PCA connected with the first three flares ended at McMurdo on 6 August at 2000 UT. For the northern hemisphere we could not determine the end of the first PCA and the beginning of the next on because, according to the vertical sounding data, total absorption was observed up to 10 August. PCA related to the flare of 7 August started at McMurdo at 0100 UT on 8 August and reached its maximum (5.5 dB) at 0000-0300 UT on 9 August, and by 1100 UT on 9 August it stopped. In the northern hemisphere, PCA ended on 10 August at 1800 UT at Godhavn; at 1100 UT at Thule ($\phi = N89.1^\circ$). In the auroral zone, a total absorption was observed up to 11 August but due to auroral absorption the end of the PCA was not determined.

It is of interest that at Godhavn the PCA started 2 hours after the proton flux of energy between 6-21 Mev had increased by one order of magnitude and reached 100 particles per $cm^{-2} sec^{-1}$, while at McMurdo, at the same latitude in the southern hemisphere, it started on the next day when the proton flux had increased by two orders of magnitude. Delay of PCA relative to the commencement of the proton flux increase in the northern hemisphere is apparently connected with the time of day. The great delay of PCA in the southern hemisphere is obscure. It is also not clear why PCA on 5, 6 and 9 August were of considerably smaller value than on 4 August, although the proton flux on those days was more than on 4 August. It is possible that the proton flux of 5, 6 and 9 August consisted of more energetic protons (>10 Mev) playing a lesser role in the ionization of the lower ionosphere.

The third significant effect of the flares in the lower ionosphere was the auroral absorption which we have not considered because we had no auroral zone riometer records.

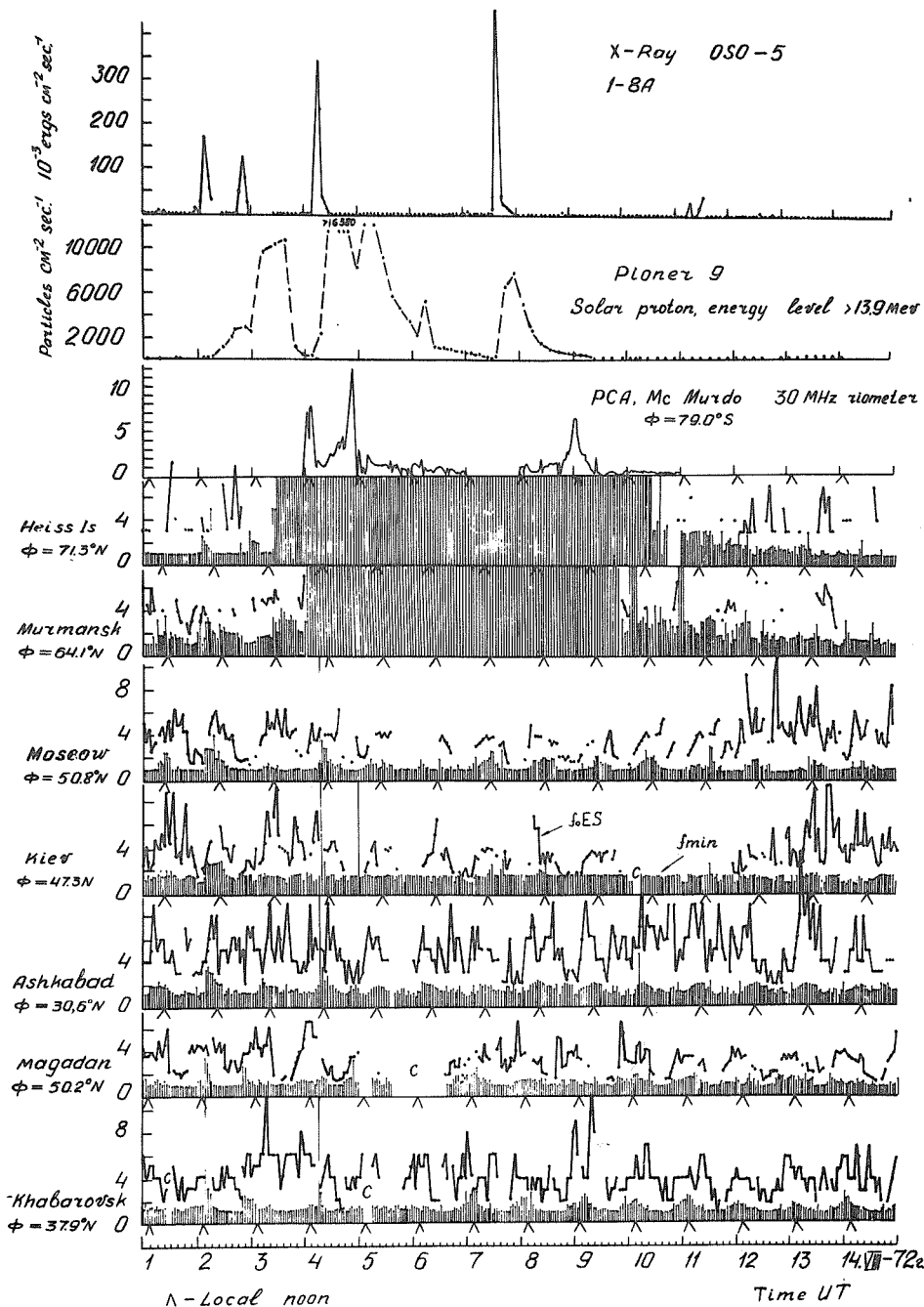


Fig. 1. X-rays (OSO-5), protons (Pioneer 9), McMurdo riometer, and fmin and fEs data from seven stations for the period 1 - 14 August 1972.

The fourth effect in the lower ionosphere was the change of fEs in middle latitudes. During the disturbance from 4 to 10 August, a decrease of fEs by 2-3 MHz was observed at Moscow, Kiev and Ashkhabad (Figure 1). Such effect of Es is typical for great summer disturbances [Zherebtsov and Kurilov, 1970]. A decrease of fEs of the same order was observed during the storms of 15-16 August 1959, 30-31 August 1966 and others. During strong disturbances the mechanism of Es-formation becomes weaker at middle latitudes.

The next ionospheric effect is the disturbances in the F-region connected with the radiation of low-energy solar plasma, with the increase of solar wind. They occur simultaneously with magnetic disturbances. Figure 2 shows the variations of solar wind velocity according to the data of Pioneer 9, Kp, Dst (H) [Lincoln *et al.*, 1972], $\Delta f_o F_2$ for mid-latitude stations (Table 3) and $\Delta h_p F_2$ for Moscow. It follows from Figure 2 that from 4 to 13 August two great magneto-ionospheric disturbances were observed with a sudden commencement at 0119 UT on 4 August and at 2354 UT on 8 August. The first very strong disturbance consisted of three disturbances with sc at 0119, 0220 and 2054 UT on 4 August, superimposed on each other. It continued 83 hours, till 1200 UT on 7 August. After every strong flare

an enhancement of magnetic and ionospheric disturbance occurred. The first disturbance started 46 hours after the flare of 0316 UT 2 August, the second one 30 hours after the flare of 1958 UT 2 August, the third 15 hours after the flare of 0605 UT 4 August, and the fourth 33 hours after the flare of 1505 UT 7 August. The flare of 11 August was observed at the solar limb ($W90^\circ$). Therefore it did not cause an ionosphere-magnetic storm.

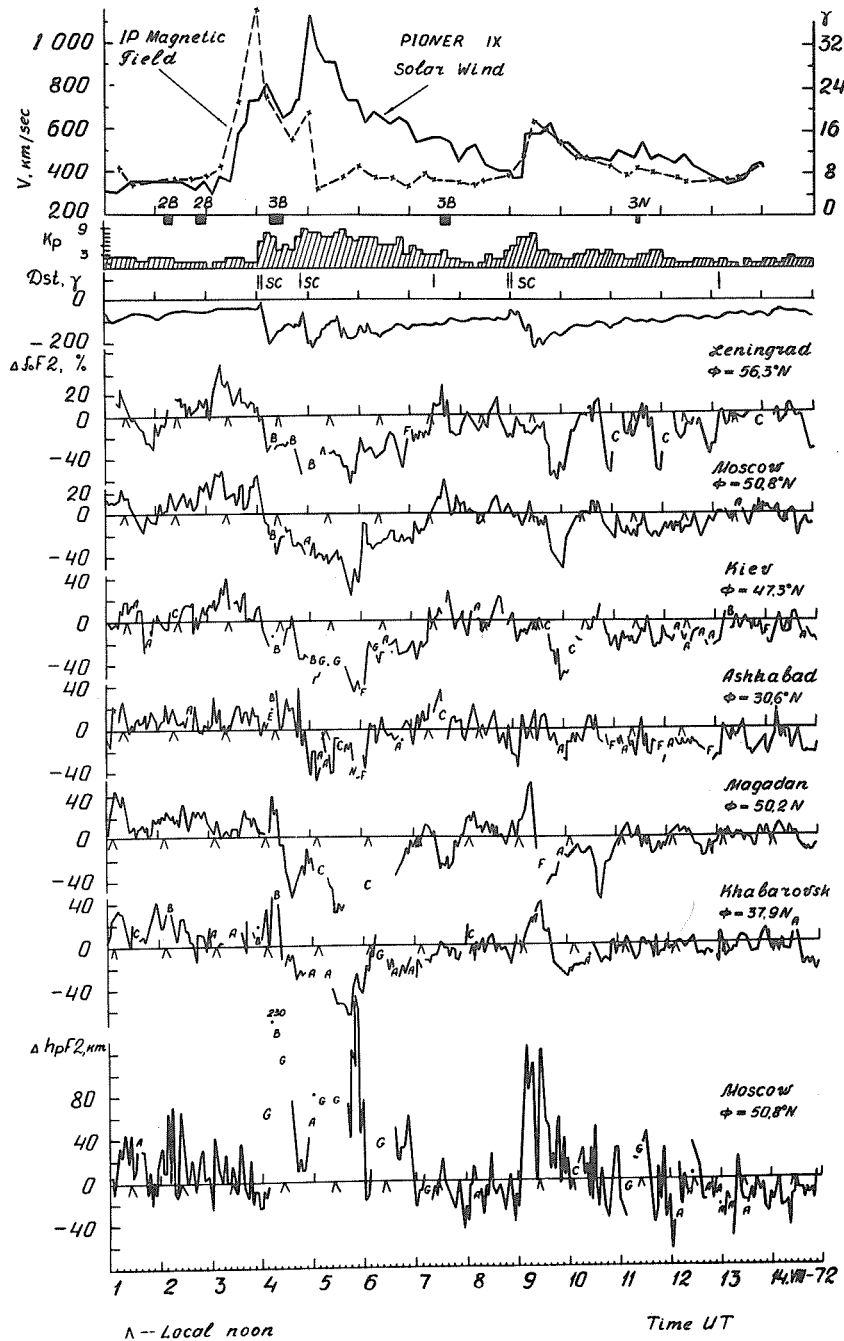


Fig. 2. Solar wind velocity (Pioneer 9), Kp, Dst, $\Delta f_o F_2$ for mid-latitude stations, and $\Delta h_p F_2$ for Moscow for the period 1 - 14 August 1972.

As is seen from the delay and the value of sc-geomagnetic disturbance, the most intensive shock-wave was caused by the flare of 4 August. It was propagated with a very great velocity $\sim 2800 \text{ km/sec}^{-1}$, impinging on the Earth for a period of 15 hours; it caused a huge sc (189 γ) and a very active storm consisting of gigantic pulsations even at middle latitudes. Shock-wave velocity from all flares considerably exceeded the solar wind velocity (Table 2). However, the greatest excess velocity (more than twice) was observed after the flares of 4 and 7 August.

On 3 August (the day before the first sc), foF2 increased by 20-40% at middle latitudes (Leningrad, Moscow, Kiev). On 3 August and on the previous day, the Earth's magnetic field was quiet ($\Sigma kp = 10$). An increase of foF2 before magnetic storm commencement has been observed earlier [Gontcharova *et al.*, 1970], but the causes of this phenomenon are not clear as yet. The interplanetary magnetic field was disturbed on 3 August: from 2230 UT 2 August up to 0600 UT 3 August there was a change of field direction from 340° to 098° [Lincoln *et al.*, 1972]. At 0400 UT 3 August the field increase started. About 1100 UT the field jumped from 20 to 84 γ . During the change of magnetic field direction a considerable increase of proton flux was observed. From 0230 to 0600 UT, flux energy >13.9 Mev increased from 2670 to 9750 particles $cm^{-2} sec^{-1}$. The increase of foF2 on 3 August was apparently connected with the growth of the interplanetary field.

Since the time of sc at 0119 UT on 4 August the disturbance was developing according to the known laws. On the night side of the Earth (at Leningrad, Moscow, Kiev) immediately after sc there were observed: a decrease of foF2 and an increase of hpF2, while on the day side (at Magadan and Khabarovsk), an increase of foF2. With sunset at these stations, a decrease of foF2 was observed. At lower latitudes (at Ashkhabad, $\phi = N30.6^\circ$) foF2 decreased only 19 hours after sc. Maximum decrease of foF2 (60-75%) at all stations was observed on 5 August during nighttime; the most intensive at Moscow (Table 4). At the same time the maximum increase of hpF2 took place. The first ionospheric disturbance ended at Leningrad simultaneously with the magnetic disturbance on 7 August at 1200 UT, but somewhat earlier at stations at lower latitudes (Table 4).

Table 4
Ionospheric Disturbances on 4 and 9 August 1972

Station	Ionospheric Disturbance					Ionospheric Disturbance				
	Start Aug. 4 UT	End Aug. UT	Time of maximum decrease foF2	$\Delta foF2$ (%)	Duration (Hours)	Start Aug. 9 UT	End Aug. UT	Time of maximum decrease foF2	$\Delta foF2$ (%)	Duration (Hours)
Leningrad	02 7 12	Aug. 5	20	-62	82	17 13 04	Aug. 9	22	-60	83
Moscow	02 7 09	5	20	-75	79	17 13 02	9	23	-50	81
Kiev	02 7 07	5	20	-65	77	17 13 04	9	22	-55	83
Ashkhabad	20 6 04	N	F	N	F	17 13 04	A		(-30F)	83
Magadan	08 7 04	C		C	68	09 13 00	F		F	87
Khabarovsk	09 7 11	5	17	-62	75	17 10 21	9	24	30	28

Where: A - Measurement influenced by, or impossible because of, the presence of a lower thin layer, for example, Es.
C - Measurement influenced by, or impossible because of, any non-ionospheric reason.
F - Measurement influenced by, or impossible because of, the presence of spread echos.
N - Conditions are such that the measurements cannot be interpreted.

The second disturbance (like the first one) started at near midnight hours (2354 UT on 8 August), but it was developing in a somewhat different way. After sc on the day side (at Magadan, Khabarovsk), an increase of foF2 took place, and on the night side, a small decrease only at Leningrad. At this at Moscow the F2-layer rose and hpF2 increased for 100-120 km, with normal values of foF2.

A sharp decrease of foF2 started at 1700 UT on 9 August when the height of the F-region had already lowered, approaching normal. Maximum decrease of foF2 (50-60%) was observed at 1900-2400 UT on 9 August when hpF2 values were increased by 10-60 km. An active period of ionospheric disturbance at 1900-2400 UT was observed every day up to 12 August, most clearly expressed at Leningrad. During active periods, hpF2 values were changing within ± 40 -50 km from the median. The disturbance continued for 83 hours till 0400 UT on 13 August. The most active disturbance was observed at Leningrad ($-\Delta foF2 = 60\%$).

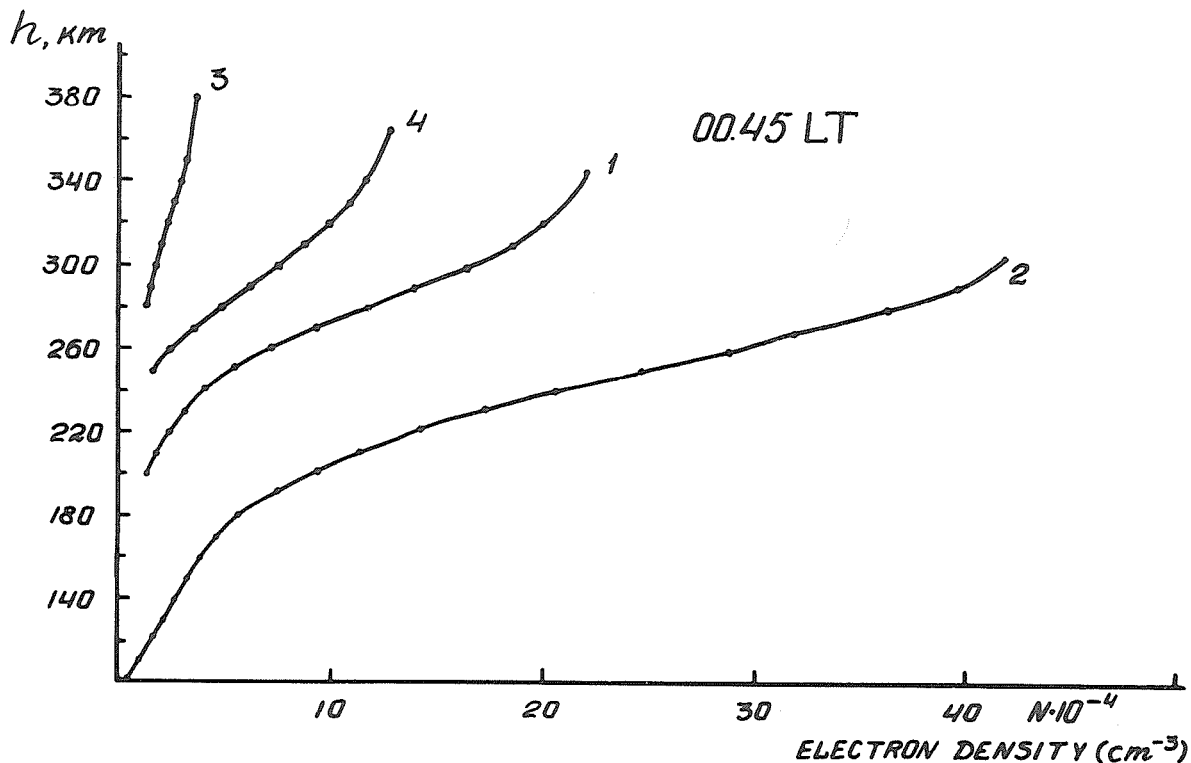
During the first disturbance of 4-7 August the greatest activity of disturbance was at Moscow ($\phi = N50.8^\circ$) and it was decreasing with the decrease of latitude but not as sharply as on 9 August, from 75% in Moscow down to 62% in Khabarovsk (Table 4). Activity of the second disturbance was the least; therefore its maximum occurred at higher latitudes ($\phi = N56.3^\circ$).

During the first disturbance the F-region suffered the changes characteristic of other great disturbances (July 1959; March-April 1960; August 1966; May 1967). During the second disturbance the change of F-region was unusual. The rise of F-region maximum without considerable change of electron concentration has been observed earlier [Shapiro and Shashunkina, 1967]; however, the mechanism of such changes is not clear as yet.

A characteristic phenomenon during strong disturbances is a maximum of F-region disturbance at middle latitudes [Zevakina et al., 1971]. It is assumed that it is connected with processes at the plasmasphere boundary, and with the dynamics of the equatorial ring current. Replenishment of the equatorial belt with particles causes (besides the enhancement of ring current) also an enhancement of particle flux along the lines of force for $L < 4$. Precipitation of particles into the upper ionosphere, as is known, causes an additional ionization. During the initial period of disturbance, before the upper atmosphere heating, this mechanism of ionization changes in the F-region apparently played an essential role, not only at high but at middle latitudes as well. With heating, the processes in the ionosphere become more complicated.

Using ionization changes with height one can determine parameters of the fluxes causing these changes [Rees 1969]. For this we have considered the change of $N(h)$ profiles for night hours at 15-minute intervals for the Moscow station. Figure 3 represents $N(h)$ profiles for 0045 UT in the quiet period of 2 August (1), in the positive phase of 4 August (2) and in the main phase of 6-7 August (3,4). Figure 3 shows that, during the main phase of disturbance, a sharp decrease is observed for both the total electron content ($n_1=1.6 \times 10^7 \text{ cm}^{-2}$, $n_3=3.0 \times 10^6 \text{ cm}^{-2}$, $n_4=9.6 \times 10^6 \text{ cm}^{-2}$) and the ionization at all levels relative to quiet conditions. Besides that, the whole layer is lifted upward and its geometry is changed. During the positive phase (2) an increase of total electron content takes place ($n_2=3.1 \times 10^7 \text{ cm}^{-2}$), and at all levels the electron concentration is growing, and $h_{\text{max}}^{\text{F2}}$ is decreasing as compared with a quiet day, the layer geometry being changed insignificantly.

According to the data of $N(h)$ profiles for quiet periods and for positive phase, the altitudinal profiles of ion-formation velocity $q(h)$ conditioning such changes in electron concentration were calculated.



MOSCOW. August, 1972.

Fig. 3. $N(h)$ profiles for 0045 UT on quiet day 2 August (1), positive phase of disturbance on 4 August (2), and the main phase 6-7 August (3,4).

For calculations of $q(h)$, the model of the neutral atmosphere of Jacchia [1964] was applied. For each level, starting from 110 km and up to $\sim h_{\max}^{F2}$ with steps of 10 km, the continuity equations were solved

$$\frac{\partial N}{\partial t} = q - \alpha N M^+ - D \quad (1)$$

$$\frac{\partial M^+}{\partial t} = M_2 (N - M^+) - \alpha N M^+ \quad (2)$$

where N , M^+ , M_2 are the concentrations of electrons, ions and neutral molecules, respectively, α is the average weighted coefficient of dissociative recombination taken equal to $2 \times 10^{-7} \left(\frac{300}{T_e} \right) \text{sec}^{-1}$; γ is the average weighted coefficient of ion-molecular reactions velocity:

$$\gamma = \gamma_1 [O_2] + \gamma_2 [N_2] \quad (3)$$

where $\gamma_1 = 10^{-11} \text{sec}^{-1}$ according to data from laboratory experiments.

γ_2 depends on the oscillation temperature of nitrogen molecules [Schmeltekopf et al. 1967]. Assuming that the oscillation temperature of nitrogen is equal to the temperature T_e of thermal electrons, the values of γ_2 were found from Thomas [1968]. D is the term conditioned by vertical transfer of ionization:

$$-D = \frac{\partial}{\partial h} \left\{ Da \left(\frac{\partial N}{\partial h} + \frac{N}{H_i} \right) \right\} \quad (4)$$

where $H_i = \frac{K(T_e + T_i)}{2mg}$ and Da - is the coefficient of ambipolar diffusion [Dalgarno, 1964]

$$Da = 1.38 \times 10^{19} \sqrt{\frac{T}{1000}} [C]^{-1} \sin^2 y \quad (5)$$

C is the concentration of main neutral components at these altitudes from the corresponding model. Assuming $dM/dt = 0$, i.e. considering quasi-stationary approximation of the description of the processes of appearance and disappearance of charged particles [Velitchansky and Klimov, 1970], equations (1) and (2) are reduced to the relatively general form:

$$q = \frac{\partial N}{\partial t} + \alpha N \frac{\gamma M_2 N}{\gamma M_2 + \alpha N} + D \quad (6)$$

At altitudes where $\gamma M_2 \gg \alpha N$

$$q = \frac{\partial N}{\partial t} + \alpha N^2 \quad (7)$$

This relation describes the decrease of electrons in the lower part of the ionosphere. In the upper ionosphere up to h_{\max}^{F2} : $\gamma M_2 \ll \alpha N$

$$q = \frac{\partial N}{\partial t} + \gamma N M_2 + D \quad (8)$$

At intermediate heights equation (6) was applied where $\gamma M_2 \sim \alpha N$.

For quiet conditons, during the calculations of ion-formation velocity, equations (6), (7), and (8) were solved under the assumption that $T_e = T_i = T_n$, and for disturbed conditions $T_e = 2 T_n$, $T_i = 1.5 T_n$.

The value T_∞ was calculated on the basis of the Jacchia model taking account of correction for magnetic activity, and were obtained: $T_\infty = 900^\circ$ (for quiet conditions), and $T_\infty = 950^\circ$ (for positive phase).

Then the experimental profiles $q(h)$ were compared with the theoretically computed profiles $q(h)$ under different assumptions of the character of the energetic spectrum of entering electrons [Zherebtsov et al., 1970].

The best agreement with the experiment was obtained as follows:

for a quiet night the spectrum in the form $N = N_0 E \exp(-E/0.5)$
with the flux of particles within energy range from 0.1 up to 12 keV $\sim 10^8 \text{ e1 cm}^{-2} \text{sec}^{-1}$;

for the positive phase: $N = N_0 E^{0.5} \exp(-E/0.5)$

with the flux: $\sim 10^9 \text{ e1 cm}^{-2} \text{sec}^{-1}$.

REFERENCES

- DALGARNO, A. 1964 J. Atm. Terr. Phys., 26, 939.
- GONTCHAROVA, E. E. 1970 Geomagnetism i Aeronomiya, 10, 67.
R. A. ZEVAKINA
E. W. LAVROVA and
L. A. YUDOVITCH
- JACCHIA, L. G. 1964 Spec. Rept., 170.
- LINCOLN, J. V. and 1972 Preliminary compilation of data for retrospective world
H. I. LEIGHTON, ed. interval July 26 - August 14, 1972, Report UAG-21, November
1972.
- REES, M. N. 1969 Space Sci. Rev., 10, 413.
- SCHMELTEKOPF, A. H. 1967 Plan. Space Sci., 407.
F. C. FEHSENFELD
G. J. GELMAN and
E. E. FERGUSON
- SHAPIRO, B. S. and 1967 Geomagnetism i Aeronomiya, 7, 894.
V. M. SHASHUNKINA
- THOMAS, G. R. 1968 J. Atm. Terr. Phys., 30, 1429.
- VELITCHANSKY, B. N. 1973 "Investigations on Geomagnetism, Aeronomy and Solar Physics",
E. E. GONTCHAROVA Izd-vo, "Nauka".
N. N. KLIMOV
A. N. TYATUSHKIN and
L. A. YUDOVITCH
- VELITCHANSKY, B. N. and 1970 "Investigations on Geomagnetism, Aeronomy and Solar Physics",
N. M. KLIMOV Izd-vo "Nauka", 12, 130.
- ZEVAKINA, R. A. 1971 Geomagnetism i Aeronomiya, 11, 977.
E. E. GONTCHAROVA
E. N. PUSHKOVA and
L. A. YUDOVITCH
- ZHEREBTSOV, G. A. and 1970 Geomagnetism i Aeronomiya, 10, 160.
B. A. KURILOV

Ionospheric Behavior during August 2-11, 1972 Derived from
Data of the Ionosphere Vertical Sounding over Khabarovsk

by

E. G. Mirmovich
Academy of Sciences of the USSR
Soviet Geophysical Committee
World Data Center, Moscow, U.S.S.R.

The data have been obtained with an SP-3 ionosonde in Khabarovsk (geographical coordinates: N48.5, E135.2; geomagnetic coordinates: N37.9, E200.1).

Standard f-plots shown in Figures 1-10 present the general picture of ionospheric behavior during several solar flares in this period. For comparison Figure 11 shows the medians of the regular layers' frequencies, f_{min} and f_{bEs} .

Figure 12 shows f_oF_2 deviations from the median for the whole period. Of the four flares marked on Figure 12, the one on August 4 had the largest effect on the D-region (Figure 3). According to data published in "Solar-Geophysical Data" [1972], SOLRAD 10 Outstanding X-ray Events, this flare produced emission flux in the 0.5-3 Å range and the 1-8 Å range ten times and three times, respectively, as large as each of the preceding ones.

The world-wide station network recorded four magnetic storms with sudden commencements; they are marked by the letters sc on Figure 12. It is possible to distinguish four ionospheric disturbances associated with the magnetic ones. If a sharp decrease of critical frequency or of electron density in maximum F_2 is considered as a sudden commencement of ionospheric disturbance, it can be seen from Figure 12 that the delay of that decrease in reference to an sc is 0.5-1 hour. Figure 13 shows this delay in $\Delta h_p F_2$ and $\Delta f_o F_2$ for August 9; the curves are drawn using 15 minute values. In this and other cases a slight increase of $f_o F_2$ can be observed in the intervening time between the ionospheric disturbance commencement and the sc.

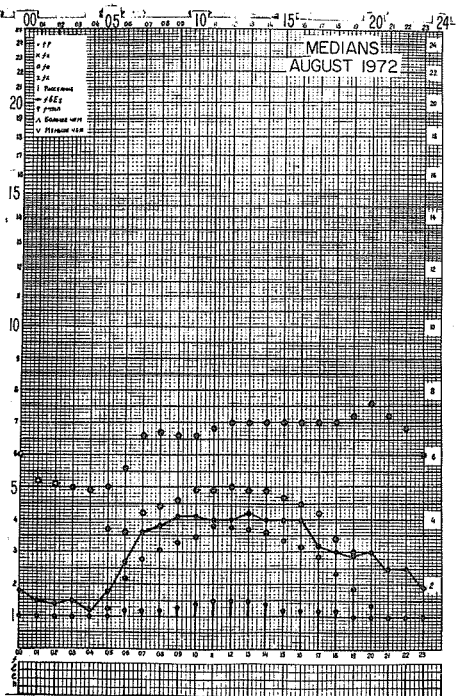
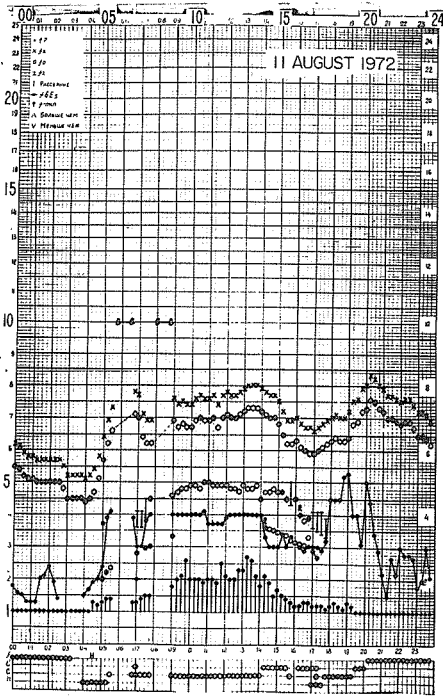
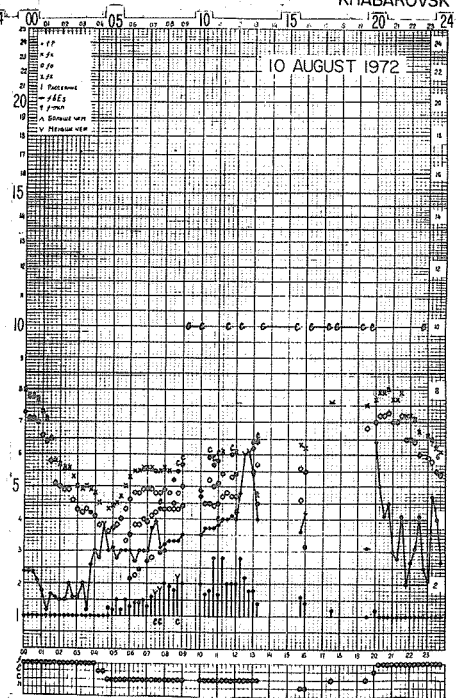
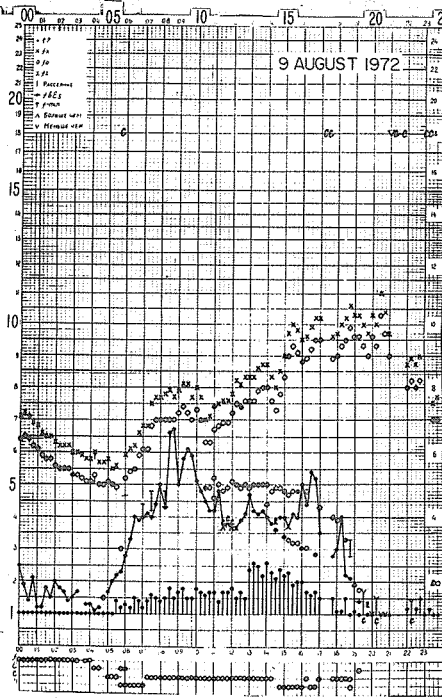
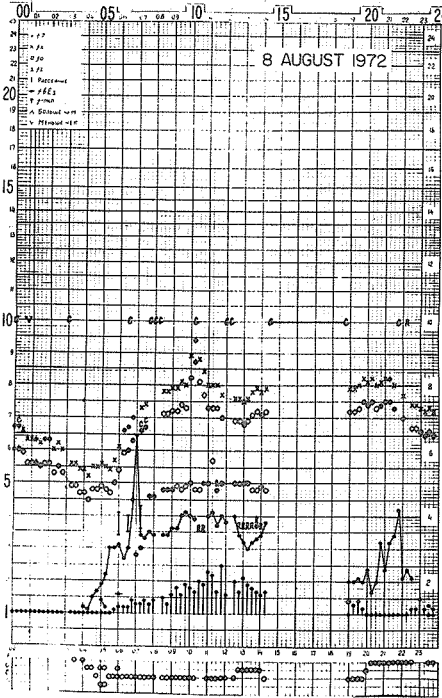
REFERENCES

- 1972 Solar-Geophysical Data, 338 Part I, October 1972;
Department of Commerce, (Boulder, Colorado, U.S.A.
80302).

IONOSPHERIC DATA

135° E

KHABAROVSK



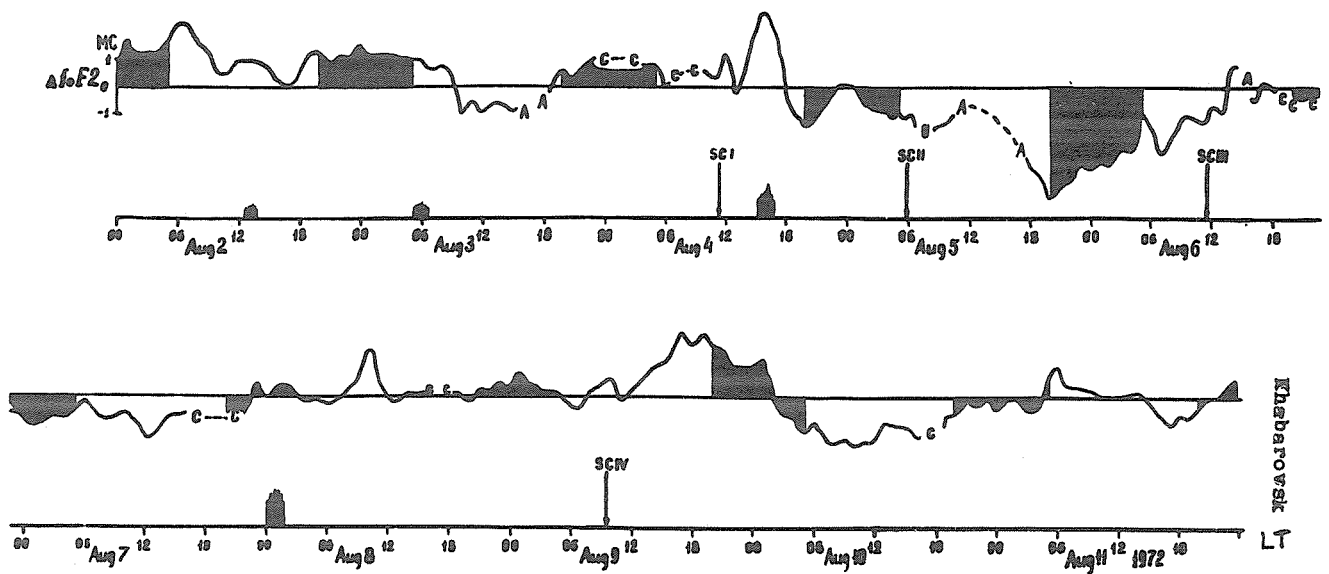


Fig. 12. Hourly deviations Δ foF2 (MHz) from the median for the period 0000 LT August 2 to 2400 LT August 11. The occurrence of solar flares () and those of the magnetic disturbance sudden commencements (sc) are marked on the time axis. The black areas below the Δ foF2 curve correspond to nighttime at Khabarovsk (2000 - 0500 LT).

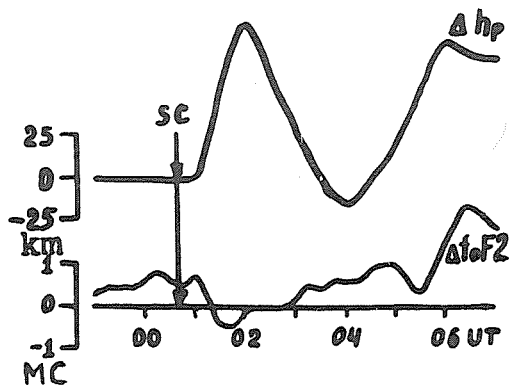


Fig. 13. The delay of the sharp change of foF2 and hpF2 in reference to the sc on August 9, 1972.

Ionospheric Report for July 24 - August 14, 1972
for Slough, South Uist and Port Stanley Observatories

by

R. W. Smith
Radio and Space Research Station
Ditton Park
Slough, Bucks, England

Slough

Apart from much blanketing by cusp-type Es on August 2 when very little was seen of the F-region all day, nothing out of the ordinary was recorded until 0500 UT on August 4 when an unusually pronounced foF1 was followed by near-G conditions at 0600 UT and then about two hours of blackout. For the next 2½ days the F-region remained highly disturbed with mostly G condition (foF2 less than foF1) by day and much oblique scatter and reflections indicating a trough-like structure by night. Daytime values of foF2 were at least 1-2 MHz below the monthly median, and the corresponding nighttime values were as much as 4 MHz down, e.g., at midnight foF2 dropped to 1.5 MHz (monthly median is normally 5.0 MHz). On August 6 foF1 was also well below the median, and for most of the stormy period complex F1 structure was present. As an example, at 1730 UT on August 5 a very distinct travelling disturbance in F1 finished up as a total-blanketing cusp-type Es. On August 7 a series of complex F1 ionograms was followed by an SID at 1600 UT which appeared to herald the return of normality to the ionosphere.

South Uist

At South Uist, which is roughly 1000 km north of Slough, blackout persisted for about 24 hours after the start of the storm and was followed by stormy high latitude conditions. Ionograms appeared normal again on August 8 although very low criticals were recorded from midnight to dawn on August 10.

Port Stanley

Nothing out of the ordinary was recorded apart from the SID of August 7.

(Ionograms were taken every hour at all three stations plus every quarter hour at Slough during the storm. They are available from World Data Center C1).

Manila Ionospheric Soundings in the Interval July 26-August 14, 1972

by

J. J. Hennessey, S. J. and Florencio Rafael, Jr.
Manila Observatory - Manila, Philippines

Throughout the active solar period July 26-August 14, 1972, departures from the median pattern of the quiet ionosphere are deserving of explicit mention. On two days, namely August 2nd and 4th, the ionosphere was severely affected, having total blackouts on each of these two days. Heavy, destructive rains and floods in Manila and environs made observing difficult. However apart from a few short power interruptions the ionosonde records were complete.

AUGUST SECOND. Manila SPA records show the start of an event at 0312 Z for the known flare starting earlier than 0316 Z [Lincoln and Leighton, 1972] i. e. within the hour prior to local noon, a period when the sun in August passed near the zenith. When Manila had its blackout Maui [Lincoln, id.] reported values for f-min at about 3.8 MHz. Before the flare Manila ionograms for the twelve hour period starting at the previous local mid-night presented full weight readings both for foF2 and fxF2. No spread echoes were found during this period but the records gave clear, fairly noise-free traces. The F2 critical frequencies followed the diurnal trend for August i. e. after mid-night, values generally dropped with some slight variation to the predawn dip. Under sunrise influence the foF2 values increased sharply and rose with the solar elevation. In comparison with values a few days both before and after, the predawn dip for foF2 on August 2 descended to the lowest value. By flare time the foF2 became slightly greater than the corresponding prenoon values of those days. Thus the change from a low predawn dip to the 0315 Z value was more rapid (frequency/time rate) than the values of days before and after. Throughout the local morning pre-flare hours, the ionograms including that at 0301 Z showed normal diurnal values for f-min. The 0315 Z ionogram gave an f-min of 4.2 MHz, an increase of absorption seen as due to the D-region with no sign of absorption effects produced in the F-region. Since the Manila records had the starting time as 0312 Z for SPAs on two paths and as 0313 Z for one SWF at 9.6 MHz and as 0314 Z for three other SWF's at 12.0, 15.0 and 18.0 MHz, the 0315 Z Manila ionogram indicated that by this time ionization density had increased in the D-region. The pronounced "h" type Es present for an hour prior to flare time also showed on the 0315 Z record with f-min Es at 4.2 MHz.

SID Event (0315 Z onwards). The 0315 Z ionogram was clearly transitional. While showing Es and a complete F-region record, there were two indications of flare effects: a) the increased f-min and b) the decrease in radio noise particularly beyond 4.5 MHz. The 0330 Z ionogram manifested the condition of nearly total blackout since radio noise from other sources operating above 4.0 MHz was missing while ionosonde echoes were all but totally obliterated. Careful inspection, however, revealed the high region of an F trace extending faintly from 9.3 MHz to 10.6 MHz. This weak trace of the F2, the only ionosonde echo, could readily be overlooked.

After the Flare. The 0345 Z recording manifested a total blackout. This single record by itself might have suggested that absorption due to the D-region extended to the vicinity of the upper frequency limit of the recorder. But weak F2 echoes appeared on the 0330 Z and the 0355 Z records. Faint as these records were they indicated that the 0345 Z record with no visible trace at all was blanketed by a D-region density capable only of occulting maximum frequencies not greatly beyond the highest frequency of the 0355 Z record. The next four records: 0359; 0400; 0401; 0405 Z showed all traces occulted. At 0410 Z the F2 layer appeared faintly indicating a decrease in D-region ionization density. The next ionograms taken at 0415, 0420 and 0425 Z showed no echoes. Just prior to this increased absorption at 0415 Z solar radio emission observed at 0411.9 Z [Lincoln, id.] facilitated production of greater D-region ionization. After 0430 Z the F-region echoes began to appear except for a reversal at 0455 Z. Solrad 10 - Explorer 44 showed a solar X-ray increase at 05 hour over that of 04 hour. [Lincoln, id.] A comparison of the foF2 values before and after the blackout (Fig. 1) manifested continuity rather than a sudden change in the F-region ionization. The Es traces after the flare stood out clearly with relatively high ftEs values. Starting at 0745 Z with a value of 14.0 MHz for ftEs, this parameter gradually increased to 18.0 MHz at 0755 Z and remained at 18.0 MHz until 0815 Z. In the F-region, storm stratification (the "L" condition) began at 0917 Z. Normally found during daylight hours this "L" condition persisted until 1045 Z.

TABLE 1. Sequence of Blackout and Recovery

Time (UT) August 2	f-min MHz	F2 Max Freq	foF2 MHz	h'min Km.	Time (UT) August 4	f-min MHz	F2 Max Freq	foF2 MHz	h'min Km.
0315	4.2	10.6	10.6	240	0614	3.7	9.5	9.5	230
0330	9.3	10.6	R	520	0625, 30, 35	TOTAL BLACKOUT			
0345	TOTAL BLACKOUT				40, 45, 50	TOTAL BLACKOUT			
0355	9.5	10.8	R	530	55, 59, 0700	TOTAL BLACKOUT			
0359, 0400	TOTAL BLACKOUT				0701	10.0	11.0	11.0	410
0401, 0405	TOTAL BLACKOUT				0705	8.0	11.0	11.0	355
0410	10.2	11.0	11.0	570	0710	7.8	11.0	11.0	345
0415, 20, 25	TOTAL BLACKOUT				0715	7.6	11.0	11.0	335
0430	9.3	10.0	R	530	0725	6.0	11.0	11.2	335
0435	9.4	10.8	11.0	535	0730	5.8	11.2	11.2	335
0440	9.7	10.0	R	540	0735	5.4	11.2	11.2	335
0445	9.6	10.8	11.0	540	0740	5.3	11.3	11.3	335
0450	8.0	10.8	R	475	0745	5.0	11.3	11.3	330
0455	TOTAL BLACKOUT				0750	4.7	11.3	11.3	300
0459	8.4	10.6	R	480	0755	4.5	11.3	11.3	300
0500	9.5	10.8	R	500	0759	4.5	11.3	11.3	300
0501	7.8	11.0	11.1	450	0800	4.8	11.0	11.3	330
0505	9.5	11.0	R	500	0801	4.3	11.2	11.2	295
0510	8.1	11.0	R	460	0805	4.8	11.0	11.1	325
0515	8.1	11.4	11.4	460	0810	4.7	11.0	11.0	320
0520	8.0	11.0	R	450	0815	4.4	11.0	11.0	310
0525	7.6	11.0	11.5	435	0820	4.3	10.8	10.8	310
0530	6.8	11.0	R	420	0825	4.4	10.7	10.7	310

AUGUST FOURTH. The second of the two major blackouts recorded on the Manila ionograms during the passage of McMath Solar Region 11976, in late July and early August, took place on August 4 starting at 0625 Z. Start of recovery came after 40 minutes. Prior to this total absence of vertical incidence reflections the ionosphere during the local night manifested some notable features of an abnormal ionosphere. In the evening hours the sporadic E appeared as the dominant feature. For example, at 1400 Z, August 3, seven sporadic-E multiples were present with no F-trace and the top Es frequency went above 13 MHz. With so many passages of the energy between the transmitter level and the E-region, the D-region was weak in ionization density, while on the contrary the E-region attained a rather high electron density of ionization, about two million electrons per cubic centimeter. The E-region critical frequency remained high throughout most of the night, but not always nor totally, blanketing the F-region. After local midnight, range spread in the F-region persisted until it changed to frequency spread near dawn. For some three hours after 1800 Z the series of ionograms indicated, by the oblique echoes, that a dense cloud of ionization was approaching the station to pass overhead. After dawn sequential Es appeared descending from E2. Also characteristic of a disturbed ionosphere was the appearance of the F-trace from about four hours before noon on the fourth until the burst of solar energy produced the blackout. A rather fine sequence of morning ionograms developed with the signs of a lunar layer. The top F-frequency was about 2 MHz lower than usual for these days; several stratified F-layers appeared; and the virtual heights went into a "W" condition, i. e. with heights in excess of 700 kilometers.

S I D. Four Manila SWF receivers respectively at 9.6, 12.0, 15.0 and 18.0 MHz recorded the start of the short wave fadeout at 0621 Z with the maximum at 0633 Z and end time at 0850 Z. The first Manila ionogram this day to present a total blackout was taken at 0625 Z. All immediately subsequent ionograms showed the continuance of the blackout until the 0701 Z ionogram when this one on high gain and contracted scale gave a faint indication of the top end of the F-region between its f-min of 10.0 MHz and its foF2 of 11.0 MHz. Within four minutes the F-layer recovery reached an f-min of 8.0 MHz at 0705 Z. The f-min remaining in the F-region decreased gradually on successive frames for two hours. During this interval a multiple of the F-trace appeared at 0900 Z while shortly after at 0910 Z the E-layer had its first appearance. From 1030 Z the Es trace came back and the echoes followed a normal pattern. F2 critical frequencies had full weight readings all through the local night to 2359 Z, August 4.

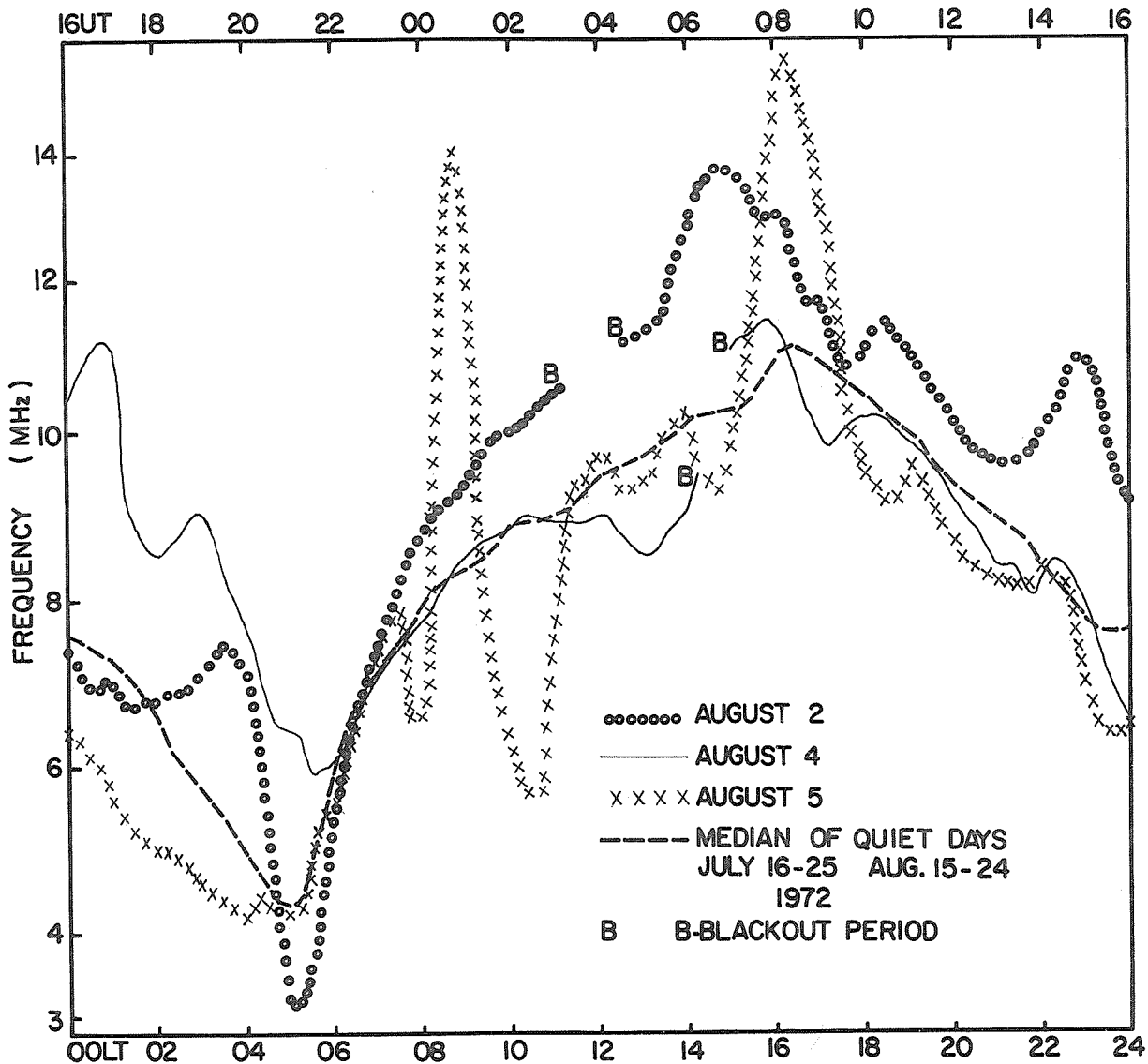


FIG. 1 PLOTS FOR f_oF_2 FOR THREE SPECIAL DAYS AND MEDIAN.

SOME OTHER ACTIVE DAYS. Due to solar activity throughout the active interval remarkable ionospheric effects were found on some other selected days. Local August 3 came a day after a SID and a day before another blackout. On this day the predawn f_oF_2 remained very high, 5.9 MHz at 2100 Z August 2. The previous blackout could have contributed to this result by limiting electron loss. Also the solar burst and flare beginning about 1958 Z had some influence particularly in the still dark ionosphere. After sunrise, from 0715 L. T. throughout the day to 1700 L. T. the ionograms were particularly free of radio noise. The presence of the F1 1/2 layer from noontime for some three hours added confirmation to the storminess. While Es was quite prominent in the daylight hours, at 1000 Z a rapid rise started in the top frequency of the Es traces. At 1015 Z this frequency went beyond the upper limit (25 MHz) of the recorder. However the Es did not blanket the F-trace which appeared from 4.5 MHz to 11 MHz. Yet fifteen minutes later, at 1030 Z, the f_oE_s remaining above 25 MHz totally blanketed the F-trace. This condition perdured through 1045 Z.

Local August 5. The rarely occurring forked trace appeared on the 0511 L. T. record. During the local night (August 4-5) hours very clear and regular F-layer characteristics were presented. The daytime hours deviated quite drastically from the usually expected variations. The foF2 plot (cf. Fig. 1) showed sharp morning rise to 14.0 MHz in a 45 minute period followed by an abnormal descent. There was an increase to noontime and then a growth to a maximum of 15.6 MHz in the afternoon hours followed by an evening drop, not according to the usual pattern. The corresponding F2 virtual heights were significantly low during the morning critical frequency peak. Afterwards the retardation of the F-region created a "W" condition at 0350 Z. Later the curve behaved in appearance as a more normal F2 layer. At the peak of foF2 at 0815Z an "L" condition for the F-trace set in which lasted until 1045 Z.

Local August 7. On this day from 0800-1045 L. T. the ionograms were regular with E, Es and F-layers present. Manila Observatory reported an Sb flare starting at 1052 E. All the following, each with starting time 1052, - SPA's on three paths, SWF's at four frequencies and SCNA's at 18 and 30 MHz - were likewise reported at Manila. At 1055 the ionosonde records grew more free of noise from extraneous radio sources; the E- and Es-layers were blanketed; the f-min increased to 5.1 MHz. The f-min remained high for nearly two hours with the 1205 L. T. f-min reaching 6.1 MHz. During this noontime two-hour period the foF2 dropped down one MHz and then returned. The traces after the dip showed retardation and stratification but were otherwise quite regular in values for the remainder of the day.

Acknowledgement:

We wish to express our gratitude to NOAA, Boulder, Colorado for providing the ionosonde and for their support of operations.

REFERENCES

Lincoln, J. V. and
H. I. Leighton

1972

Preliminary Compilation of Data for RWI July 26-
August 14, 1972, World Data Center A,
Solar-Terrestrial Physics, Report UAG-21.

HF Doppler Observations at Boulder, Colorado, August 1-12, 1972

by

G. M. Lerfald and R. B. Jurgens
NOAA, Boulder, Colorado 80302

1. Summary

An HF Doppler system has been operated near Boulder, Colorado since September 1971. The data collected during the solar and geomagnetic storm events of early August 1972 have been studied, with particular emphasis on selected time periods. In this short report we describe the Doppler system including methods of data analysis, tabulate discrete events observed on the Doppler records and present examples of results obtained by intensive analysis of certain events. Additional analysis of events occurring during the August 1972 period is planned.

2. System Description

The system description will be limited to those aspects necessary to understanding how the measurements are made and interpreted. The physical arrangement of the system includes the use of three transmitting sites and one central receiving site. If one assumes reflection from a horizontally stratified ionosphere, the midpoints of the skywave propagation path from those transmitter sites to the receiving site lie at the corners of an approximately equilateral triangle 40 km on each side.

At each transmitting site, 3 separate CW transmitters are operated. The transmissions are at frequencies of approximately 2.4, 4.8 and 6.0 MHz with approximately 2 kHz frequency between the transmitters at the respective stations to allow the signals to be separated by ordinary receivers at the receiving site. Each received signal is mixed with a local oscillator signal to give a beat frequency of a few Hertz. The signals are recorded on a slow moving analog tape recorder, and for real-time display several channels are recorded on a chart recorder. The beat frequencies are each input to a frequency to voltage converter which produces an analog output proportional to the frequency at its input. This analog signal is sampled and digitized 10 times per second, averaged by an on-line computer and an averaged sample point recorded, once every 5 seconds. The amplitude of the incoming signal for 3 of the channels is similarly sampled, digitized and recorded, making a total of 12 channels of digital data recorded for the system. The beat-frequency Doppler data recorded on analog magnetic tape are processed by an electro-mechanical spectrum analyzer which produces a paper-strip display of the beat frequencies as a function of time.

It has been found a great advantage to have available both the analog and digital data formats. This is true because the digital format is capable of representing only a single valued function of time, whereas Doppler records sometimes exhibit multiple frequency functions. In such instances, digital records could easily give misleading results if processed blindly. In practice the analog records are used as a means of checking, correcting, or rejecting sections of digital data for further processing.

A single channel of HF Doppler data provides in effect a measure of the apparent rate of change of phase path length along the propagation path. For the case of traveling ionospheric disturbances, most of the phase path length changes are believed due to the changing physical position of the ionospheric reflection point. This motion of the apparent reflection point will be in 3-dimensions, but analysis is often simplified by assuming that the reflection point remains at a stationary position on the horizontal plane and only moves vertically. The height of the reflection point is a function of the carrier frequency. For differing frequencies transmitted between common transmitter and receiver sites, the reflection points are assumed to lie along a vertical line, although in practice this may not be strictly true.

The HF Doppler system can be characterized as a means of measuring the apparent velocities of a set of reflection points. In the present system, this set consists of 9 sampling points with 3 points distributed along each of 3 verticals, which in turn intersect the corners of a horizontal equilateral triangle approximately 40 km on each side. The reflection heights are known only approximately unless other data such as ionosonde records are used to determine the height.

The uses to which HF Doppler data have been put include determination of the physical characteristics of traveling disturbances in the ionosphere. If a traveling disturbance moves as a reasonably coherent waveform across the array, one would expect to observe related variations at each of the sampling points. Also within limits imposed by the rate of data taking and relative time resolution, it should be possible to determine the apparent rate of motion and direction of motion of the disturbance.

3. HF Doppler Events August 1-12, 1972

The Doppler frequency vs. time records obtained by processing the analog magnetic tape data through a Rayspan spectrum analyzer were used to scan the data for interesting periods. Table I lists

the types and characteristics of events selected as being worth noting for possible further study or as possibly of interest to other workers.

TABLE I - LIST OF DOPPLER EVENTS AUG. 1-12, 1972

DATE	TIME (UT) Start-End	PERIOD (Range, Mins.)	COMMENTS
Aug. 1	01-04	11-18	
1	04-12	25-60	2.5 Hz p-p ampl. (4.8 MHz)
Aug. 2	04-10	30	
2	20:05	--	SFD
2	20:20-22:00	--	SWF
Aug. 3	00-03	20	
3	06-10	15-30	
Aug. 4	00-04	2-3 and 15-20	
4	01:22	--	Assoc. with Geomagn. commence.
4	02:22	--	Assoc. with reverse shock (4 Hz p-p. ampl.)
4	04-08	30-60	5.5 Hz p-p. ampl. (4.8 MHz)
4	14-24	--	Very disturbed, partial fadeout
Aug. 5	00-03	2-2½, 4-5	Came in bursts
5	03-04	2½, 5-10	
5	04-06	6	Regular
Aug. 6	01-04	12	
6	03:30-10	30-50	Doppler spreading
6	12:30-14	14	
Aug. 6-7	22-01	15-20	
Aug. 7	01-03	10-15	
Aug. 8	01-03	12-15	
Aug. 8-9	23-02	10	
Aug. 9	01-08	3	Superposed on longer period waves.
9	04-08	25-30	
9	11-16	4-5	
Aug. 11	03-09	30-50	Doppler spreading.
Aug. 11-12	22-03	12-15	

4. Sample Results

A period of time showing Doppler variations of particularly great interest occurred 0200-0400 UT on August 5, 1972. Figure 1 shows the time series variations of Doppler frequency versus time for several channels as derived from the digitally recorded data. There appear to be several "bursts" of quasi-sinusoidal oscillations with periods from 2 to 4 minutes and about 8 minutes. These digital data were processed by a spectral analysis computer program which can easily be set to use any desired time window. In the case at hand, 21-minute data samples were taken and successive shifts of 5 minutes in time made for each spectral computation. Averaging of two time-shifted spectra was then performed to obtain some smoothing and the spectra plotted. Figure 2 shows the spectra obtained where each succeeding curve is shifted along the vertical axis to avoid overlapping. As measured on Figure 2 between 0200 and 0250 UT the peaks in the power spectra occur with a period of about 4 minutes. Then, until 0400 UT the peak energy occurs with a period between 6-7- minutes.

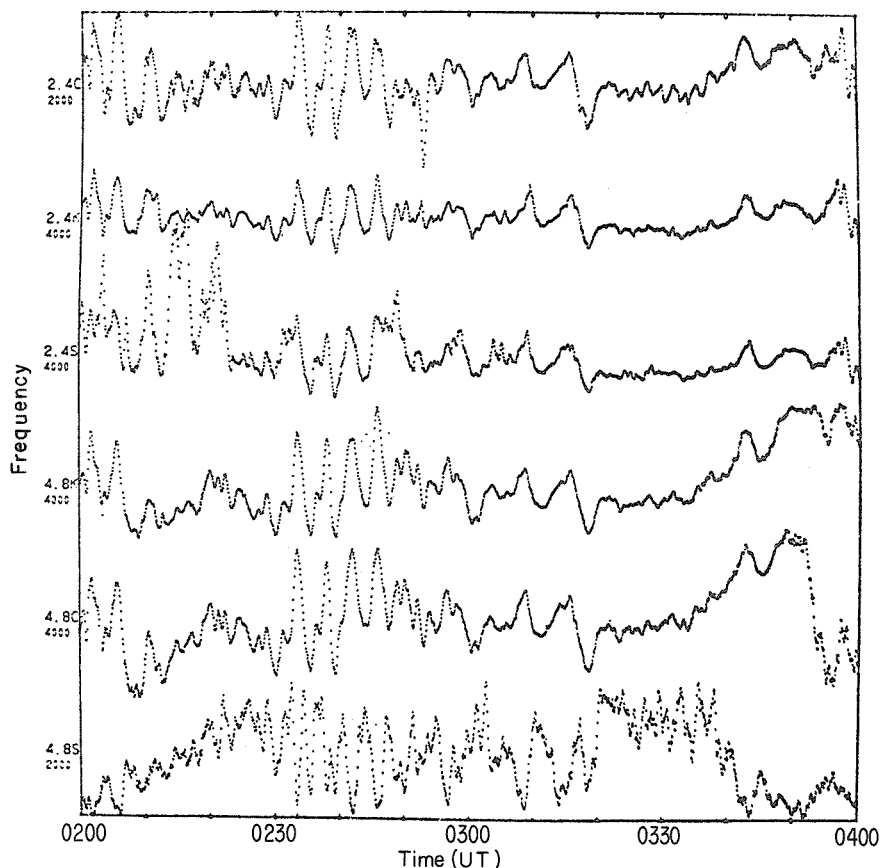


Fig. 1. Six channels of digital Doppler data from Aug. 5, 1972, 0200-0400 UT. Letter symbols for Ft. Collins, Keenesburg and Sunset are C, K and S, respectively. The numbers 2000 and 4000 refer to the vertical plotting range in digital units. 100 units equals 1 Hertz.

One of the principal uses of the spectral plots is to detect multiple spectral peaks which might indicate the presence of more than one type of wave motion or a dispersed wave train with multiple frequency components present concurrently. In this particular case, the variations are essentially monochromatic confirming the visual impression of Figure 1. When there is nearly equal power at several frequencies a cross spectrum between pairs of stations must be taken to yield the phase relation at the different frequency components.

The objective of the analysis is to infer as much as possible about the physical characteristics of the disturbances in the ionosphere giving rise to the Doppler variations. Among the characteristics of interest are the spatial dimensions, the vertical and horizontal phase velocities across the Doppler array, the phase tilt of the wavefront (if the disturbance is traveling) and the direction of travel.

The direction and speed of travel of a disturbance can be inferred from the time differences between variations of the several reflection points. The usual procedure with analog data is to pick salient features such as peaks and valleys and measure apparent time shifts from the records. The availability of digital data permits considerable sophistication and improvement over this method by the use of cross-correlation techniques and determination of lead-lag correlation values. These can be determined for any selected length of data section and the results plotted in contours of equal correlation coefficients as a function of time. Figure 3 shows such a plot where 20-minute data samples were used and the time base shifted one minute for each correlation computation. These correlation plots are obtained for each pair of stations and used as the basis for obtaining the horizontal phase velocity across the Doppler array. In the example shown, from 0200 to 0300 UT, the apparent speed across the array is too great to show a measurable delay, which has led us to speculate that the cause of these variations is not the conventional traveling disturbance but a magnetospherically related event. As seen in Figure 4, the D magnetic component at Boulder and the 2.4 MHz Doppler record from Keenesburg visually correlate, which tends to confirm this hypothesis.

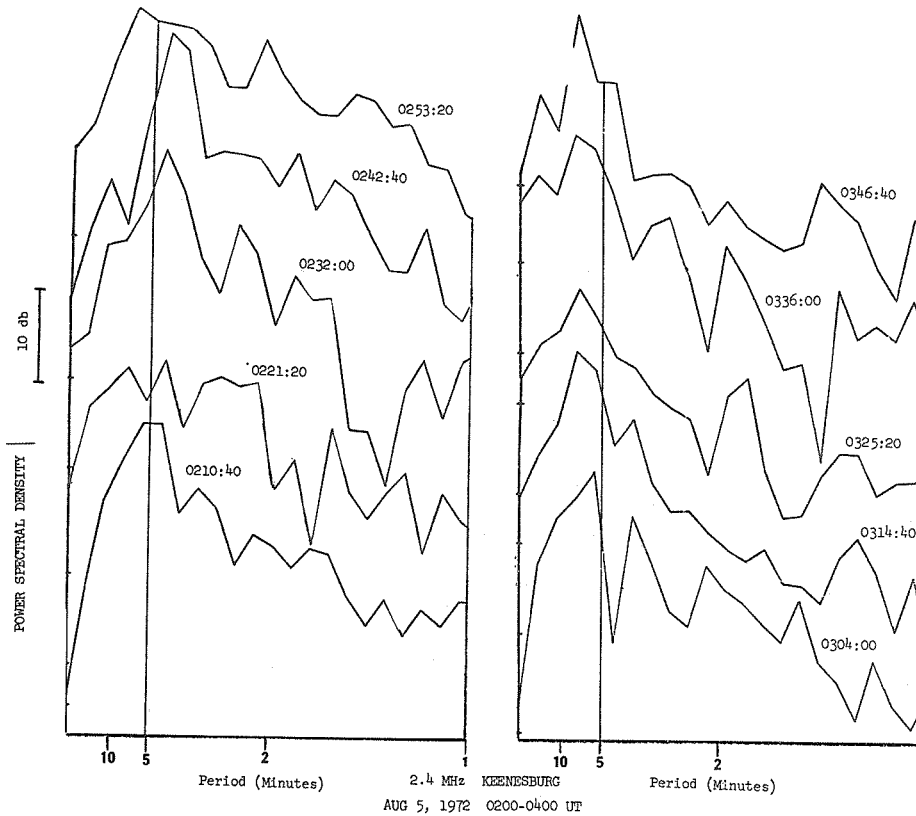


Fig. 2. Power spectral densities from the Keensburg 2.4 MHz Doppler channel for the period 0200-0400 UT, Aug. 5. Each spectrum is the average of two spectra, each computed from a data base 21 min. 20 sec. long and shifted in time by 5 min. 20 sec. The time label on each spectrum is the center of the two spectra. Spectral densities are plotted on a logarithmic axis.

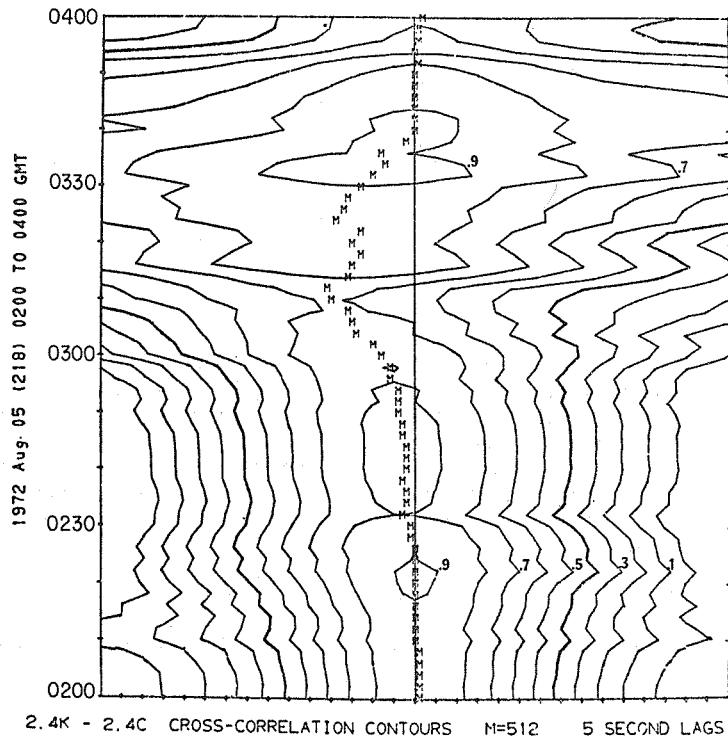


Fig. 3. Contours of equal cross-correlation as a function of lead-lag time (X-axis) and real time (Y-axis). The data used are the 2.4 MHz signals from Keensburg and Ft. Collins transmitters, respectively. Contours of positive correlation are drawn in 0.1 steps as indicated. The letter M indicates the lead or lag value at which maximum correlation exists for the analysis window used (512 points = 42 minutes). The range of lead-lag time is ± 75 seconds.

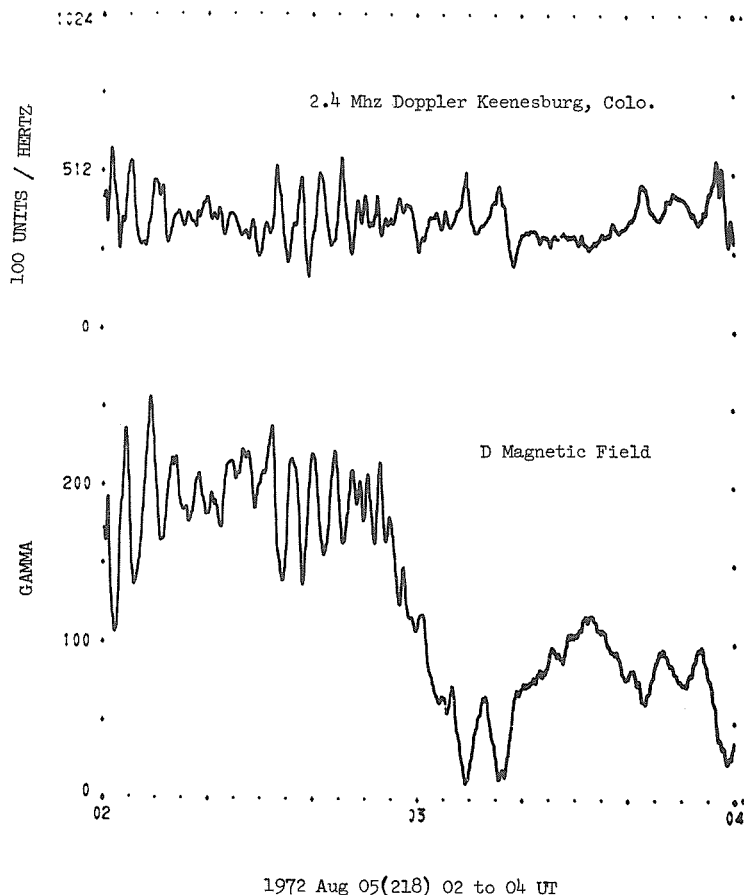


Fig. 4. Boulder D-magnetic component and the 2.4 MHz Keenesburg Doppler channel. The 4-5 minute period "bursts" between 0200-0300 occur on both records. The two records have a coherency of 1.0 at that period.

Following 0300 UT the relative delays of the Doppler channels indicate a disturbance front arriving from the north with a horizontal phase velocity of about 1200 m/sec. This is within range of characteristics of traveling disturbances associated with geomagnetically disturbed periods (see, e.g. Georges, 1967) We therefore believe that the two-hour period shown in the example represents two different kinds of events which are not directly associated.

5. Conclusions

The period August 1-12, 1972 gave rise to many interesting events recorded on the HF Doppler system at Boulder. We intend to analyze other events during the period using the methods outlined in the sample results section. We will be interested in comparisons with data collected by other workers. A joint study with the University of Alaska (R. Hunsucker, private communication) in an effort to associate specific events at the auroral oval with traveling disturbances observed at Boulder, is planned. An examination of periods with high correlation between magnetic field variations and Doppler data is also being conducted. Correlations are seen during PC 4 and PC 5 as well as long period magnetic bay events.

6. Acknowledgement

This work was supported by the Defense Advanced Research Projects Agency under ARPA Order No. 1361 and was monitored by Col. J. T. Jones.

REFERENCES

- GEORGES, T. M. 1967 Ionospheric Effects of Atmospheric Waves, ESSA Tech. Report, IER-57, ITSA-54.

HF Doppler Observations Associated with Magnetic Storm of August 4 to 6, 1972

by

T. Ichinose
Department of Electronics
Doshisha University
Kyoto, Japan

and

T. Ogawa
Ionosphere Research Laboratory
Kyoto University
Kyoto, Japan

The upper traces in Figures 1, 2 and 3 show the Doppler records observed at Doshisha University, Kyoto, Japan (N35.0, E135.8). The receiving frequencies are 5 and 10 MHz. The former is the signal from JJY and the latter is one from JJY, WWVH or BPV. The distance between the transmitting points (Koganei, Hawaii and Shanghai) and the receiving point (Kyoto) is about 360, 5700 and 1400 km, respectively.

In Figure 1 the 5 MHz radiowave from JJY is reflected by the lower F-layer at dawn. The 5 MHz radiowave in Figures 2 and 3 is reflected by the E-layer in the daytime. The 10 MHz wave is always reflected by the F-layer.

The lower trace in each figure shows the NS-component of the induction magnetogram observed by Dr. T. Saito at the Onagawa Magnetic Observatory, Miyagi, Japan.

A sudden commencement took place at 2054 UT August 4 and the Doppler shifts began at the same time. From 2054 to 2057 UT large sinusoidal oscillations with a period of 1.5 minutes were observed. The magnetic variation and the Doppler shift are in opposite phase to each other.

From 2057 to 2120 UT small amplitude oscillations with a period of 2 minutes appear on the Doppler trace, and the 10 MHz signal shows a phase lag behind the 5 MHz signal.

Figures 2 and 3 show the record on August 6 in which the Doppler shift has a good correlation with magnetic variations.

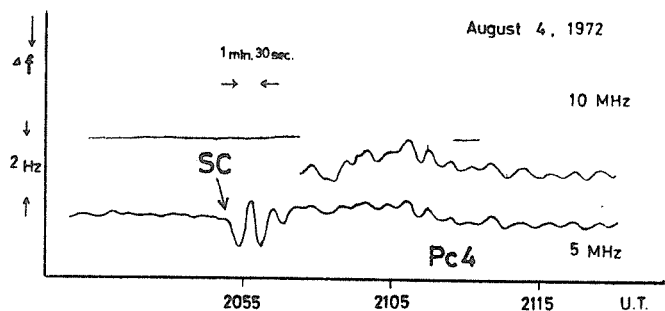


Fig. 1(a). Doppler records observed at Doshisha University on both 5 and 10 MHz for 2055-2115 UT August 4, 1972.

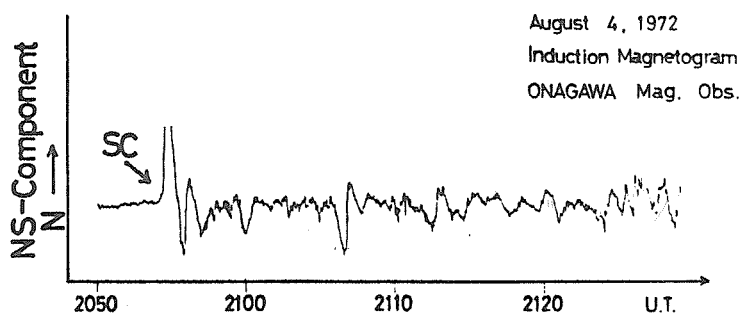


Fig. 1(b). North-South component of the induction magnetogram from Onagawa Magnetic Observatory for 2050-2120 UT August 4, 1972.

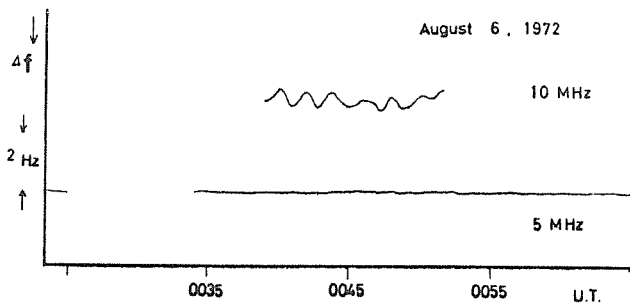


Fig. 2(a). Doppler records for 0035-0055 UT on August 6, 1972.

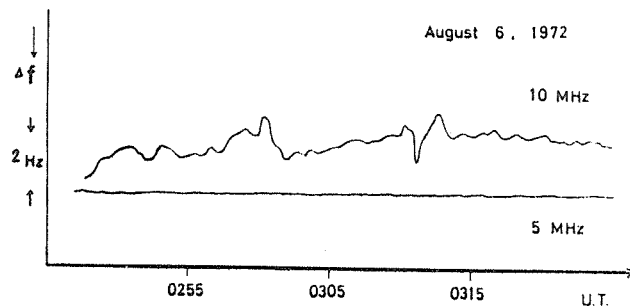


Fig. 3(a). Doppler records for 0255-0315 UT on August 6, 1972.

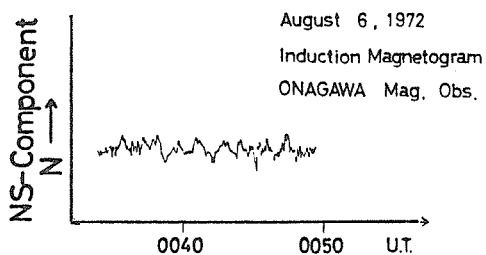


Fig. 2(b). Magnetogram for 0040-0050 UT on August 6, 1972.

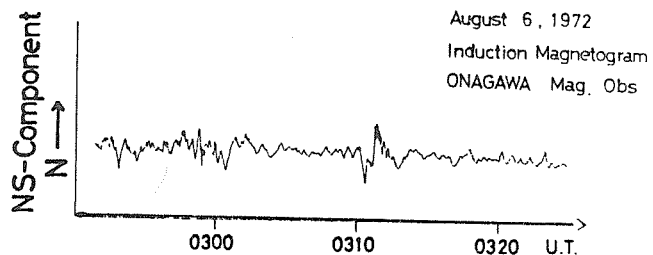


Fig. 3(b). Magnetogram for 0300-0320 UT on August 6, 1972.

SID Effects during July/August Event 1972

by

R. Knuth and K.-H. Ohle
Forschungsstelle für kosmische Elektronik
der Akademie der Wissenschaften der DDR
Observatory Neustrelitz
German Democratic Republic

This short note summarized the ionospheric effects of solar flares occurring during the July/August event 1972 as monitored at the Neustrelitz Observatory, GDR (N53°17', E13°05'). The observation methods used and their respective parameters are given in Table 1.

Table 1
Parameters of SID observation methods in Neustrelitz, GDR

Method	Frequency	Transmitter	Distance	Reflection Point	
				Geographic latitude	Geographic longitude
SFA	50 kHz	OMA Prag	380 km	N51°43'	E14°07'
SFA	155	Brasov	1200	49°38'	19°20'
SFA	164	Allouis	1000	50°09'	07°33'
SWF	2614	Norddeich	400	53°26'	10°07'
SWF	2775	Kiel	220	53°54'	11°36'
SWF	6030	Stuttgart	550	51°07'	10°58'
SCNA	25.0 MHz	Directed to	---	54°	13°
SCNA	27.6	Polar Star	---	54°	13°

During the period July 26 - August 14, 1972 in our vicinity 22 different SIDs were observed. Fourteen of them had importances ≥ 2 . This is an extremely high percentage of strong SIDs compared with the usual observations and is due to the outstanding character of the solar disturbances during this period.

Table 2 gives all data on the observed SFA (Sudden Field strength Anomalies), SWF (Short Wave Fade-Out) and SCNA (Sudden Cosmic Noise Absorption) as listed in HHI Geophysical Data [1972]; all explanations on types and importances can be found there.

Table 2
Solar Flare Effects in the Ionosphere (SID) Stations
Neustrelitz (SFA, SWF, SCNA) and Kühlungsborn (SFA, SWF)

1972 Day	S F A				S W F					S C N A			
	Start (UT)	Max. (UT)	Dur. (min.)	Imp.	Start (UT)	Max. (UT)	Dur. (min.)	Imp.	Type	Start (UT)	Max. (UT)	Dur. (min.)	Imp.
July 28	1323	1330	50	1	1324	1328	30	2	S	x	x	x	x
31	1101	1119	x	2	1100	1118	x	3	G	-	-	-	-
	1158	1205	30	1	1158	1202	25	1	S	-	-	-	-
Aug 1	0659	0708	x	1	0700	0707	x	2	S	0700	0705	15	0
	0722	0730	25	1	0724	0728	30	2	S	0723	0729	15	0
	0920	0930	50	2	0920	x	35	2	S	0916	0927	35	2
	1135	1145	x	0	1133	1140	x	0	S	x	x	x	x
	1151	1156	30	0	1151	1157	25	1	S	x	x	x	x
2	-	-	-	-	0357	x	420	3+	SL	0357	x	x	2
	1045	1056	55	2	-	-	-	-	-	-	-	-	-
4	0623	0636	200	3+	0623	x	300	3+	S	x	x	x	x
7	1056	1113	x	1	1057	1112	30	2	S	1056	1110	40	1
	1202	1207	40	0	1203	1207	20	1	S	1202	1204	20	0
	1509	1528	120	3+	1508	x	130	3+	S	1509	1525	100	3+
9	0805	0816	20	0	0809	0815	15	0	S	-	-	-	-
	-	-	-	-	0958	x	40	3	S	1003	1010	25	1
	1614	1618	30	0	1614	1620	20	1	S	1615	1620	15	0
10	1405	1412	15	0	-	-	-	-	-	-	-	-	-
11	1216	1221	x	2	x	x	x	x	x	x	x	x	x
	1233	1243	90	2	x	x	x	x	x	x	x	x	x
12	0741	0745	10	0	0733	0743	30	1	S	0733	0736	20	0
	1433	1444	80	2	1433	1442	30	2	S	1435	1440	15	1

The most spectacular events occurred between August 1 and 7, 1972. The four most disturbed days have been chosen to demonstrate in more detail what really happened in the lower ionosphere (Figures 1 - 3). In these figures the curved baselines always indicate the normal daily variations. It is well-proven [e.g. Lauter and Entzian, 1966; Ohle *et al.*, 1973] that the phase height method in the LF-range follows the height variations of a certain electron density level (for our frequencies and paths about 300 - 500 electrons/cm³). Therefore, the SFA recorded by this method can be interpreted as unusual height decreases of this constant electron density level caused by the additional solar flare ionization (Figure 1). Roughly speaking, we can assume that due to the steep electron density gradient in this region we see the height variations of the lower ionospheric border. Figures 2 and 3 in the normal manner show the absorption anomalies in the HF range (SWFs and SCNAs) caused by attenuation of these frequencies during passage through the additional ionospheric flare layer. Obviously, the strongest SIDs occurred on August 2, 4 and 7. Unfortunately, the SID of August 2 at 0357 UT is not very well expressed in SFA observations due to the high solar zenith angle, but according to SWF records had an outstanding duration of about 8 hours. The SCNA of August 7 at 1509 UT with about 9.5 dB absorption is the strongest effect of this type observed in Neustrelitz since the beginning of the cosmic noise observations in 1959. Also, the corresponding SFA with a height decrease to 66 km is probably the most intense effect recorded in Neustrelitz and Kuhlungsborn. In the past the lowest heights reached during strong solar flares for the same solar zenith angle were around 72 km! The velocity of height decrease during the initial phase from start till maximum of the effect was nearly 600 m/min, much higher than the normally found velocities of about 200 m/min [Entzian, 1966].

REFERENCES

- | | | |
|---|------|---|
| ENTZIAN, G. | 1966 | <u>Sonneneruptionseffekte im Langwellenbereich, Schriftenreihe des NKGG der DDR, Reihe II, Heft 1, 139 - 147.</u> |
| LAUTER, E. A. and
G. ENTZIAN | 1966 | <u>Überwachung der tiefen Ionosphäre mit Hilfe der Quasi-Phasenmessungen im Langwellenbereich (100-200 kHz), Schriftenreihe des NKGG der DDR, Reihe II, Heft 1, 67 - 97.</u> |
| OHLE, K. H.,
R. KNUTH
G. ENTZIAN and
J. TAUBENHEIM | 1973 | <u>On the information content of ionospheric solar flare effect observations., Part I: Experimental evidences of solar and atmospheric control of the flare effects, J. Atmos. Terr. Phys., in press.</u> |
| | 1972 | <u>Geophysikalische Beobachtungsergebnisse (Geophysical Data), Heinrich-Hertz-Institut, DDR-1199 Berlin-Adlershof.</u> |

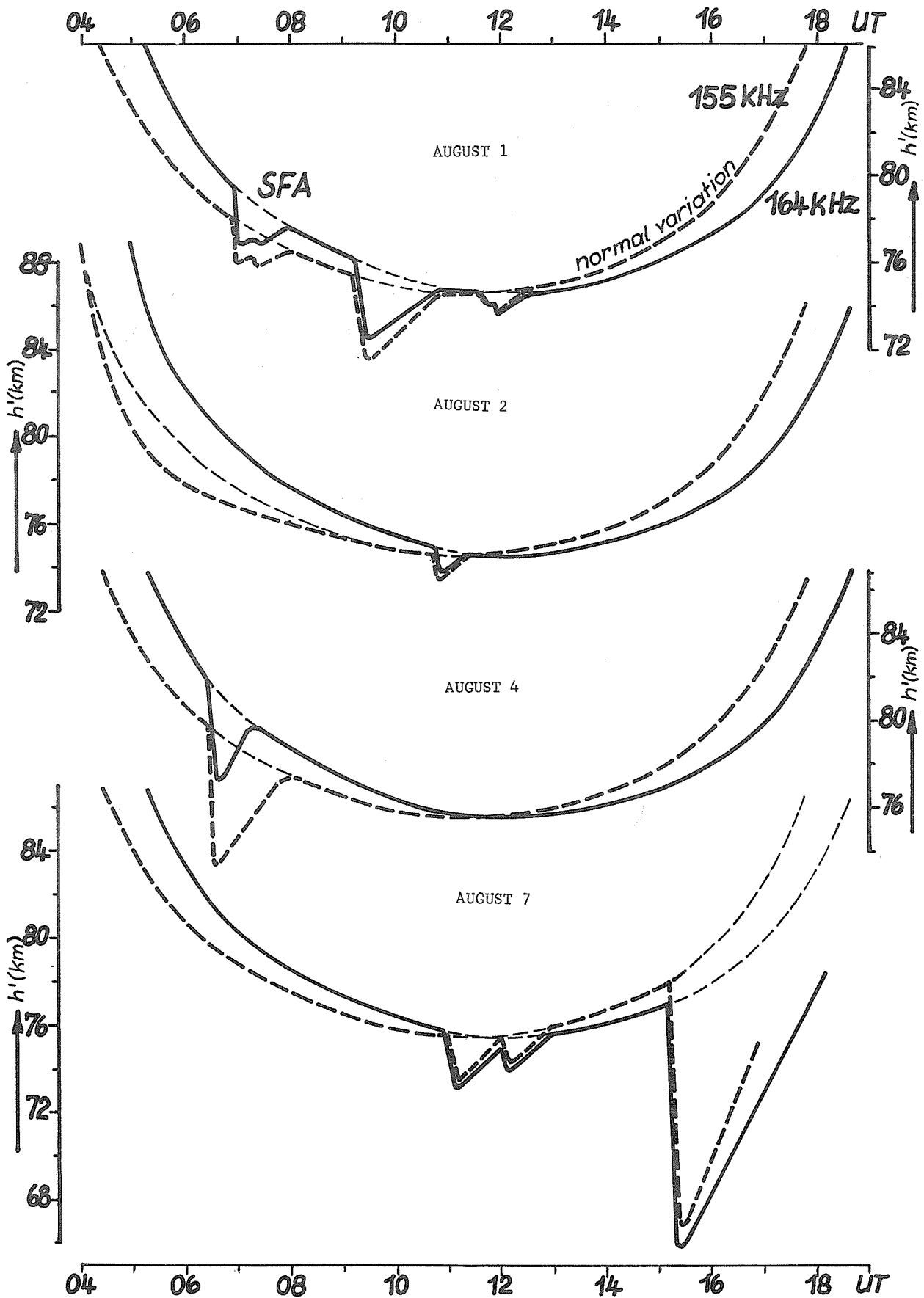


Fig. 1. Height variations of the lower ionospheric border (n_e 300 - 500 e/cm^3) deduced from SFA observations in the period August 1 - 7, 1972.

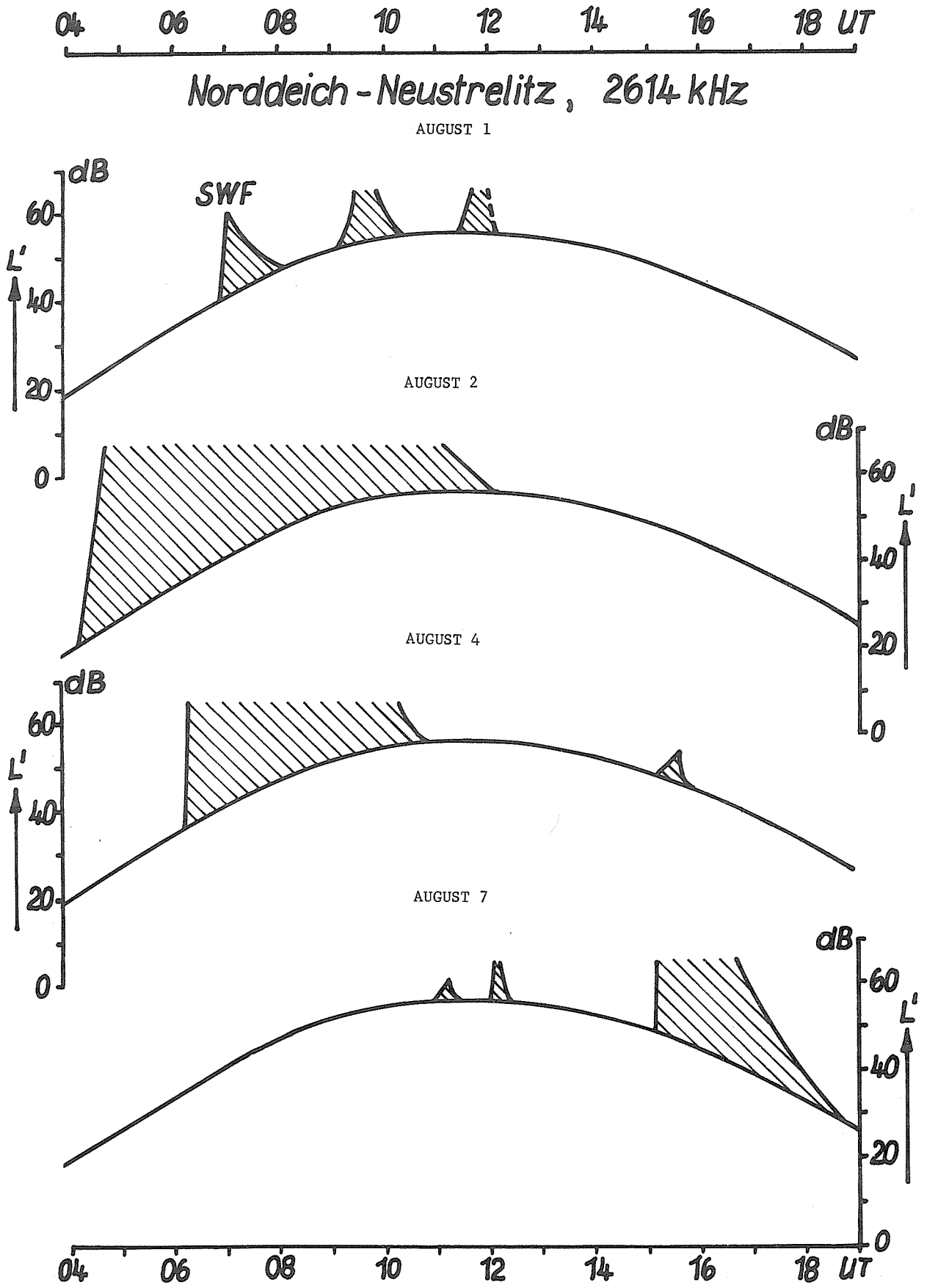


Fig. 2. Variations of ionospheric absorption in HF-range with superposed SWF in the period August 1 - 7, 1972.

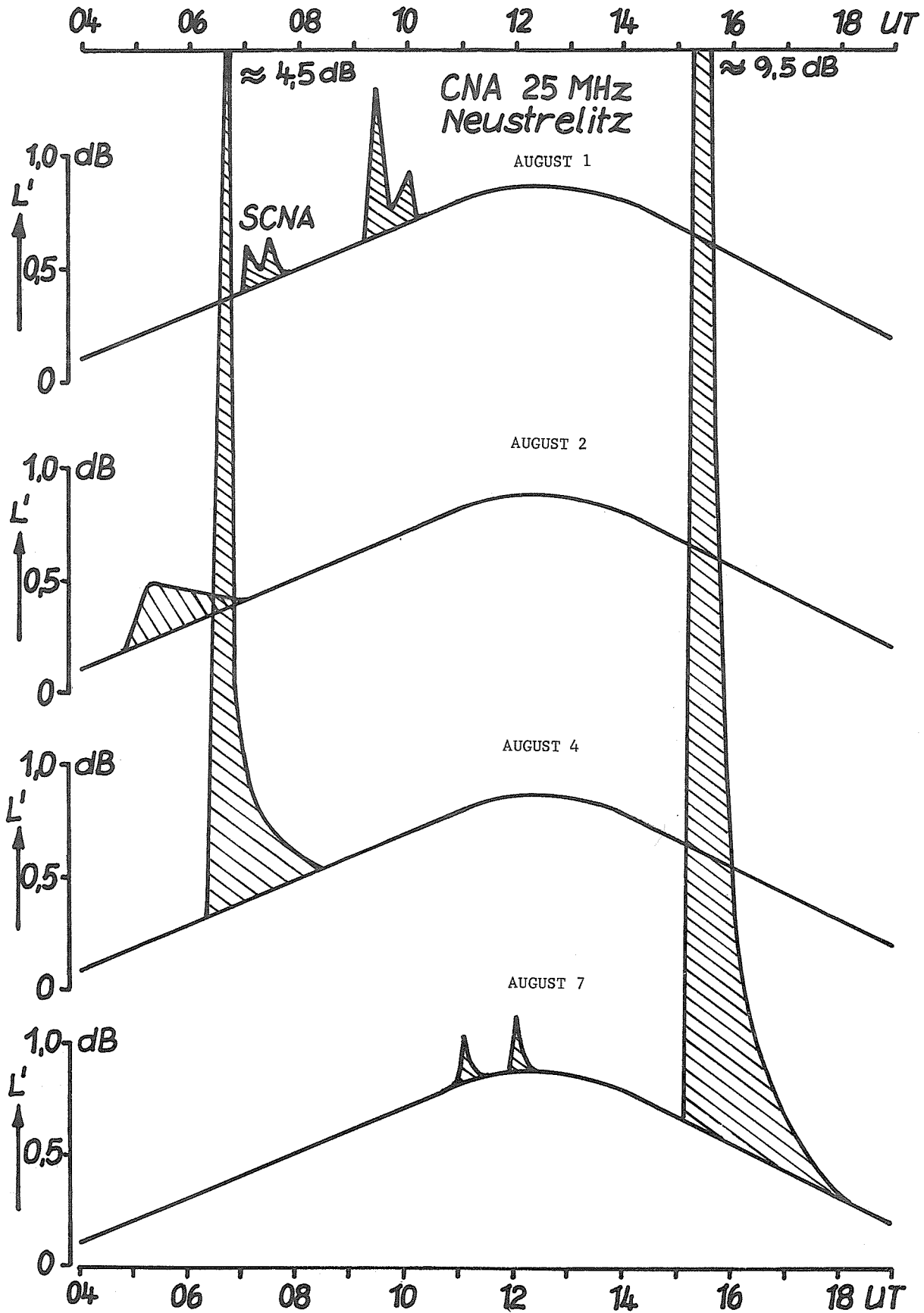


Fig. 3. Variations of ionospheric absorption according to cosmic noise observations in the period August 1 - 7, 1972.

Shortwave Fadeouts and Ionospheric Absorption Measured at Lindau
(N52.6; E8.7) in the Period 15 July to 15 August 1972

by

H. Schwentek
Max-Planck-Institut für Aeronomie
Institut für Ionosphärenphysik
D 3411 Lindau/Harz, FRG

Abstract

Results of the following observations are described: Sunspot group of 6 August 1972; solar flare effects on radio field-strength (2.61 MHz; 2.77 MHz; 6.09 MHz) and cosmic noise recordings (27.6 MHz); ionospheric absorption at 2.61 MHz.

A Short View on the Sunspots around August 1972

Two of the manifestations of the Sun's activity are the number and type of the sunspots. In August 1972 a remarkable group of sunspots appeared. As an illustration, a photograph made by an amateur is reproduced here (Fig. 1) showing this group of sunspots on 6 August 1972; a rare feature is that the spots are arranged on a circle and are joined by their penumbras. It seems as though the single spots tend to form into one very large spot.

Considering the daily variation of the sunspot number in July, August, and September 1972 (Fig. 2), two remarkable features can be noted. First, the regular, well-known variation of sunspot number due to the rotation of the sun with a period of about 28 days, appears very clearly. Secondly, the graph of sunspot numbers does not give any indication of a large disturbance in the Earth's atmosphere during the period from 2 to 8 August 1972. In fact, the variation showed its greatest amplitude even later, from 30 August to 13 September 1972. Therefore, it may be suggested that the particular congregation of the sunspots was essential.

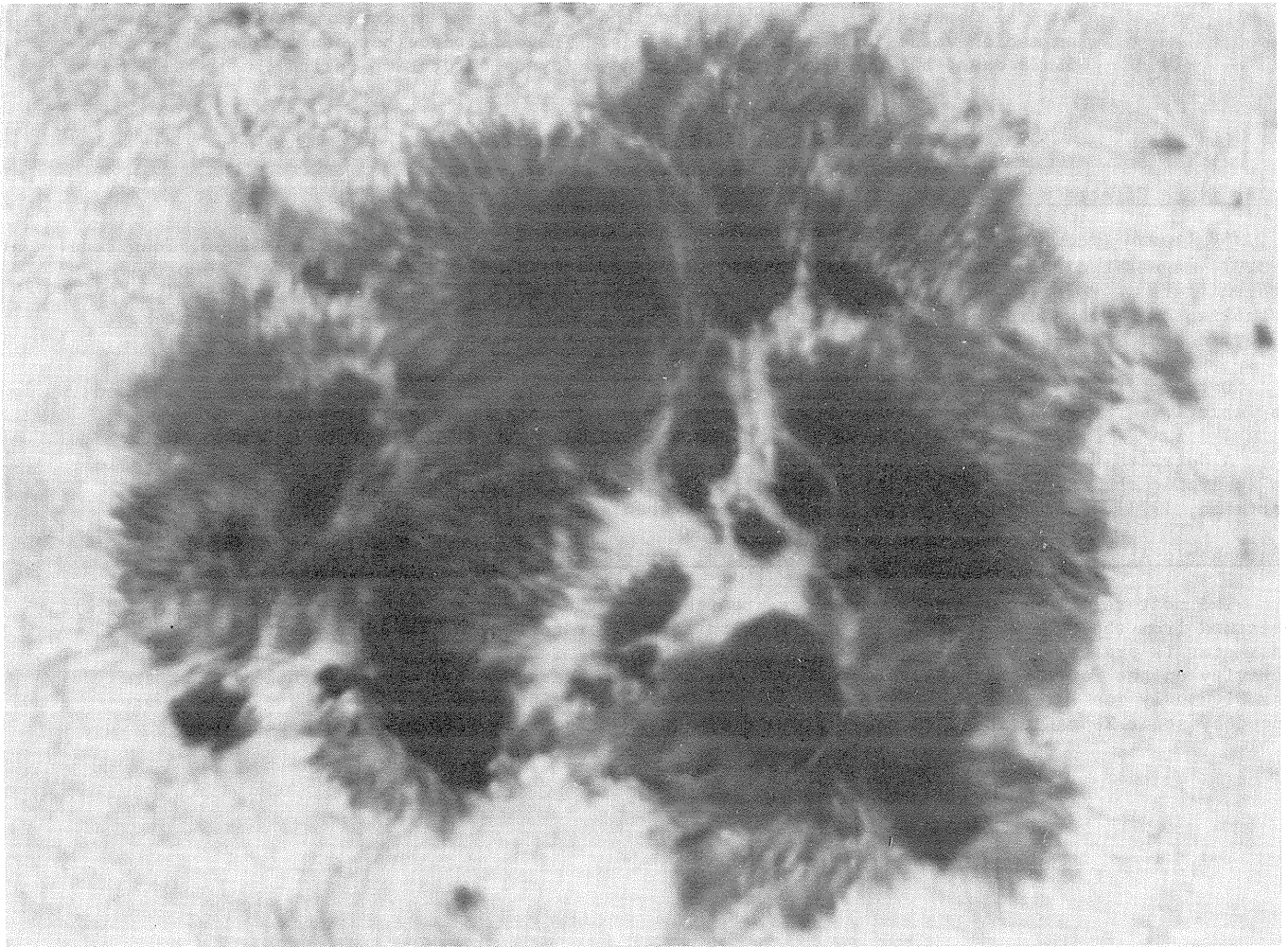


Fig. 1. Photograph of an extraordinary group of sunspots taken at 1228 UT 6 August 1972 with a refractor (17 cm; 394 cm) and a Rolleiflex SL66 camera. (Reproduced by courtesy of Dipl.-Ing. W. Bruckner, Architekt BDA, 4 Dusseldorf 1, FRG).

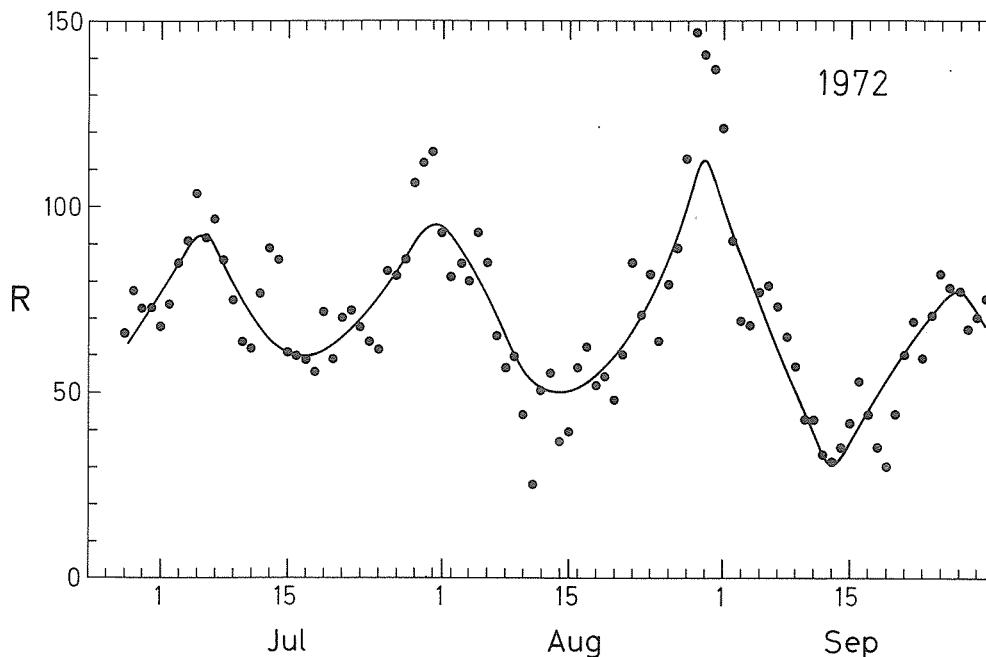


Fig. 2. Trend of the provisional daily sunspot number in July, August, and September 1972 observed at the Eidgenössische Sternwarte Zürich (Swiss Federal Observatory, Zürich, Switzerland). The curve drawn is based on median values of overlapping periods. The difference between maxima is 28 days, between minima 28 and 30 days (synodic rotation period).

Solar flare Effects on the Field-strength and Cosmic noise Recordings

At Lindau (geographical latitude N51.65, longitude E10.13; geomagnetic latitude N52.36, longitude E93.91, magnetic dip angle + 67.8°, time 15° EMT = UT + 1h) the field strength of several shortwave transmitters is recorded continuously. The transmission circuits (see Table 1) were especially established for the purpose of absorption measurements. Also, a riometer is operated [Schwentek, 1966; Schwentek and Gruschwitz, 1970; Schwentek and Timpe, 1972].

Data for shortwave fadeouts observed during the period 15 July to 15 August 1972 are summarized in Table 1.

A detailed description of the morphology of single shortwave fadeouts (Fig. 3) is most valuable in analyzing the corresponding solar X-ray flares observed by satellite [Schwentek, Kreplin, and Hartmann, 1971]. This analysis will be given later when all necessary data are available.

Ionospheric Absorption in the Period 15 July to 31 August 1972

The most reliable absorption parameter, representing the character of the day, is L ($\cos \chi = 0.2$) obtained from the diurnal variation of absorption (χ = solar zenith angle). The behavior of this parameter is presented for the period July to September 1972 in which the extreme effects of solar activity on the Earth's atmosphere occurred. The large increases in the period 6 to 14 August are unambiguously due to solar activity, that is, to particle precipitation (Fig. 4). The effects produced by solar X_E radiation (Table 1) were excluded when L ($\cos \chi = 0.2$) was determined.

REFERENCES

- | | | |
|---|------|--|
| SCHWENTEK, H. | 1966 | The determination of absorption in the ionosphere by recording the field-strength of a distant transmitter, <u>Ann. Geophys.</u> , <u>22</u> , 276 - 288. |
| SCHWENTEK, H. and
E. H. GRUSCHWITZ | 1970 | Measurements of absorption in the ionosphere on 27.6 MHz at 52°N by means of a riometer and a corner-reflector antenna directed to the celestial pole, <u>J. Atmos. Terr. Phys.</u> , <u>32</u> , 1385 - 1402. |
| SCHWENTEK, H. and
CHR. TIMPE | 1972 | The applicability of method A3 for measurements in the ionosphere at 6 MHz using only the 1 F mode, <u>J. Atmos. Terr. Phys.</u> , <u>34</u> , 867 - 876. |
| SCHWENTEK, H.,
R. W. KREPLIN, and
G. HÄRTMANN | 1971 | The trend of ionospheric absorption during shortwave fade-outs related to the trend of enhancement of solar X-ray flux, <u>Rad. Sci.</u> , <u>6</u> , 35 - 40. |

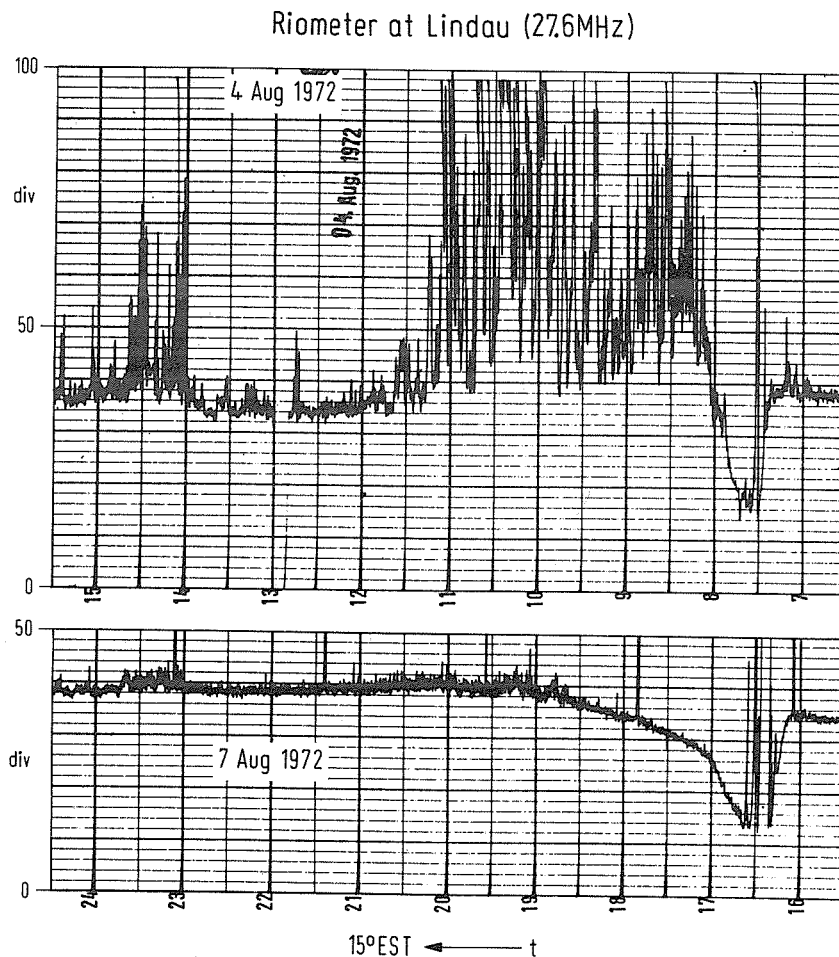


Fig. 3. Examples of the two strongest solar flare effects in August 1972 on a cosmic noise record made by a riometer of 27.6 MHz with a corner reflector antenna directed to the celestial pole. Note the intense disturbance by solar noise on A August 4, 1972 (see also the contribution by P. Czechowsky, this compilation). On August 7 the trend is also disturbed by some interference and solar noise.

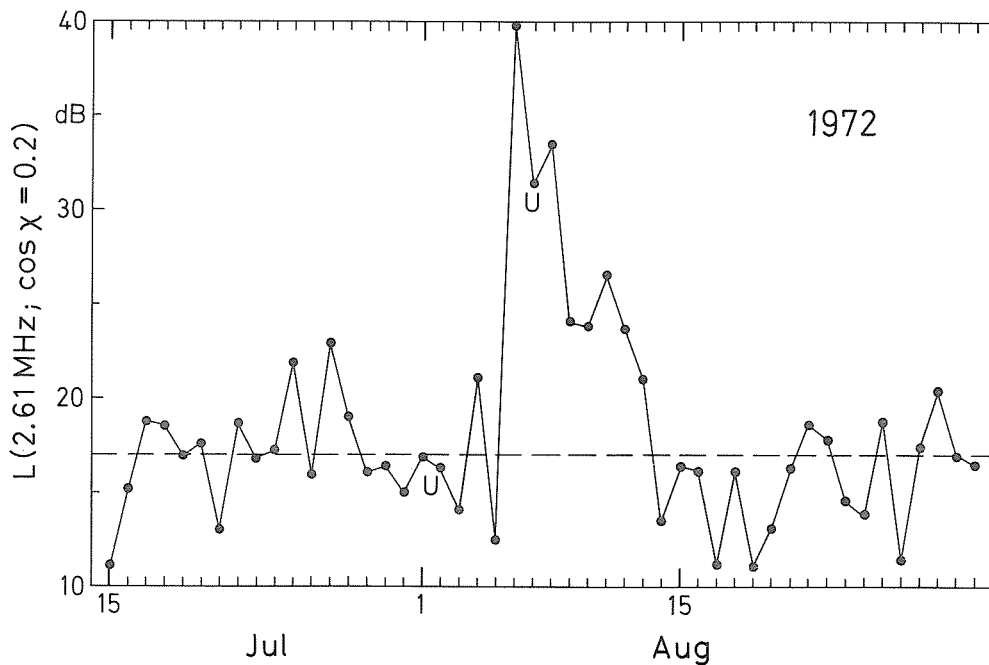


Fig. 4. Ionospheric absorption at a constant solar zenith angle $\chi = 78.5^\circ$, $L(2.61 \text{ MHz}; \cos \chi = 0.2)$; A3-circuit Norddeich-Lindau (296 km).

Table 1

Shortwave Fadeouts Observed in the Period 15 July to 15 August 1972 at Lindau

Sunrise occurred in the D-region at about 0400 UT, sunset at about 2100 UT (for 1 August: 0333 UT; 2119 UT, respectively). The most pronounced effects are underlined once, twice, or three times, corresponding to the maximum absorption measured by a riometer.

NL: A3-circuit Norddeich - Lindau, 296 km, 2.61 MHz, 1 E mode;

KL: A3-circuit Kiel - Lindau, 300 km, 2.77 MHz, 1 E mode;

LL: A3-circuit Luxemburg - Lindau, 339 km, 6.09 MHz, 1 F mode;

Rio: riometer at 27.6 MHz, corner reflector antenna directed to the celestial pole.

U: unreliable; N: not measurable; D-SWF means double SWF, that is, a second SWF started before the first ended. (See also the contribution by R. Eyfrig and J. Rottger elsewhere in this compilation.)

Date	Start	Maximum	End	Type	Absorption	Duration	Path	Remarks
1972	UT	UT	UT		dB	min		
Jul 28	13:21	13:26	13:40	S-SWF	31	19	NL	
	13:21	13:25	13:44	S-SWF	31	23	KL	
	13:21	U 13:26	U 13:40	S-SWF	16	U 19	LL	
	12:30	13:22	14:30	burst?	-	120	Rio	
<u>Jul 31</u>	11:03	U 11:15	U 12:16	V-SWF	> 36	U 73	NL	irregular
	11:03	11:14	U 11:49	V-SWF	> 47	U 46	KL	
	11:11	11:15	11:30	S-SWF	20	19	LL	11:04-11:11 slow,
	11:02	11:18	U 11:29	V-SWF	0.92	U 27	Rio	disturbed
Aug 1	06:58	07:04	07:16	D-SWF	32	U 62	NL	
	07:16	07:28	U 08:00		35			
	06:58	07:05	07:18	D-SWF	29	U 62	KL	
	07:18	07:30	U 08:00		25			
	06:57	07:04	N	S-SWF	11	N	LL	Rio: Maximum very
	07:00	07:16	N	N	0.22	N	Rio	broad

Date 1972	Start UT	Maximum UT	End UT	Type	Absorption dB	Duration min	Path	Remarks
Aug 1	11:32	11:39	12:08	S-SWF	16	36	NL	
	11:33	11:39	12:12	S-SWF	15	39	KL	
	N	11:39	N	N	N	N	LL	
	N	11:38	N	N	N	N	Rio	
Aug 2	10:45	10:48	11:07	S-SWF	10	22	NL	
	10:44	10:48	U 11:15	S-SWF	14	U 31	KL	
	10:44	10:48	N	S-SWF	U 12	N	LL	
	10:45	10:52	11:10	S-SWF	0.21	25	Rio	
<u>Aug 4</u>	06:21	N	U 12:30	S-SWF	> 42	U 369	NL	
	C	C	C	C	C	C	KL	
	06:24	N	N	S-SWF	> 28	N	LL	Rio: Disturbed by solar burst
	06:22	U 6.35/42	N	S-SWF	U 4.14	N	Rio	
Aug 7	10:57	11:09	11:45	V-SWF	U 19	48	NL	
	10:58	U 11:10	11:37	V-SWF	17	41	KL	max 11.10 - 11.20
	N	11:11	N	N	N	N	LL	
	10:58	U 11:14	U 11:34	V-SWF	0.15	U 36	Rio	
Aug 7	12:57	U 13:37	14:18	V-SWF	9	81	NL	Produced by particles?
	12:57	U 13:36	14:17	V-SWF	16	80	KL	
<u>Aug 7</u>	15:06	U 15:13?	U 17:30	S-SWF	18	U 144	NL	
	15:06	U 15:10?	U 17:37	S-SWF	15	U 151	KL	
	15:09	N	U 17:41	S-SWF	> 72	U 152	LL	
	15:07	N	U 17:40	S-SWF	4.0	U 153	Rio	disturbed
Aug 9	10:00	10:06	10:22	S-SWF	17	22	NL	
	10:03	10:08	10:20	S-SWF	18	17	KL	
<u>Aug 11</u>	N	N	N	irregular	N	12:30-15:20	NL	diurnal variation
	N	N	N	irregular	N	12:20-15:00	KL	with excessive absorption
	U 12:15	12:38-44	14:15	V-SWF	44	U 120	LL	
	U 12:28	12:38-44	U 15:00	V-SWF	2.1	U 152	Rio	Rio: Time of start extrapolated
Aug 12	07:31	07:43	U 08:08	V-SWF	22	U 37	NL	
	U 07:27	07:45	U 08:00	V-SWF	13	U 33	KL	
	N	07:45	N	N	N	N	LL	
	U 07:32	U 07:45	U 07:50	V-SWF	0.17	U 18	Rio	
Aug 12	14:31	14:40	15:24	S-SWF	31	53	NL	X _E : max 14.40
	14:33	14:40	U 15:30	S-SWF	27	U 57	KL	
	U 14:32	14:40	U 15:02	S-SWF	U 20	U 30	LL	
	14:32	14:40	15:30	S-SWF	0.30	58	Rio	

Sudden Phase Anomalies Observed at Uji

by

Y. Naito and S. Kato
Ionosphere Research Laboratory
Kyoto University, Uji, Kyoto 611, Japan

and

T. Araki
Geophysical Institute
Kyoto University, Kyoto 606, Japan

Table 1 shows SPA's observed at the Ionosphere Research Laboratory, Kyoto University (Uji, Kyoto, Japan: 34°54'N, 135°48'E) by using the VLF radio signal from NWC (North West Cape, Australia: 21°49'S, 114°10'E).

A series of SPA's began on August 1, and the maximum phase advance was recorded on August 4. Unfortunately, we could not observe the big event on August 7 because of the station break of NWC from 0000 to 0430 UT. The occurrence of SPA's increased on August 10 and 11 though the phase advances were small, and this series of SPA's seems to end on August 13.

Figure 1 shows the main features of these events. The following four types of SPA's are found in this Figure.

1. Rapidly growing and rapidly recovering types (e.g., 0618 UT, August 4).
2. Rapidly growing and slowly recovering types (e.g., 0659 UT, August 1).
3. Slowly growing and slowly recovering types (e.g., 0123 UT, August 1).
4. Multiple-peak types (e.g., 0009 and 0200 UT, August 11).

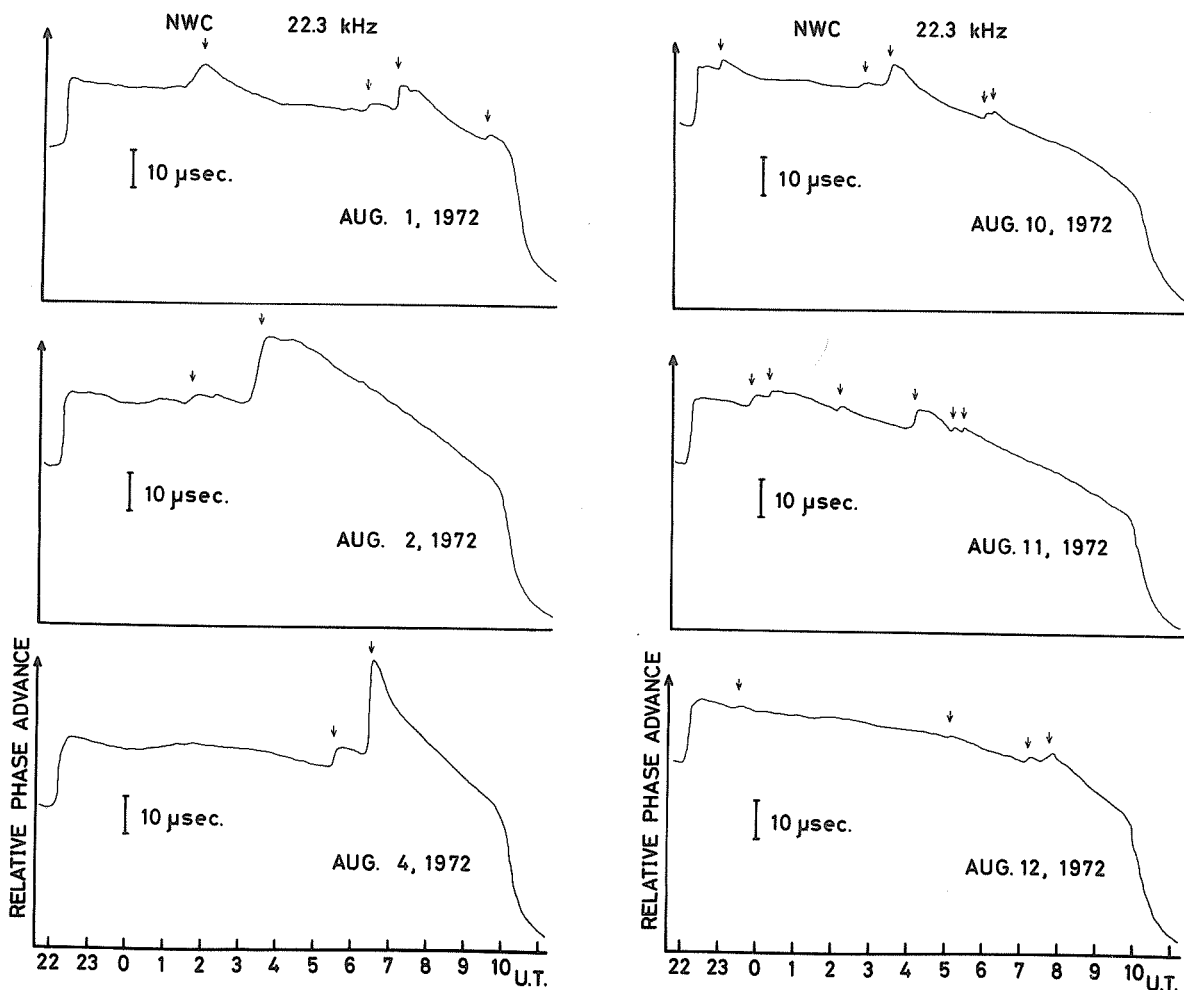


Fig. 1. The daytime phase variations of NWC signals observed at Uji, Kyoto, Japan. The arrows show SPA's. The sharp increase and decrease at 2200-2300 UT and 1000-1100 UT are the normal daily variations caused by the changes of the ionospheric reflection height during the sunrise and sunset.

Table 1
SPA's Observed at Uji from August 1 to 13, 1972

DATE	ONSET (UT)	PEAK (UT)	PHASE ADVANCE (μ sec)	REMARKS
August 1	1 0123	0157	8	
		0609	0624	3
		0659	0709	9
		0922	0945	3.5
2	0127	0145	3.5	
	0306	0340	21	
3				No SPA's observed
4	0524	0534	5.5	
	0614	0633	31.5	
5				No SPA's observed
6	0419	0423	2	
7				No SPA's observed
				Station break from 0000 to 0430 UT
8				No SPA's observed
9	2244	2251	3	
10	0224	0239	2	
	0300	0323	8.5	
	0546	0552	2.5	
	0557	0601	3.5	
	2336	0051	3.5	
11	0009	0018	5	
	0200	0206	6	
	0354	0418	9	
	0503	0506	5	
	0519	0524	6	
	2324	2329	1.5	
12	0504	0509	1.5	
	0704	0714	3	
	0727	0743	5.5	
13	0152	0206	3	
	0703	0724	1.5	

- (1) Phase advance value is defined as the phase deviation from the assumed ordinary value at the moment of maximum SPA.
(2) The multiple-peak SPA's are separately listed with each peak.

USCOMM-NOAA-ASHEVILLE, NC-7-73-1625

Publication Notice

WORLD DATA CENTER A for SOLAR-TERRESTRIAL PHYSICS REPORT UAG
(Prepared by World Data Center A for Solar-Terrestrial Physics, NOAA, Boulder, Colorado)

These reports are for sale through the National Climatic Center, Federal Building, Asheville, NC 28801, Attn: Publications. Subscription price: \$9.00 a year; \$2.50 additional for foreign mailing; single copy price varies. These reports are issued on an irregular basis with 6 to 12 reports being issued each year. Therefore, in some years the single copy rate will be less than the subscription price, and in some years the single copy rate will be more than the subscription price. Make checks and money orders payable to: Department of Commerce, NOAA.

Upper Atmosphere Geophysics Report UAG-1, "IQSY Night Airglow Data" by L. L. Smith, F. E. Roach and J. M. McKenna of Aeronomy Laboratory, ESSA Research Laboratories, July 1968, single copy price \$1.75.

Upper Atmosphere Geophysics Report UAG-2, "A Reevaluation of Solar Flares, 1964-1966" by Helen W. Dodson and E. Ruth Hedeman of McMath-Hulbert Observatory, The University of Michigan, August 1968, single copy price 30 cents.

Upper Atmosphere Geophysics Report UAG-3, "Observations of Jupiter's Sporadic Radio Emission in the Range 7.6-41 MHz, 6 July 1966 through 8 September 1968" by James W. Warwick and George A. Duik, Department of Astro-Geophysics, University of Colorado, October 1968, single copy price 30 cents.

Upper Atmosphere Geophysics Report UAG-4, "Abbreviated Calendar Record 1966-1967" by J. Virginia Lincoln, Hope I. Leighton and Dorothy K. Kropp, Aeronomy and Space Data Center, Space Disturbances Laboratory, ESSA Research Laboratories, January 1969, single copy price \$1.25.

Upper Atmosphere Geophysics Report UAG-5, "Data on Solar Event of May 23, 1967 and its Geophysical Effects" compiled by J. Virginia Lincoln, World Data Center A, Upper Atmosphere Geophysics, ESSA, February 1969, single copy price 65 cents.

Upper Atmosphere Geophysics Report UAG-6, "International Geophysical Calendars 1957-1969" by A. H. Shapley and J. Virginia Lincoln, ESSA Research Laboratories, March 1969, single copy price 30 cents.

Upper Atmosphere Geophysics Report UAG-7, "Observations of the Solar Electron Corona: February 1964-January 1968" by Richard T. Hansen, High Altitude Observatory, Boulder, Colorado and Kamuela, Hawaii, October 1969, single copy price 15 cents.

Upper Atmosphere Geophysics Report UAG-8, "Data on Solar Geophysical Activity October 24-November 6, 1968", Parts 1 and 2, compiled by J. Virginia Lincoln, World Data Center A, Upper Atmosphere Geophysics, ESSA, March 1970, single copy price (includes Parts 1 and 2) \$1.75.

Upper Atmosphere Geophysics Report UAG-9, "Data on Cosmic Ray Event of November 18, 1968 and Associated Phenomena" compiled by J. Virginia Lincoln, World Data Center A, Upper Atmosphere Geophysics, ESSA, April 1970, single copy price 55 cents.

Upper Atmosphere Geophysics Report UAG-10, "Atlas of Ionograms" edited by A. H. Shapley, ESSA Research Laboratories, May 1970, single copy price \$1.50.

Upper Atmosphere Geophysics Report UAG-11, "Catalogue of Data on Solar-Terrestrial Physics" compiled by J. Virginia Lincoln and H. Patricia Smith, World Data Center A, Upper Atmosphere Geophysics, ESSA, June 1970, single copy price \$1.50.

Upper Atmosphere Geophysics Report UAG-12, "Solar-Geophysical Activity Associated with the Major Geomagnetic Storm of March 8, 1970", Parts 1, 2 and 3, compiled by J. Virginia Lincoln and Dale B. Bucknam, World Data Center A, Upper Atmosphere Geophysics, NOAA, April 1971, single copy price (includes Parts 1-3) \$3.00.

Upper Atmosphere Geophysics Report UAG-13, "Data on the Solar Proton Event of November 2, 1969 through the Geomagnetic Storm of November 8-10, 1969" compiled by Dale B. Bucknam and J. Virginia Lincoln, World Data Center A, Upper Atmosphere Geophysics, NOAA, May 1971, single copy price 50 cents.

Upper Atmosphere Geophysics Report UAG-14, "An Experimental Comprehensive Flare Index and its Derivation for 'Major' Flares 1955-1969" by Helen W. Dodson and E. Ruth Hedeman, McMath-Hulbert Observatory, University of Michigan, July 1971, single copy price 30 cents.

Upper Atmosphere Geophysics Report UAG-15, "Catalogue of Data on Solar-Terrestrial Physics" prepared by Research Laboratories, NOAA, Boulder, Colorado, July 1971, single copy price \$1.50. (Supersedes Report UAG-11, June 1970.)

Upper Atmosphere Geophysics Report UAG-16, "Temporal Development of the Geographical Distribution of Auroral Absorption for 30 Substorm Events in each of IQSY (1964-65) and IASY (1969)" by F. T. Berkey, V. M. Driatskiy, K. Henriksen, D. H. Jelly, T. I. Shchuka, A. Theander and J. Yliniemi, September 1971, single copy price 70 cents.

Upper Atmosphere Geophysics Report UAG-17, "Ionospheric Drift Velocity Measurements at Jicamarca, Peru (July 1967 - March 1970)" by Ben B. Balsley, Aeronomy Laboratory, National Oceanic and Atmospheric Administration, Boulder, Colorado, and Ronald F. Woodman, Jicamarca Radar Observatory, Instituto Geofisico del Perú, Lima, Peru, October 1971, single copy price 35 cents.

Upper Atmosphere Geophysics Report UAG-18, "A Study of Polar Cap and Auroral Zone Magnetic Variations" by K. Kawasaki and S. I. Akasofu, Geophysical Institute, University of Alaska, June 1972, single copy price 20 cents.

Upper Atmosphere Geophysics Report UAG-19, "Reevaluation of Solar Flares 1967" by Helen W. Dodson and E. Ruth Hedeman of McMath-Hulbert Observatory, The University of Michigan, and Marta Rovira de Miceli, San Miguel Observatory, Argentina, June 1972, single copy price 15 cents.

Report UAG-20, "Catalogue of Data on Solar-Terrestrial Physics", prepared by Environmental Data Service, NOAA, Boulder, Colorado, October 1972, single copy price \$1.50. (Supersedes Report UAG-15, July 1971.)

Report UAG-21, "Preliminary Compilation of Data for Retrospective World Interval July 26 - August 14, 1972" compiled by J. Virginia Lincoln and Hope I. Leighton, World Data Center A for Solar-Terrestrial Physics, November 1972, single copy price 70 cents.

Report UAG-22, "Auroral Electrojet Magnetic Activity Indices (AE) for 1970" by Joe Haskell Allen, National Geophysical and Solar-Terrestrial Data Center, Environmental Data Service, November 1972, single copy price 75 cents.

Report UAG-23, "U.R.S.I. Handbook of Ionogram Interpretation and Reduction", Second Edition, November 1972, edited by W. R. Piggott, Radio and Space Research Station, Slough U.K., and K. Rawer, Arbeitsgruppe für Physikalische Weltraumforschung, Freiburg, G.F.R., November 1972, single copy price \$1.75.

Report UAG-24, "Data on Solar-Geophysical Activity Associated with the Major Ground Level Cosmic Ray Events of 24 January and 1 September 1971", Parts 1 and 2, compiled by Helen E. Coffey and J. Virginia Lincoln, World Data Center A for Solar-Terrestrial Physics, December 1972, single copy price (includes Parts 1 and 2) \$2.00.

Report UAG-25, "Observations of Jupiter's Sporadic Radio Emission in the Range 7.6-41 MHz, 9 September 1968 through 9 December 1971", by James W. Warwick, George A. Duik and David G. Swann, Department of Astro-Geophysics, University of Colorado, February 1973, single copy price 35¢.

Report UAG-26, "Data Compilation for the Magnetospherically Quiet Periods February 19-23 and November 29 - December 3, 1970", compiled by Helen E. Coffey and J. Virginia Lincoln, World Data Center A for Solar-Terrestrial Physics, May 1973, single copy price 70 cents.